

Catalytic Borylative Multicomponent Coupling Reactions and Novel Chemistry of Polycyclic Aromatic Hydrocarbons

Author: Hee Yeon Cho

Persistent link: <http://hdl.handle.net/2345/3398>

This work is posted on [eScholarship@BC](#),
Boston College University Libraries.

Boston College Electronic Thesis or Dissertation, 2013

Copyright is held by the author, with all rights reserved, unless otherwise noted.

Boston College

The Graduate School of Arts and Science

Department of Chemistry

CATALYTIC BORYLATIVE MULTICOMPONENT COUPLING REACTIONS

and

NOVEL CHEMISTRY OF POLYCYCLIC AROMATIC HYDROCARBONS

A dissertation

by

HEE YEON CHO

submitted in partial fulfillment of the requirements

for the degree of

Doctor of Philosophy

August 2013

© copyright by HEE YEON CHO

2013

ABSTRACT

CATALYTIC BORYLATIVE MULTICOMPONENT COUPLING REACTIONS

Hee Yeon Cho

Thesis Advisor: Professor James P. Morken

Expeditious establishment of molecular complexity in a stereoselective manner is a prominent goal in organic synthesis. In this regard, multicomponent coupling reactions have received substantial attention due to their ability to access complex molecules from simple starting materials in a single step.

Chapter 1 is a comprehensive review on catalytic bismetallative multicomponent reactions. The scope of this process in terms of both bismetallative reagents and the π -components are broad enough to be generally applied to more elaborate synthetic sequences. Particularly, contemporary applications of the bismetallative multicomponent coupling reactions, in which high enantio- and/or diastereoselectivities are displayed, have enabled the study of this area to make a significant step forward.

Chapter 2 presents nickel-catalyzed coupling reactions of aldehyde, diene, and a diboron reagent in the presence of a trialkyl phosphine ligand. Compared to borylation reactions with one π component, these borylative multicomponent reactions (involving two π components) lead to formation of a new C–C bond between the π components as well as generation of highly functionalized, stereodefined products.

Chapter 3 describes a remarkable turnover in regioselectivity of the borylative multicomponent coupling when PCy_3 is replaced with $\text{P}(\text{SiMe}_3)_3$. In particular, the products from the reactions with $\text{P}(\text{SiMe}_3)_3$ feature three contiguous stereocenters and an α -chiral allylboronate. The effect of $\text{P}(\text{SiMe}_3)_3$ ligand on the product selectivity is intriguing. According to the experimental and computational results, it has an ability to act as an electron acceptor, which will facilitate reductive elimination from the intermediate nickel complex during the course of the reaction.

In Chapter 4, we show that borylative ketone–diene coupling reactions can be accomplished in high yields and with excellent levels of diastereocontrol. This reaction occurs in a predictable fashion, yet with regioselection that is distinct from related aldehyde–diene coupling reactions. The reaction products from these coupling processes, which possess tertiary alcohol functionality and an allylic alcohol moiety, are particularly well suited for the preparation of polyketide natural products.

ABSTRACT

NOVEL CHEMISTRY OF POLYCYCLIC AROMATIC HYDROCARBONS

Hee Yeon Cho

Thesis Advisor: Professor Lawrence T. Scott

Chapter 5 presents investigations on bowl-shaped geodesic polyarenes, which are the missing links between the “classic” planar polycyclic aromatic hydrocarbons (PAHs) and the spheroidal fullerenes. The present study has shown that open geodesic polyarenes can feature chemistry inherent to both classes of aromatics. The curved π system induces unequal environments on the two faces of circumtrindene, significant strain energy to the molecule, and non-identical bond lengths. Along with the electronic effects, the stereoelectronic effect enabled the site-selective functionalization with fullerene-type chemistry. On the other hand, the edge carbons, which are not present in fullerenes, still possess reactivity of common planar PAHs.

Chapter 6 describes the intermolecular oxidative cyclotrimerization reactions of alkenes and aromatic compounds with DDQ and trifluoromethanesulfonic acid. The Scholl-type oxidation reactions involving alkenes have never been demonstrated. Moreover, the DDQ/acid system has never been used for the intermolecular oxidative cyclization reactions. This convenient non-metallic reagent system (DDQ/TfOH) is advantageous over the metal-

based Scholl-type oxidants because it eliminates the possibility of halogenation of aromatic compounds and the reduced oxidant can be reoxidized.

In Chapter 7, the regioselective formation of cyclic trimers from substituted benzenes and heteroaromatic compounds is demonstrated. This DDQ/TfOH method provides a simple and convenient synthetic route toward star-shaped oligomers containing triphenylene or isotruxene cores. Furthermore, the experimental outcome suggests that this oxidative process proceeds by an electron transfer mechanism. This is the first experimental evidence for mechanistic details on the Scholl-type oxidation.

ACKNOWLEDGEMENTS

None of this work would have been possible without help and guidance from a number of people around me. First of all, I would like to thank both of my Ph.D. advisors, Professor Lawrence T. Scott and Professor James P. Morken. I am greatly thankful to Professor Scott for supporting and guiding me throughout my time at Boston College. He taught me not only the chemistry of his own laboratory, but also how to teach chemistry in class and how to write various forms of papers. Moreover, it is unforgettable how sincerely he has shown his full respect for me when I was a student in his lab.

I also would like to thank Professor Morken for his excellent guidance and constant encouragement. Especially, when I just started my graduate study at BC, he was extremely patient with my endless questions. I was very fortunate to learn from and work with him at an earlier stage of my graduate studies, and he has been continuously supportive thereafter.

I would like to thank my committee members, Professor T. Ross Kelly and Professor Marc L. Snapper. I am grateful to them for being my thesis committee and for reading my thesis. Also, I would like to thank Professors Hoveyda, Tan, and Kingsbury for their support and inspiration during my study at Boston College. Besides, I am indebted to many other professors in the chemistry department at BC for their guidance and support.

I have been very pleased to work with a number of great coworkers in the Scott and the Morken groups. I have really appreciated their help and support in the laboratories. Last but not least, I would like to thank my parents and my family for being extremely supportive throughout my life.

Table of Contents

TABLE OF CONTENTS.....	I
LIST OF SCHEMES	XI
LIST OF TABLES	XXII
LIST OF FIGURES.....	XXIV
LIST OF ABBREVIATIONS.....	XXVI
CHAPTER 1. CATALYTIC BISMETALLATIVE MULTICOMPONENT COUPLING REACTIONS.....	1
1.1. Introduction	1
1.2. Mechanistic Considerations.....	5
1.2.1. Oxidative Cyclization Mechanism	5
1.2.2. Oxidative Addition Mechanism	6
1.3. Palladium-Catalyzed Bismetallative Multicomponent Coupling.....	8
1.3.1. Coupling of Alkyne–Alkyne and Alkyne–Alkene.....	8
1.3.2. Coupling of Allene–Allene and Allene–Alkyne	15
1.3.3. Coupling of Diene–Diene	19
1.3.4. Coupling of Aldehyde–Allene and Ketone–Allene.....	24
1.4. Platinum-Catalyzed Bismetallative Multicomponent Coupling.....	27
1.4.1. Coupling of Diene–Diene	27
1.4.2. Coupling of Aldehyde–Diene	28
1.5. Nickel Catalyzed Bismetallative Multicomponent Coupling.....	31
1.5.1. Coupling of Alkyne–Alkyne	31
1.5.2. Coupling of Aldehyde–Diene	32
1.5.2.1. Intramolecular Aldehyde–Diene Coupling	32
1.5.2.2. Intermolecular Aldehyde–Diene Coupling	37
1.5.3. Coupling of Ketone–Diene	43

1.6. Conclusions and Outlook.....	47
CHAPTER 2. NICKEL-CATALYZED MULTICOMPONENT COUPLING REACTIONS OF ALDEHYDES, DIENES, AND DIBORON REAGENTS	48
2.1. Introduction to Multicomponent Coupling Reactions	48
2.2. Background	53
2.2.1. Strecker Multicomponent Reaction	53
2.2.2. Hantzsch Multicomponent Reaction.....	55
2.2.3. Biginelli Multicomponent Reaction.....	57
2.2.4. Passerini Multicomponent Reaction	60
2.2.5. Ugi Multicomponent Reaction	62
2.2.6. Mannich Multicomponent Reaction.....	65
2.2.7. Summary	68
2.3. Method Development.....	69
2.3.1. Ni-Catalyzed Borylative Diene–Aldehyde Coupling.....	69
2.3.1.1. Project Goals	69
2.3.1.2. Reaction Optimization	72
2.3.1.3. Substrate Scope.....	75
2.3.1.3.1. Survey of Carbonyl Compounds	75
2.3.1.3.2. Survey of Unsaturated Hydrocarbons	77
2.3.1.3.3. Summary of Substrate Scope	79
2.3.1.4. Product Transformation.....	82
2.3.1.4.1. Three Component Coupling–Allylation Sequence	82
2.3.1.4.2. Determination of Relative Configurations	83
2.3.2. Ni-Catalyzed Diene Diboration	85
2.4. Mechanistic Considerations.....	86
2.4.1. Possible Mechanistic Pathways.....	86
2.4.2. Mechanistic Probe of Plausible Reaction Pathway	87
2.4.3. Proposed Catalytic Cycle	88
2.5. Conclusions and Outlook.....	90

2.6. Experimental Section	91
2.6.1. General Information	91
2.6.2. Experimental Procedures	94
2.6.2.1. General Procedure for Ni-Catalyzed Three-Component Coupling	94
2.6.2.1.1. Characterization Data and Proof of Stereochemistry	95
2.6.2.2. Procedure and Data for Ni-Catalyzed Diboration/Allylation	108
2.6.2.3. Procedure and Data for Ni-Catalyzed Diene Diboration	111
2.6.3. Representative Spectral Data	113
CHAPTER 3. LIGAND EFFECTS ON THE NICKEL-CATALYZED BORYLATIVE COUPLING REACTIONS OF ALDEHYDES AND DIENES	144
3.1. Introduction	144
3.1.1. Nickel-Catalyzed Reductive Coupling Reactions	144
3.1.2. Mechanistic Perspectives	147
3.2. Background	150
3.2.1. Reductive Coupling of Aldehyde–Diene	150
3.2.2. Reductive Coupling of Aldehyde–Alkyne	151
3.2.3. Reductive Coupling of Carbonyl–Allene	154
3.2.4. Reductive Coupling of Alkyne–Alkene	156
3.2.5. Reductive Coupling of Alkyne–Epoxide	159
3.2.6. Summary	161
3.3. Method Development	163
3.3.1. Aldehyde–Diene–Diboron Coupling with P(TMS) ₃ as a Ligand	163
3.3.1.1. Project Goals	163
3.3.1.2. Reaction Optimization	164
3.3.1.3. Substrate Scope	167
3.3.1.3.1. Survey of Carbonyl Compounds	167
3.3.1.3.2. Survey of Hydrocarbons and Diboron Reagents	171
3.3.1.3.3. Summary of Substrate Scope	174
3.3.1.4. Product Transformation	177

3.3.1.4.1. Three Component Coupling–Allylation Sequence	177
3.3.1.4.2. Determination of Relative Configurations	179
3.3.2. Catalytic Enantioselective Aldehyde–Diene–Diboron Coupling	183
3.4. Mechanistic Considerations.....	187
3.4.1. Properties of the P(TMS) ₃ Ligand	187
3.4.2. Theoretical Investigations	190
3.4.3. Proposed Reaction Mechanism	191
3.5. Conclusions and Outlook.....	193
3.6. Experimental Section	194
3.6.1. General Information	194
3.6.2. Experimental Procedures.....	197
3.6.2.1. General Procedure for Borylative Diene Aldehyde Coupling	197
3.6.2.1.1. Characterization Data and Proof of Stereochemistry.....	198
3.6.2.2. Procedure for Ni-Catalyzed Diboration/Allylation	220
3.6.2.2.1. Characterization and Proof of Stereochemistry	221
3.6.3. Representative Spectral Data.....	224
 CHAPTER 4. STEREOSELECTIVE SYNTHESIS OF TERTIARY ALCOHOLS VIA CATALYTIC BORYLATIVE COUPLING REACTIONS OF KETONES AND DIENES	 256
4.1. Introduction	256
4.1.1. Tertiary Alcohol Synthesis.....	256
4.1.2. Tertiary Alcohols from Ketones and Organometallics.....	260
4.2. Background	262
4.2.1. Asymmetric Arylation of Ketones.....	262
4.2.2. Asymmetric Alkylation of Ketones	264
4.2.3. Asymmetric Alkenylation of Ketones.....	266
4.2.4. Asymmetric Alkynylation of Ketones.....	268
4.2.5. Asymmetric Allylation/Crotylation of Ketones.....	270
4.2.6. Asymmetric Cyanosilylation of Ketones	273
4.2.7. Summary	276

4.3. Method Development.....	277
4.3.1. Catalytic Borylative Coupling Reactions of Ketones and Dienes	277
4.3.1.1. Project Goals	277
4.3.1.2. Reaction Optimization	278
4.3.1.3. Substrate Scope.....	281
4.3.1.3.1. Survey of Carbonyl Compounds	281
4.3.1.3.2. Survey of Unsaturated Hydrocarbons	284
4.3.1.3.3. Summary of Substrate Scope	285
4.3.1.4. Product Transformation.....	289
4.3.2. Ni-Catalyzed Borylative Coupling of Bisketones and Dienes.....	292
4.3.2.1. Project Goals	292
4.3.2.2. Project Descriptions	293
4.4. Mechanistic Considerations.....	295
4.4.1. Observed Product Selectivity	295
4.4.2. Proposed Reaction Pathways	296
4.5. Conclusions and Outlook.....	299
4.6. Experimental Section	300
4.6.1. General Information	300
4.6.2. Experimental Procedures.....	303
4.6.2.1. General Procedure for Borylative Ketone–Diene Coupling	303
4.6.2.2. Characterization Data and Proof of Stereochemistry	304
4.6.3. Representative Spectral Data.....	322
 CHAPTER 5. SITE-SELECTIVE FUNCTIONALIZATION OF A BOWL-SHAPED POLYCYCLIC AROMATIC HYDROCARBON (PAH)	 360
5.1. Introduction to Circumtrindene (C ₃₆ H ₁₂).....	360
5.2. Background	363
5.2.1. Nonplanar Polycyclic Aromatic Hydrocarbons (PAHs).....	363
5.2.2. Preparation of Nonplanar PAHs	366
5.2.3. Functionalization of Nonplanar PAHs	369

5.3. Synthesis of Circumtrindene	374
5.3.1. Circumtrindene from Decacyclene.....	374
5.3.2. Circumtrindene from Decacyclene Derivatives	375
5.3.2.1. Synthesis of Halogenated Decacyclenes.....	375
5.3.2.2. Pyrolysis of Halogenated Decacyclenes	380
5.3.2.3. Pyrolysis of <i>t</i> -Butylated Decacyclenes	382
5.3.2.4. Pyrolysis of <i>t</i> -Butylated and Halogenated Decacyclenes.....	385
5.3.3. Properties of Circumtrindene.....	388
5.4. Interior Functionalization of Circumtrindene	391
5.4.1. Bingel–Hirsch Reaction.....	391
5.4.2. Prato Reaction.....	394
5.4.3. Computational Studies.....	396
5.4.3.1. Frontier Molecular Orbital (FMO) Analysis	396
5.4.3.2. Electrostatic Potential (ESP) Analysis	398
5.5. Peripheral Functionalization of Circumtrindene	400
5.5.1. Ring Extension Process	401
5.5.2. Computational Studies.....	406
5.5.2.1. Magnetic Environment.....	406
5.5.2.2. Stereoelectronic Environment	409
5.5.2.2.1. Introduction to Natural Bond Orbital (NBO).....	409
5.5.2.2.2. NBO Analysis of Circumtrindene	414
5.6. Noncovalent Functionalization of Circumtrindene	417
5.6.1. Reduction with Lithium Metal.....	417
5.6.2. Complexation with Silver Ion	420
5.7. Conclusions and Outlook.....	422
5.8. Experimental Section	424
5.8.1. General Information	424
5.8.2. Experimental and Spectral Data	427
5.8.2.1. Circumtrindene	427

5.8.2.2.	Attempted Synthesis of Circumtrindene from C ₆₀ H ₆₆	433
5.8.2.3.	6-Fluoro-1-naphthoic acid.....	434
5.8.2.4.	2-Fluoronaphthalene	440
5.8.2.5.	1-(7-Fluoronaphthalen-1-yl)ethan-1-one	445
5.8.2.6.	Methyl 2-(7-fluoronaphthalen-1-yl)acetate	449
5.8.2.7.	2-(7-Fluoronaphthalen-1-yl)acetic acid	455
5.8.2.8.	2-(7-Fluoronaphthalen-1-yl)acetyl chloride	460
5.8.2.9.	8-Fluoroacenaphthylen-1(2H)-one	463
5.8.2.10.	1,7,13-trifluorodecacyclene	468
5.8.2.11.	Attempted Synthesis of Circumtrindene from C ₃₆ H ₁₅ F ₃	469
5.8.2.12.	1-(7-Chloronaphthalen-1-yl)ethan-1-one.....	470
5.8.2.13.	Methyl 2-(7-chloronaphthalen-1-yl)acetate.....	474
5.8.2.14.	2-(7-Chloronaphthalen-1-yl)acetic acid	477
5.8.2.15.	2-(7-Chloronaphthalen-1-yl)acetyl chloride.....	480
5.8.2.16.	8-Chloroacenaphthylen-1(2H)-one.....	484
5.8.2.17.	6b,7a-Dihydroacenaphtho[1,2-b]oxirene	488
5.8.2.18.	1-Acenaphthone	491
5.8.2.19.	Decacyclene.....	494
5.8.2.20.	Methyl 2-(3-(<i>tert</i> -butyl)-7-chloronaphthalen-1-yl)acetate	497
5.8.2.21.	2-(3-(<i>tert</i> -Butyl)-7-chloronaphthalen-1-yl)acetic acid	502
5.8.2.22.	2-(3-(<i>tert</i> -Butyl)-7-chloronaphthalen-1-yl)acetyl chloride	507
5.8.2.23.	4-(<i>tert</i> -Butyl)-8-chloroacenaphthylen-1(2H)-one.....	510
5.8.2.24.	5,11,17-tri- <i>tert</i> -butyl-1,7,13-trichlorodecacyclene	514
5.8.2.25.	Circumtrindene from C ₄₈ H ₃₉ Cl ₃	520
5.8.2.26.	12d,12e-(bis(ethoxycarbonyl)methylene-bridged)circumtrindene.....	521

CHAPTER 6.	INTERMOLECULAR OXIDATIVE COUPLING OF ARENES AND UNACTIVATED ALKENES LEADING TO π -CONJUGATED CYCLIC TRIMERS.....	525
6.1.	Introduction	525
6.1.1.	Oxidative Coupling of Unactivated Arenes.....	525

6.1.2. Scholl Oxidation	526
6.2. Background	529
6.2.1. Aluminum- or Copper/Aluminum-Mediated Scholl Oxidation.....	529
6.2.2. Iron-Mediated Scholl Oxidation	533
6.2.3. Molybdenum-Mediated Scholl Oxidation.....	535
6.2.4. Antimony-Mediated Scholl Oxidation.....	537
6.2.5. Thallium-Mediated Scholl Oxidation.....	539
6.2.6. DDQ/Acid-Mediated Scholl Oxidation.....	542
6.2.7. Summary	544
6.3. Method Development.....	545
6.3.1. Project Goals	545
6.3.2. Reaction Optimization.....	548
6.3.3. Substrate Scope.....	553
6.3.3.1. Survey of Unsaturated Hydrocarbons.....	553
6.3.3.2. Survey of Aromatic Compounds.....	559
6.4. Mechanistic Considerations.....	566
6.5. Conclusions and Outlook.....	569
6.6. Experimental Section	570
6.6.1. General Information	570
6.6.2. Experimental and Spectral Data	573
6.6.2.1. 4,7-Di- <i>tert</i> -butylacenaphthene.....	573
6.6.2.2. 4,7-Di- <i>tert</i> -butylacenaphthylene	575
6.6.2.3. 2,5,8,11,14,17-Hexa- <i>tert</i> -butyldecacyclene.....	577
6.6.2.4. Representative Procedure for Oxidative Coupling.....	579
6.6.2.5. 2,3,6,7,10,11-Hexamethoxytriphenylene.....	580
6.6.2.6. 2,3,6,7,10,11-Hexakis(octyloxy)triphenylene	583
6.6.2.7. 2,3,8,9,14,15-Hexahydrotriphenyleno[2,3-b:6,7-b':10,11- b'']tris-([1,4]dioxine).....	586
6.6.2.8. 2,3,6,7,10,11-Hexaethoxytriphenylene	589

6.6.2.9. 2,3,6,7,10,11-Hexakis(hexyloxy)triphenylene	593
6.6.2.10. 2,3,6,7,10,11-Hexakis(decyloxy)triphenylene.....	597
CHAPTER 7. REGIOSELECTIVE SYNTHESIS OF STAR-SHAPED POLYCYCLIC AROMATIC COMPOUNDS: EVIDENCE FOR A RADICAL CATION MECHANISM.....	601
7.1. Introduction	601
7.1.1. Conjugated Aromatic Systems in Materials Science.....	601
7.1.2. Star-Shaped Conjugated Oligomers.....	604
7.2. Background	607
7.2.1. Star-Shaped Oligomers with a Triphenylene Core	607
7.2.2. Star-Shaped Oligomers with a Truxene Core	611
7.2.3. Star-Shaped Oligomers with an Isotruxene Core.....	615
7.2.4. Star-Shaped Oligomers with a Hexaazatriphenylene (HAT) Core	616
7.2.5. Star-Shaped Oligomers with a Triazatruxene Core	619
7.2.6. Summary	622
7.3. Method Development.....	624
7.3.1. Project Goals	624
7.3.2. Oxidation toward Triphenylene Derivatives.....	625
7.3.2.1. Survey of Halogenated Anisoles	625
7.3.2.2. Survey of Substituted Aromatic Compounds.....	630
7.3.3. Oxidation toward Isotruxene Derivatives.....	633
7.3.3.1. Survey of Benzothiophenes and Thiophenes.....	633
7.3.3.2. Survey of Indoles and Benzofurans	636
7.4. Mechanistic Considerations.....	638
7.5. Conclusions and Outlook.....	643
7.6. Experimental Section	644
7.6.1. General Information	644
7.6.2. Experimental and Spectral Data	647
7.6.2.1. Representative Procedure for Oxidative Coupling of Anisoles.....	647
7.6.2.2. 2,6,11-Trichloro-3,7,10-trimethoxytriphenylene	648

7.6.2.3.	2,6,11-Tribromo-3,7,10-trimethoxytriphenylene	655
7.6.2.4.	2,6,11-Trifluoro-3,7,10-trimethoxytriphenylene	661
7.6.2.5.	2,6,11-Tribromo-3,7,10-triethoxytriphenylene	665
7.6.2.6.	2,6,11-Trichloro-3,7,10-triethoxytriphenylene	668
7.6.2.7.	2,6,11-Tribromo-3,7,10-tris(2-bromoethoxy)triphenylene.....	676
7.6.2.8.	2,6,11-Tris(2-bromoethoxy)-3,7,10-trimethoxytriphenylene.....	680
7.6.2.9.	2,6,11-Tris(3-bromopropoxy)-3,7,10-trichlorotriphenylene	683
7.6.2.10.	Representative Procedure for Coupling of Benzothiophenes	690
7.6.2.11.	Benzo[1,2- <i>b</i> :3,4- <i>b'</i> :6,5- <i>b''</i>]tris[1]benzothiophene	691
7.6.2.12.	2,7,14-Trimethylbenzo[1,2- <i>b</i> :3,4- <i>b'</i> :6,5- <i>b''</i>]tris[1]benzothiophene	697

List of Schemes

Scheme 1.1 Bismetallative Coupling with One vs. Two π -Components.....	2
Scheme 1.2 Reductive vs Bismetallative Multicomponent Coupling.....	4
Scheme 1.3 Oxidative Cyclization Mechanism	6
Scheme 1.4 Oxidative Addition Mechanism	7
Scheme 1.5 Sakurai's Intermolecular Alkyne–Alkyne Coupling (1975).....	8
Scheme 1.6 Tanaka's Intramolecular Alkyne–Alkene Coupling (1997).....	10
Scheme 1.7 Mori's Intramolecular Alkyne–Alkene Coupling (2001).....	11
Scheme 1.8 Proposed Mechanism for Enyne Cyclization (Mori, 2001).....	12
Scheme 1.9 RajanBabu's Intramolecular Alkyne–Alkyne Coupling (2000).....	12
Scheme 1.10 Enantiomers of Compound 1.27 at $-40\text{ }^{\circ}\text{C}$ (RajanBabu, 2000).....	13
Scheme 1.11 RajanBabu's Stereoselective Diyne Cyclization (2012).....	14
Scheme 1.12 Proposed Origin of Stereoselectivity (RajanBabu, 2012).....	15
Scheme 1.13 Kang's Intramolecular Allene–Allene Coupling (2000).....	16
Scheme 1.14 Rationale for Stereochemical Outcome (Kang, 2000).....	17
Scheme 1.15 RajanBabu's Intramolecular Allene–Alkyne Coupling (2001).....	18
Scheme 1.16 Yu's Intramolecular Allene–Allene Coupling (2004).....	18
Scheme 1.17 Sakurai's Intermolecular Diene–Diene Coupling (1975).....	20
Scheme 1.18 Sakurai's Disilylative Dimerization of Dienes (1984).....	21
Scheme 1.19 Synthesis of <i>dl</i> -Muscone 1.54 (Sakurai, 1984).....	21
Scheme 1.20 Tsuji's Intermolecular Diene–Diene Coupling (1992).....	22

Scheme 1.21 Tsuji's Intramolecular Diene–Diene Coupling (1995)	23
Scheme 1.22 Synthesis and ORTEP Drawing of 1.63 (Tsuji, 1995)	23
Scheme 1.23 Rationale for Stereochemical Outcome (Kang, 2002)	26
Scheme 1.24 Miyaura's Intermolecular Diene–Diene Coupling (1996).....	28
Scheme 1.25 Proposed Mechanism for Pt-Catalyzed Coupling (Ito, 1998).....	30
Scheme 1.26 Ito's Ni-Catalyzed Alkyne Dimerization (1998).....	31
Scheme 1.27 Proposed Mechanism for Alkyne Dimerization (Ito, 1998).....	32
Scheme 1.28 Mori's Intramolecular Aldehyde–Diene Coupling (2002).....	33
Scheme 1.29 Yu's Sequential Four-Component Coupling (2005).....	34
Scheme 1.30 Rationale for Stereochemical Outcome (Yu, 2005).....	35
Scheme 1.31 Mori and Sato's Aldehyde–Diene Coupling (2007).....	36
Scheme 1.32 Proposed Mechanism for Cho–Morken Coupling (2008).....	39
Scheme 1.33 Ligand Effect on Regioselectivity (Morken, 2010)	40
Scheme 1.34 Morken's Intermolecular Ketone–Diene Coupling (2011).....	44
Scheme 1.35 Mechanistic Rationale for Borylative Multicomponent Coupling (2011).....	46
Scheme 2.1 Multicomponent Coupling Reactions.....	49
Scheme 2.2 Strecker Multicomponent Reaction.....	54
Scheme 2.3 Jacobsen's Asymmetric Acyl-Strecker Reaction.....	55
Scheme 2.4 Hantzsch Multicomponent Reaction	55
Scheme 2.5 Gong's Asymmetric Hantzsch Reaction.....	57
Scheme 2.6 Biginelli Multicomponent Reaction	58
Scheme 2.7 Zhu's Asymmetric Biginelli Reaction	59
Scheme 2.8 Chen's Asymmetric Biginelli Reaction.....	60

Scheme 2.9 Passerini Multicomponent Reaction	61
Scheme 2.10 Schreiber's Asymmetric Passerini Reaction.....	61
Scheme 2.11 Zhu's Asymmetric Passerini Reaction.....	62
Scheme 2.12 Ugi Multicomponent Reaction.....	63
Scheme 2.13 Carreira's Ugi Reaction.....	64
Scheme 2.14 Zhu's Asymmetric Three-Component Ugi Reaction.....	65
Scheme 2.15 Mannich Multicomponent Reaction	66
Scheme 2.16 Dondori's Mannich Reaction	67
Scheme 2.17 Córdova's Asymmetric Mannich Reaction.....	68
Scheme 2.18 Diboration of One π Component.....	70
Scheme 2.19 Diboration of Two π Components.....	71
Scheme 2.20 Expected Products from Borylative Aldehyde–Diene Coupling	71
Scheme 2.21 Initial Investigation on Borylative Aldehyde–Diene Coupling.....	72
Scheme 2.22 Survey of Aromatic Aldehydes for Borylative Coupling Reactions	76
Scheme 2.23 Survey of Aliphatic Aldehydes for Borylative Coupling Reactions	76
Scheme 2.24 Survey of Dienes for Borylative Coupling Reactions.....	77
Scheme 2.25 Survey of Alkynes and Alkenes for Borylative Coupling Reactions	78
Scheme 2.26 Borylative Aldehyde– <i>cis</i> -Piperylene Coupling.....	78
Scheme 2.27 NMR Experiments for Diene Isomerization	79
Scheme 2.28 Three-Component Coupling and Subsequent Allylation.....	83
Scheme 2.29 Ozonolysis of a Coupling Product.....	83
Scheme 2.30 Multistep Transformation of a Coupling Product.....	84
Scheme 2.31 Acetonide Analysis of a Coupling Product Derivative.....	84

Scheme 2.32 Nickel-Catalyzed Diene Diboration.....	85
Scheme 2.33 Oxidative Cyclization Mechanism.....	86
Scheme 2.34 Sequential Diboration–Allylation Mechanism.....	87
Scheme 2.35 Sequential Diboration–Allylation Experiments.....	88
Scheme 2.36 Proposed Catalytic Cycle for Borylative Aldehyde–Diene Coupling.....	89
Scheme 3.1 Isolated Nickelacyclic Intermediate.....	148
Scheme 3.2 Catalytic Cycle for Reductive Coupling Reactions.....	149
Scheme 3.3 Intramolecular Aldehyde–Diene Coupling.....	150
Scheme 3.4 Intermolecular Aldehyde–Diene Coupling.....	151
Scheme 3.5 Intramolecular Aldehyde–Alkyne Coupling.....	152
Scheme 3.6 Total Synthesis of D-Erythro-sphingosine.....	153
Scheme 3.7 Enantioselective Aldehyde–Alkyne Coupling.....	154
Scheme 3.8 Intramolecular Aldehyde–Allene Coupling.....	155
Scheme 3.9 Intramolecular Ketone–Allene Coupling.....	156
Scheme 3.10 Intramolecular Alkyne–Alkene Coupling.....	157
Scheme 3.11 Intermolecular Alkyne–Alkene Coupling.....	158
Scheme 3.12 Intermediate Nickelacyclic Enolate.....	159
Scheme 3.13 Intermolecular Coupling of Alkyne–Epoxide.....	159
Scheme 3.14 Key Step in the Synthesis of (–)-Cyatha-3,12-diene.....	160
Scheme 3.15 Total Synthesis of (–)-Gloeosporone.....	161
Scheme 3.16 A Regioisomeric Product for the Borylative Aldehyde–Diene Coupling.....	163
Scheme 3.17 Initial Investigations toward 1,3-Diol Synthesis.....	166
Scheme 3.18 Survey of Aromatic Aldehydes for 1,3-Diol Synthesis.....	168

Scheme 3.19 Survey of Heterocyclic Aromatic Aldehydes for 1,3-Diol Synthesis	168
Scheme 3.20 Survey of Aliphatic Aldehydes for 1,3-Diol Synthesis.....	169
Scheme 3.21 Survey of Carbonyl Compounds for 1,3-Diol Synthesis.....	170
Scheme 3.22 Survey of Chiral Aldehydes for 1,3-Diol Synthesis	170
Scheme 3.23 Coupling Reaction with an α -Chiral Aldehyde and the Felkin–Ahn Model	171
Scheme 3.24 Survey of Dienes for 1,3-Diol Synthesis	172
Scheme 3.25 Survey of Alkynes and Alkenes for 1,3-Diol Synthesis.....	172
Scheme 3.26 Three-Component Coupling Reaction with <i>cis</i> -Piperylene.....	173
Scheme 3.27 Three-Component Coupling Reaction with Isoprene	173
Scheme 3.28 Survey of Diboron Reagents for Borylative Aldehyde–Isoprene Coupling	174
Scheme 3.29 Three Component Coupling with $P(TMS)_3$ and Subsequent Allylation	178
Scheme 3.30 Proposed Transition State for the Subsequent Allylation Step.....	178
Scheme 3.31 Synthesis and Analysis of Acetonide Derived from a Coupling Product.....	179
Scheme 3.32 Acetonide Analysis of a Coupling Product	180
Scheme 3.33 Multistep Transformation of a Coupling Product	180
Scheme 3.34 Synthetic Plan for the Enantioenriched Authentic Compound.....	181
Scheme 3.35 Synthetic Route to Compound 3.10	181
Scheme 3.36 Synthetic Route to the Enantioenriched Authentic Compound	182
Scheme 3.37 Chiral Monodentate Phosphine/Phosphoramidite Ligand Screening.....	183
Scheme 3.38 Chiral Bidentate Phosphine Ligand Screening.....	184
Scheme 3.39 Chiral Nitrogen Ligand Screening	185
Scheme 3.40 Chiral PN Ligand and NHC Ligand Screening.....	186
Scheme 3.41 Original Design for Optically-Active Chiral Phosphine Ligands.....	186

Scheme 3.42 Palladium-Catalyzed Aryl Amination	187
Scheme 3.43 Proposed Reaction Pathways for Borylative Aldehyde–Diene Coupling	192
Scheme 4.1 Enantioselective Tertiary Alcohol Synthesis	259
Scheme 4.2 Organometallic Addition to a Ketone	261
Scheme 4.3 Fu’s Arylation of Ketones	262
Scheme 4.4 Ishihara’s Arylation of Ketones	263
Scheme 4.5 Gau’s Arylation of Ketones	264
Scheme 4.6 Yus’ Alkylation of Ketones.....	265
Scheme 4.7 Shibasaki’s Alkylation of α -Ketoesters.....	266
Scheme 4.8 Walsh’s Alkenylation of Ketones	267
Scheme 4.9 Shibasaki’s Alkenylation of Ketones.....	268
Scheme 4.10 Cozzi’s Alkynylation of Ketones	269
Scheme 4.11 Chan’s Alkynylation of Ketones.....	269
Scheme 4.12 Tagliavini’s Allylation of Ketones.....	271
Scheme 4.13 Shibasaki’s Allylation of Ketones	271
Scheme 4.14 Yamamoto’s Crotylation of Ketones.....	272
Scheme 4.15 Sigman’s Allylation of Ketones	273
Scheme 4.16 Choi’s Cyanosilylation of Ketones	274
Scheme 4.17 Snapper and Hoveyda’s Cyanosilylation of Ketones.....	275
Scheme 4.18 Borylative Ketone–Diene Coupling Reactions	277
Scheme 4.19 Initial Investigations on Ketone–Diene Coupling Reactions	278
Scheme 4.20 Spirobiindane-Derived Ligand for Borylative Ketone–Diene Coupling.....	280
Scheme 4.21 Survey of Acetophenone Derivatives for Borylative Ketone–Diene Coupling	281

Scheme 4.22 Survey of Aromatic Ketones for Borylative Ketone–Diene Coupling	282
Scheme 4.23 Survey of Halogenated Aromatic Ketones for Borylative Ketone–Diene Coupling.....	282
Scheme 4.24 Survey of Various Ketones for Borylative Ketone–Diene Coupling	283
Scheme 4.25 Attempted Experiments for Borylative Pyruvate–Diene Coupling	283
Scheme 4.26 Survey of Aliphatic Ketones for 1,5-Diol Synthesis.....	284
Scheme 4.27 Survey of Dienes for Borylative Ketone–Diene Coupling.....	285
Scheme 4.28 Borylative Coupling of Acetophenone and Isoprene.....	285
Scheme 4.29 Attempts to Protect the Coupling Product with Acetonide	290
Scheme 4.30 Acetal Analysis for Relative Configurations	291
Scheme 4.31 Borylative Coupling Reactions with Bis-Electrophiles	292
Scheme 4.32 Intramolecular Allylation with Bisketone–Diene Coupling	293
Scheme 4.33 Proposed Reaction Pathway for Borylative Bisketone–Diene Coupling.....	294
Scheme 4.34 Observed Effects of Substrate Sterics on Product Selectivity	295
Scheme 4.35 Proposed Reaction Mechanism for Less Hindered Carbonyls	297
Scheme 4.36 Proposed Reaction Mechanism for More Hindered Carbonyls.....	298
Scheme 5.1 Covalent Functionalization of Circumtrindene	362
Scheme 5.2 Bingel–Hirsch Reaction of C ₆₀ -Fullerene.....	371
Scheme 5.3 Prato Reaction of C ₆₀ -Fullerene.....	372
Scheme 5.4 Carbene Addition to Corannulene.....	372
Scheme 5.5 Dimethylation of Diindenochrysene.....	373
Scheme 5.6 Synthesis of Circumtrindene with FVP	374
Scheme 5.7 Pyrolysis of Circumtrindene at 1100 °C at Different Pressures	375
Scheme 5.8 HF Homo-Elimination	377

Scheme 5.9 Synthetic Route to Trifluorodecacyclene	378
Scheme 5.10 Synthetic Route to Trichlorodecacyclene	379
Scheme 5.11 Pyrolysis of Trifluorodecacyclene	381
Scheme 5.12 Pyrolysis of Trichlorodecacyclene.....	381
Scheme 5.13 Synthesis of Hexa- <i>t</i> -butyldecacyclene	384
Scheme 5.14 Pyrolysis of Hexa- <i>t</i> -butyldecacyclene	385
Scheme 5.15 Synthesis of <i>tert</i> -Butylated Trichlorodecacyclene	387
Scheme 5.16 Pyrolysis of <i>tert</i> -Butylated Trichlorodecacyclene	388
Scheme 5.17 Bingel–Hirsch Reaction of Circumtrindene.....	392
Scheme 5.18 Proposed Mechanism for the Bingel–Hirsch Reaction of Circumtrindene.....	393
Scheme 5.19 Prato Reaction of Circumtrindene.....	395
Scheme 5.20 Selected Electrophilic Aromatic Substitution Reactions	400
Scheme 5.21 Site-Selective Peripheral Monobromination of Circumtrindene	404
Scheme 5.22 Suzuki Coupling and Ring Closing Reactions toward Indenocircumtrindene.....	405
Scheme 5.23 Suzuki Coupling of Brominated Circumtrindene	407
Scheme 5.24 Reduction of Corannulene	418
Scheme 5.25 Reduction of Circumtrindene	419
Scheme 5.26 Preparation of Ag(I)–Circumtrindene Complex.....	421
Scheme 6.1 Scholl Reaction (Original Report by Scholl)	527
Scheme 6.2 Aluminum-Mediated Intramolecular Oxidation	530
Scheme 6.3 Preparation of Dehydrohelicenes.....	531
Scheme 6.4 Copper/Aluminum-Mediated Intramolecular Oxidation	532
Scheme 6.5 Various Planar Conformations of Oligophenylene	533

Scheme 6.6 Iron-Mediated Intermolecular Oxidation	534
Scheme 6.7 Iron-Mediated Intramolecular Oxidation	535
Scheme 6.8 Molybdenum-Mediated Intramolecular Oxidation.....	536
Scheme 6.9 Molybdenum-Mediated Intermolecular Oxidation.....	537
Scheme 6.10 Antimony-Mediated Intermolecular Oxidation.....	538
Scheme 6.11 Antimony-Mediated Cyclization and Dimerization	539
Scheme 6.12 Thallium-Mediated Intramolecular Oxidation.....	540
Scheme 6.13 Synthesis of (\pm)-Ocoteine	541
Scheme 6.14 Thallium-Mediated Intermolecular Oxidation.....	541
Scheme 6.15 Rathore's Hexabenzocoronene Synthesis	542
Scheme 6.16 Chen & Liu's Fjord Region Oxidation	543
Scheme 6.17 Triple Aldol Condensation Reaction	545
Scheme 6.18 Oxidative Coupling toward Triply-Annulated Benzene Rings.....	546
Scheme 6.19 Trimerization of Acenaphthylene Derivatives.....	547
Scheme 6.20 Synthesis of <i>Tert</i> -butylated Acenaphthylene.....	548
Scheme 6.21 Initial Investigations on Oxidative Cyclotrimerization	549
Scheme 6.22 Oxidative Cyclotrimerization of Cyclic Alkenes	555
Scheme 6.23 Oxidative Cyclotrimerization of Phenanthrene	555
Scheme 6.24 Oxidative Cyclotrimerization of Acyclic Alkenes	556
Scheme 6.25 One-pot Operation for DDQ Oxidation and Oxidative Cyclotrimerization.....	557
Scheme 6.26 Sonogashira Coupling of 4- <i>tert</i> -Butylphenylacetylene	558
Scheme 6.27 Oxidative Cyclotrimerization of Alkyne.....	559
Scheme 6.28 Oxidative Cyclotrimerization of Veratrole Derivatives.....	560

Scheme 6.29 Oxidative Cyclotrimerization of Dialkoxy/Difluoroalkoxy Benzenes.....	561
Scheme 6.30 Oxidative Cyclotrimerization of Benzodioxoles	562
Scheme 6.31 Oxidative Cyclotrimerization of Disubstituted Benzenes	563
Scheme 6.32 Possible Oxidation Route for Catechol.....	563
Scheme 6.33 Oxidative Cyclotrimerization of Aromatic Compounds	564
Scheme 6.34 Oxidative Cyclotrimerization of Benzo-18-crown-6.....	565
Scheme 6.35 Electron Transfer Mechanism for Oxidative Cyclotrimerization	567
Scheme 6.36 Proton Transfer Mechanism for Oxidative Cyclotrimerization.....	568
Scheme 7.1 Synthesis of Triphenylene by Oxidative Dehydrogenation	608
Scheme 7.2 Trimerization of Benzyne	609
Scheme 7.3 Preparation of Functionalized Triphenylenes	610
Scheme 7.4 Synthesis of Truxene	612
Scheme 7.5 Synthesis of Truxene from 1-Indanone	613
Scheme 7.6 Preparation of Functionalized Truxenes	614
Scheme 7.7 Synthesis of Isotruxene	615
Scheme 7.8 Preparation of Hexaazatriphenylene Derivatives.....	617
Scheme 7.9 Preparation of Functionalized Hexaazatriphenylene	618
Scheme 7.10 Synthesis of Triazatruxene	620
Scheme 7.11 Preparation of Triazatruxene Derivatives.....	621
Scheme 7.12 Preparations and Properties of Six-Armed Triazatruxenes	622
Scheme 7.13 Oxidative Coupling toward Triphenylene Derivatives	624
Scheme 7.14 Oxidative Coupling toward Truxene/Isotruxene Derivatives	625
Scheme 7.15 Oxidative Cyclotrimerization of 2-Chloroanisole.....	626

Scheme 7.16 Oxidative Cyclotrimerization of Halogenated Anisoles and Phenetoles.....	627
Scheme 7.17 Oxidative Cyclotrimerization of 2-Fluoroanisole	628
Scheme 7.18 Oxidative Cyclotrimerization of Halogenated Trifluoromethoxy Benzenes.....	629
Scheme 7.19 Oxidative Cyclotrimerization of Halogenated Anisole Derivatives	630
Scheme 7.20 Oxidative Cyclotrimerization of Dialkoxy Benzene.....	631
Scheme 7.21 Oxidative Cyclotrimerization of Anisole Derivatives.....	632
Scheme 7.22 Oxidative Cyclotrimerization of Monosubstituted Aromatic Compounds.....	633
Scheme 7.23 Oxidative Cyclotrimerization of Benzothiophene	634
Scheme 7.24 Oxidative Cyclotrimerization of Halogenated Benzothiophenes.....	635
Scheme 7.25 Oxidative Cyclotrimerization of 5-Methyl-1-benzothiophene.....	635
Scheme 7.26 Oxidative Cyclotrimerization of 2,3-Dimethylthiophene.....	636
Scheme 7.27 Oxidative Cyclotrimerization of Benzofuran	636
Scheme 7.28 Oxidative Cyclotrimerization of Indole and its Derivatives	637
Scheme 7.29 Dimer Formation via Electron Transfer Mechanism.....	639
Scheme 7.30 Trimer Formation via Electron Transfer Mechanism.....	640
Scheme 7.31 Dimer Formation via Proton Transfer Mechanism.....	641
Scheme 7.32 Trimer Formation via Proton Transfer Mechanism.....	642

List of Tables

Table 1.1 Kang's Intramolecular Carbonyl–Allene Coupling (2002).....	25
Table 1.2 Ito's Intermolecular Aldehyde–Diene Coupling (1998).....	29
Table 1.3 Morken's Intermolecular Aldehyde–Diene Coupling (2008)	38
Table 1.4 Aldehyde–Diene Coupling for 1,3-Diols (Morken, 2010).....	41
Table 1.5 Saito and Sato's Enantioselective Coupling Reactions (2012).....	43
Table 1.6 Ketone–Diene Coupling for 1,5-Diol Synthesis (Morken, 2011).....	45
Table 2.1 Screen of Ligands for Borylative Aldehyde–Diene Coupling	73
Table 2.2 Survey of Solvents for Borylative Aldehyde–Diene Coupling.....	74
Table 2.3 Effect of Temperature on Borylative Aldehyde–Diene Coupling.....	74
Table 2.4 Influence of Concentration on Borylative Aldehyde–Diene Coupling	75
Table 2.5 Ni-Catalyzed Borylative Aldehyde–Piperylene Coupling.....	80
Table 2.6 Ni-Catalyzed Borylative Aldehyde–Diene Coupling	81
Table 2.7 Ni-Catalyzed Borylative Coupling with Aliphatic Aldehydes	82
Table 3.1 Survey of Ligands for 1,3-Diol Synthesis.....	165
Table 3.2 Screen of Solvents for 1,3-Diol Synthesis	166
Table 3.3 Influence of Temperature on 1,3-Diol Synthesis.....	167
Table 3.4 Stereoselective 1,3-Diol Synthesis with Benzaldehyde Derivatives.....	175
Table 3.5 Stereoselective 1,3-Diol Synthesis with Aromatic Aldehydes	176
Table 3.6 Stereoselective 1,3-Diol Synthesis with Aliphatic Aldehydes	177
Table 3.7 CO IR Stretching for Nickel–Phosphine Complexes.....	189

Table 3.8 Carbon NMR Data for Phosphine Ligands	190
Table 4.1 Effects of Reaction Temperature on Borylative Ketone–Diene Coupling.....	279
Table 4.2 Screen of Ligands for Borylative Ketone–Diene Coupling	280
Table 4.3 Borylative Ketone–Diene Coupling with Acetophenone Derivatives.....	286
Table 4.4 Borylative Ketone–Diene Coupling with Methyl Ketones.....	287
Table 4.5 Borylative Ketone–Piperylene Coupling Reactions	288
Table 4.6 Borylative Ketone–Diene Coupling Reactions.....	289
Table 5.1 Calculated and Experimentally-Obtained NMR Chemical Shifts.....	408
Table 6.1 Screen of Acids for Oxidative Cyclotrimerization.....	550
Table 6.2 Screen of Oxidants for Oxidative Cyclotrimerization.....	551
Table 6.3 Effect of Temperature on Oxidative Cyclotrimerization	552
Table 6.4 Influence of Concentrations on Oxidative Cyclotrimerization.....	553

List of Figures

Figure 2.1 Synthetic Target Molecules – Microtubule Stabilizers	72
Figure 3.1 <i>P</i> -Chiral Ferrocenyl Phosphine	154
Figure 3.2 Potential Synthetic Target – Discodermolide	164
Figure 3.3 X-Ray Analysis of the P(TMS) ₃ Ligand	188
Figure 3.4 Tungsten–Phosphine Complexes	189
Figure 3.5 NBO Analysis of Phosphine Ligands	191
Figure 4.1 Biologically Related Molecules Containing Tertiary Alcohol Functionality	257
Figure 4.2 Synthetic Targets in Natural Products	278
Figure 4.3 Rationale for the Observed Reactivity of the Diol	290
Figure 4.4 Potential Synthetic Target for Borylative Bisketone–Diene Coupling	293
Figure 5.1 Circumtrindene (C ₃₆ H ₁₂)	361
Figure 5.2 Prototypical Open and Closed Geodesic Polyarenes	364
Figure 5.3 Planar vs Pyramidalized π System	365
Figure 5.4 POAV Angles of C ₆₀ -Fullerene, Corannulene, and Diindenochoyrene	366
Figure 5.5 Flash Vacuum Pyrolysis Apparatus	367
Figure 5.6 Selected Examples of Geodesic Polyarenes Synthesized by FVP	369
Figure 5.7 Incorporation of Halogens in the Fjord Regions	376
Figure 5.8 Decacyclene with Solubilizing Group	383
Figure 5.9 <i>Tert</i> -Butylated and Halogenated Decacyclenes	386
Figure 5.10 POAV Angle and Bond Lengths of Circumtrindene	389

Figure 5.11 LUMO Orbital Map of Circumtrindene (B3LYP/6-31G*)	398
Figure 5.12 Electrostatic Potentials on the Surfaces of Circumtrindene (B3LYP/6-31G*).....	398
Figure 5.13 Monoindeno, Diindeno, and Triindeno Substituted Circumtrindene	402
Figure 5.14 Two Different Rim Carbon Atoms on Circumtrindene	403
Figure 5.15 Chemical Shifts of <i>ortho</i> -Methyl Groups in Compounds 5.40 and 5.41	408
Figure 5.16 Canonical Molecular Orbitals of Fullerene-C ₆₀	411
Figure 5.17 Natural Bond Orbitals of Fullerene-C ₆₀	411
Figure 5.18 Hierarchy of Orbitals.....	412
Figure 5.19 Consequence of the Curvature	414
Figure 5.20 Reference System for NBO Analysis.....	415
Figure 5.21 NBO Analysis for Hyperconjugation	416
Figure 5.22 X-Ray Structure of Corannulene Tetraanion	419
Figure 6.1 Triphenylene Core in Discotic Liquid Crystals	547
Figure 7.1 Structure Types of Conjugated Oligomers	604
Figure 7.2 Star-Shaped Oligomers with a Silicon Core.....	605
Figure 7.3 Polycyclic Ring Cores of Star-Shaped Oligomers	606
Figure 7.4 Discotic Liquid Crystals.....	611
Figure 7.5 Functionalized Isotruxenes	616
Figure 7.6 Carbazole and Triazatruxene.....	619

List of Abbreviations

Å	angstrom
Ac	acetyl
acac	acetylacetonyl
anhyd	anhydrous
<i>anti</i>	against, opposite
AO	atomic orbital
aq	aqueous
Ar	aryl (substituted aromatic ring)
atm	atmosphere
B ₂ (cat) ₂	bis(catecholato)diboron
B ₂ (pin) ₂	bis(pinacolato)diboron
B3LYP	Becke 3-Parameter (Exchange), Lee, Yang and Parr
BINAP	2,2'-bis(diphenylphosphino)-1,1'-binaphthyl
BINOL	1,1'-bi-2-naphthol
BIPHEP	2,2'-bis(diphenylphosphino)-6,6'-dimethoxy-1,1'biphenyl
Bn	benzyl
Boc	<i>tert</i> -butoxycarbonyl
BOX	bis(oxazoline)
bp	boiling point
br	broad or broadened (spectra)
Bu	butyl

Bz	benzoyl
C	Celsius
cat	catechol
cat.	catalytic
Cbz	benzyloxycarbonyl
<i>cis</i>	<i>L.</i> , on the same side
cm ⁻¹	wavenumbers
cod	cyclooctadiene
Cp	cyclopentadienyl
Cy	cyclohexyl
δ	NMR chemical shift in parts per million downfield from a standard
d	day
	deuteron
	doublet (spectra)
D	dextrorotatory (absolute configuration)
DAIB	dimethylamino isoborneol
DART	direct analysis in real time
dba	dibenzylidene acetone
DBU	1,8-diazabicyclo[5.4.0]undec-7-ene
DCE	1,2-dichloroethane
DCM	dichloromethane
dd	doublet of doublets (spectra)
DDQ	2,3-dichloro-5,6-dicyano-1,4-benzoquinone
DEAD	diethyl azodicarboxylate

DFT	density functional theory
DHP	dihydropyridine
DHPM	dihydropyrimidine
DIBAL	di- <i>iso</i> -butylaluminum hydride
DIPEA	<i>N,N</i> -diisopropylethylamine (Hünig's base)
DMAc	<i>N,N</i> -dimethylacetamide
DMAP	4- <i>N,N</i> -dimethylaminopyridine
DMF	<i>N,N</i> -dimethylformamide
DMP	Dess–Martin periodinane
DMS	dimethylsulfide
DMSO	dimethylsulfoxide
dppb	1,4-bis(diphenylphosphino)butane
dppe	1,2-bis(diphenylphosphino)ethane
dppf	1,1'-bis(diphenylphosphino)ferrocene
dppp	1,3-bis(diphenylphosphino)propane
dr	diastereomeric ratio
Duphos	1,2-bis(phospholano)benzene
<i>E</i>	energy
	<i>Ger.</i> , entgegen (configuration)
EDG	electron-donating group
ee	enantiomeric excess
E_h	hartree (unit)
EI	electron impact ionization
eq	equation

equiv	equivalent
er	enantiomeric ratio
ESI	electrospray ionization
ESP	electrostatic potential
ESR	electron spin resonance
Et	ethyl
Et ₂ O	diethyl ether
EtOAc	ethyl acetate
eu	entropy unit
EWG	electron-withdrawing group
FMO	frontier molecular orbital
FT	Fourier transform
FVP	flash vacuum pyrolysis
g	gram
G	Gibbs energy
GC-MS	gas chromatography-mass spectrometry
GIAO	gauge independent atomic orbital
GLC	gas liquid chromatography
h	hour
<i>h</i>	Planck's constant
<i>H</i>	enthalpy
HAT	hexaazatriphenylene
HBC	hexabenzocoronene
HF	Hartree-Fock

HMBC	heteronuclear multiple bond coherence
HMO	Hückel molecular orbital
$h\nu$	irradiation with light (h is Planck's constant, and ν is the photon frequency)
HOMO	highest occupied molecular orbital
HPLC	high performance liquid chromatography
HRMS	high resolution mass spectrometry
Hz	hertz
i	iso
IMes	1,3-bis(2,4,6-trimethylphenyl)imidazolium
IPA	isopropyl alcohol
Ipc	<i>iso</i> -pinocampheyl
IR	infrared spectroscopy
J	coupling constant (NMR spectroscopy)
kcal	kilocalorie
λ	wavelength
L	levorotatory (absolute configuration)
L	ligand
	liter
LAH	lithium aluminum hydride
LCD	liquid crystal display
LDA	lithium diisopropylamide
lit.	literature
LG	leaving group
LRMS	low resolution mass spectrometry

LUMO	lowest unoccupied molecular orbital
μ	dipole moment
	micro (10^{-6})
m	medium (spectra)
	meter
	milli (10^{-3})
	multiplet (spectra)
<i>m</i>	meta
M	molarity (mol/L)
<i>m/z</i>	mass to charge ratio
MALDI	matrix-assisted laser desorption ionization
<i>m</i> -CPBA	<i>meta</i> -chloroperoxybenzoic acid
Me	methyl
MEM	2-methoxyethoxymethyl
Mes	mesityl
MHz	megahertz
min	minute
mmol	millimole
mol	mole
MOM	methoxymethyl
mp	melting point
MP2	second-order Møller–Plesset perturbation theory
Ms	mesyl (methanesulfonyl)
MS	molecular sieves

<i>n</i>	normal total number of individuals
NA	not applicable
NaHMDS	sodium bis(trimethylsilyl)amid
NBO	natural bond orbital
NBS	<i>N</i> -bromosuccinimide
nbd	norbornadiene
NCS	<i>N</i> -chlorosuccinimide
ND	not determined
nm	nanometer
NHC	<i>N</i> -heterocyclic carbene
NMO	<i>N</i> -methyilmorpholino- <i>N</i> -oxide
NMR	nuclear magnetic resonance
NOESY	nuclear Overhauser enhancement spectroscopy
NR	no reaction
<i>o</i>	<i>ortho</i>
<i>o</i> -DCB	1,2-dichlorobenzene
ORTEP	Oak Ridge thermal ellipsoid plot
p	negative logarithm (as in pH)
<i>p</i>	<i>para</i>
PAH	polycyclic aromatic hydrocarbon
Ph	phenyl (C ₆ H ₅)
phthal	phthalimide
pin	pinacol

Piv	pivaloyl
PM3	parameterized model 3
PMA	phosphomolybdic acid
PMB	<i>para</i> -methoxybenzyl
POAV	π -orbital axis vector
ppm	parts per million
ppt	precipitate
Pr	propyl
PyBOX	2,6-bis(oxazoliny)pyridine
q	quartet (spectra)
qn	quintet (spectra)
QUINAP	1-(2-diphenylphosphino-1-naphthyl)isoquinoline
R	radical group (carbon-based substituent)
R	rectus (configuration)
<i>rac</i>	racemic
ref	reference
rel	relative
R_f	retention factor
rt	room temperature
s	second
	singlet (spectra)
	strong (spectra)
S	entropy
	sinister (configuration)

salen	<i>N,N'</i> -bis(3,5-di- <i>tert</i> -butylsalicylidene)-1,2-cyclohexanediamine
sat.	saturated
SET	single electron transfer
SFC	supercritical fluid chromatography
<i>syn</i>	together, same side
t	triplet (spectra)
<i>t</i>	temperature (in degrees Celsius)
	tertiary
	time
TBAF	tetra- <i>n</i> -butylammonium fluoride
TBDPS	<i>tert</i> -butyldiphenylsilyl
TBS	<i>tert</i> -butyldimethylsilyl
TCE	1,1,2,2-tetrachloroethane
TEA	triethylamine
Tf	trifluoromethanesulfonyl
TFA	trifluoroacetic acid
T_g	glass-transition temperature
THF	tetrahydrofuran
TIPS	tri- <i>iso</i> -propylsilyl
TLC	thin-layer chromatography
TM	transition metal
TMS	tetramethylsilane
	trimethylsilyl
TOF	time of flight

TPAP	tetrapropylammonium perruthenate
<i>trans</i>	<i>L.</i> , on the opposite side
Ts	<i>para</i> -toluenesulfonate
TTFA	thallium(III) trifluoroacetate
UV	ultraviolet
vis	visible
w	weak (spectra)
wt	weight
X	heteroatom or pseudohalide
y	yield
Z	<i>Ger.</i> , zusammen (configuration)

Chapter 1. Catalytic Bismetallative Multicomponent Coupling Reactions

1.1. Introduction

Catalytic reactions have played an indispensable role in organic chemistry for the last several decades. In particular, catalytic multicomponent reactions have attracted a lot of attention due to their efficiency and expediency towards complex molecule synthesis. The presence of bimetallic reagents (*e.g.* B–B, Si–Si, B–Si, Si–Sn, etc.) in this process renders the products enriched with various functional groups and multiple stereocenters. For this reason, catalytic bismetallative coupling is considered an effective method to generate the functional and stereochemical complexity of simple hydrocarbon substrates. This review highlights key developments of transition-metal catalyzed bismetallative reactions involving multiple π components. Specifically, it will highlight the scope, synthetic applications, and proposed mechanistic pathways of this process.

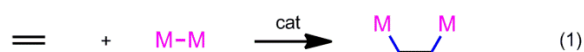
Catalytic multicomponent reactions are regarded as one of the most attractive strategies for organic synthesis, since they can generate molecular diversity and complexity from simple substrates.^{1,2} Recent investigations in this area have revealed that the

¹ For reviews, see: (a) Ikeda, S.-I., "Nickel-Catalyzed Intermolecular Domino Reactions," *Accounts of Chemical Research* **2000**, *33*, 511-519. (b) Ganem, B., "Strategies for Innovation in Multicomponent Reaction Design," *Accounts of Chemical Research* **2009**, *42*, 463-472. (c) Touré, B. B.; Hall, D. G., "Natural Product Synthesis Using Multicomponent Reaction Strategies," *Chemical Reviews* **2009**, *109*, 4439-4486. .

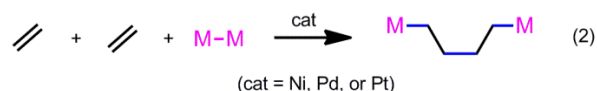
incorporation of bimetallic reagents (*e.g.* R₂B–BR₂, R₃Si–SiR₃, R₂B–SiR₃, R₃Si–SnR₃, etc.) into this process provides access to functionalized products in a stereo- and regioselective fashion.^{3,4} The resulting organometallic compounds are synthetically valuable intermediates due to their versatility and reactivity in organic synthesis.^{4a} Compared to bismetallation of one π -component (Scheme 1.1, eq. 1), bismetallation of two (or more) π -components (Scheme 1.1, eq. 2) is particularly noteworthy because the complexity generation should facilitate complex molecule syntheses.

Scheme 1.1 Bismetallative Coupling with One vs. Two π -Components

Bismetallation of one π -component (ref. 3a, Morken 2007)



Bismetallation of two π -components (this review)



² For more recent reviews, see: (a) Biggs-Houck, J. E.; Younai, A.; Shaw, J. T., "Recent Advances in Multicomponent Reactions for Diversity-Oriented Synthesis," *Current Opinion in Chemical Biology* **2010**, *14*, 371-382. (b) de Graaff, C.; Ruijter, E.; Orru, R. V., "Recent Developments in Asymmetric Multicomponent Reactions," *Chemical Society Reviews* **2012**, *41*, 3969-4009. (c) Pellissier, H., "Stereocontrolled Domino Reactions," *Chemical Reviews* **2012**, *113*, 442-524.

³ For reviews, see: (a) Beletskaya, I.; Moberg, C., "Element-Element Addition to Alkynes Catalyzed by the Group 10 Metals," *Chemical Reviews* **1999**, *99*, 3435-3462. (b) Suginome, M.; Ito, Y., "Transition-Metal-Catalyzed Additions of Silicon-Silicon and Silicon-Heteroatom Bonds to Unsaturated Organic Molecules," *Chemical Reviews* **2000**, *100*, 3221-3256.

⁴ For more recent reviews, see: (a) Burks, H. E.; Morken, J. P., "Catalytic Enantioselective Diboration, Disilation and Silaboration: New Opportunities for Asymmetric Synthesis," *Chemical Communications* **2007**, 4717-4725. (b) Ohmura, T.; Suginome, M., "Silylboranes as New Tools in Organic Synthesis," *Bulletin of the Chemical Society of Japan* **2009**, *82*, 29-49. (c) Oestreich, M.; Hartmann, E.; Mewald, M., "Activation of the Si-B Inter-element Bond: Mechanism, Catalysis, and Synthesis," *Chemical Reviews* **2012**, *113*, 402-441.

The coupling reactions of organometallic reagents with two π components were pioneered by Mori^{5,6} and Tamaru^{7,8} (Scheme 1.2, eq. 1). These reductive coupling reactions, involving organometallic reagents ($M-R$) or metal hydrides ($M-H$), have attracted a lot of attention and have been well explored in the past couple of decades.^{9,10,11} However, the

⁵ (a) Sato, Y.; Takimoto, M.; Hayashi, K.; Katsuhara, T.; Takagi, K.; Mori, M., "Novel Stereoselective Cyclization Via. Pi-Allylnickel Complex Generated from 1,3-Diene and Hydride Nickel Complex," *Journal of the American Chemical Society* **1994**, *116*, 9771-9772. (b) Sato, Y.; Takimoto, M.; Mori, M., "Remarkable Regio-Controlled Effect of 1, 3-Diene as a Ligand on Nickel-Promoted Cyclization," *Tetrahedron Letters* **1996**, *37*, 887-890.

⁶ For more recent works, see: (a) Sato, Y.; Takanashi, T.; Hoshiba, M.; Mori, M., "Nickel(0)-Catalyzed Diene-Aldehyde Cyclization," *Tetrahedron Letters* **1998**, *39*, 5579-5582. (b) Sato, Y.; Takimoto, M.; Mori, M., "Further Studies on Nickel-Promoted or -Catalyzed Cyclization of 1,3-Diene and a Tethered Carbonyl Group," *Journal of the American Chemical Society* **2000**, *122*, 1624-1634.

⁷ (a) Kimura, M.; Ezoe, A.; Shibata, K.; Tamaru, Y., "Novel and Highly Regio- and Stereoselective Nickel-Catalyzed Homoallylation of Benzaldehyde with 1,3-Dienes," *Journal of the American Chemical Society* **1998**, *120*, 4033-4034. (b) Kimura, M.; Ezoe, A.; Tanaka, S.; Tamaru, Y., "Nickel-Catalyzed Homoallylation of Aldehydes in the Presence of Water and Alcohols," *Angewandte Chemie International Edition* **2001**, *40*, 3600-3602.

⁸ (c) Shibata, K.; Kimura, M.; Shimizu, M.; Tamaru, Y., "Nickel-Catalyzed Intramolecular Homoallylation of ω -Dienyl Aldehyde," *Organic Letters* **2001**, *3*, 2181-2183. (d) Ikeda, S. I., "Nickel-Catalyzed Coupling of Carbonyl Compounds and Alkynes or 1,3-Dienes: An Efficient Method for the Preparation of Allylic, Homoallylic, and Bishomoallylic Alcohols," *Angewandte Chemie International Edition* **2003**, *42*, 5120-5122.

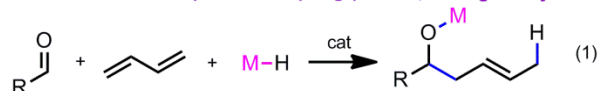
⁹ For selected reviews, see: (a) Montgomery, J., "Nickel-Catalyzed Reductive Cyclizations and Couplings," *Angewandte Chemie International Edition* **2004**, *43*, 3890-3908. (b) Moslin, R. M.; Miller-Moslin, K.; Jamison, T. F., "Regioselectivity and Enantioselectivity in Nickel-Catalysed Reductive Coupling Reactions of Alkynes," *Chemical Communications* **2007**, 4441-4449. (c) Jeganmohan, M.; Cheng, C. H., "Cobalt- and Nickel-Catalyzed Regio- and Stereoselective Reductive Coupling of Alkynes, Allenes, and Alkenes with Alkenes," *Chemistry—A European Journal* **2008**, *14*, 10876-10886.

¹⁰ For selected experimental works, see: (a) Shintani, R.; Okamoto, K.; Otomaru, Y.; Ueyama, K.; Hayashi, T., "Catalytic Asymmetric Arylative Cyclization of Alkynals: Phosphine-Free Rhodium/Diene Complexes as Efficient Catalysts," *Journal of the American Chemical Society* **2005**, *127*, 54-55. (b) Knapp-Reed, B.; Mahandru, G. M.; Montgomery, J., "Access to Macrocyclic Endocyclic and Exocyclic Allylic Alcohols by Nickel-Catalyzed Reductive Cyclization of Ynals," *Journal of the American Chemical Society* **2005**, *127*, 13156-13157.

coupling of bimetallic reagents ($M-M$) with two π components (Scheme 1.2, eq. 2) has gained relatively less attention in spite of its obvious potential for providing an efficient method in multiple bond-forming reactions. This review focuses on the major developments in the bimetallic multicomponent coupling reactions that are catalyzed by group 10 transition metals.

Scheme 1.2 Reductive vs Bimetallic Multicomponent Coupling

Reductive multicomponent coupling (ref. 6a, Montgomery 2004)



Bimetallic multicomponent coupling (this review)



¹¹ (a) Komanduri, V.; Krische, M. J., "Enantioselective Reductive Coupling of 1,3-Enynes to Heterocyclic Aromatic Aldehydes and Ketones via Rhodium-Catalyzed Asymmetric Hydrogenation: Mechanistic Insight into the Role of Brønsted Acid Additives," *Journal of the American Chemical Society* **2006**, *128*, 16448-16449. (b) Jayanth, T. T.; Cheng, C. H., "Nickel-Catalyzed Coupling of Arynes, Alkenes, and Boronic Acids: Dual Role of the Boronic Acid," *Angewandte Chemie International Edition* **2007**, *46*, 5921-5924.

1.2. Mechanistic Considerations

1.2.1. Oxidative Cyclization Mechanism

Several different mechanistic pathways have been suggested for the bimetallic multicomponent coupling reactions that are catalyzed by Ni, Pd, or Pt. One possible mechanism (oxidative cyclization mechanism)^{12, 13} among them commences with the coordination of the π -components with the catalyst **1.1** and the subsequent formation of a metalocyclic intermediate **1.2** (Scheme 1.3).^{14, 15, 16} In the presence of bimetallic reagents, this

¹² Cho, H. Y.; Morken, J. P., "Diastereoselective Construction of Functionalized Homoallylic Alcohols by Ni-Catalyzed Diboron-Promoted Coupling of Dienes and Aldehydes," *Journal of the American Chemical Society* **2008**, *130*, 16140-16141.

¹³ For DFT studies on relevant coupling reactions, see: McCarren, P.; Liu, P.; Cheong, P. H.-Y.; Jamison, T. F.; Houk, K., "Mechanism and Transition-State Structures for Nickel-Catalyzed Reductive Alkyne-Aldehyde Coupling Reactions," *Journal of the American Chemical Society* **2009**, *131*, 6654-6655. (b) Liu, P.; McCarren, P.; Cheong, P. H.-Y.; Jamison, T. F.; Houk, K., "Origins of Regioselectivity and Alkene-Directing Effects in Nickel-Catalyzed Reductive Couplings of Alkynes and Aldehydes," *Journal of the American Chemical Society* **2010**, *132*, 2050-2057. (c) Liu, P.; Montgomery, J.; Houk, K., "Ligand Steric Contours to Understand the Effects of N-Heterocyclic Carbene Ligands on the Reversal of Regioselectivity in Ni-Catalyzed Reductive Couplings of Alkynes and Aldehydes," *Journal of the American Chemical Society* **2011**, *133*, 6956-6959.

¹⁴ A nickelacyclic complex comprising an aldehyde, a diene, a nickel, and a phosphine ligand was characterized by X-ray crystallography: Ogoshi, S.; Tonomori, K.-I.; Oka, M.-A.; Kurosawa, H., "Reversible Carbon-Carbon Bond Formation between 1,3-Dienes and Aldehyde or Ketone on Nickel(0)," *Journal of the American Chemical Society* **2006**, *128*, 7077-7086.

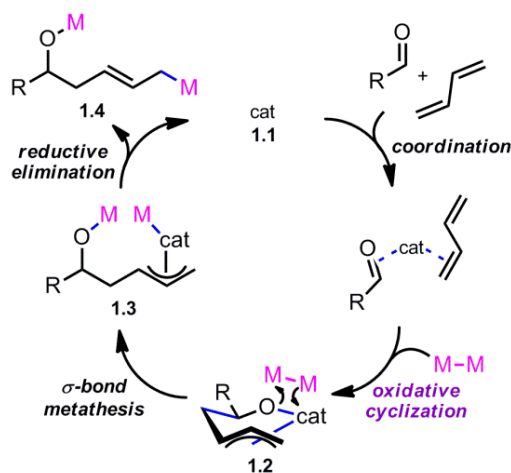
¹⁵ For related studies, see: (a) Ogoshi, S.; Arai, T.; Ohashi, M.; Kurosawa, H., "Nickeladihydrofuran. Key Intermediate for Nickel-Catalyzed Reaction of Alkyne and Aldehyde," *Chemical Communications* **2008**, 1347-1349. (b) Tamaki, T.; Nagata, M.; Ohashi, M.; Ogoshi, S., "Synthesis and Reactivity of Six-Membered Oxa-Nickelacycles: A Ring-Opening Reaction of Cyclopropyl Ketones," *Chemistry—A European Journal* **2009**, *15*, 10083-10091.

¹⁶ (a) Ogoshi, S.; Hoshimoto, Y.; Ohashi, M., "Nickel-Catalyzed Tishchenko Reaction Via Hetero-Nickelacycles by Oxidative Cyclization of Aldehydes with Nickel(0) Complex," *Chemical Communications*

cyclic intermediate (**1.2**) may undergo σ -bond metathesis forming a bismetallic complex **1.3**.

Finally, reductive elimination would afford the product **1.4** and regenerate the catalyst (**1.1**).

Scheme 1.3 Oxidative Cyclization Mechanism



1.2.2. Oxidative Addition Mechanism

In some cases, however, the initial oxidation of the catalyst (**1.1**) occurs by its insertion to bismetallic reagents (oxidative addition mechanism, Scheme 1.4).^{17,18} Next, insertion to one π -component of substrate **1.5** would give an intermediate complex **1.6**. The

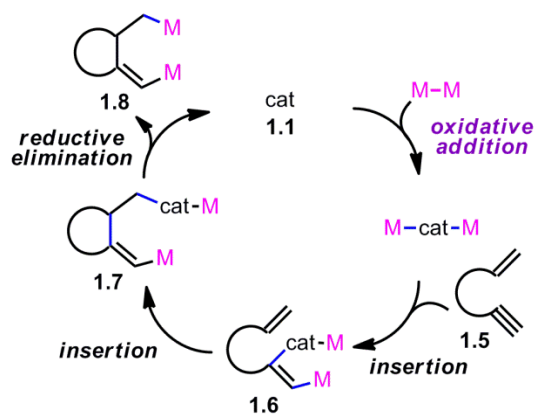
2010, *46*, 3354-3356. (b) Ohashi, M.; Taniguchi, T.; Ogoshi, S., "[3+3] Cyclodimerization of Methylene-cyclopropanes: Stoichiometric and Catalytic Reactions of Nickel (0) with Electron-Deficient Alkylidene-cyclopropanes," *Organometallics* **2010**, *29*, 2386-2389.

¹⁷ (a) Mori, M.; Hirose, T.; Wakamatsu, H.; Imakuni, N.; Sato, Y., "Palladium-Catalyzed Bismetallative Cyclization of Enynes," *Organometallics* **2001**, *20*, 1907-1909. (b) Sato, Y.; Saito, N.; Mori, M., "Ni(0)-Catalyzed Bismetallative Cyclization of 1,3-Diene and a Tethered Aldehyde in the Presence of $\text{Bu}_3\text{SnSiMe}_3$," *Chemistry Letters* **2002**, 18-19.

¹⁸ (a) Sato, Y.; Imakuni, N.; Mori, M., "Pd(0)-Catalyzed Bismetallative Cyclization of Enynes in the Presence of $\text{Bu}_3\text{SnSiMe}_3$ Using N-Heterocyclic Carbene as a Ligand," *Advanced Synthesis & Catalysis* **2003**, *345*, 488-491. (b) Saito, N.; Mori, M.; Sato, Y., "Nickel(0)-Catalyzed Disilylative and Silastannyllative Cyclizations of 1,3-Diene and Tethered Aldehyde," *Journal of Organometallic Chemistry* **2007**, *692*, 460-471.

intermediate **1.6** then can undergo additional insertion reaction with the other π -component of the substrate to generate cyclic intermediate **1.7**. Lastly, reductive elimination of **1.7** would afford the product **1.8** and restarts the catalytic cycle.

Scheme 1.4 Oxidative Addition Mechanism



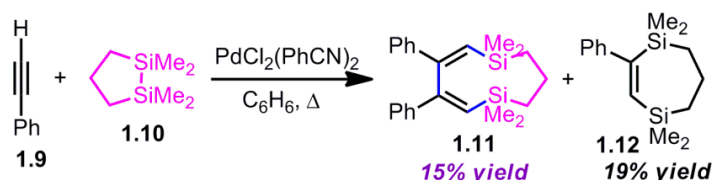
The above-described catalytic cycles represent some of the most typical reaction pathways suggested for this process, but they are not meant to be comprehensive. As in most organic reactions, proposed mechanisms for these reactions can be varied depending on catalysts, substrates, and other reaction conditions. More detailed mechanistic considerations for each category of the process will be discussed accordingly in the corresponding sections.

1.3. Palladium-Catalyzed Bimetallative Multicomponent Coupling

1.3.1. Coupling of Alkyne–Alkyne and Alkyne–Alkene

The Pd-catalyzed bimetallative alkyne–alkyne coupling and alkyne–alkene coupling have been investigated in a variety of contexts by several research groups. One of the earliest observations of this type of coupling was reported by Sakurai (Scheme 1.5).¹⁹ The main goal of their paper was to investigate the properties of silicon–silicon bond of 1,2-disilacycloalkanes, focusing on the donor ability of the Si–Si bond. During their study of cycloaddition reactions of organodisilane reagents to various acetylenes, it was observed that the disilane reagent (**1.10**) can participate in a coupling reaction between two acetylenes (**1.9**) to give **1.11** (15% yield), along with a byproduct (**1.12**). Although the yield from the two π -components product was not great, their result demonstrated the potential of bimetallic reagents towards multicomponent reactions.

Scheme 1.5 Sakurai's Intermolecular Alkyne–Alkyne Coupling (1975)



¹⁹ Sakurai, H.; Kamiyama, Y.; Nakadaira, Y., "Novel $[\sigma + \pi]$ Reactions of Hexaorganodisilanes with Acetylenes Catalyzed by Palladium Complexes," *Journal of the American Chemical Society* **1975**, 97, 931-932.

More synthetically useful methods in this type of reaction were developed later by Tanaka,²⁰ Lautens,²¹ Mori,¹⁷ and RajanBabu.^{22,23} The Tanaka group (Scheme 1.6) observed intramolecular alkyne–alkene coupling reactions that are promoted by a *B–Si* reagent in the presence of a palladium catalyst.^{20a} An intramolecular π component coupling reaction with 4,4-bis(ethoxycarbonyl)hep-6-en-1-yne (**1.13**) and **1.14** was catalyzed by Pd₂(dba)₃ and ETPO (4-ethyl-2,6,7-trioxa-1-phospha-bicyclo[2.2.2]octane) to afford **1.15** in 84% yield (determined by ¹H NMR). Along with the desired cyclization product, the formation of a byproduct (9% yield, not shown), which was speculated to have come from silaboration of the triple bond, was also observed by ¹H NMR.

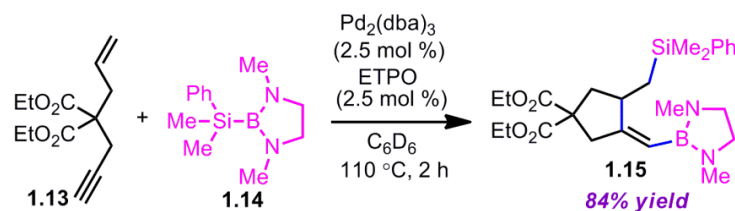
²⁰ (a) Onozawa, S.-Y.; Hatanaka, Y.; Tanaka, M., "Palladium-Catalysed Borylsilylation of Alkynes and Borylsilylative carbocyclization of Diynes and an Enyne Compound," *Chemical Communications* **1997**, 1229-1230. (b) Onozawa, S.-Y.; Hatanaka, Y.; Choi, N.; Tanaka, M., "Palladium-Catalyzed Borylstannylative Carbocyclization of Diynes and an Enyne Compound," *Organometallics* **1997**, *16*, 5389-5391. (c) Onozawa, S.-Y.; Hatanaka, Y.; Tanaka, M., "Regio- and Stereoselective 1,4-Borylstannation of 1,3-Dienes Promoted by Palladium Catalysts," *Tetrahedron Letters* **1998**, *39*, 9043-9046.

²¹ (a) Lautens, M.; Mancuso, J., "Silylstannation-Cyclization of 1,6-Enynes Using Palladium(0) and Palladium(II) Catalysis," *Synlett* **2002**, *2002*, 0394-0398. (b) Mancuso, J.; Lautens, M., "Mild Procedure for the Catalytic Bis(Stannylation) of Alkynes with Hexaalkylditins," *Organic Letters* **2003**, *5*, 1653-1655.

²² Warren, S.; Chow, A.; Fraenkel, G.; RajanBabu, T. V., "Axial Chirality in 1,4-Disubstituted (*Z,Z*)-1,3-Dienes. Surprisingly Low Energies of Activation for the Enantiomerization in Synthetically Useful Fluxional Molecules," *Journal of the American Chemical Society* **2003**, *125*, 15402-15410.

²³ For related works, see: (a) Kumareswaran, R.; Shin, S.; Gallou, I.; RajanBabu, T., "Silylstannylation of Allenes and Silylstannylation-Cyclization of Allenynes. Synthesis of Highly Functionalized Allylstannanes and Carbocyclic and Heterocyclic Compounds," *The Journal of Organic Chemistry* **2004**, *69*, 7157-7170. (b) Singidi, R. R.; Kutney, A. M.; Gallucci, J. C.; RajanBabu, T., "Stereoselective Cyclization of Functionalized 1,*n*-Diynes Mediated by [X–Y] Reagents [X–Y = R₃Si–SnS'₃ or (R₂N)₂B–SnR'₃]: Synthesis and Properties of Atropisomeric 1,3-Dienes," *Journal of the American Chemical Society* **2010**, *132*, 13078-13087.

Scheme 1.6 Tanaka's Intramolecular Alkyne–Alkene Coupling (1997)

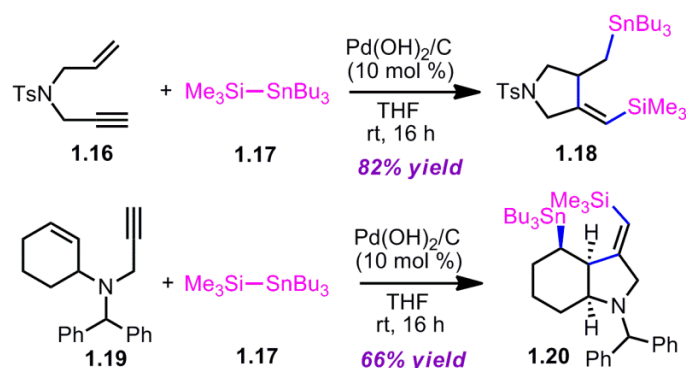


In Mori's work (Scheme 1.7),^{17a, 24, 25} enyne **1.16** was reacted with 1.5 equivalents of $\text{Me}_3\text{Si-SnBu}_3$ (**1.17**) in the presence of 10 mol % of $\text{Pd}(\text{OH})_2$ on charcoal at room temperature to furnish the bismetallation product **1.18** in 82% yield. With the use of $\text{Pd}_2(\text{dba})_3$ as a ligand (3 mol %) under the same reaction conditions, the product was obtained in a slightly lower yield (57%). Also, a saturated indole moiety **1.20** was constructed (66% yield, with $\text{Pd}(\text{OH})_2/\text{C}$) from a tertiary amine-substituted enyne **1.19** in a stereoselective fashion. In this study, it was observed that using a palladium catalyst in the *absence* of phosphine ligands tends to suppress alkyne bismetallation, which is undesired.

²⁴ For related works, see: (a) Rossi, E.; Arcadi, A.; Abbiati, G.; Attanasi, O. A.; De Crescentini, L., "Sequential Base-Promoted Annulation/Palladium-Catalyzed Domino 1,5-Enyne Arylation and Vinylation of α -Propargylaminohydrazones," *Angewandte Chemie International Edition* **2002**, *41*, 1400-1402. (b) Muraoka, T.; Matsuda, I.; Itoh, K., "Rhodium-Catalyzed Silylative Cyclization of 1,6-Heptadiyne Derivatives: A Versatile Route for the Synthesis of a 1,2-Dialkylidenecyclopentane Skeleton," *Organometallics* **2002**, *21*, 3650-3660.

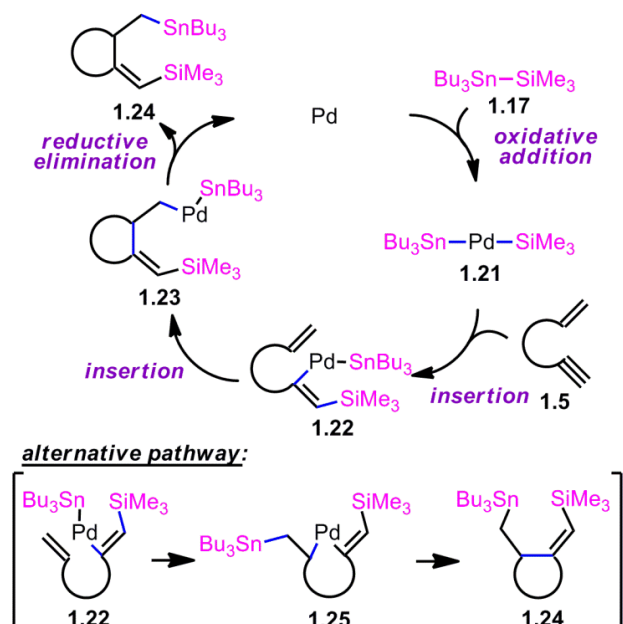
²⁵ (a) Yamamoto, Y.; Kuwabara, S.; Ando, Y.; Nagata, H.; Nishiyama, H.; Itoh, K., "Palladium(0)-Catalyzed Cyclization of Electron-Deficient Enynes and Eneidyne," *The Journal of Organic Chemistry* **2004**, *69*, 6697-6705. (b) Jung, I. G.; Seo, J.; Lee, S. I.; Choi, S. Y.; Chung, Y. K., "Reductive Cyclization of Dienes and Enynes Catalyzed by Allyl Platinum N-Heterocyclic Carbene Complexes," *Organometallics* **2006**, *25*, 4240-4242.

Scheme 1.7 Mori's Intramolecular Alkyne–Alkene Coupling (2001)



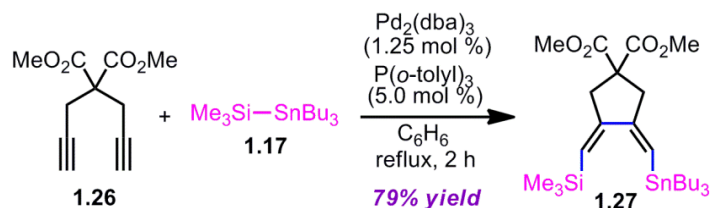
Two possible pathways for this process were considered as illustrated in Scheme 1.8. The reaction commences with oxidative addition of $\text{Me}_3\text{Si-SnBu}_3$ (**1.17**) to a Pd catalyst to give **1.21**, which is followed by an insertion of the alkyne moiety of **1.5** into the Pd–Si bond to form intermediate **1.22**. Then, an insertion of the alkene portion of **1.22** into the Pd–C bond occurs intramolecularly to afford a Pd complex **1.23**. Finally, reductive elimination would furnish cyclized product **1.24**, and the palladium catalyst is regenerated. Mori and co-workers also consider an alternate pathway; it involves the formation of **1.25**, which is an insertion product of the alkene into the Pd–Sn bond of **1.22**. From the intermediate complex **1.25**, however, the identical cyclized product **1.24** will be afforded via reductive elimination.

Scheme 1.8 Proposed Mechanism for Enyne Cyclization (Mori, 2001)



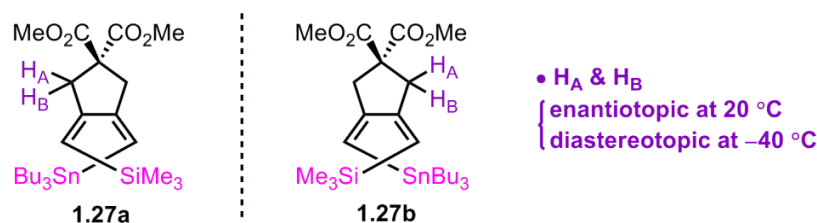
One of RajanBabu's many contributions in this field is the preparation of functionalized bisalkylidenes from 1,6-diyne, as described in Scheme 1.9.²² The construction of a (*Z,Z*)-1,3-diene **1.27** (79% yield) was accomplished by a reaction of di-*O*-methyl dipropargylmalonate (**1.26**) with $\text{Me}_3\text{Si-SnBu}_3$ (**1.17**) with a catalytic amount of $\text{Pd}_2(\text{dba})_3$ and $\text{P}(o\text{-tolyl})_3$.

Scheme 1.9 RajanBabu's Intramolecular Alkyne-Alkyne Coupling (2000)



One of the interesting features of this molecule is that sterically-encumbered silicon and tin groups enforce a nonplanar/helically chiral structure for such a diene (Scheme 1.10). The fluxional nature and stereochemistry of the (*Z,Z*)-1,3-diene **1.27** were analyzed by NMR spectroscopy. The ^1H NMR shows two distinctive sets of signals for H_A and H_B at $-40\text{ }^\circ\text{C}$, while broad signals for the ring methylene protons appeared at $20\text{ }^\circ\text{C}$. Except for a highly unlikely conformational equilibrium involving the cyclopentane, such chirality must have originated from the helical arrangement of substituents in the (*Z,Z*)-diene **1.27**.

Scheme 1.10 Enantiomers of Compound 1.27 at $-40\text{ }^\circ\text{C}$ (RajanBabu, 2000)

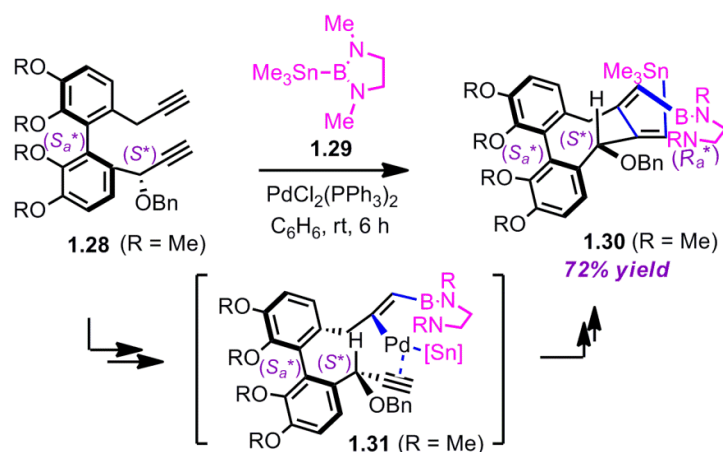


In a recent study, the RajanBabu group explored more details of the stereochemistry in these cyclization reactions.²⁶ For this study, cyclization reactions of diynes with a *B-Sn* reagent **1.29** were investigated. The regio- and stereoselectivities of this process were rationalized by the assumption that the addition of **1.29** to the diyne substrate **1.28** occurs at the less substituted, electron-rich alkyne forming a C–B bond in the product **1.30** (Scheme

²⁶ (a) Gong, W.; Singidi, R. R.; Gallucci, J. C.; RajanBabu, T., "On the Stereochemistry of Acetylide Additions to Highly Functionalized Biphenylcarbaldehydes and Multi-Component Cyclization of 1,*n*-Diyne. Syntheses of Dibenzocyclooctadiene Lignans," *Chemical Science* **2012**, 3, 1221-1230. (b) Singidi, R. R.; RajanBabu, T., "Borostannylation of Alkynes and Enynes. Scope and Limitations of the Reaction and Utility of the Adducts," *Organic Letters* **2010**, 12, 2622-2625. (c) Singidi, R. R.; RajanBabu, T., "Catalyzed Cyclizations Leading to Enrichment of Functionality and Chirality. A General Approach to Dibenzocyclooctadiene Lignans from α,ω -Diyne," *Organic Letters* **2008**, 10, 3351-3354.

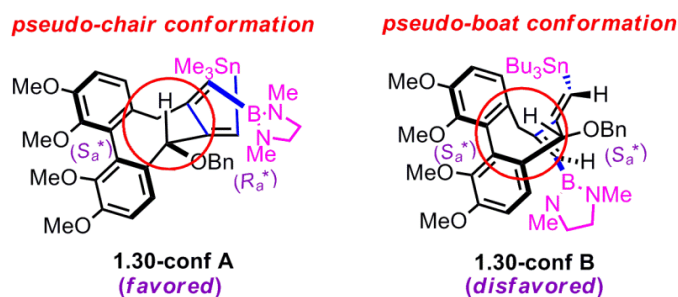
1.11). The cyclization via carbometalation of the palladium intermediate **1.31**, followed by reductive elimination, will result in the formation of C–Sn bond in the product **1.30**.

Scheme 1.11 RajanBabu's Stereoselective Diyne Cyclization (2012)



In this report, the group speculated that the cyclization step with the carbometalation process is the stereoselectivity-determining step and proposed a possible origin of stereoselectivity (Scheme 1.12). When the 7,8-bisalkylidenecyclooctadiene moiety of the product **1.30** is formed via carbometalation, the configuration of the newly-formed axial chiral element (R_a) is determined. Obviously, the (S_a, R_a) configuration of the product (**1.30-conf A**) and, thereby, its transition state have relatively strain-free pseudo-chair conformation, compared to more strained pseudo-boat conformation (**1.30-conf B**).

Scheme 1.12 Proposed Origin of Stereoselectivity (RajanBabu, 2012)

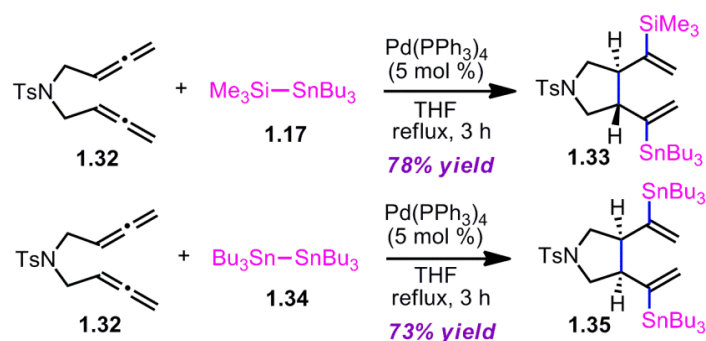


1.3.2. Coupling of Allene–Allene and Allene–Alkyne

Pd-catalyzed bimetallic coupling reactions of allene–allene with bimetallic reagents was first demonstrated by the Kang group.²⁷ His group demonstrated that silylstannanes (*Si–Sn*) or distannanes (*Sn–Sn*) can promote the palladium-catalyzed addition–cyclization reaction of tethered bis(allenes). As described in Scheme 1.13, the cyclization reaction proceeds with bis(allene) **1.32** and (trimethylsilyl)tributylstannane (**1.17**) in the presence of Pd(Ph₃P)₄ (5 mol %) to afford a *trans*-fused cyclized product **1.33** in 78% yield. On the other hand, when distannane Bu₃Sn–SnBu₃ (**1.34**) was used for this process with the same bis(allene) **1.32** and Pd(PPh₃)₄ (5 mol %), a *cis*-fused distannane **1.35** was obtained in 73% yield.

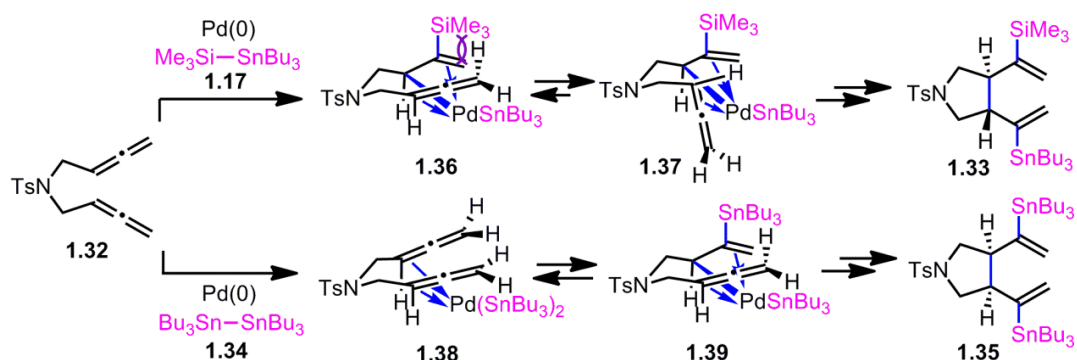
²⁷ Kang, S.-K.; Baik, T.-G.; Kulak, A. N.; Ha, Y.-H.; Lim, Y.; Park, J., "Palladium-Catalyzed Carbocyclization/Silastannylation and Distannylation of Bis(Allenenes)," *Journal of the American Chemical Society* **2000**, 122, 11529-11530.

Scheme 1.13 Kang's Intramolecular Allene–Allene Coupling (2000)



The different stereochemical outcomes between two bismetallic reagents (i.e. *cis* vs *trans* fusion at ring junction) were rationalized in this report (Scheme 1.14). For the *Si–Sn* reagent, allylpalladium complex **1.37** is formed by the addition of the $\text{Bu}_3\text{Sn–Pd–SiMe}_3$ species to the allene moiety. Intermediate **1.37** should be favored over **36** due to the steric hindrance of the nearby TMS (trimethylsilyl) group. The cyclization reaction of this intermediate (**1.37**) and subsequent reductive elimination would result in the *trans* bicyclic product **1.33**. In the case of the *Sn–Sn* reagent, however, the chelated σ -allylpalladium intermediate **1.39** is preferably formed from the coordinated compound **1.38**. Then, the rapid carbocyclization of **1.39** and reductive elimination would give the *cis*-fused bicycle **1.35**. It is conjectured that the differentiation between the two types of the reagents comes from the different bond lengths (C–Sn bond vs. C–Si bond). In other words, the steric encumbrance of the TMS group in those allylpalladium complexes is more severe than that of the Bu_3Sn group due to the shorter bond length of the C–Si bond.

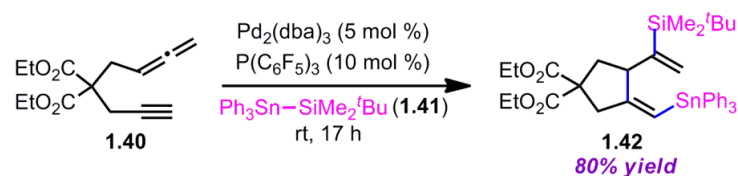
Scheme 1.14 Rationale for Stereochemical Outcome (Kang, 2000)



With the same types of organometallic reagents (i.e. *Si-Sn* and *Sn-Sn*), RajanBabu and co-workers showed that allene and alkyne can be coupled intramolecularly with a palladium catalyst (Scheme 1.15).²⁸ In the presence of $\text{Ph}_3\text{Sn-SiMe}_2^t\text{Bu}$ (**1.41**), $\text{Pd}_2(\text{dba})_3\cdot\text{CHCl}_3$ and $\text{P}(\text{C}_6\text{F}_5)_3$, alleneyne **1.40** was cleanly transformed into the cyclic product **1.42** in 80% yield at room temperature. It was found that the source of Pd affects the efficiency of the reaction in the order of the following: $(\text{C}_6\text{F}_5)_3\text{P}$: $(\text{PhCN})_2\text{PdCl}_2 \approx [\text{Pd}(\text{allyl})\text{Cl}]_2/\text{AgOTf} > \text{Pd}_2(\text{dba})_3\cdot\text{CHCl}_3 \gg \text{PdCl}_2$. It was also observed that the silyltin reagents are generally superior to other bismetallating reagents (*Sn-Sn* or *Sn-B*) for the cyclization of allenynes.

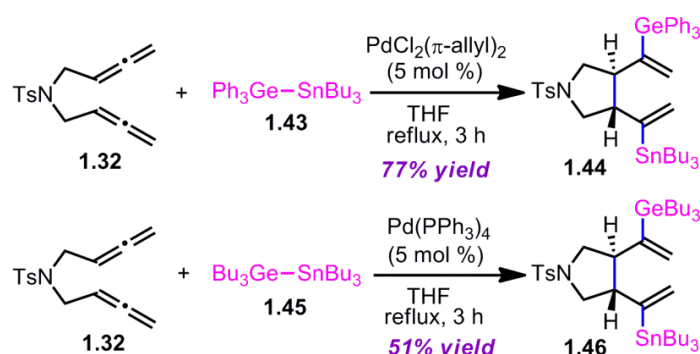
²⁸ Shin, S.; RajanBabu, T. V., "Regio- and Stereochemical Control in Bis-Functionalization-Cyclization: Use of Alleneyne Precursors for Carbocyclic and Heterocyclic Synthesis," *Journal of the American Chemical Society* **2001**, 123, 8416-8417.

Scheme 1.15 RajanBabu's Intramolecular Allene-Alkyne Coupling (2001)



For the coupling of allene-allene, *Ge-Sn* reagents can also participate as a coupling component; this process was investigated by Yu *et al* (Scheme 1.16).²⁹ They pointed out that the stereochemistry of the products is dependent on the *Ge-Sn* reagents and the catalysts that are used in the reactions. Bis(allene) **1.32** can react with $\text{Ph}_3\text{Ge-SnBu}_3$ (**1.43**) with a catalytic amount of $(\pi\text{-allyl})_2\text{PdCl}_2$ (5 mol %) to afford the *trans*-cyclized product **1.44** (77% yield). On the other hand, the same bis(allene) **1.32** furnished the *cis*-cyclized product **1.46** (51% yield) when it was reacted with $\text{Bu}_3\text{Ge-SnBu}_3$ (**1.45**) in the presence of $\text{Pd}(\text{PPh}_3)_4$.

Scheme 1.16 Yu's Intramolecular Allene-Allene Coupling (2004)



²⁹ Hong, Y.-T.; Yoon, S.-K.; Kang, S.-K.; Yu, C.-M., "A Stereoselective Carbocyclization of Bis(Allenenes) with Germylstannane Catalyzed by Palladium Complexes," *European Journal of Organic Chemistry* **2004**, 2004, 4628-4635.

1.3.3. Coupling of Diene–Diene

Among these bismetallative multicomponent coupling reactions, the Pd-catalyzed bismetallative coupling of diene–diene is one of the most frequently-observed reaction categories from various contexts. Earliest studies were reported by Sakurai et al., in which dienes are intermolecularly coupled in the presence of cyclic disilane reagents to make allyl silanes (Scheme 1.17).³⁰ Since the initial Sakurai report, preliminary observations of this type of coupling were reported by a number of research groups: Kumada,³¹ West,³² Seyferth,³³ Manners,³⁴ and Ando³⁵ groups. Then, more synthetically meaningful applications of this method were examined by the Tsuji group.³⁶

³⁰ Sakurai, H.; Kamiyama, Y.; Nakadaira, Y., "The Palladium Complex-Catalyzed Reactions of Hexaorganodisilanes with Dienes," *Chemistry Letters* **1975**, *4*, 887-890.

³¹ Tamao, K.; Okazaki, S.; Kumada, M., "Fluorinated Polysilanes. Palladium Catalyzed 1,4-Addition of Fluorodisilanes to Conjugated Diene and Enone Systems," *Journal of Organometallic Chemistry* **1978**, *146*, 87-93.

³² Carlson, C. W.; West, R., "Ring-Insertion and Ring-Opening Reactions of Octaethylcyclotetrasilane," *Organometallics* **1983**, *2*, 1801-1807.

³³ Seyferth, D.; Goldman, E. W.; Escudié, J., "The Chemistry of Octamethyl-1,2-Disilacyclobutane. Some Si–Si Cleavage and Insertion Reactions," *Journal of Organometallic Chemistry* **1984**, *271*, 337-352.

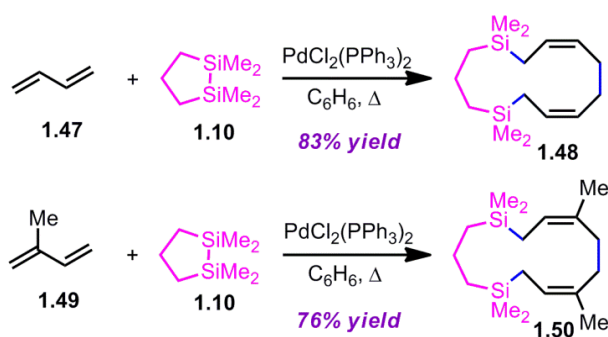
³⁴ Finckh, W.; Tang, B. Z.; Lough, A.; Manners, I., "Synthesis and Properties of Organometallic Rings and Macrocycles Containing Ferrocene, Silicon, and Unsaturated Hydrocarbon Units: X-Ray Crystal Structures of the Novel Ferrocenophanes $\text{Fe}(\eta\text{-C}_5\text{H}_4)_2(\text{SiMe}_2)_2(\text{CH}=\text{CH})$ and *Trans,Trans*- $\text{Fe}(\eta\text{-C}_5\text{H}_4)_2(\text{SiMe}_2)_2(\text{CH}_2\text{CH}=\text{CHCH}_2)_2$," *Organometallics* **1992**, *11*, 2904-2911.

³⁵ Kusakawa, T.; Kabe, Y.; Nestler, B.; Ando, W., "Palladium-Catalyzed Disilane Metathesis Reactions of 1,2-Disilacyclobutanes," *Organometallics* **1995**, *14*, 2556-2564.

³⁶ (a) Tsuji, Y.; Kakehi, T., "Palladium-Catalysed Dimerization-Double Stannation of 1,3-Dienes Using Hexamethyldistannane," *Journal of the Chemical Society, Chemical Communications* **1992**, 1000-1001. (b)

According to Sakurai's account,³⁰ when 1,3-butadiene (**1.47**) was treated with 1,1,2,2-tetramethyl-1,2-disilacyclopentane (**1.10**) in the presence of a Pd(II) catalyst, 1,1,5,5-tetramethyl-1,5-disilacyclotrideca-7,11-diene (**1.48**) was obtained in 83% yield (Scheme 1.17). Isoprene (**1.49**) also gave the corresponding allyl silane **1.50** in 76% yield under the same reaction conditions.

Scheme 1.17 Sakurai's Intermolecular Diene–Diene Coupling (1975)



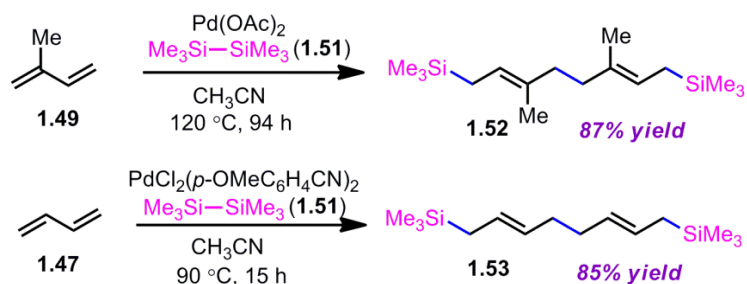
Besides the cyclic organodisilane **1.10**, acyclic organodisilanes have been utilized for diene–diene coupling reactions by the Sakurai group (Scheme 1.18).³⁷ The reaction of hexamethyldisilane (**1.51**) with isoprene (**1.49**) in the presence of a catalytic amount of Pd(OAc)₂ afforded 1,8-disilyloctadiene **1.52** (87% yield) in a regio- and stereoselective fashion. Also, 1,3-butadiene (**1.47**) can participate in this coupling reaction with hexamethyldisilane (**1.51**) and a palladium catalyst, PdCl₂(*p*-MeOC₆H₄CN)₂, to afford **1.53** in

Obora, Y.; Tsuji, Y.; Kawamura, T., "Dimerization-Double Silylation of 1,3-Dienes Using Organodisilanes Catalyzed by a Palladium Complex," *Organometallics* **1993**, *12*, 2853-2856.

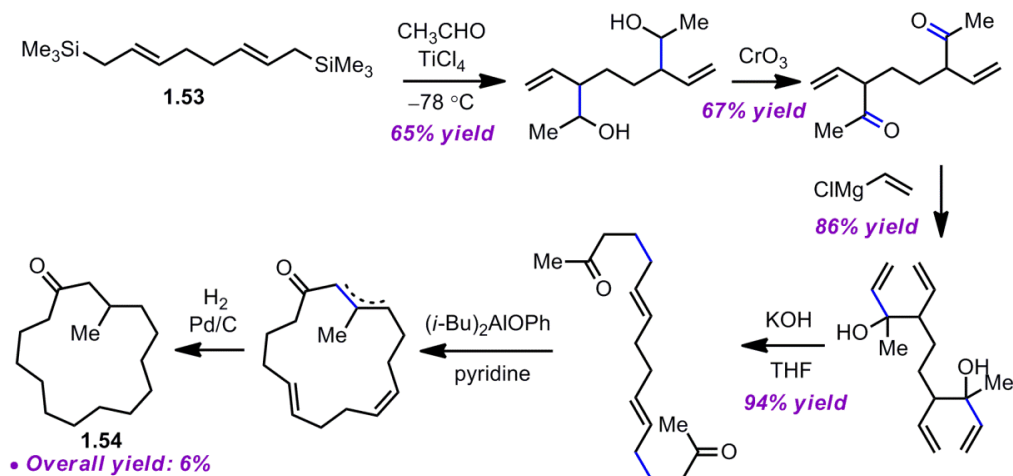
³⁷ Sakurai, H.; Eriyama, Y.; Kamiyama, Y.; Nakadaira, Y., "Reaction of Organodisilanes with Dienes Catalyzed by Transition Metal Complexes. Preparation of 1,8-Bis(trimethylsilyl) Octa-2,6-Diene and Its Use in the Synthesis of *dl*-Muscone," *Journal of Organometallic Chemistry* **1984**, *264*, 229-237.

85% yield. The coupling product **1.53** was used as a starting material for the synthesis of *dl*-muscone (**1.54**),³⁸ as described in Scheme 1.19.

Scheme 1.18 Sakurai's Disilylative Dimerization of Dienes (1984)



Scheme 1.19 Synthesis of *dl*-Muscone 1.54 (Sakurai, 1984)

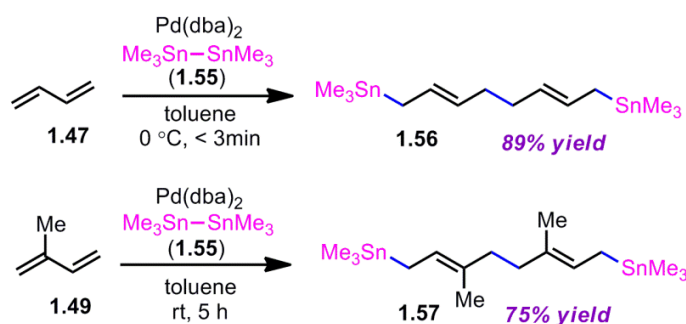


The Tsuji group investigated coupling reactions of 1,3-dienes with use of distannane and disilane reagents in the presence of a palladium catalyst (Scheme 1.20).³⁶ Employing

³⁸ Kamat, V. P.; Hagiwara, H.; Katsumi, T.; Hoshi, T.; Suzuki, T.; Ando, M., "Ring Closing Metathesis Directed Synthesis of (*R*)-(-)-Muscone from (+)-Citronellal," *Tetrahedron* **2000**, *56*, 4397-4403.

hexamethyldistannane (**1.55**), 1,3-butadiene (**1.47**), and a catalytic amount of Pd(dba)₂, Tsuji and co-workers were able to prepare a single isomer of double-stannated dimer **1.56** in 89% yield. Under the same conditions, a reaction with isoprene (**1.49**) furnished the coupling product **1.57** (75% yield) in a highly regio- and stereoselective manner.

Scheme 1.20 Tsuji's Intermolecular Diene–Diene Coupling (1992)

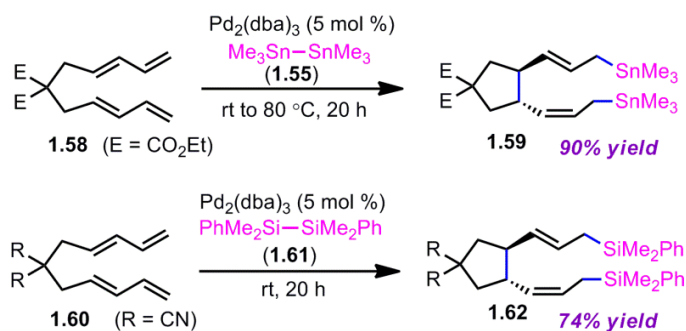


Intramolecular coupling reactions of dienes were also surveyed by the Tsuji group (Scheme 1.21).³⁹ The Pd-catalyzed reaction of Me₃Sn–SnMe₃ (**1.55**) with ethoxycarbonyl-substituted bisdiene **1.58** afforded the cyclized/distannylated product **1.59** in 90% yield in a highly regio- and stereoselective manner. A disilane reagent, Bu₃Si–SiBu₃ (**1.61**), also promoted intramolecular coupling of cyano-substituted bisdiene **1.60** to provide **1.62** in 89% yield with a catalytic amount of Pd(dba)₂. The stereochemistry of the alkenes of the product was confirmed by 2D heteronuclear multiple bond coherence (HMBC) spectra; the stereochemistry at the ring junctions was determined by X-ray crystallography of urethane

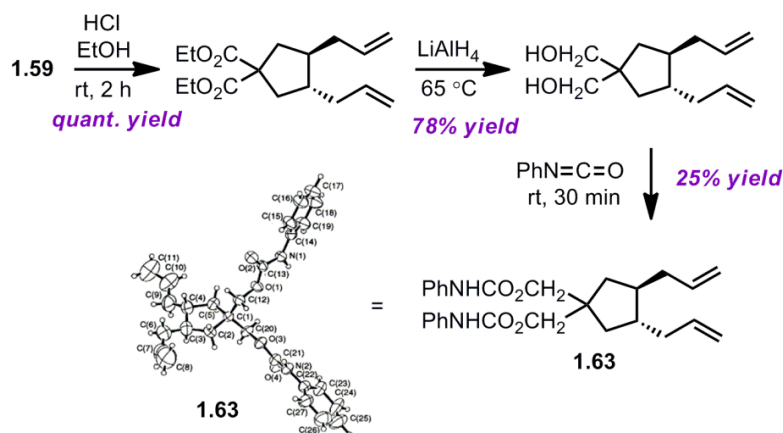
³⁹ Obora, Y.; Tsuji, Y.; Kakehi, T.; Kobayashi, M.; Shinkai, Y.; Ebihara, M.; Kawamura, T., "Palladium Complex-Catalysed Carbocyclization–Distannylation, –Disilylation and –Silastannylation of Bis-Dienes Using Distannanes, Disilanes and Silylstannanes," *Journal of the Chemical Society, Perkin Transactions 1* **1995**, 599–608.

1.63, which was transformed from the product 1.59. The X-ray structure (ORTEP drawing with 30% probability ellipsoids) and the derivatization details of diester 1.59 to diurethane 1.63 are described in Scheme 1.22.

Scheme 1.21 Tsuji's Intramolecular Diene–Diene Coupling (1995)



Scheme 1.22 Synthesis and ORTEP Drawing of 1.63 (Tsuji, 1995)



1.3.4. Coupling of Aldehyde–Allene and Ketone–Allene

The Pd-catalyzed coupling reactions of carbonyl–allene with a *Si–Sn* reagent were demonstrated by Kang et al. (Table 1.1).⁴⁰ Allene aldehyde **1.64** efficiently underwent silastannylation of multiple π components to produce *cis*-cyclopentanol **1.65** (71% yield), when it was treated with Me₃Si–SnBu₃ in the presence of (π -allyl)₂PdCl₂ at ambient temperature (entry 1). This method was also effective for the preparation of cyclohexanol derivatives; allene aldehyde **1.66** was transformed into *cis*-cyclohexanol **1.67** under the same reaction conditions in 62% yield (entry 2). In addition to these aldehyde–allene couplings, they tackled more challenging tasks, ketones–allene couplings (entries 3 & 4). More sterically hindered and less reactive allene ketones, **1.68** and **1.70**, smoothly cyclized to give the corresponding coupling products **1.69** and **1.71**, respectively, when they were reacted with 1.1 equivalents of Me₃Si–SnBu₃ (**1.17**) and 5 mol % of (π -allyl)₂PdCl₂.

⁴⁰ Kang, S.-K.; Ha, Y.-H.; Ko, B.-S.; Lim, Y.; Jung, J., "Palladium-Catalyzed Regio- and Diastereoselective Tandem Silastannylation/Allyl Addition of Allene Aldehydes and Allene Ketones: Synthesis of *Cis* Cyclopentanols and Cyclohexanols," *Angewandte Chemie International Edition* **2002**, *41*, 343-345.

Table 1.1 Kang's Intramolecular Carbonyl–Allene Coupling (2002)⁴¹

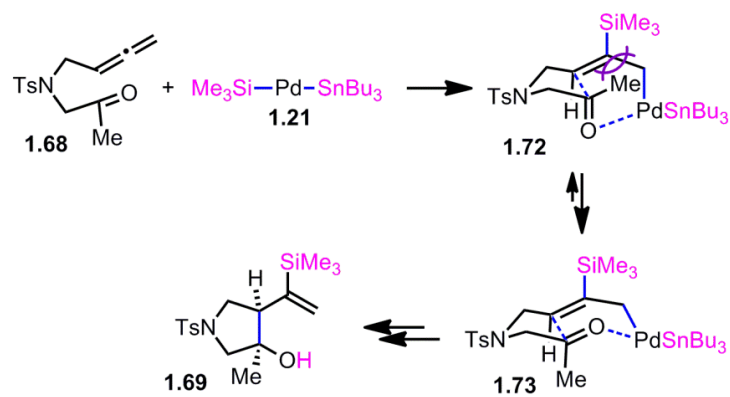
Entry	Allene carbonyl	Product	Yield (%)
1			71
2			62
3			67
4			67

The presumed mechanism of this process is illustrated in Scheme 1.23. The *Si*–*Sn* reagent **1.17** will oxidatively add to the palladium catalyst to form $\text{Me}_3\text{Si-Pd-SnBu}_3$ (**1.21**); then, it will add to the allene moiety of **1.68** to give a palladium complex **1.73**, which is in a more stable conformation than **1.72**. Subsequently, the σ - or π -allyl Pd complex **1.73** would undergo intramolecular allylation to the carbonyl and reductive elimination to afford *cis*-cyclopentanol **1.69**. It is speculated that the stereochemistry of the reaction originated from the energy difference between intermediates **1.72** and **1.73**. In other words, the steric

⁴¹ Reaction conditions: 1.0 equiv. of allene carbonyls, 1.1 equiv of $\text{Me}_3\text{Si-SnBu}_3$ (**1.17**), 5 mol % of $(\pi\text{-allyl})_2\text{Pd}_2\text{Cl}_2$, THF, room temperature, 10 min.

interference between the TMS and the methyl group may render intermediate **1.73** more stable than **1.72**.

Scheme 1.23 Rationale for Stereochemical Outcome (Kang, 2002)



1.4. Platinum-Catalyzed Bismetallative Multicomponent Coupling

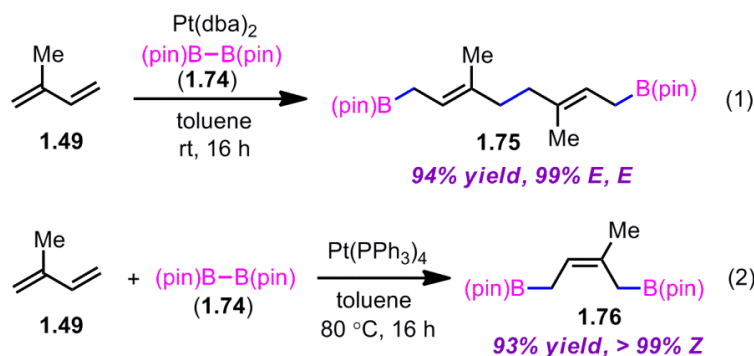
Platinum (Pt) catalyzed bismetallative multicomponent reactions are relatively sparse, compared to other group 10 transition metal catalyzed reactions (Pd or Ni). The main contributors in this section are the Miyaura group for diene–diene coupling (section 1.4.1) and the Ito group for aldehyde–diene coupling reactions (section 1.4.2).

1.4.1. Coupling of Diene–Diene

Pt-catalyzed diborylative coupling reactions of diene–diene were examined by Miyaura et al (Scheme 1.24).⁴² The reaction of isoprene (**1.49**) with bis(pinacolato)diboron (**1.74**) that is catalyzed by Pt(dba)₂ afforded a borylated dimer product **1.75** in 94% yield. The process shows high stereoselectivity as well as great regioselectivity; only the (*E,E*) isomer was observed in this reaction (eq. 1). This three-component coupling product was obtained as a major product only when Pt(dba)₂ was used as a catalyst. When Pt(PPh₃)₄ was employed as a catalyst in the same reaction, on the other hand, the 1:1 adduct of B₂(pin)₂ and diene (**1.76**) was formed exclusively (eq. 2).

⁴² Ishiyama, T.; Yamamoto, M.; Miyaura, N., "Platinum(0)-Catalysed Diboration of Alka-1,3-Dienes with Bis(Pinacolato) Diboron," *Chemical Communications* **1996**, 2073-2074.

Scheme 1.24 Miyaura's Intermolecular Diene–Diene Coupling (1996).



1.4.2. Coupling of Aldehyde–Diene

Pt-catalyzed silaborative intermolecular coupling reactions of aldehyde–diene were accomplished by the Ito group (Table 1.2).^{43,44,45} It was observed that benzaldehyde (**1.78**), 2,3-dimethyl-1,3-butadiene (**1.79**), and silylborane **1.77** can be coupled in the presence of Pt(CH₂=CH₂)(PPh₃)₂ at 120 °C to give **1.80** in 85% yield (entry 1). An unsymmetrical diene, 2-phenyl-1,3-butadiene (**1.81**), can also be employed in this process to be coupled with both

⁴³ Suginome, M.; Nakamura, H.; Matsuda, T.; Ito, Y., "Platinum-Catalyzed Silaborative Coupling of 1,3-Dienes to Aldehydes: Regio- and Stereoselective Allylation with Dienes through Allylic Platinum Intermediates," *Journal of the American Chemical Society* **1998**, *120*, 4248-4249.

⁴⁴ For a review, see: (a) Suginome, M.; Ito, Y., "Regio- and Stereoselective Synthesis of Boryl-Substituted Allylsilanes Via Transition Metal-Catalyzed Silaboration," *Journal of Organometallic Chemistry* **2003**, *680*, 43-50. For related works, see: (b) Suginome, M.; Fukuda, T.; Nakamura, H.; Ito, Y., "Synthesis of (Boryl)(Silyl)Iminomethanes by Insertion of Isonitriles into Silicon–Boron Bonds," *Organometallics* **2000**, *19*, 719-721.

⁴⁵ (a) Suginome, M.; Matsuda, T.; Yoshimoto, T.; Ito, Y., "Nickel-Catalyzed Silaboration of Small-Ring Vinylcycloalkanes: Regio- and Stereoselective (E)-Allylsilane Formation via C–C Bond Cleavage," *Organometallics* **2002**, *21*, 1537-1539. (b) Morgan, J. B.; Morken, J. P., "Platinum-Catalyzed Tandem Diboration/Asymmetric Allylboration: Access to Nonracemic Functionalized 1,3-Diols," *Organic Letters* **2003**, *5*, 2573-2575.

aromatic and aliphatic aldehydes (**1.81** and **1.84**) under similar reaction conditions to afford the coupling products **1.83** and **1.85** (entries 2 & 3). Also, this coupling reaction occurs under butadiene (**1.47**) atmosphere (1 atm) to give the correspondent product **1.86** in 63% yield with excellent stereoselectivity (entry 4). Notably, a cyclic diene **1.87** that is fixed in an *s-trans* configuration turned out to be an efficient coupling partner in this process to furnish **1.88** as a single diastereomer (entry 5).

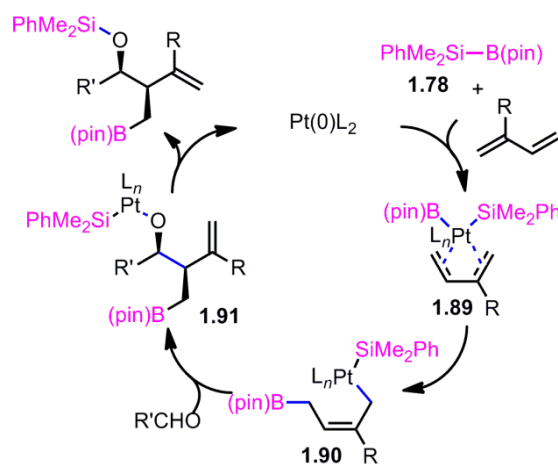
Table 1.2 Ito's Intermolecular Aldehyde-Diene Coupling (1998)⁴⁶

Entry	Aldehyde	Diene	Product	Yield	d.r.
1				85	96:4
2				83	99:1
3				71	93:7
4				63	95:5
5				60	99:1

⁴⁶ Reaction conditions: 2 mol % Pt(0), 1.5–3.0 equiv. aldehyde, hexane or octane, 80–120 °C.

The proposed mechanism for the Pt-catalyzed silaborative aldehyde–diene coupling reaction is illustrated in Scheme 1.25. The Si–B bond of **1.77** will be oxidatively added to the platinum(0) catalyst, and subsequent coordination of a diene will form a platinum(II) complex **1.89**. Then, insertion of the diene to the Pt–B bond can occur to give *cis*-crotylplatinum complex **1.90** forming a C–B bond at the terminal carbon of the less substituted alkene. Reaction of the platinum complex **1.90** with an aldehyde will form a C–C bond at the γ position to the Pt atom, which will generate an (alkoxy)(silyl)platinum(II) complex **1.91**. Finally, reductive elimination will afford the coupling product, in which a Si–O bond is present.

Scheme 1.25 Proposed Mechanism for Pt-Catalyzed Coupling (Ito, 1998)

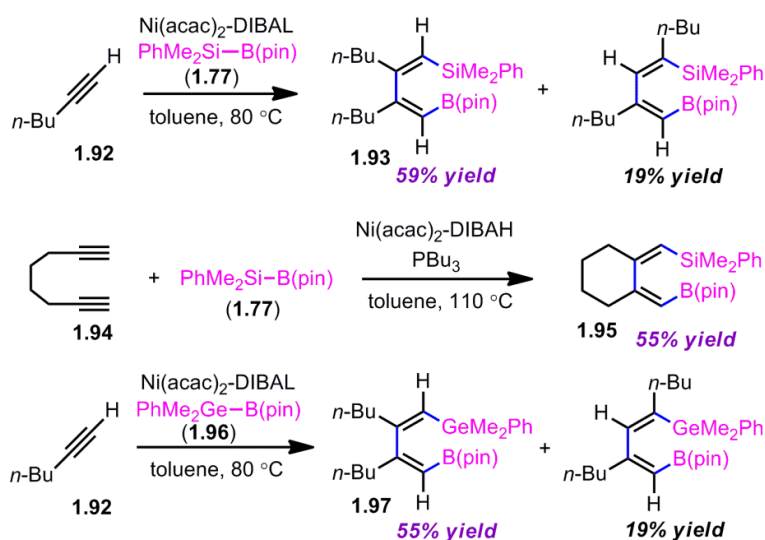


1.5. Nickel Catalyzed Bimetallative Multicomponent Coupling

1.5.1. Coupling of Alkyne–Alkyne

The Ni-catalyzed bimetallative coupling reactions of alkyne–alkyne has been introduced by the Ito group (Scheme 1.26).⁴⁷ It was demonstrated that a nickel(0) catalyst can couple two 1-hexyne (**1.92**) molecules with a *B*–*Si* reagent (**1.77**) in a regio- and stereoselective manner to provide **1.93** as a major product. This silaborative dimerization was applied to intramolecular cyclization of diyne (**1.94**) to afford **1.95** in 55% yield. The diyne dimerization with a germlyborane (*Ge*–*B*) reagent **1.96** was also reported; a head-to-head dimer **1.97** was obtained as a major product.

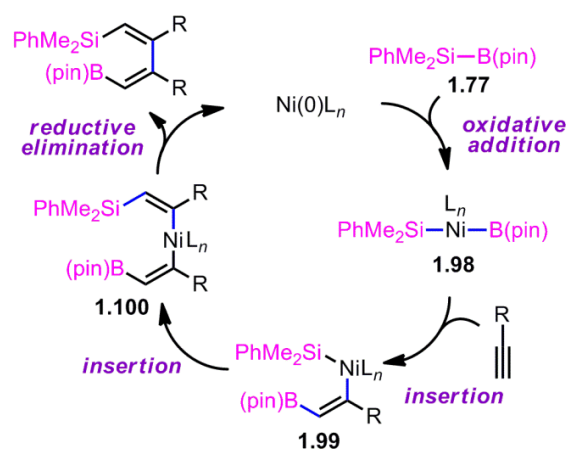
Scheme 1.26 Ito's Ni-Catalyzed Alkyne Dimerization (1998).



⁴⁷ Suginome, M.; Matsuda, T.; Ito, Y., "Nickel-Catalyzed Silaborative Dimerization of Alkynes," *Organometallics* **1998**, *17*, 5233-5235.

Based on the observed experimental results, they suggest the following catalytic cycle for a plausible mechanism for this process (Scheme 1.27). According to their speculation, an oxidative addition of the Si–B bond onto the Ni(0) complex generates the (silyl)(boryl)Ni(II) intermediate (**1.98**). Then, an alkyne undergoes *cis*-insertion into the B–Ni bond of the Ni(II) complex. The resulting vinyl-substituted nickel(II) intermediate (**1.99**) participates in another *cis*-insertion event to furnish **1.100**. Finally, reductive elimination would give the product.

Scheme 1.27 Proposed Mechanism for Alkyne Dimerization (Ito, 1998)



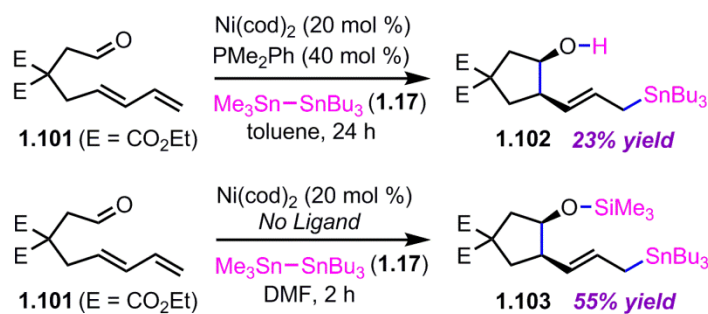
1.5.2. Coupling of Aldehyde–Diene

1.5.2.1. Intramolecular Aldehyde–Diene Coupling

The intramolecular coupling of 1,3-diene and a tethered aldehyde was studied by the Mori group (Scheme 1.28).^{17b} With the use of Ni(cod)₂ and PMe₂Ph, a cyclic alcohol **1.102** (23% yield) was formed from a reaction of **1.101** and Bu₃Sn–SiMe₃ (**1.17**) in toluene. The product

formed in this process was sensitive to the ligands and solvents that are used in the reactions. The coupling reaction from the same starting material (**1.101**) with DMF as a solvent in the absence of any phosphine ligands afforded **1.103** as a sole product in 55% yield.

Scheme 1.28 Mori's Intramolecular Aldehyde–Diene Coupling (2002)



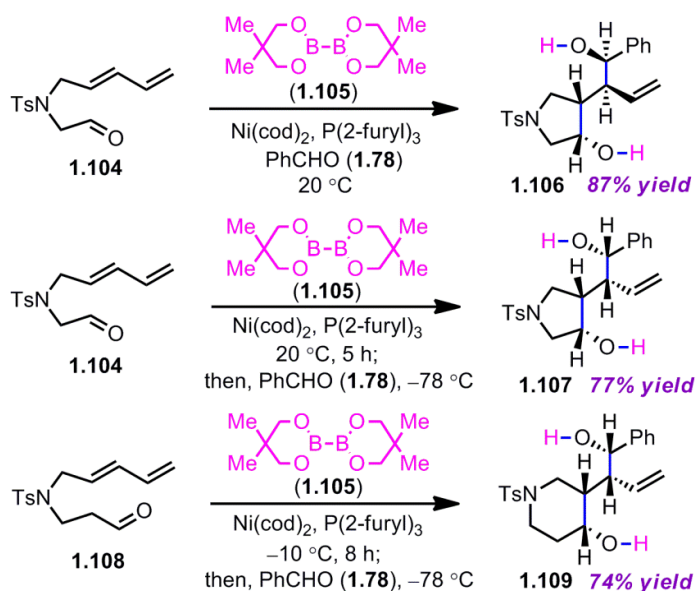
The Yu group examined sequential four-component coupling reactions (i.e. coupling of an aldehyde, a diene, and a diboron reagent followed by allylboration with another aldehyde) as shown in Scheme 1.29.^{48, 49} The reaction of a diene-aldehyde **1.104**, benzaldehyde (**1.78**), and a diboron reagent **1.105** at 20 °C in the presence of Ni(cod)₂ and P(2-furyl)₃ afforded **1.106** in 87% yield. An unexpected stereochemical inversion of the product was observed at different reaction temperatures; when the subsequent allylation with benzaldehyde (**1.78**) was carried out at –78 °C (instead of at 20 °C), compound **1.107**

⁴⁸ Yu, C.-M.; Youn, J.; Yoon, S.-K.; Hong, Y.-T., "A Highly Stereoselective Sequential Allylic Transfer Reaction of Diene with Diboronyl Reagent and Aldehydes Promoted by Nickel Catalyst," *Organic Letters* **2005**, *7*, 4507-4510.

⁴⁹ Similar sequential three-component coupling reactions (i.e. coupling of a diene and a diboron reagent followed by allylboration with an aldehyde) have also been reported by our laboratory: Miller, S. P.; Morgan, J. B.; Felix J. Nepveux V, A.; Morken, J. P., "Catalytic Asymmetric Carbohydroxylation of Alkenes by a Tandem Diboration/Suzuki Cross-Coupling/Oxidation Reaction," *Organic Letters* **2004**, *6*, 131-133.

was obtained as a single isomer. Additionally, a six-membered ring moiety (**1.109**) can be prepared by this process from a diene-aldehyde **1.108**, benzaldehyde (**1.78**), and **1.105** in the presence of a nickel catalyst (74% yield). This method is particularly noteworthy given its efficiency for installing four contiguous stereogenic centers in a single operation.

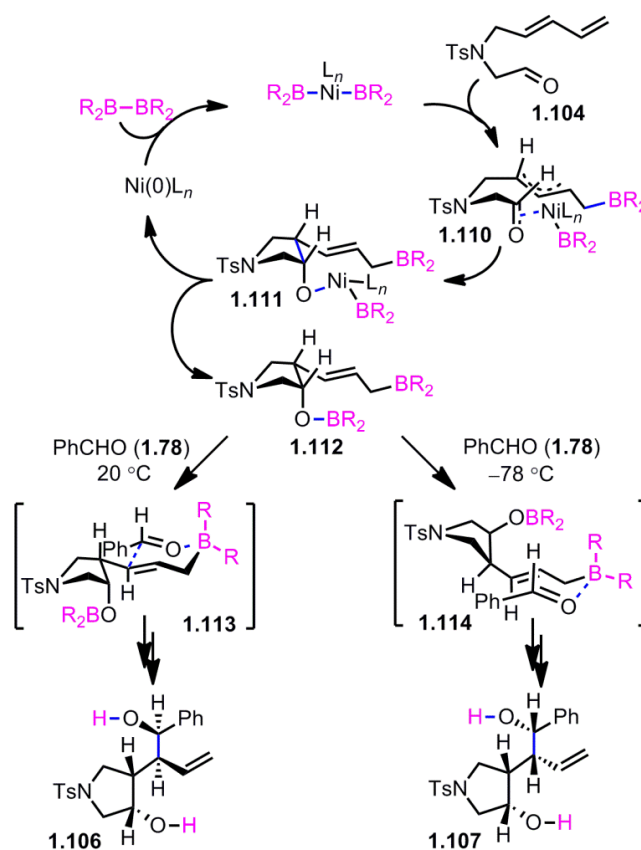
Scheme 1.29 Yu's Sequential Four-Component Coupling (2005)



The origin of the contrasting stereochemical outcomes, which vary depending on the temperatures, is speculated by the proposed pathways that are depicted in Scheme 1.30. The reaction begins with oxidative addition of the nickel catalyst to the diboron reagent. Then, diene insertion giving a π -allyl complex **1.110** and carbonyl insertion forming **1.111** would occur sequentially. After reductive elimination to give **1.112**, a subsequent intermolecular allylation with benzaldehyde (**1.78**) will furnish either **1.106** or **1.107** depending on the temperature for this step. The source of the stereochemical control is not revealed in this

report, but subtle geometrical preferences of two intermediates **1.113** and **1.114** at two different temperatures are described in Scheme 1.30.

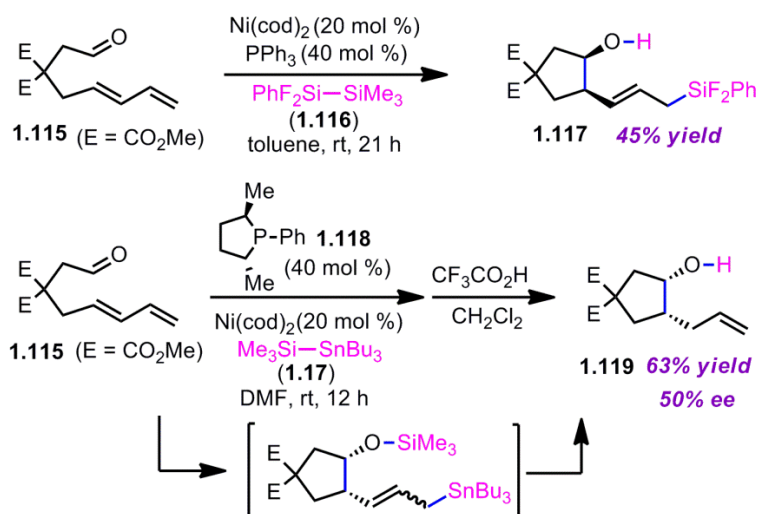
Scheme 1.30 Rationale for Stereochemical Outcome (Yu, 2005)



The Mori and Sato's laboratories investigated intramolecular disilylative and silastannylative coupling reactions of 1,3-diene and a tethered aldehyde (Scheme 1.31).^{17d} As for disilane reagents, it is known that halogenated disilane reagents tend to be more reactive

toward transition metal catalysts.⁵⁰ Disilylative coupling of **1.115** and $\text{PhF}_2\text{Si-SiMe}_3$ (**1.116**) in the presence of 20 mol % of $\text{Ni}(\text{cod})_2$ and 40 mol % of PPh_3 furnished **1.117** (45% yield) in a completely regio- and stereoselective manner. It is worth mentioning that catalytic enantioselective cyclizations were attempted in this study. With the use of $\text{Ni}(\text{cod})_2$ and a chiral ligand **1.118**,⁵¹ the reaction of **1.115** and $\text{Me}_3\text{Si-SnBu}_3$ (**1.17**) in DMF afforded **1.119** as a mixture of enantiomers.

Scheme 1.31 Mori and Sato's Aldehyde-Diene Coupling (2007)



⁵⁰ (a) Hayashi, T.; Matsumoto, Y.; Ito, Y., "Palladium-Catalyzed 1,4-Disilylation of α,β -Unsaturated Ketones with 1,1-Dichloro-1-Phenyl-2,2,2-Trimethyldisilane," *Tetrahedron Letters* **1988**, 29, 4147-4150. (b) Ozawa, F.; Sugawara, M.; Hayashi, T., "A New Reactive System for Catalytic Bis-Silylation of Acetylenes and Olefins," *Organometallics* **1994**, 13, 3237-3243.

⁵¹ Burk, M. J.; Feaster, J. E.; Harlow, R. L., "New Electron-Rich Chiral Phosphines for Asymmetric Catalysis," *Organometallics* **1990**, 9, 2653-2655.

1.5.2.2. Intermolecular Aldehyde–Diene Coupling

The intermolecular Ni-catalyzed diastereoselective bismetallative aldehyde–diene coupling reactions were demonstrated by our laboratory.^{12, 52} The coupling reactions of aldehydes, dienes, and $B_2(\text{pin})_2$ (**1.74**) lead to stereoselective formation of homoallylic boronic esters, which are synthetically valuable motifs (Table 1.3).^{12, 53} Various aromatic aldehydes (**1.78**, **1.122**, and **1.124**) are coupled a 1,3-diene **1.120** and $B_2(\text{pin})_2$ (**1.74**) to give **1.121**, **1.123**, and **1.125**, respectively (entries 1–3); a reaction with an aliphatic aldehyde **1.126** affords **1.127** in a moderate yield (entry 4). Different diene substrates (**1.128** and **1.49**) also undergo the diboron-promoted three-component coupling reactions giving **1.129** and **1.130** under the same reaction conditions (entries 5–6). These reactions feature efficient preparatory methods for functionally and stereochemically enriched allylboronates.

⁵² Cho, H. Y.; Morken, J. P., "Ni-Catalyzed Borylative Diene–Aldehyde Coupling: The Remarkable Effect of $P(\text{SiMe}_3)_3$," *Journal of the American Chemical Society* **2010**, *132*, 7576-7577.

⁵³ For related studies, see: (a) Sumida, Y.; Yorimitsu, H.; Oshima, K., "Nickel-Catalyzed Borylation of Aryl Cyclopropyl Ketones with Bis(Pinacolato)Diboron to Synthesize 4-Oxoalkylboronates," *The Journal of Organic Chemistry* **2009**, *74*, 3196-3198. (b) Yang, C.-M.; Jeganmohan, M.; Parthasarathy, K.; Cheng, C.-H., "Highly Selective Nickel-Catalyzed Three-Component Coupling of Alkynes with Enones and Alkenyl Boronic Acids: A Novel Route to Substituted 1, 3-Dienes," *Organic Letters* **2010**, *12*, 3610-3613. (c) Beaver, M. G.; Jamison, T. F., "Ni(II) Salts and 2-Propanol Effect Catalytic Reductive Coupling of Epoxides and Alkynes," *Organic Letters* **2011**, *13*, 4140-4143.

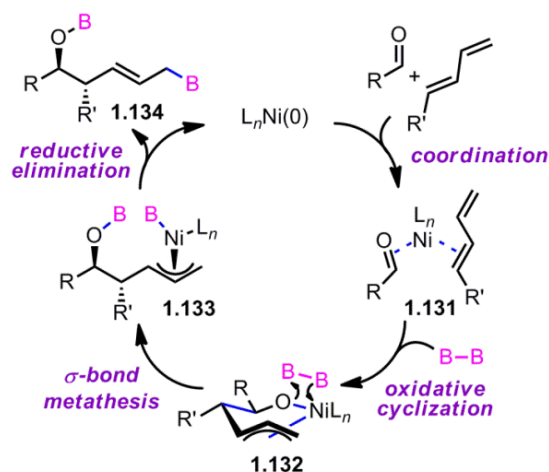
Table 1.3 Morken's Intermolecular Aldehyde–Diene Coupling (2008)⁵⁴

Entry	Aldehyde	Diene	Product	Yield	d.r.
1	1.78	1.120	1.121	66	>20:1
2	1.122	1.120	1.123	63	>20:1
3	1.124	1.120	1.125	63	>20:1
4	1.126	1.120	1.127	47	>20:1
5	1.78	1.128	1.129	70	>20:1
6	1.78	1.49	1.130	68	N/A

Based on the mechanistic studies on these coupling reactions as well as relevant reductive coupling reactions, we propose the following catalytic cycle for the our coupling reactions (Scheme 1.32). Initial oxidative cyclization will lead to the formation of nickelacyclic intermediate **1.132** from a nickel complex **1.131**. In the presence of diboron reagent, subsequent σ -bond metathesis will yield intermediate **1.133**. Then, reductive elimination will generate an allylic boronic ester **1.134** and restart the catalytic cycle.

⁵⁴ Reaction conditions: 5 mol % Ni(cod)₂, 10 mol % PCy₃, 1.1 equiv. diene, 1.2 equiv. B₂(pin)₂, 0.2 M THF, rt, 6 h. Then, oxidation with H₂O₂ and NaOH. (b) Modified reaction conditions: 10 mol % Ni(cod)₂, 10 mol % P(OEt)₃. Acetylation improved the isolated yield.

Scheme 1.32 Proposed Mechanism for Cho–Morken Coupling (2008)

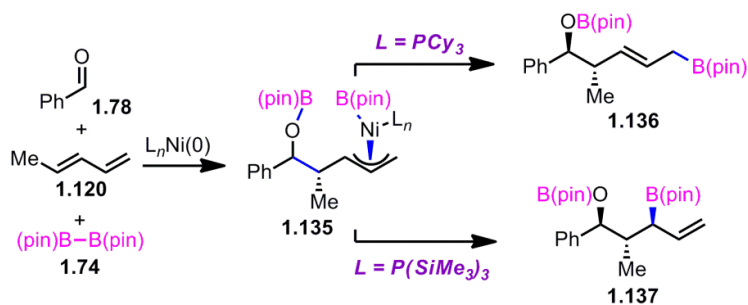


To our surprise, the regioselectivity of the products in this process is reversed with the replacement of the ligand. In the presence of $P(\text{SiMe}_3)_3$ as a ligand, the nickel-catalyzed coupling of benzaldehyde (**1.78**), 1,3-pentadiene (**1.120**), and $B_2(\text{pin})_2$ (**1.74**) afforded terminal boronate **1.137**, which is regioisomeric to the product **1.136** that comes from the reaction with PCy_3 (Scheme 33).⁵² The ligand effect that is shown in this study is rationalized by unique characteristics of $P(\text{SiMe}_3)_3$. The electron accepting ability of $P(\text{SiMe}_3)_3$ was witnessed by both Bartik⁵⁵ and Helm.⁵⁶ The large cone angle of the ligand, together with its electron accepting property, will accelerate reductive elimination of **1.135** to form **1.137**, ahead of allyl isomerization that will lead to the formation of **1.136**.

⁵⁵ Bartik, T.; Himmler, T.; Schulte, H. G.; Seevogel, K., "Substituenteneinflüsse Auf Die Basizität Von Phosphorliganden in $R_3P-Ni(CO)_3$ -Komplexen," *Journal of Organometallic Chemistry* **1984**, 272, 29-41.

⁵⁶ McCampbell, T.; Kinkel, B.; Miller, S.; Helm, M., "Group 6 Metal Carbonyl Complexes of a Bulky Phosphine: The Crystal Structures of Tris(Trimethylsilyl)Phosphine-M(0)Pentacarbonyl, M = Chromium, Molybdenum, and Tungsten," *Journal of Chemical Crystallography* **2006**, 36, 271-275.

Scheme 1.33 Ligand Effect on Regioselectivity (Morken, 2010)



Using P(SiMe₃)₃ as a ligand, various aldehydes can be coupled with 1,3-pentadiene and B₂(pin)₂ (1.74) with excellent stereoselectivity by this process (Table 1.4). Generally, aromatic and heteroaromatic aldehydes (1.78 and 1.139) efficiently undergo the Ni-catalyzed coupling reactions with *trans*-piperylene (1.120) and bis(pinacolato)diboron (1.74) to provide 1.138 and 1.140 with great diastereoselectivities (entries 1–2). The coupling with aliphatic aldehydes (1.126 and 1.142) also turned out to be effective to afford 1.141 and 1.143 under the same reaction conditions (entries 3–4). In addition, an α -chiral aldehyde (1.144) was reacted with the Felkin selectivity to give 1.145 thereby revealing the potential for asymmetric synthesis (entry 5).

Table 1.4 Aldehyde–Diene Coupling for 1,3-Diols (Morken, 2010)⁵⁷

Entry	Aldehyde	Product	Yield	d.r.
1			67	>20:1
2			55	>20:1
3			58	>20:1
4			50	>20:1
5			49	6:1

An outstanding accomplishment in this area was made by Saito and Sato in 2012; Ni-catalyzed enantio- and diastereoselective bimetallic aldehyde–diene couplings were demonstrated (Table 1.5).⁵⁸ A silylborane reagent, PhMe₂Si–B(pin) (1.77), was employed in this process along with 1,3-dienes and aldehydes in the presence of a nickel catalyst and a chiral phosphine ligand (1.147). Reactions with aldehydes that possess electron-donating groups (1.148 and 1.150) furnished the corresponding products (1.149 and 1.151) in good

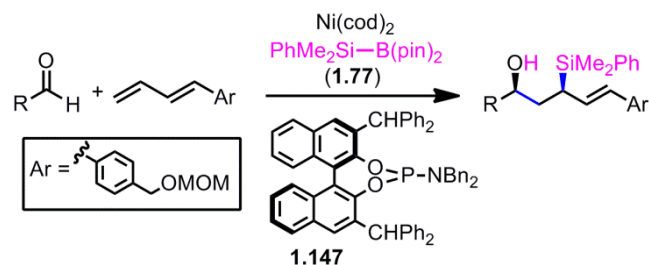
⁵⁷ Reaction conditions: 10 mol % Ni(cod)₂, 15 mol % P(*t*-Bu)₃, 3.0 equiv. diene, 3.0 equiv. B₂(pin)₂ (1.74), 0.2 M THF, rt, 12 h. Then, oxidative workup with H₂O₂ and NaOH.

⁵⁸ Saito, N.; Kobayashi, A.; Sato, Y., "Nickel-Catalyzed Enantio- and Diastereoselective Three-Component Coupling of 1,3-Dienes, Aldehydes, and a Silylborane Leading to α -Chiral Allylsilanes," *Angewandte Chemie International Edition* **2012**, *51*, 1228-1231.

yields and with high enantioselectivities (entries 1–2). However, a reaction of an aldehyde with an electron-withdrawing group (**1.152**) exhibited a decreased yield (29% yield) giving **1.153**, even though the enantiopurity was still good (85% *ee*, entry 3). Aliphatic aldehydes (**1.142** and **1.155**) also participate in this process to give the corresponding products (**1.154** and **1.156**) with great enantioselectivities (entries 4–5). These reactions provide a new tool to prepare optically active α -chiral allylsilanes.^{59,60}

⁵⁹ For selected works for synthesis of enantioenriched α -chiral allylsilanes, see: (a) Fukuda, K.; Miyashita, M.; Tanino, K., "Practical Synthesis of (*E*)- and (*Z*)-2-Silyl-3-Penten-1-ols with High Enantiopurity," *Tetrahedron Letters* **2010**, *51*, 4523-4525. (b) Li, D.; Tanaka, T.; Ohmiya, H.; Sawamura, M., "Synthesis of α -Arylated Allylsilanes through Palladium-Catalyzed γ -Selective Allyl–Aryl Coupling," *Organic Letters* **2010**, *12*, 3344-3347.

⁶⁰ (a) Aggarwal, V. K.; Binanzer, M.; de Ceglie, M. C.; Gallanti, M.; Glasspoole, B. W.; Kendrick, S. J.; Sonawane, R. P.; Vázquez-Romero, A.; Webster, M. P., "Asymmetric Synthesis of Tertiary and Quaternary Allyl- and Crotylsilanes Via the Borylation of Lithiated Carbamates," *Organic Letters* **2011**, *13*, 1490-1493. (b) Takeda, M.; Shintani, R.; Hayashi, T., "Enantioselective Synthesis of α -Tri- and α -Tetrasubstituted Allylsilanes by Copper-Catalyzed Asymmetric Allylic Substitution of Allyl Phosphates with Silylboronates," *The Journal of Organic Chemistry* **2013**, *78*, 5007-5017.

Table 1.5 Saito and Sato's Enantioselective Coupling Reactions (2012)⁶¹

Entry	Aldehyde	Product	Yield	ee
1	1.148	1.149	89	96
2	1.150	1.151	92	92
3	1.152	1.153	29	85
4	1.142	1.154	68	96
5	1.155	1.156	74	94

1.5.3. Coupling of Ketone–Diene

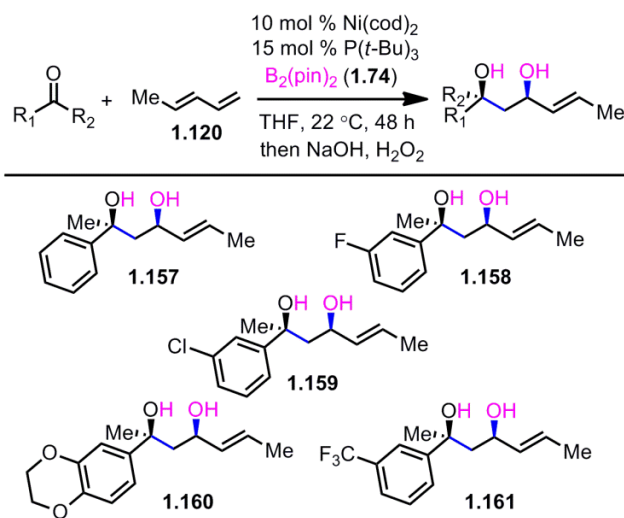
The Ni-catalyzed diborylative coupling reactions of ketone–diene have been reported by the authors' laboratory (Scheme 1.34).⁶² The report has shown that ketones, less sterically-biased substrates, can participate in this process with high regio- and stereoselectivities to afford tertiary alcohols. Initial inquiry involved acetophenone, (*E*)-1,3-

⁶¹ Reaction conditions: 10 mol % Ni(cod)₂, 10 mol % **1.147**, 1 equiv. diene, 2.5 equiv. aldehyde, 2.5 equiv. PhMe₂Si–B(pin) (**1.77**), DMF, room temperature.

⁶² Cho, H. Y.; Yu, Z.; Morken, J. P., "Stereoselective Borylative Ketone–Diene Coupling," *Organic Letters* **2011**, *13*, 5267–5269.

pentadiene (**1.120**), $B_2(\text{pin})_2$ (**1.74**) with a nickel catalyst, which provided a tertiary alcohol **1.157** (76% yield) in a highly stereoselective fashion. As described in Scheme 1.34, halogenated aromatic methyl ketones are accommodated in this reaction (compounds **1.158**, **1.159**) as are the ketones with both electron-donating and electron-withdrawing substituents (compounds **1.160**, **1.161**). In all cases, excellent diastereoselectivity (> 20:1) was observed in the reaction products.

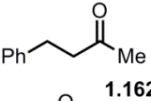
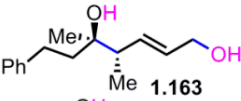
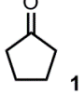
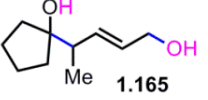
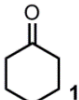

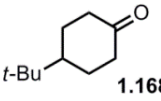
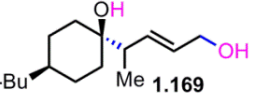
Scheme 1.34 Morken's Intermolecular Ketone–Diene Coupling (2011)



While reactions with aromatic methyl ketones furnish the 1,3-diols regioselectively, reactions of aliphatic ketones afford regioisomeric 1,5-diols (Table 1.6). For instance, the reaction with 4-phenyl-2-butanone (**1.162**) and 1,3-pentadiene gave the derived 1,5-diol **1.163** in 69% yield (entry 1). Also, constrained cyclic ketones (**1.164** and **1.166**) are found to undergo smooth coupling with the diene to afford 1,5-diols (**1.165** and **1.167**, entries 2–3).

Notably, the coupling product **1.169** from **1.168** is acquired by preferred equatorial attack of the diene to the ketone electrophile (entry 4).

Table 1.6 Ketone–Diene Coupling for 1,5-Diol Synthesis (Morken, 2011)⁶³

Entry	Ketone	Product	Yield	d.r.
$\text{R}_1\text{C(=O)R}_2 + \text{Me-CH=CH}_2 \xrightarrow[\text{then NaOH, H}_2\text{O}_2]{\text{10 mol \% Ni(cod)}_2, \text{15 mol \% P}(t\text{-Bu)}_3, \text{B}_2(\text{pin})_2 \text{ (1.74), THF, 22 }^\circ\text{C, 48 h}}$				
1			69	7:1
2			56	N/A
3			52	N/A
4			53	>20:1

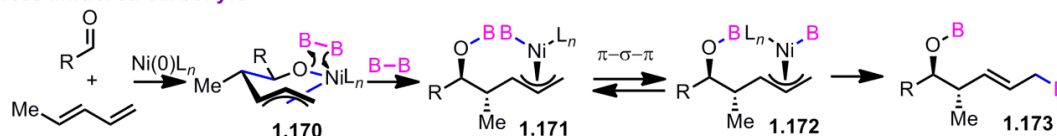
Based on the observations from these ketone–diene reactions along with the aldehyde–diene couplings (section 1.5.2.2.), both of which are reported by our laboratory, we suggest the following mechanistic rationale for the borylative multicomponent coupling reactions (Scheme 1.35). With non-hindered carbonyls (i.e. substrates in Tables 1.3, 1.4, and 1.6), reaction will proceed to give nickelacycle **1.170**. Then, subsequent σ -bond metathesis would form π -allyl complex **1.171**. Prior to reductive elimination, this intermediate may

⁶³ Reaction conditions: 10 mol % Ni(cod)₂, 15 mol % P(*t*-Bu)₃, 2.0 equiv. diene, 2.0 equiv. B₂(pin)₂ (**74**), 0.2 M THF, rt, 48 h. Then, oxidative workup with H₂O₂ and NaOH.

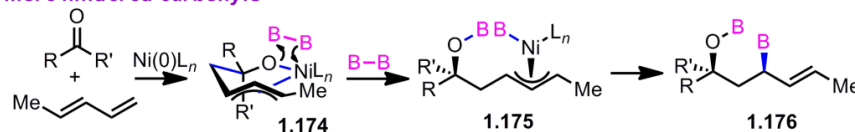
undergo π - σ - π isomerization to give **1.172**, which would afford product **1.173**. However, in the case of more hindered carbonyls (i.e. substrates in Scheme 1.34), the less substituted end of the diene would add to the carbonyl giving **1.174** due to the steric effects. The 1,3-diol **1.176** is furnished by subsequent σ -bond metathesis with **1.174** and reductive elimination of **1.175**. In this case, the π - σ - π isomerization is likely impeded with the substituted π -allyl complex.

Scheme 1.35 Mechanistic Rationale for Borylative Multicomponent Coupling (2011)

less hindered carbonyls



more hindered carbonyls



1.6. Conclusions and Outlook

Catalytic bismetallative coupling reactions involving multiple π -components are considered an effective method to build complex molecules. This one-step process features C–C bond formation, functionalization with bismetallic reagents, and the control of regio- and stereoselectivities.

The scope of this process in terms of both bismetallic reagents and the π -components are broad enough to be generally applied to more elaborate synthetic sequences. In particular, contemporary applications of the bismetallative multicomponent coupling reactions, in which high enantio- and/or diastereoselectivities are displayed, have enabled the study of this area to make a significant step forward.

Despite these considerable improvements, there is still much room for further progress in this field. Especially, investigations in more detailed mechanisms and application developments for biologically-active molecule syntheses will be of great interest.

Chapter 2. Nickel-Catalyzed Multicomponent Coupling Reactions of Aldehydes, Dienes, and Diboron Reagents

2.1. Introduction to Multicomponent Coupling Reactions

A multicomponent coupling reaction¹ is defined as a reaction in which three or more reactants combine in a single reaction event to afford a product that displays features of all reagents (Scheme 2.1).^{2,3} In other words, the functionalities of the multiple starting materials join through covalent bonds via a multicomponent coupling process. Multicomponent coupling reactions have great advantages of synthetic efficiency and operational simplicity, in addition to rapid generation of structural complexity in a single step.⁴ Some of the most useful features of multicomponent coupling reactions include selectivity, synthetic

¹ (a) Ugi, I.; Dömling, A.; Hörl, W., "Multicomponent Reactions in Organic Chemistry," *Endeavour* **1994**, *18*, 115-122. (b) Armstrong, R. W.; Combs, A. P.; Tempest, P. A.; Brown, S. D.; Keating, T. A., "Multiple-Component Condensation Strategies for Combinatorial Library Synthesis," *Accounts of Chemical Research* **1996**, *29*, 123-131. (c) Bienaymé, H.; Hulme, C.; Oddon, G.; Schmitt, P., "Maximizing Synthetic Efficiency: Multi-Component Transformations Lead the Way," *Chemistry—A European Journal* **2000**, *6*, 3321-3329.

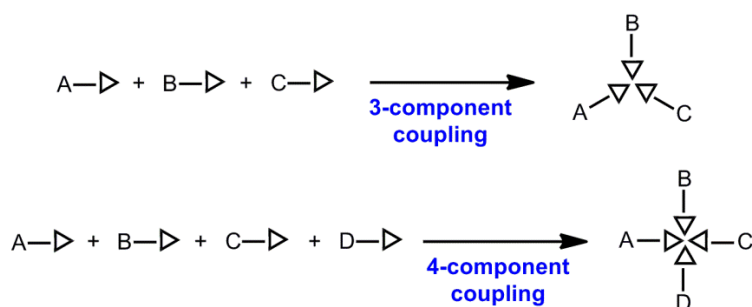
² For selected reviews, see: (a) de Graaff, C.; Ruijter, E.; Orru, R. V., "Recent Developments in Asymmetric Multicomponent Reactions," *Chemical Society Reviews* **2012**, *41*, 3969-4009 (b) Pellissier, H. I. n., "Stereocontrolled Domino Reactions," *Chemical Reviews* **2012**, *113*, 442-524.

³ (a) Biggs-Houck, J. E.; Younai, A.; Shaw, J. T., "Recent Advances in Multicomponent Reactions for Diversity-Oriented Synthesis," *Current Opinion in Chemical Biology* **2010**, *14*, 371-382. (b) Ikeda, S.-I., "Nickel-Catalyzed Intermolecular Domino Reactions," *Accounts of Chemical Research* **2000**, *33*, 511-519.

⁴ Ganem, B., "Strategies for Innovation in Multicomponent Reaction Design," *Accounts of Chemical Research* **2009**, *42*, 463-472.

convergency, and atom-economy. As a consequence, this step-economical process has played a central role in the development of modern synthetic methodology by reducing the number of synthetic steps while maximizing the accumulation of structural and functional complexity.⁵

Scheme 2.1 Multicomponent Coupling Reactions



The experimental simplicity of the multicomponent coupling reactions render these processes a great tool for systematic variations and automatization.⁶ In this regard, multicomponent reactions are particularly useful for combinatorial chemistry⁷ and

⁵ Touré, B. B.; Hall, D. G., "Natural Product Synthesis Using Multicomponent Reaction Strategies," *Chemical Reviews* **2009**, *109*, 4439-4486.

⁶ (a) Cargill, J. F.; Lebl, M., "New Methods in Combinatorial Chemistry – Robotics and Parallel Synthesis," *Current Opinion in Chemical Biology* **1997**, *1*, 67-71. (b) Powers, D. G.; Coffen, D. L., "Convergent Automated Parallel Synthesis," *Drug Discovery Today* **1999**, *4*, 377-383. (c) Kirschning, A.; Monenschein, H.; Wittenberg, R., "Functionalized Polymers—Emerging Versatile Tools for Solution-Phase Chemistry and Automated Parallel Synthesis," *Angewandte Chemie International Edition* **2001**, *40*, 650-679.

⁷ (a) Dolle, R. E., "Comprehensive Survey of Combinatorial Library Synthesis: 2002," *Journal of Combinatorial Chemistry* **2003**, *5*, 693-753. (b) Kennedy, J. P.; Williams, L.; Bridges, T. M.; Daniels, R. N.; Weaver, D.; Lindsley, C. W., "Application of Combinatorial Chemistry Science on Modern Drug Discovery," *Journal of Combinatorial Chemistry* **2008**, *10*, 345-354.

diversity-oriented synthesis.^{8, 9} So far, multicomponent coupling approaches have been employed in the synthesis of large libraries of biologically active compounds and densely functionalized molecules.¹⁰ Furthermore, the identification of therapeutic protein targets has been achieved with a method utilizing high-throughput screening of numerous candidates.¹¹ With other advantages of these processes such as high selectivities and environmental friendliness, the multicomponent coupling reactions are quite close to the realm of the ideal synthesis.^{2a, 12}

⁸ (a) Schreiber, S. L., "Target-Oriented and Diversity-Oriented Organic Synthesis in Drug Discovery," *Science* **2000**, *287*, 1964-1969. (b) Wessjohann, L.; Ruijter, E., "Macrocycles Rapidly Produced by Multiple Multicomponent Reactions Including Bifunctional Building Blocks (MiBs)," *Molecular Diversity* **2005**, *9*, 159-169.

⁹ (a) Burke, M. D.; Schreiber, S. L., "A Planning Strategy for Diversity-Oriented Synthesis," *Angewandte Chemie International Edition* **2004**, *43*, 46-58. (b) Spandl, R. J.; Bender, A.; Spring, D. R., "Diversity-Oriented Synthesis; a Spectrum of Approaches and Results," *Organic & Biomolecular Chemistry* **2008**, *6*, 1149-1158.

¹⁰ (a) Ghose, A. K.; Viswanadhan, V. N.; Wendoloski, J. J., "A Knowledge-Based Approach in Designing Combinatorial or Medicinal Chemistry Libraries for Drug Discovery. 1. A Qualitative and Quantitative Characterization of Known Drug Databases," *Journal of Combinatorial Chemistry* **1999**, *1*, 55-68. (b) Kerns, E. H., "High Throughput Physicochemical Profiling for Drug Discovery," *Journal of Pharmaceutical Sciences* **2001**, *90*, 1838-1858. (c) Colombo, M.; Peretto, I., "Chemistry Strategies in Early Drug Discovery: An Overview of Recent Trends," *Drug Discovery Today* **2008**, *13*, 677-684.

¹¹ (a) Reetz, M. T., "Combinatorial and Evolution-Based Methods in the Creation of Enantioselective Catalysts," *Angewandte Chemie International Edition* **2001**, *40*, 284-310. (b) Moaddel, R.; Wainer, I. W., "Immobilized Nicotinic Receptor Stationary Phases: Going with the Flow in High-Throughput Screening and Pharmacological Studies," *Journal of Pharmaceutical and Biomedical Analysis* **2003**, *30*, 1715-1724. (c) Gennari, C.; Piarulli, U., "Combinatorial Libraries of Chiral Ligands for Enantioselective Catalysis," *Chemical Reviews* **2003**, *103*, 3071-3100.

¹² (a) Wender, P. A.; Bi, F. C.; Gamber, G. G.; Gosselin, F.; Hubbard, R. D.; Scanio, M. J.; Sun, R.; Williams, T. J.; Zhang, L., "Toward the Ideal Synthesis. New Transition Metal-Catalyzed Reactions Inspired by Novel Medicinal Leads," *Pure and Applied Chemistry* **2002**, *74*, 25-31. (b) Wender, P. A.; Baryza, J. L.; Brenner, S. E.; Clarke, M. O.; Gamber, G. G.; Horan, J. C.; Jessop, T. C.; Kan, C.; Pattabiraman, K.; Williams, T. J., "Inspirations from Nature. New Reactions, New Therapeutic Leads, and New Drug Delivery Systems,"

The history of multicomponent coupling reactions goes back to the nineteenth century. Although it would be difficult to identify the first example of a multicomponent coupling reaction, the reaction developed by Adolf Strecker in 1850 is considered the first multicomponent reaction.¹³ The reactions of Arthur Hantzsch (1882)¹⁴ and Pietro Biginelli (1891)¹⁵ are also some of the earliest examples for multicomponent processes. Then, it was with the work of Ugi and co-workers¹⁶ that the concept of the multicomponent coupling reaction began to be appreciated as an important tool in synthetic organic chemistry. In addition, the reactions of Passerini¹⁷ and Mannich¹⁸ are also well-known multicomponent reactions.

In the following section of this chapter (Section 2.2), these “classical” multicomponent reactions and their new variants will be surveyed. More “modern-type” multicomponent reactions will not be considered in this chapter; one category of those recent

Pure and Applied Chemistry **2003**, *75*, 143-155. (c) Gaich, T.; Baran, P. S., "Aiming for the Ideal Synthesis," *The Journal of Organic Chemistry* **2010**, *75*, 4657-4673.

¹³ Strecker, A., "Ueber Die Künstliche Bildung Der Milchsäure Und Einen Neuen, Dem Glycocol Homologen Körper," *Justus Liebigs Annalen der Chemie* **1850**, *75*, 27-45.

¹⁴ Hantzsch, A., "Ueber Die Synthese Pyridinartiger Verbindungen Aus Acetessigäther Und Aldehydammoniak," *Justus Liebigs Annalen der Chemie* **1882**, *215*, 1-82.

¹⁵ Biginelli, P., "Ueber Aldehyduramide Des Acetessigäthers," *Berichte der Deutschen Chemischen Gesellschaft* **1891**, *24*, 1317-1319.

¹⁶ Ugi, I., "Versuche Mit Isonitrilen," *Angewandte Chemie International Edition* **1959**, *71*, 386-386.

¹⁷ Passerini, M., "Isonitriles. I. Compound of *p*-Isonitrileazobenzene with Acetone and Acetic Acid," *Gazzetta Chimica Italiana* **1921**, *51*, 126-129.

¹⁸ Mannich, C.; Krösche, W., "Ueber Ein Kondensationsprodukt Aus Formaldehyd, Ammoniak Und Antipyrin," *Archiv der Pharmazie* **1912**, *250*, 647-667.

processes was presented in Chapter 1 (titled as “Catalytic Bimetallative Multicomponent Coupling Reactions”), and another type of the non-classical multicomponent reactions will be described in Chapter 3 (titled as “Nickel-Catalyzed Reductive Coupling Reactions”).

2.2. Background

2.2.1. Strecker Multicomponent Reaction

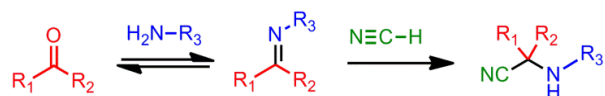
The Strecker reaction, one of the earliest examples of the multicomponent coupling reactions, is a three component reaction of carbonyl compounds, amines, and cyanide sources to furnish α -aminonitriles (Scheme 2.2).¹³ The reaction begins with a formation of imine by condensation of a carbonyl compound and an amine component. Then, the cyanide adds to the intermediate imine to form the product, α -aminonitrile. Both diastereoselective and enantioselective variants of this reaction have been developed.^{19, 20} The Kobayashi group developed the first transition metal-catalyzed enantioselective Strecker reaction in 2000.²¹ Also, the first organocatalytic variant of this reaction was reported by the groups of Pan and List in 2007.²²

¹⁹ For selected examples, see: (a) Stout, D. M.; Black, L. A.; Matier, W. L., "Asymmetric Strecker Synthesis: Isolation of Pure Enantiomers and Mechanistic Implications," *The Journal of Organic Chemistry* **1983**, *48*, 5369-5373. (b) Kunz, H.; Sager, W.; Schanzenbach, D.; Decker, M., "Carbohydrates as Chiral Templates: Stereoselective Strecker Synthesis of D- α -Amino Nitriles and Acids Using O-Pivaloylated D-Galactosylamine as the Auxiliary," *Liebigs Annalen der Chemie* **1991**, *1991*, 649-654. (c) Harwood, L. M.; Drew, M. G. B.; Hughes, D. J.; Vickers, R. J., "Diastereocontrolled Strecker Reaction Using (S)-5-Phenylmorpholin-2-One," *Journal of the Chemical Society, Perkin Transactions 1* **2001**, 1581-1583.

²⁰ (a) Ma, D.; Ding, K., "Synthesis of Enantiopure α,α -Disubstituted Amino Acids from the Asymmetric Strecker Reaction Products of Aldehydes," *Organic Letters* **2000**, *2*, 2515-2517. (b) Ooi, T.; Uematsu, Y.; Maruoka, K., "Asymmetric Strecker Reaction of Aldimines Using Aqueous Potassium Cyanide by Phase-Transfer Catalysis of Chiral Quaternary Ammonium Salts with a Tetranaphthyl Backbone," *Journal of the American Chemical Society* **2006**, *128*, 2548-2549.

²¹ (a) Ishitani, H.; Komiyama, S.; Hasegawa, Y.; Kobayashi, S., "Catalytic Asymmetric Strecker Synthesis. Preparation of Enantiomerically Pure α -Amino Acid Derivatives from Aldimines and Tributyltin

Scheme 2.2 Strecker Multicomponent Reaction



The Jacobsen group developed acyl-Strecker reaction, in which acyl cyanide was substituted for highly toxic HCN (Scheme 2.3).²³ In this asymmetric acyl-Strecker process, the thiourea-catalyzed reaction of aldehydes, amines, and acyl cyanides afforded α -amino nitriles in good yields with great enantioselectivities. The resulting α -amino nitriles were readily transformed to α -amino acids by acidic hydrolysis and hydrogenolysis. Another organocatalytic approach that involves a proline-derived catalyst was developed by the Feng group.²⁴

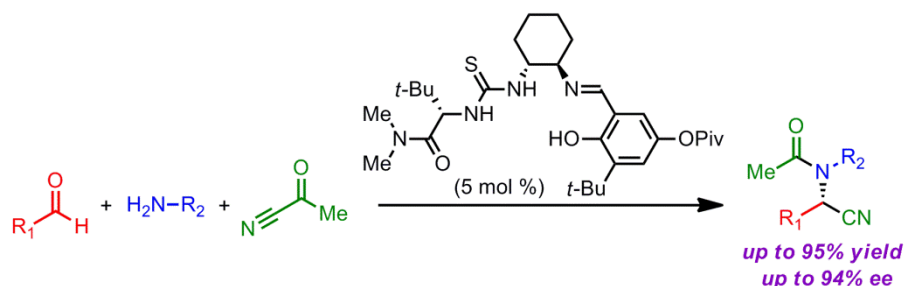
Cyanide or Achiral Aldehydes, Amines, and Hydrogen Cyanide Using a Chiral Zirconium Catalyst," *Journal of the American Chemical Society* **2000**, *122*, 762-766. (b) Kobayashi, S.; Ishitani, H., "Novel Binuclear Chiral Zirconium Catalysts Used in Enantioselective Strecker Reactions," *Chirality* **2000**, *12*, 540-543.

²² Pan, S. C.; List, B., "Catalytic Asymmetric Three-Component Acyl-Strecker Reaction," *Organic Letters* **2007**, *9*, 1149-1151.

²³ Sigman, M. S.; Jacobsen, E. N., "Schiff Base Catalysts for the Asymmetric Strecker Reaction Identified and Optimized from Parallel Synthetic Libraries," *Journal of the American Chemical Society* **1998**, *120*, 4901-4902.

²⁴ Wen, Y.; Gao, B.; Fu, Y.; Dong, S.; Liu, X.; Feng, X., "Asymmetric Three-Component Strecker Reactions Catalyzed by Trans-4-Hydroxy-L-Proline-Derived N,N' -Dioxides," *Chemistry—A European Journal* **2008**, *14*, 6789-6795.

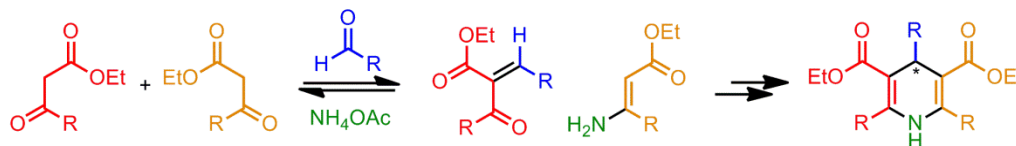
Scheme 2.3 Jacobsen's Asymmetric Acyl-Strecker Reaction



2.2.2. Hantzsch Multicomponent Reaction

In the Hantzsch dihydropyridine (DHP) synthesis, an aldehyde, two β -ketoesters, and an ammonia source are coupled to give dihydropyridines (Scheme 2.4).¹⁴ Due to dihydropyridines' biological activity, the pharmaceutical utility of these compounds will be substantially increased with developments of asymmetric synthesis of DHPs. One of the biggest challenges in the developments of this reaction is the facile epimerization at C4 position. For this reason, the low selectivities were observed for asymmetric Hantzsch reactions when harsh reaction conditions were applied.²⁵

Scheme 2.4 Hantzsch Multicomponent Reaction



²⁵ (a) Ramón, D. J.; Yus, M., "Asymmetric Multicomponent Reactions (AMCRs): The New Frontier," *Angewandte Chemie International Edition* **2005**, *44*, 1602-1634. (b) Evans, C. G.; Gestwicki, J. E., "Enantioselective Organocatalytic Hantzsch Synthesis of Polyhydroquinolines," *Organic Letters* **2009**, *11*, 2957-2959.

Recently, both highly diastereoselective and enantioselective Hantzsch reactions have been developed. The diastereoselective Hantzsch reaction was reported by the Dondoni group in 2009.²⁶ In their reaction, either (*S*)- or (*R*)-proline was used as a catalyst (10 mol %), and the targeted products, DHP C-glucoconjugates, were formed with great diastereoselectivity (> 95% *de*).

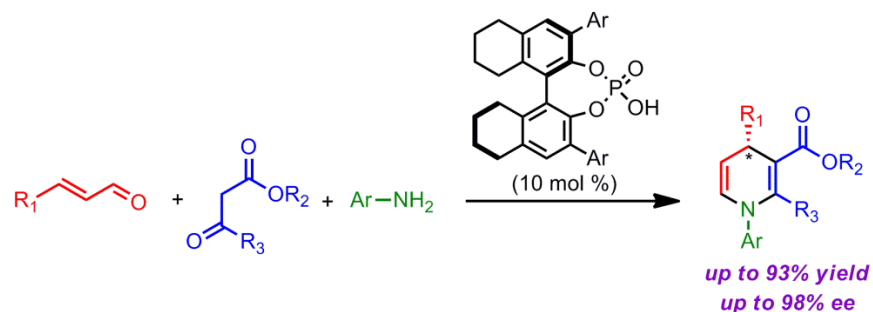
Both Jorgensen²⁷ and Gong²⁸ groups reported asymmetric organocatalytic Hantzsch-type reactions for the construction of dihydropyridines (DHPs). In Jorgensen's asymmetric reactions, the optically-active DHPs were furnished with great enantioselectivity (95% *ee*) in the presence of (*S*) or (*R*)-proline as a catalyst. On the other hand, the Gong group employed a chiral Brønsted acid as a catalyst for the coupling of α,β -unsaturated aldehyde, β -ketoester, and an amine (Scheme 2.5). The desired products, enantioenriched DHPs, were obtained with both high efficiency (up to 93% yield) and great selectivities (98% *ee*).

²⁶ Ducatti, D. R. B.; Massi, A.; Noseda, M. D.; Duarte, M. E. R.; Dondoni, A., "Dihydropyridine C-Glycoconjugates by Organocatalytic Hantzsch Cyclocondensation. Stereoselective Synthesis of α -Threofuranose C-Nucleoside Enantiomers," *Organic & Biomolecular Chemistry* **2009**, *7*, 1980-1986.

²⁷ Franke, P. T.; Johansen, R. L.; Bertelsen, S.; Jørgensen, K. A., "Organocatalytic Enantioselective One-Pot Synthesis and Application of Substituted 1,4-Dihydropyridines—Hantzsch Ester Analogues," *Chemistry – An Asian Journal* **2008**, *3*, 216-224.

²⁸ Jiang, J.; Yu, J.; Sun, X.-X.; Rao, Q.-Q.; Gong, L.-Z., "Organocatalytic Asymmetric Three-Component Cyclization of Cinnamaldehydes and Primary Amines with 1,3-Dicarbonyl Compounds: Straightforward Access to Enantiomerically Enriched Dihydropyridines," *Angewandte Chemie International Edition* **2008**, *47*, 2458-2462. (b) Yu, J.; Shi, F.; Gong, L.-Z., "Brønsted-Acid-Catalyzed Asymmetric Multicomponent Reactions for the Facile Synthesis of Highly Enantioenriched Structurally Diverse Nitrogenous Heterocycles," *Accounts of Chemical Research* **2011**, *44*, 1156-1171.

Scheme 2.5 Gong's Asymmetric Hantzsch Reaction



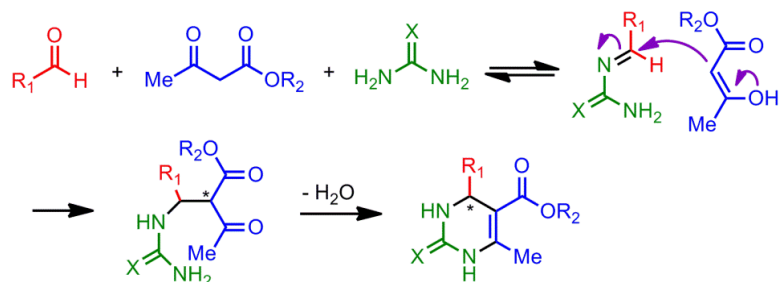
2.2.3. Biginelli Multicomponent Reaction

The Biginelli reaction,¹⁵ which is a three-component process involving aldehyde, (thio)urea, and β -ketoester, affords functionalized dihydropyrimidines (DHPMs) as described in Scheme 2.6. It has been known that a number of compounds containing dihydropyrimidines have biological activities such as antibacterial, antiviral, anti-inflammatory, and anti-tumor properties.²⁹ Consequently, these Biginelli reaction products are considered valuable compounds for the developments of new medicines in pharmaceutical industries.³⁰

²⁹ (a) Atwal, K. S.; Swanson, B. N.; Unger, S. E.; Floyd, D. M.; Moreland, S.; Hedberg, A.; O'Reilly, B. C., "Dihydropyrimidine Calcium Channel Blockers. 3. 3-Carbamoyl-4-Aryl-1,2,3,4-Tetrahydro-6-Methyl-5-Pyrimidinecarboxylic Acid Esters as Orally Effective Antihypertensive Agents," *Journal of Medicinal Chemistry* **1991**, *34*, 806-811. (b) Rovnyak, G. C.; Atwal, K. S.; Hedberg, A.; Kimball, S. D.; Moreland, S.; Gougoutas, J. Z.; O'Reilly, B. C.; Schwartz, J.; Malley, M. F., "Dihydropyrimidine Calcium Channel Blockers. 4. Basic 3-Substituted-4-Aryl-1,4-Dihydropyrimidine-5-Carboxylic Acid Esters. Potent Antihypertensive Agents," *Journal of Medicinal Chemistry* **1992**, *35*, 3254-3263.

³⁰ Maliga, Z.; Kapoor, T. M.; Mitchison, T. J., "Evidence That Monastrol Is an Allosteric Inhibitor of the Mitotic Kinesin Eg5," *Chemistry & Biology* **2002**, *9*, 989-996.

Scheme 2.6 Biginelli Multicomponent Reaction



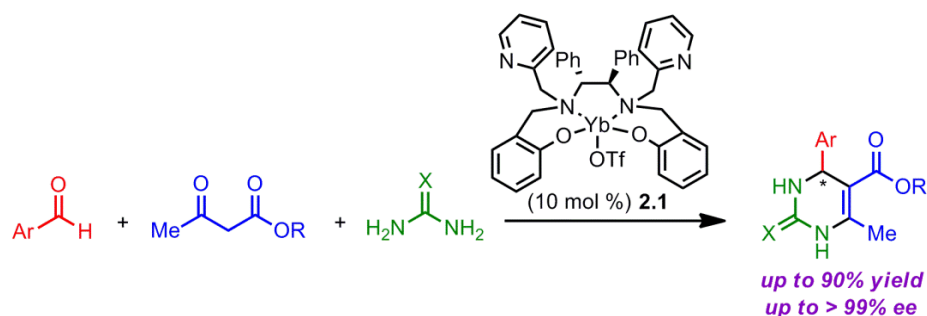
With regard to the mechanism of the Biginelli reaction, it involves imine formation from an aldehyde and a urea; then, the resulting imine undergoes a Mannich-type reaction with an enol of the β -ketoester.³¹ The configuration of the stereogenic center (C4) is crucial for the DHPM's biological properties.³² Hence, developments of highly enantioselective variants of this reaction will be particularly desirable.

The enantioselective Biginelli reactions were first developed by the Zhu group (Scheme 2.7), in which a chiral ytterbium (Yb) Lewis acid (**2.1**) was employed as a catalyst (10 mol %). With this method, a variety of optically-active dihydropyrimidines (DHPMs) were afforded with great yields (up to 90% yield) and enantioselectivities (up to 99% *ee*). Remarkably, the ytterbium catalyst **2.1** was able to be reused without any loss of enantiopurity after it was recovered from controlled pH extraction.

³¹ (a) Kappe, C. O., "Recent Advances in the Biginelli Dihydropyrimidine Synthesis. New Tricks from an Old Dog," *Accounts of Chemical Research* **2000**, *33*, 879-888. (b) Aron, Z. D.; Overman, L. E., "The Tethered Biginelli Condensation in Natural Product Synthesis," *Chemical Communications* **2004**, 253-265.

³² DeBonis, S.; Simorre, J.-P.; Crevel, I.; Lebeau, L.; Skoufias, D. A.; Blangy, A.; Ebel, C.; Gans, P.; Cross, R.; Hackney, D. D.; Wade, R. H.; Kozielski, F., "Interaction of the Mitotic Inhibitor Monastrol with Human Kinesin Eg5," *Biochemistry* **2002**, *42*, 338-349.

Scheme 2.7 Zhu's Asymmetric Biginelli Reaction



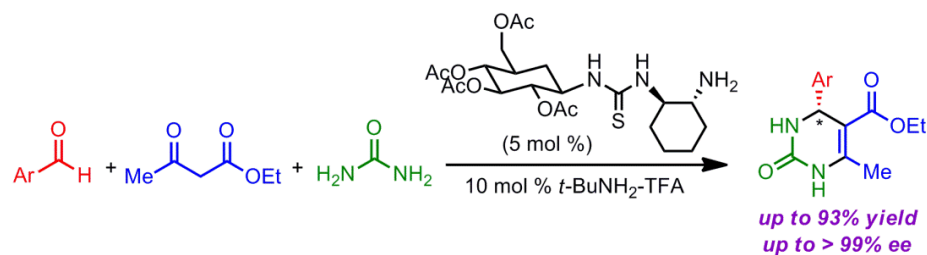
In 2009, the Chen group demonstrated that a chiral amine-thiourea catalyst can promote asymmetric Biginelli reactions (Scheme 2.8).³³ Both the intermediate imine and the carbonyl compound were activated by the amine-thiourea catalyst; the key nucleophilic attack was efficiently catalyzed by this bifunctional catalyst.³⁴ Various aromatic aldehydes can participate in this process to furnish enantio-enriched dihydropyrimidines (DHPMs) with high enantioselectivities (up to > 99% *ee*) and good yields (up to 93% yield). Recently, the same group (Chen and co-workers) reported that this asymmetric Biginelli reaction can be performed in aqueous media.³⁵

³³ Wang, Y.; Yang, H.; Yu, J.; Miao, Z.; Chen, R., "Highly Enantioselective Biginelli Reaction Promoted by Chiral Bifunctional Primary Amine-Thiourea Catalysts: Asymmetric Synthesis of Dihydropyrimidines," *Advanced Synthesis & Catalysis* **2009**, 351, 3057-3062.

³⁴ Li, X.; Deng, H.; Luo, S.; Cheng, J.-P., "Organocatalytic Three-Component Reactions of Pyruvate, Aldehyde and Aniline by Hydrogen-Bonding Catalysts," *European Journal of Organic Chemistry* **2008**, 2008, 4350-4356.

³⁵ Wang, Y.; Yu, J.; Miao, Z.; Chen, R., "Bifunctional Primary Amine-Thiourea-TfOH (BPAT-TfOH) as a Chiral Phase-Transfer Catalyst: The Asymmetric Synthesis of Dihydropyrimidines," *Organic & Biomolecular Chemistry* **2011**, 9, 3050-3054.

Scheme 2.8 Chen's Asymmetric Biginelli Reaction



2.2.4. Passerini Multicomponent Reaction

Passerini reaction¹⁷ is a three-component coupling process of carbonyl compounds, carboxylic acids, and isocyanides to give α -acyloxy carboxamides (Scheme 2.9). This reaction features mild reaction conditions, broad substrate scope, and highly variable inputs; it is suitable for generation of molecular complexity and diversity.³⁶ Despite the extensive studies on the mechanism of this reaction, the exact identity of the reaction intermediates are still under debate.³⁷ The proposed intermediates include hemiacetals,³⁸ *N*-protonated isocyanides,³⁹ zwitterionic adducts,¹⁷ and hydrogen-bonded adducts.⁴⁰

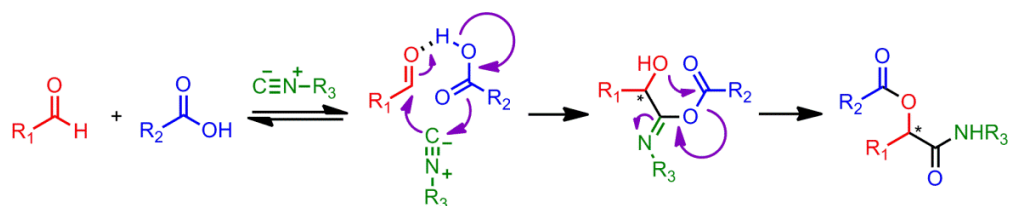
³⁶ Yue, T.; Wang, M.-X.; Wang, D.-X.; Masson, G.; Zhu, J., "Brønsted Acid Catalyzed Enantioselective Three-Component Reaction Involving the α Addition of Isocyanides to Imines," *Angewandte Chemie International Edition* **2009**, *48*, 6717-6721.

³⁷ Yue, T.; Wang, M.-X.; Wang, D.-X.; Zhu, J., "Asymmetric Synthesis of 5-(1-Hydroxyalkyl)Tetraoles by Catalytic Enantioselective Passerini-Type Reactions," *Angewandte Chemie International Edition* **2008**, *47*, 9454-9457.

³⁸ (a) Hagedorn, I.; Eholzer, U., "Isonitrile, VII. Einstufige Synthese Von α -Hydroxysäure-Amiden Durch Abwandlung Der Passerini-Reaktion," *Chemische Berichte* **1965**, *98*, 936-940. (b) Hagedorn, I.; Eholzer, U.; Winkelmann, H. D., "Beitrag Zur Isonitril-Chemie," *Angewandte Chemie* **1964**, *76*, 583-584.

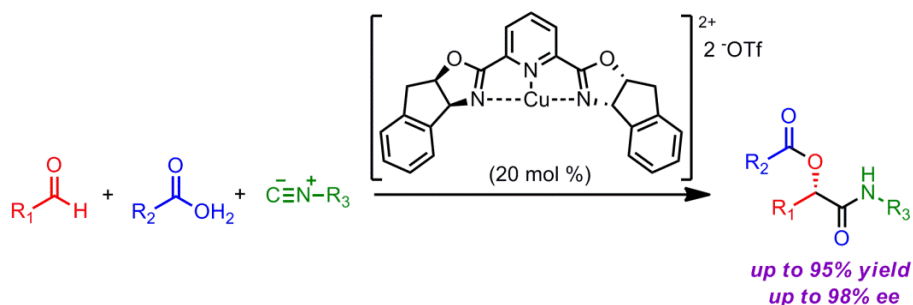
³⁹ Ugi, I., "The α -Addition of Immonium Ions and Anions to Isonitriles Accompanied by Secondary Reactions," *Angewandte Chemie International Edition* **1962**, *1*, 8-21.

Scheme 2.9 Passerini Multicomponent Reaction



An enantioselective variant of this reaction was developed by Schreiber and co-workers (Scheme 2.10).⁴¹ For this reaction, a chiral Cu(II)-PyBOX complex was employed as a catalyst. In the presence of the Lewis acidic catalyst, aldehyde, benzoic acid, and isocyanide were coupled to afford the Passerini adduct with excellent yields (up to 95% yield) and great enantioselectivities (up to 98% *ee*). In this report, the synthetic utility of this method was also presented; successive Passerini/intramolecular Diels–Alder reactions afforded tricyclic lactone skeletons with a proper choice of starting materials.

Scheme 2.10 Schreiber's Asymmetric Passerini Reaction

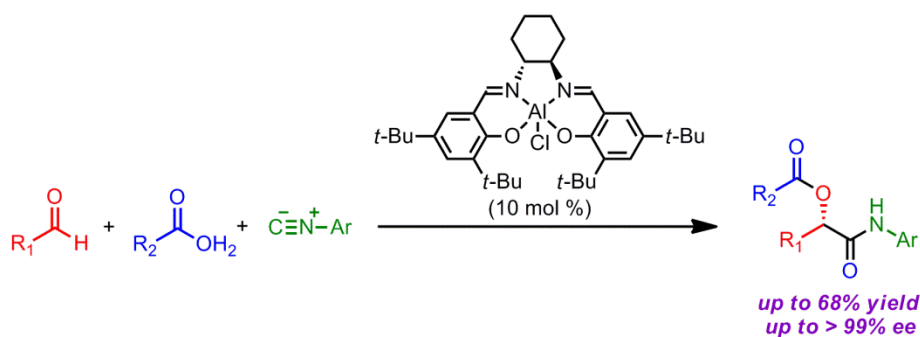


⁴⁰ Baker, R. H.; Stanonis, D., "The Passerini Reaction. III. Stereochemistry and Mechanism" *Journal of the American Chemical Society* **1951**, *73*, 699-702.

⁴¹ Andreana, P. R.; Liu, C. C.; Schreiber, S. L., "Stereochemical Control of the Passerini Reaction," *Organic Letters* **2004**, *6*, 4231-4233.

More recently, the Zhu group demonstrated that more readily available Al-salen complex can catalyze this process (Scheme 2.11).⁴² In this system, the uncatalyzed background reaction was suppressed by lowering the temperature (-60 °C). Under optimized reaction conditions, the desired products, α -acyloxy carboxamides, were obtained with great enantioselectivity (up to > 99% *ee*) and good yields (up to 68% yield).

Scheme 2.11 Zhu's Asymmetric Passerini Reaction



2.2.5. Ugi Multicomponent Reaction

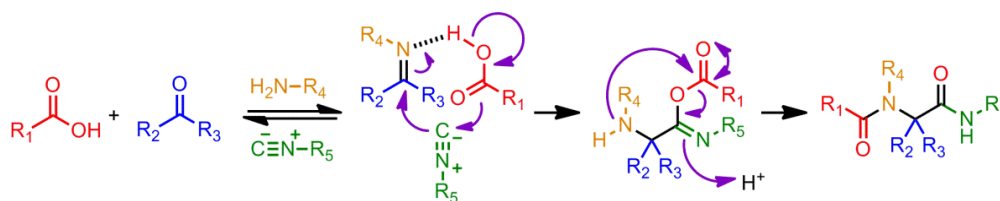
In addition to the Passerini reaction, the Ugi reaction¹⁶ is another multicomponent reaction that employs isocyanide reagents as a one of the coupling components (Scheme 2.12).⁴³ The Ugi process is one of the most frequently utilized multicomponent reactions; it has been widely acknowledged as a powerful synthetic tool in medicinal chemistry. The Ugi four-component reaction allows the synthesis of α -amino acid derivatives by a condensation

⁴² Wang, S.-X.; Wang, M.-X.; Wang, D.-X.; Zhu, J., "Catalytic Enantioselective Passerini Three-Component Reaction," *Angewandte Chemie International Edition* **2008**, *47*, 388-391.

⁴³ Dömling, A.; Ugi, I., "Multicomponent Reactions with Isocyanides," *Angewandte Chemie International Edition* **2000**, *39*, 3168-321.

of carbonyl compounds (usually aldehydes), amines, carboxylic acids (or an alcohol), and isocyanides. The generally-accepted mechanism suggests that the process begins with formation of imine from the carbonyl compound and the amine, and then the isocyanide is reacted with this imine as well as the carboxylic acid. Finally, the intra intramolecular acyl transfer from oxygen to nitrogen (known as the Mumm rearrangement)⁴⁴ affords substituted α -amino acid derivatives.

Scheme 2.12 Ugi Multicomponent Reaction



Due to the high diversity that comes from the Ugi process, a significant amount of effort has been made to study and develop this process; it has been investigated more than any other multicomponent reaction.⁴⁵ A number of diastereoselective Ugi reactions have been reported. Among them, the reactions with chiral amines (as a coupling component) give the most promising results;⁴⁶ the Dyker group showed that the diastereoselective Ugi

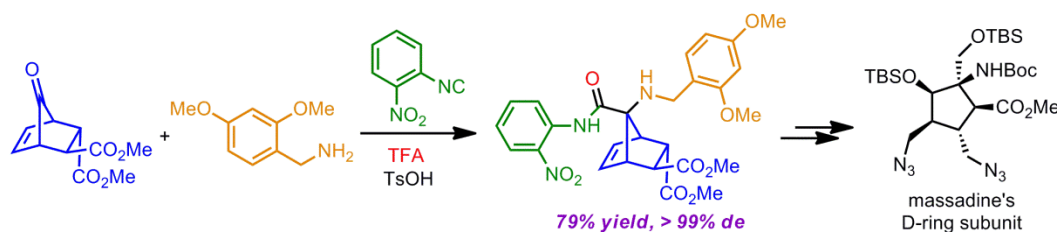
⁴⁴ Mumm, O., "Umsetzung Von Säureimidchloriden Mit Salzen Organischer Säuren Und Mit Cyankalium," *Berichte der Deutschen Chemischen Gesellschaft* **1910**, 43, 886-893.

⁴⁵ Orru, R. V. A.; de Greef, M., "Recent Advances in Solution-Phase Multicomponent Methodology for the Synthesis of Heterocyclic Compounds," *Synthesis* **2003**, 2003, 1471-1499.

⁴⁶ (a) Ugi, I.; Demharter, A.; Hörl, W.; Schmid, T., "Ugi Reactions with Trifunctional α -Amino Acids, Aldehydes, Isocyanides and Alcohols," *Tetrahedron* **1996**, 52, 11657-11664. (b) Ugi, I.; Horl, W.; Hanusch-Kompa, C.; Schmid, T.; Herdtweck, E., "MCR 6: Chiral 2,6-Piperazinediones via Ugi Reactions with Alpha-Amino Acids, Carbonyl Compounds, Isocyanides and Alcohols," *Heterocycles* **1998**, 47, 965-975.

reaction can be applied to synthesize optically pure isoindoles and dihydroisoquinolines.⁴⁷ More recently, the Carreira group successfully demonstrated that the diastereoselective Ugi reaction can construct the core fragment of a natural product, massadine, with the use of an enantio-enriched norbornene as a chiral auxiliary (Scheme 2.13).⁴⁸

Scheme 2.13 Carreira's Ugi Reaction



On the other hand, enantioselective variants of the four-component Ugi reaction have never been reported. Instead, several asymmetric “Ugi-type” reactions, in which three coupling components are combined, have been demonstrated. One of the enantioselective three-component Ugi reactions was reported by Zhu and co-workers as shown in Scheme 2.14.⁴⁹ In this method, an α -isocyanoacetamide replaces the carboxylic acid component, and it also possesses the isocyanide moiety. In the presence of a chiral phosphoric acid as a

(c) Linderman, R. J.; Binet, S.; Petrich, S. R., "Enhanced Diastereoselectivity in the Asymmetric Ugi Reaction Using a New "Convertible" Isonitrile," *The Journal of Organic Chemistry* **1998**, *64*, 336-337.

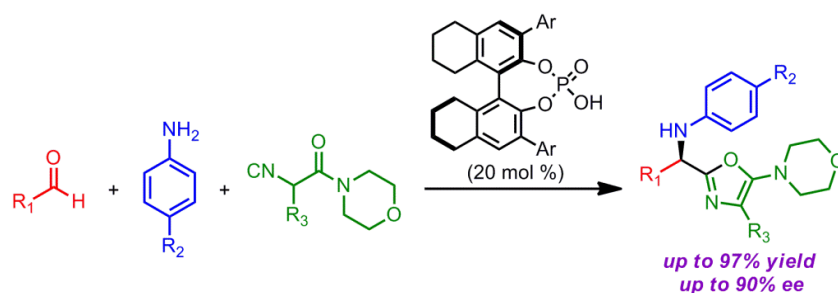
⁴⁷ Kadzimirsz, D.; Hildebrandt, D.; Merz, K.; Dyker, G., "Isoindoles and Dihydroisoquinolines by Gold-Catalyzed Intramolecular Hydroamination of Alkynes," *Chemical Communications* **2006**, 661-662.

⁴⁸ Chinigo, G. M.; Breder, A.; Carreira, E. M., "Ugi-4-Component Reaction Enabling Rapid Access to the Core Fragment of Massadine," *Organic Letters* **2010**, *13*, 78-81.

⁴⁹ Yue, T.; Wang, M.-X.; Wang, D.-X.; Masson, G.; Zhu, J., "Brønsted Acid Catalyzed Enantioselective Three-Component Reaction Involving the A Addition of Isocyanides to Imines," *Angewandte Chemie International Edition* **2009**, *48*, 6717-6721.

catalyst, the targeted products, enantio-enriched aminooxazoles, were furnished with high selectivities (up to 90% *ee*) and great yields (up to 97% yield).

Scheme 2.14 Zhu's Asymmetric Three-Component Ugi Reaction



2.2.6. Mannich Multicomponent Reaction

The Mannich reaction¹⁸ is a three-component coupling process involving ammonia, a non-enolizable aldehyde, and an enolizable carbonyl compound, which leads to β -amino-carbonyl compounds (Scheme 2.15). These products from the Mannich reaction, β -amino carbonyls, are known to be useful synthetic building blocks for pharmaceutical compounds and natural products.⁵⁰ Furthermore, optically pure β -amino carbonyl compounds have shown great potential as a ligand for enantioselective catalysis.⁵¹ A number of groups

⁵⁰ Trost, B. M.; Fleming, I.; Schreiber, S. L.; Heathcock, C. H.; Pattenden, G.; Semmelhack, M. F.; Paquette, L. A.; Winterfeldt, E.; Ley, S. V. *Comprehensive Organic Synthesis: Selectivity, Strategy and Efficiency in Modern Organic Synthesis*; Pergamon: Oxford, 1991.

⁵¹ (a) Li, X.; Yeung, C.-h.; Chan, A. S. C.; Yang, T.-K., "New 1,3-Amino Alcohols Derived from Ketopinic Acid and Their Application in Catalytic Enantioselective Reduction of Prochiral Ketones," *Tetrahedron: Asymmetry* **1999**, *10*, 759-763. (b) Kochi, T.; Tang, T. P.; Ellman, J. A., "Development and Application of a New General Method for the Asymmetric Synthesis of *syn*- and *anti*-1, 3-Amino Alcohols," *Journal of the American Chemical Society* **2003**, *125*, 11276-11282. (c) Escorihuela, J.; Burguete, M. I.; Luis, S. V., "New Advances in Dual Stereocontrol for Asymmetric Reactions," *Chemical Society Reviews* **2013**, *42*, 5595-5617.

reported their efforts toward the development of both diastereoselective and enantioselective variants of the Mannich reaction. One of their goals is to invent novel glycopeptide-based medicines for the treatment of cancer, bacterial infections, and inflammatory processes.⁵²

Scheme 2.15 Mannich Multicomponent Reaction



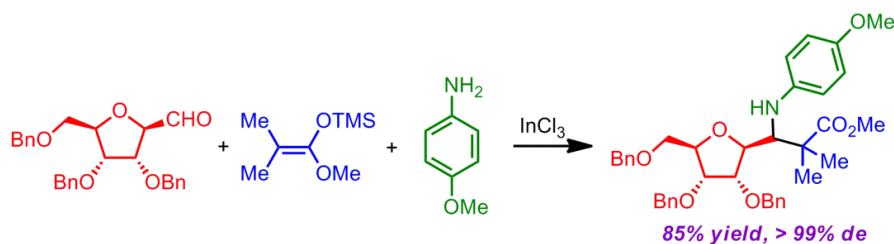
The diastereoselective Mannich reactions were developed with various optically active starting materials. The Dondoni group employed a range of chiral C-glycosyl aldehydes as a coupling component in the diastereoselective Mannich reactions (Scheme 2.16).⁵³ In this reaction, InCl_3 promoted coupling reactions of the chiral aldehydes, *p*-methoxybenzylamines, and ketene silyl acetals to furnish optically pure C-glycosyl α,α -dimethyl β -amino esters with great diastereoselectivities and excellent yields. On the other hand, the Yang group utilized chiral amines as one of the coupling components for the

⁵² (a) Danker, K.; Fischer, A.; Reutter, W. In *Carbohydrate-Based Drug Discovery*; Wiley-VCH Verlag GmbH & Co. KGaA, 2005. (b) Islam, T.; Linhardt, R. J. In *Carbohydrate-Based Drug Discovery*; Wiley-VCH Verlag GmbH & Co. KGaA, 2005.

⁵³ Dondoni, A.; Massi, A., "Design and Synthesis of New Classes of Heterocyclic C-Glycoconjugates and Carbon-Linked Sugar and Heterocyclic Amino Acids by Asymmetric Multicomponent Reactions (AMCRs)," *Accounts of Chemical Research* **2006**, 39, 451-463.

Mannich reaction.⁵⁴ In their study, various aldehydes and silyl ketene acetals were coupled with optically active amines to furnish 6-alkylated piperidinone and 2-piperidines in an enantio-enriched form.

Scheme 2.16 Dondori's Mannich Reaction



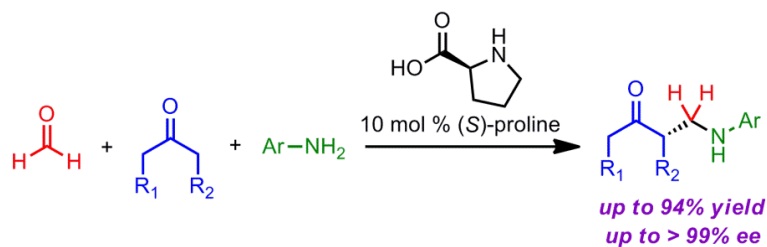
The enantioselective variant of Mannich reaction was reported by Córdova and co-workers (Scheme 2.17).⁵⁵ They demonstrated that (*S*)- or (*R*)-proline can catalyze enantioselective Mannich reaction of formaldehyde, various ketones, and aryl amines to afford α -aminomethylated ketones with great enantiomeric excess (up to 99% *ee*) and good yields (up to 94% yield). In addition, the Gong group utilized a chiral phosphoric acid to catalyze the asymmetric Mannich reaction to provide β -amino carbonyl compounds with excellent stereoselectivities (up to 98% *ee* and 96% *de*) and yields (up to > 99%).⁵⁶

⁵⁴ Yang, Y.; Phillips, D. P.; Pan, S., "A Stereoselective Approach to 6-Alkylated Piperidinone & 2-Piperidine via Three-Component Vinylogous Mannich Reactions (VMR) and a Concise Synthesis of (*S*)-Anabasine," *Tetrahedron Letters* **2011**, 52, 1549-1552.

⁵⁵ Ibrahim, I.; Casas, J.; Córdova, A., "Direct Catalytic Enantioselective α -Aminomethylation of Ketones," *Angewandte Chemie International Edition* **2004**, 43, 6528-6531.

⁵⁶ Guo, Q.-X.; Liu, H.; Guo, C.; Luo, S.-W.; Gu, Y.; Gong, L.-Z., "Chiral Brønsted Acid-Catalyzed Direct Asymmetric Mannich Reaction," *Journal of the American Chemical Society* **2007**, 129, 3790-3791.

Scheme 2.17 Córdoba's Asymmetric Mannich Reaction



2.2.7. Summary

Classical multicomponent coupling reactions (*i.e.* Strecker, Hantzsch, Biginelli, Passerini, Ugi, and Mannich reactions) and their modern developments have been described in this section. Despite its long history (over 100 years), major progress in the multicomponent coupling process regarding efficient stereoselective synthesis has been accomplished in recent years. Considering the usefulness and advantages of this process for pharmaceutical industries and medicinal chemistry, continuous improvements and developments of these reactions with novel techniques are unquestionably expected. In particular, with use of the newest knowledge about transition-metal catalysts or organocatalysts, the developments of such enantioselective processes will be greatly facilitated.

2.3. Method Development

2.3.1. Ni-Catalyzed Borylative Diene–Aldehyde Coupling⁵⁷

2.3.1.1. Project Goals

Diboration reactions with various π components have been extensively explored in our laboratory.^{58,59} Diboration of unsaturated systems has attracted a lot of attention since it can functionalize prochiral hydrocarbon substrates giving functionally- and stereochemically-enriched products. More specifically, diboration reactions of alkenes,⁶⁰

⁵⁷ Portions of this project described here have been published: Cho, H. Y.; Morken, J. P., "Diastereoselective Construction of Functionalized Homoallylic Alcohols by Ni-Catalyzed Diboron-Promoted Coupling of Dienes and Aldehydes," *Journal of the American Chemical Society* **2008**, *130*, 16140-16141.

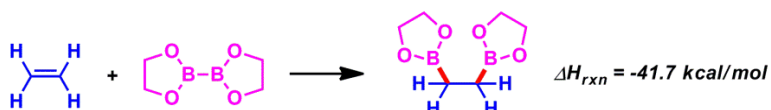
⁵⁸ For selected initial investigations, see: (a) Morgan, J. B.; Miller, S. P.; Morken, J. P., "Rhodium-Catalyzed Enantioselective Diboration of Simple Alkenes," *Journal of the American Chemical Society* **2003**, *125*, 8702-8703. (b) Miller, S. P.; Morgan, J. B.; Felix J. Nepveux V, A.; Morken, J. P., "Catalytic Asymmetric Carbohydroxylation of Alkenes by a Tandem Diboration/Suzuki Cross-Coupling/Oxidation Reaction," *Organic Letters* **2004**, *6*, 131-133.

⁵⁹ (a) Ballard, C. E.; Morken, J. P., "Platinum-Catalyzed Tandem Diboration/Intramolecular Allylboration: Diastereoselective Access to Cyclohexanes Bearing 1,3-Diols," *Synthesis* **2004**, *2004*, 1321-1324. (b) Pelz, N. F.; Woodward, A. R.; Burks, H. E.; Sieber, J. D.; Morken, J. P., "Palladium-Catalyzed Enantioselective Diboration of Prochiral Allenes," *Journal of the American Chemical Society* **2004**, *126*, 16328-16329.

⁶⁰ (a) Baker, R. T.; Nguyen, P.; Marder, T. B.; Westcott, S. A., "Transition Metal Catalyzed Diboration of Vinylarenes," *Angewandte Chemie International Edition* **1995**, *34*, 1336-1338. (b) Iverson, C. N.; Smith, M. R., "Efficient Olefin Diboration by a Base-Free Platinum Catalyst," *Organometallics* **1997**, *16*, 2757-2759.

dienes,⁶¹ allenes,⁶² and enones⁶³ provide versatile intermediates that can participate in stereoselective reaction sequences. According to the results from DFT calculations,⁶⁴ diboration of one π component is calculated to be exothermic by 41.7 kcal/mol (Scheme 2.18).

Scheme 2.18 Diboration of One π Component



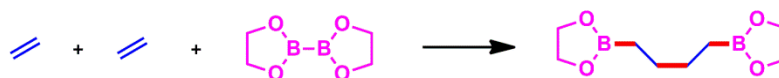
As a useful extension of this methodology, we were interested in developing diboration reactions involving two π components (*i.e.* multicomponent coupling reactions), instead of one π component. As described in Scheme 2.19, when two π components are coupled with a diboron reagent, the process will furnish highly functionalized reaction products with concomitant construction of a new carbon–carbon bond.

⁶¹ (a) Ishiyama, T.; Yamamoto, M.; Miyaura, N., "Diboration of Alkenes with Bis(Pinacolato) Diboron Catalysed by A platinum(0) Complex," *Chemical Communications* **1997**, 689-690. (b) Morgan, J. B.; Morken, J. P., "Platinum-Catalyzed Tandem Diboration/Asymmetric Allylboration: Access to Nonracemic Functionalized 1,3-Diols," *Organic Letters* **2003**, 5, 2573-2575.

⁶² (a) Ishiyama, T.; Kitano, T.; Miyaura, N., "Platinum(0)-Catalyzed Diboration of Allenes with Bis(Pinacolato)Diboron," *Tetrahedron Letters* **1998**, 39, 2357-2360. (b) Yang, F.-Y.; Cheng, C.-H., "Unusual Diboration of Allenes Catalyzed by Palladium Complexes and Organic Iodides: A New Efficient Route to Biboronic Compounds," *Journal of the American Chemical Society* **2001**, 123, 761-762.

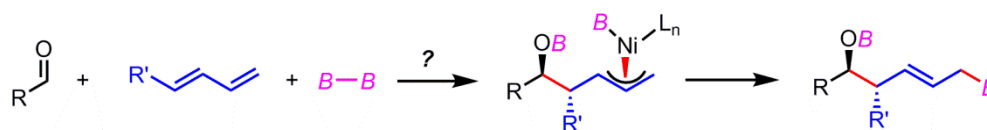
⁶³ (a) G. Lawson, Y.; J. Gerald Lesley, M.; C. Norman, N.; R. Rice, C.; B. Marder, T., "Platinum Catalysed 1,4-Diboration of α,β -Unsaturated Ketones," *Chemical Communications* **1997**, 2051-2052. (b) Takahashi, K.; Ishiyama, T.; Miyaura, N., "Addition and Coupling Reactions of Bis(Pinacolato)Diboron Mediated by CuCl in the Presence of Potassium Acetate," *Chemistry Letters* **2000**, 29, 982-983.

⁶⁴ (a) Cui, Q.; Musaev, D. G.; Morokuma, K., "Molecular Orbital Study of the Mechanism of Platinum(0)-Catalyzed Alkene and Alkyne Diboration Reactions," *Organometallics* **1997**, 16, 1355-1364. (b) Sakaki, S.; Kikuno, T., "Reaction of BX_2-BX_2 ($X = H$ or OH) with $M(Ph_3)_2$ ($M = Pd$ or Pt). A Theoretical Study of the Characteristic Features," *Inorganic Chemistry* **1997**, 36, 226-229.

Scheme 2.19 Diboration of Two π Components

Considering the oxophilic nature of boron, we thought that a reasonable starting point for this study would be coupling reactions of aldehydes, dienes, and diboron reagents. According to the speculated reaction pathway (Scheme 2.20), these processes would afford products that contain multiple stereocenters as well as an allylboronate moiety, which is a synthetically versatile functional group.

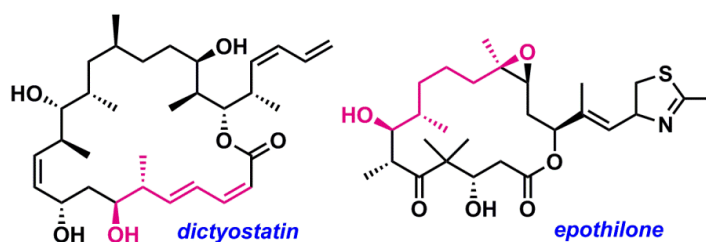
Scheme 2.20 Expected Products from Borylative Aldehyde–Diene Coupling



The resulting allylic alcohols, which are obtained after oxidative workup, can be found as key motifs in various natural products and biologically relevant molecules. Some of those examples are illustrated in Figure 2.1. In particular, microtubule stabilizers are known as highly effective drugs for the treatment of many types of cancers including breast, ovarian, and lung cancers as well as head and neck tumors.⁶⁵

⁶⁵ Risinger, A. L.; Mooberry, S. L., "Taccalonolides: Novel Microtubule Stabilizers with Clinical Potential," *Cancer Letters* **2010**, 291, 14-19.

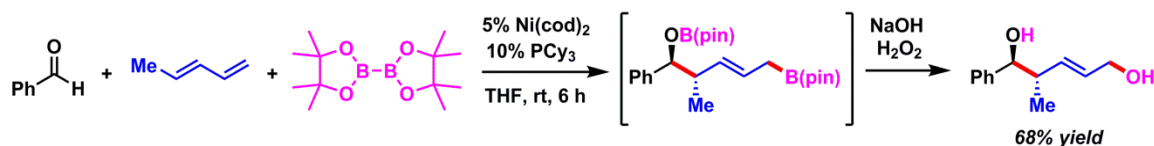
Figure 2.1 Synthetic Target Molecules – Microtubule Stabilizers



2.3.1.2. Reaction Optimization

Initial experiments involved the nickel-catalyzed, room temperature reaction of bis(pinacolato)diboron, *trans*-1,3-pentadiene and benzaldehyde (Scheme 2.21). To our great pleasure, it was observed that this process furnished a compound possessing two stereocenters, a *trans* alkene moiety, and allylic/homoallylic alcohol functionalities as a major reaction product.

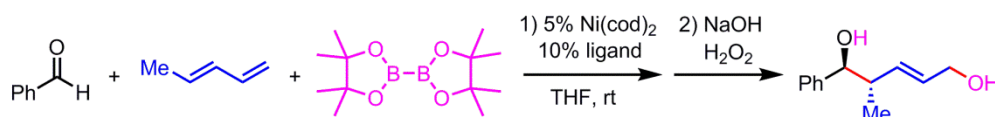
Scheme 2.21 Initial Investigation on Borylative Aldehyde–Diene Coupling



Immediately after the initial observation, extensive optimization reactions were conducted. As shown in Table 2.1, various phosphine ligands were surveyed for this coupling reaction. When no ligand was added to the coupling reaction, poor yield and selectivity were observed (entry 1). The reaction with P(t-Bu)₃ gave the highest yield, but the diastereoselectivity was not high (entry 2). When PCy₃ was employed as a ligand, the

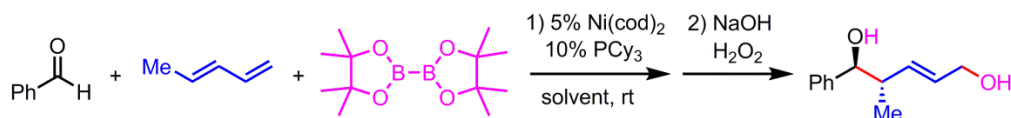
product was formed with good efficiency and selectivity (entry 3). We also examined $P(NMe_2)_3$, PPh_3 , and $PMePh_2$ for this process, but the reactions with these ligands exhibited either poor selectivity or low efficiency (entries 4–6).

Table 2.1 Screen of Ligands for Borylative Aldehyde–Diene Coupling



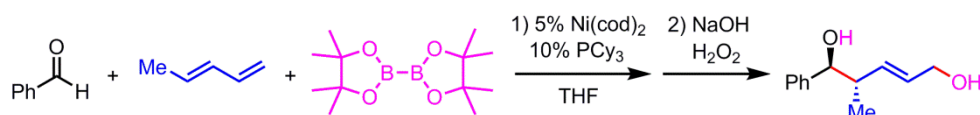
entry	ligand	yield (%)	dr
1	none	39%	1:1
2	$P(t-Bu)_3$	71%	6:1
3	PCy_3	67%	> 20:1
4	$P(NMe_2)_3$	16%	> 20:1
5	PPh_3	63%	5:1
6	$PMePh_2$	31%	4:1

The results from solvent screening experiments suggested that tetrahydrofuran (THF) is the most effective medium for this system (Table 2.2, entry 1). The reactions in toluene or ethyl acetate also afforded the desired product with reasonable efficiency, but they were not better than THF (entries 2–3). In addition, mixed solvent systems (THF/DMF or THF/acetonitrile) were not suitable for this process (entries 4–5).

Table 2.2 Survey of Solvents for Borylative Aldehyde–Diene Coupling

entry	solvent	yield (%)	dr
1	THF	66%	> 20:1
2	toluene	48%	> 20:1
3	EtOAc	45%	10:1
4	THF:DMF (1:1)	< 10%	nd
5	THF:CH ₃ CN (1:1)	< 10%	nd

Furthermore, temperature of the reaction was also crucial for high selectivity and efficiency of the process (Table 2.3). While the reaction at 0 °C was not productive (entry 1), the reaction proceeded well at ambient temperature with high selectivity (entry 2). At 60 °C, we observed some loss of selectivity and generation of more byproducts (entry 3).

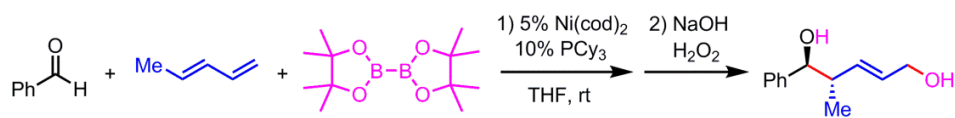
Table 2.3 Effect of Temperature on Borylative Aldehyde–Diene Coupling

entry	temperature	yield (%)	dr
1	0 °C	< 10%	nd
2	rt	66%	> 20:1
3	60 °C	53%	8:1

The effects of reaction concentrations on product efficiency/selectivity were also examined (Table 2.4). When the concentration of the reaction mixture was 0.05 M, the multicomponent reaction did not proceed (entry 1). The optimal concentration of the

reaction turned out to be 0.2 M, which resulted in the best yield and selectivity of the process (entry 2). At a higher concentration (0.5 M), the desired product was formed in a lower yield due to the formation of a significant amount of byproducts (entry 3).

Table 2.4 Influence of Concentration on Borylative Aldehyde–Diene Coupling



entry	concentration	yield (%)	dr
1	0.05 M	< 10%	nd
2	0.2 M	66%	> 20:1
3	0.5 M	23%	nd

After extensive optimization of these reaction parameters (ligand, solvent, temperature, and concentration), the optimal set of reaction conditions was found to include PCy₃ as the ligand, THF as the solvent, at room temperature and a substrate concentration of 0.2 M.

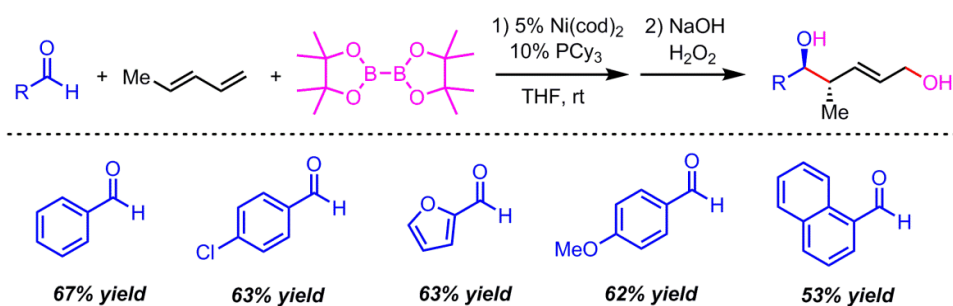
2.3.1.3. Substrate Scope

2.3.1.3.1. Survey of Carbonyl Compounds

Under the optimized reaction conditions, a number of different substrates (both carbonyl compounds and unsaturated hydrocarbons) were explored for this system. The survey started with diverse aromatic aldehydes, as described in Scheme 2.22. The aromatic

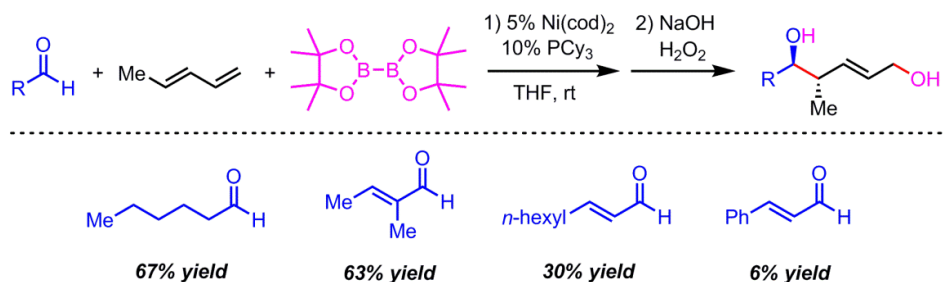
aldehydes possessing various electronic/steric components were good substrates for the system giving the desired products in good yields (53–67%).

Scheme 2.22 Survey of Aromatic Aldehydes for Borylative Coupling Reactions



Furthermore, we observed that some aliphatic aldehydes also participate in this process giving synthetically more useful reaction products (Scheme 2.23). A reaction with hexanal furnished the desired product with good efficiency (67% yield). Some α,β -unsaturated aldehydes also engaged this process with reasonable productivity; however, the reaction involving *trans*-cinnamaldehyde gave the corresponding product in only 6% yield.

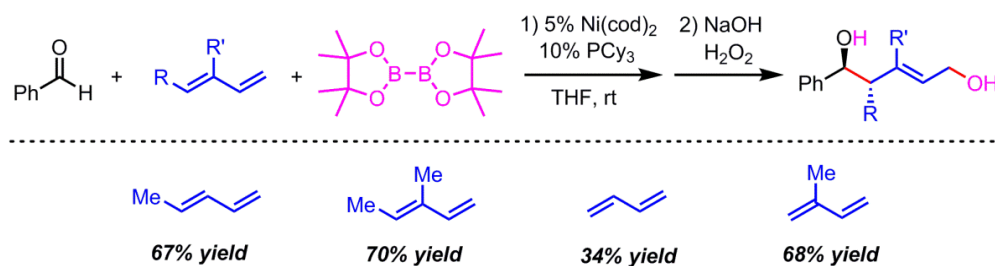
Scheme 2.23 Survey of Aliphatic Aldehydes for Borylative Coupling Reactions



2.3.1.3.2. Survey of Unsaturated Hydrocarbons

Different kinds of unsaturated hydrocarbon substrates were examined for this process. The reactions with various dienes turned out to be an effective tool to prepare the corresponding allylic alcohols (Scheme 2.24). The pentadienes, *trans*-piperylene and 3-methylpentadiene, afforded the corresponding products in good yields (67% and 70% yield, respectively) when they were reacted with benzaldehyde and diboron reagent. While butadiene has a moderate reactivity toward the coupling reaction (34% yield), isoprene functioned as an effective coupling partner in the process to give trisubstituted alkene in 68% yield.

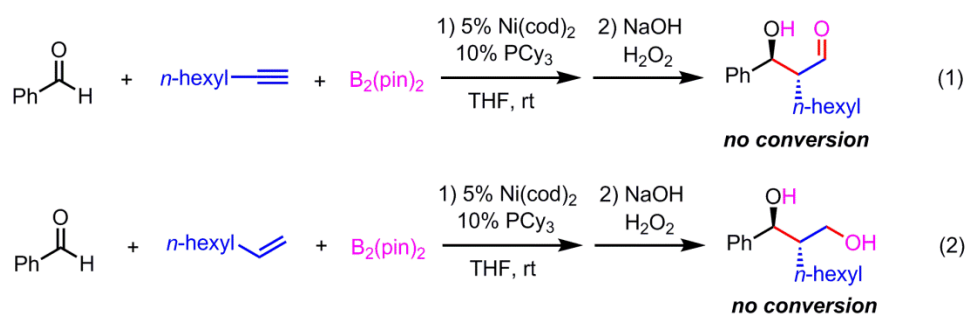
Scheme 2.24 Survey of Dienes for Borylative Coupling Reactions



After the encouraging results with the dienes, we were also curious if other types of unsaturated hydrocarbons would participate in this process. However, when 1-octyne or 1-octene was employed as a coupling partner in this process, the reactions did not produce any

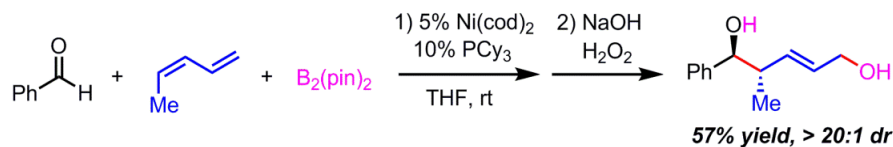
desired products (Scheme 2.25). It is likely due to the lower reactivity of alkynes or alkenes, compare to that of dienes, toward formation of a metallocyclic intermediate.⁶⁶

Scheme 2.25 Survey of Alkynes and Alkenes for Borylative Coupling Reactions



Having known that *trans*-piperylene is efficiently transformed into the desired product in the coupling reaction with benzaldehyde in a stereoselective fashion (see Scheme 2.24), we wanted to examine the effect of the change in the configuration of the starting material on both reactivity and stereoselectivity. Surprisingly, when *cis*-piperylene was employed in this process, the product possessed the same configuration as that of the product from *trans*-piperylene (Scheme 2.26).

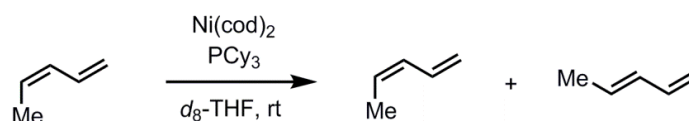
Scheme 2.26 Borylative Aldehyde–*cis*-Piperylene Coupling



⁶⁶ For more details, see the mechanistic investigations in Section 2.4.

One possible explanation for this result is that isomerization of the starting material (from *cis*- to *trans*-diene) occurs during the course of the reaction, and the *trans*-diene would be more rapidly incorporated into the product. To examine this hypothesis, NMR experiments were conducted (Scheme 2.27). When *cis*-pentadiene was treated with the nickel catalyst in the absence of benzaldehyde and $B_2(\text{pin})_2$, it was observed that a portion of the *cis*-piperylene was isomerized to *trans*-piperylene. A plausible mechanism for this isomerization would be the well-established π - σ - π process involving the nickel- π -allyl intermediate.⁶⁷

Scheme 2.27 NMR Experiments for Diene Isomerization



2.3.1.3.3. Summary of Substrate Scope

As presented so far, a number of aldehydes and dienes participate in this stereoselective diboron-promoted diene-aldehyde coupling. Under the optimized reaction conditions, benzaldehyde, *trans*-1,3-pentadiene and $B_2(\text{pin})_2$ were effectively coupled and, after oxidative work-up (NaOH , H_2O_2), the allylic alcohol product was obtained in good yield and stereoselectivity (Table 2.5, entry 1). In general, aromatic aldehydes tend to be effective substrates with $B_2(\text{pin})_2$ and *trans*-piperylene (entries 1-5). All the products from

⁶⁷ Consiglio, G.; Waymouth, R. M., "Enantioselective Homogeneous Catalysis Involving Transition-Metal-Allyl Intermediates," *Chemical Reviews* **1989**, 89, 257-276.

these aromatic aldehydes exhibited good efficiency (53–67% yield) as well as high selectivity (> 20:1 dr).

Table 2.5 Ni-Catalyzed Borylative Aldehyde–Piperylene Coupling

entry	aldehyde	diene	product	yield	dr
1				67%	> 20:1
2				63%	> 20:1
3				63%	> 20:1
4				62%	> 20:1
5				53%	> 20:1

With the more sterically-hindered 3-methylpenta-1,3-diene, versatile trisubstituted alkenes were furnished (Table 2.6, entries 1 and 2). Within the limits of detection of NMR spectra, these products were obtained as single stereoisomers with respect to the stereocenters and the alkene. With butadiene, reaction yields suffered, even with further optimization of reaction conditions (entry 3). In contrast to butadiene, isoprene reacted with comparable efficiency as compared to 1,3-pentadiene and furnished a single alkene

stereoisomer as determined by ^1H NMR analysis of the oxidation product (entry 4). With this substrate, the use of $\text{P}(\text{OEt})_3$ as the ligand was critical - with PCy_3 , a significant amount of a double allylation product, incorporating two equivalents of the aldehyde, was obtained.

Table 2.6 Ni-Catalyzed Borylative Aldehyde–Diene Coupling

entry	aldehyde	diene	product	yield	dr
1				70%	> 20:1
2				65%	> 20:1
3				34%	NA
4				68%	NA

The results in Table 2.7 demonstrate that the reaction is not necessarily limited to aromatic aldehydes; both saturated and α,β -unsaturated aldehydes participate in the reaction, although yields were diminished with these substrates (Table 2.7, entries 1 and 2). The lower reactivity of these substrates is likely due to the lower electrophilicity of aliphatic aldehydes, compared to that of aromatic aldehydes.

Table 2.7 Ni-Catalyzed Borylative Coupling with Aliphatic Aldehydes

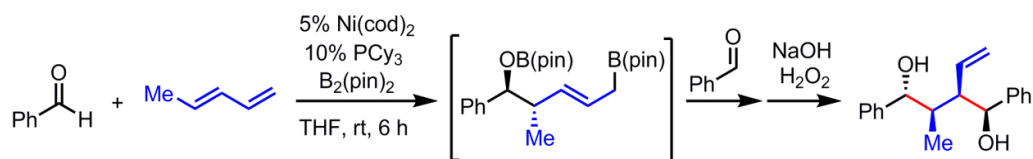
entry	aldehyde	diene	product	yield	dr
1				47%	> 20:1
2				24%	> 20:1

2.3.1.4. Product Transformation

2.3.1.4.1. Three Component Coupling–Allylation Sequence

The products of this process, allylic boronates, are known to undergo allylation reactions in the presence of carbonyl compounds. To probe this feature of the coupling product, we conducted a reaction described in Scheme 2.28; instead of oxidative work-up of the resulting allylboronate, an additional equivalent of aldehyde was added to the coupling product. From this process, the expected product, incorporating 2 equiv of aldehyde and 1 equiv of diene, was obtained as a major reaction product. The initial experiments suggested that the yield of this process was 40% (unoptimized). However, the reaction conditions of this sequence were not further optimized.

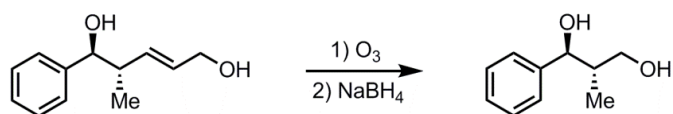
Scheme 2.28 Three-Component Coupling and Subsequent Allylation



2.3.1.4.2. Determination of Relative Configurations

The stereochemical outcome of the coupling reactions (*i.e.* the *anti*-relationship of the substituents at the stereocenters) was determined by comparison of the NMR spectral data of the derivatized product to literature values. As depicted in Scheme 2.29, the alkene moiety of the product (from the coupling of benzaldehyde and pentadiene) can be cleaved by an ozonolysis–reduction sequence to afford a 1,3-diol. The NMR data of the product were in agreement with literature values.⁶⁸

Scheme 2.29 Ozonolysis of a Coupling Product

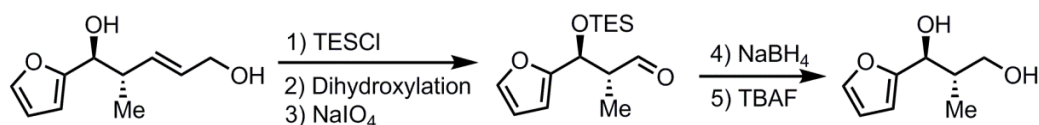


In some cases, the derivatization to the corresponding diol required a multiple-step process instead of the single-step operation of ozonolysis–reduction (Scheme 2.30). When the product from 2-furaldehyde and pentadiene was subjected to an ozonolysis reaction, a rupture of the furan ring was observed. Therefore, dihydroxylation of the alkene and

⁶⁸ For more details, see the Experimental Section (Section 2.6).

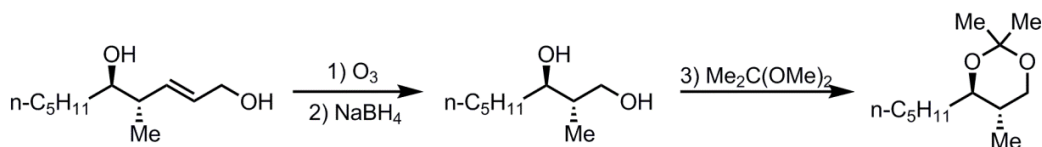
subsequent periodate cleavage of the 1,2-glycol sequence were employed after the alcohol was protected with a silyl group. Then, the reduction of the aldehyde with sodium borohydride afforded a known 1,3-diol.

Scheme 2.30 Multistep Transformation of a Coupling Product



When the derivative of the product was not a known compound, the resulting ozonolysis–reduction product (a 1,3-diol) was transformed to an acetonide (Scheme 2.31). The coupling constant between the two protons at the stereocenters (10.5 Hz) was indicative for the *anti*-stereochemistry of the product.

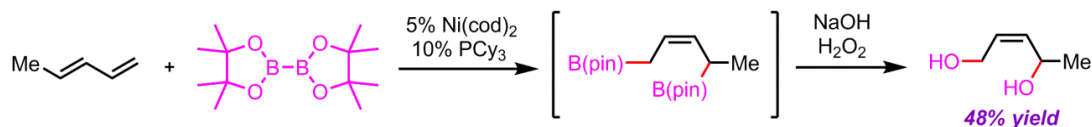
Scheme 2.31 Acetonide Analysis of a Coupling Product Derivative



2.3.2. Ni-Catalyzed Diene Diboration

As introduced previously, catalytic diboration of unsaturated hydrocarbons has attracted a lot of attention due to the synthetic utility of the products. In particular, the 1,4-diboration of 1,3-dienes allows for the transformation of simple hydrocarbons to synthetically valuable allyl diboronate intermediates.⁶⁹ During the investigation of the nickel-catalyzed borylative coupling reactions, we found that Ni(cod)₂, in the presence of PCy₃, promotes the 1,4-diboration of a 1,3-diene with bis(pinacolato)diboron (Scheme 2.32).⁷⁰

Scheme 2.32 Nickel-Catalyzed Diene Diboration



The outcome of this reaction suggested that catalytic diene diboration can be conducted with a convenient and inexpensive catalytic system. Moreover, this process was highly selective in terms of both regiochemical and stereochemical outcomes.

⁶⁹ (a) Ishiyama, T.; Yamamoto, M.; Miyaura, N., "Platinum(0)-Catalysed Diboration of Alka-1,3-Dienes with Bis(Pinacolato)Diboron," *Chemical Communications* **1996**, 2073-2074. (b) Clegg, W.; R. F. Johann, T.; B. Marder, T.; C. Norman, N.; Guy Orpen, A.; M. Peakman, T.; J. Quayle, M.; R. Rice, C.; J. Scott, A., "Platinum-Catalysed 1,4-Diboration of 1,3-Dienes," *Journal of the Chemical Society, Dalton Transactions* **1998**, 1431-1438.

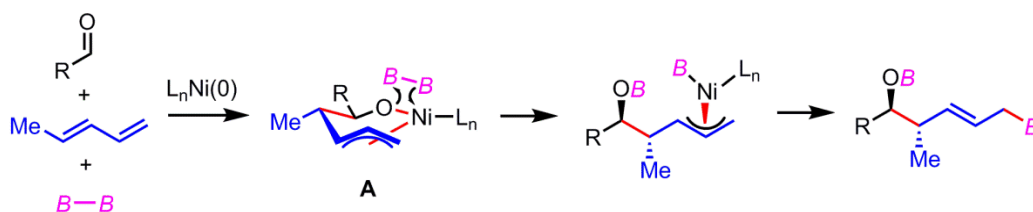
⁷⁰ For Ni-catalyzed silylboration of dienes, see: (a) Suginome, M.; Matsuda, T.; Yoshimoto, T.; Ito, Y., "Stereoselective 1,4-Silylboration of 1,3-Dienes Catalyzed by Nickel Complexes," *Organic Letters* **1999**, *1*, 1567-1569. (b) Gerdin, M.; Moberg, C., "Enantioselective Platinum-Catalyzed Silicon-Boron Addition to 1,3-Cyclohexadiene," *Advanced Synthesis & Catalysis* **2005**, *347*, 749-753.

2.4. Mechanistic Considerations

2.4.1. Possible Mechanistic Pathways

In the hopes of gathering information that could lead to the development of a methodology with greater efficiency and scope, we made efforts toward mechanistic investigations on the borylative multicomponent process. Considering the products that were experimentally obtained and the mechanistic studies on similar reductive coupling reactions,⁷¹ we proposed two plausible mechanistic pathways. One of them would be oxidative cyclization mechanism (Scheme 2.33), in which the initial nickelacyclic complex (**A**) serves as a key intermediate of the process. Subsequent transmetalation and reductive elimination will furnish the observed products.

Scheme 2.33 Oxidative Cyclization Mechanism

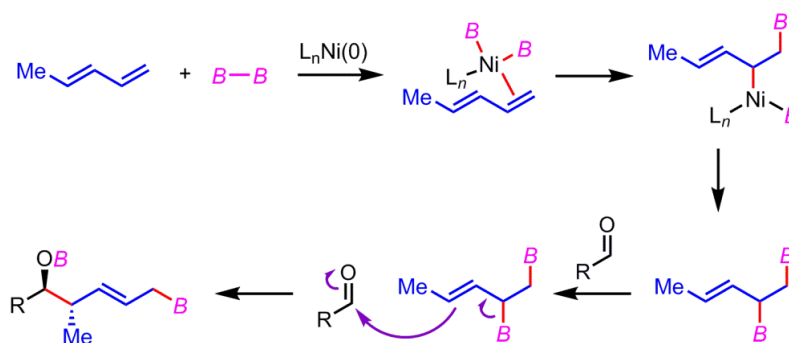


An alternative mechanism involves sequential diboration and allylation reactions, as described in Scheme 2.34. In this pathway, a diene undergoes a catalytic diboration process yielding a 1,2-bisboronate as a reaction intermediate. Then, the intermediate bisboronate is

⁷¹ For more details on reductive coupling reactions, see Sections 3.1 and 3.2 of this thesis.

involved in a subsequent allylation reaction with an aldehyde, which will afford the observed product.

Scheme 2.34 Sequential Diboration–Allylation Mechanism

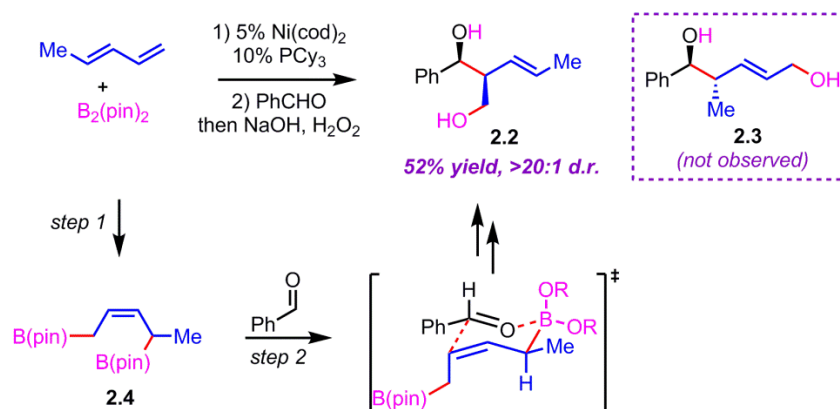


2.4.2. Mechanistic Probe of Plausible Reaction Pathway

To probe features of the proposed mechanisms, the experiments in Scheme 2.35 were carried out. When *trans*-1,3-pentadiene and $B_2(\text{pin})_2$ were allowed to react with the catalyst for 48 hours, prior to the addition of benzaldehyde, addition product **2.2** was obtained.⁷² This addition product is regioisomeric with respect to compound **2.3**, which is the observed product from the borylative multicomponent coupling process (see Table 2.5, entry 1). Formation of compound **2.2** appears most likely to result from sequential Ni-catalyzed 1,4 diene diboration to give **2.4**, followed by selective aldehyde allylation (as depicted in Scheme 2.35). This conjecture was also supported by the outcome in the diene diboration process, in which only 1,4 diboration of diene was observed (see Section 2.3.2).

⁷² With 6 h reaction time for the first step, a mixture of **1** and **2** resulted.

Scheme 2.35 Sequential Diboration–Allylation Experiments



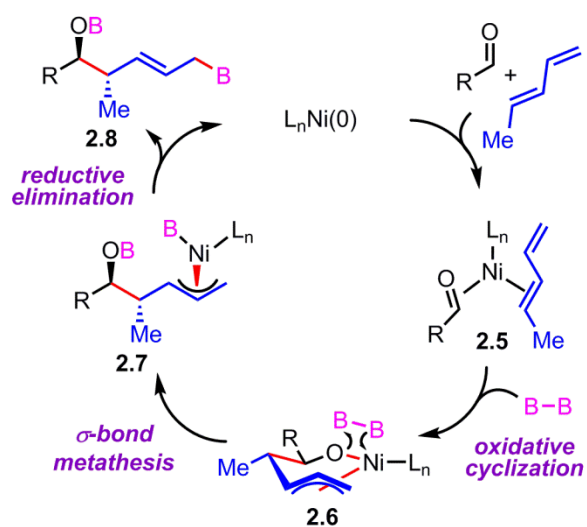
The fact that the three-component reaction takes a different course than the process in Scheme 2.34 (Sequential Diboration–Allylation Mechanism) suggests that a sequential diene diboration followed by aldehyde allylation does not operate in this borylative multicomponent coupling; a more likely mechanism is related to that in Scheme 2.33 (Oxidative Cyclization Mechanism).

2.4.3. Proposed Catalytic Cycle

Based on the mechanistic investigations on the borylative multicomponent process, we propose a plausible catalytic cycle for this process as described in Scheme 2.36. Initial coordination of an aldehyde and a diene by a nickel catalyst would lead to formation of complex **2.5**. Then, oxidative cyclization will result in the formation of nickelacyclic intermediate **2.6**. In the presence of a diboron reagent, subsequent σ -bond metathesis between intermediate **2.6** and the diboron reagent will generate a nickel– π -allyl complex **2.7**.

Finally, reductive elimination will produce an allylic boronic ester **2.8** and restart the catalytic cycle by regenerating a nickel(0) catalyst.

Scheme 2.36 Proposed Catalytic Cycle for Borylative Aldehyde–Diene Coupling



2.5. Conclusions and Outlook

We have demonstrated that diboron reagents can be used to facilitate stereoselective intermolecular coupling of dienes and aldehydes. Compared to borylation reactions with one π component, these borylative multicomponent reactions (involving two π components) lead to formation of a new C–C bond between the π components as well as generation of highly functionalized, stereodefined products.

The reaction products, which are functionally- and stereochemically-enriched, are particularly well suited for the construction of polyketide natural products and other useful chiral materials. Particularly, further studies in asymmetric catalysis and in alternate transformations of the allyl boron product will be greatly useful for building complex molecules in a stereoselective fashion.

2.6. Experimental Section

2.6.1. General Information

All reactions were performed in oven- or flame-dried glassware fitted with rubber septa under a positive pressure of nitrogen, unless otherwise stated. Air- and moisture-sensitive liquids were transferred via syringe or stainless steel cannula. Organic solvents were concentrated by rotary evaporation at various temperatures, unless otherwise noted. All work-up and purification procedures were carried out with reagent grade solvents under typical bench-top conditions. Analytical thin-layer chromatography (TLC) was performed using glass plates, which are pre-coated with silica gel 60 F254 (0.25 mm thickness) impregnated with a fluorescent indicator (254 nm). TLC plates were visualized by exposure to UV (ultraviolet) light, and then were stained with phosphomolybdic acid (PMA) in ethanol, potassium permanganate (KMnO₄) in water, or cerium(IV) sulfate and ammonium molybdate in sulfuric acid (CAM). Liquid chromatography was performed using forced flow (flash chromatography)⁷³ on silica gel (porosity = 60 Å, particle size = 40-63 μm) purchased from Silicycle. Medium pressure gradient chromatography was performed on a Teledyne Isco CombiFlash automated flash chromatography system with a 200-780 nm UV-vis variable wavelength detector.

⁷³ Still, W. C.; Kahn, M.; Mitra, A., "Rapid Chromatographic Technique for Preparative Separations with Moderate Resolution," *The Journal of Organic Chemistry* **1978**, *43*, 2923-2925.

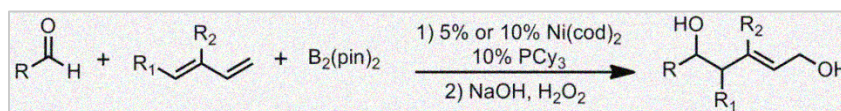
Tetrahydrofuran (THF), dichloromethane, and diethyl ether were purified using a Pure Solv MD-4 solvent purification system from Innovative Technology Inc. Bis(pinacolato)diboron [B₂(pin)₂] was obtained from AllyChem Co., Ltd. and recrystallized from pentane prior to use. Aldehydes were purchased from Aldrich and distilled or recrystallized prior to use. Bis(1,5-cyclooctadiene)nickel(0) [Ni(cod)₂] and tricyclohexylphosphine (PCy₃) were purchased from Strem Chemicals, Inc. Piperylene (1,3-pentadiene) and 3-methyl-1,3-pentadiene were purchased from ChemSampCo. All other reagents were purchased from Sigma Aldrich, Acros, Strem, Alfa Aesar, Fisher, or TCI America and used without further purification.

Proton nuclear magnetic resonance (¹H NMR) spectra were recorded on either a Varian Gemini-400 (400 MHz), or a Varian Inova-500 (500 MHz) spectrometer. Proton chemical shifts are reported in ppm (parts per million, δ scale) downfield from tetramethylsilane and are referenced to residual protium in the NMR solvent as the internal standard (CHCl₃: 7.26 ppm). Data are reported as follows: chemical shift, integration, multiplicity (s = singlet, d = doublet, t = triplet, q = quartet, br = broad, m = multiplet), coupling constants (Hz), and assignment. ¹³C NMR spectra were recorded on either a Varian Gemini-400 (100 MHz), or a Varian Inova-500 (125 MHz) spectrometer with complete proton decoupling. Carbon chemical shifts are reported in ppm (parts per million, δ scale) downfield from tetramethylsilane and are referenced to the NMR solvent resonance as the internal standard (CDCl₃: 77.16 ppm). Infrared (IR) spectra were recorded on a Bruker alpha spectrophotometer, ν_{\max} cm⁻¹. Bands are characterized as broad (br), strong (s), medium (m),

and weak (w). High resolution mass spectrometry (HRMS) was performed at the Mass Spectrometry Facility, Boston College. Melting points were determined with a Thomas-Hoover Unimelt capillary melting point apparatus and were uncorrected.

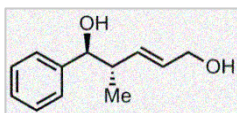
2.6.2. Experimental Procedures

2.6.2.1. General Procedure for Ni-Catalyzed Three-Component Coupling



An oven-dried 20 mL scintillation vial, equipped with a magnetic stir-bar, was charged with Ni(cod)₂ (0.05 mmol or 0.10 mmol), PCy₃ (0.10 mmol), and THF (5 mL, 0.2 M) in a dry box under an argon atmosphere. After stirring for 5 min, the aldehyde (1.0 mmol), diene (1.1 mmol) and B₂(pin)₂ (1.2 mmol or 2.0 mmol) were added sequentially. The vial was sealed with a polypropylene cap and removed from the dry box. The reaction mixture was then allowed to stir at ambient temperature for 6 h or 14 h. After this time, the mixture was cooled to 0 °C (ice-water bath), and 4 mL of 3 M NaOH and 3 mL of 30% H₂O₂ were added dropwise with caution. The mixture was then allowed to stir at ambient temperature for 10 h. The resulting solution was cooled to 0 °C and quenched by the addition of 2 mL of saturated aqueous Na₂S₂O₃. The two-phase mixture was extracted with ethyl acetate (3 x 30 mL), and the combined organic layers were dried over anhydrous Na₂SO₄. The drying agent was removed by filtration and the solvent was evaporated *in vacuo*. The crude material was purified by silica gel chromatography (hexanes/EtOAc) to afford the title compounds.

2.6.2.1.1. Characterization Data and Proof of Stereochemistry



(2*E*, 4*S*^{*}, 5*S*^{*})-4-methyl-5-phenyl-pent-2-ene-1,5-diol. The reaction was

performed according to the general procedure with 13.8 mg (0.05 mmol) of Ni(cod)₂, 28.0 mg (0.10 mmol) of PCy₃, 106 mg (1.0 mmol) of

benzaldehyde, 74.9 mg (1.1 mmol) of *trans*-1,3-pentadiene, and 305 mg (1.2 mmol) of B₂(pin)₂

in THF (5.0 mL) for 6 h, followed by oxidation, to afford the title compound as a colorless oil

(126 mg, 66% yield). R_f = 0.22 (1:1 hexanes:EtOAc); ¹H NMR (400 MHz, CDCl₃): δ 0.84 (3H, d,

J = 6.8 Hz, CHCH₃), 2.22 (1H, br s, OH), 2.46 (1H, br s, OH), 2.48 (1H, m, CHCH₃), 4.11 (2H,

d, *J* = 5.2 Hz, CHCH₂OH), 4.33 (1H, d, *J* = 8.0 Hz, C₆H₅CH), 5.68 (1H, dd, *J* = 15.6 Hz, 8.0 Hz,

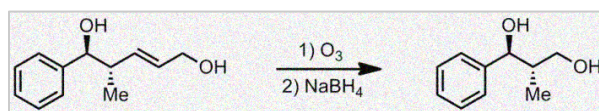
C₆H₅CHCHCH), 5.78 (1H, dt, *J* = 15.6 Hz, 5.6 Hz, CHCH₂OH), 7.26-7.36 (5H, m, CHC₆H₅); ¹³C

NMR (100 MHz, CDCl₃): δ 142.7, 134.5, 131.2, 128.4, 127.8, 126.9, 78.5, 63.6, 44.8, 17.2; IR

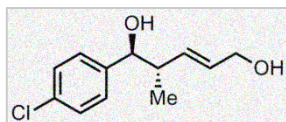
(neat): 3333 (br), 2964 (w), 2928 (w), 2871 (w), 1494 (m), 1058 (s), 700 (s) cm⁻¹; HRMS (ESI+)

Calculated for C₁₂H₁₆O₂ (M + NH₄)⁺: 210.1501, found: 210.1494.

Proof of stereochemistry. The relative configuration was assigned as *anti* by comparison of the ¹H NMR spectrum with that reported in the literature,⁷⁴ after conversion of the title compound into a 1,3-diol by ozonolysis/reduction as shown below.



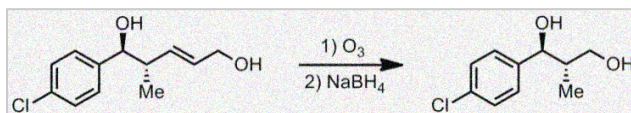
⁷⁴ Pietruszka, J.; Schöne, N., "New 1,3-Disubstituted Enantiomerically Pure Allylboronic Esters by Johnson Rearrangement of Boron-Substituted Allyl Alcohols," *European Journal of Organic Chemistry* **2004**, 2004, 5011-5019.



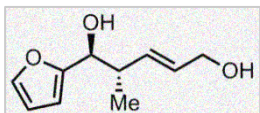
(2E, 4S*, 5S*)-5-(4-chlorophenyl)-4-methyl-pent-2-ene-1,5-diol.

The reaction was performed according to the general procedure with 13.8 mg (0.05 mmol) of Ni(cod)₂, 28.0 mg (0.10 mmol) of PCy₃, 141 mg (1.0 mmol) of 4-chlorobenzaldehyde, 74.9 mg (1.1 mmol) of *trans*-1,3-pentadiene, and 305 mg (1.2 mmol) of B₂(pin)₂ in THF (5.0 mL) for 6 h, followed by oxidation, to afford the title compound as a white solid (143 mg, 63% yield). R_f = 0.22 (1:1 hexanes:EtOAc); mp 65-66 °C; ¹H NMR (400 MHz, CDCl₃): δ 0.86 (3H, d, *J* = 6.8 Hz, CHCH₃), 2.03 (1H, br s, OH), 2.44 (1H, m, CHCH₃), 2.51 (1H, br s, OH), 4.13 (2H, t, *J* = 4.8 Hz, CHCH₂OH), 4.33 (1H, d, *J* = 7.6 Hz, ArCH), 5.66 (1H, dd, *J* = 15.2 Hz, 8.0 Hz, ArCHCHCH), 5.78 (1H, dt, *J* = 15.2 Hz, 5.6 Hz, CHCH₂OH), 7.26 (2H, d, *J* = 8.8 Hz, ArH), 7.32 (2H, d, *J* = 6.8 Hz, ArH); ¹³C NMR (100 MHz, CDCl₃): δ 141.1, 133.9, 133.5, 131.5, 128.5, 128.2, 77.7, 63.5, 44.9, 17.0; IR (neat): 3345 (br), 2964 (w), 2928 (w), 2872 (w), 1490 (s), 1409 (m), 1089 (s), 1013 (s), 972 (s), 825 (s) cm⁻¹; HRMS (ESI+) Calculated for C₁₂H₁₅ClO₂ (M + NH₄)⁺: 244.1113, found: 244.1104.

Proof of stereochemistry. The relative configuration was assigned as *anti* by comparison of the ¹H NMR spectrum with that reported in the literature,⁷⁵ after conversion of the title compound into a 1,3-diol by ozonolysis/reduction as shown below.



⁷⁵ Hayashi, Y.; Aratake, S.; Okano, T.; Takahashi, J.; Sumiya, T.; Shoji, M., "Combined Proline-Surfactant Organocatalyst for the Highly Diastereo- and Enantioselective Aqueous Direct Cross-Aldol Reaction of Aldehydes," *Angewandte Chemie International Edition* **2006**, *45*, 5527-5529.



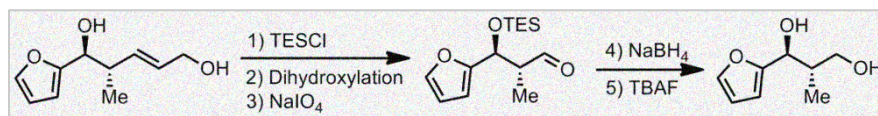
(2E, 4S*, 5S*)-5-furan-2-yl-4-methyl-pent-2-ene-1,5-diol. The

reaction was performed according to the general procedure with 13.8 mg (0.05 mmol) of Ni(cod)₂, 28.0 mg (0.10 mmol) of PCy₃, 96.1 mg (1.0 mmol) of 2-furaldehyde, 74.9 mg (1.1 mmol) of *trans*-1,3-pentadiene, and 305 mg (1.2 mmol) of B₂(pin)₂ in THF (5.0 mL) for 6 h, followed by oxidation, to afford the title compound as a light yellow oil (114 mg, 63% yield). R_f = 0.17 (1:1 hexanes:EtOAc); ¹H NMR (400 MHz, CDCl₃): δ 0.92 (3H, d, J = 6.8 Hz, CHCH₃), 2.00 (1H, br s, OH), 2.43 (1H, br s, OH), 2.71 (1H, m, CHCH₃), 4.12 (2H, d, J = 5.6 Hz, CHCH₂OH), 4.40 (1H, d, J = 7.6 Hz, ArCH), 5.67 (1H, dd, J = 15.6 Hz, 8.0 Hz, ArCHCHCH), 5.80 (1H, dt, J = 15.6 Hz, 5.6 Hz, CHCH₂OH), 6.26 (1H, dd, J = 3.2 Hz, 0.8 Hz, ArH), 6.33 (1H, dd, J = 3.2 Hz, 1.6 Hz, ArH), 7.38 (1H, dd, J = 1.6 Hz, 0.8 Hz, ArH); ¹³C NMR (100 MHz, CDCl₃): δ 155.2, 142.1, 133.8, 131.4, 110.2, 107.4, 71.9, 63.6, 42.3, 16.8; IR (neat): 3345 (br), 2969 (w), 2930 (w), 2874 (w), 1505 (w), 1456 (m), 1376 (m), 1149 (m), 1008 (s), 973 (s), 736 (s), 599 (m) cm⁻¹; HRMS (ESI+) Calculated for C₁₀H₁₄O₃ (M + NH₄)⁺: 200.1290, found: 200.1287.

Proof of stereochemistry. The relative configuration was assigned as *anti* by comparison of the ¹H NMR spectrum with that reported in the literature,⁷⁶ after conversion of the title

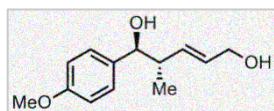
⁷⁶ Christlieb, M.; Davies, J. E.; Eames, J.; Hooley, R.; Warren, S., "The Stereoselective Synthesis of Oxetanes; Exploration of a New, Mitsunobu-Style Procedure for the Cyclisation of 1,3-Diols," *Journal of the Chemical Society, Perkin Transactions 1* **2001**, 2983-2996.

compound into a 1,3-diol by bis-TES protection, dihydroxylation,⁷⁷ oxidative cleavage, reduction, and deprotection as described below.⁷⁸



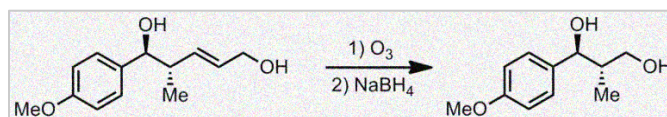
⁷⁷ The dihydroxylation procedure was adapted from: Ohmori, K.; Nishiyama, S.; Yamamura, S., "Synthetic Studies on Bryostatins, Potent Antineoplastic Agents: Synthesis of the C₁₇ □ C₂₇ Fragment of C₂₀ Oxygenated Bryostatins," *Tetrahedron Letters* **1995**, 36, 6519-6522.

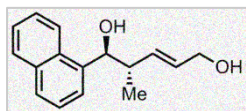
⁷⁸ Ozonolysis of the title compound led to rupture of the furan ring.

(2E, 4S*, 5S*)-5-(4-methoxyphenyl)-4-methyl-pent-2-ene-1,5-diol.

The reaction was performed according to the general procedure with 13.8 mg (0.05 mmol) of Ni(cod)₂, 28.0 mg (0.10 mmol) of PCy₃, 136 mg (1.0 mmol) of 4-methoxybenzaldehyde, 74.9 mg (1.1 mmol) of *trans*-1,3-pentadiene, and 305 mg (1.2 mmol) of B₂(pin)₂ in THF (5.0 mL) for 6 h, followed by oxidation, to afford the title compound as a colorless oil (138 mg, 62% yield). R_f = 0.14 (1:1 hexanes:EtOAc); ¹H NMR (400 MHz, CDCl₃): δ 0.82 (3H, d, *J* = 6.8 Hz, CHCH₃), 1.94 (1H, br s, OH), 2.26 (1H, br s, OH), 2.46 (1H, m, CHCH₃), 3.80 (3H, s, C₆H₄OCH₃), 4.13 (2H, s, CHCH₂OH), 4.28 (1H, d, *J* = 8.4 Hz, ArCH), 5.68 (1H, dd, *J* = 15.2 Hz, 8.0 Hz, C₆H₄CHCHCH), 5.79 (1H, dt, *J* = 15.2 Hz, 5.6 Hz, CHCH₂OH), 6.87 (2H, d, *J* = 8.4 Hz, ArH), 7.23 (2H, d, *J* = 8.8 Hz, ArH); ¹³C NMR (100 MHz, CDCl₃): δ 159.3, 134.9, 134.8, 131.1, 128.0, 113.9, 78.1, 63.7, 55.5, 44.9, 17.2; IR (neat): 3351 (br), 2960 (w), 2931 (w), 2871 (w), 1611 (m), 1511 (s), 1456 (m), 1302 (m), 1244 (s), 1174 (s), 1030 (s), 971 (s), 829 (s) cm⁻¹; HRMS (ESI⁺) Calculated for C₁₃H₁₈O₃ (M + NH₄)⁺: 240.1609, found: 240.1600.

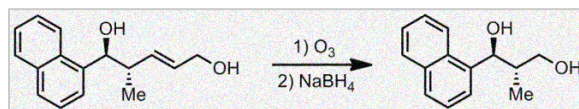
Proof of stereochemistry. The relative configuration was assigned as *anti* by comparison of the ¹H NMR spectrum with that reported in the literature,⁷⁵ after conversion of the title compound into a 1,3-diol by ozonolysis/reduction as shown below.

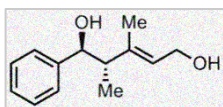




(2E, 4S*, 5S*)-4-methyl-5-naphthalen-1-yl-pent-2-ene-1,5-diol. The reaction was performed according to the general procedure with 13.8 mg (0.05 mmol) of $\text{Ni}(\text{cod})_2$, 28.0 mg (0.10 mmol) of PCy_3 , 156 mg (1.0 mmol) of 1-naphthaldehyde, 74.9 mg (1.1 mmol) of *trans*-1,3-pentadiene, and 305 mg (1.2 mmol) of $\text{B}_2(\text{pin})_2$ in THF (5.0 mL) for 6 h, followed by oxidation, to afford the title compound as an off-white oil (128 mg, 53% yield). $R_f = 0.25$ (1:1 hexanes:EtOAc); ^1H NMR (400 MHz, CDCl_3): δ 0.96 (3H, d, $J = 6.8$ Hz, CHCH_3), 1.78 (1H, br s, OH), 2.35 (1H, br s, OH), 2.84 (1H, m, CHCH_3), 4.13 (2H, t, $J = 4.4$ Hz, CHCH_2OH), 5.18 (1H, d, $J = 6.8$ Hz, ArCH), 5.76 (2H, m, CHCHCH_2OH) 7.44-7.55 (4H, m, ArH), 7.78 (1H, d, $J = 8.0$ Hz, ArH), 7.87 (1H, d, $J = 7.2$ Hz, ArH), 8.15 (1H, d, $J = 7.6$ Hz, ArH); ^{13}C NMR (100 MHz, CDCl_3): δ 138.5, 134.2, 134.0, 131.2, 131.0, 129.1, 128.3, 126.0, 125.6, 125.3, 124.6, 123.6, 75.4, 63.7, 43.9, 17.7; IR (neat): 3357 (br), 2965 (w), 2928 (w), 2871 (w), 1454 (w), 1373 (w), 995 (m), 972 (m), 799 (m), 778 (s) cm^{-1} ; HRMS (ESI+) Calculated for $\text{C}_{16}\text{H}_{18}\text{O}_2$ ($\text{M} + \text{NH}_4$) $^+$: 260.1648, found: 260.1650.

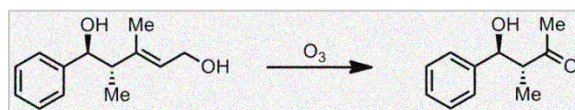
Proof of stereochemistry. The relative configuration was assigned as *anti* by comparison of the ^1H NMR spectrum with that reported in the literature,⁷⁵ after conversion of the title compound into a 1,3-diol by ozonolysis/reduction as illustrated below.



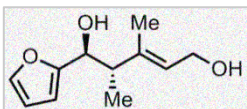


(2E, 4S*, 5S*)-3,4-dimethyl-5-phenyl-pent-2-ene-1,5-diol. The reaction was performed according to the general procedure with 27.5 mg (0.10 mmol) of Ni(cod)₂, 28.0 mg (0.10 mmol) of PCy₃, 106 mg (1.0 mmol) of benzaldehyde, 90.3 mg (1.1 mmol) of *trans*-3-methyl-1,3-pentadiene, and 508 mg (2.0 mmol) of B₂(pin)₂ in THF (5.0 mL) for 14 h, followed by oxidation, to afford the title compound as colorless crystals (144 mg, 70% yield). R_f = 0.18 (1:1 hexanes:EtOAc); mp 52-54 °C; ¹H NMR (400 MHz, CDCl₃): δ 0.74 (3H, d, *J* = 7.2 Hz, CHCH₃), 1.73 (3H, s, CHCCH₃), 2.41 (1H, m, CHCH₃), 2.45 (1H, br s, OH), 2.57 (1H, br s, OH), 4.13 (1H, dd, *J* = 12.0 Hz, 6.4 Hz, CHCH_aH_bOH), 4.24 (1H, dd, *J* = 12.4 Hz, 7.2 Hz, CHCH_aH_bOH), 4.38 (1H, d, *J* = 9.6 Hz, C₆H₅CH), 5.64 (1H, t, *J* = 6.8 Hz, CCHCH₂OH), 7.26-7.35 (5H, m, CHC₆H₅); ¹³C NMR (100 MHz, CDCl₃): δ 142.8, 140.8, 128.4, 127.9, 127.1, 126.9, 76.7, 59.1, 51.2, 16.1, 12.7; IR (neat): 3346 (br), 3029 (w), 2966 (w), 2875 (w), 1454 (m), 1384 (w), 1060 (m), 995 (s), 754 (s), 700 (s), 573 (m) cm⁻¹; HRMS (ESI+) Calculated for C₁₃H₁₈O₂ (M + NH₄)⁺: 224.1651, found: 224.1651.

Proof of stereochemistry. The relative configuration was assigned as *anti* by comparison of the ¹H NMR spectrum with that reported in the literature,⁷⁹ after conversion of the title compound into a ketone by ozonolysis as shown below. The alkene configuration was assigned as (*E*) by NOESY analysis.

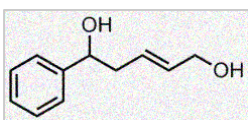


⁷⁹ Schetter, B.; Ziemer, B.; Schnakenburg, G.; Mahrwald, R., "Tetranuclear Binol-Titanium Complex in Selective Direct Aldol Additions," *The Journal of Organic Chemistry* **2008**, *73*, 813-819.



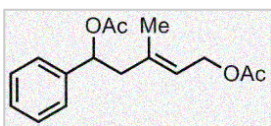
(*2E*, *4S*^{*}, *5S*^{*})-5-furan-2-yl-3,4-dimethyl-pent-2-ene-1,5-diol. The reaction was performed according to the general procedure with 27.5 mg (0.10 mmol) of Ni(cod)₂, 28.0 mg (0.10 mmol) of PCy₃, 96.1 mg (1.0 mmol) of 2-furaldehyde, 90.3 mg (1.1 mmol) of *trans*-3-methyl-1,3-pentadiene, and 508 mg (2.0 mmol) of B₂(pin)₂ in THF (5.0 mL) for 14 h, followed by oxidation, to afford the title compound as a light yellow oil (128 mg, 65% yield). *R*_f = 0.11 (1:1 hexanes:EtOAc); ¹H NMR (400 MHz, CDCl₃): δ 0.84 (3H, d, *J* = 6.8 Hz, CHCH₃), 1.68 (3H, s, CHCCH₃), 1.82 (1H, br t, *J* = 5.2 Hz, OH), 2.33 (1H, d, *J* = 3.6 Hz, OH), 2.70 (1H, m, CHCH₃), 4.14-4.26 (2H, m, CHCH₂OH), 4.49 (1H, dd, *J* = 9.6 Hz, 4.0 Hz ArCH), 5.64 (1H, t, *J* = 6.8 Hz, CHCH₂OH), 6.28 (1H, dd, *J* = 3.2 Hz, 0.8 Hz, ArH), 6.33 (1H, dd, *J* = 3.2 Hz, 1.6 Hz, ArH), 7.39 (1H, dd, *J* = 2.0 Hz, 0.8 Hz, ArH); ¹³C NMR (100 MHz, CDCl₃): δ 155.1, 142.2, 140.2, 127.1, 110.2, 107.7, 69.8, 59.2, 48.6, 16.0, 12.6; IR (neat): 3345 (br), 2967 (w), 2931 (w), 2877 (w), 1664 (w), 1504 (w), 1378 (m), 1185 (m), 1007 (s), 735 (s), 599 (s) cm⁻¹; HRMS (ESI⁺) Calculated for C₁₁H₁₆O₃ (M – H₂O + H)⁺: 179.1068, found: 179.1072.

Stereochemistry. The relative configuration was assigned as *anti* by analogy. The alkene configuration was assigned as (*E*) by NOESY analysis.



(E)-5-phenyl-pent-2-ene-1,5-diol. The reaction was performed according to the general procedure with 27.5 mg (0.10 mmol) of Ni(cod)₂, 28.0 mg (0.10 mmol) of PCy₃, 106 mg (1.0 mmol) of benzaldehyde, 1.1 mmol of 1,3-butadiene,⁸⁰ and 305 mg (1.2 mmol) of B₂(pin)₂ in THF (5.0 mL) for 14 h, followed by oxidation, to afford the title compound as a light yellow oil (61.2 mg, 34% yield). R_f = 0.16 (1:1 hexanes:EtOAc); ¹H NMR (400 MHz, CDCl₃): δ 1.61 (1H, br s, OH), 2.18 (1H, br s, OH), 2.51 (2H, t, J = 6.0 Hz, C₆H₅CHCH₂), 4.10 (2H, br s, CHCH₂OH), 4.74 (1H, t, J = 6.4 Hz, C₆H₅CH), 5.70 (1H, dt, J = 15.6 Hz, 6.4 Hz, C₆H₅CHCH₂CH), 5.78 (1H, dt, J = 15.6 Hz, 5.2 Hz, CHCHCH₂OH), 7.26-7.40 (5H, m, CHC₆H₅); ¹³C NMR (100 MHz, CDCl₃): δ 144.0, 132.9, 128.6, 128.4, 127.7, 125.9, 73.8, 63.6, 42.3; IR (neat): 3334 (br), 3029 (w), 2924 (m), 2856 (m), 1493 (w), 1454 (m), 1045 (m), 1002 (s), 972 (s), 758 (m), 700 (s) cm⁻¹; HRMS (ESI+) Calculated for C₁₁H₁₄O₂ (M + NH₄)⁺: 196.1350, found: 196.1338.

⁸⁰ Gaseous 1,3-butadiene was dissolved in anhydrous THF using a cold finger condenser at -78 °C. The concentration of the 1,3-butadiene solution was determined by ¹H NMR prior to use.



(E)-3-methyl-5-phenyl-pent-2-ene-1,5-diol diacetate.⁸¹ The reaction

was performed according to the general procedure with 27.5 mg (0.10

mmol) of Ni(cod)₂, 16.6 mg (0.10 mmol) of P(OEt)₃, 106 mg (1.0 mmol)

of benzaldehyde, 74.9 mg (1.1 mmol) of isoprene, and 305 mg (1.2 mmol) of B₂(pin)₂ in THF

(5.0 mL) for 14 h, followed by oxidation, to give a crude diol as a yellow oil. To the crude

diol, 73.3 mg (0.6 mmol) of 4-(dimethylamino)pyridine, 4 mL of dichloromethane, and 1.12

mL (8.0 mmol) of triethylamine were added. The reaction mixture was cooled to 0 °C, and

then 0.94 mL (10 mmol) of acetic anhydride was added. The mixture was allowed to stir at

ambient temperature for 14 h. The solvent was evaporated *in vacuo* and the crude product

was passed through a pad of silica gel with 10:1 hexanes:EtOAc as the eluent. After ¹H NMR

analysis of the crude product, it was purified by silica gel chromatography to afford the title

compound as a light yellow oil (188 mg, 68% yield). R_f = 0.36 (4:1 hexanes:EtOAc); ¹H NMR

(400 MHz, CDCl₃): δ 1.73 (3H, s, C₆H₅CHCH₂CCH₃), 2.03 (3H, s, OCOCH₃), 2.05 (3H, s,

OCOCH₃), 2.43 (1H, dd, J = 14.0 Hz, 5.2 Hz, C₆H₅CHCH_aH_b), 2.63 (1H, dd, J = 14.0 Hz, 8.4 Hz,

C₆H₅CHCH_aH_b), 4.53 (2H, d, J = 6.8 Hz, CCHCH₂OAc), 5.34 (1H, t, J = 7.2 Hz, CCHCH₂OAc),

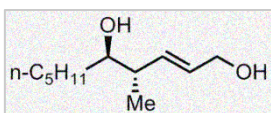
5.91 (1H, dd, J = 8.8 Hz, 5.2 Hz, C₆H₅CH), 7.26-7.34 (5H, m, CHC₆H₅); ¹³C NMR (100 MHz,

CDCl₃): δ 171.0, 170.2, 140.3, 137.5, 128.5, 128.1, 126.5, 122.5, 74.0, 61.2, 46.8, 21.3, 21.1, 17.0; IR

⁸¹ An additional acylation step was employed to ease manipulation; the corresponding diol could not be separated from triethyl phosphate by column chromatography. The acylation procedure was adapted from: Pelz, N. F.; Morken, J. P., "Modular Asymmetric Synthesis of 1,2-Diols by Single-Pot Allene Diboration/Hydroboration/Cross-Coupling," *Organic Letters* **2006**, *8*, 4557-4559.

(neat): 1733 (s), 1439 (w), 1368 (m), 1225 (s), 1021 (s), 972 (m), 758 (m), 700 (m), 608 (m), 545

(m) cm^{-1} ; HRMS (ESI+) Calculated for $\text{C}_{16}\text{H}_{20}\text{O}_4$ ($\text{M} + \text{NH}_4$)⁺: 294.1703, found: 294.1705.



(2*E*, 4*S*^{*}, 5*S*^{*})-4-methyl-dec-2-ene-1,5-diol. The reaction was

performed according to the general procedure with 27.5 mg (0.10

mmol) of Ni(cod)₂, 28.0 mg (0.10 mmol) of PCy₃, 100 mg (1.0 mmol)

of hexanal, 74.9 mg (1.1 mmol) of *trans*-1,3-pentadiene, and 305 mg (1.2 mmol) of B₂(pin)₂ in

THF (5.0 mL) for 14 h, followed by oxidation,⁸² to afford the title compound as a colorless oil

(86.8 mg, 47% yield). *R*_f = 0.29 (1:1 hexanes:EtOAc); ¹H NMR (400 MHz, CDCl₃): δ 0.89 (3H, t,

J = 6.4 Hz, CH₂CH₂CH₂CH₃), 1.04 (3H, d, *J* = 7.2 Hz, CHCH₃), 1.30-1.49 (10H, m, aliphatic &

2×OH), 2.23 (1H, m, n-C₅H₁₁CHCH), 3.41 (1H, m, n-C₅H₁₁CH), 4.14 (2H, t, *J* = 5.6 Hz,

CHCHCH₂OH), 5.65 (1H, dd, *J* = 15.6 Hz, 7.6 Hz, n-C₅H₁₁CHCHCH), 5.72 (1H, dt, *J* = 15.6 Hz,

5.6 Hz, CHCH₂OH); ¹³C NMR (100 MHz, CDCl₃): δ 134.2, 130.7, 75.3, 63.7, 42.7, 34.6, 32.1,

25.6, 22.8, 16.9, 14.2; IR (neat): 3345 (br), 2958 (s), 2930 (s), 2860 (s), 1458 (m), 1377 (w), 1122

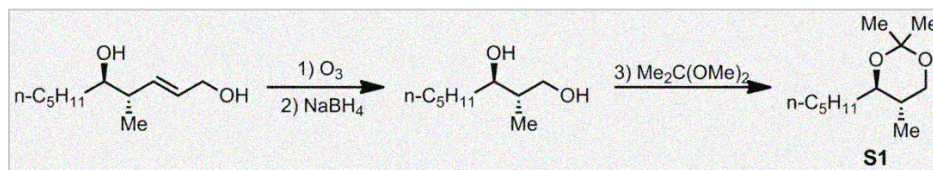
(w), 974 (s), 733 (m) cm⁻¹; HRMS (ESI⁺) Calculated for C₁₁H₂₂O₂ (M + NH₄)⁺: 204.1969, found:

204.1964.

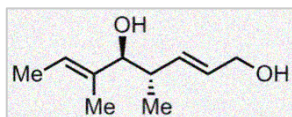
Proof of stereochemistry. The relative configuration was assigned as *anti* by ¹H NMR

analysis of the derived ketal (**S1**), after ozonolysis, reduction, and acetonide protection of the

title compound as shown below.

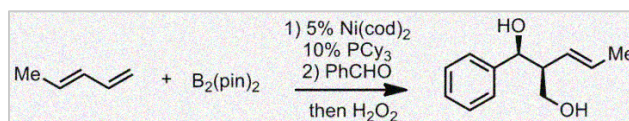


⁸² After aqueous work-up, the crude product was subjected to oxidative cleavage (NaIO₄) for better purification since the title compound was not separated well from pinacol by column chromatography.

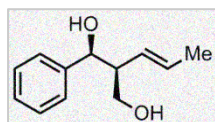


(2E, 4S*, 5S*)-4,6-dimethyl-octa-2,6-diene-1,5-diol. The reaction was performed according to the general procedure with 27.5 mg (0.10 mmol) of Ni(cod)₂, 28.0 mg (0.10 mmol) of PCy₃, 84.1 mg (1.0 mmol) of *trans*-2-methyl-2-butenal, 74.9 mg (1.1 mmol) of *trans*-1,3-pentadiene, and 305 mg (1.2 mmol) of B₂(pin)₂ in THF (5.0 mL) for 14 h, followed by oxidation, to afford the title compound as a colorless oil (40.2 mg, 24% yield). R_f = 0.19 (1:1 hexanes:EtOAc); ¹H NMR (400 MHz, CDCl₃): δ 0.85 (3H, d, *J* = 6.8 Hz, OHCHCHCH₃), 1.60 (3H, s, CH₃CHCCH₃), 1.62 (3H, d, *J* = 6.8 Hz, HOCHCCHCH₃), 1.75 (1H, br t, *J* = 5.6 Hz, OH), 1.81 (1H, br s, OH), 2.33 (1H, m, OHCHCHCH₃), 3.64 (1H, d, *J* = 9.2 Hz, OHCH), 4.13 (2H, t, *J* = 5.6 Hz, CH₂OH), 5.47 (1H, q, *J* = 6.4 Hz, OHCHCCHCH₃), 5.62 (1H, dd, *J* = 15.6 Hz, 8.0 Hz, OHCH₂CHCH), 5.77 (1H, dt, *J* = 15.6 Hz, 6.0 Hz, OHCH₂CHCH); ¹³C NMR (100 MHz, CDCl₃): δ 135.9, 135.2, 130.9, 123.4, 82.1, 63.7, 40.8, 17.3, 13.3, 10.8; IR (neat): 3358 (br), 2970 (m), 2924 (m), 2865 (m), 1668 (w), 1452 (m), 1379 (m), 1056 (w), 971 (s), 912 (w), 824 (m) cm⁻¹; HRMS (ESI+) Calculated for C₁₀H₁₈O₂ (M + NH₄)⁺: 188.1651, found: 188.1651.

2.6.2.2. Procedure and Data for Ni-Catalyzed Diboration/Allylation

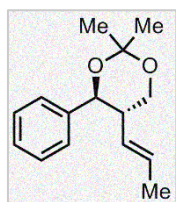
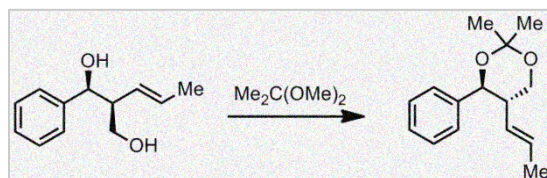


An oven-dried 20 mL scintillation vial, equipped with a magnetic stir-bar, was charged with Ni(cod)₂ (13.8 mg, 0.05 mmol), PCy₃ (28.0 mg, 0.10 mmol), and THF (5 mL) in a dry box under an argon atmosphere. After stirring for 5 min, *trans*-1,3-pentadiene (68.1 mg, 1.0 mmol) and B₂(pin)₂ (305 mg, 1.2 mmol) were added. The vial was sealed with a polypropylene cap and removed from the dry box. The reaction mixture was then allowed to stir at ambient temperature for 48 h. After this time, benzaldehyde (1.0 mmol, 106 mg) was added to the reaction mixture under an inert atmosphere, and stirred at ambient temperature. After stirring for 10 h, the mixture was cooled to 0 °C (ice-water bath), and 4 mL of 3 M NaOH and 3 mL of 30% H₂O₂ were added dropwise with caution. The mixture was then allowed to stir at ambient temperature for 14 h. The resulting solution was cooled to 0 °C and quenched by the addition of 2 mL of saturated aqueous Na₂S₂O₃. The two-phase mixture was extracted with ethyl acetate (3 x 30 mL), and the combined organic layers were dried over anhydrous Na₂SO₄. The drying agent was removed by filtration and the solvent was evaporated *in vacuo*. The crude material was purified by silica gel chromatography (1:1 hexanes:EtOAc) to afford the diol as an off-white solid (98.9 mg, 52% yield).



(*E*, 1*S*^{*}, 2*S*^{*})-1-phenyl-2-(1-propenyl)-propane-1,3-diol. $R_f = 0.46$ (1:1 hexanes:EtOAc); mp 91-92 °C; $^1\text{H NMR}$ (400 MHz, CDCl_3): δ 1.59 (3H, d, $J = 7.2$ Hz, CHCHCH_3), 2.42 (1H, br t, $J = 5.6$ Hz, OH), 2.60 (1H, m, CHCH_2OH), 2.66 (1H, br s, OH), 3.74 (1H, m, $\text{CHCH}_a\text{H}_b\text{OH}$), 3.79 (1H, m, $\text{CHCH}_a\text{H}_b\text{OH}$), 4.75 (1H, d, $J = 7.6$ Hz, $\text{C}_6\text{H}_5\text{CH}$), 5.23 (1H, dd, $J = 15.2$ Hz, 8.8 Hz, $\text{C}_6\text{H}_5\text{CHCHCH}$), 5.45 (1H, dq, $J = 15.2$ Hz, 6.8 Hz, CHCHCH_3), 7.26-7.36 (5H, m, CHC_6H_5); $^{13}\text{C NMR}$ (100 MHz, CDCl_3): δ 143.0, 129.3, 128.4, 127.9, 127.7, 126.7, 78.1, 65.3, 51.4, 18.3; IR (neat): 3340 (br), 3030 (w), 2917 (m), 2882 (w), 1725 (w), 1494 (w), 1452 (m), 1026 (s), 968 (s), 759 (m), 700 (s) cm^{-1} ; HRMS (ESI⁺) Calculated for $\text{C}_{12}\text{H}_{16}\text{O}_2$ ($\text{M} + \text{NH}_4$)⁺: 210.1503, found: 210.1494.

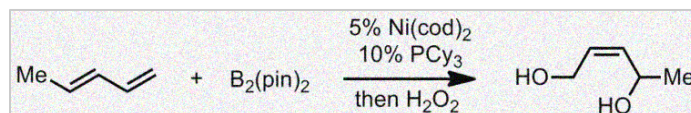
Proof of stereochemistry. The relative configuration was assigned as *syn* by $^1\text{H NMR}$ of the derived ketal, after acetonide protection of the title compound as shown below.



(*E*, 4*S*^{*}, 5*S*^{*})-2,2-dimethyl-4-phenyl-5-propenyl-[1,3]dioxane. An off-white solid. $R_f = 0.66$ (4:1 hexanes:EtOAc); mp 88-90 °C; $^1\text{H NMR}$ (400 MHz, CDCl_3): δ 1.49 (3H, s, OCCH_3), 1.52 (3H, d, $J = 6.4$ Hz, CHCHCH_3), 1.57 (3H, s, OCCH_3), 2.51 (1H, m, $\text{C}_6\text{H}_5\text{CHCH}$), 3.84 (1H, dd, $J = 8.0$ Hz, 3.6 Hz, $\text{C}_6\text{H}_5\text{CHCHCH}_a\text{H}_b$), 3.87 (1H, t, $J = 12.0$ Hz, $\text{C}_6\text{H}_5\text{CHCHCH}_a\text{H}_b$), 4.59 (1H, d, $J = 10.4$ Hz, $\text{C}_6\text{H}_5\text{CH}$), 5.05 (1H, dd, $J = 15.6$ Hz, 8.0 Hz, $\text{C}_6\text{H}_5\text{CHCHCH}$), 5.26 (1H, dq, $J = 15.6$ Hz, 6.4 Hz,

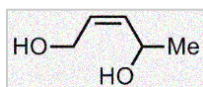
CHCHCH₃), 7.24-7.33 (5H, m, CHC₆H₅); ¹³C NMR (100 MHz, CDCl₃): δ 140.5, 129.2, 128.2, 127.9, 127.6, 126.6, 98.7, 64.7, 45.2, 30.1, 29.9, 19.2, 18.4; IR (neat): 3030 (w), 2992 (m), 2921 (m), 2856 (m), 1453 (m), 1379 (s), 1196 (s), 1164 (s), 1110 (s), 1083 (s), 879 (s), 698 (s) cm⁻¹; LRMS (ESI+) Calculated for C₁₅H₂₀O₂ (M + H)⁺: 233.154, found: 233.196.

2.6.2.3. Procedure and Data for Ni-Catalyzed Diene Diboration



An oven-dried 20 mL scintillation vial, equipped with a magnetic stir-bar, was charged with Ni(cod)₂ (13.8 mg, 0.05 mmol), PCy₃ (28.0 mg, 0.10 mmol), and THF (5 mL) in a dry box under an argon atmosphere. After stirring for 5 min, *trans*-1,3-pentadiene (68.1 mg, 1.0 mmol) and B₂(pin)₂ (305 mg, 1.2 mmol) were added. The vial was sealed with a polypropylene cap and removed from the dry box. The reaction mixture was then allowed to stir at ambient temperature for 48 h. After this time, the mixture was cooled to 0 °C (ice-water bath), and 4 mL of 3 M NaOH and 3 mL of 30% H₂O₂ (dropwise with caution) were added. The mixture was then allowed to stir at ambient temperature for 10 h. The resulting solution was cooled to 0 °C and quenched by the addition of 2 mL of saturated aqueous Na₂S₂O₃. The two-phase mixture was extracted with ethyl acetate (5 x 30 mL), and the combined organic layers were dried over anhydrous Na₂SO₄. The drying agent was removed by filtration and the solvent was evaporated *in vacuo*. The crude material was purified by silica gel chromatography to afford **S3** as a colorless oil (48.7 mg, 48% yield).

(Z)-pent-2-ene-1,4-diol. R_f = 0.12 (1:2 hexanes:EtOAc); ¹H NMR (400

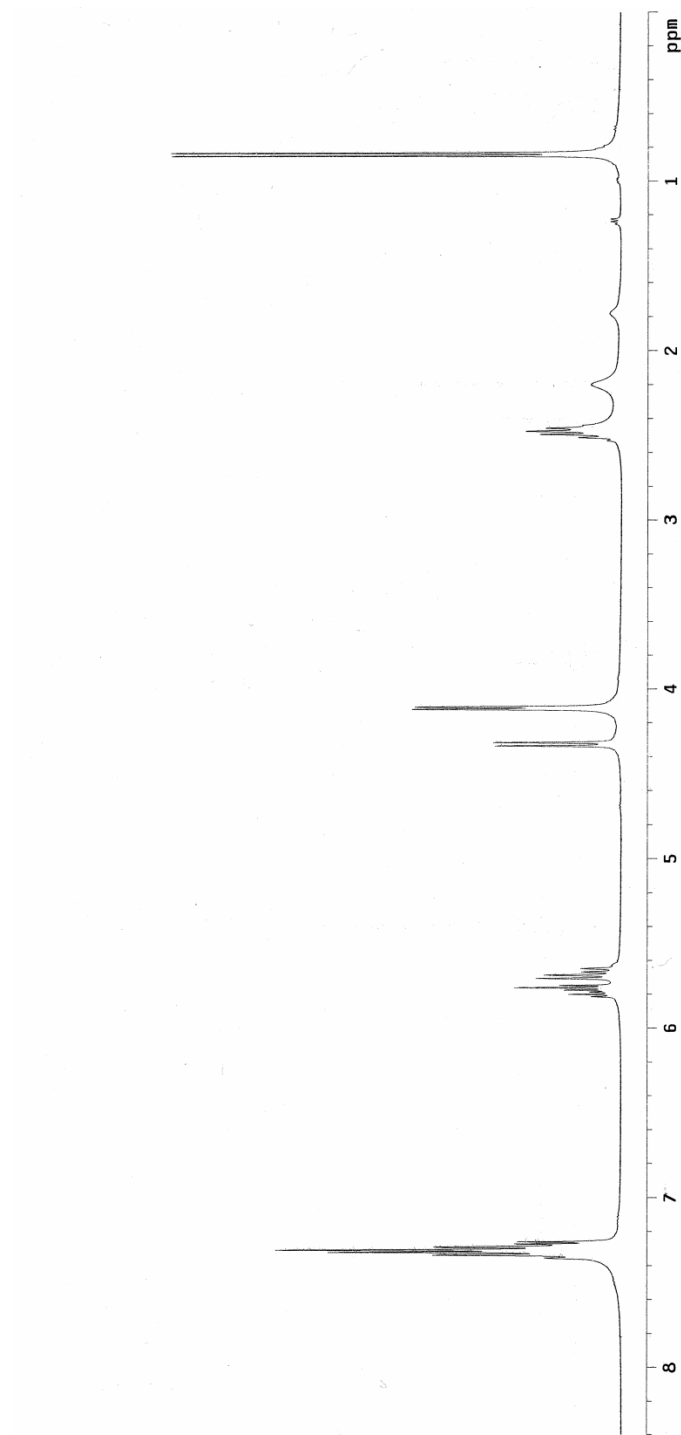
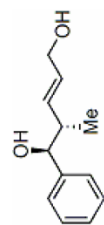


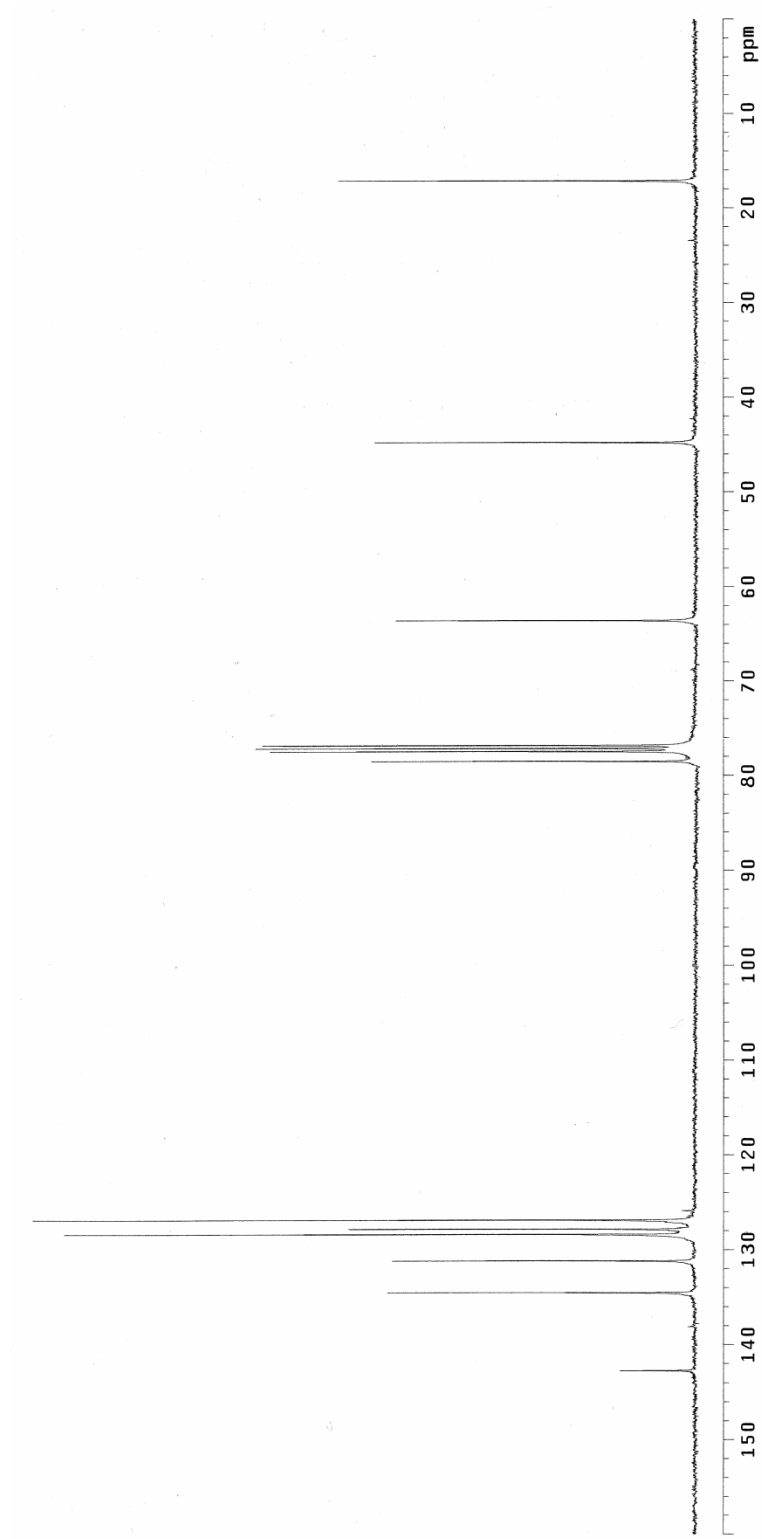
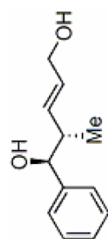
MHz, CDCl₃): δ 1.23 (3H, d, *J* = 6.0 Hz, OHCHCH₃), 3.70 (2H, br s, OH),

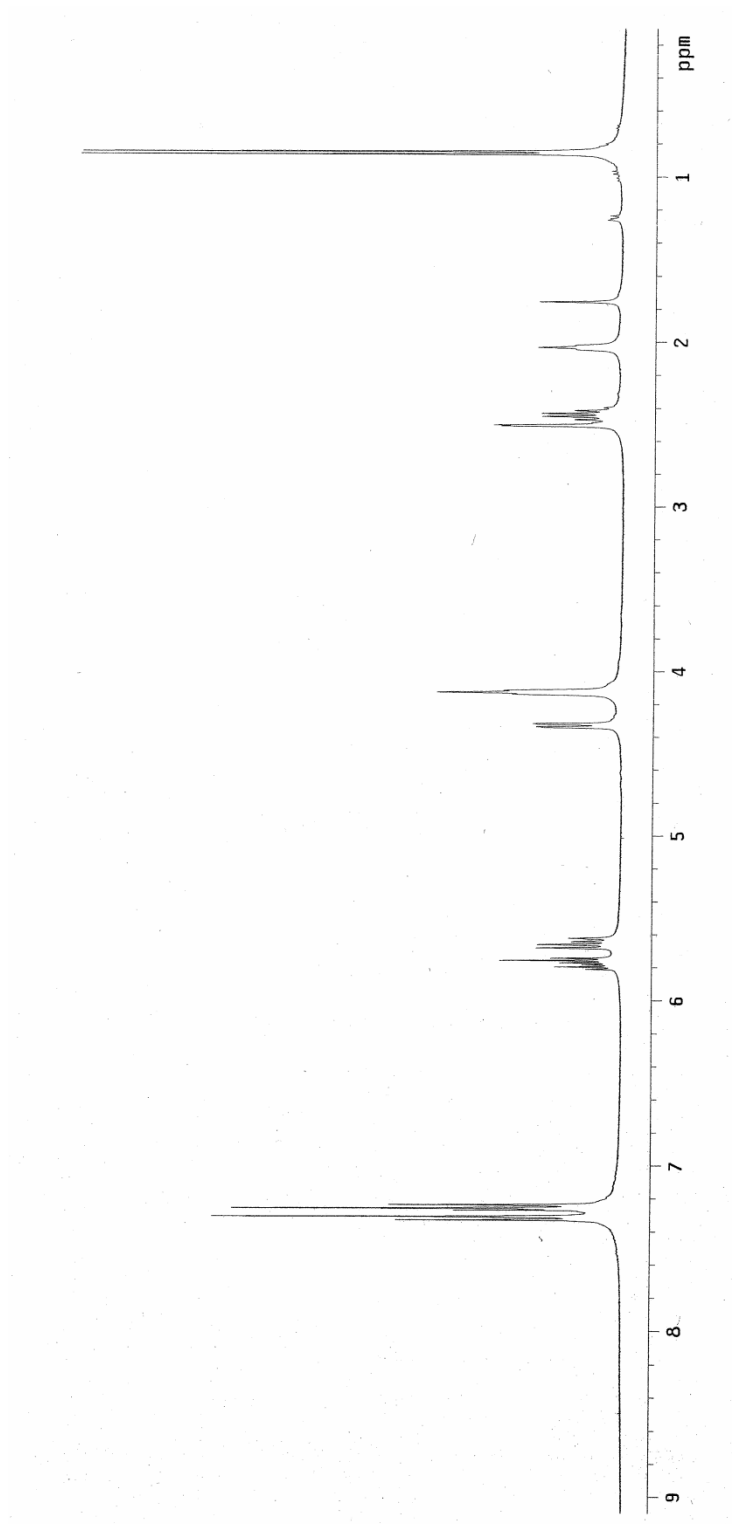
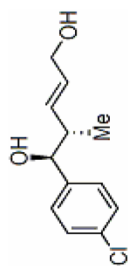
4.04 (1H, dd, *J* = 13.2 Hz, 5.2 Hz, CHCH_aH_bOH), 4.28 (1H, dd, *J* = 13.2 Hz, 8.0 Hz, CHCH_aH_bOH), 4.62 (1H, quintet, *J* = 7.2 Hz, OHCHCH₃), 5.55 (1H, dd, *J* = 11.2 Hz, 8.0 Hz,

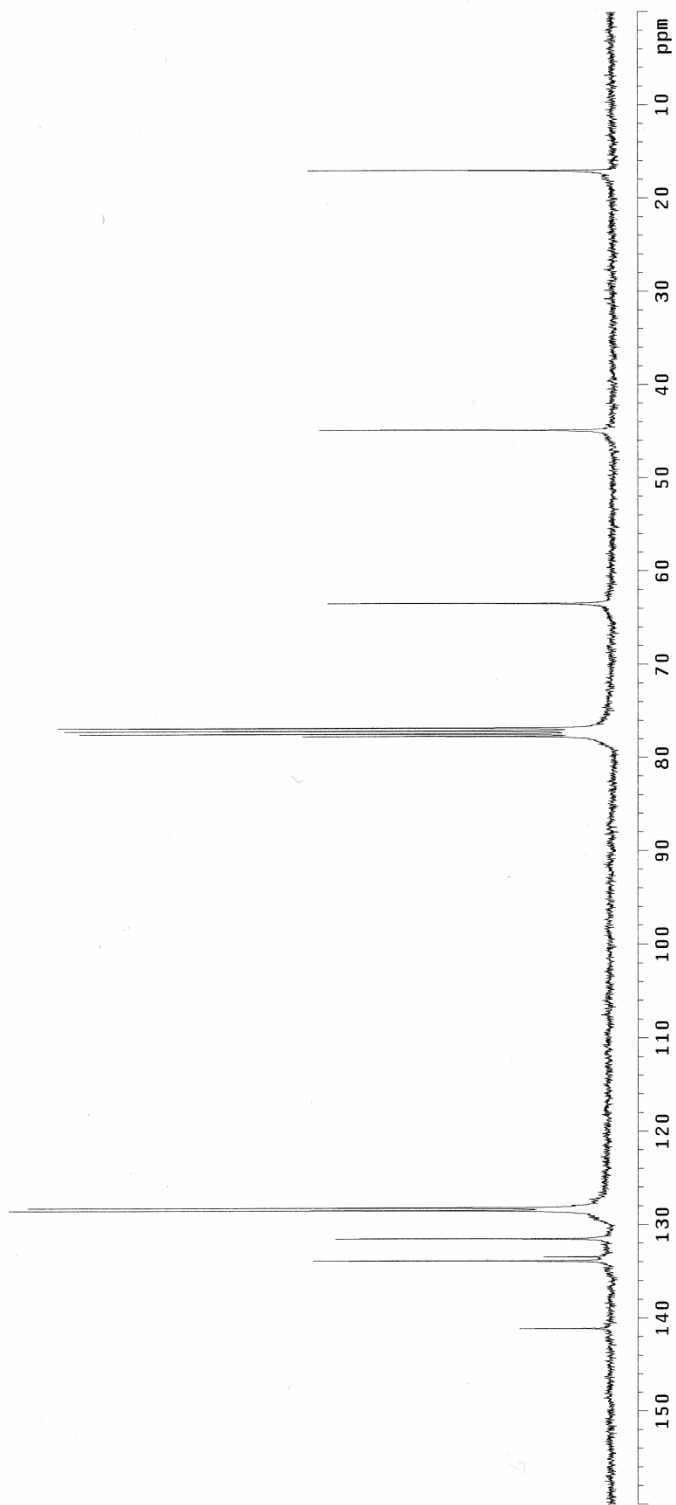
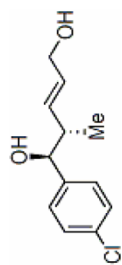
CHCHCHCH₃), 5.62 (1H, m, OHCH₂CHCH); ¹³C NMR (100 MHz, CDCl₃): δ 136.5, 129.4, 63.9, 58.5, 23.7; IR (neat): 3299 (br), 2959 (m), 2923 (s), 2854 (m), 1459 (w), 1375 (w), 1292 (w), 1060 (m), 1025 (s), 999 (m), 733 (m) cm⁻¹; HRMS (ESI+) Calculated for C₅H₁₀O₂ (M + NH₄)⁺: 120.1033, found: 120.1025.

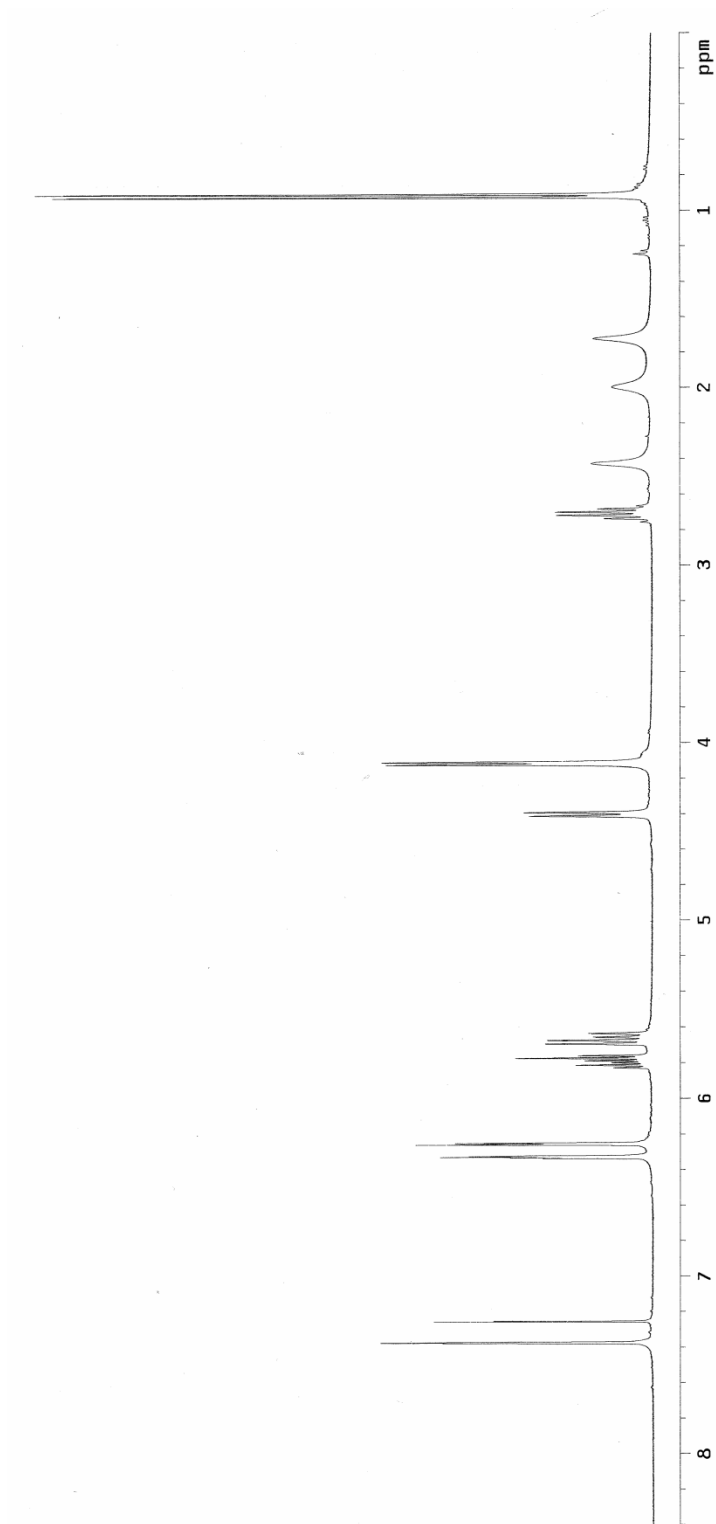
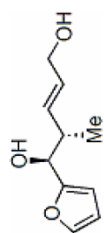
2.6.3. Representative Spectral Data

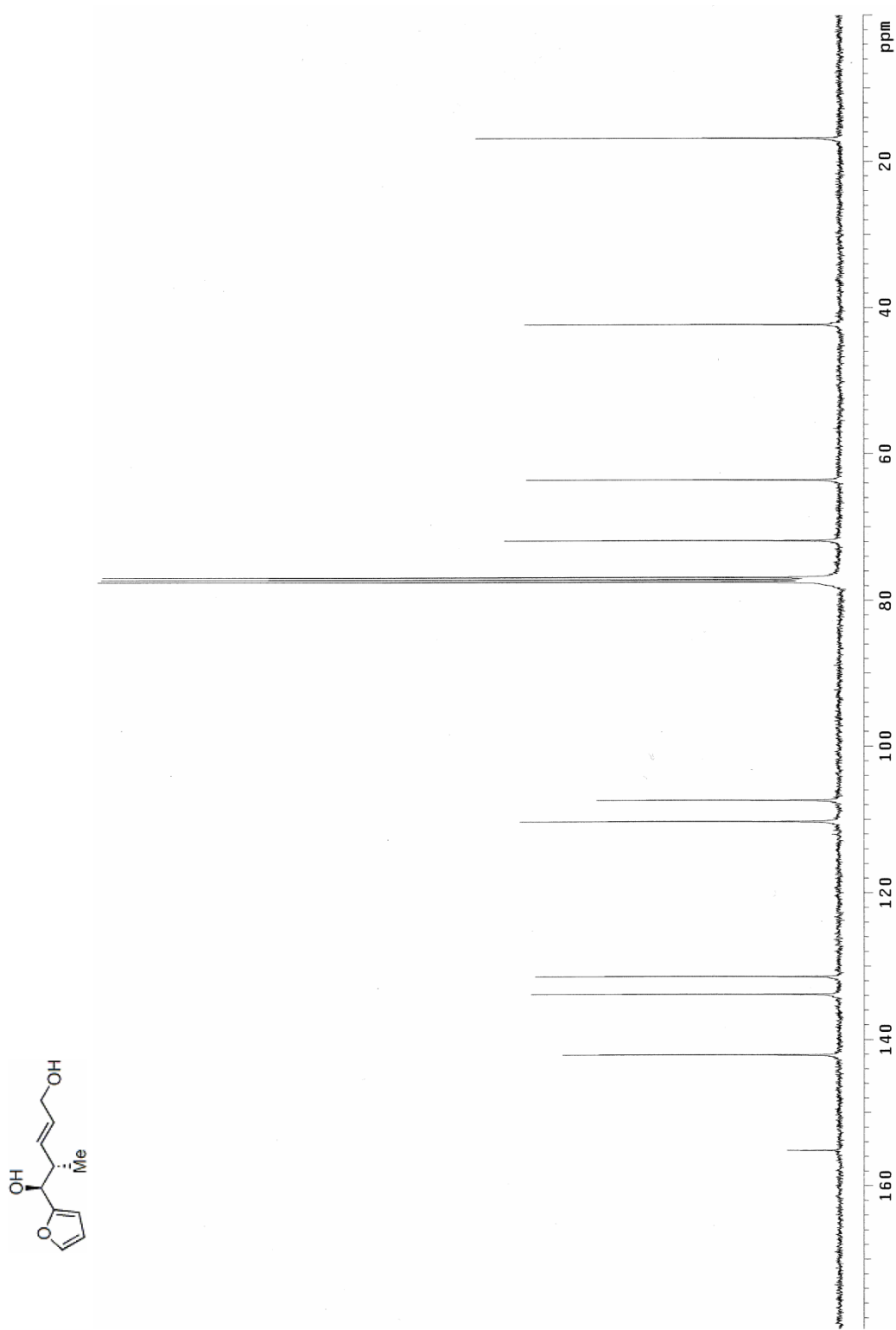


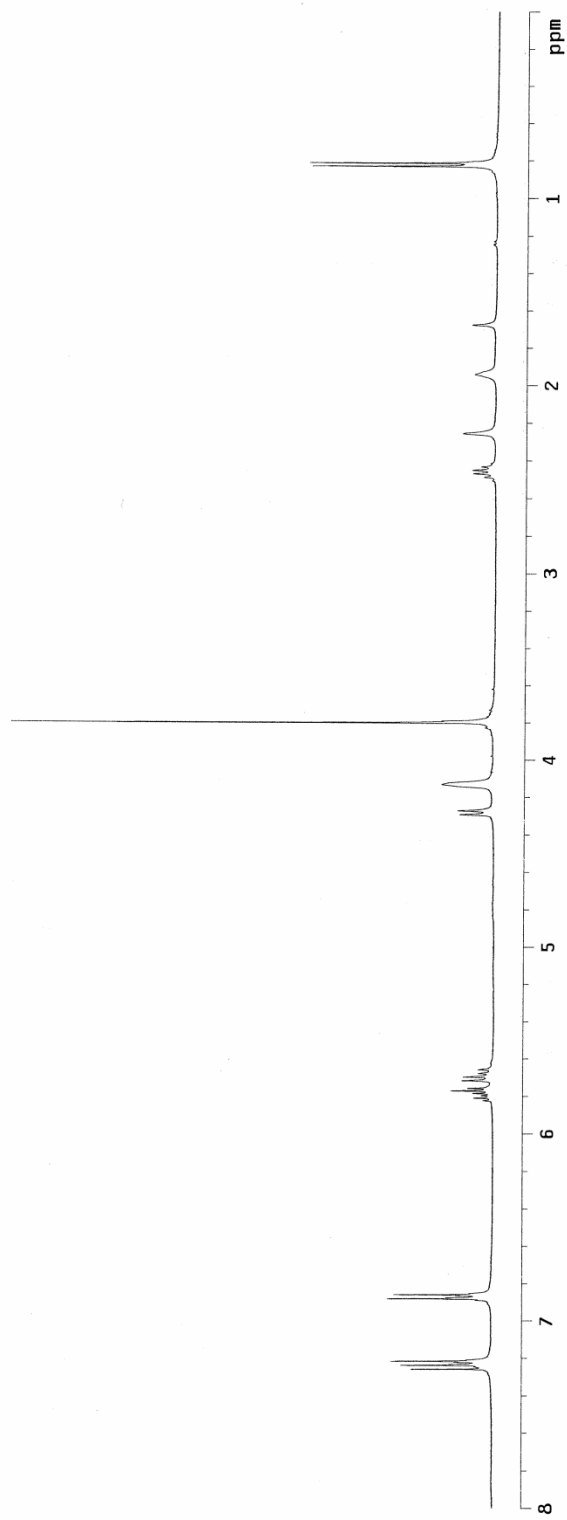
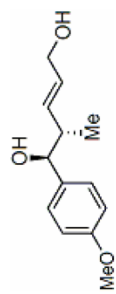


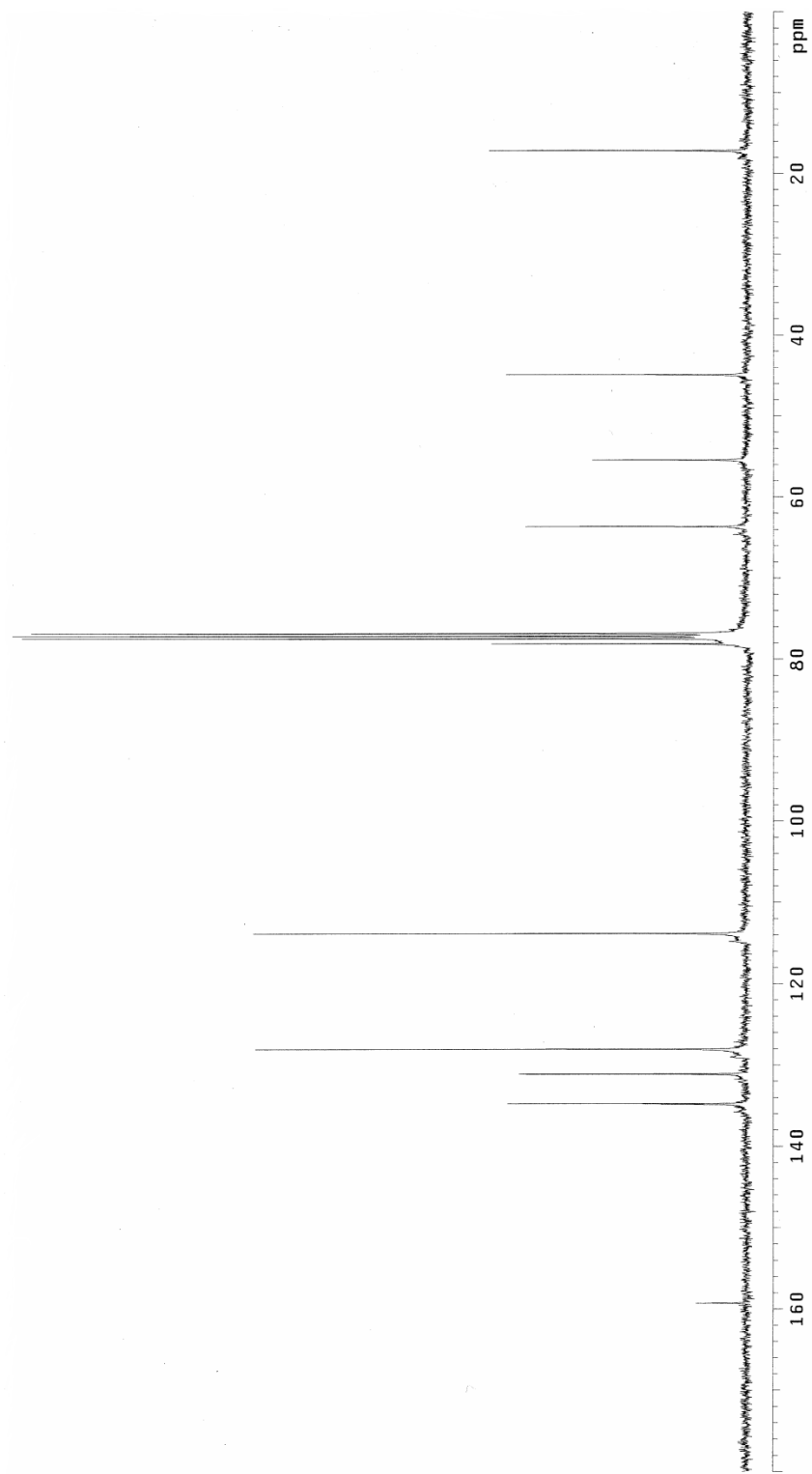
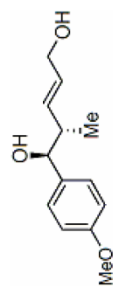


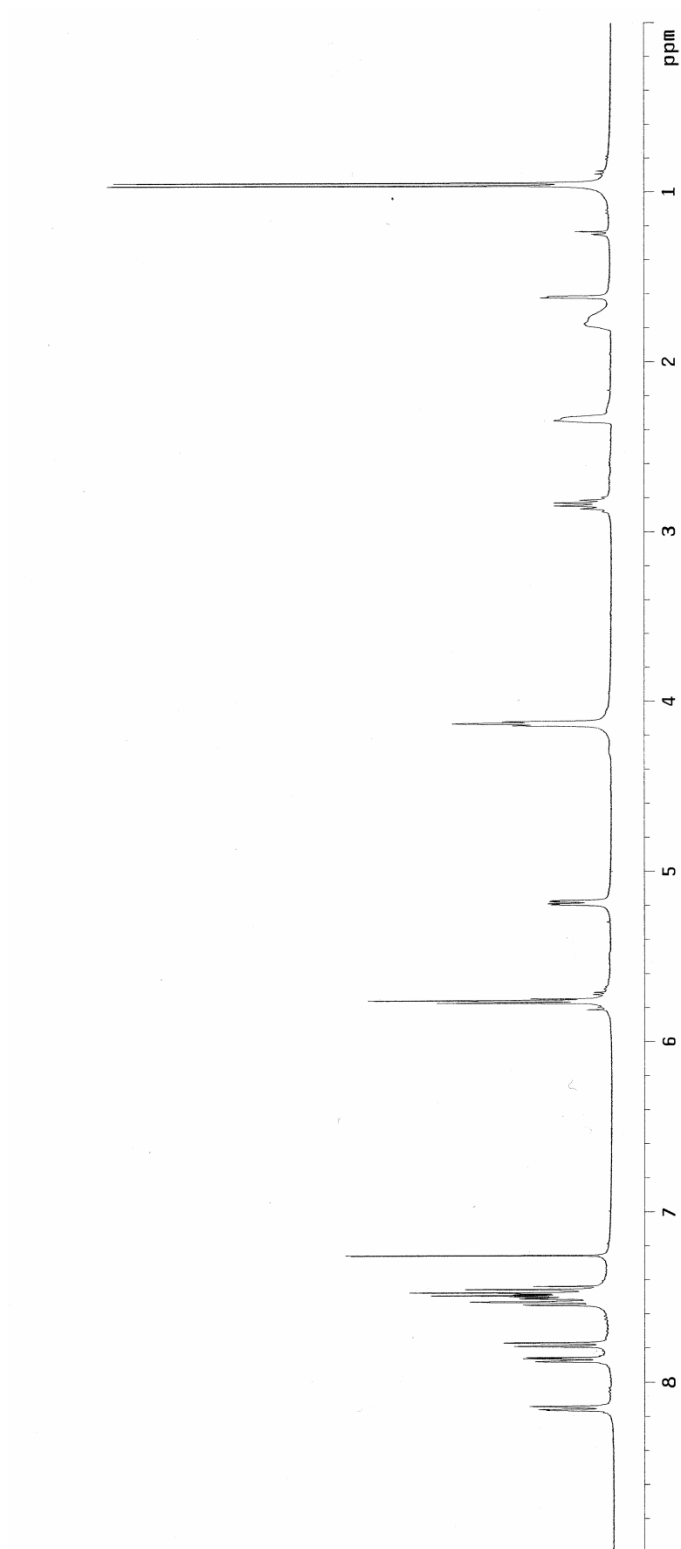
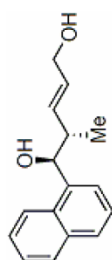


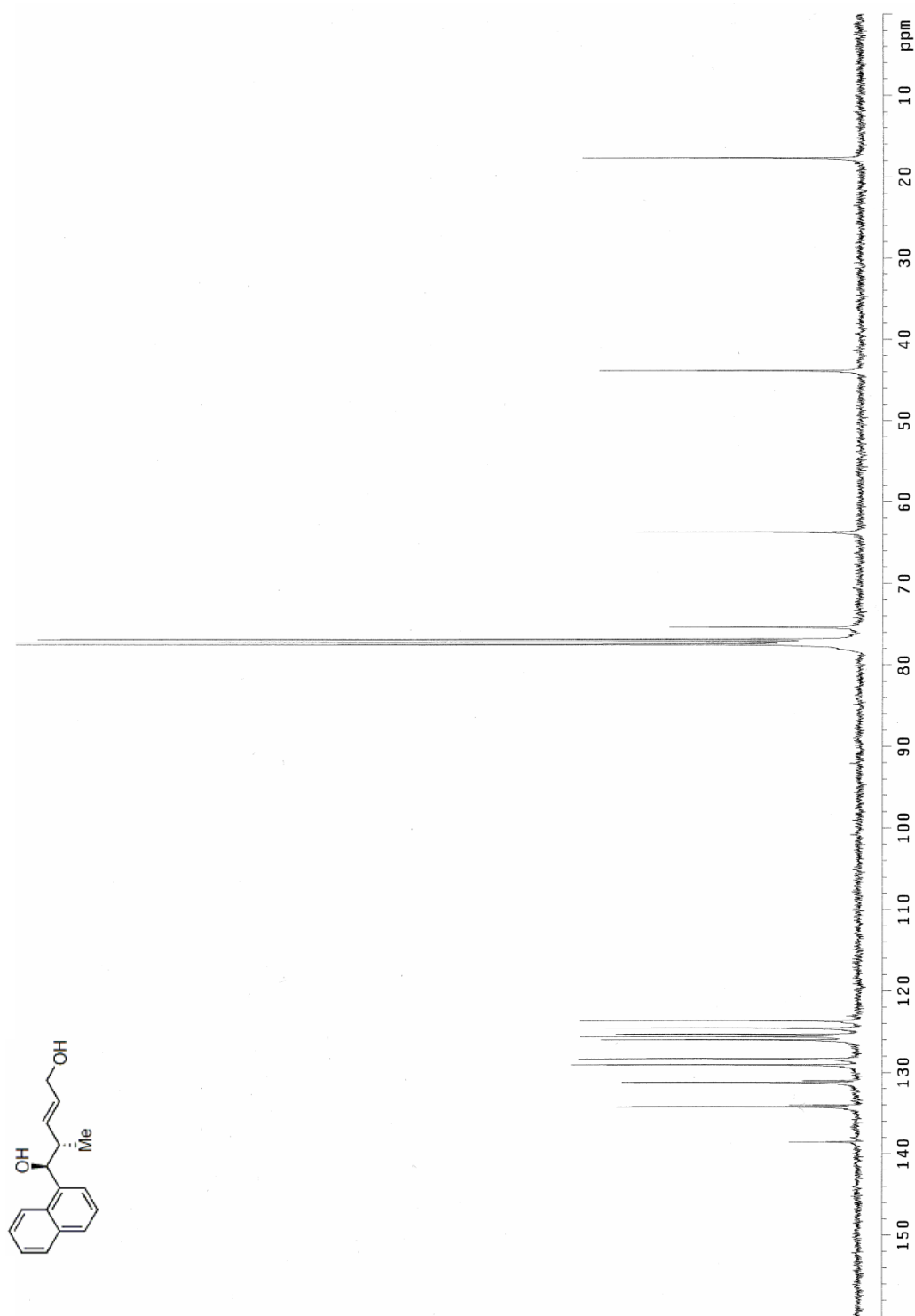


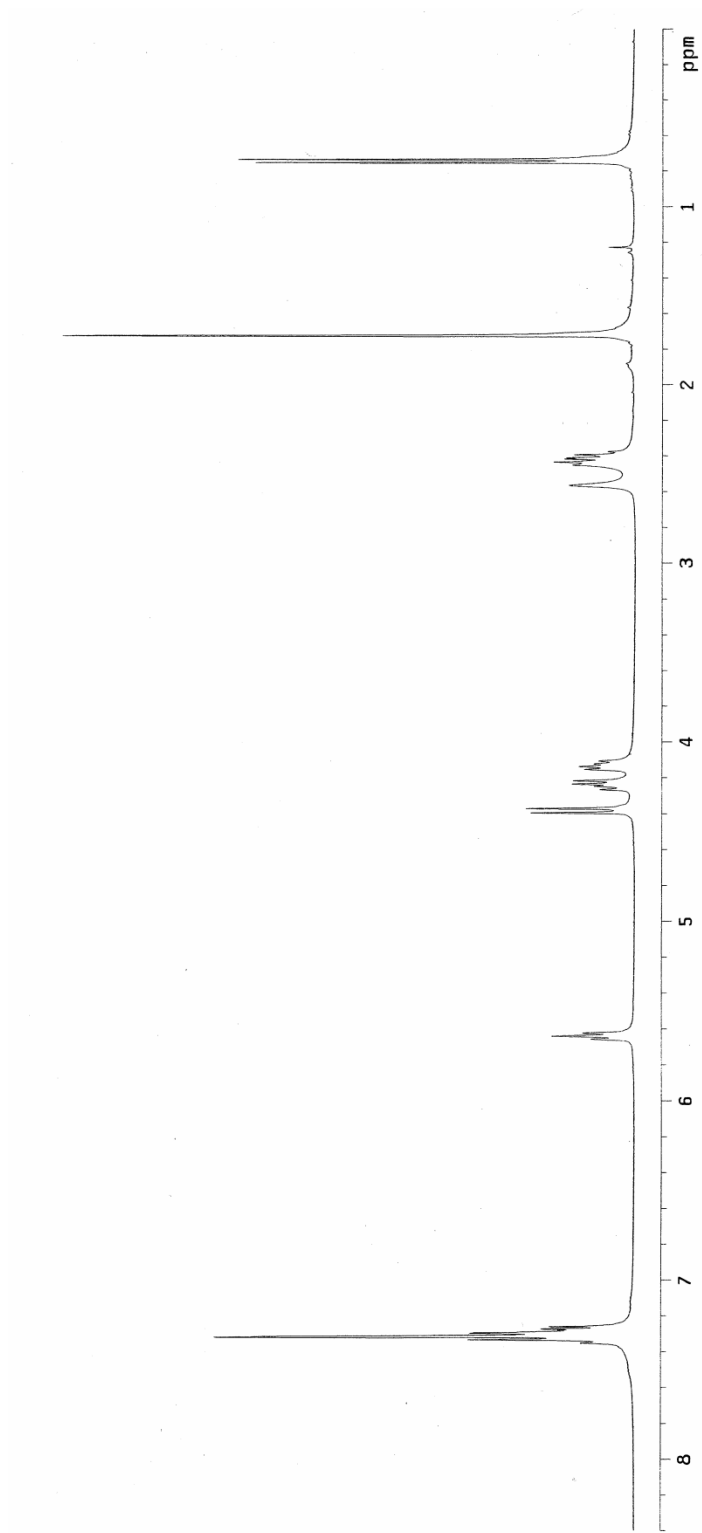
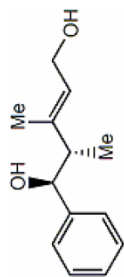


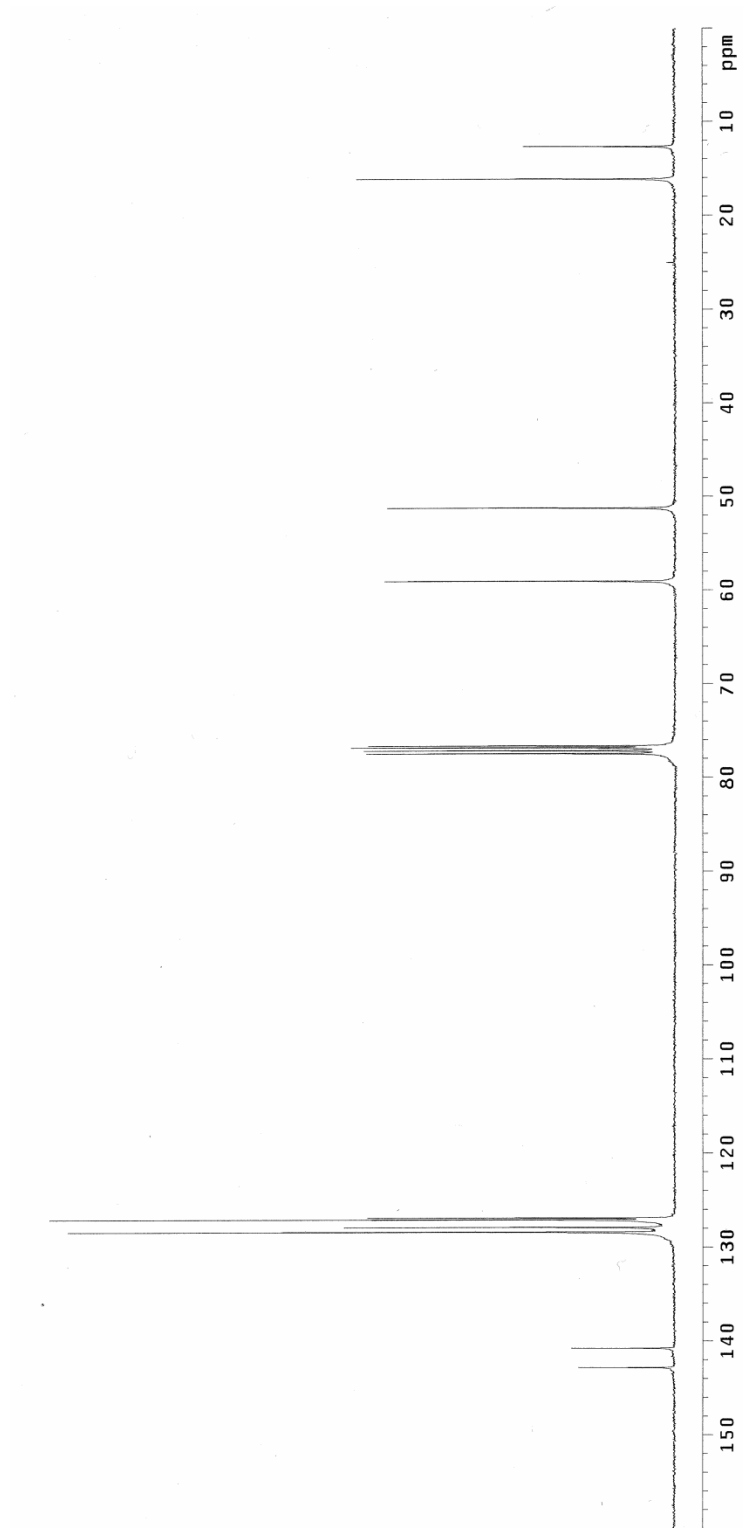
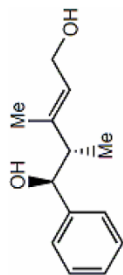


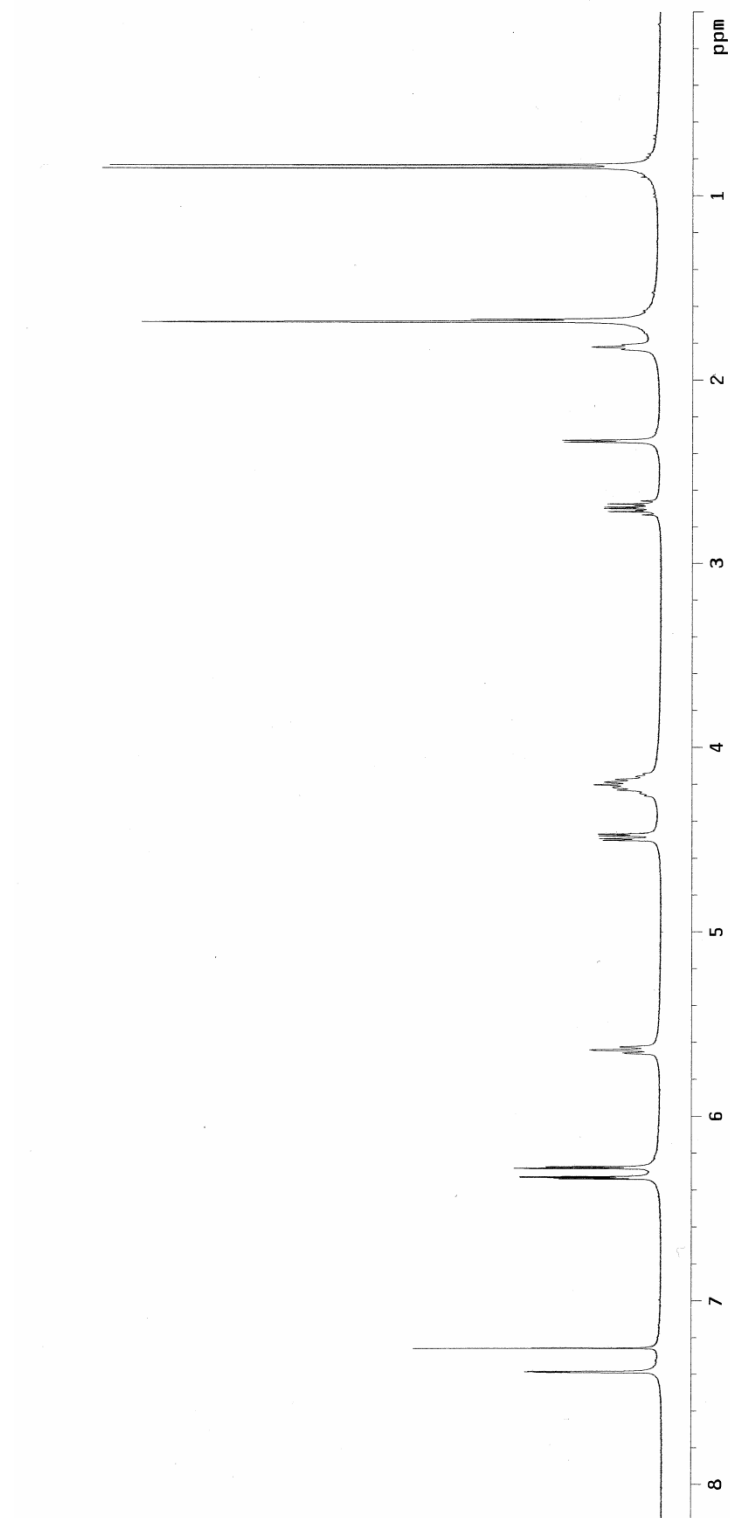
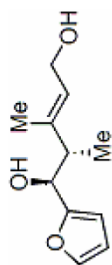


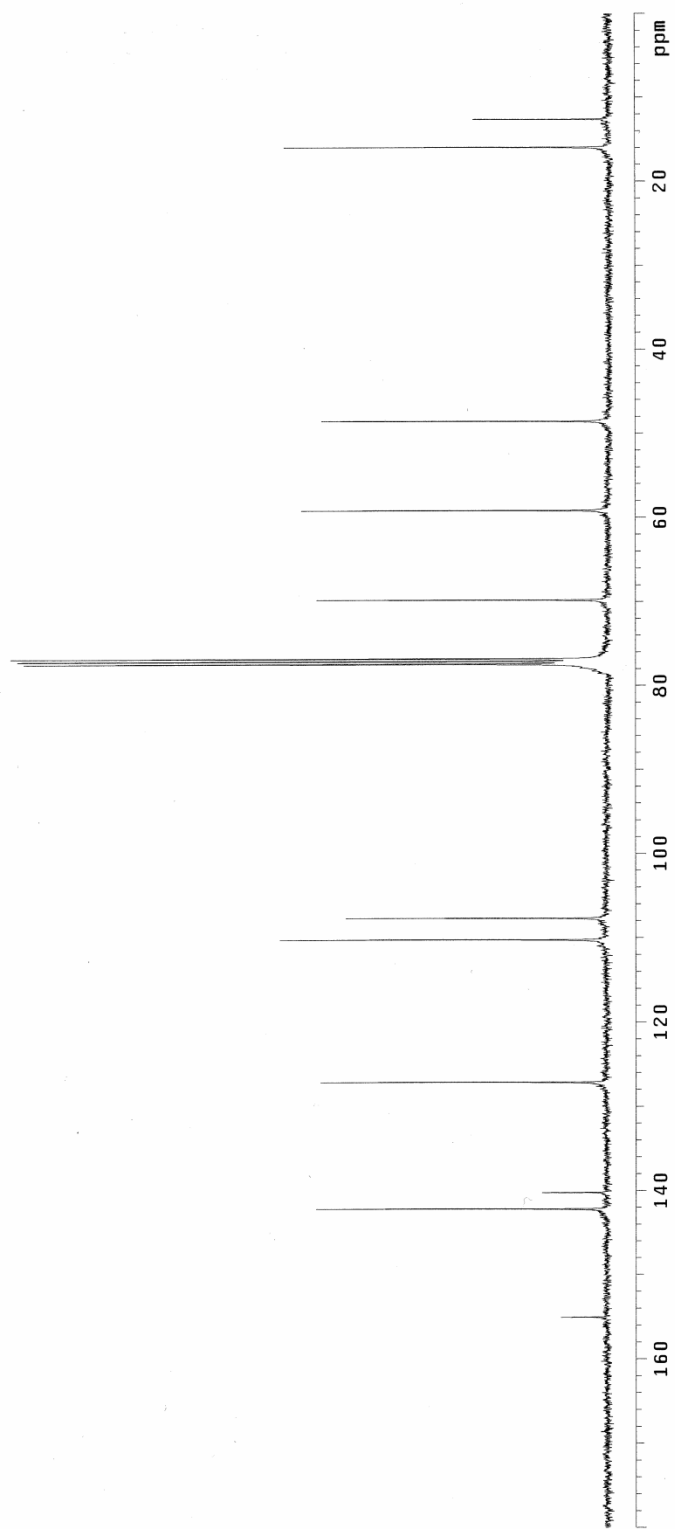
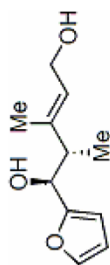


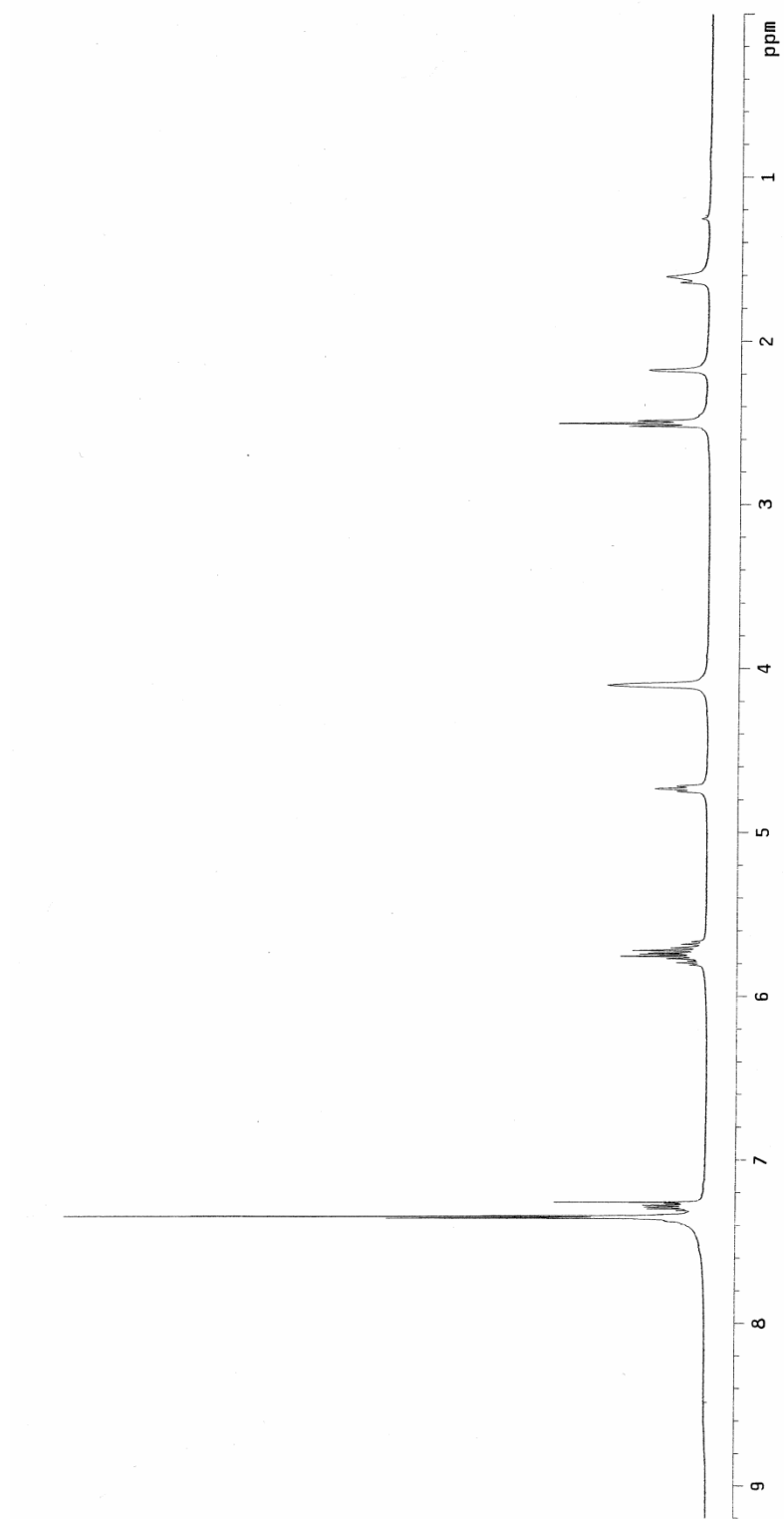
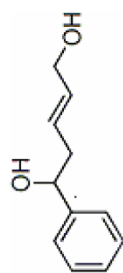


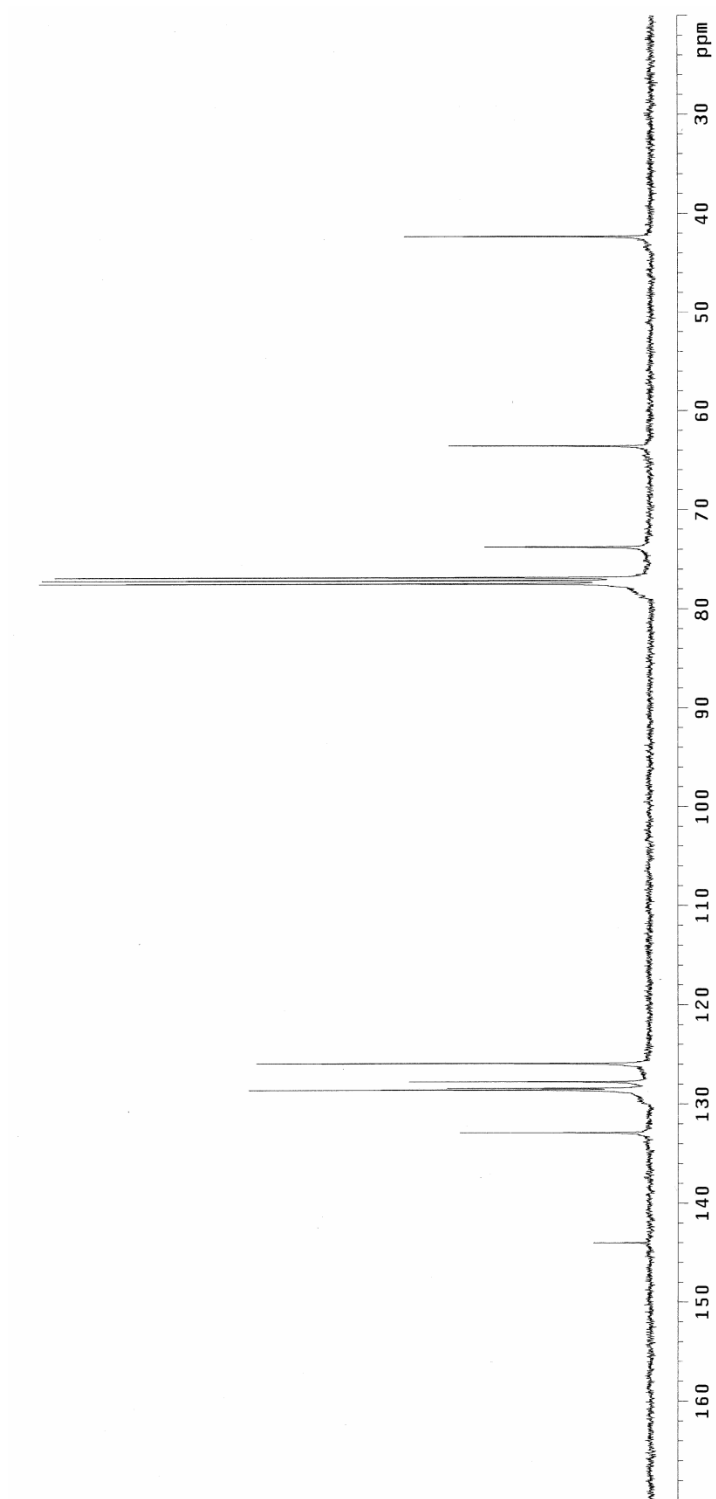
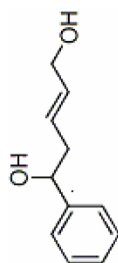


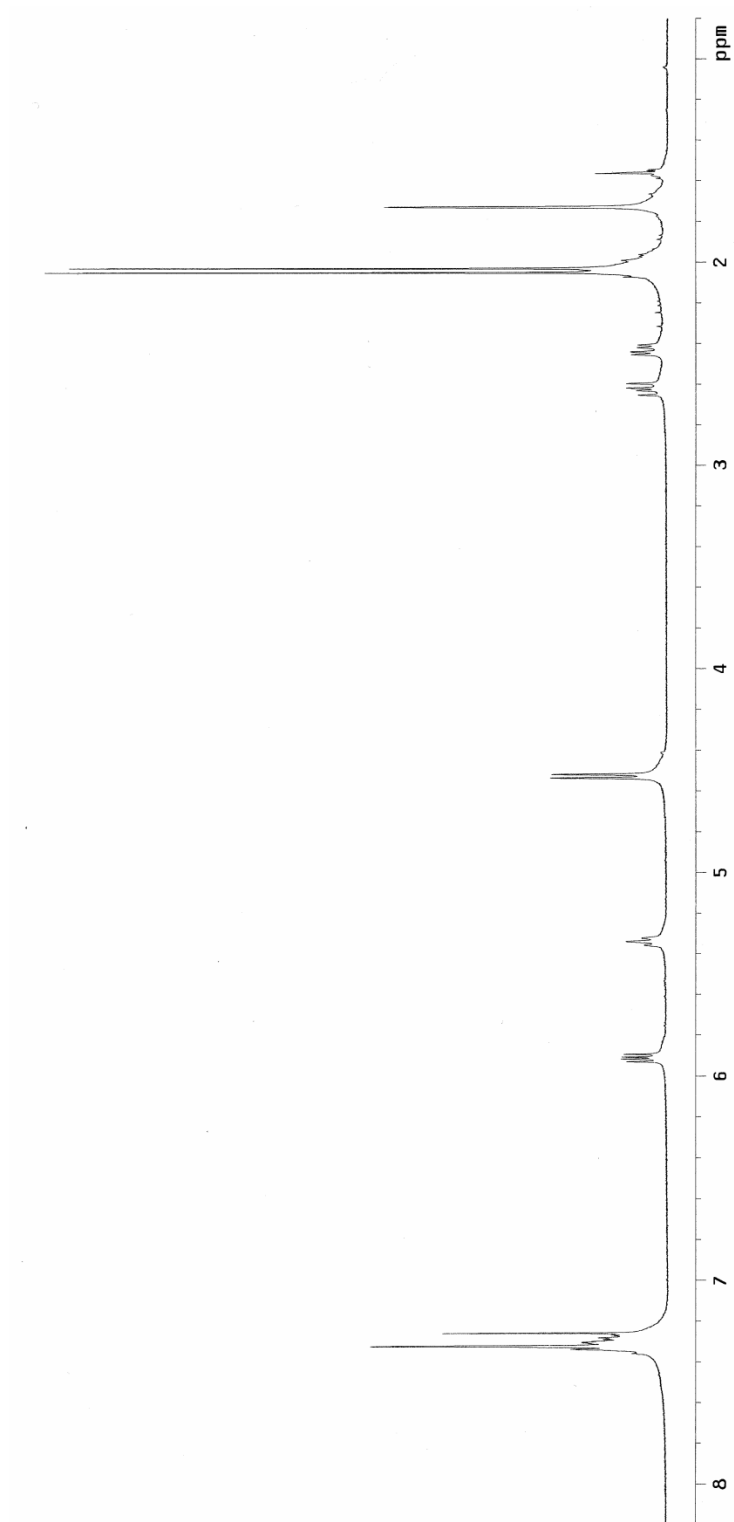
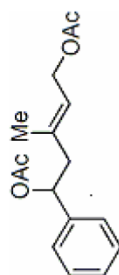


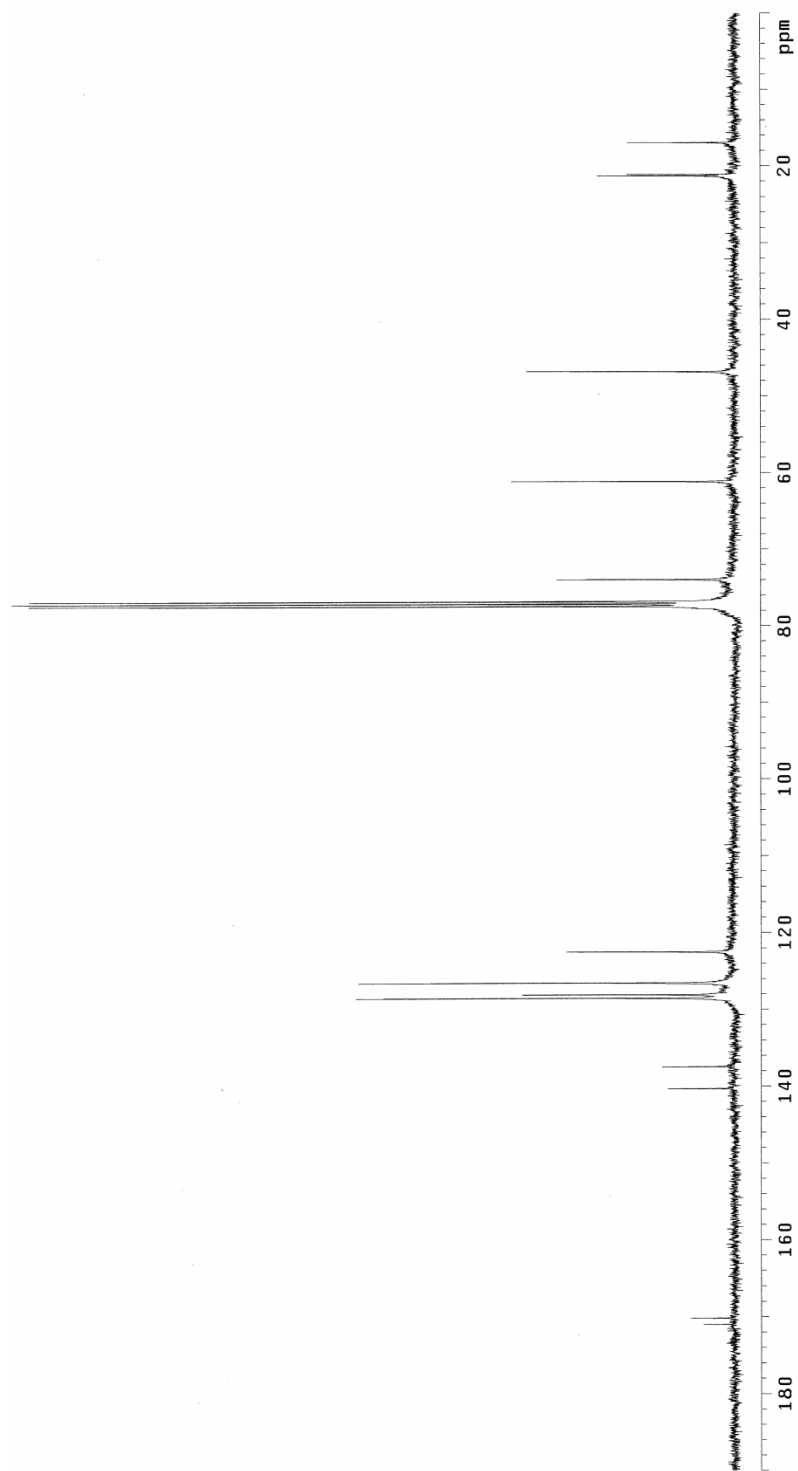
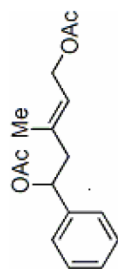


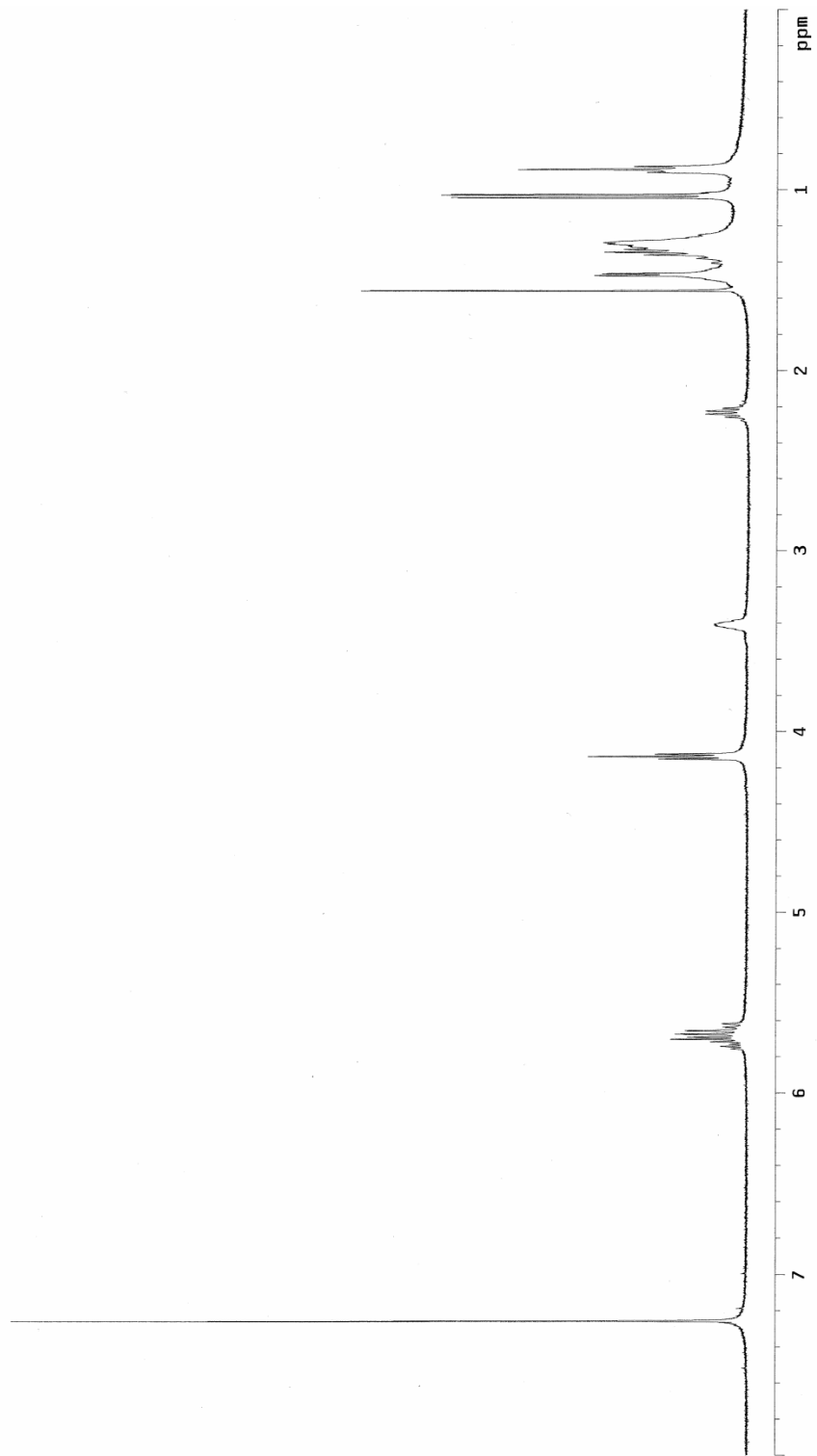
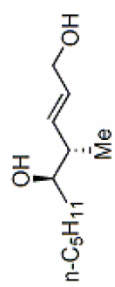


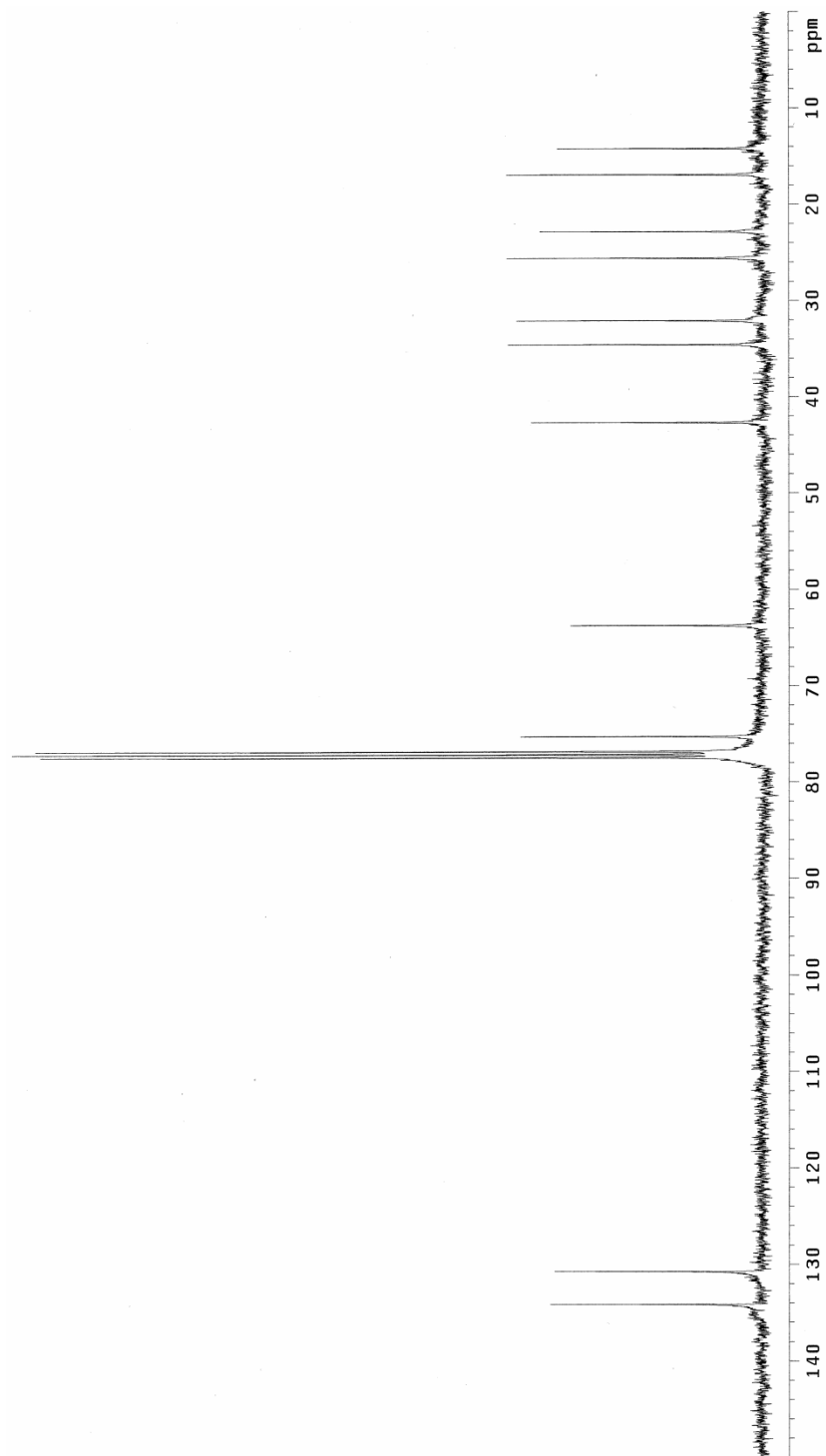
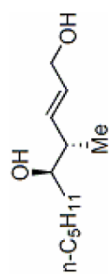


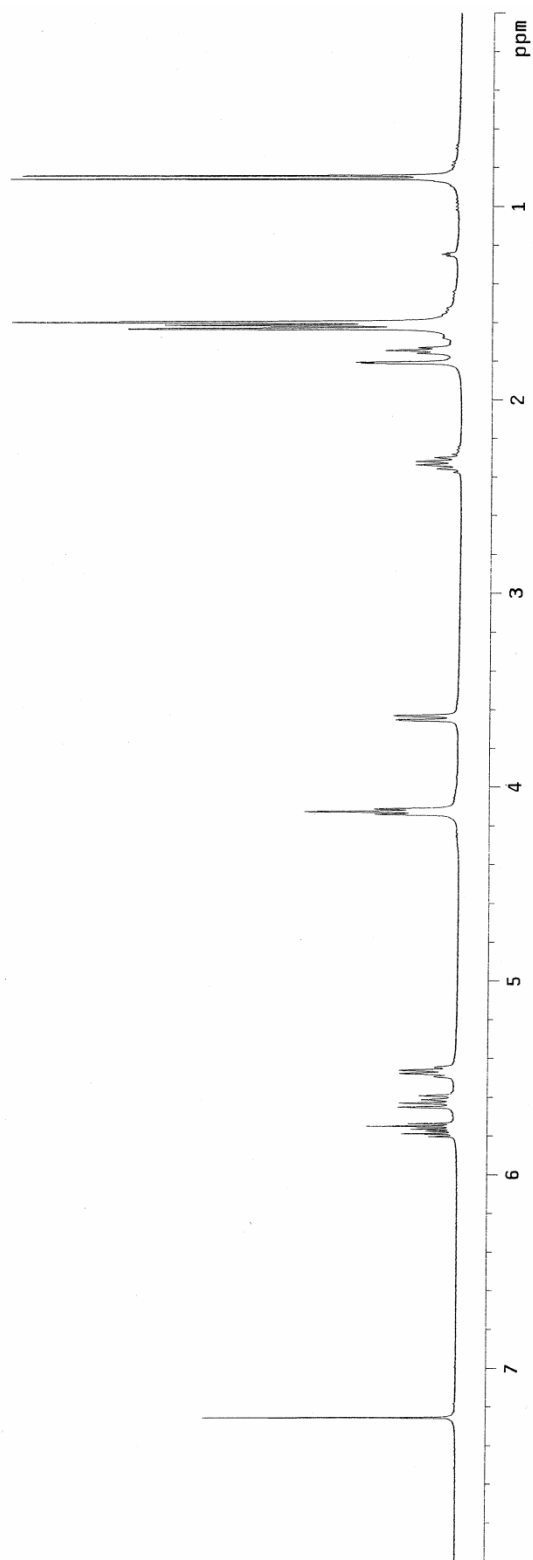
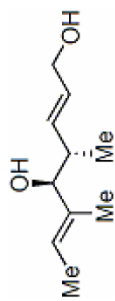


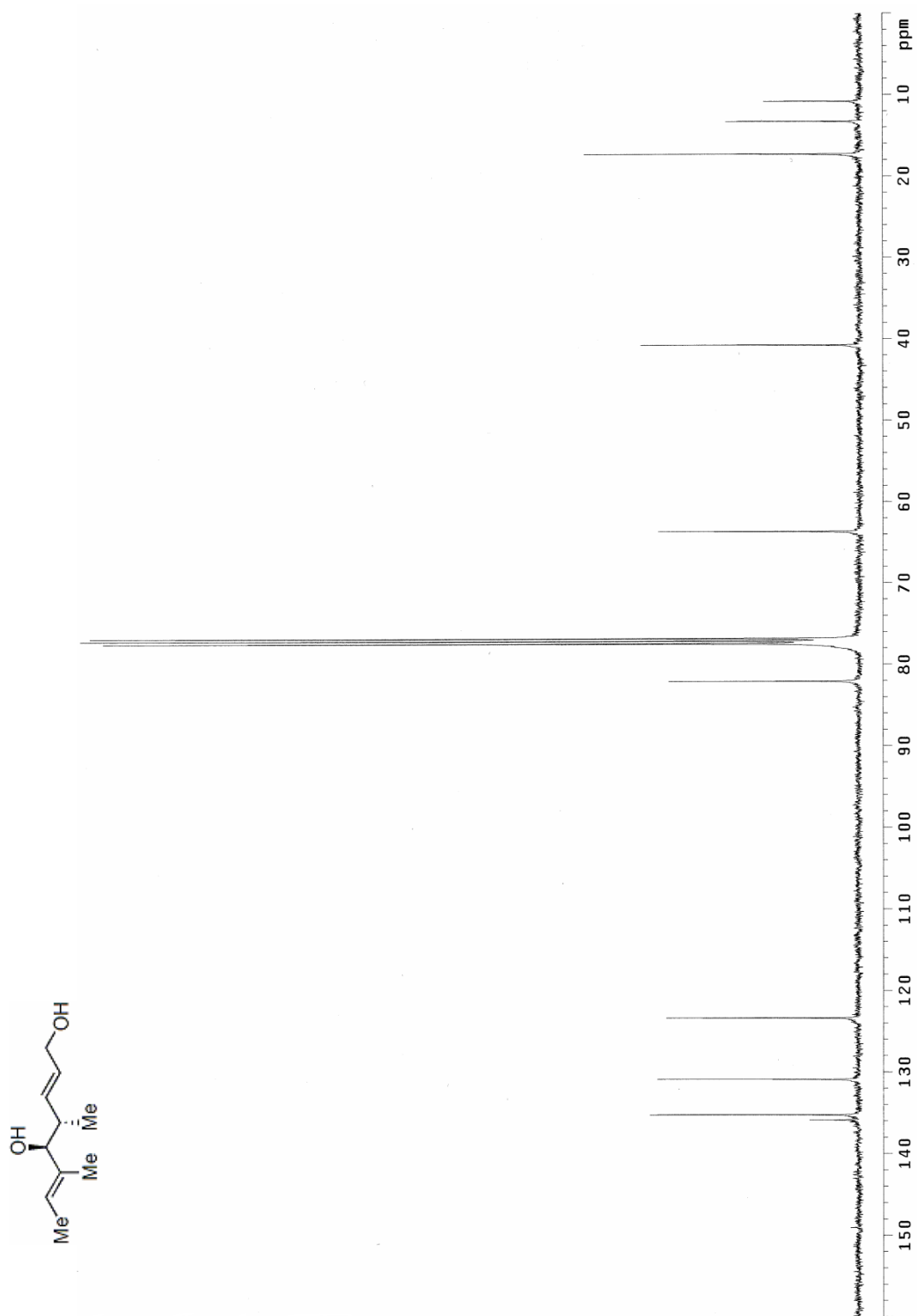


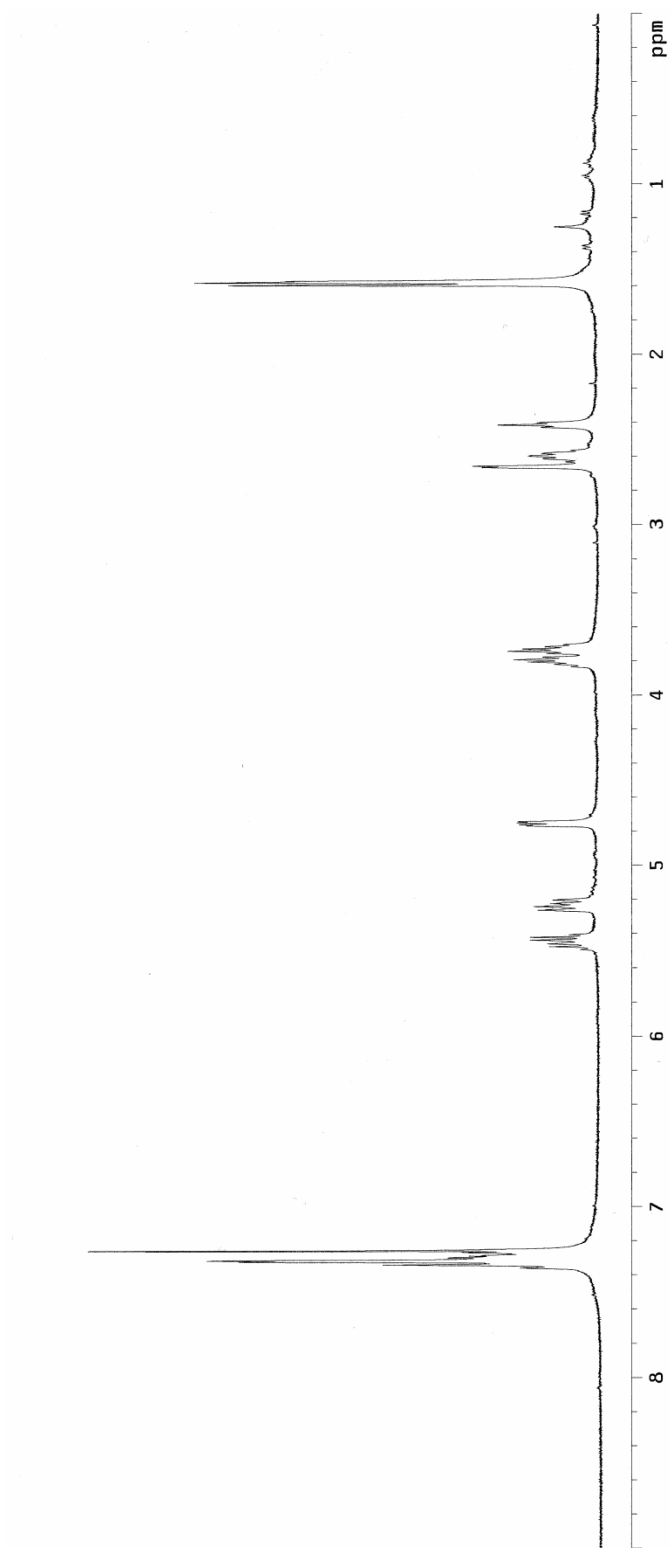
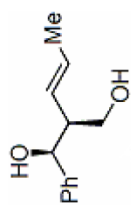


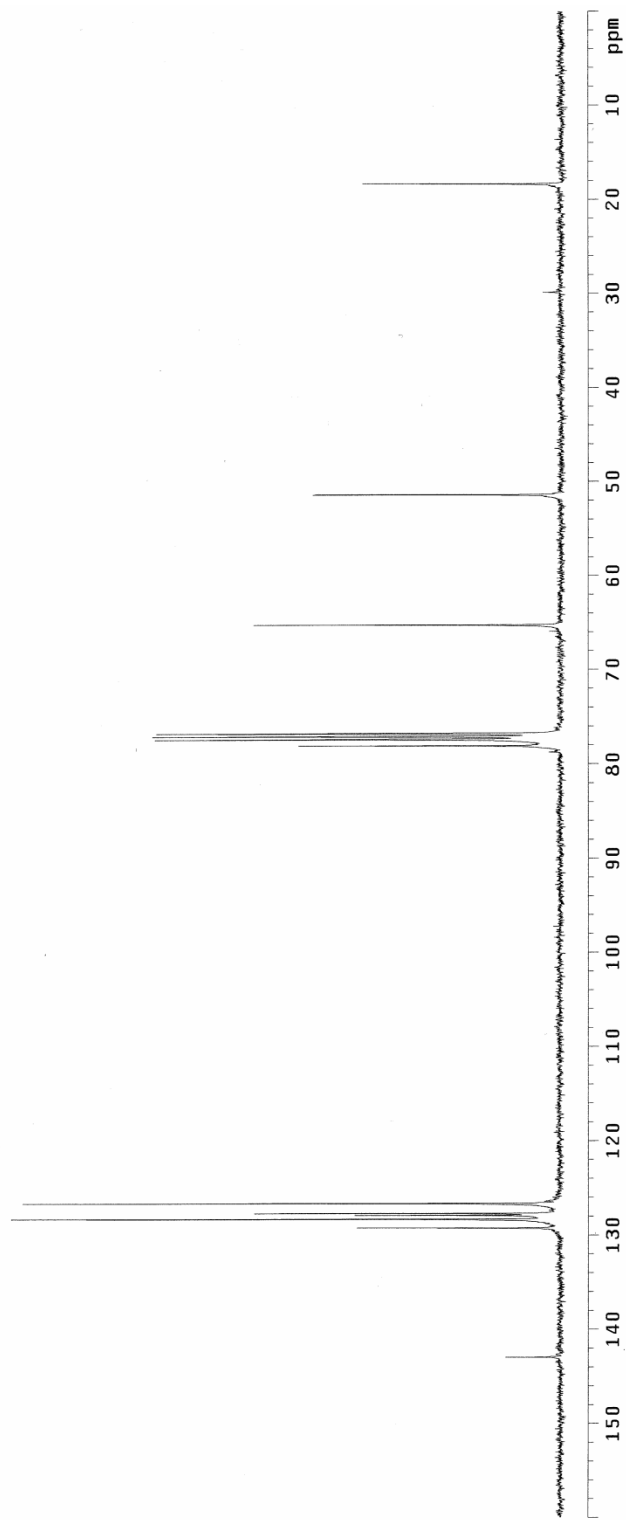
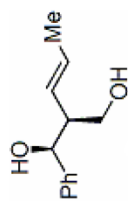


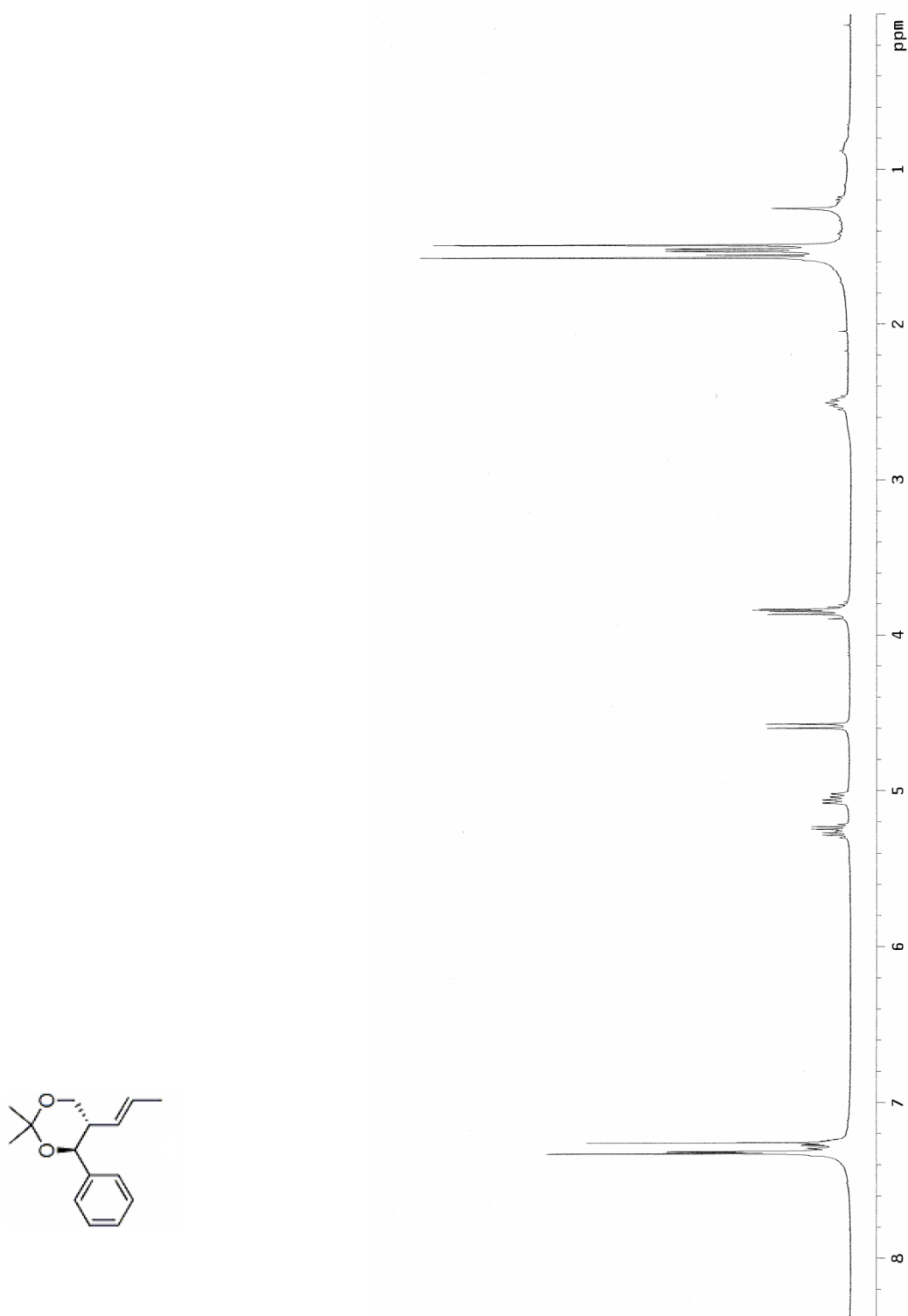


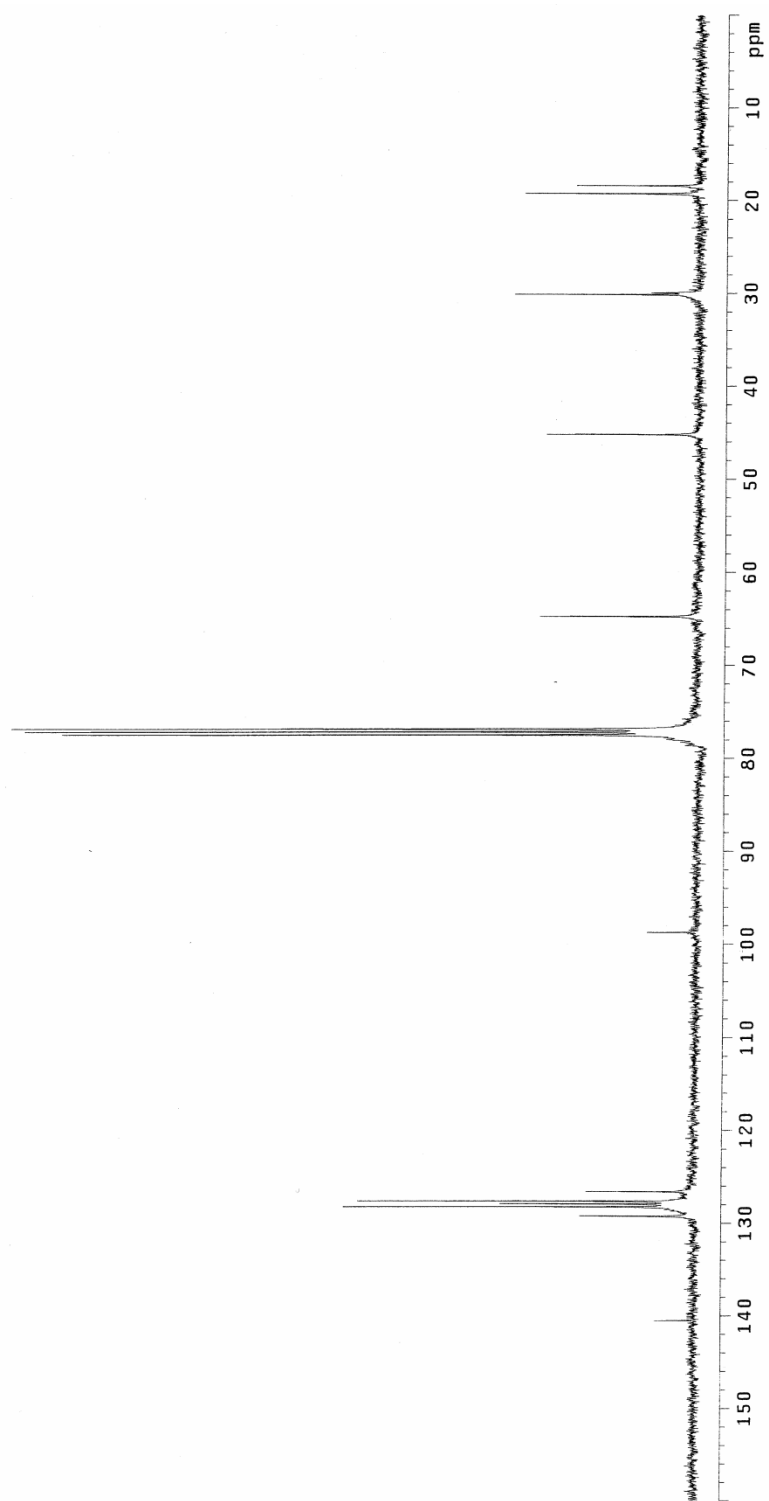
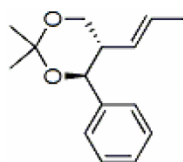


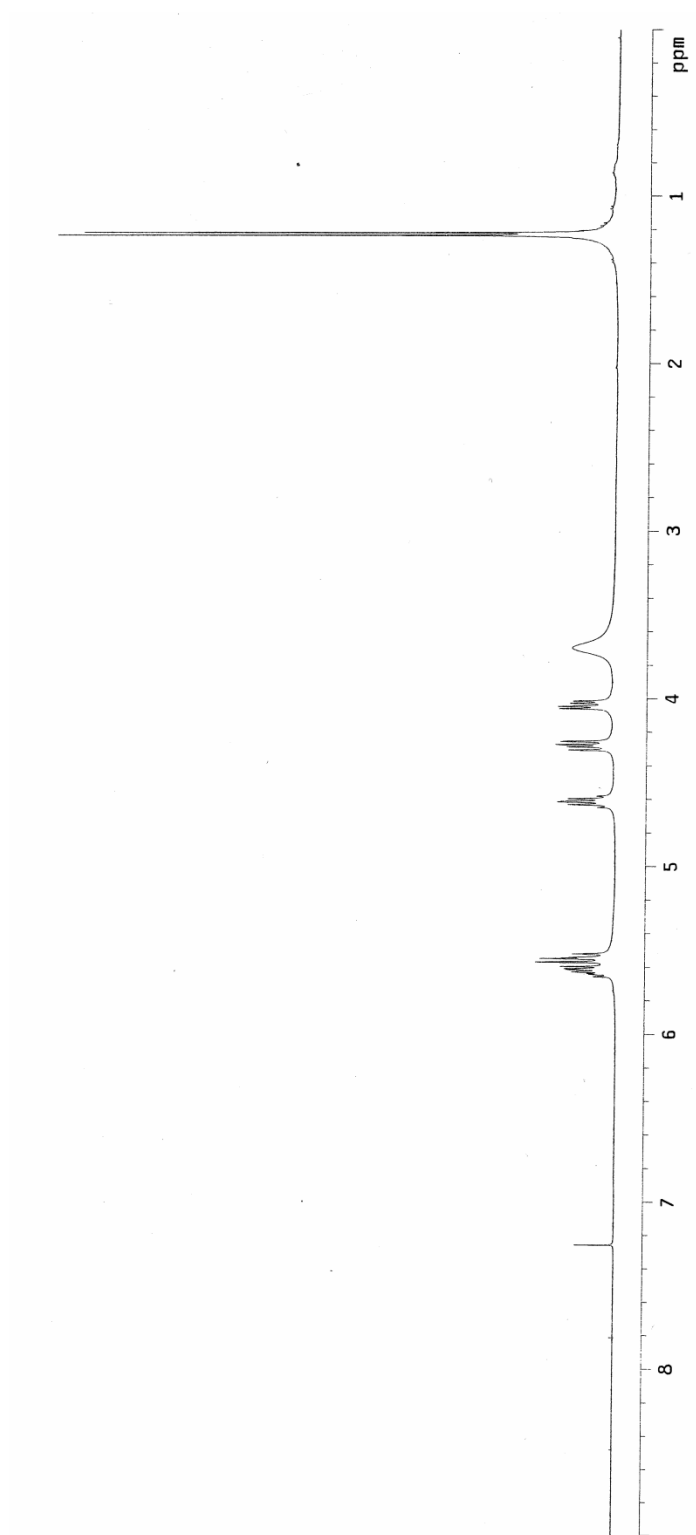
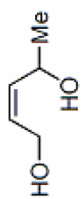


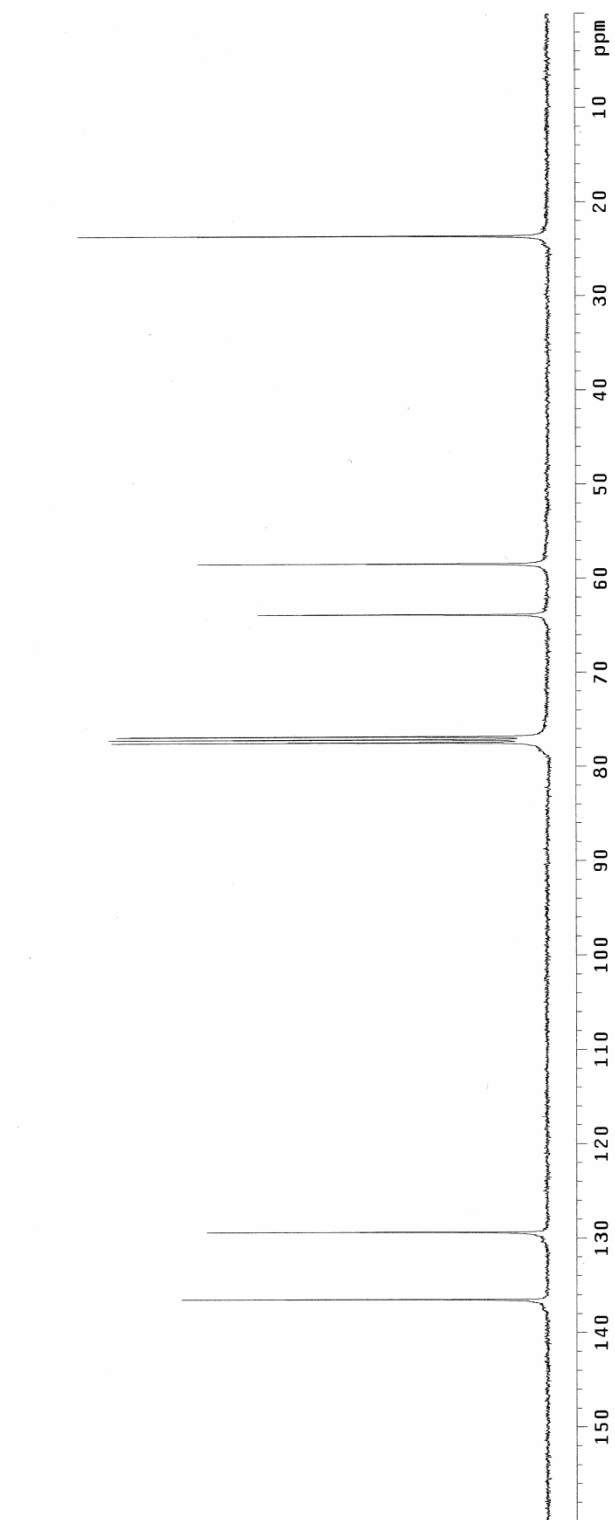
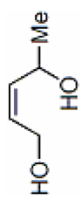


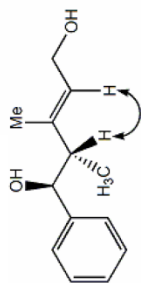
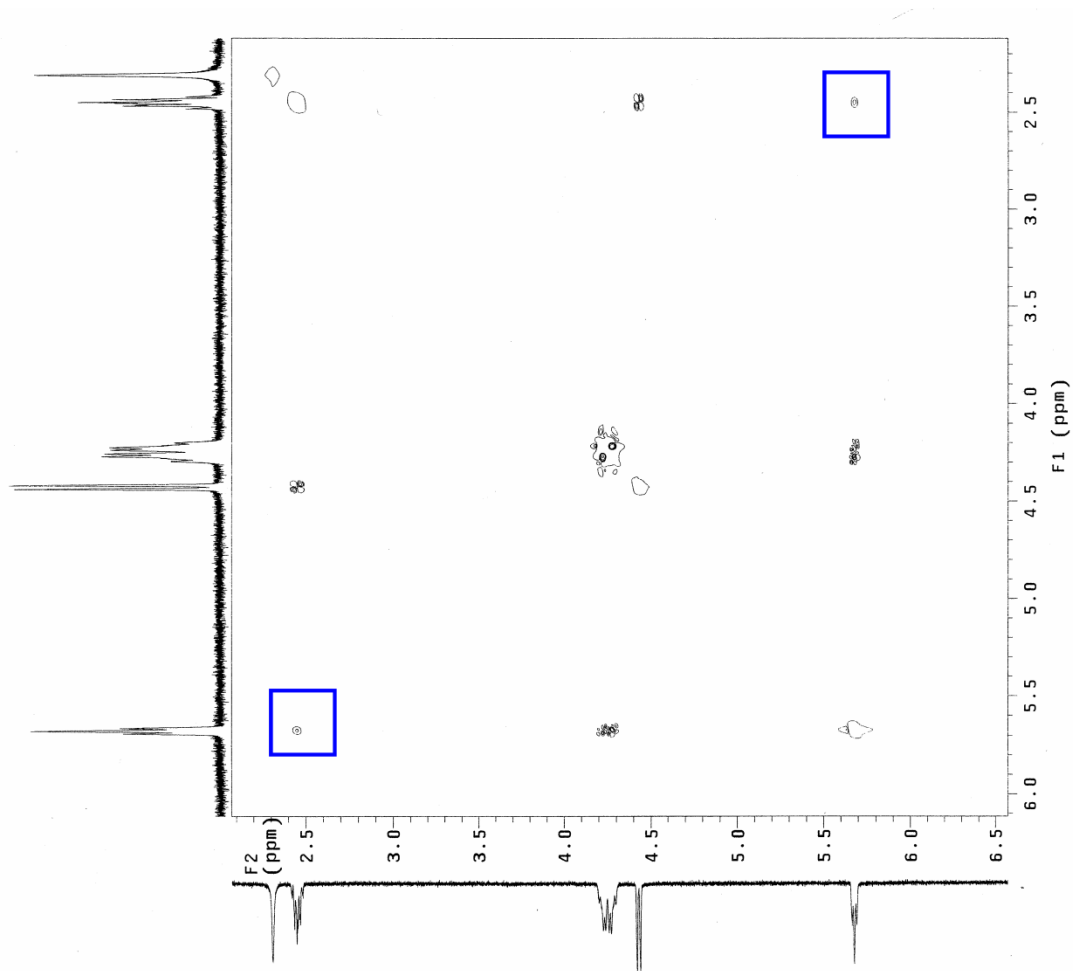


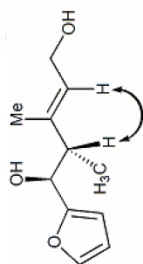
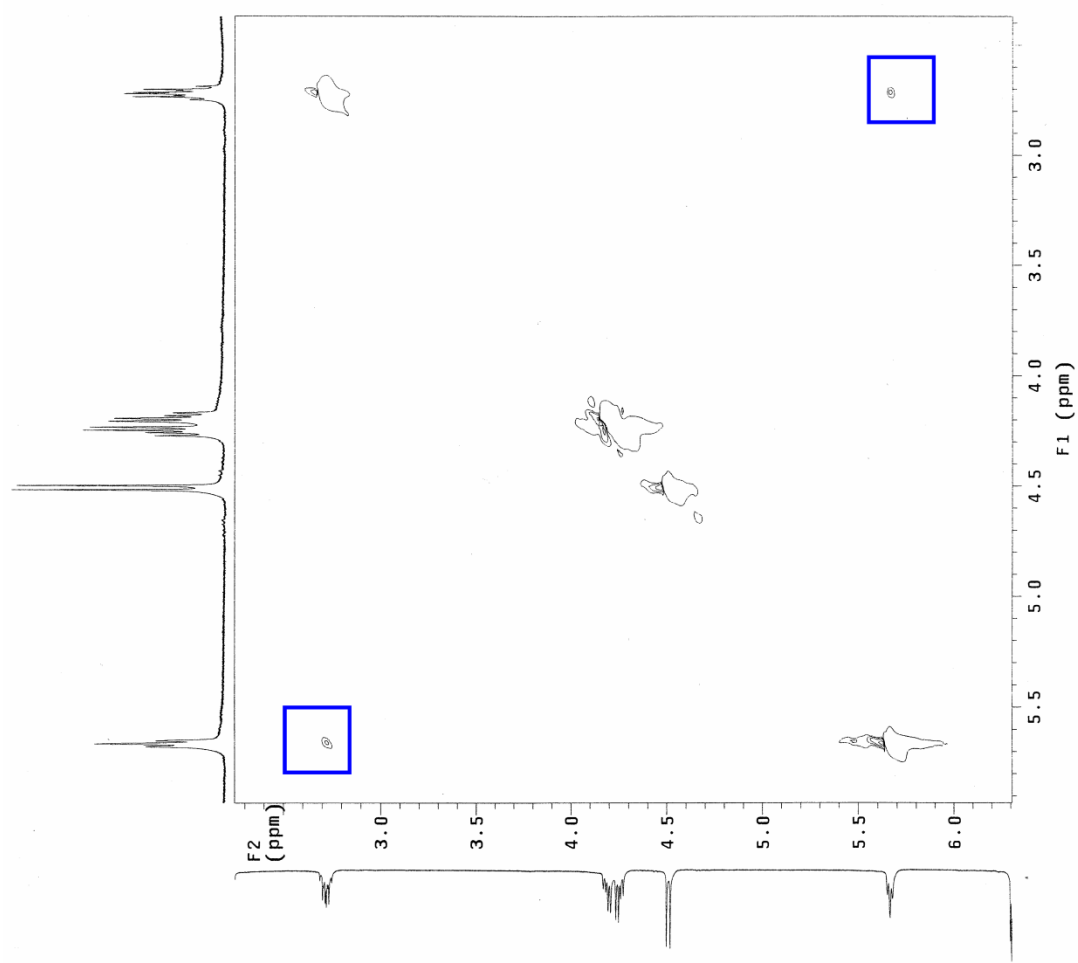


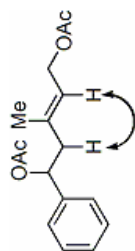
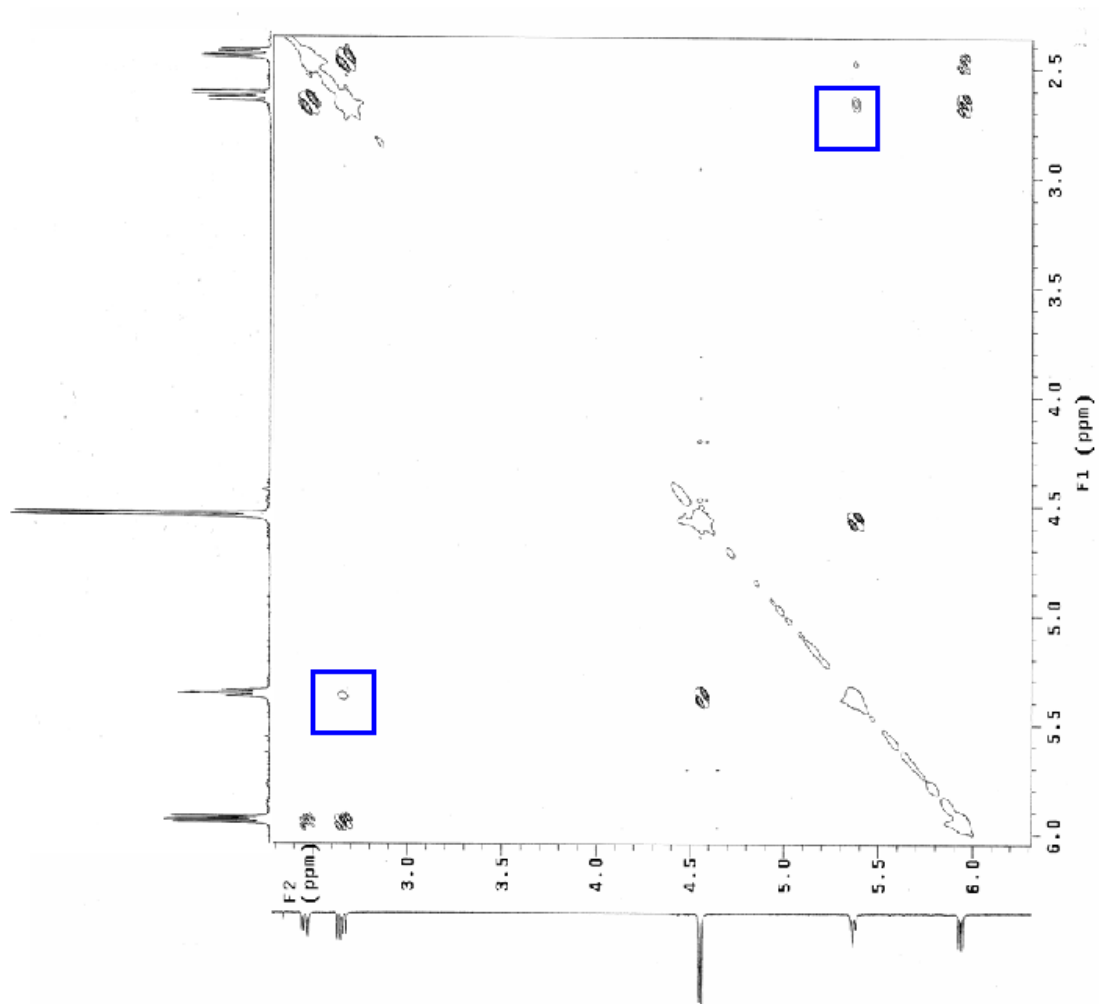












Chapter 3. Ligand Effects on the Nickel-Catalyzed Borylative Coupling

Reactions of Aldehydes and Dienes

3.1. Introduction

3.1.1. Nickel-Catalyzed Reductive Coupling Reactions

Among various types of multicomponent coupling reactions in organic chemistry,¹ catalytic reductive multicomponent coupling reactions are the most relevant processes to our studies in terms of reaction mechanism. The catalytic reductive coupling reactions involving multiple coupling components have attracted a lot of attention and have been extensively explored for the last couple of decades,^{2,3,4} since these reactions allow a wide range of

¹ Two other types of multicomponent coupling reactions—catalytic bimetallic multicomponent coupling reactions and classical (and named) multicomponent coupling reactions—are presented in Chapters 1 and 2, respectively.

² For reviews, see: (a) Montgomery, J., "Nickel-Catalyzed Reductive Cyclizations and Couplings," *Angewandte Chemie International Edition* **2004**, *43*, 3890-3908. (b) Moslin, R. M.; Miller-Moslin, K.; Jamison, T. F., "Regioselectivity and Enantioselectivity in Nickel-Catalyzed Reductive Coupling Reactions of Alkynes," *Chemical Communications* **2007**, 4441-4449. (c) Montgomery, J., "Nickel-Catalyzed Cyclizations, Couplings, and Cycloadditions Involving Three Reactive Components," *Accounts of Chemical Research* **2000**, *33*, 467-473.

³ (a) Jeganmohan, M.; Cheng, C. H., "Cobalt- and Nickel-Catalyzed Regio- and Stereoselective Reductive Coupling of Alkynes, Allenes, and Alkenes with Alkenes," *Chemistry—A European Journal* **2008**, *14*, 10876-10886. (b) Iida, H.; Krische, M. In *Metal Catalyzed Reductive C–C Bond Formation*; Krische, M., Ed.; Springer Berlin Heidelberg, 2007; Vol. 279.

⁴ (a) Ikeda, S. i., "Nickel-Catalyzed Coupling of Carbonyl Compounds and Alkynes or 1, 3-Dienes: An Efficient Method for the Preparation of Allylic, Homoallylic, and Bishomoallylic Alcohols," *Angewandte Chemie International Edition* **2003**, *42*, 5120-5122. (b) Ikeda, S.-I., "Nickel-Catalyzed Intermolecular Domino Reactions," *Accounts of Chemical Research* **2000**, *33*, 511-519.

coupling reactions with multiple π components and organometallic reagents. In this process, various starting materials (e.g. carbonyl compounds, alkenes, alkynes, allenes, alkynes, alkenes, and epoxides) can be coupled in the presence of organometallic reagents leading to highly stereo- and regioselective product formation.

Some examples of these reactions include alkyne–alkyne coupling,^{5, 6} alkyne–alkene coupling,^{7, 8} alkene–alkene coupling,⁹ carbonyl–alkyne coupling,^{10, 11, 12} carbonyl–diene

⁵ For selected examples, see: (a) Lappert, M. F.; Nile, T. A.; Takahashi, S., "Homogeneous Catalysis : II. Ziegler Systems as Catalysts for Hydrosilylation," *Journal of Organometallic Chemistry* **1974**, *72*, 425-439. (b) Tamao, K.; Kobayashi, K.; Ito, Y., "Nickel(0)-Catalyzed Cyclization of 1,7-Diynes via Hydrosilation: One-Step Synthesis of 1,2-Dialkylidencyclohexanes with a (Z)-Vinylsilane Moiety," *Journal of the American Chemical Society* **1989**, *111*, 6478-6480.

⁶ (a) Tamao, K.; Kobayashi, K.; Ito, Y., "Nickel(0)-Mediated Intramolecular Cyclizations of Enynes, Dienynes, Bis-Dienes, and Diynes," *Synlett* **1992**, *1992*, 539-546. (b) Sugimoto, M.; Matsuda, T.; Ito, Y., "Nickel-Catalyzed Silaborative Dimerization of Alkynes," *Organometallics* **1998**, *17*, 5233-5235.

⁷ For selected examples, see: (a) Ikeda, S.-i.; Sato, Y., "Synthesis of Stereodefined Enynes by the Nickel-Catalyzed Coupling Reaction of Alkynyltins, Alkynes, and Enones," *Journal of the American Chemical Society* **1994**, *116*, 5975-5976. (b) Ikeda, S.-I.; Kondo, K.; Sato, Y., "Nickel-Catalyzed Tandem Coupling of A,B-Enones, Alkynes, and Alkynyltins for the Regio- and Stereoselective Synthesis of Conjugated Enynes," *The Journal of Organic Chemistry* **1996**, *61*, 8248-8255. (c) Amarasinghe, K. K. D.; Chowdhury, S. K.; Heeg, M. J.; Montgomery, J., "Structure of an η^1 Nickel O-Enolate: Mechanistic Implications in Catalytic Enyne Cyclizations," *Organometallics* **2001**, *20*, 370-372.

⁸ For reviews, see: (a) Montgomery, J.; Amarasinghe, K. K.; Chowdhury, S. K.; Oblinger, E.; Seo, J.; Savchenko, A. V., "Nickel-Catalyzed Cyclizations of Alkynyl Enones and Alkynyl Enals," *Pure and Applied Chemistry* **2002**, *74*, 129-133. (b) Miller, K. M.; Molinaro, C.; Jamison, T. F., "Catalytic Reductive Carbon–Carbon Bond-Forming Reactions of Alkynes," *Tetrahedron: Asymmetry* **2003**, *14*, 3619-3625

⁹ For selected examples, see: (a) Nomura, N.; Jin, J.; Park, H.; RajanBabu, T. V., "The Hydrovinylation Reaction: A New Highly Selective Protocol Amenable to Asymmetric Catalysis," *Journal of the American Chemical Society* **1998**, *120*, 459-460. (b) Radetich, B.; RajanBabu, T. V., "Catalyzed Cyclization of A, Ω -Dienes: A Versatile Protocol for the Synthesis of Functionalized Carbocyclic and Heterocyclic Compounds," *Journal of the American Chemical Society* **1998**, *120*, 8007-8008. (c) Savchenko, A. V.; Montgomery, J., "Organozinc/Nickel(0)-Promoted Cyclizations of Bis-Enones," *The Journal of Organic Chemistry* **1996**, *61*, 1562-1563.

coupling,¹³ carbonyl–allene coupling,¹⁴ and alkyne–epoxide coupling.¹⁵ Furthermore, enantioselective variants have also been developed for some of these coupling reactions.¹⁶ In

¹⁰ For selected examples, see: (a) Oblinger, E.; Montgomery, J., "A New Stereoselective Method for the Preparation of Allylic Alcohols," *Journal of the American Chemical Society* **1997**, *119*, 9065-9066. (b) Takimoto, M.; Shimizu, K.; Mori, M., "Nickel-Promoted Alkylative or Arylative Carboxylation of Alkynes," *Organic Letters* **2001**, *3*, 3345-3347.

¹¹ (a) Mahandru, G. M.; Liu, G.; Montgomery, J., "Ligand-Dependent Scope and Divergent Mechanistic Behavior in Nickel-Catalyzed Reductive Couplings of Aldehydes and Alkynes," *Journal of the American Chemical Society* **2004**, *126*, 3698-3699. (b) Shimizu, K.; Takimoto, M.; Mori, M., "Novel Synthesis of Heterocycles Having a Functionalized Carbon Center via Nickel-Mediated Carboxylation: Total Synthesis of Erythrocarine," *Organic Letters* **2003**, *5*, 2323-2325.

¹² For more examples, see: (a) Huang, W.-S.; Chan, J.; Jamison, T. F., "Highly Selective Catalytic Intermolecular Reductive Coupling of Alkynes and Aldehydes," *Organic Letters* **2000**, *2*, 4221-4223. (b) Miller, K. M.; Luanphaisarnnont, T.; Molinaro, C.; Jamison, T. F., "Alkene-Directed, Nickel-Catalyzed Alkyne Coupling Reactions," *Journal of the American Chemical Society* **2004**, *126*, 4130-4131. (c) Patel, S. J.; Jamison, T. F., "Catalytic Three-Component Coupling of Alkynes, Imines, and Organoboron Reagents," *Angewandte Chemie International Edition* **2003**, *42*, 1364-1367.

¹³ For selected examples, see: (a) Shibata, K.; Kimura, M.; Shimizu, M.; Tamaru, Y., "Nickel-Catalyzed Intramolecular Homoallylation of ω -Dienyl Aldehyde," *Organic Letters* **2001**, *3*, 2181-2183. (b) Sato, Y.; Saito, N.; Mori, M., "Ni(0)-Catalyzed Bismetallative Cyclization of 1,3-Diene and a Tethered Aldehyde in the Presence of $\text{Bu}_3\text{SnSiMe}_3$," *Chemistry Letters* **2002**, *31*, 18-19. (c) Sato, Y.; Saito, N.; Mori, M., "A Novel Asymmetric Cyclization of ω -Formyl-1,3-Dienes Catalyzed by a Zerovalent Nickel Complex in the Presence of Silanes," *Journal of the American Chemical Society* **2000**, *122*, 2371-2372.

¹⁴ For selected examples, see: (a) Kang, S.-K.; Yoon, S.-K., "Cis-Stereoselective Nickel-Catalyzed Cyclization/Alkylation and Arylation Reactions of Allenyl-Aldehydes and -Ketones with Organozinc Reagents," *Chemical Communications* **2002**, 2634-2635. (b) Montgomery, J.; Song, M., "Preparation of Homoallylic Alcohols by Nickel-Catalyzed Cyclizations of Allenyl Aldehydes," *Organic Letters* **2002**, *4*, 4009-4011.

¹⁵ For selected examples, see: (a) Molinaro, C.; Jamison, T. F., "Nickel-Catalyzed Reductive Coupling of Alkynes and Epoxides," *Journal of the American Chemical Society* **2003**, *125*, 8076-8077. (b) Woodin, K. S.; Jamison, T. F., "Total Synthesis of Pumiliotoxins 209F and 251D via Late-Stage, Nickel-Catalyzed Epoxide-Alkyne Reductive Cyclization," *The Journal of Organic Chemistry* **2007**, *72*, 7451-7454. (c) O'Brien, K. C.; Colby, E. A.; Jamison, T. F., "Synthesis of C13–C22 of Amphidinolide T2 Via Nickel-Catalyzed Reductive Coupling of an Alkyne and a Terminal Epoxide," *Tetrahedron* **2005**, *61*, 6243-6248

¹⁶ For selected examples, see: (a) Ikeda, S.-I.; Cui, D.-M.; Sato, Y., "Nickel-Catalyzed Asymmetric Multiple-Component Tandem Coupling. Effects of Simple Monodentate Oxazolines as Chiral Ligands," *Journal of the American Chemical Society* **1999**, *121*, 4712-4713. (b) Colby, E. A.; Jamison, T. F., "P-Chiral,

addition, synthetic applications of the methods toward total synthesis of biologically-active molecules have also been reported.^{17, 18, 19}

3.1.2. Mechanistic Perspectives

Nickel-catalyzed dimerizations and oligomerizations of alkynes and dienes have one of the longest histories in organic synthesis.²⁰ Since the pioneering work of Reppe²¹ and

Monodentate Ferrocenyl Phosphines, Novel Ligands for Asymmetric Catalysis," *The Journal of Organic Chemistry* **2002**, *68*, 156-166.

¹⁷ For selected examples, see: (a) Sato, Y.; Saito, N.; Mori, M., "Stereoselective Synthesis of Nitrogen-Containing Heterocycles via Nickel-Catalyzed Cyclization of 1,3-Diene and Aldehyde: Formal Total Synthesis of (-)-Elaeokanine C," *Tetrahedron* **1998**, *54*, 1153-1168. (b) Sato, Y.; Takimoto, M.; Mori, M., "Total Synthesis of Prostaglandin F₂α via Nickel-Promoted Stereoselective Cyclization of 1,3-Diene and Aldehyde," *Synlett* **1997**, 1997, 734-736.

¹⁸ (a) Seo, J.; Fain, H.; Blanc, J.-B.; Montgomery, J., "Nickel-Catalyzed Cyclizations of Enolate Equivalents: Application to the Synthesis of Angular Triquinanes," *The Journal of Organic Chemistry* **1999**, *64*, 6060-6065. (b) Sato, Y.; Takimoto, M.; Mori, M., "Total Synthesis of Prostaglandin F₂ Using Nickel-Catalyzed Stereoselective Cyclization of 1,3-Diene and Tethered Aldehyde via Transmetalation of Nickelacycle with Diisobutylaluminum Acetylacetonate," *Chemical & Pharmaceutical Bulletin* **2000**, *48*, 1753-1760.

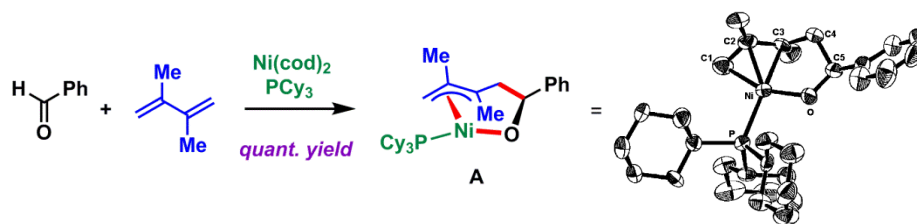
¹⁹ For more examples, see: (a) Colby, E. A.; O'Brien, K. C.; Jamison, T. F., "Synthesis of Amphidinolide T1 via Catalytic, Stereoselective Macrocyclization," *Journal of the American Chemical Society* **2004**, *126*, 998-999. (b) Trenkle, J. D.; Jamison, T. F., "Macrocyclization by Nickel-Catalyzed, Ester-Promoted, Epoxide-Alkyne Reductive Coupling: Total Synthesis of (-)-Gloeosporone," *Angewandte Chemie International Edition* **2009**, *48*, 5366-5368.

²⁰ For reviews, see: a) Reppe, W.; v. Kutepow, N.; Magin, A., "Cyclization of Acetylenic Compounds," *Angewandte Chemie International Edition* **1969**, *8*, 727-733. (b) Wilke, G., "Contributions to Organo-Nickel Chemistry," *Angewandte Chemie International Edition* **1988**, *27*, 185-206.

²¹ (a) Reppe, W.; Schlichting, O.; Klager, K.; Toepel, T., "Cyclisierende Polymerisation Von Acetylen I Über Cyclooctatetraen," *Justus Liebigs Annalen der Chemie* **1948**, *560*, 1-92. (b) Reppe, W.; Vetter, H., "Carbonylierung VI. Synthesen Mit Metallcarbonylwasserstoffen," *Justus Liebigs Annalen der Chemie* **1953**, *582*, 133-161.

Wilke,²² nickel catalysis has been investigated in various contexts and its mechanisms have also been explored. Regarding the catalytic reductive multicomponent coupling, the generally proposed mechanism suggests that it involves a metallocyclic intermediate, which is formed by oxidative cyclization of the π components and the catalyst. As the evidence for this hypothesis, a nickelacyclic intermediate (**A**) of Ni-catalyzed aldehyde–diene coupling was isolated and analyzed with X-ray crystallography by Ogoshi and co-workers (Scheme 3.1).²³ This nickelacyclic complex was prepared from benzaldehyde, a 1,3-butadiene, Ni(cod)₂, and a phosphine ligand in deuterated THF. The result suggests that the reaction proceeds with oxidative cyclization giving the allylalkoxynickel complex as a key intermediate.

Scheme 3.1 Isolated Nickelacyclic Intermediate



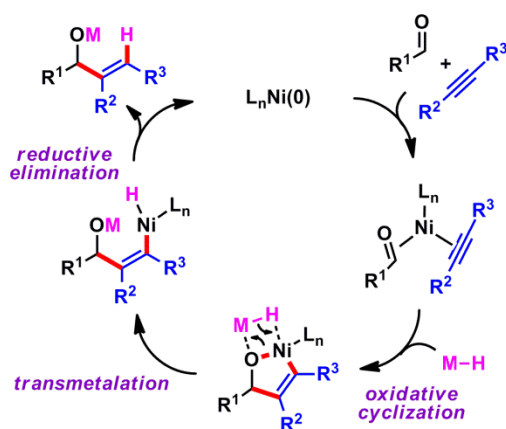
Several mechanistic investigations have been performed to probe more details of this process. In one recent study, Jamison and Houk proposed a mechanistic pathway and corresponding intermediates for the coupling of aldehyde and alkyne, in which the energies

²² (a) Wilke, G., "Neues Über Cyclische Butadienoligomere," *Angewandte Chemie-International Edition* **1960**, 72, 581-582. (b) Bogdanović, B.; Kröner, M.; Wilke, G., "Übergangsmetallkomplexe, I. Olefin-Komplexe Des Nickels(0)," *Justus Liebigs Annalen der Chemie* **1966**, 699, 1-23.

²³ Ogoshi, S.; Tonomori, K.-I.; Oka, M.-A.; Kurosawa, H., "Reversible Carbon–Carbon Bond Formation between 1,3-Dienes and Aldehyde or Ketone on Nickel(0)," *Journal of the American Chemical Society* **2006**, 128, 7077-7086.

of each intermediate were computed by DFT calculations (Scheme 3.2).²⁴ In this report, they have suggested that the oxidative cyclization step, which leads to formation of the nickeladihydrofuran intermediate, is the rate-determining step. Also, the details of the transition state of this step (oxidative cyclization) including orbital interactions have been examined.

Scheme 3.2 Catalytic Cycle for Reductive Coupling Reactions



In the following sections, some representative examples of these reductive coupling reactions will be introduced; more specifically, nickel-catalyzed coupling reactions of two π -components and an organometallic reagent will be presented.

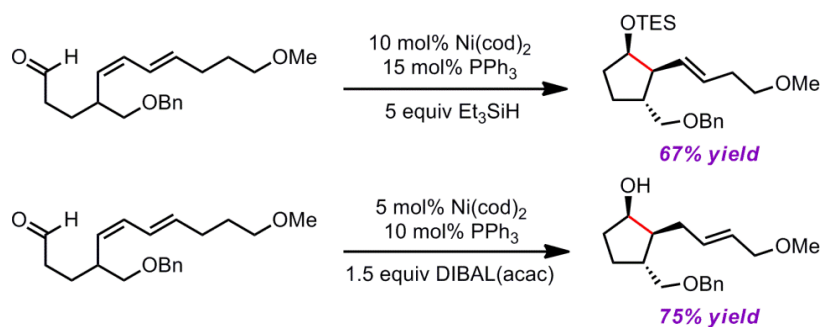
²⁴ McCarren, P. R.; Liu, P.; Cheong, P. H.-Y.; Jamison, T. F.; Houk, K. N., "Mechanism and Transition-State Structures for Nickel-Catalyzed Reductive Alkyne–Aldehyde Coupling Reactions," *Journal of the American Chemical Society* **2009**, *131*, 6654-6655.

3.2. Background

3.2.1. Reductive Coupling of Aldehyde–Diene

The Mori group has extensively investigated Ni-catalyzed reductive coupling reactions involving aldehydes, dienes and reducing agents.^{25, 26} Some intramolecular variants of this type of coupling reaction are described in Scheme 3.3. In these studies, a dienal and triethylsilane or DIBAL were coupled in the presence of a Ni(0)-phosphine catalyst. It was observed that the product selectivity (*i.e.* formation of homoallylic alcohol vs. bishomoallylic alcohol) was dependent on the reducing agent employed in the reaction.

Scheme 3.3 Intramolecular Aldehyde–Diene Coupling

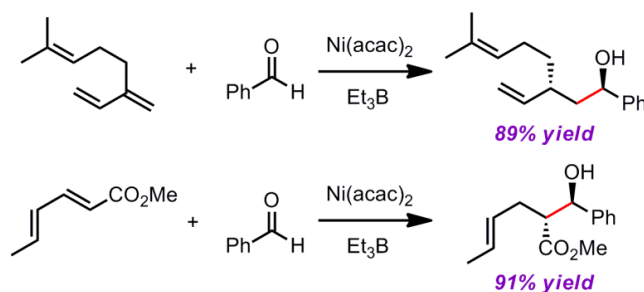


²⁵ (a) Sato, Y.; Takimoto, M.; Mori, M., "Further Studies on Nickel-Promoted or -Catalyzed Cyclization of 1,3-Diene and a Tethered Carbonyl Group," *Journal of the American Chemical Society* **2000**, 122, 1624-1634. (b) Sato, Y.; Takimoto, M.; Hayashi, K.; Katsuhara, T.; Takagi, K.; Mori, M., "Novel Stereoselective Cyclization Via π -Allylnickel Complex Generated from 1,3-Diene and Hydride Nickel Complex," *Journal of the American Chemical Society* **1994**, 116, 9771-9772.

²⁶ (a) Sato, Y.; Sawaki, R.; Mori, M., "Dramatic Influence on the Olefinic Geometry in the Nickel(0)-Catalyzed Coupling Reaction of 1,3-Dienes and Aldehydes Using N-Heterocyclic Carbene as a Ligand," *Organometallics* **2001**, 20, 5510-5512. (b) Sato, Y.; Takanashi, T.; Hoshihara, M.; Mori, M., "Nickel(0)-Catalyzed Diene-Aldehyde Cyclization," *Tetrahedron Letters* **1998**, 39, 5579-5582.

Intermolecular coupling reactions of aldehyde–diene have been reported by Tamaru and co-workers (Scheme 3.4).²⁷ The substrate scope is broad in terms of both coupling partners. Also, either triethylborane (Et₃B) or diethyl zinc (ZnEt₂) can be used as a reducing agent depending on the substrates. The authors have suggested that the reaction mechanism involves formation of a nickelacyclic intermediate with two π -components and the nickel catalyst; then, subsequent β -hydride elimination and reductive elimination would give the product.

Scheme 3.4 Intermolecular Aldehyde–Diene Coupling



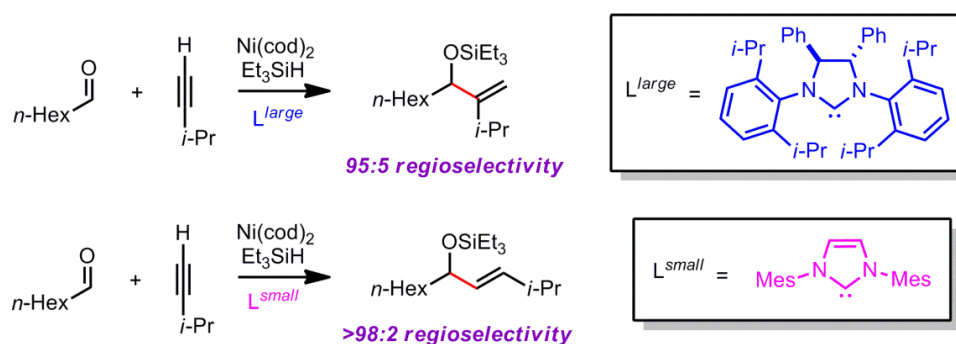
3.2.2. Reductive Coupling of Aldehyde–Alkyne

Montgomery and co-workers have developed a number of coupling reactions involving aldehydes, alkynes, and reducing reagents and made substantial effort to examine

²⁷ (a) Kimura, M.; Ezo, A.; Shibata, K.; Tamaru, Y., "Novel and Highly Regio- and Stereoselective Nickel-Catalyzed Homoallylation of Benzaldehyde with 1,3-Dienes," *Journal of the American Chemical Society* **1998**, *120*, 4033-4034. (b) Kimura, M.; Fujimatsu, H.; Ezo, A.; Shibata, K.; Shimizu, M.; Matsumoto, S.; Tamaru, Y., "Nickel-Catalyzed Homoallylation of Aldehydes and Ketones with 1,3-Dienes and Complementary Promotion by Diethylzinc or Triethylborane," *Angewandte Chemie International Edition* **1999**, *38*, 397-400.

the regioselectivity of the reductive coupling reactions.²⁸ With careful optimization of the ligand structure, they have observed that the regioselectivity of the reaction is strongly governed by the size of the ligands (Scheme 3.5).^{28c} Compared to their previous reports, the impact of ligand size effects in this work is significant enough to override the substrate-derived influences with both biased- and unbiased-alkynes.

Scheme 3.5 Intramolecular Aldehyde–Alkyne Coupling



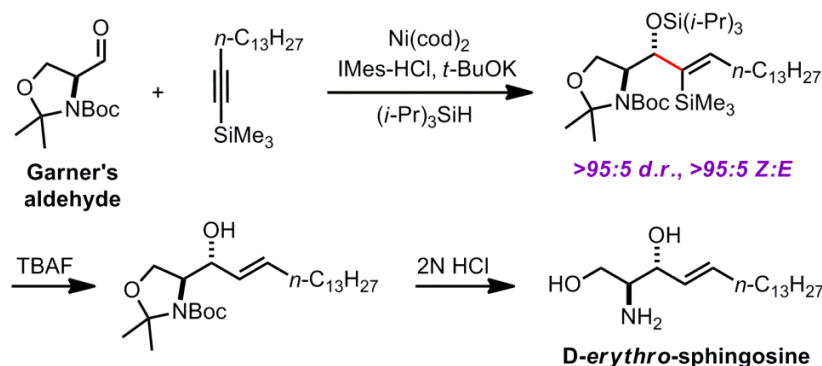
A synthetic application of the reductive aldehyde–alkyne coupling has also been demonstrated by this group (Scheme 3.6).²⁹ Through the key Ni-catalyzed reductive aldehyde–alkyne coupling reaction, *D-erythro*-sphingosine was prepared by a short reaction

²⁸ (a) Chaulagain, M. R.; Sormunen, G. J.; Montgomery, J., "New N-Heterocyclic Carbene Ligand and Its Application in Asymmetric Nickel-Catalyzed Aldehyde/Alkyne Reductive Couplings," *Journal of the American Chemical Society* **2007**, *129*, 9568-9569. (b) Malik, H. A.; Chaulagain, M. R.; Montgomery, J., "Cooperativity of Regiochemistry Control Strategies in Reductive Couplings of Propargyl Alcohols and Aldehydes," *Organic Letters* **2009**, *11*, 5734-5737. (c) Malik, H. A.; Sormunen, G. J.; Montgomery, J., "A General Strategy for Regiocontrol in Nickel-Catalyzed Reductive Couplings of Aldehydes and Alkynes," *Journal of the American Chemical Society* **2010**, *132*, 6304-6305.

²⁹ Sa-ei, K.; Montgomery, J., "Diastereoselective Nickel-Catalyzed Reductive Couplings of Aminoaldehydes and Alkynylsilanes: Application to the Synthesis of *D-Erythro*-Sphingosine," *Tetrahedron* **2009**, *65*, 6707-6711.

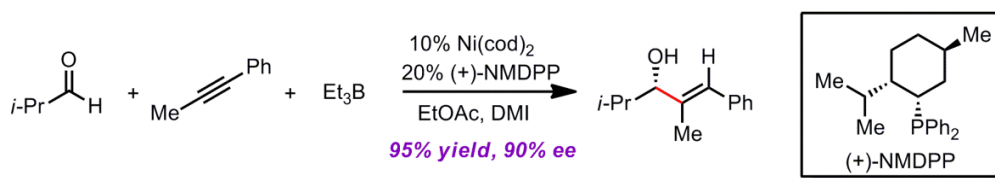
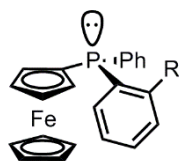
sequence from an aminoaldehyde and a silylalkyne. The reductive coupling of Garner's aldehyde and an alkynyl silane with triisopropylsilane as the reducing agent furnished an unsaturated *anti*-1,2-aminoalcohol with great diastereoselectivities (>95:5 *dr*, >95:5 *Z:E*). The resulting coupling product was converted to the target molecule by silyl deprotection and HCl-mediated deprotection.

Scheme 3.6 Total Synthesis of D-Erythro-sphingosine



An enantioselective variant of this reaction was developed by the Jamison group. High enantioselectivity (90% *ee*) with great yield (95% yield) was observed in the coupling of an aldehyde, an aromatic alkyne (aryl-C≡C-alkyl) and triethylborane when a chiral phosphine ligand, (+)-neomenthyl-diphenylphosphine (NMDPP), was employed. They have also demonstrated that another class of chiral ligand, *P*-chiral ferrocenyl phosphine (Figure 3.1), can catalyze similar processes, when dialkyl substituted alkynes (alkyl-C≡C-alkyl) are one of the coupling partners.

Scheme 3.7 Enantioselective Aldehyde–Alkyne Coupling

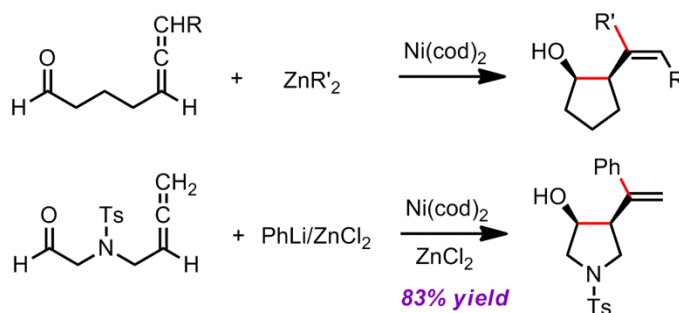
Figure 3.1 *P*-Chiral Ferrocenyl Phosphine

3.2.3. Reductive Coupling of Carbonyl–Allene

The first cyclization reactions of allenyl aldehydes with organic zinc leading to homoallylic alcohols were reported by Montgomery and co-workers (Scheme 3.8).^{14b} This process furnishes synthetically versatile homoallylic alcohols in a stereoselective fashion. The reaction is compatible with both mono-substituted and 1,3-disubstituted allenes; notably, the reactions with disubstituted allenes afford trisubstituted alkenes stereoselectively. It was observed that the cyclopentane core was formed with *cis*-substitution, and the favored alkene geometry was (*Z*) configuration in most cases. This strategy was utilized in the total

synthesis of (-)- α -kainic Acid³⁰ and (+)-testudinariol A³¹ to construct the fundamental carbon skeleton of the molecules.

Scheme 3.8 Intramolecular Aldehyde–Allene Coupling

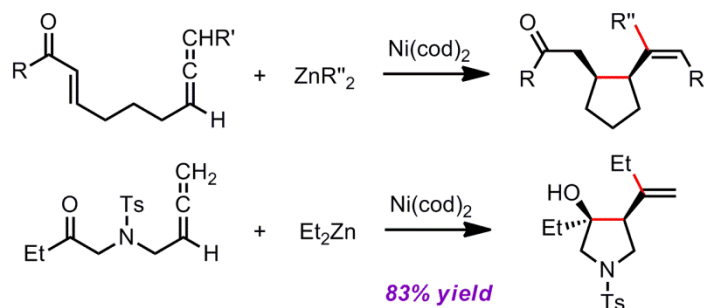


Furthermore, the Montgomery group demonstrated that more sterically-hindered substrates, ketones, are also compatible with this system (Scheme 3.9).^{14b} Both cyclopentane rings and substituted pyrrolidine core were prepared from the cyclization reactions. As observed in the case of aldehydes, the ring substituents were favored to be *cis* to each other and the alkenes were formed with (*Z*)-configuration. To install a phenyl group in the coupling product, a combination of two reagents—PhLi and ZnCl₂—was employed. In addition to the Montgomery group, the Kang group^{14a} has also examined some of these cyclization reactions of allene–aldehyde with organozinc reagents.

³⁰ Chevliakov, M. V.; Montgomery, J., "A Stereodivergent Approach to (-)- α -Kainic Acid and (+)- α -Allokainic Acid Utilizing the Complementarity of Alkyne and Allene Cyclizations," *Journal of the American Chemical Society* **1999**, 121, 11139-11143.

³¹ Amarasinghe, K. K. D.; Montgomery, J., "Enantioselective Total Synthesis of (+)-Testudinariol a Using a New Nickel-Catalyzed Allenyl Aldehyde Cyclization," *Journal of the American Chemical Society* **2002**, 124, 9366-9367.

Scheme 3.9 Intramolecular Ketone–Allene Coupling



3.2.4. Reductive Coupling of Alkyne–Alkene

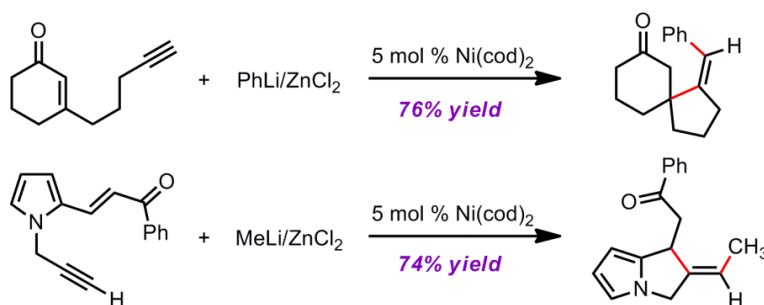
The coupling reactions of alkynes and alkenes with organometallic reagents have been investigated in various contexts. Regarding the organometallic reagents for these reactions, organozinc,³² organoaluminum,³³ or organozirconium³⁴ reagents can be employed for this process. The Montgomery group presented intramolecular coupling of alkynes and alkenes with organozinc reagents (Scheme 3.10).³² From this process, highly substituted alkenes are furnished in a stereoselective manner.

³² (a) Montgomery, J.; Savchenko, A. V., "Nickel-Catalyzed Cyclizations of Alkynyl Enones with Concomitant Stereoselective Tri- or Tetrasubstituted Alkene Introduction," *Journal of the American Chemical Society* **1996**, *118*, 2099-2100. (b) Montgomery, J.; Oblinger, E.; Savchenko, A. V., "Nickel-Catalyzed Organozinc-Promoted Carbocyclizations of Electron-Deficient Alkenes with Tethered Unsaturation," *Journal of the American Chemical Society* **1997**, *119*, 4911-4920. (c) Montgomery, J.; Chevliakov, M. V.; Briemann, H. L., "Nickel-Catalyzed Heterocycle Construction with Stereoselective Exocyclic Alkene Introduction," *Tetrahedron* **1997**, *53*, 16449-16462.

³³ Chevliakov, M. V.; Montgomery, J., "Nickel and Palladium Catalysis in the Stereoselective Synthesis of Functionalized Pyrrolidines: Enantioselective Formal Synthesis of (+)- α -Allokainic Acid," *Angewandte Chemie International Edition* **1998**, *37*, 3144-3146.

³⁴ Ni, Y.; Amarasinghe, K. K. D.; Montgomery, J., "Nickel-Catalyzed Cyclizations and Couplings with Vinylzirconium Reagents," *Organic Letters* **2002**, *4*, 1743-1745.

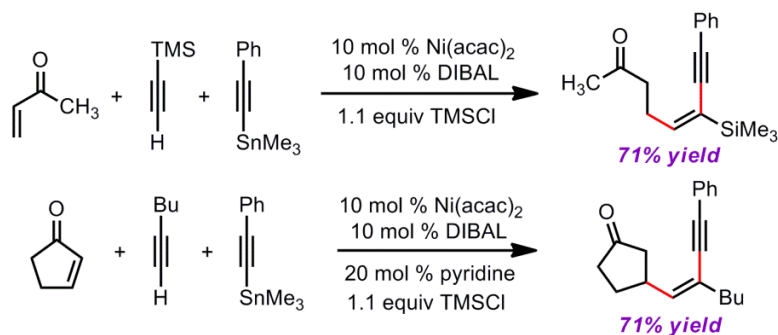
Scheme 3.10 Intramolecular Alkyne–Alkene Coupling



The intermolecular coupling reactions of alkynes, enones, and organometallic reagents were developed by Ikeda and co-workers (Scheme 3.11).^{7a,b} This nickel-catalyzed coupling of α,β -enones with monosubstituted alkynes, alkynyltin reagents, and TMSCl lead to the construction of two carbon–carbon bonds to afford enol silyl ethers. The resulting enol ethers were then hydrolyzed to give conjugated enynes with great regio- and stereoselectivities. When alkynylzinc reagents were used in place of alkynyltin reagents, the yields and regioselectivities were lowered.³⁵

³⁵ Ikeda, S.-I.; Kondo, K.; Sato, Y., "Nickel-Catalyzed Tandem Coupling of Enones, Alkynes, Alkynylzincs, and Chlorotrimethylsilane," *Chemistry Letters* **1999**, 28, 1227-1228.

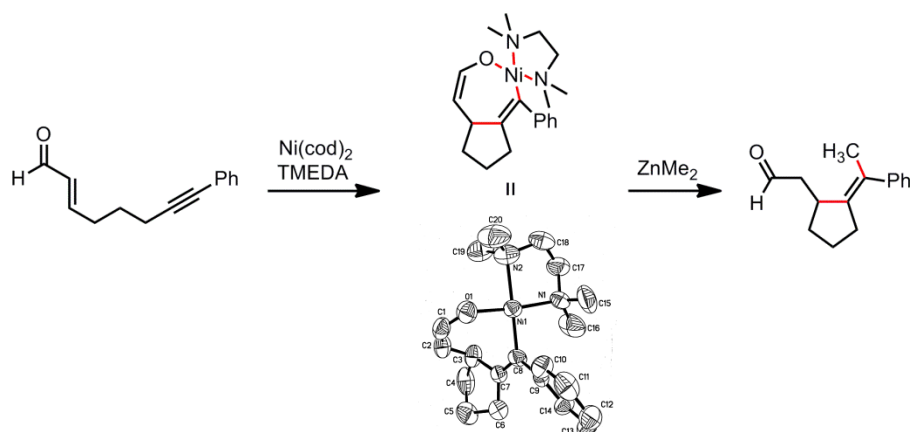
Scheme 3.11 Intermolecular Alkyne–Alkene Coupling



The proposed mechanism for the alkyne–enone coupling process involves nickelacyclic intermediate derived from the oxidative cyclization of an alkyne, an enone, and a nickel catalyst. After this intermediate is formed, subsequent transmetalation and reductive elimination will provide the observed products. To probe this mechanistic pathway, in particular the key oxidative cyclization step, the Montgomery group synthesized and isolated the nickelacyclic intermediate of this process (Scheme 3.12).³⁶ The X-ray crystallography analysis revealed that the intermediate complex was the η^1 -(O)-bound enolate, as expected from the proposed catalytic cycle.

³⁶ Amarasinghe, K. K. D.; Chowdhury, S. K.; Heeg, M. J.; Montgomery, J., "Structure of an η^1 Nickel O-Enolate: Mechanistic Implications in Catalytic Enyne Cyclizations," *Organometallics* **2001**, 20, 370-372.

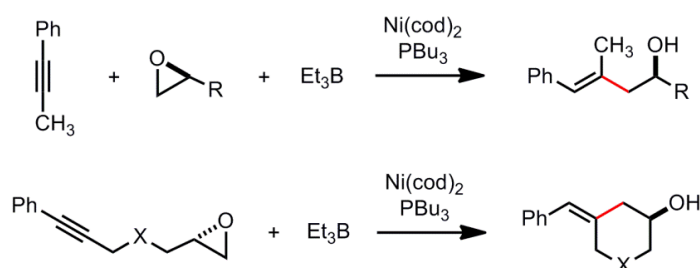
Scheme 3.12 Intermediate Nickelacyclic Enolate



3.2.5. Reductive Coupling of Alkyne–Epoxide

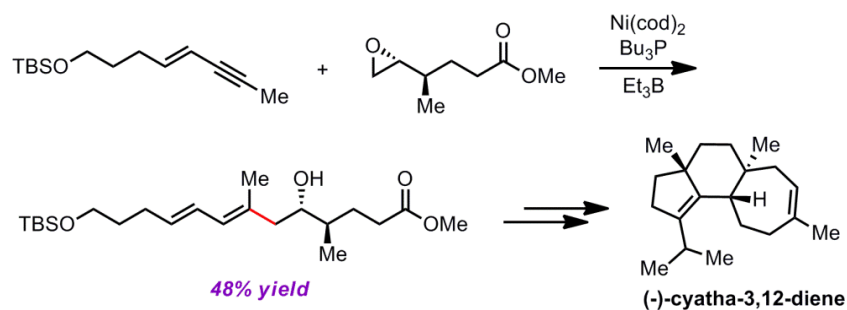
The coupling reactions of epoxides and alkynes were accomplished by Jamison and co-workers both inter- and intramolecularly.^{15a, 19a} In this process, triethylborane (Et_3B) is employed as a reducing agent to couple alkynes with epoxides in the presence of Ni(0)-phosphine catalyst (Scheme 3.13). The process is effective with internal alkynes, and the use of optically-pure epoxides affords enantio-enriched homoallylic alcohols. This reaction also proceeds in an intramolecular fashion to furnish five- or six-membered rings.

Scheme 3.13 Intermolecular Coupling of Alkyne–Epoxide



In recent studies by Jamison and co-workers, the reductive epoxide–alkyne coupling reactions have been applied to natural product syntheses. The group made considerable efforts to utilize this method for the preparation of a key intermediate for the total synthesis of (–)-cyatha-3,12-diene (Scheme 3.14).³⁷ The desired coupling product, enantiomerically-pure 3,5-dien-1-ol, was obtained from simple starting materials. Regarding the stereochemistry of the process, retention of the epoxide configuration was observed. Although the yield was moderate (48% yield), this one-step process provided the key carbon skeleton for the target molecule in an enantio-enriched form.

Scheme 3.14 Key Step in the Synthesis of (–)-Cyatha-3,12-diene

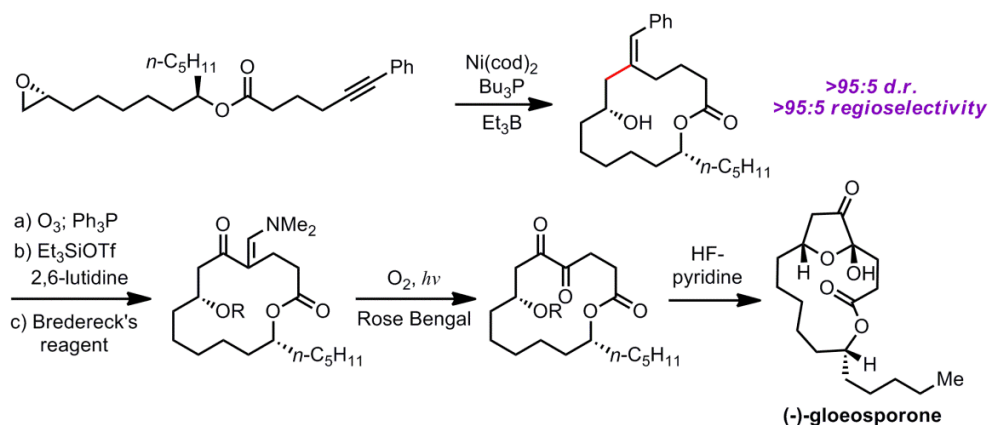


Another application of this methodology has also been reported, where epoxides and alkynes that are tethered in one molecule are assembled to furnish large rings (Scheme

³⁷ Sparling, B. A.; Simpson, G. L.; Jamison, T. F., "Strategic Use of Nickel(0)-Catalyzed Enyne–Epoxide Reductive Coupling toward the Synthesis of (–)-Cyatha-3,12-Diene," *Tetrahedron* **2009**, *65*, 3270–3280.

3.15).³⁸ This intramolecular epoxide–alkyne coupling employed triethylborane (Et₃B) as a reducing reagent and Ni(cod)₂ as a catalyst. The key macrocyclization in the total synthesis of (–)-gloeosporone proceeded with high regio- and stereoselectivity.

Scheme 3.15 Total Synthesis of (–)-Gloeosporone



3.2.6. Summary

Representative examples of nickel-catalyzed reductive coupling reactions and their synthetic applications are presented. This type of reaction has made a significant impact on complex molecule synthesis with stereo- and regioselective C–C bond formation. In particular, mechanistic investigations and experimental evidence are the most relevant to our study of bimetallic multicomponent coupling reactions. All things considered, these two classes of reactions (*i.e.* reductive and bimetallic coupling) undergo similar catalytic

³⁸ Trenkle, J. D.; Jamison, T. F., "Macrocyclization by Nickel-Catalyzed, Ester-Promoted, Epoxide–Alkyne Reductive Coupling: Total Synthesis of (–)-Gloeosporone," *Angewandte Chemie International Edition* **2009**, *48*, 5366–5368.

cycles involving the oxidative cyclization as a key step. However, the targeted products from these processes are exclusive to each other due to the different organometallic reagents employed. Further investigations in both areas will provide more useful strategies for the synthesis of valuable and versatile synthetic intermediates.

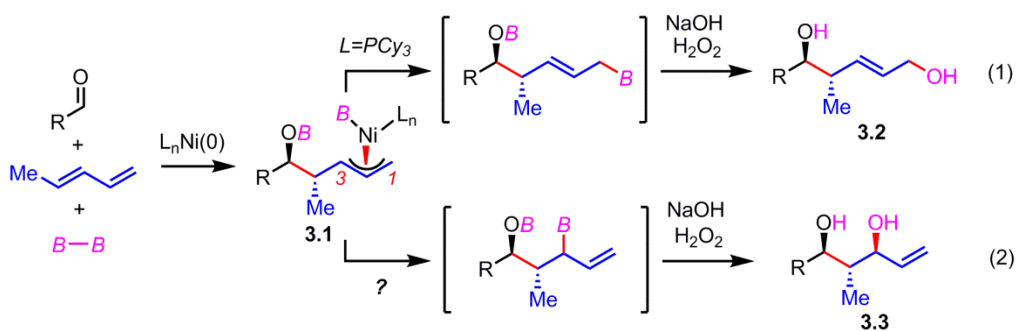
3.3. Method Development

3.3.1. Aldehyde–Diene–Diboron Coupling with P(TMS)₃ as a Ligand³⁹

3.3.1.1. Project Goals

After the investigations on the borylative multicomponent coupling reactions of aldehydes and dienes (as described in Chapter 2), we sought to develop a method that can furnish other regioisomers as a reaction product. We observed that, in the presence of PCy₃ as a ligand, compound **3.2** was formed as a reaction product, presumably from reductive elimination of **3.1** forming a bond between C1 and boron (Scheme 3.16, eq 1). We were curious about the possibility for bond formation between boron and C3, instead of C1, leading to compound **3.3** (eq 2, Scheme 3.16).

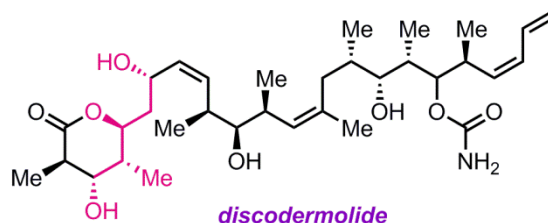
Scheme 3.16 A Regioisomeric Product for the Borylative Aldehyde–Diene Coupling



³⁹ Portions of this project described here have been published: Cho, H. Y.; Morken, J. P., "Ni-Catalyzed Borylative Diene–Aldehyde Coupling: The Remarkable Effect of P(SiMe₃)₃," *Journal of the American Chemical Society* **2010**, 132, 7576–7577.

The structural features of compound **3.3** – three contiguous stereocenters, an α -chiral allylboronate,⁴⁰ and a functional group pattern that maps onto polyketides – made this a compelling inquiry. More specifically, the carbon skeleton possessing such consecutive stereocenters can be found in the structure of discodermolide (Figure 3.2), which would be a potential synthetic target for this methodology. Discodermolide is known as a potent inhibitor of cancer cell growth.⁴¹

Figure 3.2 Potential Synthetic Target – Discodermolide



3.3.1.2. Reaction Optimization

Initial exploratory studies focused on the nickel catalyzed reaction between one equivalent each of 1,3-pentadiene, benzaldehyde, and $B_2(\text{pin})_2$. While PCy_3 promoted formation of terminal boronate **3.2** (analysis after oxidative workup with hydrogen peroxide,

⁴⁰ For selected synthesis, see: (a) Fang, G. Y.; Aggarwal, V. K., "Asymmetric Synthesis of α -Substituted Allyl Boranes and Their Application in the Synthesis of Iso-Agatharesinol," *Angewandte Chemie International Edition* **2007**, *46*, 359-362. (b) Carosi, L.; Hall, D. G., "Catalytic Enantioselective Preparation of α -Substituted Allylboronates: One-Pot Addition to Functionalized Aldehydes and a Route to Chiral Allylic Trifluoroborate Reagents," *Angewandte Chemie International Edition* **2007**, *46*, 5913-5915.

⁴¹ (a) Gunasekera, S. P.; Gunasekera, M.; Longley, R. E.; Schulte, G. K., "Discodermolide: A New Bioactive Polyhydroxylated Lactone from the Marine Sponge *Discodermia Dissoluta*," *The Journal of Organic Chemistry* **1990**, *55*, 4912-4915. (b) ter Haar, E.; Kowalski, R. J.; Hamel, E.; Lin, C. M.; Longley, R. E.; Gunasekera, S. P.; Rosenkranz, H. S.; Day, B. W., "Discodermolide, a Cytotoxic Marine Agent That Stabilizes Microtubules More Potently Than Taxol," *Biochemistry* **1996**, *35*, 243-250.

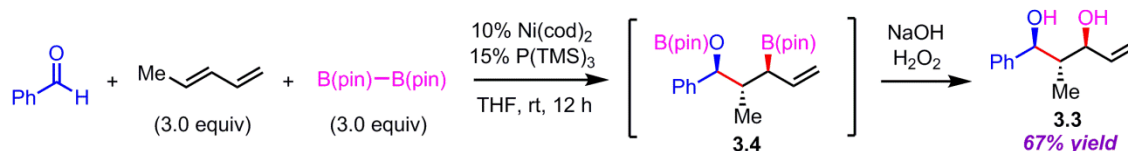
Table 3.1, entry 1), other alkyl and aryl phosphines, and simple phosphites were either ineffective or resulted in poor selectivity (entries 2–5). However, when commercially available $P(\text{SiMe}_3)_3$ was employed, compound **3.3** was observed with excellent selectivity (entry 6).

Table 3.1 Survey of Ligands for 1,3-Diol Synthesis

entry	ligand	3.2		3.3	
		yield (%)	dr	yield (%)	dr
1	PCy ₃	69%	> 20:1	-	-
2	PEt ₃	20%	7:1	34%	2:1
3	PMe ₂ Ph	20%	3:1	-	-
4	PMe ₃	19%	2:1	55%	4:1
5	P(OEt) ₃	40%	4:1	-	-
6	P(SiMe ₃) ₃	5%	7:1	67%	> 20:1

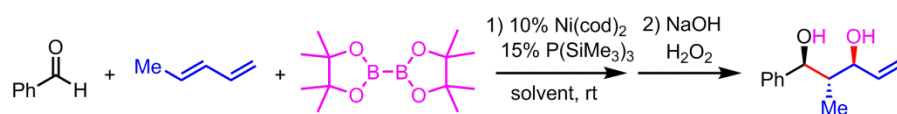
In this coupling reaction employing $P(\text{TMS})_3$ as a ligand, by-products comprising two aldehydes and one diene, or two dienes and one aldehyde, were also observed (detected by mass spectrometry). We speculated that reaction of **3.4** (shown in Scheme 3.17) with unreacted aldehyde might compete with the catalytic process at later stages of reaction and deliver some of these by-products. For this reason, the concentrations of $B_2(\text{pin})_2$ and pentadiene were increased from 1 equiv to 3 equiv (Scheme 3.17). This strategy furnished better conditions for this three-component process.

Scheme 3.17 Initial Investigations toward 1,3-Diol Synthesis



The solvent screening results indicated that tetrahydrofuran (THF) is the best medium for this system (Table 3.2, entry 1). The coupling reactions in diethyl ether or ethyl acetate also afforded the desired product with reasonable efficiency, but they were not better than that in THF (entries 2–3). In addition, the mixed solvent systems (THF/acetonitrile or THF/DMF) were not suitable for this process (entries 4–5).

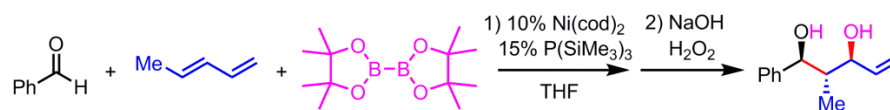
Table 3.2 Screen of Solvents for 1,3-Diol Synthesis



entry	solvent	yield (%)	dr
1	THF	66%	> 20:1
2	diethyl ether	50%	15:1
3	EtOAc	38%	10:1
4	THF:CH ₃ CN (1:1)	< 20%	nd
5	THF:DMF (1:1)	< 10%	nd

The temperature of the reaction mixture was also a critical factor for better selectivity and efficiency (Table 2.3). While the coupling reaction at 4 °C was not productive (entry 1), the reaction proceeded well at ambient temperature with high selectivity (entry 2). At an increased temperature, 60 °C, we observed some loss of selectivity and decreased yield due to formation of more byproducts (entry 3).

Table 3.3 Influence of Temperature on 1,3-Diol Synthesis



entry	temperature	yield (%)	dr
1	4 °C	< 30%	nd
2	rt	67%	> 20:1
3	60 °C	43%	7:1

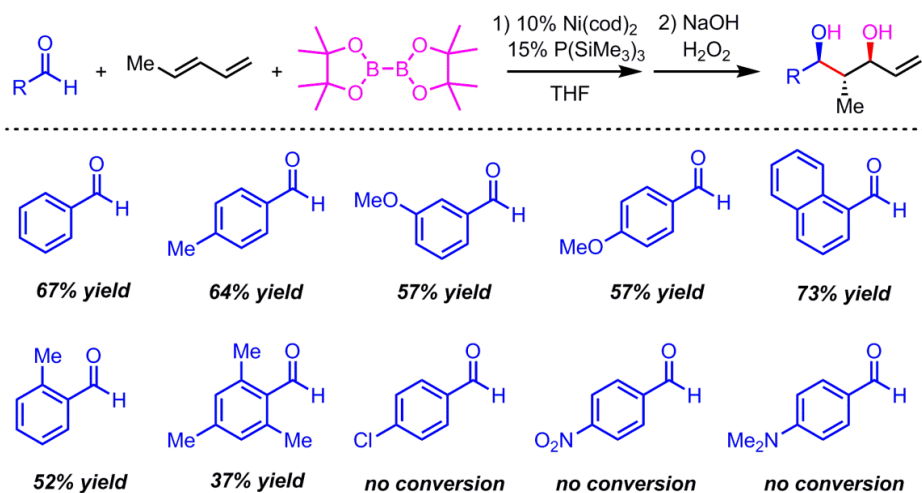
After extensive optimization of these reaction parameters (ligand, concentration, solvent, and temperature), the optimal set of reaction conditions was found to include $P(\text{TMS})_3$ as the ligand, 3 equiv of $B_2(\text{pin})_2/\text{diene}$, THF as the solvent, and ambient temperature for reaction mixture.

3.3.1.3. Substrate Scope

3.3.1.3.1. Survey of Carbonyl Compounds

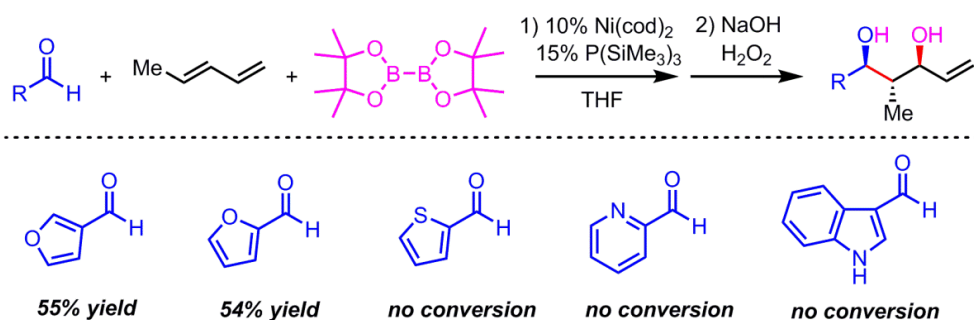
Under these optimized reaction conditions, a number of different substrates (both carbonyl compounds and unsaturated hydrocarbons) were examined for this coupling reaction. The investigation began with various aromatic aldehydes, as depicted in Scheme 3.18. The aromatic aldehydes possessing electron-neutral or electron-donating groups were good substrates for the system giving the desired products in moderate to good yields (37–67%). However, the aldehydes with electron-withdrawing groups (i.e. 4-chlorobenzaldehyde or 4-nitrobenzaldehyde) did not show any reactivity in this process. Also, 4-dimethylaminobenzaldehyde was not an effective coupling partner, either.

Scheme 3.18 Survey of Aromatic Aldehydes for 1,3-Diol Synthesis



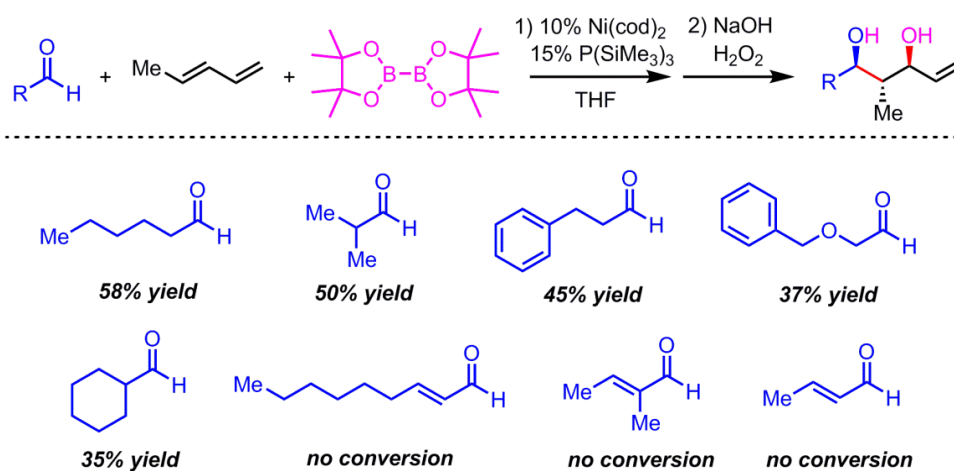
In addition, a variety of heterocyclic aromatic aldehydes were also surveyed (Scheme 3.19). While both furaldehydes (i.e. 2-furaldehyde and 3-furaldehyde) participate in this process giving the corresponding products in good yield, other S- or N-heteroaromatic aldehydes (i.e. thiophene aldehyde, 2-pyridyl aldehyde, and 3-indole aldehyde) did not afford any desired products in these reactions.

Scheme 3.19 Survey of Heterocyclic Aromatic Aldehydes for 1,3-Diol Synthesis



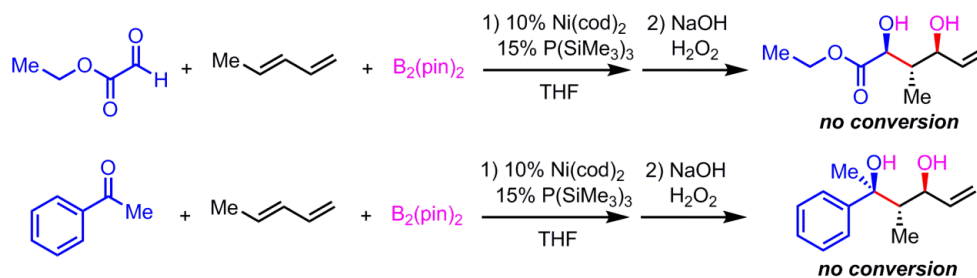
Furthermore, we observed that several aliphatic aldehydes can be good candidates for these processes (Scheme 3.20). The reactions with alkyl-substituted aldehydes proceeded well giving the products in 35–58% yield. On the other hand, the α,β -unsaturated aldehydes were not converted into the desired products in the coupling reactions.

Scheme 3.20 Survey of Aliphatic Aldehydes for 1,3-Diol Synthesis



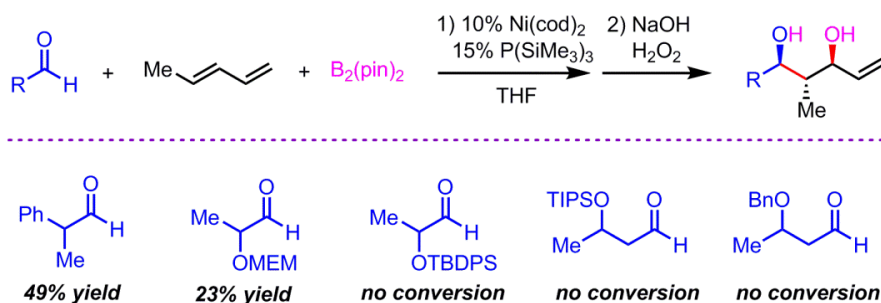
Some more challenging substrates for this process, such as ethyl glyoxalate and ketones, were also examined (Scheme 3.21). The coupling reactions with these substrates could afford products that contain more synthetically challenging moieties. Unfortunately, neither of these reactions afforded the corresponding products in this process.

Scheme 3.21 Survey of Carbonyl Compounds for 1,3-Diol Synthesis



In the hopes of applying this method for asymmetric synthesis, we next examined the reactivity of several chiral aldehydes. As shown in Scheme 3.22, a couple of simple α -chiral aldehydes were found to be effective; but, the α -chiral aldehyde containing a silyl ether was not reactive. In addition, the β -chiral aldehydes were not transformed into the desired products in these multicomponent coupling reactions.

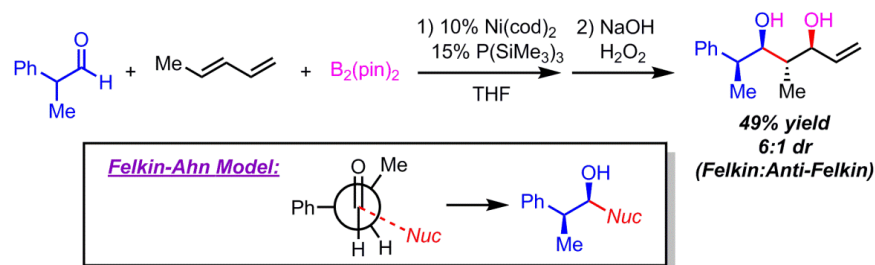
Scheme 3.22 Survey of Chiral Aldehydes for 1,3-Diol Synthesis



More details on the reaction with an α -chiral aldehyde, 2-phenylpropanaldehyde, were studied (Scheme 3.23). The investigations on the relative stereochemistry of this reaction product revealed that the chiral aldehyde reacted with Felkin selectivity (6:1 dr). As illustrated in the box of Scheme 3.23, the phenyl group serves as a large group, and the

nucleophile (i.e. the diene in this case) approaches the carbonyl carbon away from the large group. The stereoselection of this process opened the possibility that this method can be utilized in asymmetric synthesis.

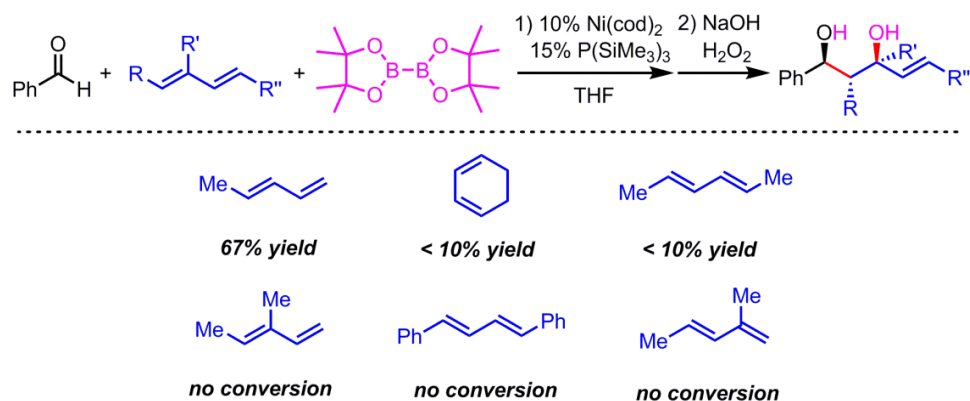
Scheme 3.23 Coupling Reaction with an α -Chiral Aldehyde and the Felkin–Ahn Model



3.3.1.3.2. Survey of Hydrocarbons and Diboron Reagents

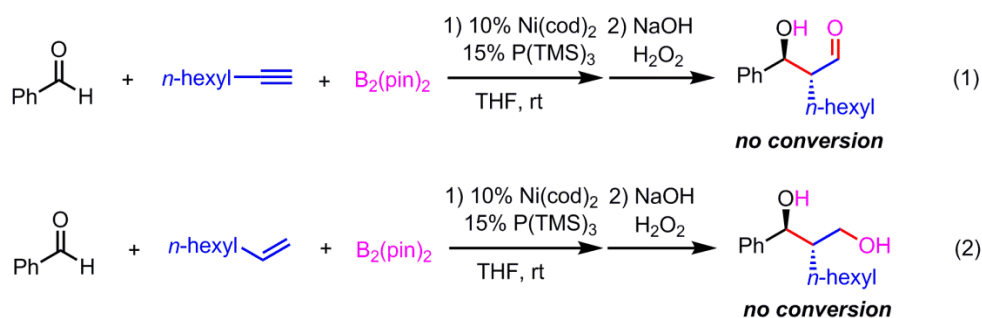
Various unsaturated hydrocarbon substrates were examined for this coupling reaction. The survey began with diverse dienes since the reaction involving dienes would be an effective tool to prepare corresponding allylic alcohols (Scheme 3.24). It was observed that *trans*-piperylene was one of the best nucleophiles in this process affording the corresponding product in 67% yield. However, other dienes, which include 1,3-cyclohexadiene, 2,4-hexadiene, and substituted pentadienes, were not reactive enough in this type of reaction.

Scheme 3.24 Survey of Dienes for 1,3-Diol Synthesis



Also, we questioned if other types of unsaturated hydrocarbons, such as alkenes or alkynes, could participate in this process. However, when 1-octyne or 1-octene was reacted with benzaldehyde and $B_2(\text{pin})_2$ in the presence of the nickel catalyst, the reaction did not furnish any coupling products (Scheme 3.25).

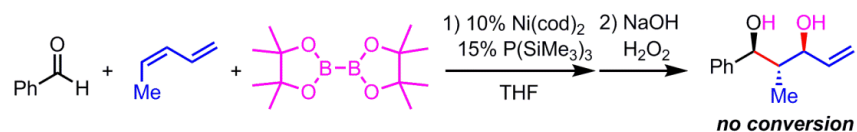
Scheme 3.25 Survey of Alkynes and Alkenes for 1,3-Diol Synthesis



As described in the previous chapter (Section 2.3.1.3.2.), when *cis*-piperylene was employed in this coupling reaction with PCy_3 as a ligand, we observed it is isomerized to *trans*-piperylene and thus afforded that the same product as that from the reaction with

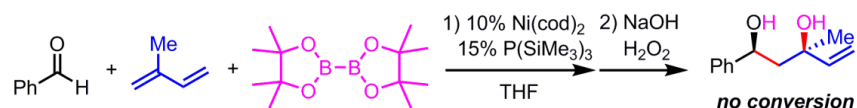
trans-piperylene. However, when *cis*-piperylene was reacted in the multicomponent reaction with $\text{P}(\text{TMS})_3$ as a ligand, we did not observe any coupling products formed from this process (Scheme 3.26).

Scheme 3.26 Three-Component Coupling Reaction with *cis*-Piperylene



Among potential hydrocarbon candidates for this coupling reaction, we were particularly interested in isoprene because the reaction involving isoprene would furnish a product containing tertiary alcohol functionality (Scheme 3.27). Unfortunately, when isoprene was subjected to the three-component reaction with $\text{P}(\text{TMS})_3$ as a ligand, it was not converted to the corresponding product.

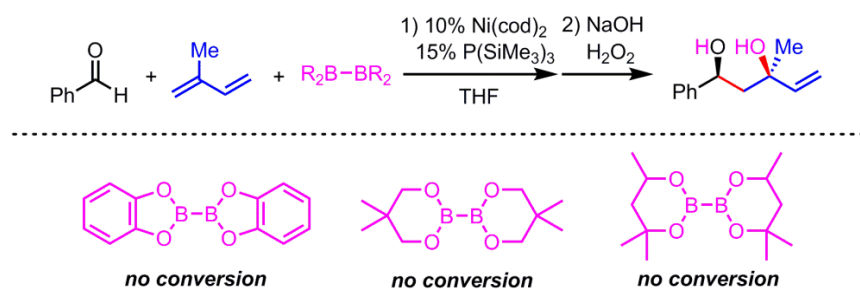
Scheme 3.27 Three-Component Coupling Reaction with Isoprene



Hoping that a more reactive diboron reagent would promote this coupling, we employed $\text{B}_2(\text{cat})_2$ in the reaction of benzaldehyde, isoprene, and the nickel catalyst (Scheme 3.28). However, the reaction with $\text{B}_2(\text{cat})_2$ still did not afford a coupling product. We also tried bis(neopentylglycolato)diboron and bis(hexyleneglycolato)diboron as a diboron

reagent to facilitate this process. But, neither of these agents was able to promote the coupling reaction with isoprene.

Scheme 3.28 Survey of Diboron Reagents for Borylative Aldehyde–Isoprene Coupling



3.3.1.3.3. Summary of Substrate Scope

As presented in the previous section, a number of aldehydes participate in the stereoselective borylative coupling reactions. Under the optimized reaction conditions, benzaldehyde, *trans*-1,3-pentadiene and $\text{B}_2(\text{pin})_2$ were effectively coupled in the presence of $\text{Ni}(\text{cod})$ and $\text{P}(\text{TMS})_3$ and, after oxidative work-up (NaOH , H_2O_2), the 1,3 diol product was obtained in good yield and stereoselectivity (Table 3.4, entry 1).⁴² In general, benzaldehyde derivatives tend to be effective substrates for the reaction with $\text{B}_2(\text{pin})_2$ and *trans*-piperylene (entries 2-4). All the products from these aldehydes showed good efficiency (57–64% yield) as well as high selectivity (> 20:1 dr).

⁴² For recent diol construction using organoboron reagents, see: (a) González, A. Z.; Román, J. G.; Alicea, E.; Canales, E.; Soderquist, J. A., "Borabicyclo[3.3.2]Decanes and the Stereoselective Asymmetric Synthesis of 1,3-Diol Stereotriads from 1,3-Diborylpropenes," *Journal of the American Chemical Society* **2008**, *131*, 1269-1273. (b) Chen, M.; Handa, M.; Roush, W. R., "Enantioselective Synthesis of 2-Methyl-1,2-*Syn*- and 2-Methyl-1,2-*Anti*-3-Butenediols via Allene Hydroboration–Aldehyde Allylboration Reaction Sequences," *Journal of the American Chemical Society* **2009**, *131*, 14602-14603.

Table 3.4 Stereoselective 1,3-Diol Synthesis with Benzaldehyde Derivatives

entry	aldehyde	diene	product	yield	dr
1				67%	> 20:1
2				64%	> 20:1
3				57%	> 20:1
4				57%	> 20:1

Furthermore, the more sterically-encumbered 1-naphthaldehyde effectively participated in this process to furnish the allylic alcohol in 73% yield with > 20:1 dr (Table 3.5, entry 1). In addition, a couple of heteroaromatic aldehydes (3-furaldehyde and 2-furaldehyde) turned out to be an adequate coupling partner for this process to give the corresponding 1,3-diols in around 55% yield with great selectivities (entries 2 and 3).

Table 3.5 Stereoselective 1,3-Diol Synthesis with Aromatic Aldehydes

entry	aldehyde	diene	product	yield	dr
1				73%	> 20:1
2				55%	> 20:1
3				54%	> 20:1

The data in Table 3.6 indicate that this coupling reaction is not necessarily limited to aromatic aldehydes; both several aliphatic aldehydes can be coupled with pentadiene and diboron reagent (Table 3.6). Both hexanal and isobutyraldehyde were efficiently transformed into the corresponding products in the coupling reactions with great selectivities (entries 1 and 2). When hydrocinnamaldehyde was subjected to the coupling reaction, it furnished the 1,3-diol in good yield with excellent selectivity (entry 3). Finally, benzyloxyacetaldehyde was an acceptable electrophile in this process; its reaction afforded the allylic alcohol in 37% yield with > 20:1 dr (entry 4).

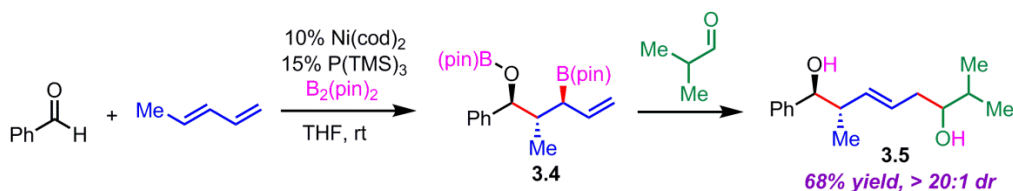
Table 3.6 Stereoselective 1,3-Diol Synthesis with Aliphatic Aldehydes

entry	aldehyde	diene	product	yield	dr
1				58%	> 20:1
2				50%	> 20:1
3				45%	> 20:1
4				37%	> 20:1

3.3.1.4. Product Transformation

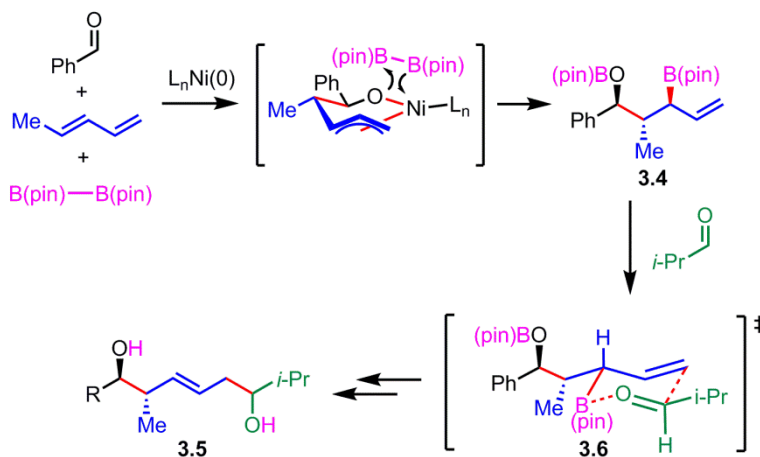
3.3.1.4.1. Three Component Coupling–Allylation Sequence

As mentioned in the previous section, the allylboronate product of this coupling (i.e. compound **3.4**) possesses an α -chiral allylic boronate, a motif that often engages in highly selective carbonyl allylation reactions. To probe the capacity for structures such as **3.4** to participate in stereoselective allylations, benzaldehyde and 1,3-pentadiene were subjected to borylative coupling and, after 12 hours, isobutyraldehyde was added to the reaction mixture (Scheme 3.29). This single-pot reaction sequence delivered 1,6-diol **3.5** in good yield, as a single regioisomer, and with excellent levels of 1,5-stereoselection (>20:1 dr) and olefin stereocontrol.

Scheme 3.29 Three Component Coupling with P(TMS)₃ and Subsequent Allylation

Considering the olefin configuration in the reaction product, it appears plausible that boronate **3.4** reacts with isobutyraldehyde by way of transition structure **3.6** with the appendage at the α position of the boronate occupying a pseudoequatorial position.^{43, 44}

Scheme 3.30 Proposed Transition State for the Subsequent Allylation Step



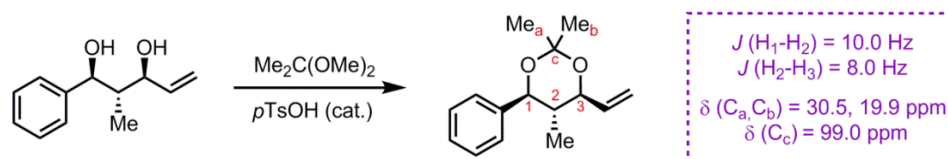
⁴³ Large boron ligands (i.e. tetraphenylethylene glycol) favor the axial orientation whereas small ligands (propanediol) favor the equatorial orientation. See: (a) W. Hoffman, R.; Weidmann, U., "Zur "Cis-Präferenz" Bei Der Addition Von Butenyl-Metallverbindung an Ketone Und Aldehyde," *Journal of Organometallic Chemistry* **1980**, 195, 137-146. (b) Flamme, E. M.; Roush, W. R., "Enantioselective Synthesis of 1,5-Anti- and 1,5-Syn-Diols Using a Highly Diastereoselective One-Pot Double Allylboration Reaction Sequence," *Journal of the American Chemical Society* **2002**, 124, 13644-13645.

⁴⁴ In the presence of Lewis acids, the equatorial orientation of the α -substituents is preferred. See: Carosi, L.; Lachance, H.; Hall, D. G., "Additions of Functionalized α -Substituted Allylboration to Aldehydes under the Novel Lewis and Brønsted Acid Catalyzed Manifolds," *Tetrahedron Letters* **2005**, 46, 8981-8985.

3.3.1.4.2. Determination of Relative Configurations

The stereochemical outcome of the coupling reactions (i.e. *anti-anti* relationship of the substituents at the stereocenters) was determined by the NMR analysis of the acetonide that was prepared from a coupling product (Scheme 3.31). The coupling product, 1,3-diol, was transformed to an acetonide, and both ^1H and ^{13}C NMR spectra of the acetonide were taken. Both the coupling constants in the proton NMR and the chemical shifts in the carbon NMR suggested the relative configuration of the product must be the *anti-anti* relationship.⁴⁵

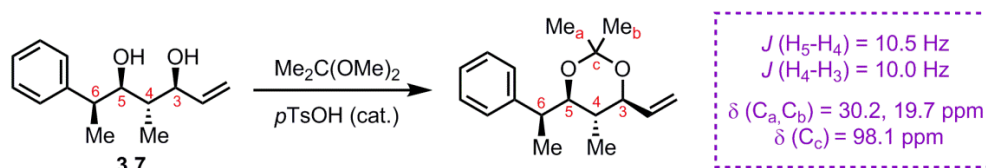
Scheme 3.31 Synthesis and Analysis of Acetonide Derived from a Coupling Product



Another coupling product **3.7**, which was made by the reaction of 2-phenylpropionaldehyde and *trans*-piperylene, was also transformed to an acetonide. Then, the acetonide was analyzed by NMR spectroscopy to prove the relative stereochemistry between C3–C4 as well as C4–C5 of compound **3.7** (Scheme 3.32).

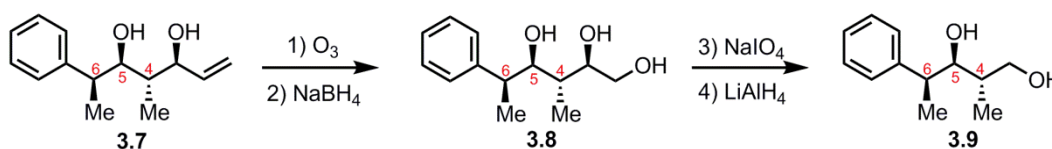
⁴⁵ For ^{13}C NMR chemical shift correlations in 1,3-diol acetonides, see: (a) Rychnovsky, S. D.; Skalitzky, D. J., "Stereochemistry of Alternating Polyol Chains: ^{13}C NMR Analysis of 1,3-Diol Acetonides," *Tetrahedron Letters* **1990**, *31*, 945-948. (b) Evans, D. A.; Rieger, D. L.; Gage, J. R., " ^{13}C NMR Chemical Shift Correlations in 1,3-Diol Acetonides. Implications for the Stereochemical Assignment of Propionate-Derived Polyols," *Tetrahedron Letters* **1990**, *31*, 7099-7100. (c) Rychnovsky, S. D.; Rogers, B. N.; Richardson, T. I., "Configurational Assignment of Polyene Macrolide Antibiotics Using the [^{13}C]Acetonide Analysis," *Accounts of Chemical Research* **1998**, *31*, 9-17.

Scheme 3.32 Acetonide Analysis of a Coupling Product



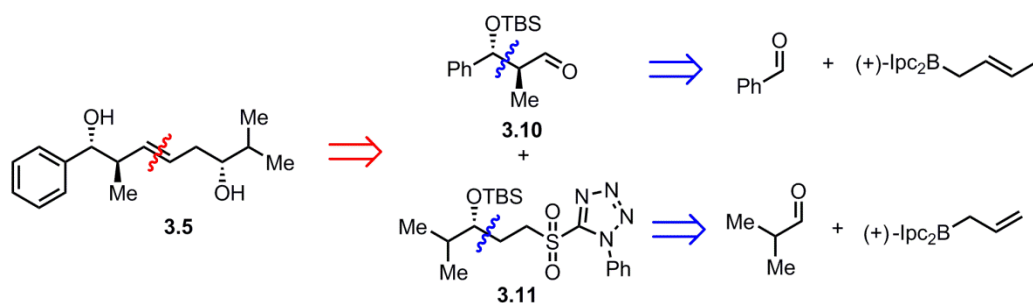
The relative configuration between C5–C6 in compound **3.7** was determined after the coupling product (**3.7**) was derivatized into compound **3.9** (Scheme 3.33). The diol, compound **3.9**, was prepared from compound **3.8** by the sodium periodate cleavage/reduction sequence from compound **3.8**. We were able to access the triol (**3.8**) via the ozonolysis/reduction sequence with a starting material of compound **3.7**.

Scheme 3.33 Multistep Transformation of a Coupling Product



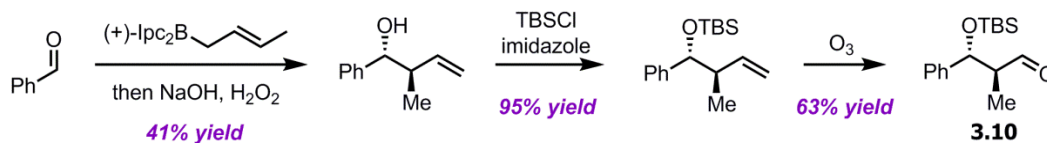
In order to prove the stereochemistry of the allylation product (**3.5**), we planned to synthesize the identical compound with well-established procedures. The key disconnections for the enantioselective synthesis of compound **3.5** are described in Scheme 3.34. The double bond of compound **3.5** can be formed by the Julia–Kocięski reaction of compounds **3.10** and **3.11**. The carbon skeletons of these two components (**3.10** and **3.11**) can be constructed by Brown crotylation or allylation in a stereoselective fashion.

Scheme 3.34 Synthetic Plan for the Enantioenriched Authentic Compound



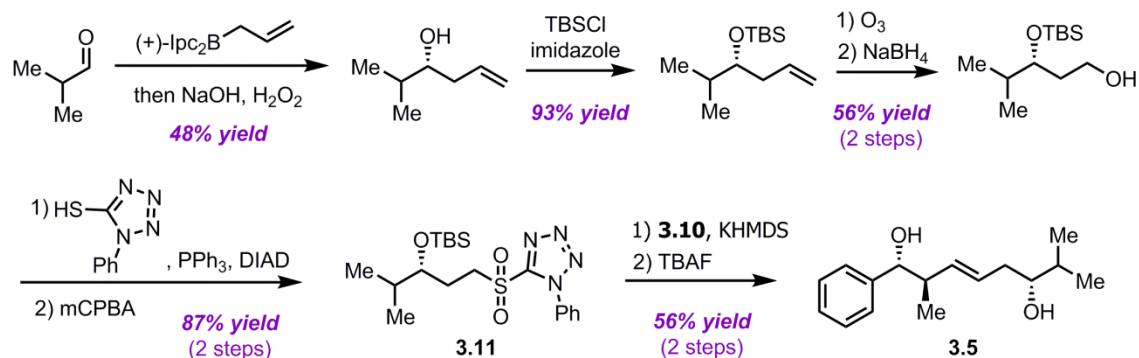
The detailed synthetic route to compound **3.10** is described in Scheme 3.35. The Brown crotylation reaction between benzaldehyde and (+)-(*E*)-crotyl bis(isopinocampheyl)borane afforded the corresponding homoallylic alcohol in 41% yield. This alcohol was transformed to compound **3.10** by a silyl protection (95% yield) followed by ozonolysis (63% yield).

Scheme 3.35 Synthetic Route to Compound 3.10



Then, another coupling partner for the Julia olefination (compound **3.11**) was synthesized by the route that is described in Scheme 3.36. We started with the Brown allylation reaction with isobutyraldehyde and (+)-allyl bis(isopinocampheyl)borane to furnish the corresponding homoallylic alcohol in 48% yield. Compound **3.11** could be accessed from this alcohol via a silyl protection (93% yield), the ozonolysis/reduction sequence (56% yield), and the Mitsunobu/oxidation reactions (87% yield).

Scheme 3.36 Synthetic Route to the Enantioenriched Authentic Compound



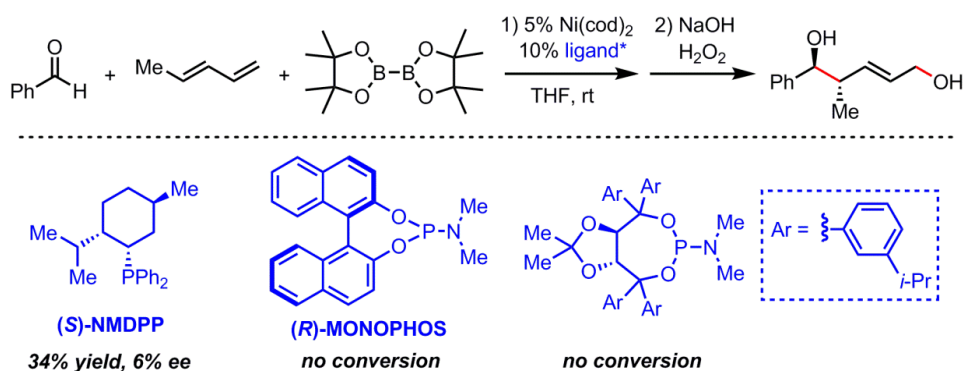
Then, the last step of the synthesis (Julia–Kocięski reaction)⁴⁶ was conducted with these two coupling partners (compounds **3.10** and **3.11**, Scheme 3.36). The olefination followed by silyl deprotection furnished compound **3.5** in 56% yield. The NMR analyses (both proton and carbon NMRs) confirmed the stereochemical relationship of compound **3.5**.

⁴⁶ (a) Julia, M.; Paris, J.-M., "Syntheses a L'aide De Sulfones V⁽⁺⁾-Methode De Synthese Generale De Doubles Liaisons," *Tetrahedron Letters* **1973**, *14*, 4833-4836. (b) Blakemore, P. R.; Cole, W. J.; Kocięski, P. J.; Morley, A., "A Stereoselective Synthesis of *Trans*-1,2-Disubstituted Alkenes Based on the Condensation of Aldehydes with Metallated 1-Phenyl-1*H*-Tetrazol-5-yl Sulfones," *Synlett* **1998**, 26-28.

3.3.2. Catalytic Enantioselective Aldehyde–Diene–Diboron Coupling

One of the major objectives in this project was to develop catalytic enantioselective multicomponent coupling reactions. To achieve this goal, extensive screening experiments with optically-active chiral ligands were conducted. A chiral monodentate phosphine ligand, (*S*)-NMDPP, afforded the 1,5 diol in 34% yield and 6% ee (Scheme 3.37). Neither of the phosphoramidite ligands shown in Scheme 3.37 produced the desired coupling product under these conditions.

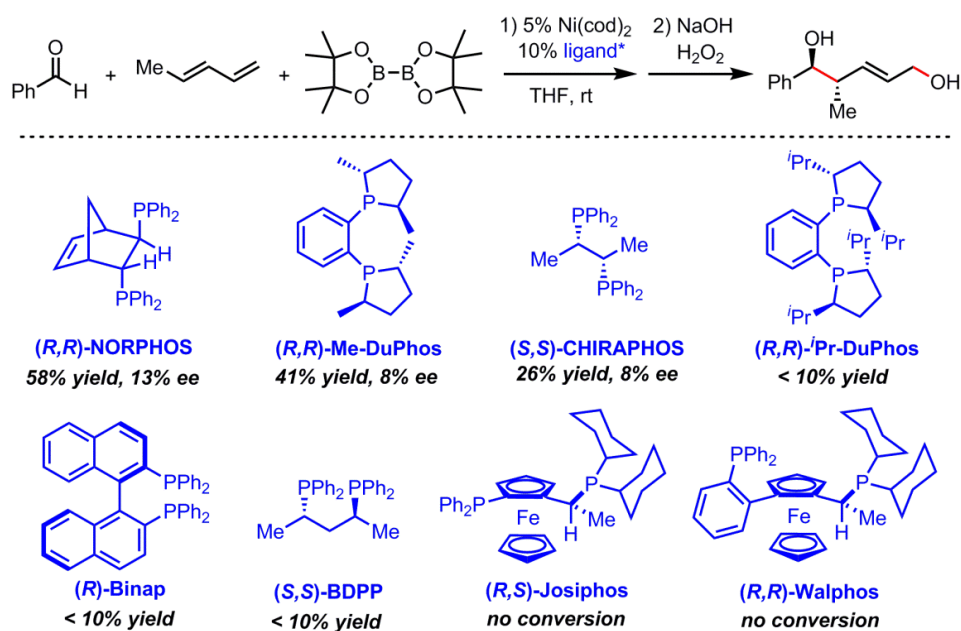
Scheme 3.37 Chiral Monodentate Phosphine/Phosphoramidite Ligand Screening



Various bidentate phosphine ligands were also surveyed for this multicomponent coupling process (Scheme 3.38). The reaction with (*R,R*)-NORPHOS gave the 1,5-diol in 58% yield and 13% ee. The reactions with (*R,R*)-Me-DuPhos and (*S,S*)-CHIRAPHOS afforded the desired product in moderate yields; but, the selectivity was poor (8% ee). When the reaction was conducted with (*R,R*)-*i*-Pr-DuPhos, (*R*)-BINAP, or (*S,S*)-BDPP as a ligand, the product was formed in less than 10% yield. Additionally, we did not observe any products formed

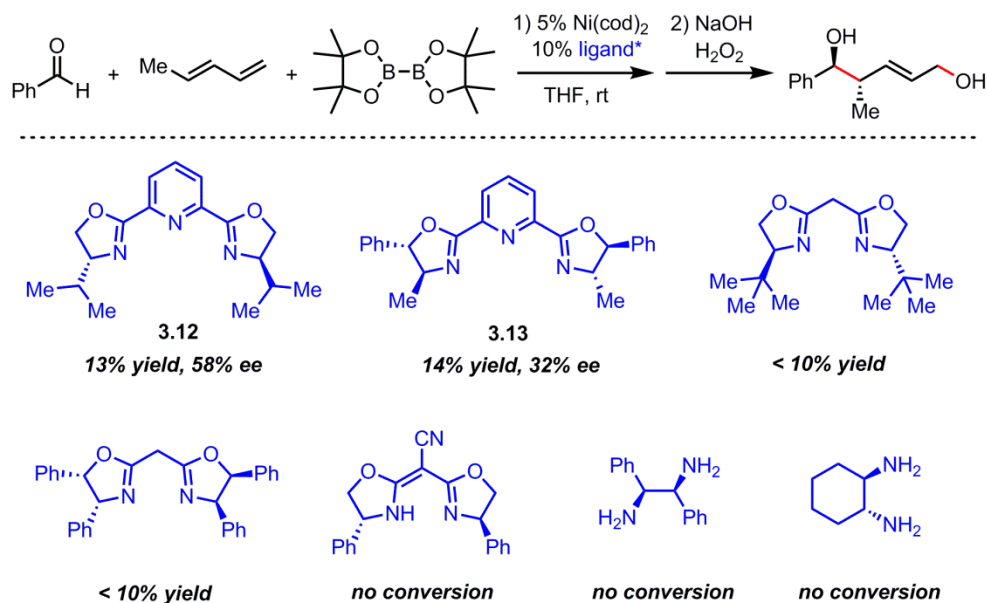
form the reactions with the ferrocene-based phosphine ligands [(*R,S*)-Josiphos and (*R,R*)-Walphos].

Scheme 3.38 Chiral Bidentate Phosphine Ligand Screening



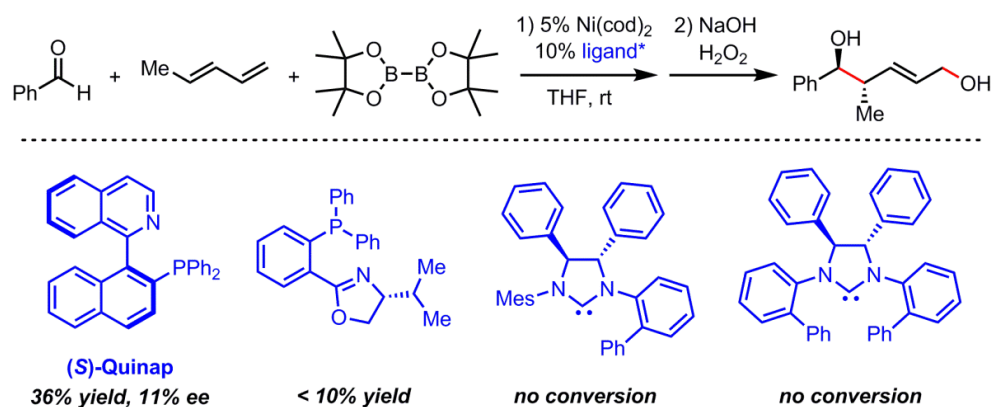
Some of the best selectivities were observed when PyBOX ligands were employed in the coupling reactions. When the reaction was carried out with a PyBOX ligand **3.12**, the 1,5 diol was afforded in 13% yield and 58% ee (Scheme 3.39). Also, another PyBOX ligand **3.13** furnished the product with 32% ee in the aldehyde–diene–diboron coupling reaction. The Box ligands shown in Scheme 3.39 gave the product in less than 10% yield, and the reaction with diamine ligands produced any products in the process.

Scheme 3.39 Chiral Nitrogen Ligand Screening



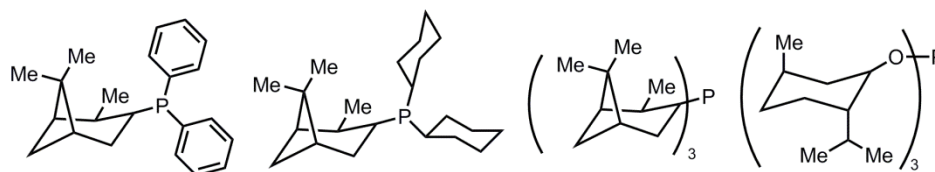
In addition, some chiral PN ligands and NHC ligands were also examined for the borylative coupling reactions (Scheme 3.40). The reaction with (*S*)-QUINAP as a ligand afforded the diol product in 36% yield, but the ee was only 11%. The other PN ligand in Scheme 3.40 gave the 1,5 diol in less than 10% yield. We also examined some chiral *N*-heterocyclic carbene (NHC) ligands. Neither of the NHC ligands shown in Scheme 3.40 showed any catalytic activities toward the borylative multicomponent coupling reactions.

Scheme 3.40 Chiral PN Ligand and NHC Ligand Screening



During the course of investigations with commercially available chiral ligands, we also designed some chiral phosphine ligands (Scheme 3.41). Considering that PCy_3 is one of the best ligands for this multicomponent coupling reaction, these chiral monodentate phosphine ligands that are analogous to tricyclohexylphosphine are likely to work well in this process. These ligands were synthesized in oxidized forms (i.e. phosphine oxides), but they were not employed in these borylative coupling reactions due to the difficulties in the reduction step.

Scheme 3.41 Original Design for Optically-Active Chiral Phosphine Ligands

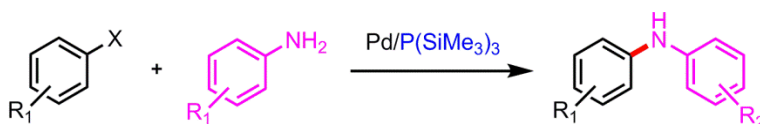


3.4. Mechanistic Considerations

3.4.1. Properties of the P(TMS)₃ Ligand

As described in the previous sections, we observed the reversal in regioselectivity when it is used in place of PCy₃ or P(*t*-Bu)₃ during the investigations on the borylative aldehyde–diene coupling reaction. In the hopes of obtaining insights on the reactivities of this unique ligand, we next sought to investigate the properties of the P(TMS)₃ ligand. P(SiMe₃)₃ is a relatively unknown ligand in transition metal catalysis. The only reported use of P(TMS)₃ ligand can be found in the Pd-catalyzed aryl amination reaction (Scheme 3.42).⁴⁷

Scheme 3.42 Palladium-Catalyzed Aryl Amination



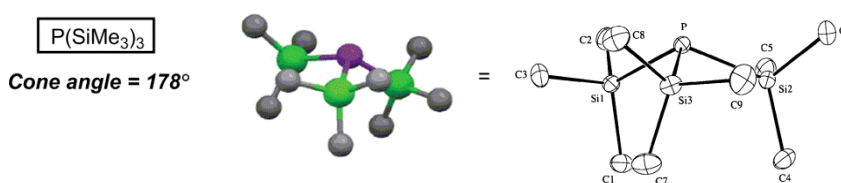
Data in Table 3.1 reveal that smaller ligands may favor formation of **3.3** (see entries 2 and 4 in Table 3.1), which might suggest that P(SiMe₃)₃ simply serves as a precursor to PH₃ (reaction with adventitious moisture).⁴⁸ However, *in situ* ³¹P NMR analysis of reactions in the

⁴⁷ Richter, A. M. and Lischewski, V. *Chemical Abstracts* **2001**, 135, 152619; DE Patent 19,963,009, 1991.

⁴⁸ Conversion of P(SiMe₃)₃ complexes to PH₃ complexes by treatment with Brønsted acids: (a) Haupt, H. J.; Krampe, O.; Flörke, U., "Darstellung Und Molekülstrukturen Von Oligofunktionalen Dirheniumcarbonylderivaten Aus Dirheniumnonacarbonylphosphan," *Zeitschrift für Anorganische und Allgemeine Chemie* **1996**, 622, 807-812. (b) Vogel, U.; Timoshkin, A. Y.; Schwan, K.-C.; Bodensteiner, M.; Scheer, M., "The Formation of Lewis Acid/Base Stabilised Phosphanyltriellanes – a Theoretical and Experimental Study," *Journal of Organometallic Chemistry* **2006**, 691, 4556-4564.

presence of $\text{P}(\text{SiMe}_3)_3$ shows that the preponderance of the ligand remains unmodified (^{31}P $\delta = -251.4$ ppm) over the course of the catalytic reaction.⁴⁹ As far as the steric environment of the $\text{P}(\text{TMS})_3$ ligand is concerned, the X-ray analysis of the ligand suggests that the cone angle of the phosphine is 178° (Figure 3.3).⁵⁰

Figure 3.3 X-Ray Analysis of the $\text{P}(\text{TMS})_3$ Ligand



The fact that the cone angle of $\text{P}(\text{SiMe}_3)_3$ is similar to that of $\text{P}(t\text{-Bu})_3$ (178° versus 182°) suggests that the difference in regioselectivity observed with these ligands most likely arises from electronic rather than steric differences between the carbon- and the silicon-based structures. Helm and co-workers investigated the IR frequency of the CO group (A_1 CO stretching) in the tungsten– $\text{P}(\text{TMS})_3$ complex (Figure 3.4).⁵¹ The IR analysis of the CO

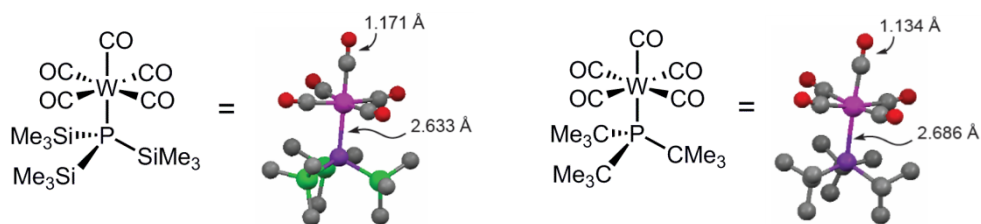
⁴⁹ An analogous experiment with PCy_3 shows that the majority of PCy_3 is uncoordinated during catalytic reactions as well.

⁵⁰ Bruckmann, J.; Kruger, C., "Tris(*n*-Butyl)Phosphine, Tris(*Tert*-Butyl)Phosphine and Tris-(Trimethylsilyl)Phosphine," *Acta Crystallographica Section C: Crystal Structure Communications* **1995**, *51*, 1152-1155.

⁵¹ McCampbell, T. A.; Kinkel, B. A.; Miller, S. M.; Helm, M. L., "Group 6 Metal Carbonyl Complexes of a Bulky Phosphine: The Crystal Structures of Tris(Trimethylsilyl)Phosphine-M(0) Pentacarbonyl, M= Chromium, Molybdenum, and Tungsten," *Journal of Chemical Crystallography* **2006**, *36*, 271-275.

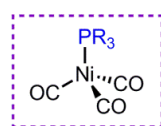
stretching of the tungsten complex with $\text{P}(\text{TMS})_3$ suggested that $\text{P}(\text{TMS})_3$ and $\text{P}(t\text{-Bu})_3$ are electronically similar.⁵²

Figure 3.4 Tungsten–Phosphine Complexes



The investigations on the CO IR stretching of nickel–phosphine complexes were conducted by Bartik and co-workers (Table 3.7).⁵³ The IR data in Table 3.7 also indicated that $\text{P}(\text{TMS})_3$ and trialkylphosphines are electronically similar ligands.

Table 3.7 CO IR Stretching for Nickel–Phosphine Complexes



PR_3	ν_{CO} (cm^{-1})
$\text{P}(t\text{-Bu})_3$	2056.1
$\text{P}(\text{SiMe}_3)_3$	2056.9
PCy_3	2057.5
PEt_3	2062.4
PMe_3	2064.6
PPh_3	2069.3
$\text{P}(\text{OEt})_3$	2077.7

⁵² Pickardt, J.; Rösch, L.; Schumann, H., "Die Kristallstruktur Von Pentacarbonyl(Tri-Tert-Butylphosphin)Wolfram Und Tricarbonyl(Tri-Tert-Butylphosphin)Nickel," *Zeitschrift für Anorganische und Allgemeine Chemie* **1976**, 426, 66-76.

⁵³ Bartik, T.; Himmler, T.; Schulte, H. G.; Seevogel, K., "Substituenteneinflüsse Auf Die Basizität Von Phosphorliganden in $\text{R}_3\text{P-Ni}(\text{CO})_3$ -Komplexen," *Journal of Organometallic Chemistry* **1984**, 272, 29-41.

Bodner and coworkers reported carbon NMR resonances for nickel–phosphine complexes as shown in Table 3.8.⁵⁴ In this set of data, it is suggested that P(TMS)₃ is less electron-rich than either PCy₃ or P(*t*-Bu)₃.

Table 3.8 Carbon NMR Data for Phosphine Ligands

PR ₃	Δδ from Ni(CO) ₄ (ppm)
P(<i>t</i> -Bu) ₃	6.37
PCy ₃	6.32
P(SiMe ₃) ₃	5.67
PEt ₃	5.54
PMe ₃	5.05
PPh ₃	4.30
P(OEt) ₃	3.61

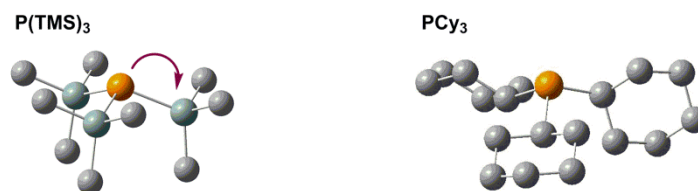
3.4.2. Theoretical Investigations

Because the reported data regarding the electronic properties of phosphine ligands are conflicting, we next sought to investigate the donor–acceptor interactions of the phosphine ligands with NBO analysis (Figure 3.5).⁵⁵ The calculated NBO energies revealed that there is a significant interaction between the donor orbital of phosphine lone-pair and the acceptor orbital of σ^* of Si–C bond in the P(TMS)₃ ligand. However, such hyperconjugative interactions were not observed in the tricyclohexylphosphine ligand.

⁵⁴ Bodner, G. M.; May, M. P.; McKinney, L. E., "A Fourier Transform Carbon-13 NMR Study of the Electronic Effects of Phosphorus, Arsenic, and Antimony Ligands in Transition-Metal Carbonyl Complexes," *Inorganic Chemistry* **1980**, *19*, 1951-1958.

⁵⁵ For more details on NBO analysis, please refer to Section 5.5.2.2.1 "Introduction to Natural Bond Orbital (NBO)" in this thesis.

Figure 3.5 NBO Analysis of Phosphine Ligands



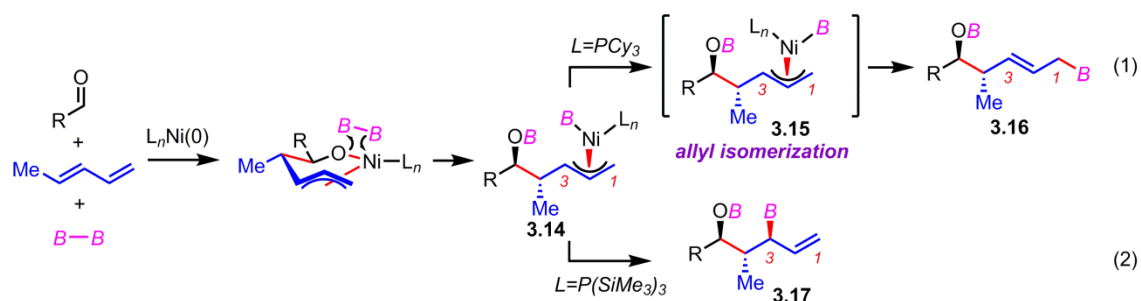
The NBO data suggest that when $\text{P}(\text{TMS})_3$ forms a complex with a nickel catalyst, this silicon-based ligand can act as an electron acceptor due to the hyperconjugative interaction between the donor and acceptor orbitals.

3.4.3. Proposed Reaction Mechanism

Based on the results from both experimental and theoretical investigations, we formulated a tentative hypothesis for the reaction pathways of the borylative aldehyde–diene coupling reactions (Scheme 3.43). In the case of reaction with PCy_3 , the intermediate nickel-allyl complex (**3.14**) would be isomerized to complex **3.15** via allyl isomerization.⁵⁶ Then, subsequent reductive elimination of **3.15** would afford product **3.16** by forming a bond between C1 and the boryl group (eq 1, Scheme 3.43).

⁵⁶ Consiglio, G.; Waymouth, R. M., "Enantioselective Homogeneous Catalysis Involving Transition-Metal-Allyl Intermediates," *Chemical Reviews* **1989**, *89*, 257-276.

Scheme 3.43 Proposed Reaction Pathways for Borylative Aldehyde–Diene Coupling



In the case of $P(\text{TMS})_3$, however, reductive elimination of complex **3.14** would directly furnish product **3.17** by forming a bond between C3 and the boryl group (eq 2, Scheme 3.43). The large cone angle of $P(\text{SiMe}_3)_3$, combined with an ability to act as an electron acceptor, may facilitate reductive elimination of **3.17** from **3.14**, prior to allyl isomerization required for formation of **3.16**. Consistent with this hypothesis, the borylative coupling reaction with tris(2,4-di-*tert*-butylphenyl)phosphite as the ligand⁵⁷ also furnished **3.17** selectively, albeit in an inferior yield relative to $P(\text{SiMe}_3)_3$.

⁵⁷ Cone angle = 215°, see: Crous, R.; Datt, M.; Foster, D.; Bennie, L.; Steenkamp, C.; Huyser, J.; Kirsten, L.; Steyl, G.; Roodt, A., "Rhodium Hydride Formation in the Presence of a Bulky Monophosphite Ligand: A Spectroscopic and Solid-State Investigation," *Dalton Transactions* **2005**, 1108-1116.

3.5. Conclusions and Outlook

Borylative diene–aldehyde coupling reaction provides an efficient single-step route to complex molecules that possess multiple stereogenic centers and functional group handles. During the study of this process, we observed a remarkable turnover in regioselectivity of the borylative multicomponent coupling when PCy₃ is replaced with P(SiMe₃)₃. In particular, the products from the reactions with P(SiMe₃)₃ feature three contiguous stereocenters and an α -chiral allylboronate.

Utilizing this α -chiral allylboronate product, a single-pot reaction sequence delivers 1,6-diol as a single regioisomer and with excellent levels of 1,5-stereoiduction. The results of enantioselective borylative diene–aldehyde couplings are preliminary; however, bulky PyBOX ligands seem most promising in terms of enantioselectivities.

The effect of P(SiMe₃)₃ ligand on the product selectivity is intriguing. According to the experimental and computational results, it has an ability to act as an electron acceptor, which will prevent allyl isomerization and facilitate reductive elimination from the intermediate nickel complex during the course of the reaction.

3.6. Experimental Section

3.6.1. General Information

All reactions were performed in oven- or flame-dried glassware fitted with rubber septa under a positive pressure of nitrogen, unless otherwise stated. Air- and moisture-sensitive liquids were transferred via syringe or stainless steel cannula. Organic solvents were concentrated by rotary evaporation at various temperatures, unless otherwise noted. All work-up and purification procedures were carried out with reagent grade solvents under typical bench-top conditions. Analytical thin-layer chromatography (TLC) was performed using glass plates, which are pre-coated with silica gel 60 F254 (0.25 mm thickness) impregnated with a fluorescent indicator (254 nm). TLC plates were visualized by exposure to UV (ultraviolet) light, and then were stained with phosphomolybdic acid (PMA) in ethanol, potassium permanganate (KMnO₄) in water, or cerium(IV) sulfate and ammonium molybdate in sulfuric acid (CAM). Liquid chromatography was performed using forced flow (flash chromatography)⁵⁸ on silica gel (porosity = 60 Å, particle size = 40-63 μm) purchased from Silicycle. Medium pressure gradient chromatography was performed on a Teledyne Isco CombiFlash automated flash chromatography system with a 200-780 nm UV-vis variable wavelength detector.

⁵⁸ Still, W. C.; Kahn, M.; Mitra, A., "Rapid Chromatographic Technique for Preparative Separations with Moderate Resolution," *The Journal of Organic Chemistry* **1978**, *43*, 2923-2925.

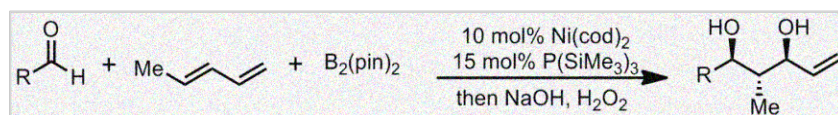
Tetrahydrofuran (THF), dichloromethane, and diethyl ether were purified using a Pure Solv MD-4 solvent purification system from Innovative Technology Inc. Bis(pinacolato)diboron [$B_2(\text{pin})_2$] was obtained from AllyChem Co., Ltd. and recrystallized from pentane prior to use. Aldehydes were purchased from Aldrich and distilled or recrystallized prior to use. Bis(1,5-cyclooctadiene)nickel(0) [$Ni(\text{cod})_2$] and tricyclohexylphosphine (PCy_3) were purchased from Strem Chemicals, Inc. Piperylene (1,3-pentadiene) and 3-methyl-1,3-pentadiene were purchased from ChemSampCo. All other reagents were purchased from Sigma Aldrich, Acros, Strem, Alfa Aesar, Fisher, or TCI America and used without further purification.

Proton nuclear magnetic resonance (^1H NMR) spectra were recorded on either a Varian Gemini-400 (400 MHz), or a Varian Inova-500 (500 MHz) spectrometer. Proton chemical shifts are reported in ppm (parts per million, δ scale) downfield from tetramethylsilane and are referenced to residual protium in the NMR solvent as the internal standard (CHCl_3 : 7.26 ppm). Data are reported as follows: chemical shift, integration, multiplicity (s = singlet, d = doublet, t = triplet, q = quartet, br = broad, m = multiplet), coupling constants (Hz), and assignment. ^{13}C NMR spectra were recorded on either a Varian Gemini-400 (100 MHz), or a Varian Inova-500 (125 MHz) spectrometer with complete proton decoupling. Carbon chemical shifts are reported in ppm (parts per million, δ scale) downfield from tetramethylsilane and are referenced to the NMR solvent resonance as the internal standard (CDCl_3 : 77.16 ppm). Infrared (IR) spectra were recorded on a Bruker alpha spectrophotometer, ν_{max} cm^{-1} . Bands are characterized as broad (br), strong (s), medium (m),

and weak (w). High resolution mass spectrometry (HRMS) was performed at the Mass Spectrometry Facility, Boston College. Melting points were determined with a Thomas-Hoover Unimelt capillary melting point apparatus and were uncorrected.

3.6.2. Experimental Procedures

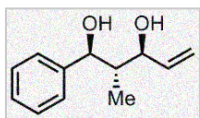
3.6.2.1. General Procedure for Borylative Diene Aldehyde Coupling



An oven-dried 20 mL scintillation vial, equipped with a magnetic stir-bar, was charged with Ni(cod)₂ (0.10 mmol), P(SiMe₃)₃ (0.15 mmol),⁵⁹ and THF (5 mL, 0.2 M) in a dry box under an argon atmosphere. After stirring for 5 min, the aldehyde (1.0 mmol), *trans*-1,3-pentadiene (1.1 mmol or 3.0 mmol) and B₂(pin)₂ (1.2 mmol or 3.0 mmol) were added sequentially. The vial was sealed with a polypropylene cap and removed from the dry box. The reaction mixture was then allowed to stir at ambient temperature for 12 h. After this time, the mixture was cooled to 0 °C (ice-water bath), and 4 mL of 3 M NaOH and 3 mL of 30% H₂O₂ were added dropwise with caution. The mixture was then allowed to stir at ambient temperature for 10 h. The resulting solution was cooled to 0 °C and quenched by the addition of 2 mL of saturated aqueous Na₂S₂O₃. The two-phase mixture was extracted with ethyl acetate (3 × 30 mL), and the combined organic layers were dried over anhydrous Na₂SO₄. The drying agent was removed by filtration and the solvent was evaporated *in vacuo*. The crude material was purified by silica gel chromatography (hexanes/EtOAc) to afford the title compounds.

⁵⁹ P(SiMe₃)₃ is highly pyrophoric; it should be handled with great caution.

3.6.2.1.1. Characterization Data and Proof of Stereochemistry



(1S*,2S*,3S*)-2-methyl-1-phenylpent-4-ene-1,3-diol. The reaction was

performed according to the general procedure with 27.5 mg (0.10 mmol) of

Ni(cod)₂, 37.5 mg (0.15 mmol) of P(SiMe₃)₃, 106 mg (1.0 mmol) of

benzaldehyde, 204.4 mg (3.0 mmol) of *trans*-1,3-pentadiene, and 761.8 mg (3.0 mmol) of

B₂(pin)₂ in THF (5.0 mL) for 12 h, followed by oxidation, to afford the title compound (**6**) as a

white solid (128 mg, 67% yield). R_f = 0.52 (1:1 hexanes:EtOAc); mp 79-80 °C; ¹H NMR (400

MHz, CDCl₃): δ 7.36-7.26 (5H, m, CHC₆H₅), 5.91 (1H, ddd, *J* = 18.0 Hz, 10.4 Hz, 7.6 Hz,

CH₂CH), 5.29 (1H, d, *J* = 17.2 Hz, CHCHCH_aH_b), 5.20 (1H, d, *J* = 10.4 Hz, CHCHCH_aH_b), 4.59

(1H, d, *J* = 8.4 Hz, ArCH), 4.20 (1H, dd, *J* = 8.8 Hz, 7.2 Hz, CH₂CHCH), 3.34 (1H, br s, OH),

3.16 (1H, br s, OH), 2.02-1.92 (1H, m, CHCH₃), 0.53 (3H, d, *J* = 6.8 Hz, CHCH₃); ¹³C NMR (100

MHz, CDCl₃): δ 143.2, 139.5, 128.5, 128.0, 127.2, 116.9, 80.4, 79.0, 44.8, 13.7; IR (neat): 3323 (br),

3029 (w), 2965 (w), 2923 (m), 2854 (w), 1493 (w), 1454 (m), 1378 (w), 1324 (m), 1278 (m), 1091

(m), 1014 (s), 924 (s), 763 (s), 699 (s) cm⁻¹; HRMS (ESI+) calculated for C₁₂H₁₅O [M-H₂O+H]⁺:

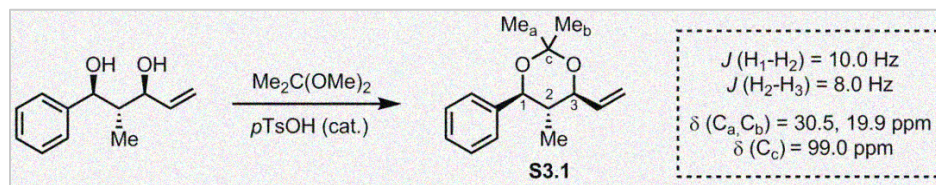
175.1122, found: 175.1121.

Proof of Stereochemistry. The relative configuration was assigned as *anti* (C₁-C₂)/*anti* (C₂-C₃)

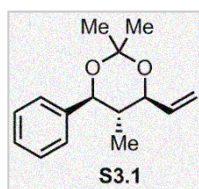
by analysis of the spectral data, after conversion of the title compound into **S3.1** as shown

below.⁶⁰

⁶⁰ For ¹³C NMR chemical shift correlations in 1,3-diol acetonides, see: (a) Rychnovsky, S. D.; Skaltitzky, D. J., "Stereochemistry of Alternating Polyol Chains: ¹³C NMR Analysis of 1,3-Diol Acetonides,"



(4*S*^{*},5*S*^{*},6*S*^{*})-2,2,5-trimethyl-4-phenyl-6-vinyl-1,3-dioxane (S3.1). A

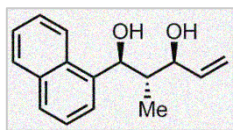


flame-dried 10 mL round-bottom flask, equipped with a magnetic stir-bar, was charged with the diol (93 mg, 0.50 mmol), 2,2-dimethoxypropane (2 mL, 0.25 M), and *p*-toluenesulfonic acid (9 mg, 0.05 mmol). After stirring

at ambient temperature for 30 min, a saturated aqueous NaHCO₃ solution was added. The reaction mixture was extracted with diethyl ether (3 × 10 mL) and the organic layer was washed with brine. The combined organic layers were dried over anhydrous Na₂SO₄. The drying agent was removed by filtration and the solvent was evaporated *in vacuo*. The crude product was purified by silica gel chromatography to afford **S1** as a colorless oil. *R*_f = 0.68 (4:1 hexanes:EtOAc); ¹H NMR (400 MHz, CDCl₃): δ 7.39-7.26 (5H, m, CHC₆H₅), 5.81 (1H, ddd, *J* = 17.6 Hz, 10.0 Hz, 7.2 Hz, CH₂CH), 5.32 (1H, d, *J* = 17.6 Hz, CHCHC_{H_a}H_b), 5.25 (1H, d, *J* = 10.4 Hz, CHCHC_{H_a}H_b), 4.47 (1H, d, *J* = 10.0 Hz, ArCH), 4.08 (1H, dd, *J* = 8.0 Hz, 7.2 Hz, CH₂CHCH), 1.65-1.55 (1H, m, CH₃CH), 1.60 (3H, s, CCH₃), 1.52 (3H, s, CCH₃), 0.62 (3H, d, *J* = 6.8 Hz, CHCHCH₃); ¹³C NMR (100 MHz, CDCl₃): δ 140.6, 137.1, 128.5, 128.1, 127.8, 118.3, 99.0,

Tetrahedron Letters **1990**, *31*, 945-948. (b) Evans, D. A.; Rieger, D. L.; Gage, J. R., "¹³C NMR Chemical Shift Correlations in 1,3-Diol Acetonides. Implications for the Stereochemical Assignment of Propionate-Derived Polyols," *Tetrahedron Letters* **1990**, *31*, 7099-7100. (c) Rychnovsky, S. D.; Rogers, B. N.; Richardson, T. L., "Configurational Assignment of Polyene Macrolide Antibiotics Using the [¹³C]Acetonide Analysis," *Accounts of Chemical Research* **1998**, *31*, 9-17.

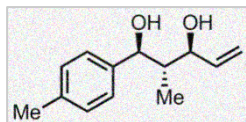
78.5, 77.4, 40.3, 30.5, 19.9, 12.5; IR (neat): 3064 (w), 3029 (w), 2990 (m), 2936 (w), 2873 (m), 1494 (w), 1454 (m), 1379 (s), 1255 (s), 1227 (m), 1199 (s), 1172 (s), 1105 (m), 1053 (s), 1022 (m), 936 (s), 755 (s), 699 (s), 543 (m) cm^{-1} ; HRMS (ESI+) calculated for $\text{C}_{12}\text{H}_{13}$ $[\text{M}-\text{acetone}-\text{H}_2\text{O}+\text{H}]^+$: 157.1022, found: 157.1017.



(1S*,2S*,3S*)-2-methyl-1-(naphthalen-1-yl)pent-4-ene-1,3-diol. The

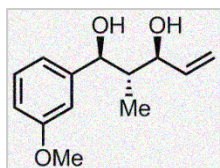
reaction was performed according to the general procedure with 27.5 mg (0.10 mmol) of Ni(cod)₂, 37.5 mg (0.15 mmol) of P(SiMe₃)₃, 156.2 mg (1.0 mmol) of 1-naphthaldehyde, 204.4 mg (3.0 mmol) of *trans*-1,3-pentadiene, and 761.8 mg (3.0 mmol) of B₂(pin)₂ in THF (5.0 mL) for 12 h, followed by oxidation, to afford the title compound as a white solid (176 mg, 73% yield). R_f = 0.50 (1:1 hexanes:EtOAc); mp 132-134 °C; ¹H NMR (500 MHz, CDCl₃): δ 8.37 (1H, d, *J* = 8.0 Hz, ArH), 7.87 (1H, d, *J* = 6.5 Hz, ArH), 7.80 (1H, d, *J* = 8.0 Hz, ArH), 7.55-7.45 (4H, m, ArH), 5.93 (1H, ddd, *J* = 17.5 Hz, 10.0 Hz, 7.5 Hz, CH₂CH), 5.28 (1H, d, *J* = 10.0 Hz, CHCHCH_aH_b), 5.32 (1H, d, *J* = 17.0 Hz, CHCHCH_aH_b), 5.20 (1H, d, *J* = 11.0 Hz, ArCH), 4.29 (1H, dd, *J* = 8.0 Hz, *J* = 7.5 Hz, CH₂CHCH), 3.66 (1H, br s, OH), 3.58 (1H, br s, OH), 2.37-2.32 (1H, m, CHCH₃), 0.49 (3H, d, *J* = 6.5 Hz, CHCH₃); ¹³C NMR (125 MHz, CDCl₃): δ 139.4, 138.9, 134.1, 131.3, 129.0, 128.6, 126.0, 125.7, 125.6, 125.4, 124.2, 116.9, 79.5, 78.4, 44.8, 14.1; IR (neat): 3308 (br), 3048 (w), 2968 (w), 2926 (w), 1596 (w), 1510 (w), 1457 (m), 1395 (m), 1376 (m), 1095 (w), 1016 (m), 993 (m), 927 (w), 800 (s), 778 (s) cm⁻¹; HRMS (ESI+) calculated for C₁₆H₂₂NO₂ [M+NH₄]⁺: 260.16505, found: 260.16502.

Stereochemistry. The relative configuration was assigned as *anti* (C₁-C₂)/*anti* (C₂-C₃) by analogy.



(1S*,2S*,3S*)-2-methyl-1-(*p*-tolyl)pent-4-ene-1,3-diol. The reaction was performed according to the general procedure with 27.5 mg (0.10 mmol) of Ni(cod)₂, 37.5 mg (0.15 mmol) of P(SiMe₃)₃, 120.2 mg (1.0 mmol) of *p*-tolualdehyde, 204.4 mg (3.0 mmol) of *trans*-1,3-pentadiene, and 761.8 mg (3.0 mmol) of B₂(pin)₂ in THF (5.0 mL) for 12 h, followed by oxidation, to afford the title compound as a colorless oil (131 mg, 64% yield). R_f = 0.55 (1:1 hexanes:EtOAc); ¹H NMR (400 MHz, CDCl₃): δ 7.22 (2H, d, *J* = 8.4 Hz, ArH), 7.15 (2H, d, *J* = 8.0 Hz, ArH), 5.88 (1H, ddd, *J* = 17.2 Hz, 10.0 Hz, 7.2 Hz, CH₂CH), 5.27 (1H, d, *J* = 16.8 Hz, CHCHCH_aH_b), 5.18 (1H, d, *J* = 10.4 Hz, CHCHCH_aH_b), 4.52 (1H, d, *J* = 9.2 Hz, ArCH), 4.16 (1H, dd, *J* = 8.0 Hz, *J* = 7.6 Hz, CH₂CHCH), 3.53 (1H, br s, OH), 3.41 (1H, br s, OH), 2.35 (3H, s, ArCH₃), 2.00-1.90 (1H, m, CHCH₃), 0.52 (3H, d, *J* = 6.8 Hz, CHCH₃); ¹³C NMR (100 MHz, CDCl₃): δ 140.3, 139.5, 137.7, 129.2, 127.1, 116.8, 80.3, 78.9, 44.8, 21.3, 13.6; IR (neat): 3327 (br), 2968 (w), 2923 (w), 1514 (w), 1457 (m), 1419 (m), 1325 (w), 1304 (w), 1278 (w), 1202 (w), 1090 (m), 1016 (s), 925 (m), 817 (s) cm⁻¹; HRMS (ESI⁺) calculated for C₁₃H₂₂NO₂ [M+NH₄]⁺: 224.1650, found: 260.1641.

Stereochemistry. The relative configuration was assigned as *anti* (C₁-C₂)/*anti* (C₂-C₃) by analogy.

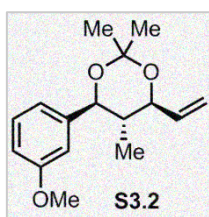
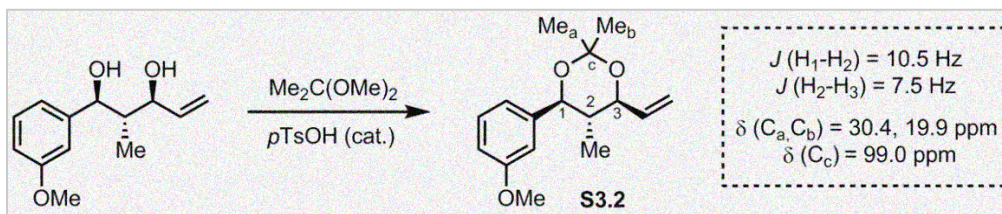


(1S*,2S*,3S*)-1-(3-methoxyphenyl)-2-methylpent-4-ene-1,3-diol. The

reaction was performed according to the general procedure with 27.5 mg (0.10 mmol) of Ni(cod)₂, 37.5 mg (0.15 mmol) of P(SiMe₃)₃, 136.2 mg (1.0 mmol) of *m*-anisaldehyde, 204.4 mg (3.0 mmol) of *trans*-1,3-

pentadiene, and 761.8 mg (3.0 mmol) of B₂(pin)₂ in THF (5.0 mL) for 12 h, followed by oxidation, to afford the title compound as a colorless oil (127 mg, 57% yield). R_f = 0.42 (1:1 hexanes:EtOAc); ¹H NMR (400 MHz, CDCl₃): δ 7.26 (1H, t, *J* = 7.2 Hz, ArH), 6.92 (1H, d, *J* = 7.6 Hz, ArH), 6.91 (1H, s, ArH), 6.84 (1H, d, *J* = 8.0 Hz, ArH), 5.90 (1H, ddd, *J* = 17.2 Hz, 10.4 Hz, 7.6 Hz, CH₂CH), 5.28 (1H, d, *J* = 17.2 Hz, CHCHCH_aH_b), 5.19 (1H, d, *J* = 10.0 Hz, CHCHCH_aH_b), 4.55 (1H, d, *J* = 8.8 Hz, ArCH), 4.18 (1H, dd, *J* = 8.0 Hz, 7.6 Hz, CH₂CHCH), 3.82 (3H, s, ArOCH₃), 3.40 (1H, br s, OH), 3.22 (1H, br s, OH), 2.00-1.90 (1H, m, CHCH₃), 0.55 (3H, d, *J* = 6.8 Hz, CHCH₃); ¹³C NMR (100 MHz, CDCl₃): δ 160.0, 144.8, 139.5, 129.5, 119.7, 116.9, 113.6, 112.6, 80.4, 79.0, 55.4, 44.9, 13.6; IR (neat): 3345 (br), 2968 (w), 2935 (w), 2896 (w), 2836 (w), 1601 (m), 1587 (m), 1487 (m), 1457 (m), 1436 (m), 1260 (s), 1157 (w), 1020 (s), 955 (s), 954 (w), 928 (w), 703 (w) cm⁻¹; HRMS (ESI+) calculated for C₁₃H₂₂NO₃ [M+NH₄]⁺: 240.1600, found: 240.1605.

Proof of Stereochemistry. The relative configuration was assigned as *anti* (C₁-C₂)/*anti* (C₂-C₃) by analysis of the spectral data, after conversion of the title compound into **S3.2** as shown below.



(4*S*^{*},5*S*^{*},6*S*^{*})-4-(3-methoxyphenyl)-2,2,5-trimethyl-6-vinyl-1,3-dioxane

(S3.2). $R_f = 0.58$ (4:1 hexanes:EtOAc); $^1\text{H NMR}$ (500 MHz, CDCl_3): δ 7.25

(1H, t, $J = 8.0$ Hz, ArH), 6.95 (1H, d, $J = 8.0$ Hz, ArH), 6.94 (1H, s, ArH),

6.84 (1H, d, $J = 8.5$ Hz, ArH), 5.81 (1H, ddd, $J = 17.0$ Hz, 10.0 Hz, 7.0 Hz,

CH₂CH), 5.33 (1H, d, $J = 17.0$ Hz, CHCHCH_aH_b), 5.25 (1H, d, $J = 10.0$ Hz, CHCHCH_aH_b), 4.45

(1H, d, $J = 10.5$ Hz, ArCH), 4.07 (1H, t, $J = 7.5$ Hz, CH₂CHCH), 3.82 (3H, s, ArOCH₃), 1.60 (3H,

s, CCH₃), 1.64-1.58 (1H, m, CH₃CH), 1.52 (3H, s, CCH₃), 0.63 (3H, d, $J = 6.5$ Hz, CHCHCH₃);

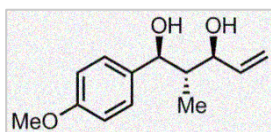
$^{13}\text{C NMR}$ (125 MHz, CDCl_3): δ 159.9, 142.1, 137.1, 129.4, 120.3, 118.4, 113.8, 113.2, 99.0, 78.4,

77.5, 55.4, 40.2, 30.4, 19.9, 12.5; IR (neat): 3079 (w), 2991 (m), 2963 (w), 2936 (w), 2873 (w), 2836

(w), 1857 (m), 1489 (m), 1456 (m), 1435 (m), 1407 (m), 1379 (s), 1288 (s), 1200 (s), 1171 (m), 992

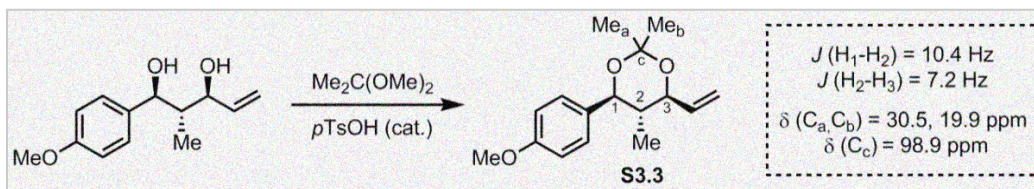
(m), 926 (m), 903 (m), 782 (m), 700 (m) cm^{-1} ; HRMS (ESI⁺) calculated for C₁₃H₁₅O [M-

acetone-OH]⁺: 187.1123, found: 187.1129.

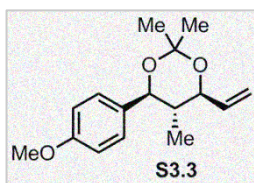
(1S*,2S*,3S*)-1-(4-methoxyphenyl)-2-methylpent-4-ene-1,3-diol.

The reaction was performed according to the general procedure with 27.5 mg (0.10 mmol) of Ni(cod)₂, 37.5 mg (0.15 mmol) of P(SiMe₃)₃, 136.2 mg (1.0 mmol) of *p*-anisaldehyde, 204.4 mg (3.0 mmol) of *trans*-1,3-pentadiene, and 761.8 mg (3.0 mmol) of B₂(pin)₂ in THF (5.0 mL) for 12 h, followed by oxidation, to afford the title compound as a colorless oil (126 mg, 57% yield). R_f = 0.35 (1:1 hexanes:EtOAc); ¹H NMR (400 MHz, CDCl₃): δ 7.27 (2H, d, *J* = 7.2 Hz, ArH), 6.88 (2H, d, *J* = 8.8 Hz, ArH), 5.90 (1H, ddd, *J* = 17.2 Hz, 10.0 Hz, 7.2 Hz, CH₂CH), 5.28 (1H, d, *J* = 17.2 Hz, CHCHCH_aH_b), 5.19 (1H, d, *J* = 10.4 Hz, CHCHCH_aH_b), 4.54 (1H, d, *J* = 8.8 Hz, ArCH), 4.18 (1H, t, *J* = 8.0 Hz, CH₂CHCH), 3.81 (3H, s, ArOCH₃), 3.28 (1H, br s, OH), 3.18 (1H, br s, OH), 1.98-1.90 (1H, m, CHCH₃), 0.52 (3H, d, *J* = 6.8 Hz, CHCH₃); ¹³C NMR (100 MHz, CDCl₃): δ 159.4, 139.5, 135.5, 128.3, 116.8, 113.9, 80.1, 78.9, 55.5, 44.9, 13.7; IR (neat): 3349 (br), 2965 (w), 2932 (w), 2837 (w), 1612 (m), 1586 (w), 1513 (m), 1460 (w), 1396 (w), 1303 (w), 1246 (s), 1175 (m), 1033 (s), 927 (w), 831 (m) cm⁻¹; HRMS (ESI+) calculated for C₁₃H₂₂NO₃ [M+NH₄]⁺: 240.15997, found: 240.15991.

Proof of Stereochemistry. The relative configuration was assigned as *anti* (C₁-C₂)/*anti* (C₂-C₃) by analysis of the spectral data, after conversion of the title compound into **S3.3** as shown below.



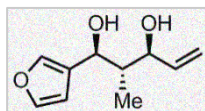
(4*S*^{*},5*S*^{*},6*S*^{*})-4-(4-methoxyphenyl)-2,2,5-trimethyl-6-vinyl-1,3-di-



oxane (S3.3). $R_f = 0.56$ (4:1 hexanes:EtOAc); $^1\text{H NMR}$ (500 MHz, CDCl_3): δ 7.30 (2H, d, $J = 8.8$ Hz, ArH), 6.88 (2H, d, $J = 8.8$ Hz, ArH), 5.81 (1H, ddd, $J = 17.6$ Hz, 10.4 Hz, 7.2 Hz, CH_2CH), 5.32 (1H, d, $J =$

17.2 Hz, $\text{CHCHCH}_a\text{H}_b$), 5.24 (1H, d, $J = 10.4$ Hz, $\text{CHCHCH}_a\text{H}_b$), 4.42 (1H, d, $J = 10.4$ Hz, ArCH), 4.06 (1H, t, $J = 7.2$ Hz, CH_2CHCH), 3.80 (3H, s, ArOCH_3), 1.64-1.56 (1H, m, CH_3CH), 1.59 (3H, s, CCH_3), 1.50 (3H, s, CCH_3), 0.61 (3H, d, $J = 6.8$ Hz, CHCHCH_3); $^{13}\text{C NMR}$ (125 MHz, CDCl_3): δ 159.5, 137.2, 132.9, 128.9, 118.2, 113.9, 98.9, 78.0, 77.5, 55.5, 40.3, 30.5, 19.9, 12.5; IR (neat): 2991 (m), 2962 (w), 2936 (w), 2909 (w), 2873 (w), 2837 (w), 1613 (m), 1586 (w), 1514 (s), 1461 (m), 1379 (s), 1301 (m), 1249 (s), 1229 (m), 1200 (s), 1171 (s), 1099 (m), 1054 (s), 1035 (s), 991 (w), 936 (m), 886 (m), 830 (s) cm^{-1} ; HRMS (ESI+) calculated for $\text{C}_{13}\text{H}_{15}\text{O}$ [$\text{M}-\text{acetone}-\text{OH}]^+$: 187.1123, found: 187.1120.

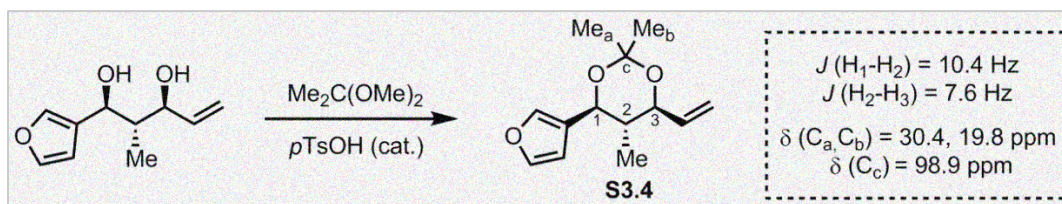
(1*S**,2*S**,3*S**)-1-(furan-3-yl)-2-methylpent-4-ene-1,3-diol. The reaction



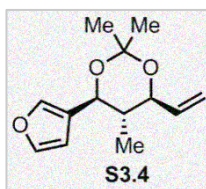
was performed according to the general procedure with 27.5 mg (0.10 mmol) of Ni(cod)₂, 37.5 mg (0.15 mmol) of P(SiMe₃)₃, 96.1 mg (1.0 mmol)

of 3-furaldehyde, 204.4 mg (3.0 mmol) of *trans*-1,3-pentadiene, and 761.8 mg (3.0 mmol) of B₂(pin)₂ in THF (5.0 mL) for 12 h, followed by oxidation, to afford the title compound as a colorless oil (100 mg, 55% yield). R_f = 0.34 (1:1 hexanes:EtOAc); ¹H NMR (400 MHz, CDCl₃): δ 7.40 (2H, s, ArH), 6.44 (1H, s, ArH), 5.91 (1H, ddd, *J* = 17.2 Hz, 10.4 Hz, 7.2 Hz, CH₂CH), 5.28 (1H, d, *J* = 17.6 Hz, CHCHCH_aH_b), 5.20 (1H, d, *J* = 10.4 Hz, CHCHCH_aH_b), 4.65 (1H, d, *J* = 8.8 Hz, ArCH), 4.14 (1H, t, *J* = 7.2 Hz, CH₂CHCH), 3.15 (1H, br s, OH), 2.89 (1H, br s, OH), 1.99-1.89 (1H, m, CHCH₃), 0.65 (3H, d, *J* = 7.2 Hz, CHCH₃); ¹³C NMR (100 MHz, CDCl₃): δ 143.6, 140.1, 139.5, 127.6, 117.1, 108.8, 78.8, 71.9, 44.0, 13.5; IR (neat): 3350 (br), 2967 (w), 2929 (w), 2554 (w), 1502 (w), 1405 (w), 1380 (m), 1318 (w), 1239 (w), 1158 (m), 1022 (s), 874 (s), 794 (s), 750 (w), 730 (w), 600 (s) cm⁻¹; HRMS (ESI+) calculated for C₁₀H₁₃O₂ [M-H₂O+H]⁺: 165.0915, found: 165.0910.

Proof of Stereochemistry. The relative configuration was assigned as *anti* (C₁-C₂)/*anti* (C₂-C₃) by analysis of the spectral data, after conversion of the title compound into **S3.4** as shown below.

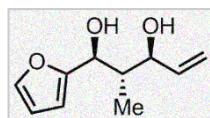


(4S*,5S*,6S*)-4-(furan-3-yl)-2,2,5-trimethyl-6-vinyl-1,3-dioxane (S3.4). R_f



= 0.61 (4:1 hexanes:EtOAc); $^1\text{H NMR}$ (500 MHz, CDCl_3): δ 7.44 (1H, s, ArH), 7.39 (1H, s, ArH), 6.45 (1H, s, ArH), 5.80 (1H, ddd, $J = 17.6$ Hz, 10.4 Hz, 7.2 Hz, CH_2CH), 5.32 (1H, d, $J = 17.2$ Hz, $\text{CHCHCH}_a\text{H}_b$), 5.25 (1H, d,

$J = 10.4$ Hz, $\text{CHCHCH}_a\text{H}_b$), 4.51 (1H, d, $J = 10.4$ Hz, ArCH), 4.03 (1H, t, $J = 7.6$ Hz, CH_2CHCH), 1.65-1.55 (1H, m, CH_3CH), 1.57 (3H, s, CCH_3), 1.48 (3H, s, CCH_3), 0.69 (3H, d, $J = 6.8$ Hz, CHCHCH_3); $^{13}\text{C NMR}$ (125 MHz, CDCl_3): δ 143.4, 140.5, 137.1, 125.3, 118.3, 109.1, 98.9, 77.2, 70.3, 39.4, 30.4, 19.8, 12.7; IR (neat): 2990 (w), 2964 (w), 2938 (w), 2874 (w), 1502 (w), 1459 (w), 1378 (m), 1337 (w), 1253 (m), 1200 (s), 1172 (s), 1159 (s), 1136 (m), 1105 (m), 1091 (m), 1051 (s), 1020 (s), 945 (w), 918 (s), 872 (s), 788 (s), 600 (s) cm^{-1} ; HRMS (ESI+) calculated for $\text{C}_{10}\text{H}_{13}\text{O}_2$ $[\text{M}-\text{acetone}+\text{H}]^+$: 165.0915, found: 165.0915.



(1S*,2S*,3S*)-1-(furan-2-yl)-2-methylpent-4-ene-1,3-diol. The reaction

was performed according to the general procedure with 27.5 mg (0.10

mmol) of Ni(cod)₂, 37.5 mg (0.15 mmol) of P(SiMe₃)₃, 96.1 mg (1.0 mmol)

of 2-furaldehyde, 204.4 mg (3.0 mmol) of *trans*-1,3-pentadiene, and 761.8 mg (3.0 mmol) of

B₂(pin)₂ in THF (5.0 mL) for 12 h, followed by oxidation, to afford the title compound as a

colorless oil (98 mg, 54% yield). R_f = 0.42 (1:1 hexanes:EtOAc); ¹H NMR (500 MHz, CDCl₃): δ

7.39 (1H, dd, *J* = 1.5 Hz, 0.5 Hz, ArH), 6.34 (1H, dd, *J* = 3.0 Hz, 2.0 Hz, ArH), 6.28 (1H, d, *J* =

3.0 Hz, ArH), 5.90 (1H, ddd, *J* = 17.5 Hz, 10.5 Hz, 7.5 Hz, CH₂CH), 5.28 (1H, d, *J* = 17.0 Hz,

CHCHCH_aH_b), 5.21 (1H, d, *J* = 10.5 Hz, CHCHCH_aH_b), 4.67 (1H, d, *J* = 9.0 Hz, ArCH), 4.16

(1H, dd, *J* = 8.0 Hz, 7.5 Hz, CH₂CHCH), 3.37 (1H, br s, OH), 2.74 (1H, br s, OH), 2.21-2.12 (1H,

m, CHCH₃), 0.64 (3H, d, *J* = 7.0 Hz, CHCH₃); ¹³C NMR (125 MHz, CDCl₃): δ 155.5, 142.2, 139.3,

117.2, 110.2, 107.5, 78.6, 73.0, 43.0, 13.2; IR (neat): 3430 (br), 2968 (w), 2931 (w), 1732 (m), 1565

(w), 1504 (w), 1458 (m), 1380 (m), 1320 (m), 1231 (m), 1149 (s), 1070 (s), 990 (s), 926 (s), 883 (m),

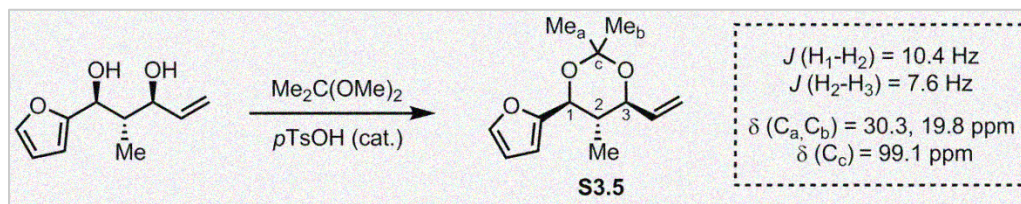
815 (m), 737 (m), 700 (m), 599 (w) cm⁻¹; HRMS (ESI+) calculated for C₁₀H₁₃O₂ [M-H₂O+H]⁺:

165.0916, found: 165.0917.

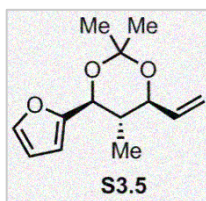
Proof of Stereochemistry. The relative configuration was assigned as *anti* (C₁-C₂)/*anti* (C₂-C₃)

by analysis of the spectral data, after conversion of the title compound into **S3.5** as shown

below.

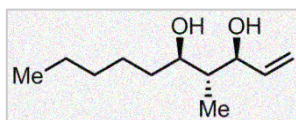


(4*S,5*S**,6*S**)-4-(furan-2-yl)-2,2,5-trimethyl-6-vinyl-1,3-dioxane (S3.5).**



$R_f = 0.61$ (4:1 hexanes:EtOAc); $^1\text{H NMR}$ (400 MHz, CDCl_3): δ 7.39 (1H, dd, $J = 0.4 \text{ Hz}, 1.2 \text{ Hz}$ ArH), 6.38-6.30 (2H, m, ArH), 5.81 (1H, ddd, $J = 17.6 \text{ Hz}, 10.4 \text{ Hz}, 7.2 \text{ Hz}$, CH_2CH), 5.32 (1H, d, $J = 17.2 \text{ Hz}$,

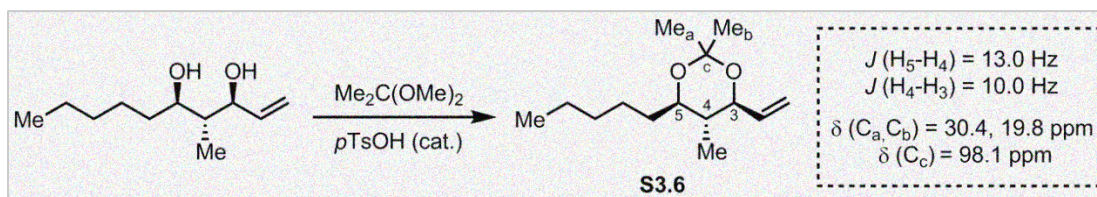
$\text{CHCHCH}_a\text{H}_b$), 5.25 (1H, d, $J = 10.4 \text{ Hz}$, $\text{CHCHCH}_a\text{H}_b$), 4.59 (1H, d, $J = 10.8 \text{ Hz}$, ArCH), 4.03 (1H, t, $J = 7.2 \text{ Hz}$, CH_2CHCH), 1.95-1.85 (1H, m, CH_3CH), 1.59 (3H, s, CCH_3), 1.49 (3H, s, CCH_3), 0.68 (3H, d, $J = 6.8 \text{ Hz}$, CHCHCH_3); $^{13}\text{C NMR}$ (100 MHz, CDCl_3): δ 153.2, 142.5, 136.9, 118.4, 110.3, 108.4, 99.1, 77.3, 71.2, 37.3, 30.3, 19.8, 12.7; IR (neat): 3079 (w), 2963 (w), 2927 (m), 2877 (w), 1720 (m), 1504 (w), 1458 (m), 1380 (m), 1259 (m), 1230 (s), 1202 (s), 1170 (s), 1103 (s), 1054 (s), 1011 (s), 991 (s), 924 (s), 886 (s), 811 (m), 739 (w), 652 (w) cm^{-1} ; HRMS (ESI+) calculated for $\text{C}_{13}\text{H}_{13}\text{O}_2$ [$\text{M}-\text{acetone}+\text{H}$] $^+$: 165.0916, found: 165.0921.

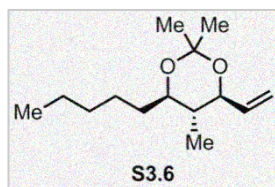


(3*S**,4*R**,5*R**)-4-methyldec-1-ene-3,5-diol. The reaction was performed according to the general procedure with 27.5 mg (0.10 mmol) of Ni(cod)₂, 37.5 mg (0.15 mmol) of P(SiMe₃)₃, 100.2 mg

(1.0 mmol) of hexanal, 74.9 mg (1.1 mmol) of *trans*-1,3-pentadiene, and 305 mg (1.2 mmol) of B₂(pin)₂ in THF (5.0 mL) for 12 h, followed by oxidation, to afford the title compound as a colorless oil (108 mg, 58% yield). *R*_f = 0.50 (1:1 hexanes:EtOAc); ¹H NMR (400 MHz, CDCl₃): δ 5.87 (1H, ddd, *J* = 17.2 Hz, 10.4 Hz, 7.2 Hz, CH₂CH), 5.24 (1H, d, *J* = 17.2 Hz, CHCHCH_aH_b), 5.18 (1H, d, *J* = 10.8 Hz, CHCHCH_aH_b), 4.08 (1H, t, *J* = 7.2 Hz, CH₂CHCH), 3.66-3.54 (1H, m, *n*-C₅H₁₁CH), 2.81 (2H, br s, 2×OH), 1.68-1.52 (1H, m, *n*-C₅H₁₁CHCH), 1.60-1.20 (8H, m, aliphatic 4×CH₂), 0.90 (3H, t, *J* = 6.4 Hz, CH₂CH₂CH₂CH₃), 0.79 (3H, d, *J* = 6.8 Hz, CHCH₃); ¹³C NMR (100 MHz, CDCl₃): δ 139.9, 116.7, 79.1, 76.4, 43.6, 35.1, 32.1, 24.7, 22.8, 14.2, 13.3; IR (neat): 3329 (br), 2955 (m), 2928 (s), 2858 (m), 1458 (m), 1422 (w), 1377 (w), 1328 (w), 1126 (w), 1089 (w), 1014 (s), 991 (s), 972 (s), 922 (w), 873 (w), 725 (w), 692 (w), 616 (w), 548 (w) cm⁻¹; HRMS (ESI+) calculated for C₁₁H₂₁O [M-H₂O+H]⁺: 169.1592, found: 169.1593.

Proof of Stereochemistry. The relative configuration was assigned as *anti* (C₅-C₄)/*anti* (C₄-C₃) by analysis of the spectral data, after conversion of the title compound into **S3.6** as shown below.



(4R*,5R*,6S*)-2,2,5-trimethyl-4-pentyl-6-vinyl-1,3-dioxane (S3.6).

$R_f = 0.63$ (4:1 hexanes:EtOAc); $^1\text{H NMR}$ (500 MHz, CDCl_3): δ 5.74

(1H, ddd, $J = 17.0$ Hz, 10.0 Hz, 7.5 Hz, CH_2CH), 5.26 (1H, d, $J = 17.0$

Hz, $\text{CHCHCH}_a\text{H}_b$), 5.19 (1H, d, $J = 10.5$ Hz, $\text{CHCHCH}_a\text{H}_b$), 3.87 (1H,

dd, $J = 10.0$ Hz, 7.5 Hz, CH_2CHCH), 3.48 (1H, td, $J = 13.0$ Hz, 2.0 Hz, $n\text{-C}_5\text{H}_{11}\text{CH}$), 1.62-1.58

(1H, m, $n\text{-C}_5\text{H}_{11}\text{CHCH}$), 1.46 (3H, s, CCH_3), 1.41 (3H, s, CCH_3), 1.39-1.20 (8H, m, aliphatic

$4 \times \text{CH}_2$), 0.89 (3H, t, $J = 6.5$ Hz, $\text{CH}_2\text{CH}_2\text{CH}_2\text{CH}_3$), 0.76 (3H, d, $J = 7.0$ Hz, CHCHCH_3); ^{13}C

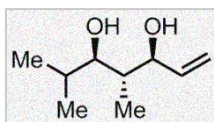
NMR (125 MHz, CDCl_3): δ 137.7, 118.1, 98.1, 74.2, 38.2, 33.2, 31.9, 30.4, 24.8, 22.8, 19.8, 14.2,

12.4; IR (neat): 2991 (m), 2955 (s), 2933 (s), 2859 (m), 1461 (w), 1378 (s), 1349 (w), 1258 (m),

1201 (s), 1174 (s), 1117 (w), 1060 (w), 1041 (w), 1022 (w), 988 (w), 965 (w), 924 (w), 892 (w),

875 (w), 837 (w), 516 (w) cm^{-1} ; HRMS (ESI+) calculated for $\text{C}_{14}\text{H}_{27}\text{O}_2$ $[\text{M}+\text{H}]^+$: 227.2021, found:

227.2011.



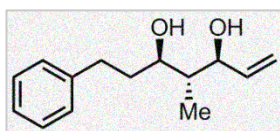
(3S*,4R*,5R*)-4,6-dimethylhept-1-ene-3,5-diol. The reaction was

performed according to the general procedure with 27.5 mg (0.10 mmol) of Ni(cod)₂, 37.5 mg (0.15 mmol) of P(SiMe₃)₃, 72.1 mg (1.0 mmol) of isobutyraldehyde, 74.9 mg (1.1 mmol) of *trans*-1,3-pentadiene, and 305 mg (1.2 mmol) of B₂(pin)₂ in THF (5.0 mL) for 12 h, followed by oxidation, to afford the title compound as a colorless oil (79 mg, 50% yield). R_f = 0.52 (1:1 hexanes:EtOAc); ¹H NMR (500 MHz, CDCl₃): δ 5.88 (1H, ddd, *J* = 17.5 Hz, 10.5 Hz, 7.5 Hz, CH₂CH), 5.25 (1H, d, *J* = 17.0 Hz, CHCHCH_aH_b), 5.18 (1H, d, *J* = 10.5 Hz, CHCHCH_aH_b), 4.12 (1H, t, *J* = 7.5 Hz, CH₂CHCH), 3.44 (1H, dd, *J* = 9.0 Hz, 2.5 Hz, (CH₃)₂CHCH), 3.09 (1H, br s, OH), 2.75 (1H, br s, OH), 1.89 (1H, heptet of doublets, *J* = 7.0 Hz, 2.5 Hz, (CH₃)₂CH), 1.76-1.64 (1H, m, CH₃CH), 1.00 (3H, d, *J* = 7.0 Hz, CHCH₃), 0.87 (3H, d, *J* = 6.5 Hz, CHCH₃), 0.78 (3H, d, *J* = 7.0 Hz, CHCH₃); ¹³C NMR (125 MHz, CDCl₃): δ 139.8, 116.9, 80.9, 79.1, 41.2, 30.0, 20.3, 14.0, 13.2; IR (neat): 3318 (br), 2962 (s), 2931 (m), 2875 (m), 1463 (s), 1415 (m), 1384 (m), 1367 (m), 1336 (w), 1319 (w), 1278 (w), 1177 (w), 1141 (w), 990 (s), 969 (s), 924 (s), 661 (w), 626 (w), 567 (w) cm⁻¹; HRMS (ESI+) calculated for C₉H₁₇O [M-H₂O+H]⁺: 141.1279, found: 141.1275.

Stereochemistry. The relative configuration was assigned as *anti* (C₅-C₄)/*anti* (C₄-C₃) by analogy.

(3S*,4R*,5R*)-4-methyl-7-phenylhept-1-ene-3,5-diol.

The



reaction was performed according to the general procedure with

27.5 mg (0.10 mmol) of Ni(cod)₂, 37.5 mg (0.15 mmol) of P(SiMe₃)₃,

134.2 mg (1.0 mmol) of hydrocinnamaldehyde, 74.9 mg (1.1 mmol) of *trans*-1,3-pentadiene,

and 305 mg (1.2 mmol) of B₂(pin)₂ in THF (5.0 mL) for 12 h, followed by oxidation, to afford

the title compound as a colorless oil (99 mg, 45% yield). R_f = 0.45 (1:1 hexanes:EtOAc); ¹H

NMR (500 MHz, CDCl₃): δ 7.30-7.17 (5H, m, CH₂C₆H₅), 5.88 (1H, ddd, J = 17.5 Hz, 10.5 Hz,

7.5 Hz, CH₂CH), 5.24 (1H, d, J = 17.0 Hz, CHCHCH_aH_b), 5.18 (1H, d, J = 10.5 Hz,

CHCHCH_aH_b), 4.07 (1H, t, J = 7.5 Hz, CH₂CHCH), 3.72-3.66 (1H, m, ArCH₂ CH₂CH), 3.15

(1H, br s, OH), 2.86 (1H, ddd, J = 13.5 Hz, 11.0 Hz, 5.5 Hz, ArCH_aH_b), 2.70 (1H, ddd, J =

16.5 Hz, 10.5 Hz, 6.5 Hz, ArCH_aH_b), 2.53 (1H, br s, OH), 1.96-1.90 (1H, m, ArCH₂CH_aH_b),

1.78-1.72 (1H, m, ArCH₂CH_aH_b), 1.74-1.55 (1H, m, CH₃CH), 0.80 (3H, d, J = 7.0 Hz, CHCH₃);

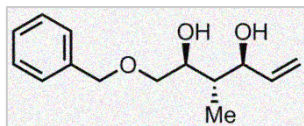
¹³C NMR (125 MHz, CDCl₃): δ 142.5, 139.9, 128.6, 128.5, 125.9, 117.0, 79.1, 75.7, 43.6, 36.9, 31.6,

13.3; IR (neat): 3331 (br), 3083 (w), 3061 (w), 3025 (m), 2923 (m), 1602 (w), 1495 (m), 1453 (s),

1377 (w), 1323 (w), 1126 (m), 1096 (m), 1030 (m), 993 (m), 967 (m), 926 (m), 847 (w), 747 (s),

699 (s) cm⁻¹; HRMS (ESI+) calculated for C₁₄H₁₉O [M-H₂O+H]⁺: 203.1435, found: 203.1426.

Stereochemistry. The relative configuration was assigned as *anti* (C₅-C₄)/*anti* (C₄-C₃) by analogy.



(2S*,3S*,4S*)-1-(benzyloxy)-3-methylhex-5-ene-2,4-diol. The

reaction was performed according to the general procedure with

27.5 mg (0.10 mmol) of Ni(cod)₂, 37.5 mg (0.15 mmol) of

P(SiMe₃)₃, 150.2 mg (1.0 mmol) of benzyloxyacetaldehyde, 74.9 mg (1.1 mmol) of *trans*-1,3-

pentadiene, and 305 mg (1.2 mmol) of B₂(pin)₂ in THF (5.0 mL) for 12 h, followed by

oxidation, to afford the title compound as a colorless oil (87 mg, 37% yield). R_f = 0.33 (1:1

hexanes:EtOAc); ¹H NMR (500 MHz, CDCl₃): δ 7.38-7.29 (5H, m, CH₂C₆H₅), 5.84 (1H, ddd, *J* =

17.6 Hz, 10.4 Hz, 7.6 Hz, CH₂CH), 5.25 (1H, d, *J* = 17.2 Hz, CHCHCH_aH_b), 5.12 (1H, d, *J* = 10.4

Hz, CHCHCH_aH_b), 4.59 (1H, d, *J* = 12.0 Hz, ArCH_aH_b), 4.54 (1H, d, *J* = 12.0 Hz, ArCH_aH_b),

4.14 (1H, t, *J* = 7.6 Hz, CH₂CHCH), 3.78 (1H, td, *J* = 7.5 Hz, 3.0 Hz, BnOCH₂CH), 3.63 (1H, dd,

J = 9.5 Hz, 3.0 Hz, BnOCH_aH_b), 3.49 (1H, br s, OH), 3.46 (1H, dd, *J* = 9.5 Hz, 7.0 Hz,

BnOCH_aH_b), 3.20 (1H, br s, OH), 1.77 (1H, sextet, *J* = 7.5 Hz, CHCH₃), 0.79 (3H, d, *J* = 7.0 Hz,

CHCH₃); ¹³C NMR (125 MHz, CDCl₃): δ 139.2, 137.9, 128.6, 127.9, 127.8, 116.7, 77.4, 74.9, 73.6,

72.8, 41.1, 12.8; IR (neat): 3409 (br), 2966 (w), 2931 (w), 2172 (w), 1724 (m), 1566 (w), 1503 (w),

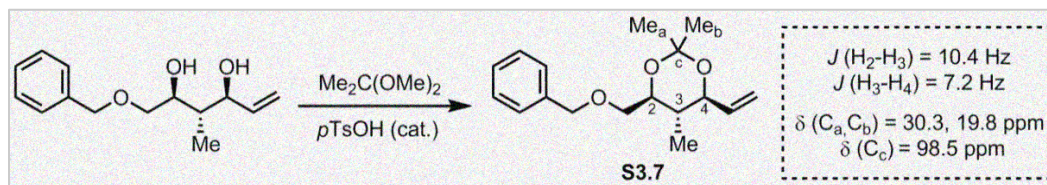
1458 (m), 1381 (m), 1319 (m), 1149 (s), 1072 (s), 990 (s), 927 (s), 816 (m), 738 (m), 702 (m) cm⁻¹;

HRMS (ESI⁺) calculated for C₁₄H₁₉O₂ [M-H₂O+H]⁺: 219.1390, found: 219.1397.

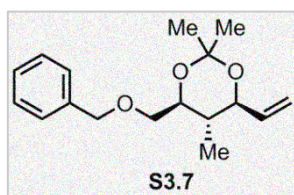
Proof of Stereochemistry. The relative configuration was assigned as *anti* (C₂-C₃)/*anti* (C₃-C₄)

by analysis of the spectral data, after conversion of the title compound into **S3.7** as shown

below.

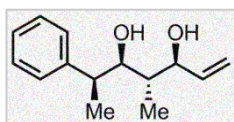


(4*S,5*S**,6*S**)-4-((benzyloxy)methyl)-2,2,5-trimethyl-6-vinyl-1,3-**



dioxane (S3.7). $R_f = 0.56$ (4:1 hexanes:EtOAc); $^1\text{H NMR}$ (400 MHz, CDCl_3): δ 7.35-7.26 (5H, m, $\text{CH}_2\text{C}_6\text{H}_5$), 5.74 (1H, ddd, $J = 17.6 \text{ Hz}$, 10.4 Hz, 7.2 Hz, CH_2CH), 5.27 (1H, d, $J = 17.2 \text{ Hz}$, $\text{CHCHCH}_a\text{H}_b$),

5.23 (1H, d, $J = 10.4 \text{ Hz}$, $\text{CHCHCH}_a\text{H}_b$), 4.64 (1H, d, $J = 12.4 \text{ Hz}$, ArCH_aH_b), 4.57 (1H, d, $J = 12.4 \text{ Hz}$, ArCH_aH_b), 3.91 (1H, dd, $J = 10.0 \text{ Hz}$, 7.2 Hz, CH_2CHCH), 3.72 (1H, ddd, $J = 10.4 \text{ Hz}$, 7.2 Hz, 4.4 Hz, BnOCH_2CH), 3.59-3.55 (2H, m, BnOCH_2), 1.58-1.44 (1H, m, CH_3CH), 1.49 (3H, s, CCH_3), 1.46 (3H, s, CCH_3), 0.76 (3H, d, $J = 6.8 \text{ Hz}$, CHCHCH_3); $^{13}\text{C NMR}$ (100 MHz, CDCl_3): δ 138.5, 137.3, 128.4, 127.9, 127.6, 118.4, 98.5, 76.9, 74.5, 73.6, 71.7, 34.9, 30.3, 19.8, 12.4; IR (neat): 3317 (br), 3066 (w), 2990 (m), 2937 (w), 2878 (w), 1721 (m), 1495 (w), 1435 (s), 1426 (s), 1312 (w), 1258 (s), 1203 (s), 1175 (s), 1112 (s), 1058 (s), 1027 (s), 991 (s), 921 (s), 895 (w), 857 (w), 749 (s) cm^{-1} ; HRMS (ESI+) calculated for $\text{C}_{14}\text{H}_{19}\text{O}_2$ [$\text{M}-\text{acetone}+\text{H}$] $^+$: 219.1390, found: 219.1390.

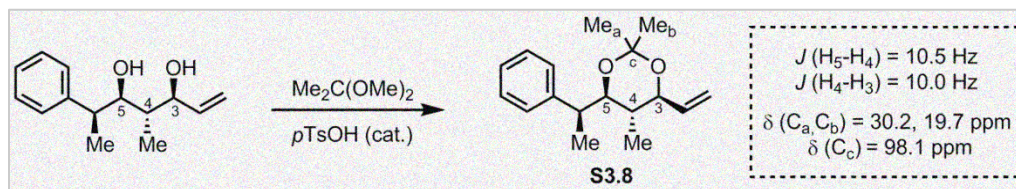


(3S*,4S*,5R*,6S*)-4-methyl-6-phenylhept-1-ene-3,5-diol. The reaction

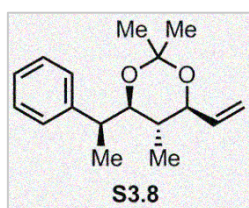
was performed according to the general procedure with 27.5 mg (0.10 mmol) of Ni(cod)₂, 37.5 mg (0.15 mmol) of P(SiMe₃)₃, 134.2 mg (1.0

mmol) of 2-phenylpropionaldehyde, 74.9 mg (1.1 mmol) of *trans*-1,3-pentadiene, and 305 mg (1.2 mmol) of B₂(pin)₂ in THF (5.0 mL) for 24 h, followed by oxidation, to afford the title compound as a colorless oil (108 mg, 49% yield). R_f = 0.51 (1:1 hexanes:EtOAc); ¹H NMR (500 MHz, CDCl₃): δ 7.37-7.34 (2H, m, aromatic), 7.29-7.24 (3H, m, aromatic), 5.89 (1H, ddd, *J* = 17.5 Hz, 10.0 Hz, 7.0 Hz, CH₂CH), 5.26 (1H, d, *J* = 17.5 Hz, CHCHCH_aH_b), 5.19 (1H, d, *J* = 10.5 Hz, CHCHCH_aH_b), 4.13 (1H, t, *J* = 7.0 Hz, CH₂CHCH), 3.66 (1H, dt, *J* = 9.0 Hz, 3.0 Hz, ArCHCH), 3.41 (1H, br s, OH), 3.11 (1H, quartet of doublets, *J* = 7.0 Hz, 3.0 Hz, ArCH), 2.30 (1H, br s, OH), 1.83 (1H, m, ArCHCHCH), 1.30 (3H, d, *J* = 7.0 Hz, ArCHCH₃), 0.93 (3H, d, *J* = 7.0 Hz, ArCHCHCH₃); ¹³C NMR (125 MHz, CDCl₃): δ 144.5, 139.5, 128.8, 128.1, 126.8, 116.8, 80.8, 78.4, 41.8, 40.8, 13.3, 11.4; IR (neat): 3346 (br), 3083 (w), 3026 (w), 2971 (m), 2931 (m), 2877 (m), 1602 (w), 1494 (m), 1452 (s), 1411 (m), 1380 (m), 1330 (w), 1133 (m), 1097 (m), 1014 (s), 993 (s), 970 (s), 924 (s), 760 (m), 701 (s), 661 (w), 548 (w) cm⁻¹; HRMS (ESI+) calculated for C₁₄H₂₁O₂ [M+H]⁺: 221.1542, found: 221.1544.

Proof of Stereochemistry. The relative stereochemistry of C₅-C₄ and C₄-C₃ was assigned as *anti* (C₅-C₄)/*anti* (C₄-C₃) by analysis of the spectral data, after conversion of the title compound into **S3.8** as shown below.



(4*R*^{*},5*S*^{*},6*S*^{*})-2,2,5-trimethyl-4-((*S*^{*})-1-phenylethyl)-6-vinyl-1,3-dio-



xane (S3.8). $R_f = 0.48$ (9:1 hexanes:Et₂O); ¹H NMR (500 MHz, CDCl₃):

δ 7.28 (4H, m, aromatic), 7.19 (1H, m, aromatic), 5.78 (1H, ddd, $J =$
17.5 Hz, 10.5 Hz, 7.5 Hz, CH₂CH), 5.28 (1H, d, $J = 17.5$ Hz,

CHCHCH_aH_b), 5.23 (1H, d, $J = 10.5$ Hz, CHCHCH_aH_b), 3.88 (1H, dd, $J = 10.0$ Hz, 7.5 Hz,

CH₂CHCH), 3.67 (1H, dd, $J = 10.5$ Hz, 2.0 Hz, ArCHCH), 2.96 (1H, quartet of doublets, $J = 7.0$

Hz, 2.0 Hz, ArCH), 1.60-1.52 (1H, m, ArCHCHCH), 1.41 (3H, s, CCH₃), 1.31 (3H, s, CCH₃),

1.26 (3H, d, $J = 7.0$ Hz, ArCHCH₃), 0.80 (3H, d, $J = 6.5$ Hz, ArCHCHCHCH₃); ¹³C NMR (125

MHz, CDCl₃): δ 146.4, 137.6, 128.1 (2 C's), 126.1, 118.4, 98.1, 77.6, 77.4, 40.4, 35.8, 30.2, 19.7,

14.0, 12.5; IR (neat): 3025 (w), 2990 (m), 2968 (m), 2936 (m), 2877 (w), 2857 (w), 1493 (w), 1453

(m), 1380 (s), 1351 (w), 1255 (s), 1202 (s), 1176 (s), 1151 (m), 1125 (m), 1096 (w), 1049 (s), 1019

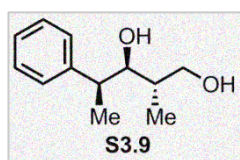
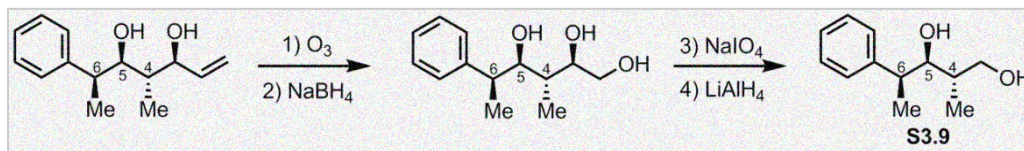
(s), 991 (m), 926 (m), 895 (m), 761 (m), 700 (s) cm⁻¹; HRMS (ESI⁺) calculated for C₁₄H₁₉O [M-

acetone+H]⁺: 203.1433, found: 203.1436.

The relative stereochemistry of C₆-C₅ and C₅-C₄ was assigned as *syn* (C₆-C₅)/*anti* (C₅-C₄) by comparison of the ¹H NMR spectrum with that reported in the literature,⁶¹ after conversion

⁶¹ (a) Matsumoto, T.; Hosoda, Y. k.; Mori, K.; Fukui, K., "The Stereochemistry of Nucleophilic Addition. V. The Reformatsky Reaction of 2-Phenylpropanal with Methyl & α -Bromopropionate," *Bulletin of*

of the title compound into **S3.9** by ozonolysis/reduction, oxidative cleavage, and LAH reduction as illustrated below.



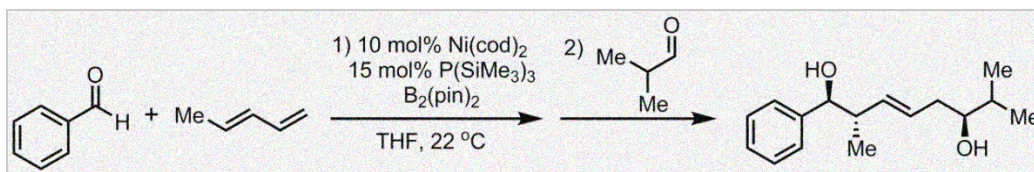
(2S*,3R*,4S*)-2-methyl-4-phenylpentane-1,3-diol (S3.9). $R_f = 0.33$ (1:1

hexanes:EtOAc); $^1\text{H NMR}$ (500 MHz, CDCl_3): δ 7.35-7.32 (2H, m, aromatic), 7.25-7.22 (3H, m, aromatic), 3.74 (1H, ddd, $J = 10.5$ Hz, 7.5

Hz, 3.0 Hz), 3.64-3.59 (2H, m), 3.03 (1H, quartet of doublets, $J = 7.0$ Hz, 4.0 Hz, ArCH), 2.86 (1H, dd, $J = 7.5$ Hz, 3.5 Hz, OH), 2.14 (1H, d, $J = 4.0$ Hz, OH), 1.83 (1H, sextet of doublets, $J = 8.0$ Hz, 3.5 Hz, OHCH₂CH), 1.32 (3H, d, $J = 7.0$ Hz, ArCHCH₃), 0.98 (3H, d, $J = 7.0$ Hz, OHCH₂CHCH₃); $^{13}\text{C NMR}$ (125 MHz, CDCl_3): δ 144.5, 128.9, 127.9, 126.4, 81.9, 68.0, 42.5, 37.0, 14.3, 13.3; IR (neat): 3346 (br), 3084 (w), 3061 (w), 3027 (w), 2964 (m), 2929 (m), 2876 (m), 1602 (w), 1494 (m), 1452 (s), 1378 (w), 1067 (m), 1016 (s), 969 (s), 911 (w), 761 (m), 701 (s), 663 (w), 550 (m) cm^{-1} . HRMS (ESI+) calculated for $\text{C}_{12}\text{H}_{19}\text{O}_2$ $[\text{M}+\text{H}]^+$: 195.1380, found: 195.1385.

the Chemical Society of Japan **1972**, 45, 3156-3160. (b) Mori, I.; Ishihara, K.; Heathcock, C. H., "Acyclic Stereoselection. 50. New Stereoselective Propanal/Propanoic Acid Synthons for Aldol Reactions," *The Journal of Organic Chemistry* **1990**, 55, 1114-1117.

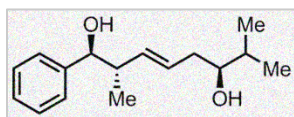
3.6.2.2. Procedure for Ni-Catalyzed Diboration/Allylation



An oven-dried 20 mL scintillation vial, equipped with a magnetic stir-bar, was charged with 27.5 mg (0.10 mmol) of Ni(cod)₂, 37.5 mg (0.15 mmol) of P(SiMe₃)₃, and THF (5 mL, 0.2 M) in a dry box under an argon atmosphere. After stirring for 5 min, 106 mg (1.0 mmol) of benzaldehyde, 204.4 mg (3.0 mmol) of *trans*-1,3-pentadiene, and 761.8 mg (3.0 mmol) of B₂(pin)₂ were added sequentially. The vial was sealed with a polypropylene cap and removed from the dry box. The reaction mixture was then allowed to stir at ambient temperature for 12 h. After this time, isobutyraldehyde (3.0 mmol, 216.3 mg) was added to the reaction mixture and stirred at ambient temperature. After stirring 48 h, the mixture was cooled to 0 °C (ice-water bath), and 4 mL of 3 M NaOH and 3 mL of 30% H₂O₂ were added dropwise with caution. The mixture was then allowed to stir at ambient temperature for 10 h. The resulting solution was cooled to 0 °C and quenched by the addition of 2 mL of saturated aqueous Na₂S₂O₃. The two-phase mixture was extracted with ethyl acetate (3 × 30 mL), and the combined organic layers were dried over anhydrous Na₂SO₄. The drying agent was removed by filtration and the solvent was evaporated *in vacuo*. The crude material was purified by silica gel chromatography (1:1 hexanes:EtOAc) to afford the diol as a colorless oil (168 mg, 68% yield).

3.6.2.2.1. Characterization and Proof of Stereochemistry

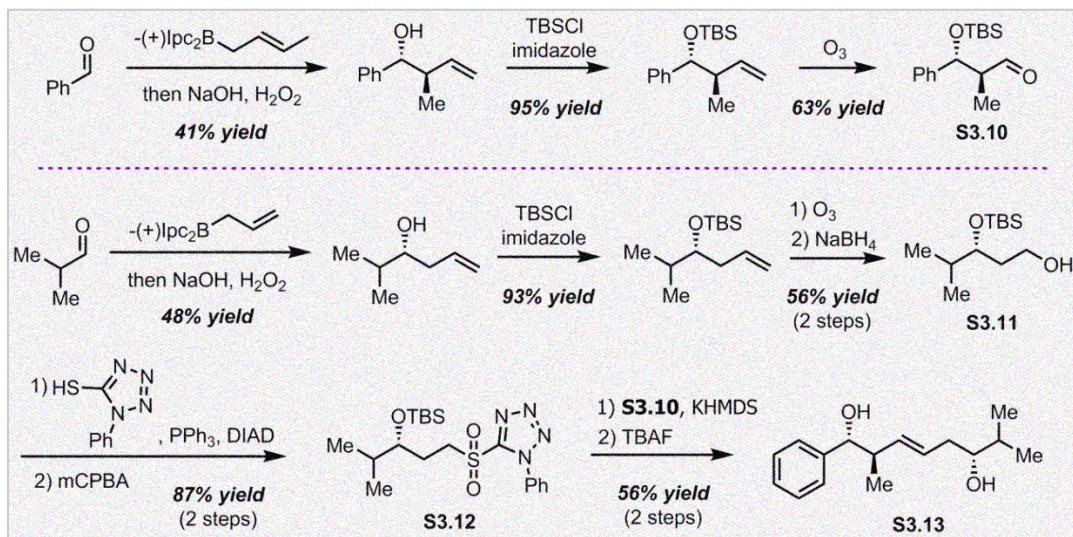
(1S*,2S*,6S*,E)-2,7-dimethyl-1-phenyloct-3-ene-1,6-diol. $R_f =$



0.55 (1:1 hexanes:EtOAc); ^1H NMR (400 MHz, CDCl_3): δ 7.38-7.26 (5H, m, $\text{CH}_2\text{C}_6\text{H}_5$), 5.57 (1H, ddd, $J = 15.2$ Hz, 8.0 Hz, 5.2 Hz,

ArCHCHCHCH), 5.47 (1H, dd, $J = 15.2$ Hz, 8.4 Hz, ArCHCHCH), 4.30 (1H, d, $J = 8.0$ Hz, ArCH), 3.36-3.31 (1H, m, ArCHCH), 2.45 (1H, dd, $J = 14.4$ Hz, 8.0 Hz, $(\text{CH}_3)_2\text{CHCH}$), 2.30 (1H, dt, $J = 13.2$ Hz, 4.8 Hz, CHCHCH_aH_b), 2.06 (1H, dt, $J = 13.6$ Hz, 8.8 Hz, CHCHCH_aH_b), 1.82 (1H, br s, OH), 1.71-1.63 (1H, m, $(\text{CH}_3)_2\text{CH}$), 1.58 (1H, br s, OH), 0.94 (3H, d, $J = 6.8$ Hz, CHCH₃), 0.93 (3H, d, $J = 6.8$ Hz, CHCH₃), 0.86 (3H, d, $J = 6.8$ Hz, CHCH₃); ^{13}C NMR (100 MHz, CDCl_3): δ 136.0, 129.5, 128.4, 127.8, 126.9, 78.3, 75.5, 45.8, 37.8, 33.5, 18.9, 17.9, 17.2; IR (neat): 3352 (br), 3029 (w), 2960 (m), 2925 (s), 2873 (m), 2855 (m), 1493 (w), 1453 (s), 1402 (w), 1332 (w), 1277 (w), 1198 (w), 1023 (m), 916 (m), 878 (w), 828 (m), 761 (m), 741 (m), 700 (s), 699 (w), 627 (w) cm^{-1} ; HRMS (ESI+) calculated for $\text{C}_{16}\text{H}_{23}\text{O}$ $[\text{M}-\text{H}_2\text{O}+\text{H}]^+$: 231.1750, found: 231.1759.

Proof of Stereochemistry. The relative configuration was assigned as *anti* ($\text{C}_1\text{-C}_2$)/*anti* ($\text{C}_2\text{-C}_6$) by analysis of the spectral data (^1H and ^{13}C NMR), after synthesis of the enantioenriched authentic compound (**S3.13**) as shown below.



The synthesis of the dihydroxylated *trans*-alkene (**S3.13**) commenced with the conversion of benzaldehyde into an enantiomerically enriched α -hydroxy aldehyde (**S3.10**) via the Brown asymmetric crotylation⁶² followed by ozonolysis. The enantiomerically enriched alcohol (**S3.11**) was prepared from isobutyraldehyde using the Brown asymmetric allylation⁶³ followed by ozonolysis/reduction. The protected alcohol (**S3.11**) was transformed to a sulfone (**S3.12**) via a two-step protocol employing sequential Mitsunobu reaction⁶⁴ and

⁶² (a) Brown, H. C.; Bhat, K. S., "Enantiomeric *Z*- and *E*-Crotyldiisopinocampheylboranes. Synthesis in High Optical Purity of All Four Possible Stereoisomers of β -Methylhomoallyl Alcohols," *Journal of the American Chemical Society* **1986**, *108*, 293-294. (b) Brown, H. C.; Bhat, K. S., "Chiral Synthesis via Organoboranes. 7. Diastereoselective and Enantioselective Synthesis of Erythro- and Threo- β -Methylhomoallyl Alcohols via Enantiomeric (*Z*)- and (*E*)-Crotylboranes," *Journal of the American Chemical Society* **1986**, *108*, 5919-5923.

⁶³ Jadhav, P. K.; Bhat, K. S.; Perumal, P. T.; Brown, H. C., "Chiral Synthesis via Organoboranes. 6. Asymmetric Allylboration via Chiral Allyldialkylboranes. Synthesis of Homoallylic Alcohols with Exceptionally High Enantiomeric Excess," *The Journal of Organic Chemistry* **1986**, *51*, 432-439.

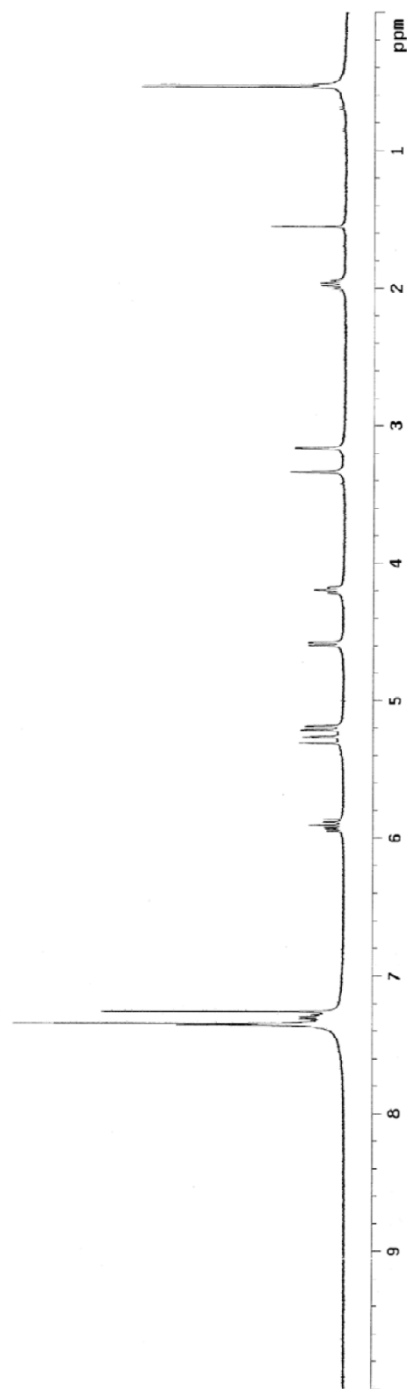
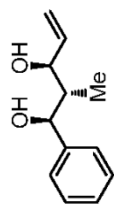
⁶⁴ (a) Mitsunobu, O.; Yamada, M.; Mukaiyama, T., "Preparation of Esters of Phosphoric Acid by the Reaction of Trivalent Phosphorus Compounds with Diethyl Azodicarboxylate in the Presence of Alcohols,"

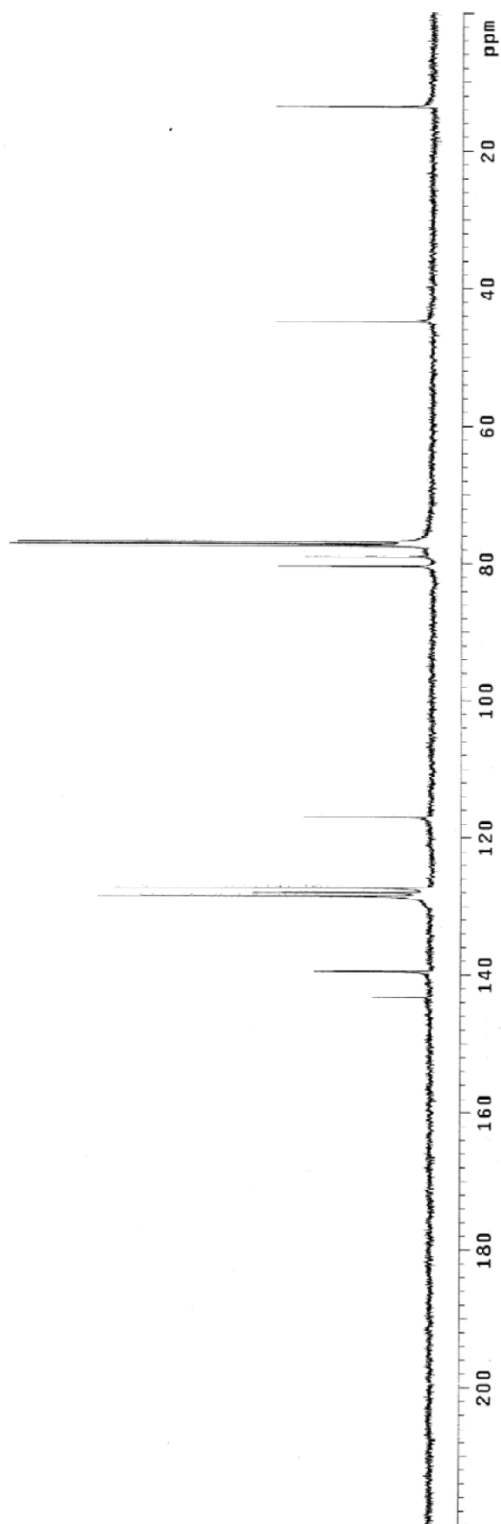
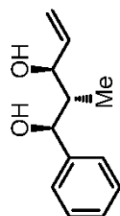
sulfide-sulfone oxidation. Finally, coupling of **S10** and **S12** with the Julia-Kocięński olefination⁶⁵ afforded the desired product (**S13**).

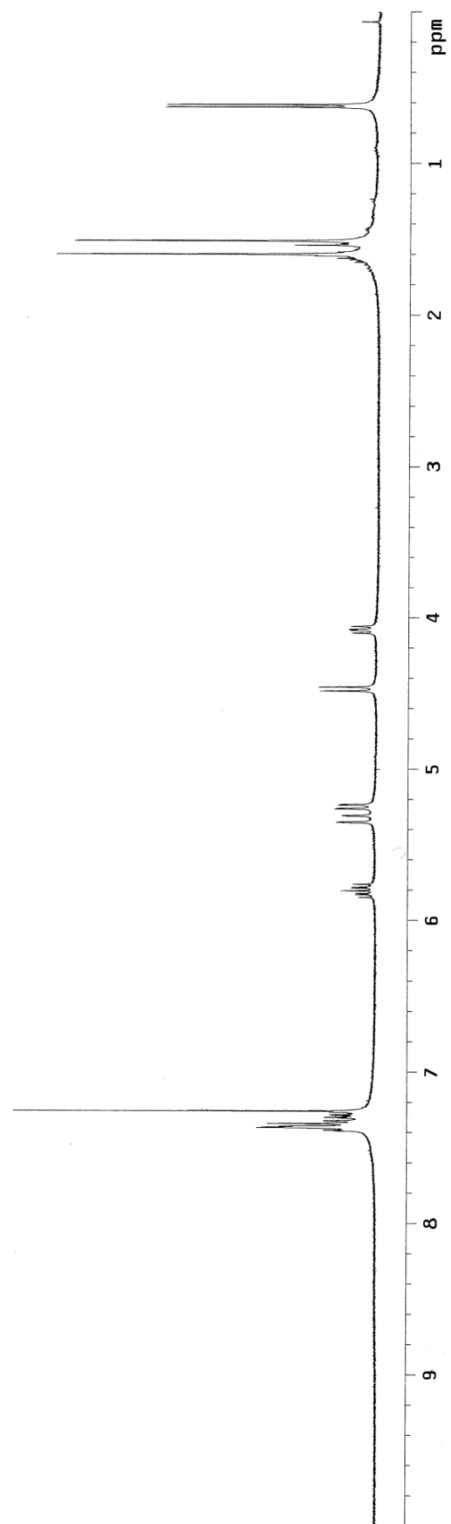
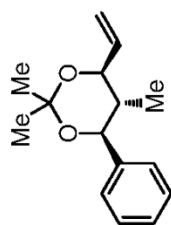
Bulletin of the Chemical Society of Japan **1967**, *40*, 935-939. (b) Mitsunobu, O.; Yamada, M., "Preparation of Esters of Carboxylic and Phosphoric Acid via Quaternary Phosphonium Salts," *Bulletin of the Chemical Society of Japan* **1967**, *40*, 2380-2382. (c) Mitsunobu, O., "The Use of Diethyl Azodicarboxylate and Triphenylphosphine in Synthesis and Transformation of Natural Products," *Synthesis* **1981**, *1981*, 1-28.

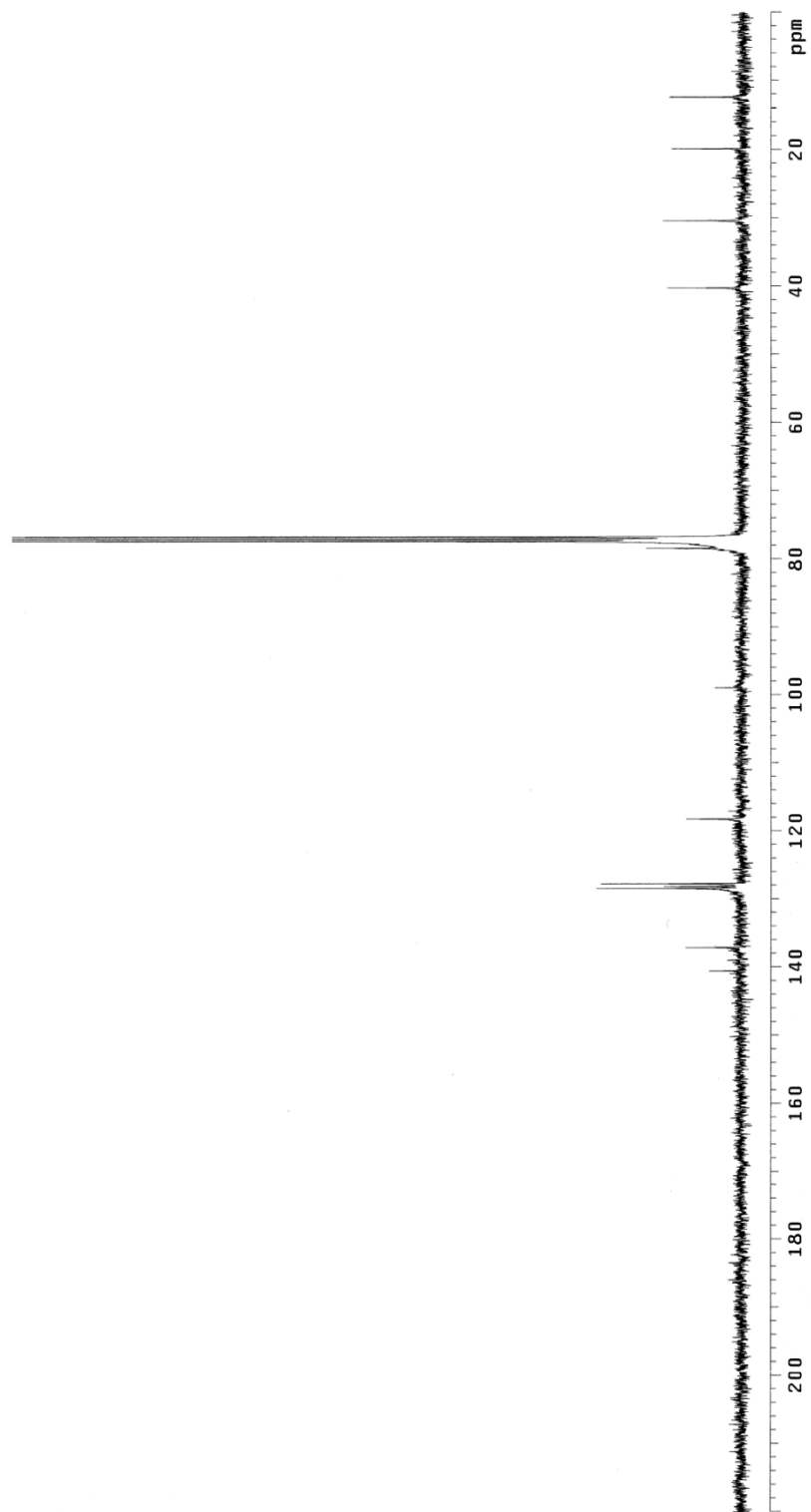
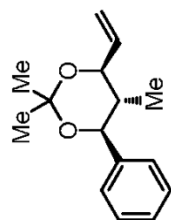
⁶⁵ (a) Julia, M.; Paris, J.-M., "Syntheses a L'aide De Sulfones V⁽⁺⁾-Methode De Synthese Generale De Doubles Liaisons," *Tetrahedron Letters* **1973**, *14*, 4833-4836. (b) Blakemore, P. R.; Cole, W. J.; Kocięński, P. J.; Morley, A., "A Stereoselective Synthesis of Trans-1,2-Disubstituted Alkenes Based on the Condensation of Aldehydes with Metallated 1-Phenyl-1H-Tetrazol-5-yl Sulfones," *Synlett* **1998**, *1998*, 26-28.

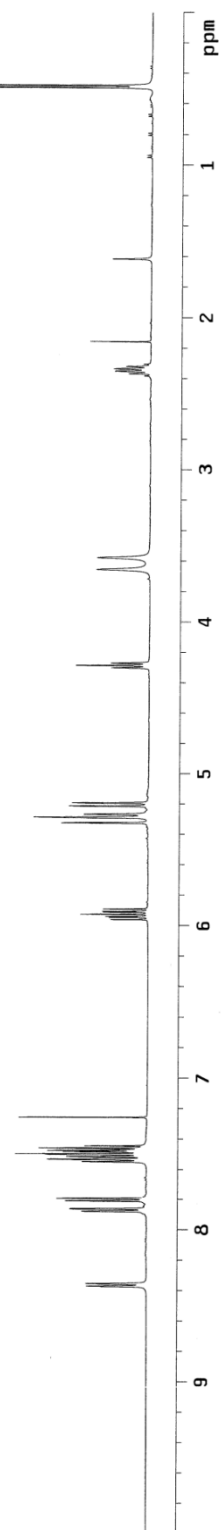
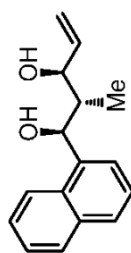
3.6.3. Representative Spectral Data

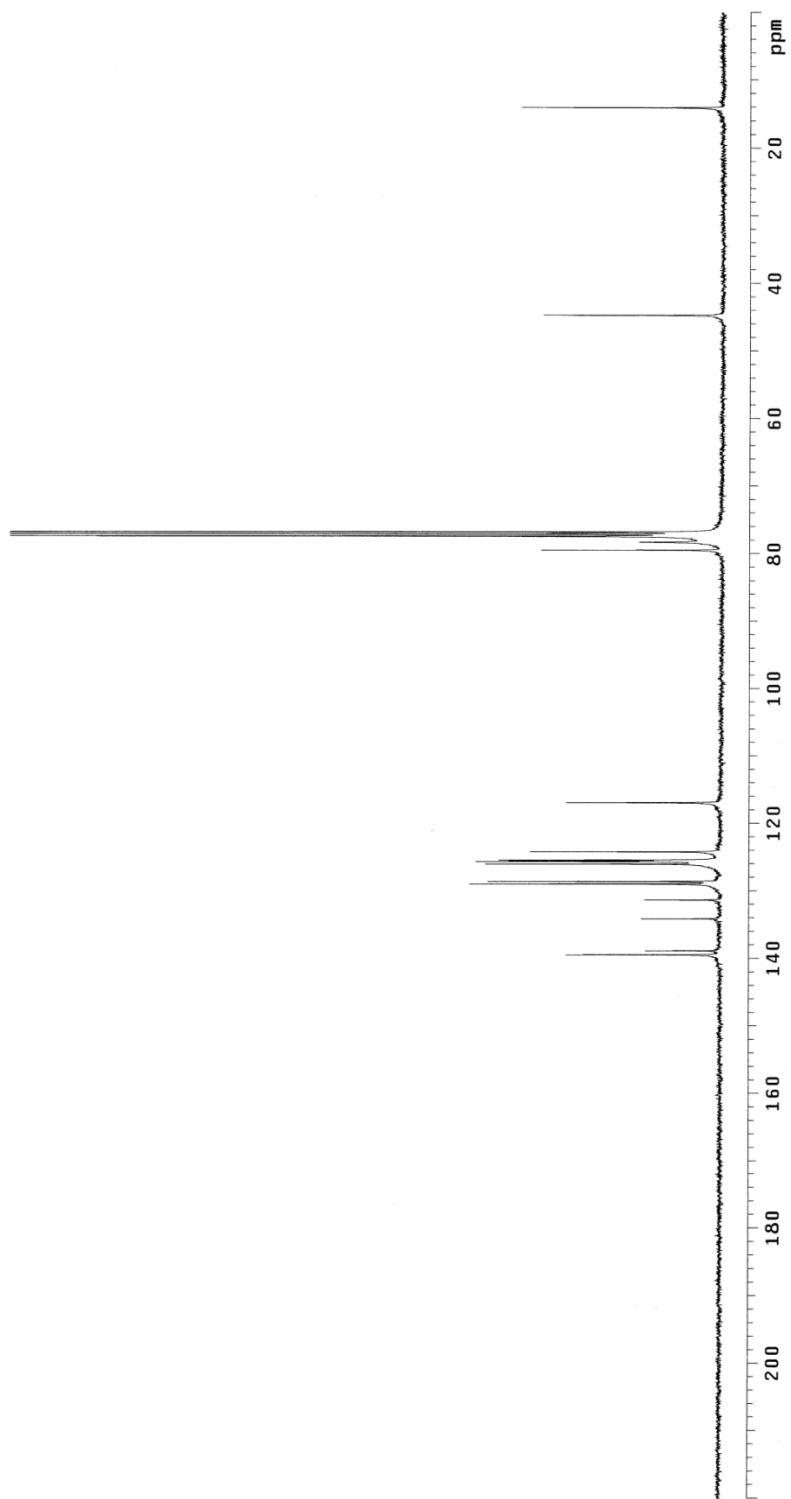
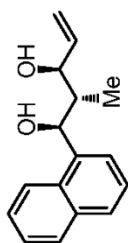


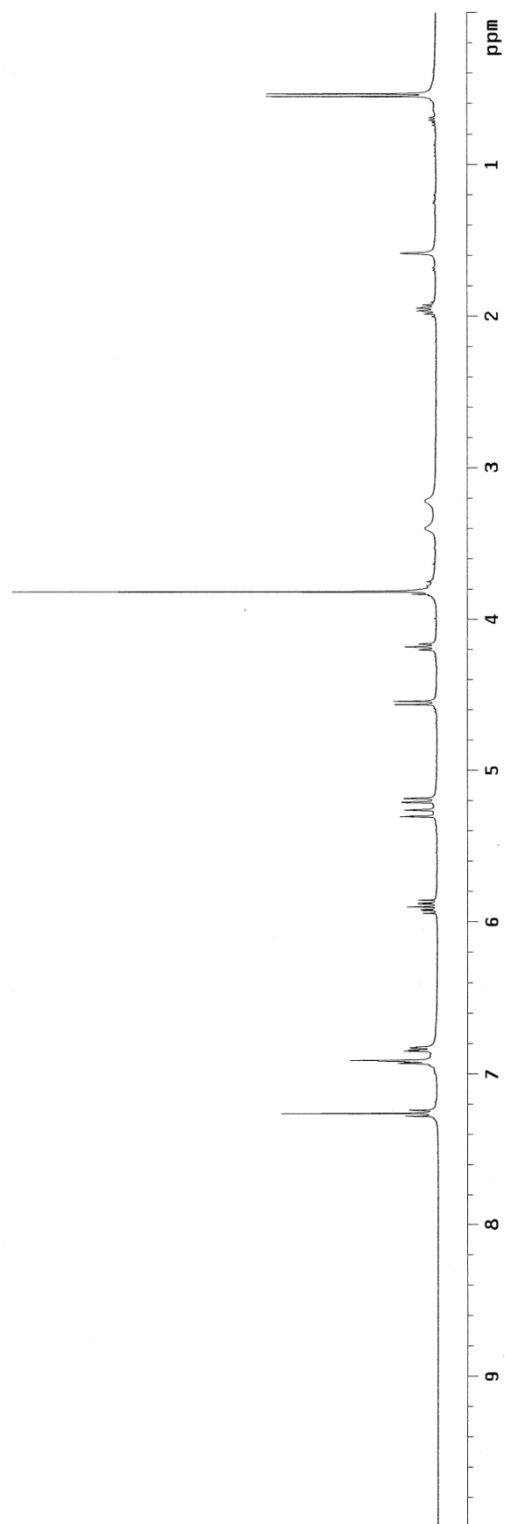
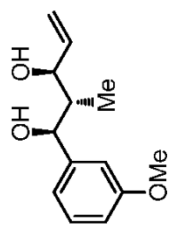


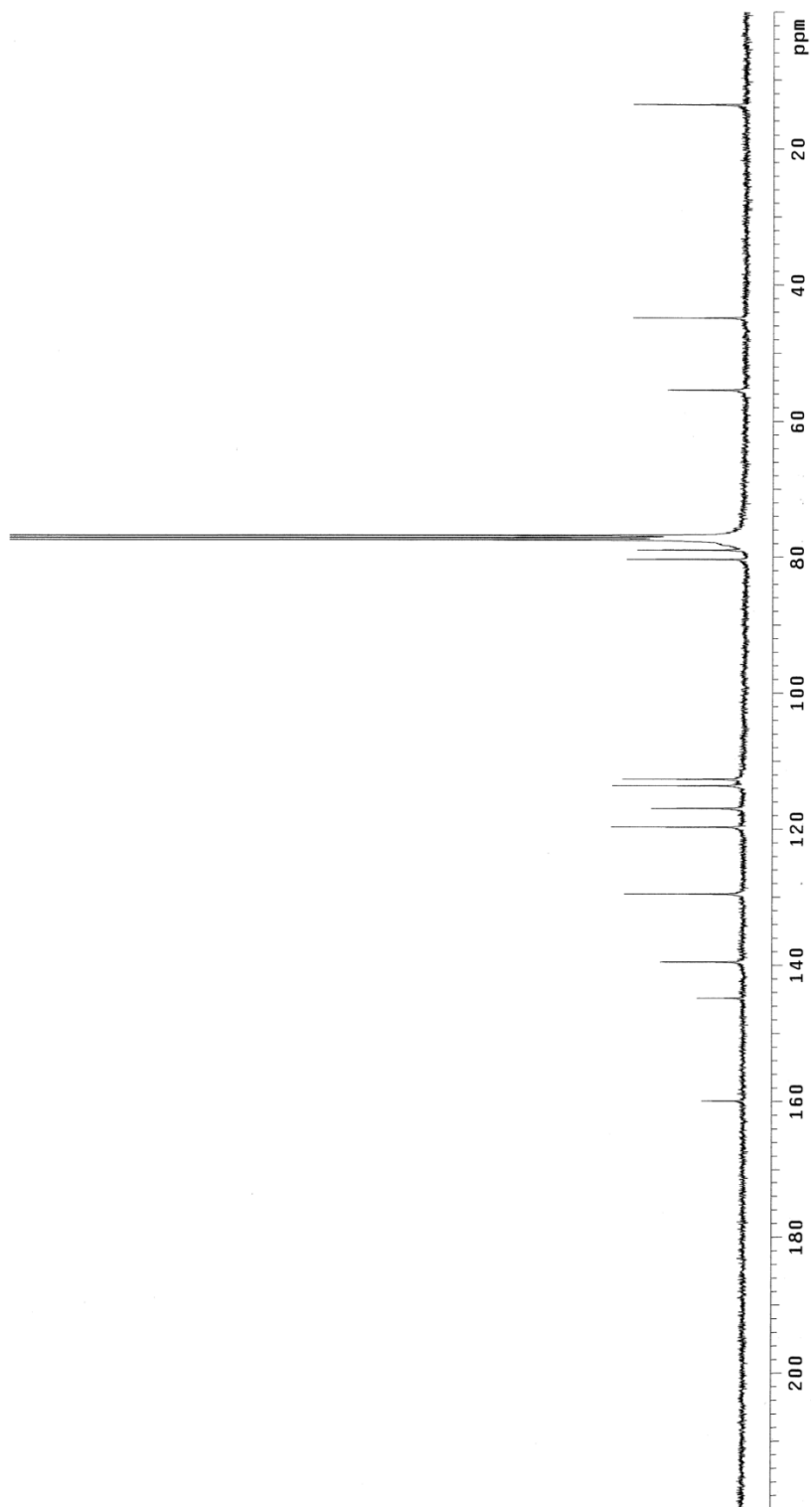
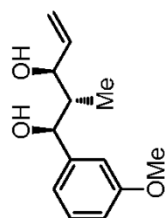


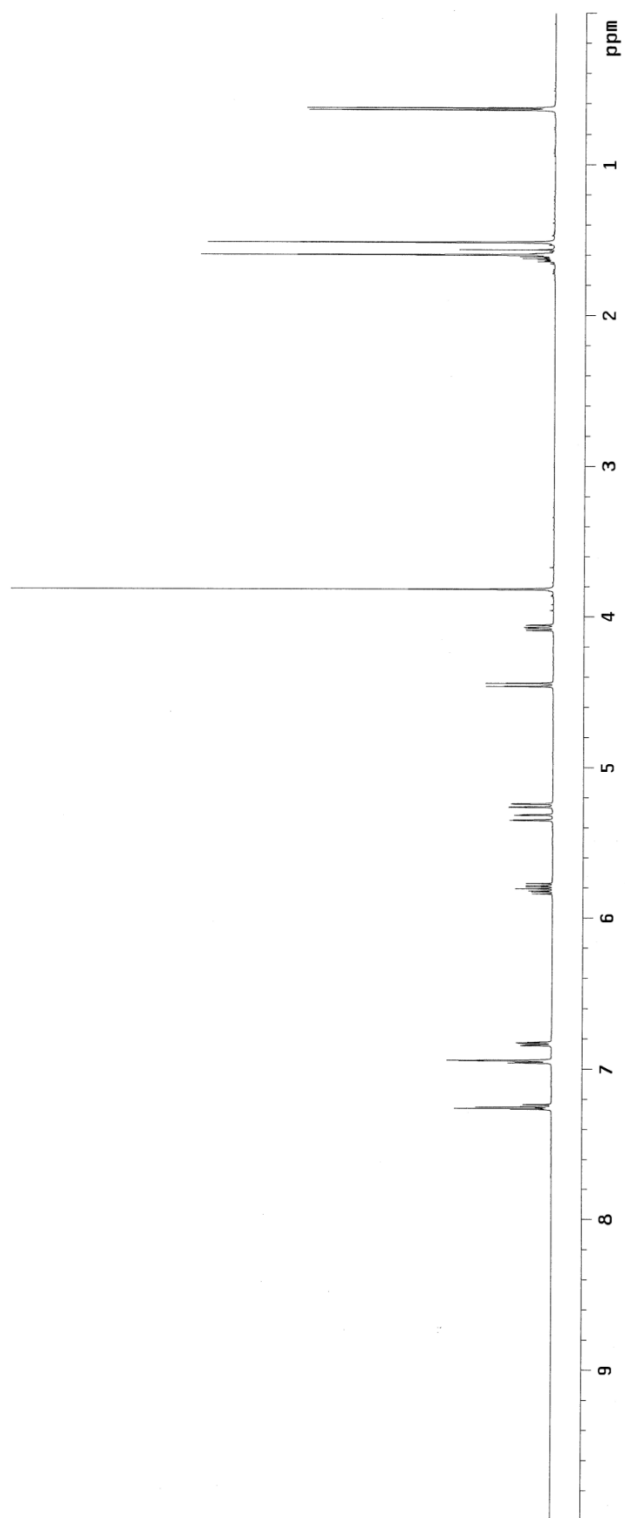
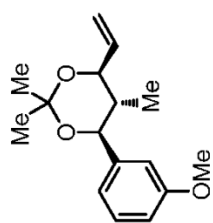


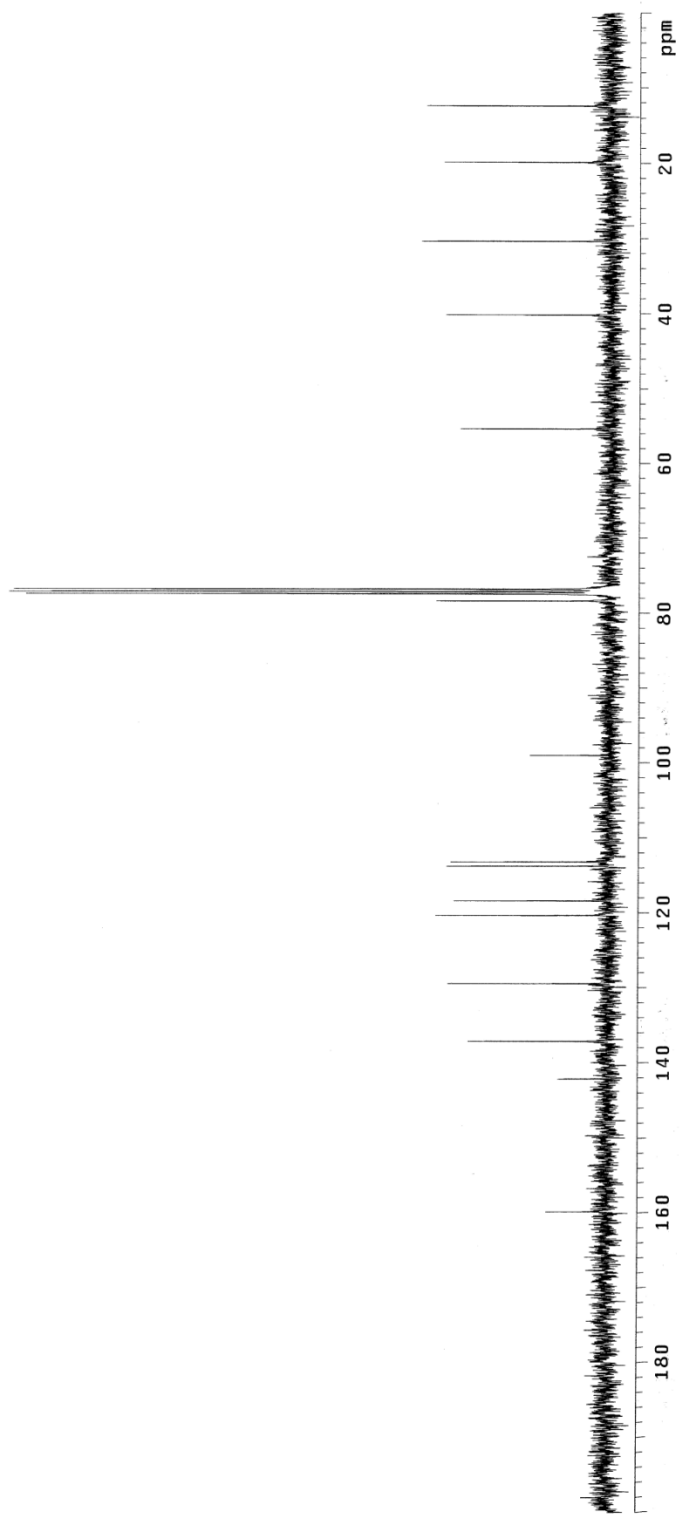
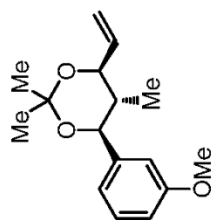


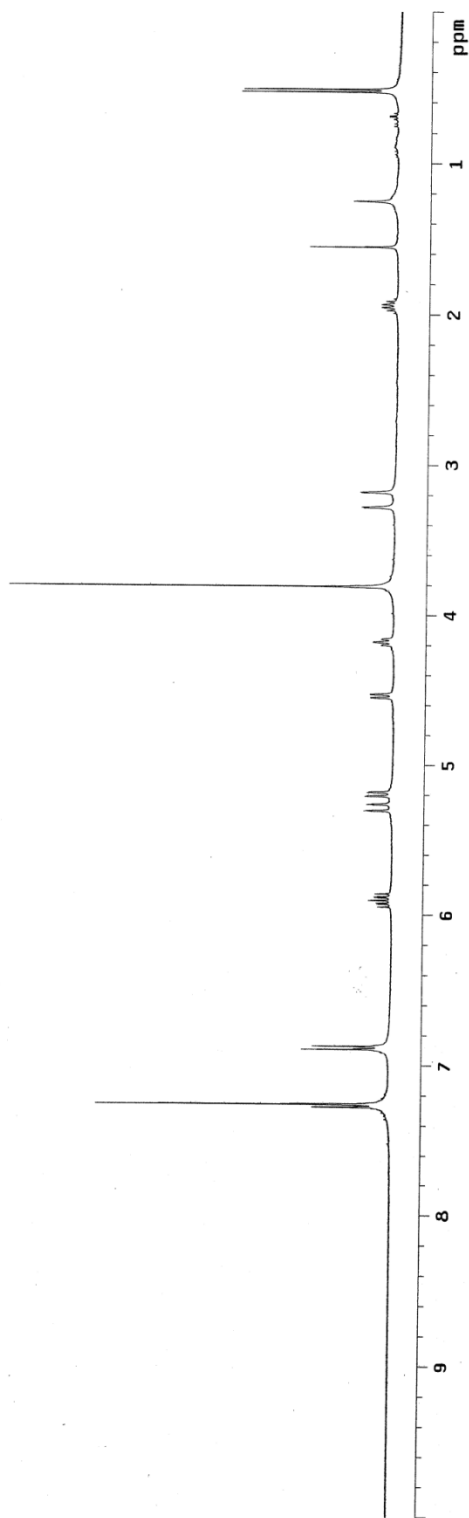
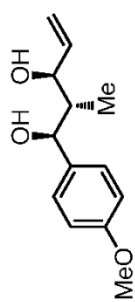


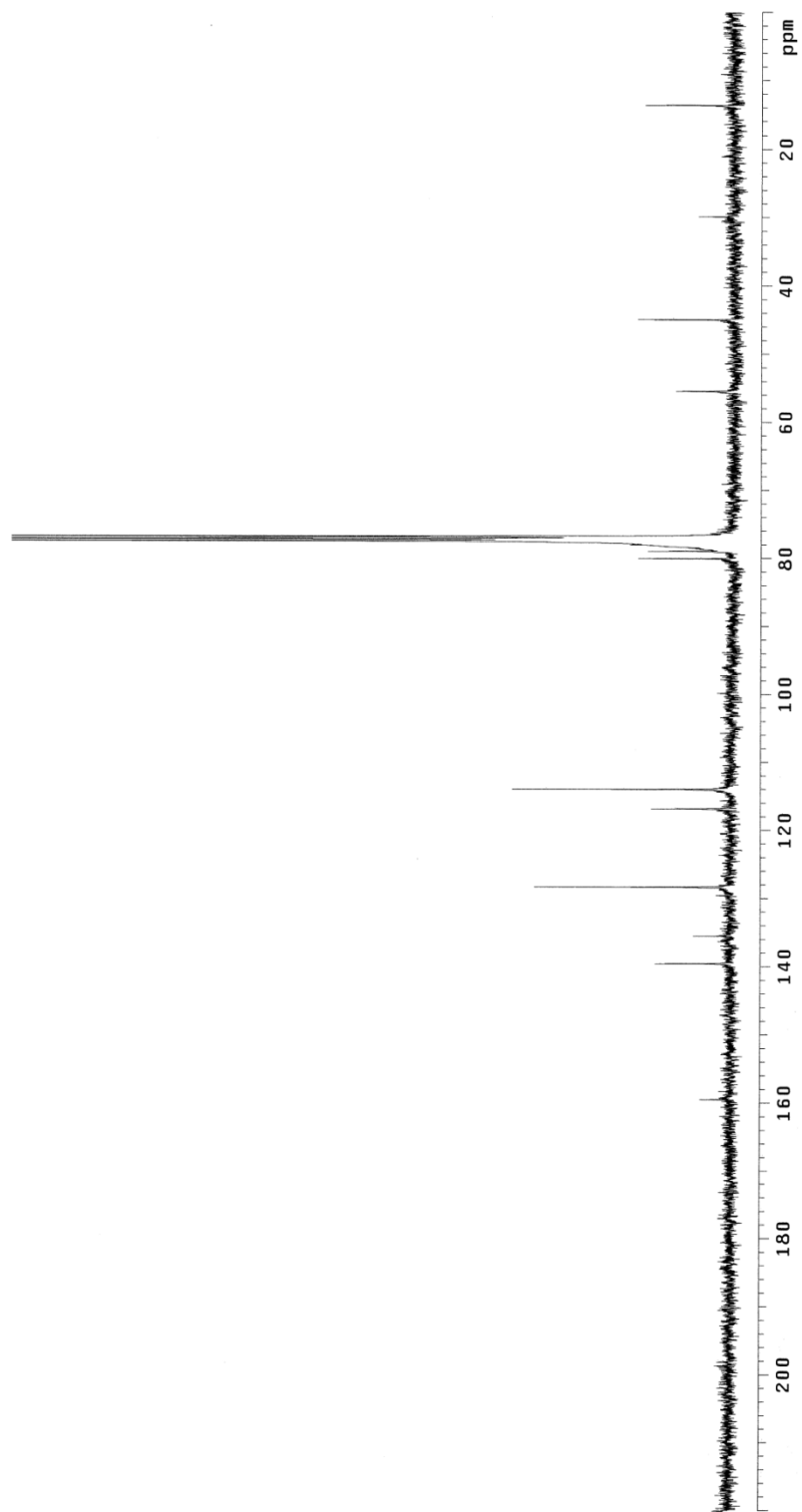
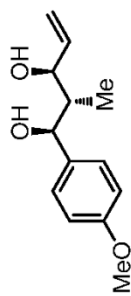


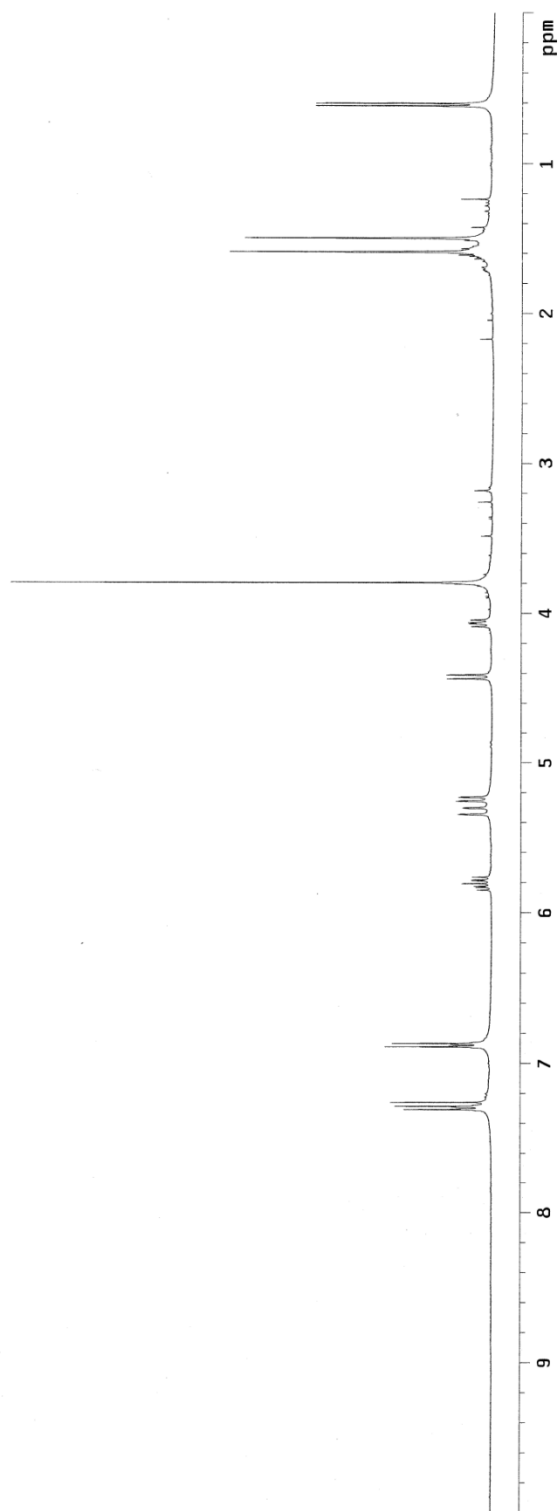
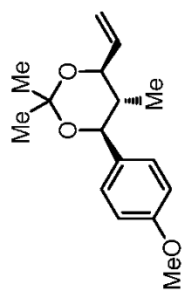


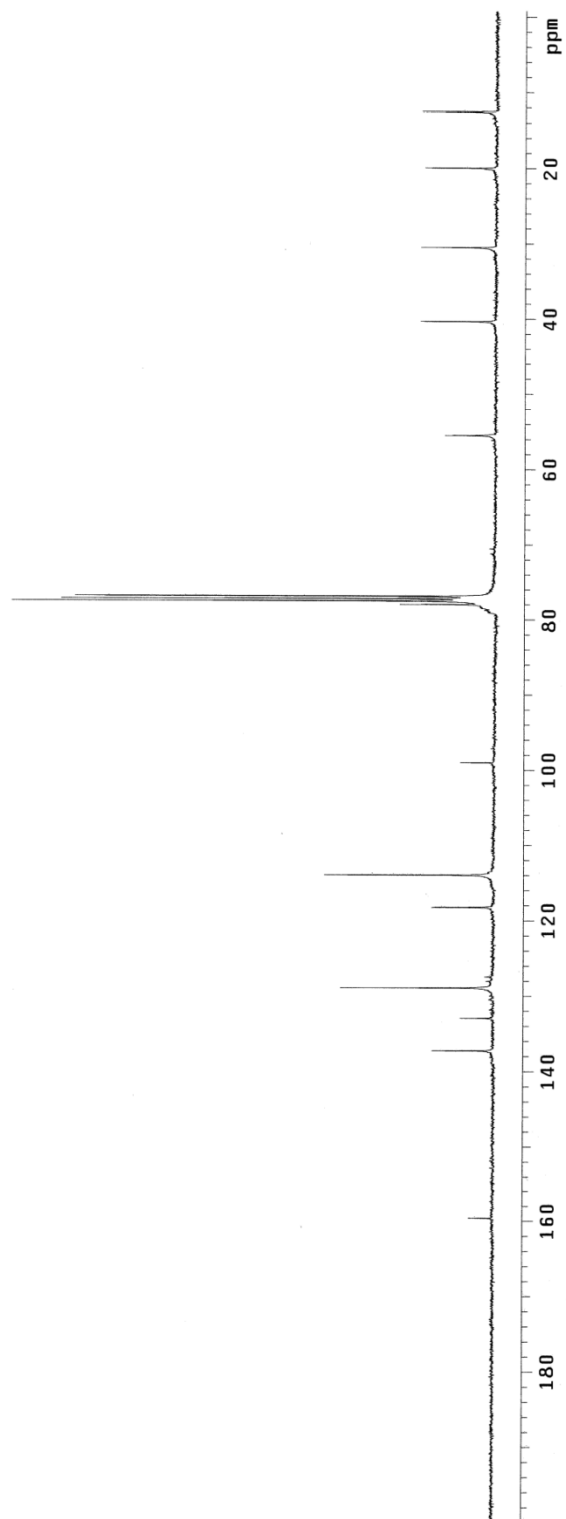
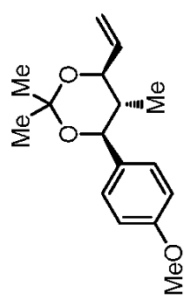


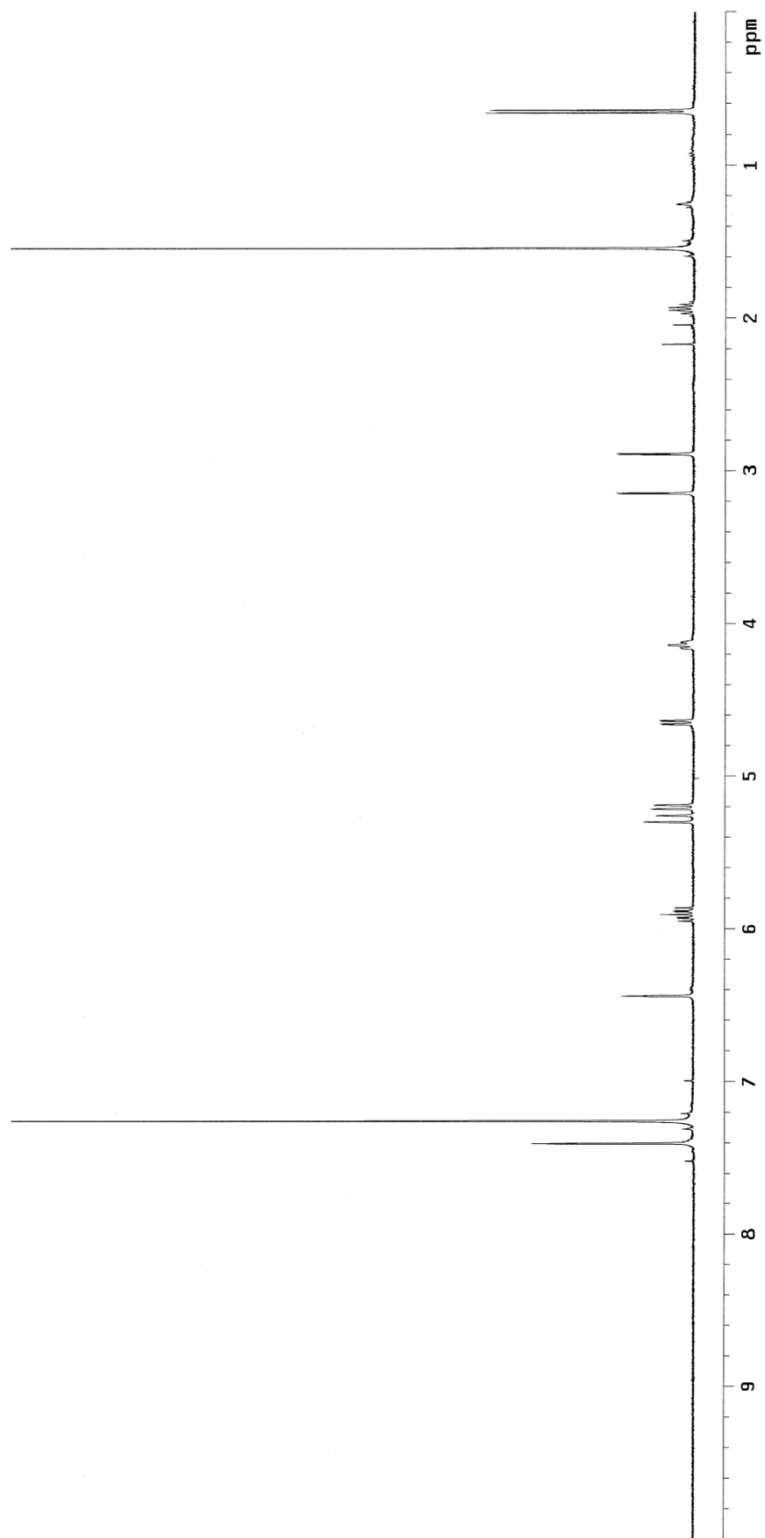
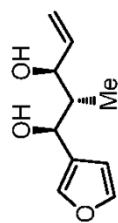


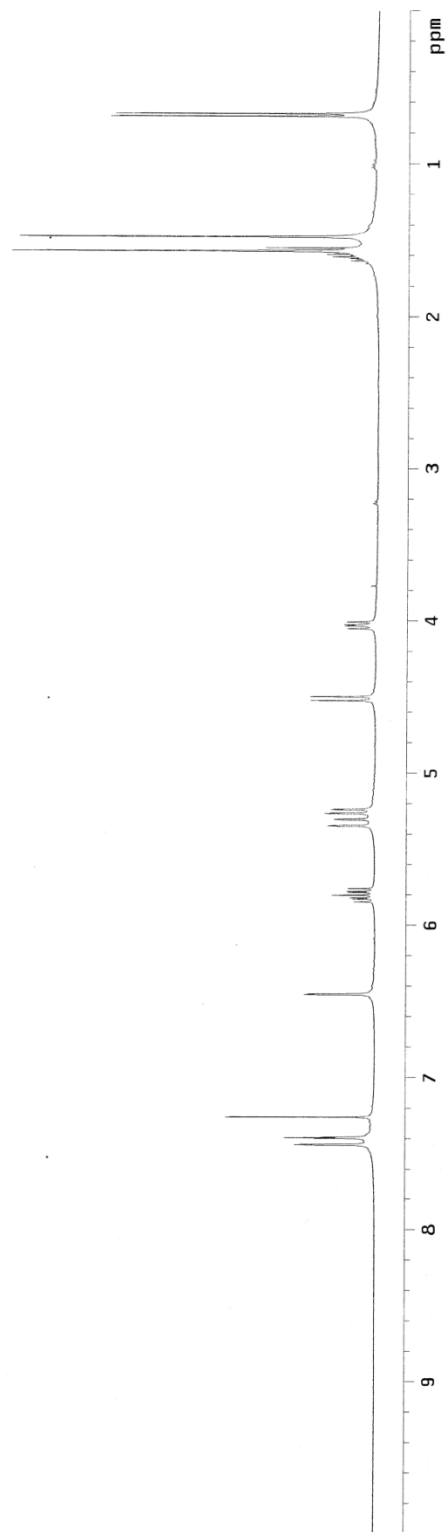
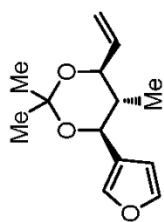


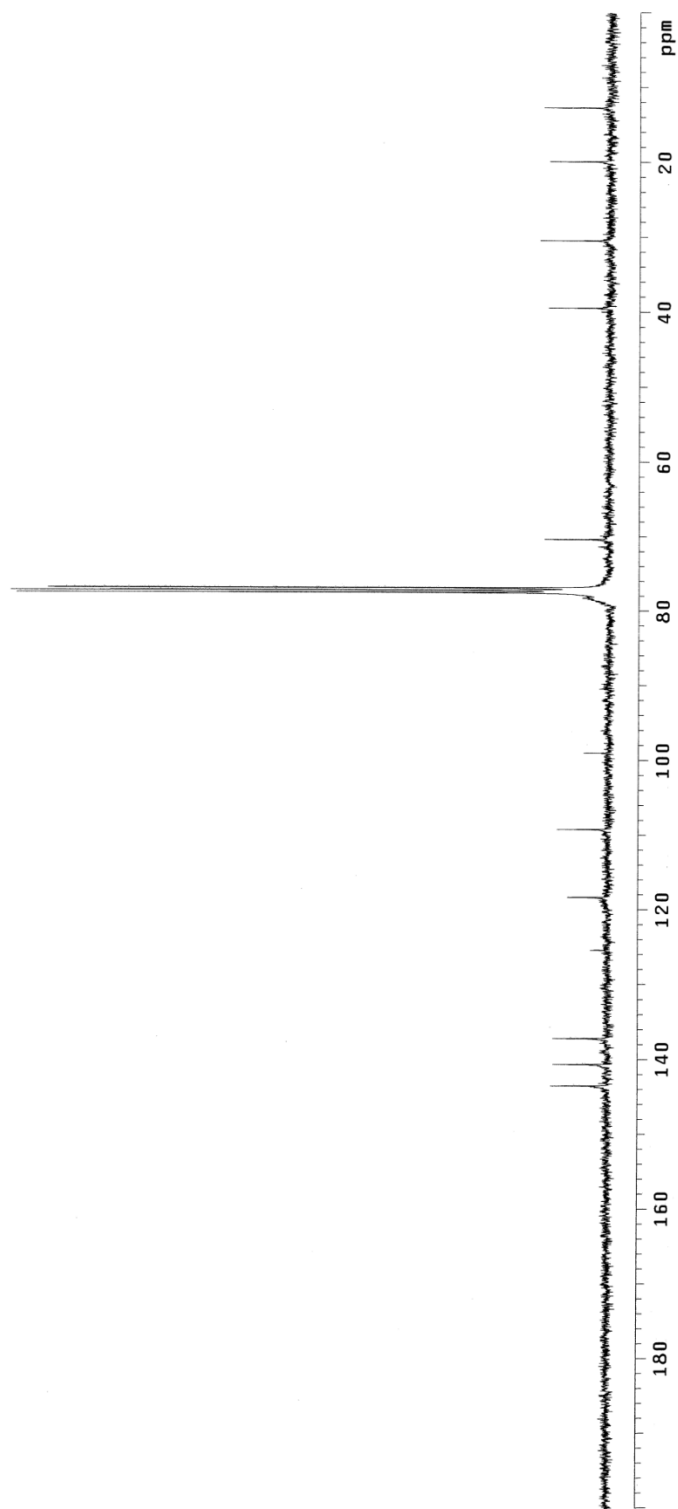
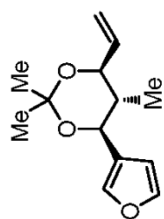


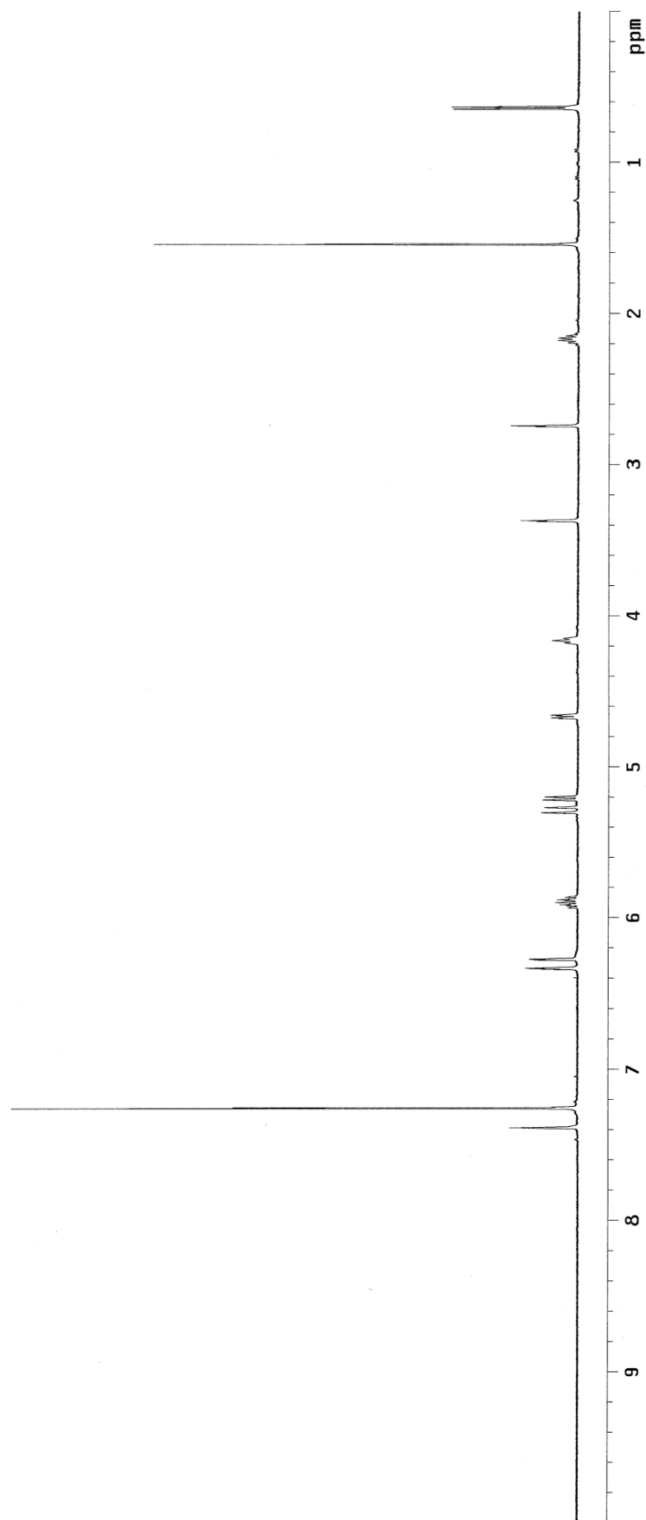
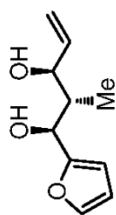


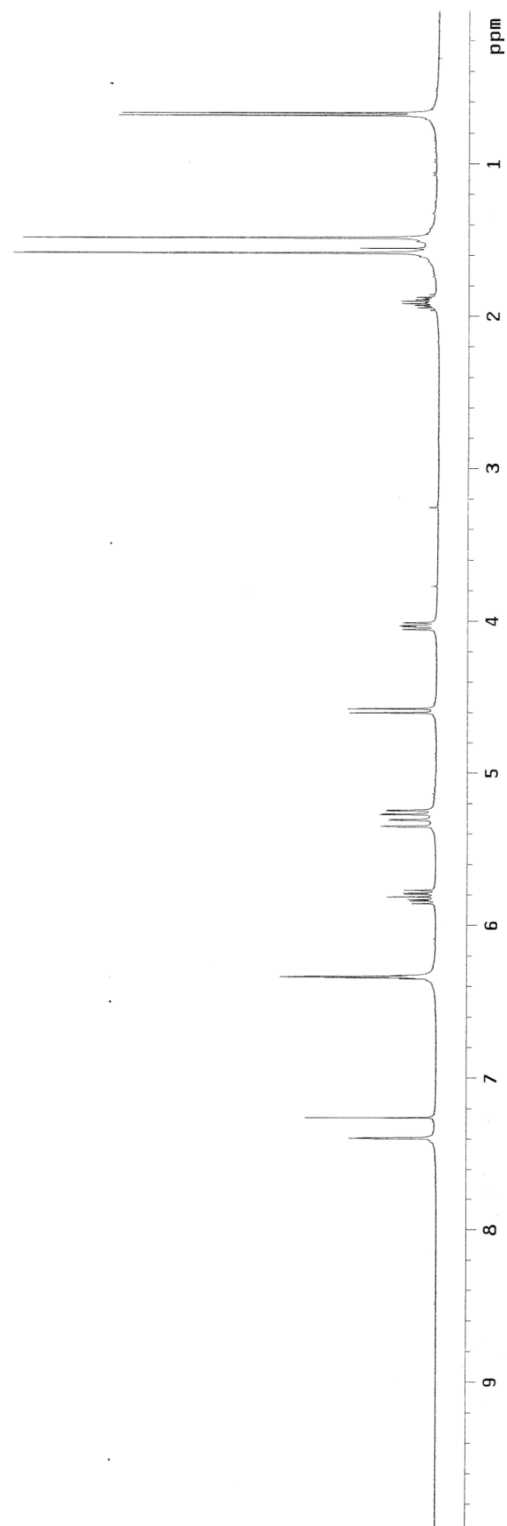
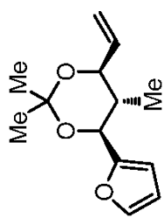


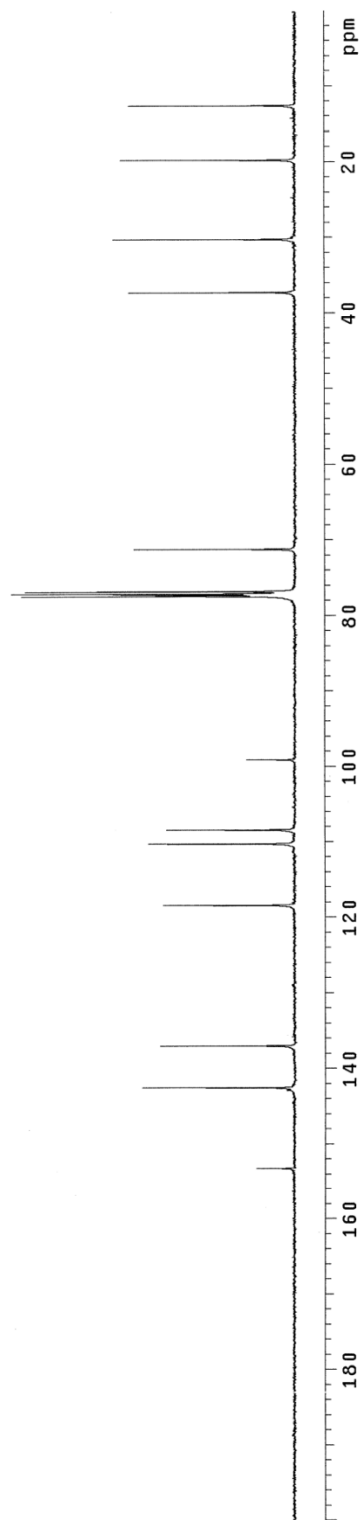
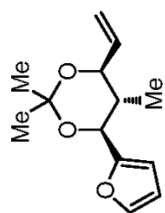


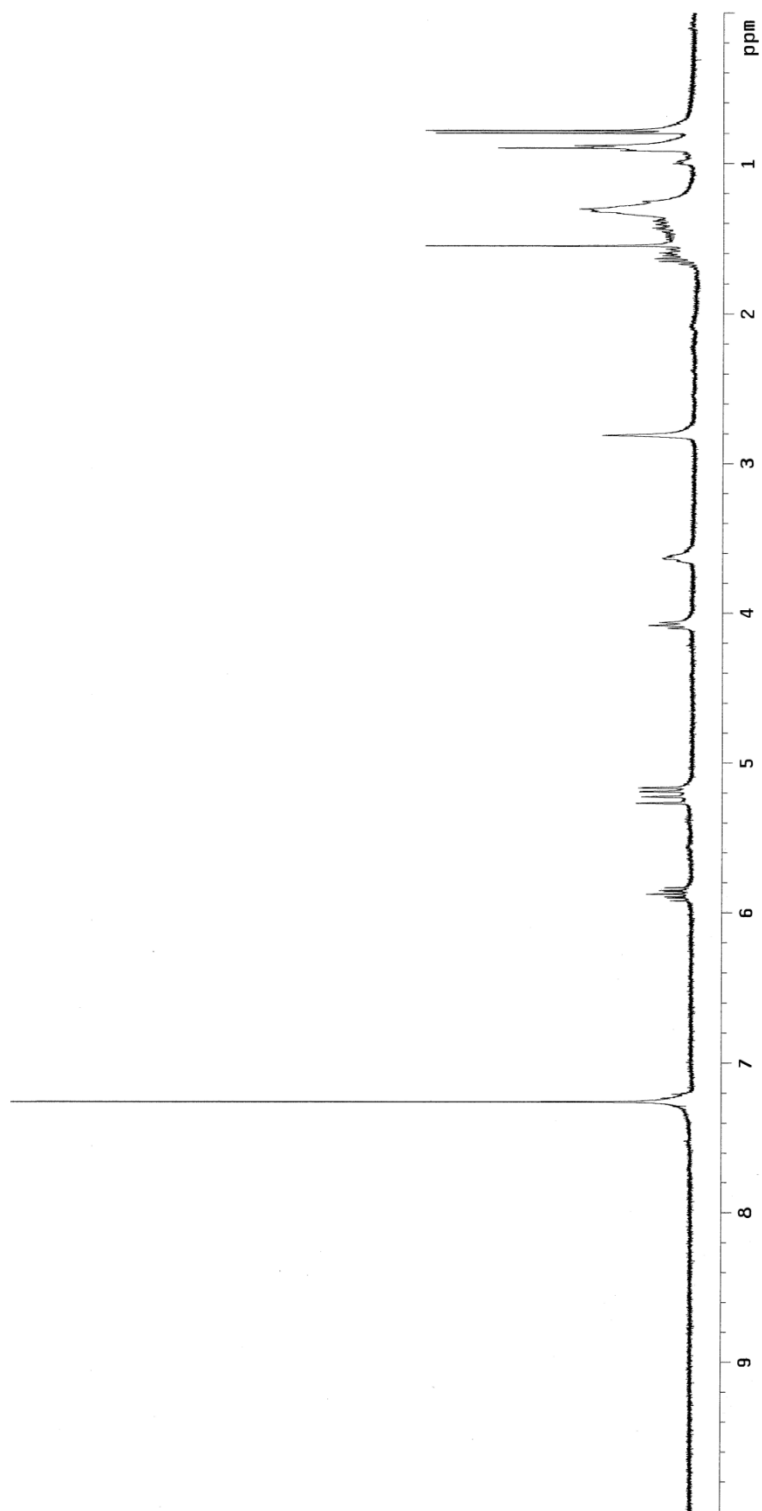
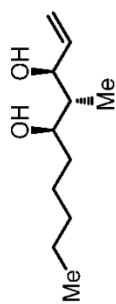


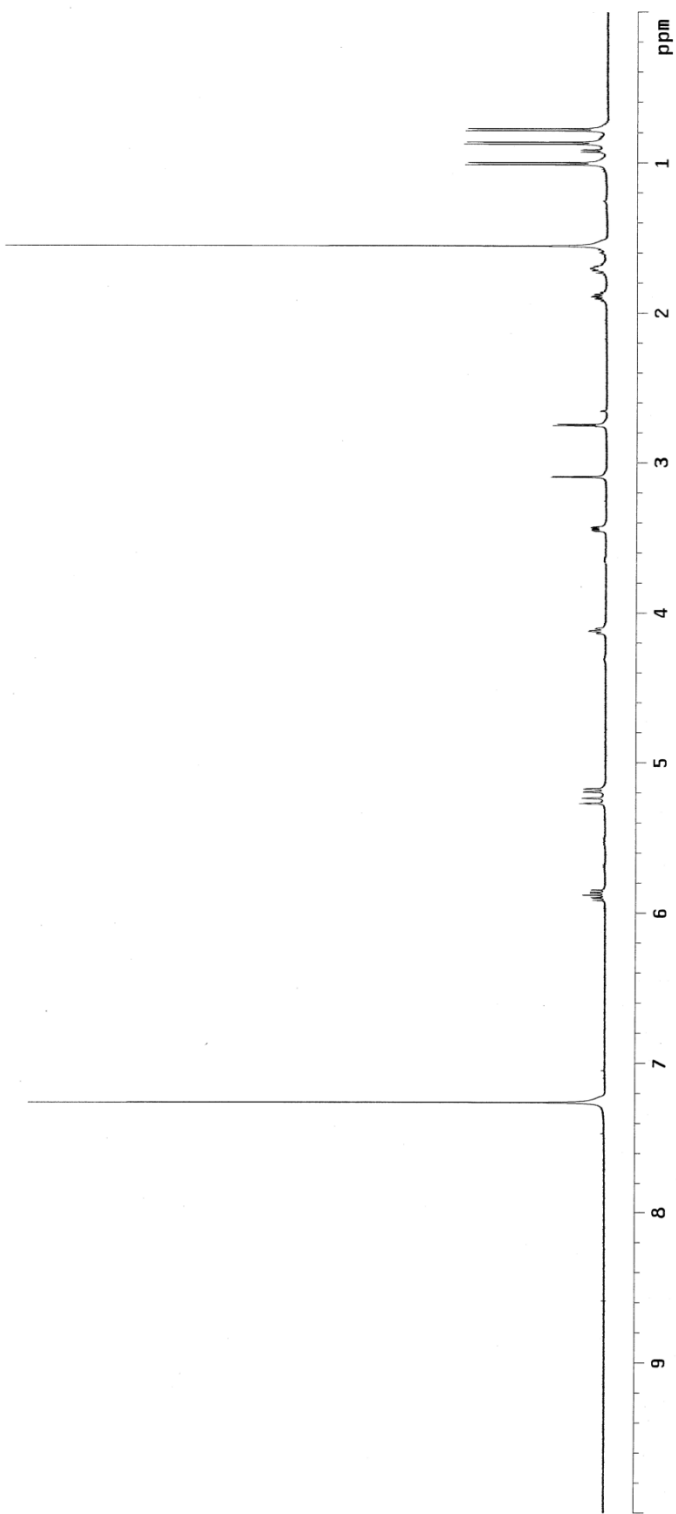
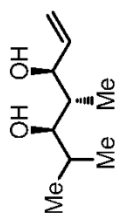


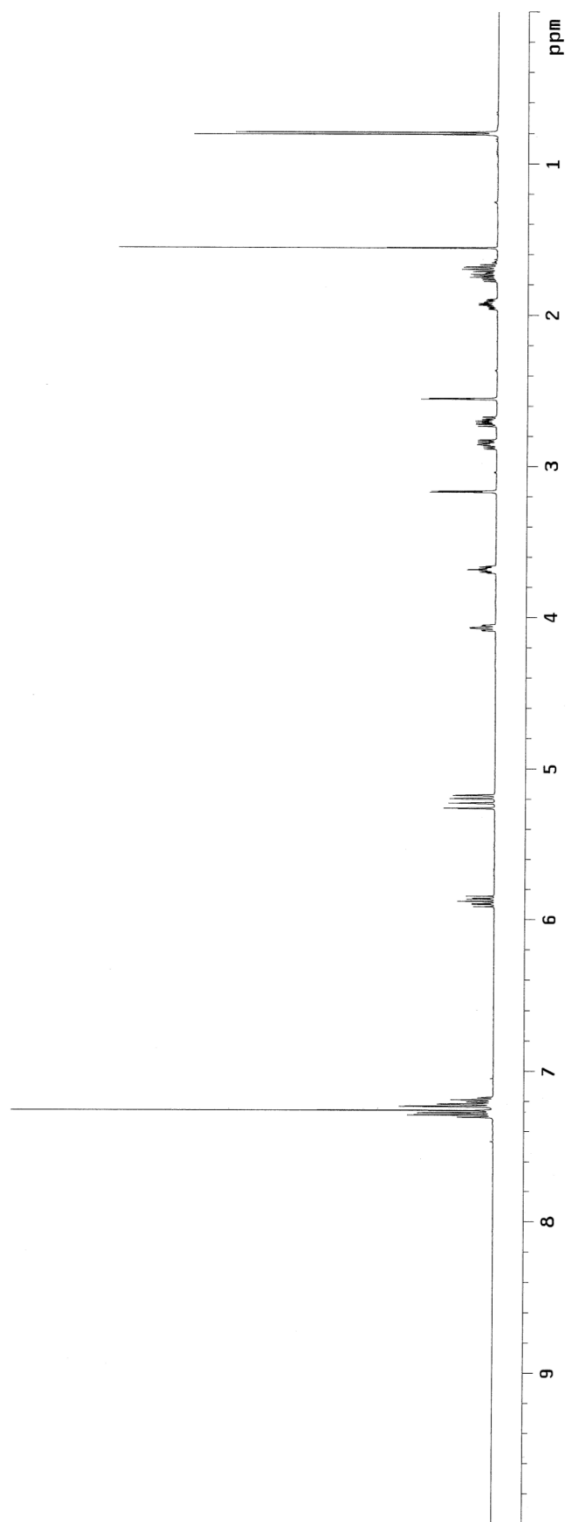
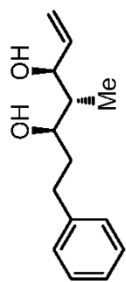


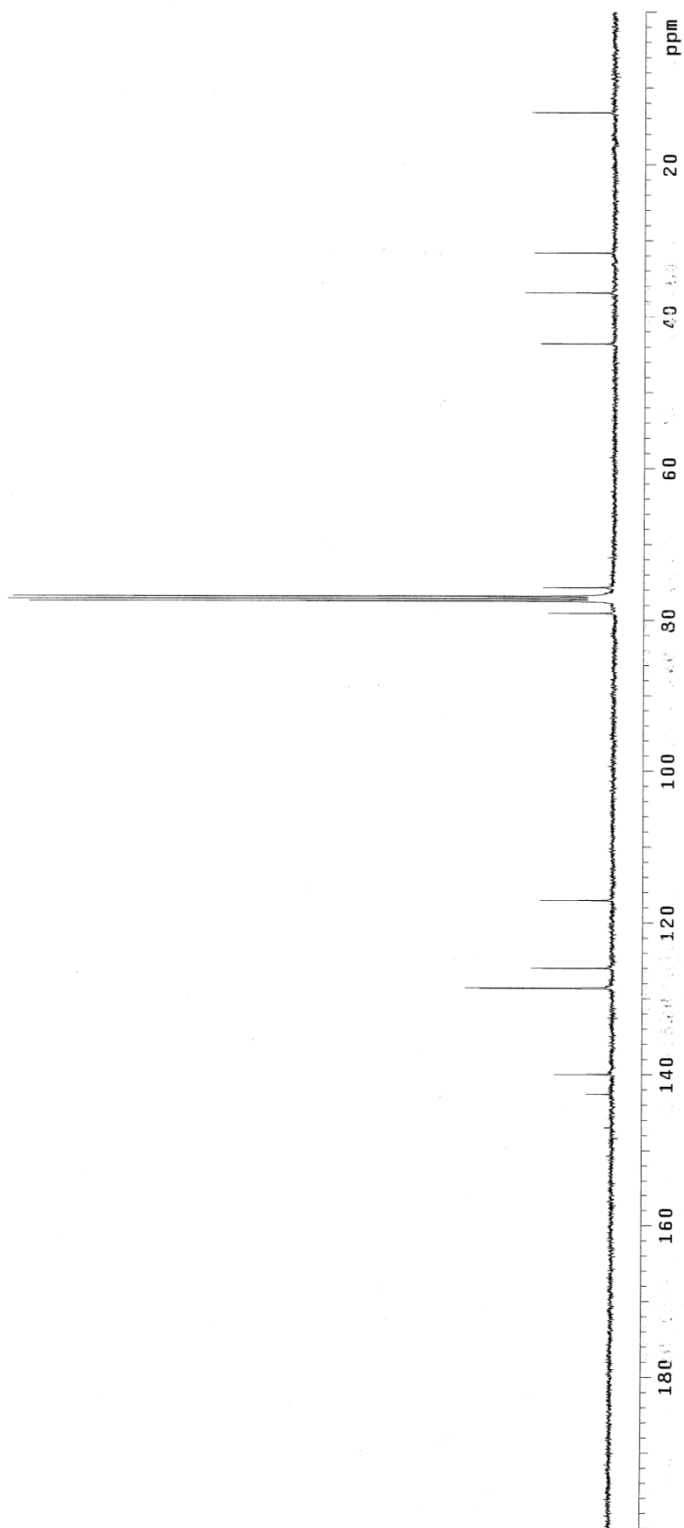
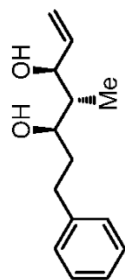


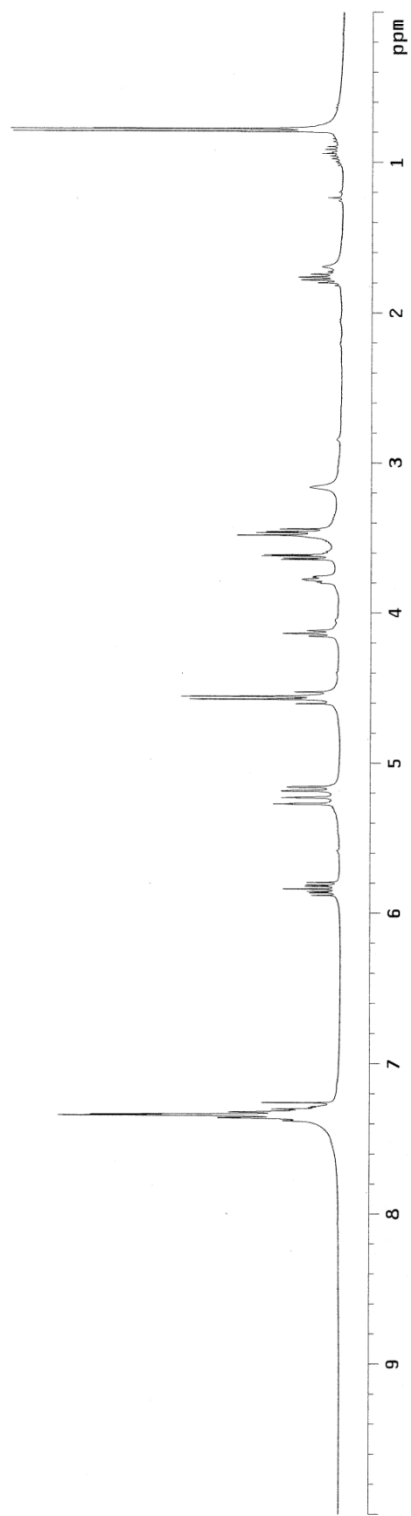
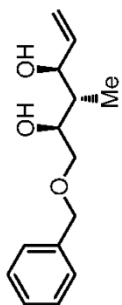


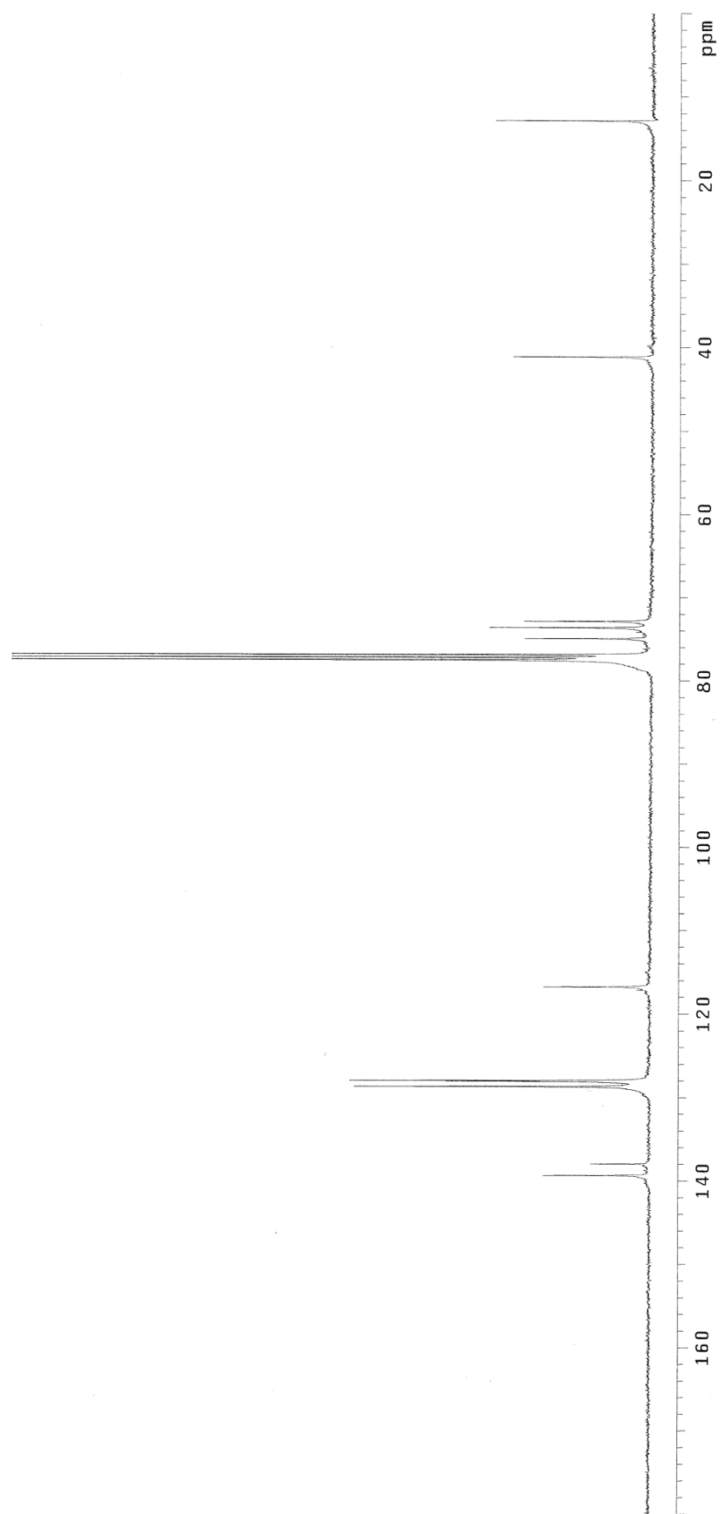
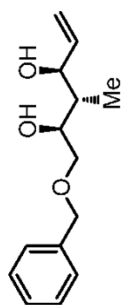


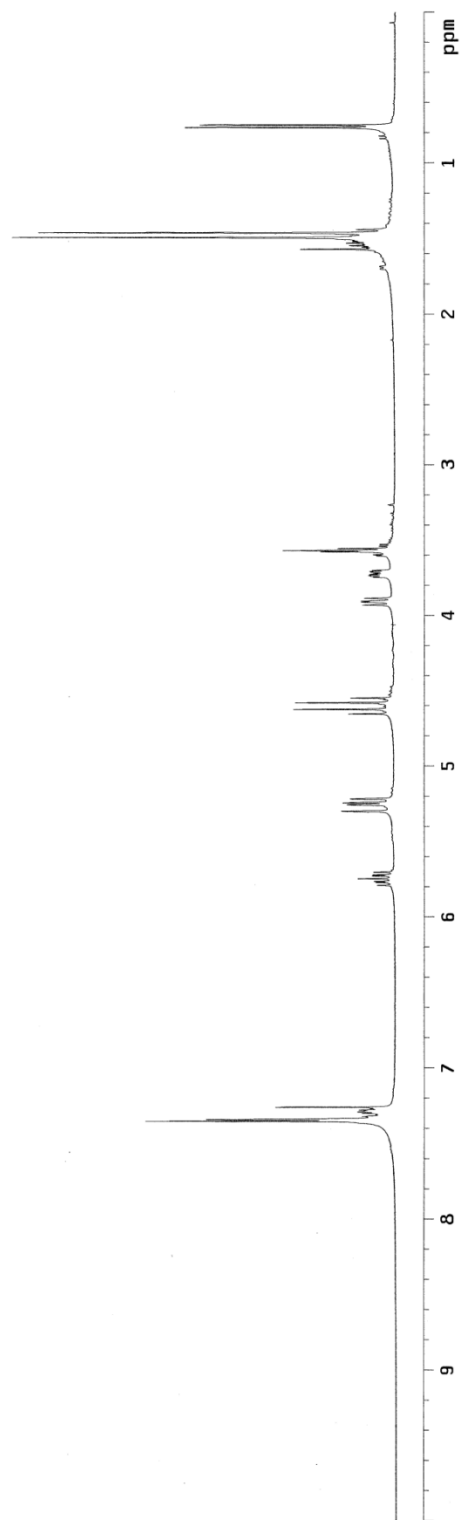
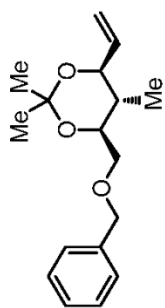


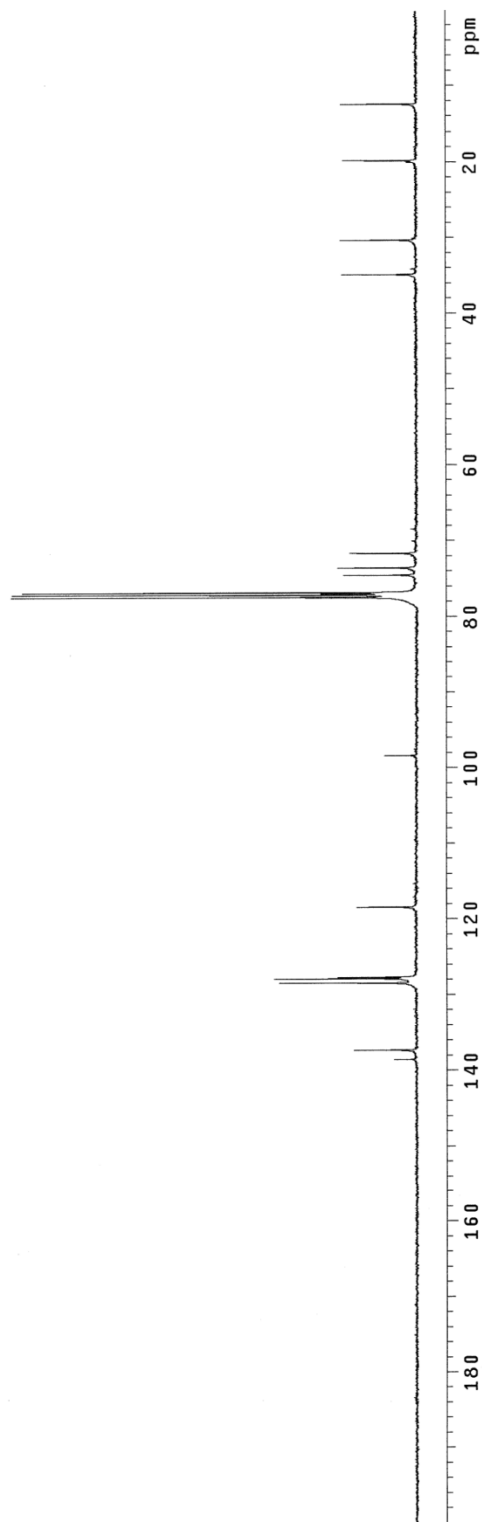
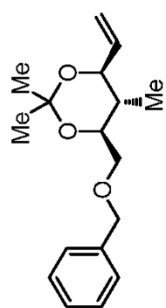


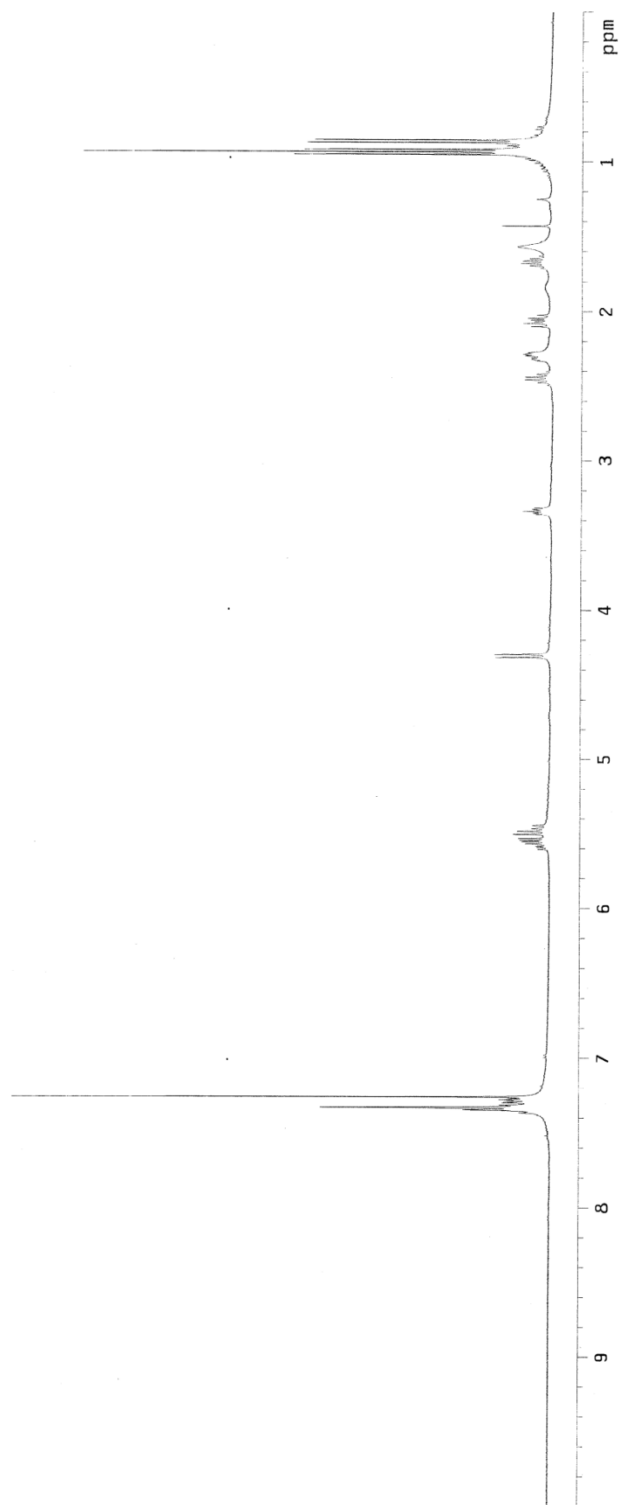
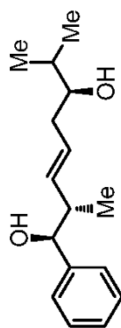


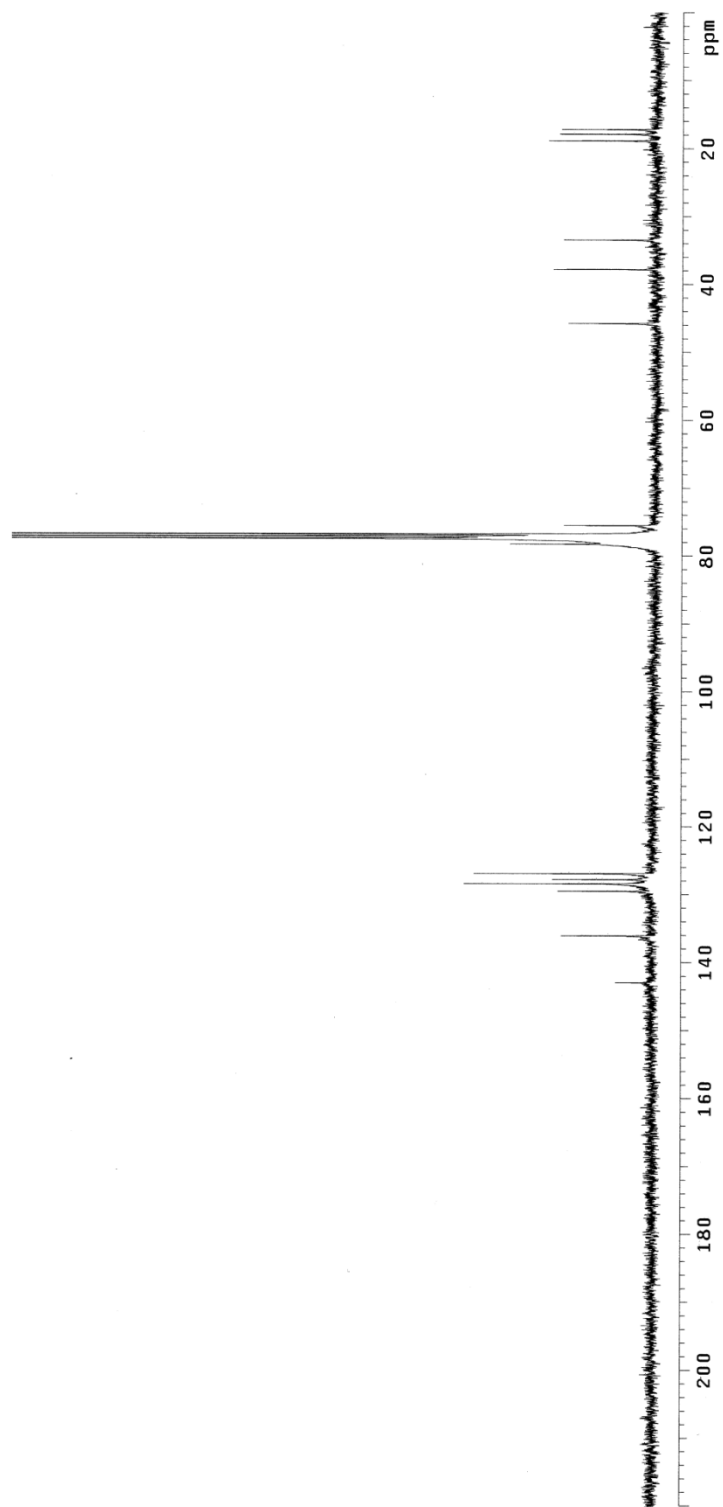
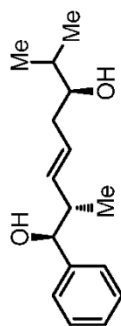


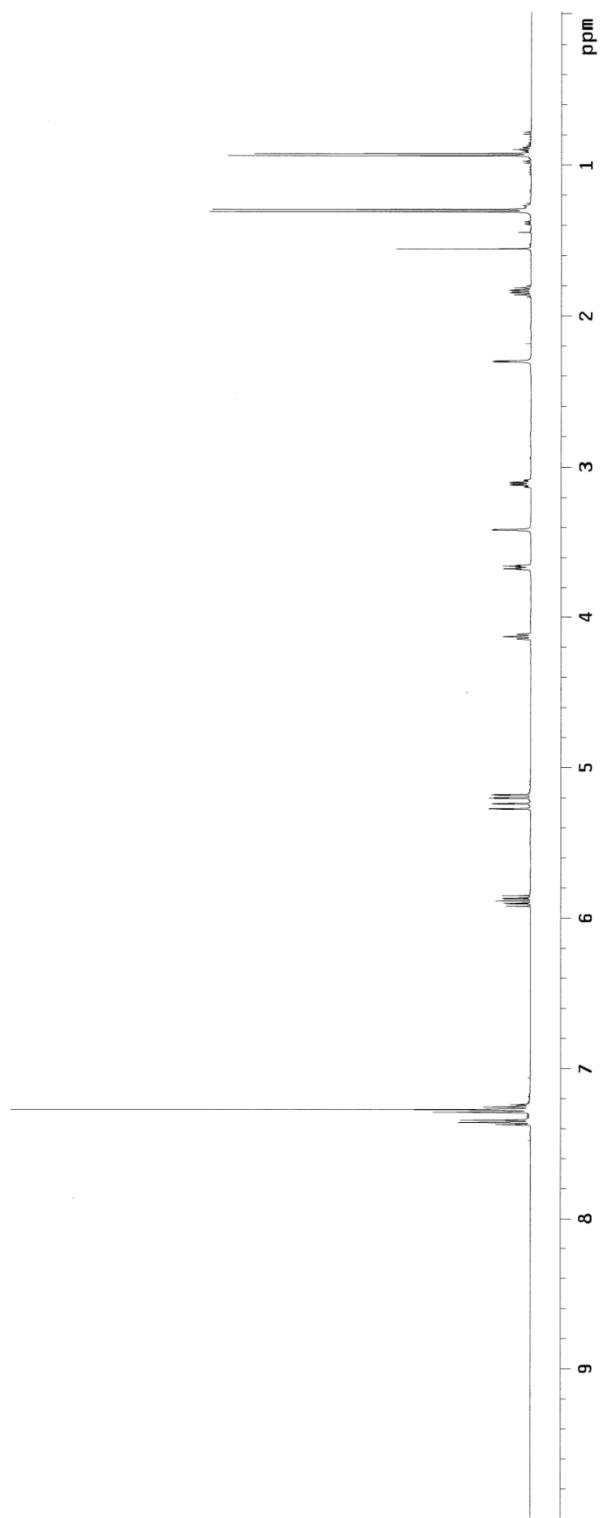
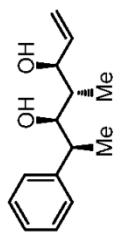


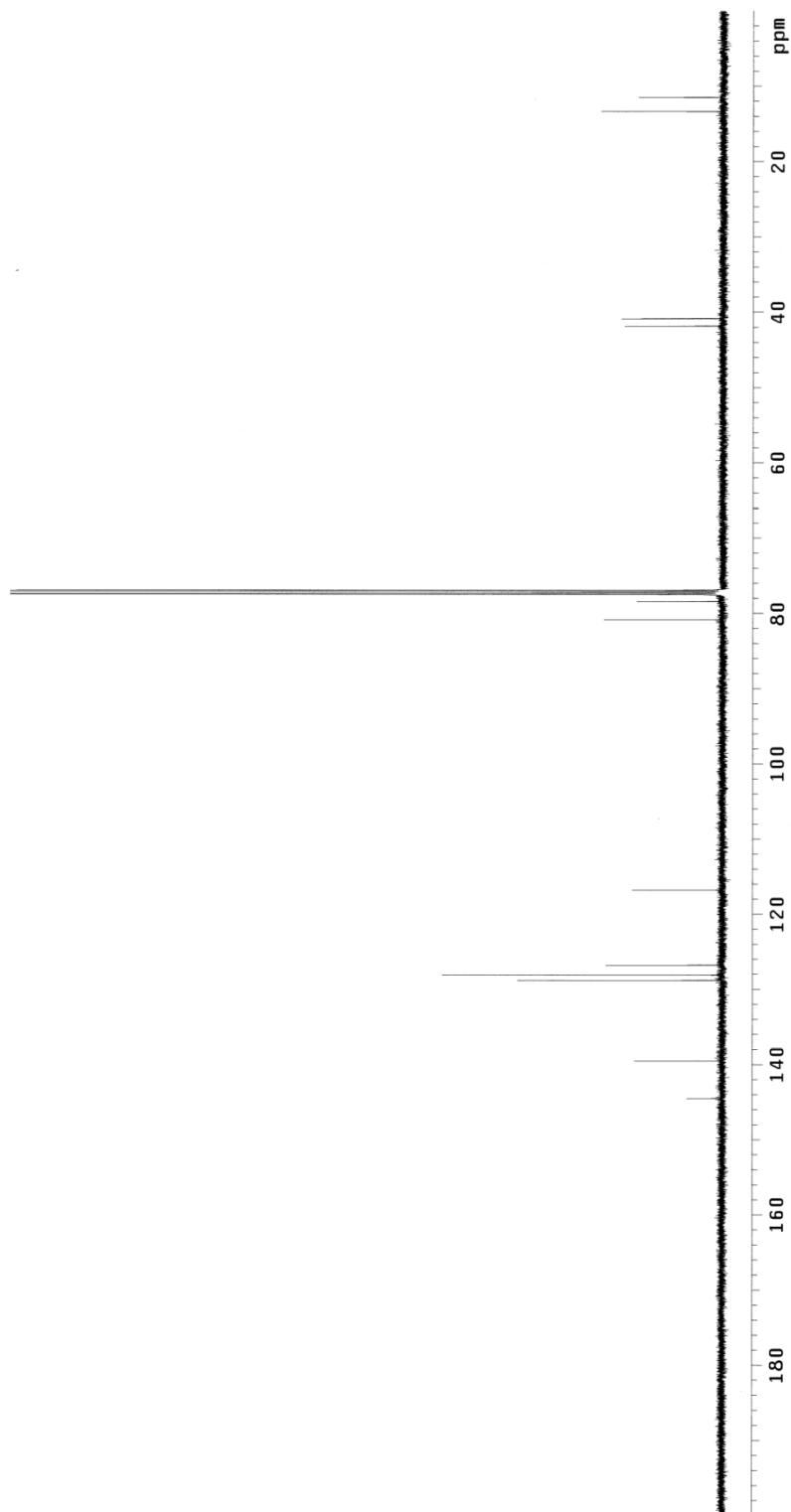
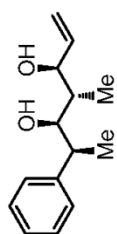












Chapter 4. Stereoselective Synthesis of Tertiary Alcohols via Catalytic Borylative Coupling Reactions of Ketones and Dienes

4.1. Introduction

4.1.1. Tertiary Alcohol Synthesis

Tertiary alcohols¹ are valuable and versatile motifs for the synthesis of natural products and medicinally active agents.^{2,3} Representative examples of biologically active molecules bearing tertiary alcohol functionality include camptothecin,⁴ tripanavir,⁵

¹ (a) Garcia, C.; Martin, V. S., "Asymmetric Addition to Ketones: Enantioselective Formation of Tertiary Alcohols," *Current Organic Chemistry* **2006**, *10*, 1849-1889. (b) Riant, O.; Hannedouche, J., "Asymmetric Catalysis for the Construction of Quaternary Carbon Centres: Nucleophilic Addition on Ketones and Ketimines," *Organic and Biomolecular Chemistry* **2007**, *5*, 873-888.

² For selected reviews on tertiary alcohol synthesis, see: (a) Hatano, M.; Ishihara, K., "Recent Progress in the Catalytic Synthesis of Tertiary Alcohols from Ketones with Organometallic Reagents," *Synthesis* **2008**, *2008*, 1647-1675. (b) Shibasaki, M.; Kanai, M., "Asymmetric Synthesis of Tertiary Alcohols and α -Tertiary Amines via Cu-Catalyzed C-C Bond Formation to Ketones and Ketimines," *Chemical Reviews* **2008**, *108*, 2853-2873.

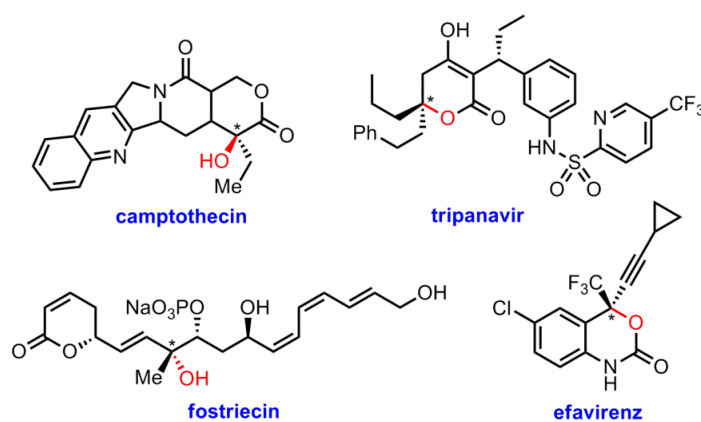
³ (a) Hatano, M.; Ishihara, K., "Catalytic Enantioselective Organozinc Addition toward Optically Active Tertiary Alcohol Synthesis," *The Chemical Record* **2008**, *8*, 143-155. (b) Adachi, S.; Harada, T., "Catalytic Enantioselective Aldol Additions to Ketones," *European Journal of Organic Chemistry* **2009**, *2009*, 3661-3671.

⁴ Wall, M. E.; Wani, M.; Cook, C.; Palmer, K. H.; McPhail, A.; Sim, G., "Plant Antitumor Agents. I. The Isolation and Structure of Camptothecin, a Novel Alkaloidal Leukemia and Tumor Inhibitor from *Camptotheca Acuminata* 1, 2," *Journal of the American Chemical Society* **1966**, *88*, 3888-3890.

⁵ Burlet, S.; Pietrancosta, N.; Laras, Y.; Garino, C.; Quelever, G.; Kraus, J.-L., "Prospects for the Resistance to HIV Protease Inhibitors: Current Drug Design Approaches and Perspectives," *Current Pharmaceutical Design* **2005**, *11*, 3077-3090.

fostriecin,⁶ and efavirenz⁷ (Figure 4.1). Notably, approximately 20 percent of the top 50 medicines possess tertiary alcohol functionality.⁸ In this regard, there has been an increasing need for development of effective methodologies to synthesize these important building blocks.^{9,10}

Figure 4.1 Biologically Related Molecules Containing Tertiary Alcohol Functionality



⁶ Tunac, J.; Graham, B.; Dobson, W., "Novel Antitumor Agents CI-920, PD 113,270 and PD 113,271. I. Taxonomy, Fermentation and Biological Properties," *The Journal of Antibiotics* **1983**, 36, 1595-1600.

⁷ Staszewski, S.; Morales-Ramirez, J.; Tashima, K. T.; Rachlis, A.; Skiest, D.; Stanford, J.; Stryker, R.; Johnson, P.; Labriola, D. F.; Farina, D., "Efavirenz Plus Zidovudine and Lamivudine, Efavirenz Plus Indinavir, and Indinavir Plus Zidovudine and Lamivudine in the Treatment of HIV-1 Infection in Adults," *New England Journal of Medicine* **1999**, 341, 1865-1873.

⁸ For more details, see: <http://cbc.arizona.edu/njardarson/group/top-pharmaceuticals-poster>.

⁹ For reviews on aligned studies in quaternary center generation, see: (a) Trost, B. M.; Jiang, C., "Catalytic Enantioselective Construction of All-Carbon Quaternary Stereocenters," *Synthesis* **2006**, 2006, 369-396. (b) Christoffers, J.; Baro, A., "Construction of Quaternary Stereocenters: New Perspectives through Enantioselective Michael Reactions," *Angewandte Chemie International Edition* **2003**, 42, 1688-1690. (c) Christoffers, J.; Mann, A., "Enantioselective Construction of Quaternary Stereocenters," *Angewandte Chemie International Edition* **2001**, 40, 4591-4597.

¹⁰ (a) Corey, E. J.; Guzman-Perez, A., "The Catalytic Enantioselective Construction of Molecules with Quaternary Carbon Stereocenters," *Angewandte Chemie International Edition* **1998**, 37, 388-401. (b) Fuji, K., "Asymmetric Creation of Quaternary Carbon Centers," *Chemical Reviews* **1993**, 93, 2037-2066.

A number of research groups have developed methods for enantioselective tertiary alcohol synthesis in various contexts (Scheme 4.1). **(a)** Sharpless asymmetric dihydroxylation of trisubstituted alkenes is one of the methods to access enantiomerically-enriched tertiary alcohols.^{11, 12} **(b)** Catalytic enantioselective aldol addition to ketones can also generate products containing tertiary alcohol functionality.^{3d, 13, 14} **(c)** Recently, enantioselective hydroxylation of oxindoles was reported; the resulting products bear tertiary alcohol groups at the alpha position.^{15, 16} **(d)** Furthermore, optically pure tertiary

¹¹ For reviews, see: (a) Kolb, H. C.; VanNieuwenhze, M. S.; Sharpless, K. B., "Catalytic Asymmetric Dihydroxylation," *Chemical Reviews* **1994**, *94*, 2483-2547. (b) Johnson, R. A.; Sharpless, K. B. In *Catalytic Asymmetric Synthesis*; John Wiley & Sons, Inc., 2005.

¹² For examples, see: (a) Jacobsen, E. N.; Marko, I.; Mungall, W. S.; Schroeder, G.; Sharpless, K. B., "Asymmetric Dihydroxylation via Ligand-Accelerated Catalysis," *Journal of the American Chemical Society* **1988**, *110*, 1968-1970. (b) Hale, K. J.; Manaviazar, S.; Peak, S. A., "Anomalous Enantioselectivity in the Sharpless Catalytic Asymmetric Dihydroxylation Reaction of 1,1-Disubstituted Allyl Alcohol Derivatives," *Tetrahedron Letters* **1994**, *35*, 425-428. (c) Gupta, P.; Fernandes, R. A.; Kumar, P., "An Asymmetric Dihydroxylation Route to (S)-Oxybutynin," *Tetrahedron Letters* **2003**, *44*, 4231-4232.

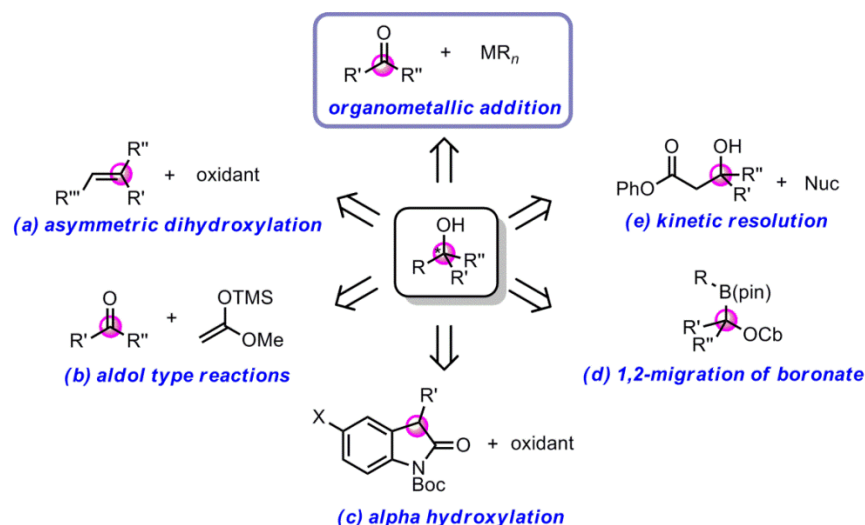
¹³ For selected examples, see: (a) Evans, D. A.; Kozłowski, M. C.; Burgey, C. S.; MacMillan, D. W. C., "C₂-Symmetric Copper(II) Complexes as Chiral Lewis Acids. Catalytic Enantioselective Aldol Additions of Enolsilanes to Pyruvate Esters," *Journal of the American Chemical Society* **1997**, *119*, 7893-7894. (b) Bøgevig, A.; Kumaragurubaran, N.; Jørgensen, K. A., "Direct Catalytic Asymmetric Aldol Reactions of Aldehydes," *Chemical Communications* **2002**, 620-621.

¹⁴ (a) Denmark, S. E.; Fan, Y., "Catalytic, Enantioselective Aldol Additions to Ketones," *Journal of the American Chemical Society* **2002**, *124*, 4233-4235. (b) Moreau, X.; Bazán-Tejeda, B.; Campagne, J.-M., "Catalytic and Asymmetric Vinylogous Mukaiyama Reactions on Aliphatic Ketones: Formal Asymmetric Synthesis of Taurospongins A," *Journal of the American Chemical Society* **2005**, *127*, 7288-7289.

¹⁵ For reviews, see: (a) Zhou, F.; Liu, Y. L.; Zhou, J., "Catalytic Asymmetric Synthesis of Oxindoles Bearing a Tetrasubstituted Stereocenter at the C-3 Position," *Advanced Synthesis and Catalysis* **2010**, *352*, 1381-1407. (b) Galliford, C. V.; Scheidt, K. A., "Pyrrolidinyl-Spirooxindole Natural Products as Inspirations for the Development of Potential Therapeutic Agents," *Angewandte Chemie International Edition* **2007**, *46*, 8748-8758. (c) Marti, C.; Carreira, E. M., "Construction of Spiro[Pyrrrolidine-3,3'-Oxindoles] – Recent Applications to the Synthesis of Oxindole Alkaloids," *European Journal of Organic Chemistry* **2003**, *2003*, 2209-2219.

alcohols can be prepared from enantio-enriched secondary alcohols by 1,2-metallate rearrangement of the boronate complex.¹⁷ (e) Also, there have been several reports on kinetic resolution of tertiary alcohols with chiral nucleophiles.¹⁸

Scheme 4.1 Enantioselective Tertiary Alcohol Synthesis



¹⁶ (a) Toullec, P. Y.; Bonaccorsi, C.; Mezzetti, A.; Togni, A., "Expanding the Scope of Asymmetric Electrophilic Atom-Transfer Reactions: Titanium- and Ruthenium-Catalyzed Hydroxylation of β -Ketoesters," *Proceedings of the National Academy of Sciences of the United States of America* **2004**, *101*, 5810-5814. (b) Ishimaru, T.; Shibata, N.; Nagai, J.; Nakamura, S.; Toru, T.; Kanemasa, S., "Lewis Acid-Catalyzed Enantioselective Hydroxylation Reactions of Oxindoles and β -Keto Esters Using DBFOX Ligand," *Journal of the American Chemical Society* **2006**, *128*, 16488-16489.

¹⁷ (a) Stymiest, J. L.; Bagutski, V.; French, R. M.; Aggarwal, V. K., "Enantiodivergent Conversion of Chiral Secondary Alcohols into Tertiary Alcohols," *Nature* **2008**, *456*, 778-782. (b) Bagutski, V.; French, R. M.; Aggarwal, V. K., "Full Chirality Transfer in the Conversion of Secondary Alcohols into Tertiary Boronic Esters and Alcohols Using Lithiation-Borylation Reactions," *Angewandte Chemie International Edition* **2010**, *49*, 5142-5145.

¹⁸ (a) Schipper, D. J.; Rousseaux, S.; Fagnou, K., "Kinetic Resolution of Quaternary and Tertiary β -Hydroxy Esters," *Angewandte Chemie International Edition* **2009**, *48*, 8343-8347. (b) Lebel, H.; Jacobsen, E. N., "Chromium Catalyzed Kinetic Resolution of 2,2-Disubstituted Epoxides," *Tetrahedron Letters* **1999**, *40*, 7303-7306. (c) Jarvo, E. R.; Evans, C. A.; Copeland, G. T.; Miller, S. J., "Fluorescence-Based Screening of Asymmetric Acylation Catalysts through Parallel Enantiomer Analysis. Identification of a Catalyst for Tertiary Alcohol Resolution," *The Journal of Organic Chemistry* **2001**, *66*, 5522-5527.

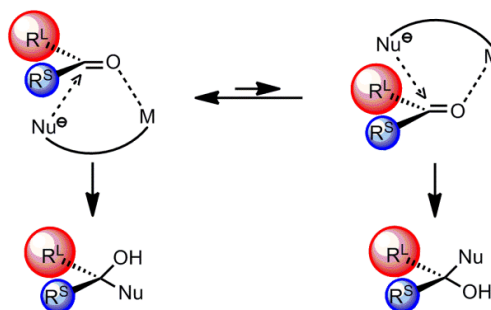
Last but not least, tertiary alcohols can be prepared by 1,2-addition of organometallic reagents to ketone electrophiles.^{1, 3a-c,19} With this method, a tetrasubstituted stereogenic center will be generated with concomitant formation of a new carbon–carbon bond. Among the six different approaches described in Scheme 4.1, the synthesis of tertiary alcohols via organometallic addition to ketones is one of the most useful and well-developed classes of the processes.

4.1.2. Tertiary Alcohols from Ketones and Organometallics

Catalytic enantioselective addition of organometallic reagents to ketones is an efficient synthetic method, since it generates a stereogenic center bearing a tertiary alcohol and constructs carbon frameworks by a new C–C bond formation. Compared to addition to aldehydes, however, addition to ketones inherently possesses a few challenges (Scheme 4.2). First, ketones are substantially less electrophilic than aldehydes, and therefore less reactive. Moreover, there are smaller differences between the two substituents of ketones (i.e. R vs R'), compared to those of aldehydes (i.e. R vs H). Consequently, when organometallic reagents approach ketones, discrimination between the two prochiral faces of ketones is more challenging due to the similar nature of the substituents.^{1b}

¹⁹ Betancort, J. M.; Garcia, C.; Walsh, P. J.; Kim, B.; Cho, M.; Woo, H.; Filippov, D.; van den Elst, H.; Tromp, C.; van der Marel, G., "Development of the First Practical Catalyst for the Asymmetric Addition of Alkyl- and Arylzinc Reagents to Ketones," *Synlett* **2004**, 15, 749-760.

Scheme 4.2 Organometallic Addition to a Ketone



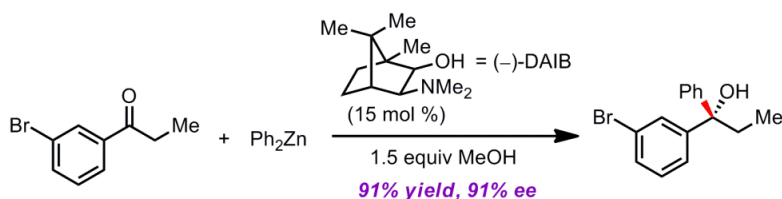
Despite the intrinsic challenges for ketone electrophiles, several research groups have tackled this difficult problem over the last couple of decades. A number of organometallic reagents have been developed for this class of reactions; organomagnesium, organolithium, organoboron, organozinc, organocopper, organosilicon, organoaluminum, and organotin reagents can participate in the process.^{3a} The reaction categories developed in this area with respect to the added substituents (R groups) include arylation, alkylation, alkenylation, alkynylation, allylation, and cyanosilylation of ketones.

4.2. Background

4.2.1. Asymmetric Arylation of Ketones

The first asymmetric arylations of ketones were reported by Fu and co-workers (Scheme 4.3).^{20,21} In this study, enantioselective arylation of ketones was achieved with Ph_2Zn in the presence of Noyori's DAIB (3-*exo*-dimethylaminoisoborneol) ligand.²² The DAIB-catalyzed reaction proceeded efficiently with great enantioselectivity (91% yield, 91% *ee*) when methanol was added. In the absence of methanol, the arylation reactions were not efficient; generation of alkoxy phenyl zinc reagent might be crucial for this process.

Scheme 4.3 Fu's Arylation of Ketones



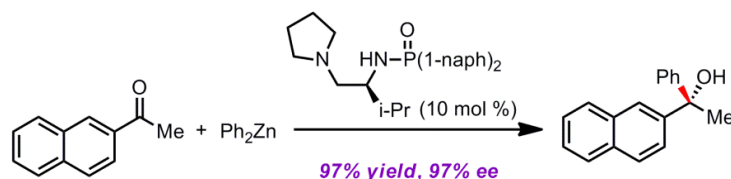
²⁰ Dosa, P. I.; Fu, G. C., "Catalytic Asymmetric Addition of ZnPh_2 to Ketones: Enantioselective Formation of Quaternary Stereocenters," *Journal of the American Chemical Society* **1998**, *120*, 445-446.

²¹ For aligned studies with aldehyde electrophiles, see: Dosa, P. I.; Ruble, J. C.; Fu, G. C., "Planar-Chiral Heterocycles as Ligands in Metal-Catalyzed Processes: Enantioselective Addition of Organozinc Reagents to Aldehydes," *The Journal of Organic Chemistry* **1997**, *62*, 444-445.

²² (a) Kitamura, M.; Suga, S.; Kawai, K.; Noyori, R., "Catalytic Asymmetric Induction. Highly Enantioselective Addition of Dialkylzincs to Aldehydes," *Journal of the American Chemical Society* **1986**, *108*, 6071-6072. (b) Noyori, R.; Suga, S.; Kawai, K.; Okada, S.; Kitamura, M., "Enantioselective Alkylation of Carbonyl Compounds. From Stoichiometric to Catalytic Asymmetric Induct Ion," *Pure and Applied Chemistry* **1988**, *60*, 1597.

More recently, the Ishihara group has demonstrated that a chiral phosphoramidate-zinc catalyst can promote the arylation of ketones with great efficiency and selectivity (Scheme 4.4).^{23, 24} The chiral ligand was conveniently prepared from an inexpensive natural amino acid, L-valine. Notably, 4'-chloroacetophenone was phenylated under the same reaction conditions to give the desired alcohol in 91% yield with 93% ee; the resulting optically-pure tertiary alcohol is the key intermediate for the synthesis of clemastine (an antihistamine drug).²⁵

Scheme 4.4 Ishihara's Arylation of Ketones



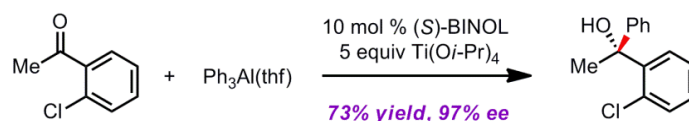
²³ Hatano, M.; Miyamoto, T.; Ishihara, K., "Highly Active Chiral Phosphoramidate-Zn(II) Complexes as Conjugate Acid-Base Catalysts for Enantioselective Organozinc Addition to Ketones," *Organic Letters* **2007**, 9, 4535-4538.

²⁴ For aligned studies with aldehyde electrophiles, see: (a) Hatano, M.; Miyamoto, T.; Ishihara, K., "Enantioselective Dialkylzinc Addition to Aldehydes Catalyzed by Chiral Zn(II)-Binolates Bearing Phosphonates and Phosphoramidates in the 3,3' -Positions," *Synlett* **2006**, 2006, 1762-1764. (b) Hatano, M.; Miyamoto, T.; Ishihara, K., "3,3'-Diphosphoryl-1,1'-Bi-2-Naphthol-Zn(II) Complexes as Conjugate Acid-Base Catalysts for Enantioselective Dialkylzinc Addition to Aldehydes," *The Journal of Organic Chemistry* **2006**, 71, 6474-6484. (c) Hatano, M.; Miyamoto, T.; Ishihara, K., "Enantioselective Addition of Organozinc Reagents to Aldehydes Catalyzed by 3,3' -Bis (Diphenylphosphinoyl)-Binol," *Advanced Synthesis & Catalysis* **2005**, 347, 1561-1568.

²⁵ (a) Jung, J. W.; Kim, H.-D., "Stereoselective Synthesis of (-)-Hydroxyclemastine as a Versatile Intermediate for the H₁ Receptor Antagonist Clemastine," *Archives of Pharmacal Research* **2007**, 30, 1521-1525. (b) Kim, S. J.; Chang, M.; Kim, H.-D., "Asymmetric Transformation of L-Homoserine Lactone to an Optically Active 2-Substituted Pyrrolidine for Clemastine," *Tetrahedron: Asymmetry* **2011**, 22, 1901-1905.

The arylation reaction has been performed not only with organozinc reagents but also with organoaluminum reagents. The first example of asymmetric arylation of ketones with organoaluminum reagents was reported by the Gau group.^{26,27} In the presence of (*S*)-BINOL and titanium(IV) isopropoxide, the organoaluminum reagent, [Ph₃Al(thf)] was effectively added to the ketone electrophile to afford a tertiary alcohol with good efficiency and high selectivity (Scheme 4.5).

Scheme 4.5 Gau's Arylation of Ketones



4.2.2. Asymmetric Alkylation of Ketones

The first catalytic enantioselective alkylation of ketones was accomplished by Yus and co-workers (Scheme 4.6).²⁸ The effectiveness of titanium-based catalyst, which is employed in this work, toward alkylation of aldehyde was previously investigated by

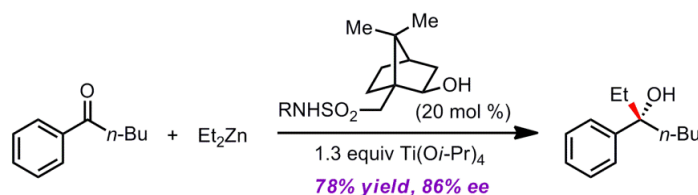
²⁶ Chen, C.-A.; Wu, K.-H.; Gau, H.-M., "Highly Enantioselective Aryl Additions of [AlAr₃(THF)] to Ketones Catalyzed by a Titanium(IV) Catalyst of (*S*)-BINOL," *Angewandte Chemie International Edition* **2007**, *46*, 5373-5376.

²⁷ For aligned studies with aldehyde electrophiles, see: Wu, K.-H.; Gau, H.-M., "Remarkably Efficient Enantioselective Titanium(IV)-(*R*)-H₈-BINOLate Catalyst for Arylations to Aldehydes by Triaryl(Tetrahydrofuran)Aluminum Reagents," *Journal of the American Chemical Society* **2006**, *128*, 14808-14809.

²⁸ (a) Ramón, D. J.; Yus, M., "First Enantioselective Addition of Dialkylzinc to Ketones Promoted by Titanium(IV) Derivatives," *Tetrahedron Letters* **1998**, *39*, 1239-1242. (b) Ramón, D. J.; Yus, M., "First Enantioselective Addition of Diethylzinc and Dimethylzinc to Prostereogenic Ketones Catalysed by Camphorsulfonamide-Titanium Alkoxide Derivatives," *Tetrahedron* **1998**, *54*, 5651-5666.

Kobayashi²⁹ and Seebach.³⁰ Various hydroxysulfonamide ligands that are derived from camphor are utilized to promote the alkylation of ketones in an enantioselective fashion (Scheme 4.6). Even though a stoichiometric amount of titanium(IV) isopropoxide was required, the reaction between 1-phenyl-1-pentanone and diethylzinc proceeded well in the presence of the hydroxysulfonamide ligand (20 mol %) with good efficiency and selectivity (78% yield, 86% ee).

Scheme 4.6 Yus' Alkylation of Ketones



Shibasaki and co-workers have investigated asymmetric dialkylzinc addition to α -ketoesters (Scheme 4.7).³¹ In this study, a chiral bifunctional catalyst³² is employed to

²⁹ Takahashi, H.; Kawakita, T.; Ohno, M.; Yoshioka, M.; Kobayashi, S., "A Catalytic Enantioselective Reaction Using a C₂-Symmetric Disulfonamide as a Chiral Ligand: Alkylation of Aldehydes Catalyzed by Disulfonamide-Ti(Oi-Pr)₄-Dialkyl Zinc System," *Tetrahedron* **1992**, *48*, 5691-5700.

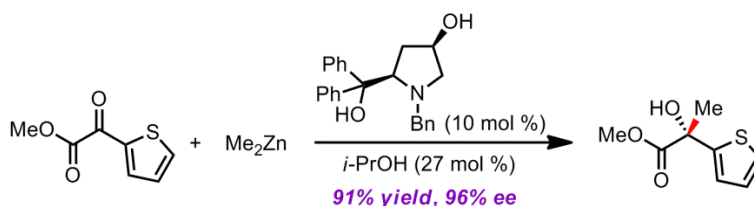
³⁰ Seebach, D.; Beck, A. K.; Schmidt, B.; Wang, Y. M., "Enantio- and Diastereoselective Titanium-Taddolate Catalyzed Addition of Diethyl and Bis(3-Buten-1-yl) Zinc to Aldehydes a Full Account with Preparative Details," *Tetrahedron* **1994**, *50*, 4363-4384.

³¹ Funabashi, K.; Jachmann, M.; Kanai, M.; Shibasaki, M., "Multicenter Strategy for the Development of Catalytic Enantioselective Nucleophilic Alkylation of Ketones: Me₂Zn Addition to α -Ketoesters," *Angewandte Chemie International Edition* **2003**, *42*, 5489-5492.

³² For reviews on bifunctional catalysts, see: (a) Gröger, H., "The Development of New Monometallic Bifunctional Catalysts with Lewis Acid and Lewis Base Properties, and Their Application in Asymmetric Cyanation Reactions," *Chemistry—A European Journal* **2001**, *7*, 5246-5251. (b) Shibasaki, M.; Kanai, M.; Funabashi, K., "Recent Progress in Asymmetric Two-Center Catalysis," *Chemical Communications* **2002**, 1989-1999.

promote the catalytic enantioselective methylation of α -ketoesters. In the presence of the chiral ligand containing multicenters (alcohols and amines), the heterocyclic α -ketoester was effectively converted into an optically pure hydroxy ester in 91% yield with significant enantiomeric excess (96% *ee*). The authors have observed that both the rate of the addition of Me_2Zn reagent and the presence of *i*-PrOH affected the reaction yield and selectivity.

Scheme 4.7 Shibasaki's Alkylation of α -Ketoesters



4.2.3. Asymmetric Alkenylation of Ketones

Asymmetric alkenylation of carbonyl compounds has attracted significant interests because the corresponding products from the process are synthetically versatile allylic alcohols.³³ In this regard, Walsh and co-workers have developed asymmetric alkenylation and dienylation of ketones (Scheme 4.8).^{34,35} The vinylzinc reagent was generated *in situ*

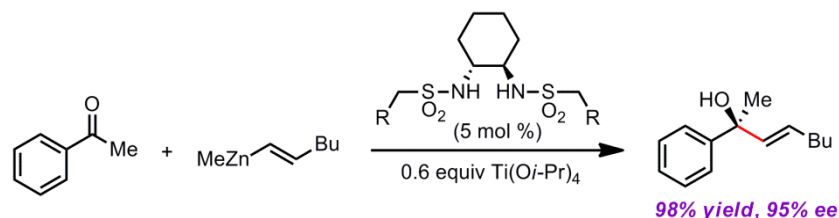
³³ (a) Pu, L.; Yu, H.-B., "Catalytic Asymmetric Organozinc Additions to Carbonyl Compounds," *Chemical Reviews* **2001**, *101*, 757-824. (b) Chen, Y. K.; Lurain, A. E.; Walsh, P. J., "A General, Highly Enantioselective Method for the Synthesis of D and L α -Amino Acids and Allylic Amines," *Journal of the American Chemical Society* **2002**, *124*, 12225-12231.

³⁴ (a) Li, H.; Walsh, P. J., "Catalytic Asymmetric Vinylation of Ketones," *Journal of the American Chemical Society* **2004**, *126*, 6538-6539. (b) Li, H.; Walsh, P. J., "Catalytic Asymmetric Vinylation and Dienylation of Ketones," *Journal of the American Chemical Society* **2005**, *127*, 8355-8361.

³⁵ For aligned studies with aldehyde electrophiles, see: Pritchett, S.; Woodmansee, D.; Gantzel, P.; Walsh, P., "Synthesis and Crystal Structures of Bis(Sulfonamido) Titanium Bis(Alkoxide) Complexes:

from the corresponding alkyne (1-hexyne) and Schwartz's reagent (Cp_2ZrClH)³⁶ via hydrozirconation of the alkyne. In the presence of a chiral bis(sulfonamide) ligand and titanium tetraisopropoxide, the vinylzinc reagent was added to acetophenone enantioselectively to furnish an optically-pure allylic tertiary alcohol (98% yield, 95% *ee*).

Scheme 4.8 Walsh's Alkenylation of Ketones



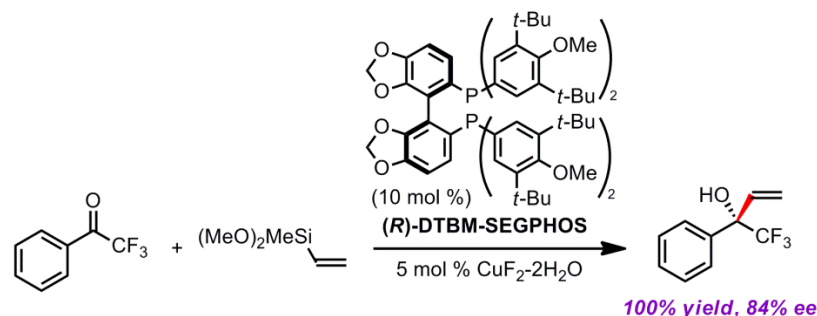
On the other hand, the Shibasaki group employed organosilicon reagents for enantioselective alkenylation (Scheme 4.9).³⁷ In this study, trifluoromethyl ketones were employed as carbonyl electrophiles, and alkenylsilanes were used as nucleophiles. In the presence of a $\text{CuF}(\text{R})\text{-DTBM-SEGPHOS}$ complex, asymmetric vinylation of 2,2,2-trifluoroacetophenone occurred with a vinylsilane reagent to afford a tertiary alcohol bearing a trifluoromethyl group (100% yield, 84% *ee*).

Mechanistic Implications in the Bis(Sulfonamide) Catalyzed Asymmetric Addition of Dialkylzinc Reagents to Aldehydes," *Journal of the American Chemical Society* **1998**, *120*, 6423-6424.

³⁶ Buchwald, S. L.; LaMaire, S. J.; Nielsen, R. B.; Watson, B. T.; King, S. M., "A Modified Procedure for the Preparation of $\text{Cp}_2\text{Zr}(\text{H})\text{Cl}$ (Schwartz's Reagent)," *Tetrahedron Letters* **1987**, *28*, 3895-3898.

³⁷ Motoki, R.; Tomita, D.; Kanai, M.; Shibasaki, M., "Catalytic Enantioselective Alkenylation and Phenylation of Trifluoromethyl Ketones," *Tetrahedron Letters* **2006**, *47*, 8083-8086.

Scheme 4.9 Shibasaki's Alkenylation of Ketones



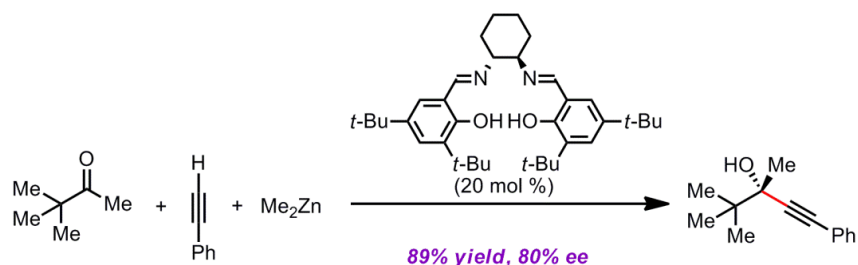
4.2.4. Asymmetric Alkynylation of Ketones

Pioneering work in asymmetric alkynylation of ketones was done by Cozzi in 2003 (Scheme 4.10).^{38, 39} Phenylacetylene was enantioselectively added to pinacolone in the presence of a chiral salen ligand and dimethylzinc to afford an optically active propargyl tertiary alcohol (89% yield, 80% *ee*). In this method, an excess amount of dimethylzinc was employed to generate a zinc(II)–salen catalyst and the zinc acetylide nucleophile. The author speculated that the Zn(II)–salen complex would act as a bifunctional catalyst by activating both the ketone substrate and the acetylide nucleophile in this system.

³⁸ Cozzi, P. G., "Enantioselective Alkynylation of Ketones Catalyzed by Zn(Salen) Complexes," *Angewandte Chemie International Edition* **2003**, *42*, 2895-2898.

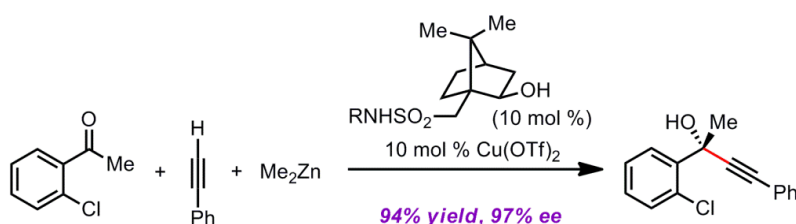
³⁹ For reviews on asymmetric alkynylation of carbonyl compounds, see: (a) Pu, L., "Asymmetric Alkynylzinc Additions to Aldehydes and Ketones," *Tetrahedron* **2003**, *59*, 9873-9886. (b) Cozzi, P. G.; Hilgraf, R.; Zimmermann, N., "Acetylenes in Catalysis: Enantioselective Additions to Carbonyl Groups and Imines and Applications Beyond," *European Journal of Organic Chemistry* **2004**, *2004*, 4095-4105. (c) Lu, G.; Li, Y.-M.; Li, X.-S.; Chan, A. S. C., "Synthesis and Application of New Chiral Catalysts for Asymmetric Alkynylation Reactions," *Coordination Chemistry Reviews* **2005**, *249*, 1736-1744.

Scheme 4.10 Cozzi's Alkynylation of Ketones



The Chan group also demonstrated that asymmetric alkyne addition to ketones can be effective under optimized reaction conditions (Scheme 4.11).⁴⁰ In this study, a chiral hydroxysulfonamide ligand²⁸ was used to promote enantioselective alkynylation of chlorinated acetophenone in the presence of phenylacetylene, dimethylzinc, and copper(II) triflate. The corresponding optically active propargylic 3° alcohol was obtained in 94% yield and 97% ee. This system exhibited a substantial improvement from previous studies in terms of the amount of catalyst (10 mol %) and the enantioselectivity (up to 97% ee).

Scheme 4.11 Chan's Alkynylation of Ketones



⁴⁰ (a) Lu, G.; Li, X.; Jia, X.; Chan, W. L.; Chan, A. S., "Enantioselective Alkynylation of Aromatic Ketones Catalyzed by Chiral Camphorsulfonamide Ligands," *Angewandte Chemie International Edition* **2003**, *42*, 5057-5058. (b) Lu, G.; Li, X.; Li, Y. M.; Kwong, F. Y.; Chan, A. S., "Highly Enantioselective Catalytic Alkynylation of Ketones—a Convenient Approach to Optically Active Propargylic Alcohols," *Advanced Synthesis & Catalysis* **2006**, *348*, 1926-1933.

4.2.5. Asymmetric Allylation/Crotylation of Ketones

Catalytic asymmetric allylation of carbonyls is one of the most pivotal synthetic methods in organic chemistry.^{41,42} However, the known methods for aldehyde allylations often cannot be applied to ketone allylation reactions. The first asymmetric allylation of ketones was achieved by Tagliavini and co-workers (Scheme 4.12).⁴³ Acetophenone and tetraallyltin underwent an asymmetric allylation reaction in the presence of a BINOL–titanium(IV) catalyst⁴⁴ to give the homoallylic tertiary alcohol with moderate enantioselectivity (77% yield, 65% *ee*). The chiral catalyst for this system was prepared from (R)-BINOL (20 mol %), dichlorotitanium(IV) isopropoxide (20 mol %), and allyltributyltin (40 mol %).

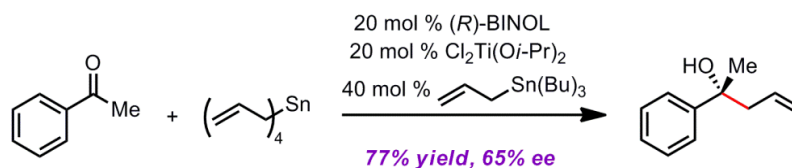
⁴¹ For reviews, see: (a) Yamamoto, Y., "Acyclic Stereocontrol via Allylic Organometallic Compounds," *Accounts of Chemical Research* **1987**, *20*, 243-249. (b) Yamamoto, Y.; Asao, N., "Selective Reactions Using Allylic Metals," *Chemical Reviews* **1993**, *93*, 2207-2293.

⁴² (a) Marshall, J. A., "Chiral Allylic and Allenic Stannanes as Reagents for Asymmetric Synthesis," *Chemical Reviews* **1996**, *96*, 31-48. (b) Denmark, S. E.; Fu, J., "Catalytic Enantioselective Addition of Allylic Organometallic Reagents to Aldehydes and Ketones," *Chemical Reviews* **2003**, *103*, 2763-2794.

⁴³ Casolari, S.; D'Addari, D.; Tagliavini, E., "BINOL-Ti-Catalyzed Synthesis of Tertiary Homoallylic Alcohols: The First Catalytic Asymmetric Allylation of Ketones," *Organic Letters* **1999**, *1*, 1061-1063.

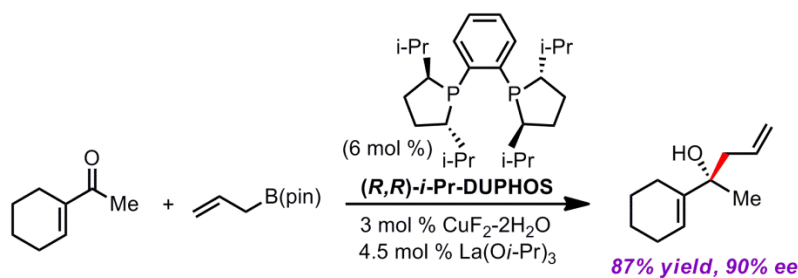
⁴⁴ Yasuda, M.; Kitahara, N.; Fujibayashi, T.; Baba, A., "Allylation of Unactivated Ketones by Tetraallyltin Accelerated by Phenol. Application to Asymmetric Allylation Using a Tetraallyltin-BINOL System," *Chemistry Letters* **1998**, *27*, 743-744.

Scheme 4.12 Tagliavini's Allylation of Ketones



Allylic boron reagents can be employed as nucleophiles in this process, as demonstrated by the Shibasaki group (Scheme 4.13).⁴⁵ In these catalytic enantioselective allylation and crotylation of ketones, $\text{CuF}-i\text{-Pr-DuPhos}$ and lanthanum(III) isopropoxide were used as a chiral catalyst and a cocatalyst, respectively. With this catalytic system, the allylation reactions on aliphatic and aromatic ketones proceeded with good enantioselectivities. The authors pointed out that the fluoride ligand on copper is crucial for catalytic efficiency since it activates the allylating reagents by a boronate complex formation. Also, the addition of lanthanum(III) isopropoxide accelerated the process, presumably by facilitating the ligand exchange between boron and copper atoms.

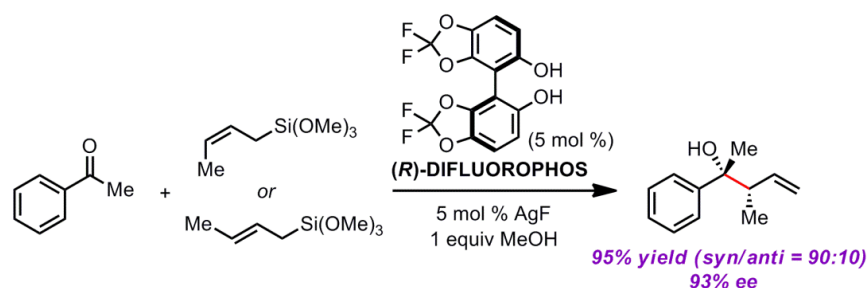
Scheme 4.13 Shibasaki's Allylation of Ketones



⁴⁵ Wada, R.; Oisaki, K.; Kanai, M.; Shibasaki, M., "Catalytic Enantioselective Allylboration of Ketones," *Journal of the American Chemical Society* **2004**, 126, 8910-8911.

Yamamoto and co-workers have reported catalytic enantioselective allylation and crotylation reactions using allyltrimethoxysilane or crotyltrimethoxysilane as nucleophiles (Sakurai–Hosomi allylation). By employing AgF–difluorophos as a catalyst, crotylation of acetophenone with trimethoxy crotylsilane furnished the corresponding homoallylic alcohol in 95% yield with 93% *ee* (Scheme 4.14).⁴⁶ The *syn*-product was obtained as a major isomer (*syn/anti* = 90:10) regardless of the configuration of the starting material (crotylsilane). In this catalytic cycle, the active nucleophile is an allyl (or crotyl)–silver species that is generated from transmetalation. The addition of methanol is critical in this process since it regenerates the silver catalyst from the silver alkoxide intermediate, which was produced by the allyl transfer from silver to a ketone.

Scheme 4.14 Yamamoto's Crotylation of Ketones

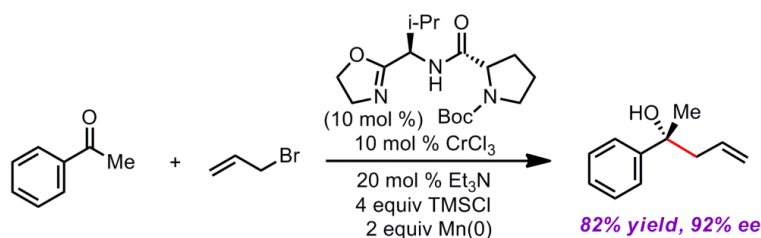


More recently, the Sigman group has demonstrated the Cr-catalyzed ketone allylation with use of allyl chromium as a nucleophile (a variant of the Nozaki–Hiyama–Kishi reaction). In the presence of chromium(III) chloride and a chiral

⁴⁶ Wadamoto, M.; Yamamoto, H., "Silver-Catalyzed Asymmetric Sakurai-Hosomi Allylation of Ketones," *Journal of the American Chemical Society* **2005**, *127*, 14556-14557.

peptide ligand, the allylation of acetophenone with allyl bromide afforded the corresponding homoallylic alcohol with good efficiency and high selectivity (Scheme 4.15).⁴⁷ Analogous crotylation reactions also proceeded with crotylbromide under the same reaction conditions.

Scheme 4.15 Sigman's Allylation of Ketones



4.2.6. Asymmetric Cyanosilylation of Ketones

Enantiomerically enriched cyanohydrins are versatile and valuable synthetic intermediates in organic synthesis as well as biological studies.^{48, 49, 50} The first chemically-

⁴⁷ (a) Miller, J. J.; Sigman, M. S., "Design and Synthesis of Modular Oxazoline Ligands for the Enantioselective Chromium-Catalyzed Addition of Allyl Bromide to Ketones," *Journal of the American Chemical Society* **2007**, *129*, 2752-2753. (b) Rajaram, S.; Sigman, M. S., "Design of Hydrogen Bond Catalysts Based on a Modular Oxazoline Template: Application to an Enantioselective Hetero Diels–Alder Reaction," *Organic Letters* **2005**, *7*, 5473-5475.

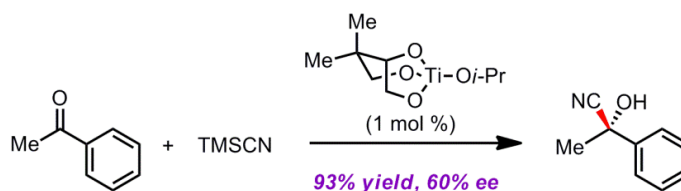
⁴⁸ For reviews, see: (a) North, M., "Synthesis and Applications of Non-Racemic Cyanohydrins," *Tetrahedron: Asymmetry* **2003**, *14*, 147-176. (b) Gregory, R. J. H., "Cyanohydrins in Nature and the Laboratory: Biology, Preparations, and Synthetic Applications," *Chemical Reviews* **1999**, *99*, 3649-3682.

⁴⁹ (a) Effenberger, F., "Synthesis and Reactions of Optically Active Cyanohydrins," *Angewandte Chemie International Edition* **1994**, *33*, 1555-1564. (b) North, M., "Catalytic Asymmetric Cyanohydrin Synthesis," *Synlett* **1993**, 1993, 807-820.

⁵⁰ For selected synthesis, see: (a) Hamashima, Y.; Kanai, M.; Shibasaki, M., "Catalytic Enantioselective Cyanosilylation of Ketones," *Journal of the American Chemical Society* **2000**, *122*, 7412-7413. (b) Hamashima, Y.; Kanai, M.; Shibasaki, M., "Catalytic Enantioselective Cyanosilylation of Ketones:

catalyzed asymmetric cyanosilylation of ketones was reported by Choi and co-workers (Scheme 4.16).⁵¹ The reaction of acetophenone and trimethylsilyl cyanide (TMSCN) in the presence of a chiral titanium catalyst furnished the corresponding cyanohydrin in a good yield with moderate selectivity (93% yield, 60% ee). The chiral catalyst that was employed in this process was prepared from (*S*)-3,3-dimethyl-1,2,4-butanetriol and titanium(IV) isopropoxide.

Scheme 4.16 Choi's Cyanosilylation of Ketones



A more efficient catalytic method for enantioselective cyanosilylation of ketones was developed by Snapper and Hoveyda (Scheme 4.17).⁵² This system employs an aluminum-based catalyst that is associated with a chiral peptide ligand. The reaction with 2-

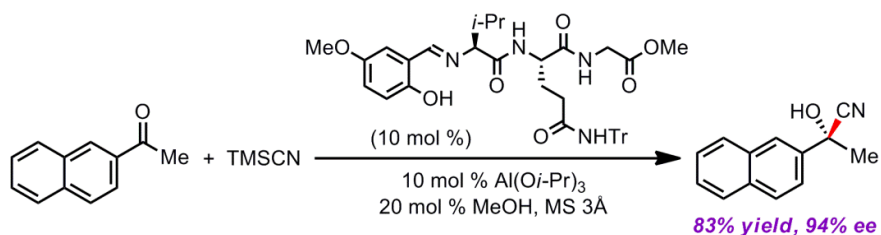
Improvement of Enantioselectivity and Catalyst Turn-over by Ligand Tuning," *Tetrahedron Letters* **2001**, *42*, 691-694. (c) Yabu, K.; Masumoto, S.; Yamasaki, S.; Hamashima, Y.; Kanai, M.; Du, W.; Curran, D. P.; Shibasaki, M., "Switching Enantiofacial Selectivities Using One Chiral Source: Catalytic Enantioselective Synthesis of the Key Intermediate for (2*S*)-Camptothecin Family by (*S*)-Selective Cyanosilylation of Ketones," *Journal of the American Chemical Society* **2001**, *123*, 9908-9909.

⁵¹ (a) Choi, M. C.; Chan, S.; Matsumoto, K., "Catalytic Asymmetric Synthesis of (*S*)-Acetophenone Cyanohydrin under High Pressure," *Tetrahedron Letters* **1997**, *38*, 6669-6672. (b) Choi, M. C.; Chan, S.-S.; Chan, M.-K.; Kim, J. C.; Iida, H.; Matsumoto, K., "Ti-Triol Catalysed Trimethylsilylcyanation of Acetophenones under High Pressure," *Heterocycles* **2004**, *62*, 643-653.

⁵² Deng, H.; Isler, M. P.; Snapper, M. L.; Hoveyda, A. H., "Aluminum-Catalyzed Asymmetric Addition of TMSCN to Aromatic and Aliphatic Ketones Promoted by an Easily Accessible and Recyclable Peptide Ligand," *Angewandte Chemie International Edition* **2002**, *41*, 1009-1012.

acetophenone and TMSCN in the presence of the chiral Al(III)–peptide complex furnished the corresponding product in 83% yield with 94% *ee*. A variety of aromatic, aliphatic, and unsaturated ketones can participate in this process with high selectivities. It was observed that the presence of the glutamine moiety and the addition of methanol are crucial for high enantioselectivities of the process. These early investigations in asymmetric cyanosilylation of ketones were soon followed by a number of different approaches that were developed in various contexts.^{53, 54}

Scheme 4.17 Snapper and Hoveyda's Cyanosilylation of Ketones



⁵³ Senanayake, C. H., "A New Lithium Alkoxide Accelerated Diastereoselective Cyanation of Ketones," *Organic Letters* **2001**, 3, 553-556. (b) Chen, F.-X.; Feng, X., "Synthesis of Racemic Tertiary Cyanohydrins," *Synlett* **2005**, 2005, 0892-0899. (c) Fukuda, Y.; Kondo, K.; Aoyama, T., "Construction of Tetrasubstituted Carbon by an Organocatalyst: Cyanation Reaction of Ketones and Ketimines Catalyzed by a Nucleophilic *N*-Heterocyclic Carbene," *Synthesis* **2006**, 2006, 2649-2652.

⁵⁴ (a) Wang, X.; Tian, S.-K., "Neutral π -Nucleophile Catalyzed Cyanation of Aldehydes and Ketones," *Synfacts* **2007**, 2007, 0872-0872. (b) Wang, X.; Tian, S.-K., "Catalytic Cyanosilylation of Ketones with Simple Phosphonium Salt," *Tetrahedron Letters* **2007**, 48, 6010-6013. (c) Khan, N.-U. H.; Agrawal, S.; Kureshy, R. I.; Abdi, S. H. R.; Singh, S.; Jasra, R. V., "Fe(Cp)₂PF₆: An Efficient Catalyst for Cyanosilylation of Carbonyl Compounds under Solvent Free Condition," *Journal of Organometallic Chemistry* **2007**, 692, 4361-4366.

4.2.7. Summary

Representative examples for the catalytic enantioselective synthesis of tertiary alcohols from ketones and organometallic reagents are presented.^{55,56} This area is rapidly growing due to the needs of optically active tertiary alcohols in scientific communities. In particular, organometallic addition to ketones represents one of the most atom-economical and generally-applicable methodologies. Despite significant advances of the methods in this area, there is still room for further improvement. Specifically, lowering catalyst loadings and broadening substrate scopes will be some of the main focuses in the future work of this class of reactions.

⁵⁵ For trifluoromethylation to ketones, see: (a) Iseki, K.; Nagai, T.; Kobayashi, Y., "Asymmetric Trifluoromethylation of Aldehydes and Ketones with Trifluoromethyltrimethylsilane Catalyzed by Chiral Quaternary Ammonium Fluorides," *Tetrahedron Letters* **1994**, 35, 3137-3138. (b) Caron, S.; Do, N. M.; Arpin, P.; Larivée, A., "Enantioselective Addition of a Trifluoromethyl Anion to Aryl Ketones and Aldehydes," *Synthesis* **2003**, 2003, 1693-1698. (c) Mizuta, S.; Shibata, N.; Akiti, S.; Fujimoto, H.; Nakamura, S.; Toru, T., "Cinchona Alkaloids/Tmaf Combination-Catalyzed Nucleophilic Enantioselective Trifluoromethylation of Aryl Ketones," *Organic Letters* **2007**, 9, 3707-3710.

⁵⁶ For a related ketoester-ene reaction, see: Mikami, K.; Kawakami, Y.; Akiyama, K.; Aikawa, K., "Enantioselective Catalysis of Ketoester-Ene Reaction of Silyl Enol Ether to Construct Quaternary Carbons by Chiral Dicationic Palladium(II) Complexes," *Journal of the American Chemical Society* **2007**, 129, 12950-12951.

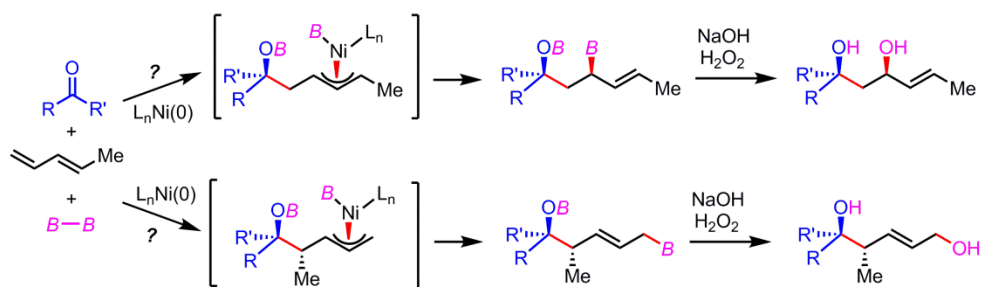
4.3. Method Development

4.3.1. Catalytic Borylative Coupling Reactions of Ketones and Dienes⁵⁷

4.3.1.1. Project Goals

In the previous two chapters (Chapters 2 and 3), stereoselective borylative aldehyde–diene coupling reactions were described. These reactions occur with exceptionally high levels of stereoselection when aldehydes are employed as substrates. Following that, we were interested in whether these processes might also apply to ketone electrophiles and to determine whether high levels of stereocontrol could be maintained (Scheme 4.18).

Scheme 4.18 Borylative Ketone–Diene Coupling Reactions

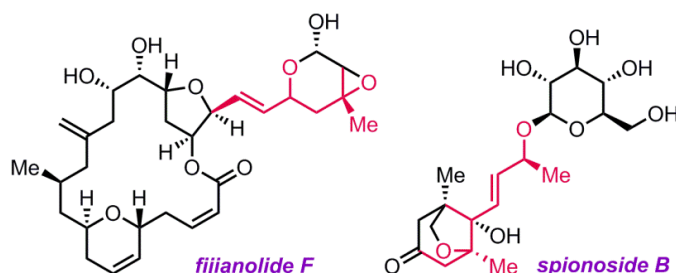


Notably, the products from the borylative ketone–diene coupling reactions would possess tertiary alcohol functionality. While construction of these functional groups is readily accomplished by nucleophilic additions to ketones, such reactions can be challenging,

⁵⁷ Portions of this project described here have been published: Cho, H. Y.; Yu, Z.; Morken, J. P., "Stereoselective Borylative Ketone–Diene Coupling," *Organic Letters* **2011**, *13*, 5267–5269.

particularly when stereocontrol is a required element. Potential synthetic targets in natural products, which contain the same carbon skeletons and functional groups as in the expected ketone–diene coupling products, are presented in Figure 4.2.

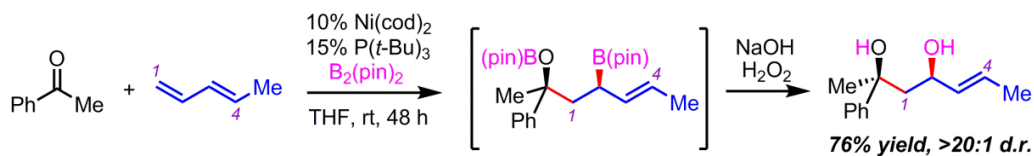
Figure 4.2 Synthetic Targets in Natural Products



4.3.1.2. Reaction Optimization

In order to initiate studies in ketone–diene coupling reactions, acetophenone was treated with (*E*)-1,3-pentadiene under conditions similar to those employed for aldehyde coupling reactions (10 mol % Ni(cod)₂, 15 mol % P(*t*-Bu)₃, 2 equiv B₂(pin)₂) and then subjected to oxidative work-up. As depicted in Scheme 4.19, this reaction occurred in good yield and with >20:1 diastereoselectivity.

Scheme 4.19 Initial Investigations on Ketone–Diene Coupling Reactions



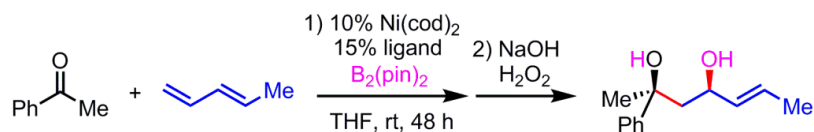
We observed a significant effect of temperature on both reactivity and selectivity in the borylative ketone–diene coupling reactions (Table 4.1). While the reaction at 0 °C was not effective (entry 1), the multicomponent coupling reaction proceeded well at room temperature with high selectivity (entry 2). At an increased temperature, 60 °C, we observed some loss of diastereoselectivity and formation of more byproducts (entry 3).

Table 4.1 Effects of Reaction Temperature on Borylative Ketone–Diene Coupling

entry	temperature	yield (%)	dr
1	0 °C	< 20%	nd
2	rt	76%	> 20:1
3	60 °C	47%	5:1

We were also inquisitive about the range of phosphine ligands that can promote this type of coupling reaction. The phosphine ligand screening results for the borylative ketone–diene coupling reactions are summarized in Table 4.2. Strikingly, none of the phosphine ligands, except for tri-*tert*-butylphosphine, afforded the desired tertiary alcohol product in this process. The high level of selectivity and reactivity of the multicomponent coupling with ketone electrophiles can be achieved only when P(*t*-Bu)₃ is employed as a ligand.

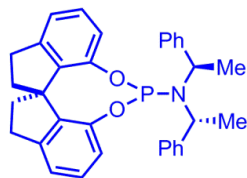
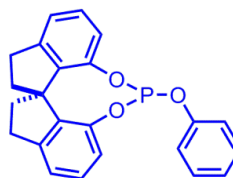
Table 4.2 Screen of Ligands for Borylative Ketone–Diene Coupling



entry	ligand	yield (%)	dr
1	PCy ₃	0%	na
2	P(<i>t</i> -Bu) ₃	71%	> 20:1
3	PPh ₃	0%	na
4	P(TMS) ₃	0%	na
5	PMe ₃	0%	na
6	P(OEt) ₃	0%	na

In addition to these achiral phosphine ligands, some optically-active chiral ligands were also examined for this process. We employed commercially available spirobiindane-derived ligands in the borylative ketone–diene coupling reactions (Scheme 4.20). However, none of those ligands promoted the coupling reactions to afford the desired products.

Scheme 4.20 Spirobiindane-Derived Ligand for Borylative Ketone–Diene Coupling

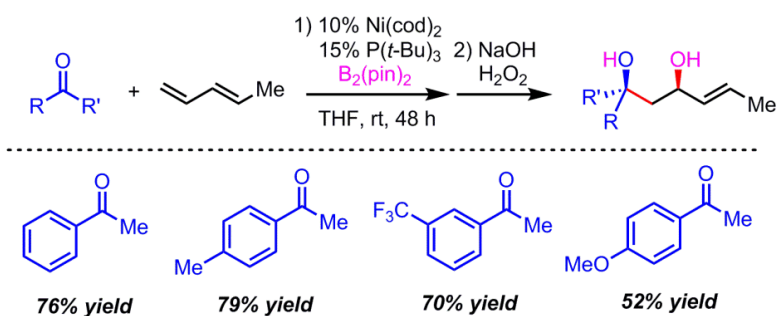
**(R)-Shiphos-PE**
no conversion**(R)-SHIP**
no conversion

4.3.1.3. Substrate Scope

4.3.1.3.1. Survey of Carbonyl Compounds

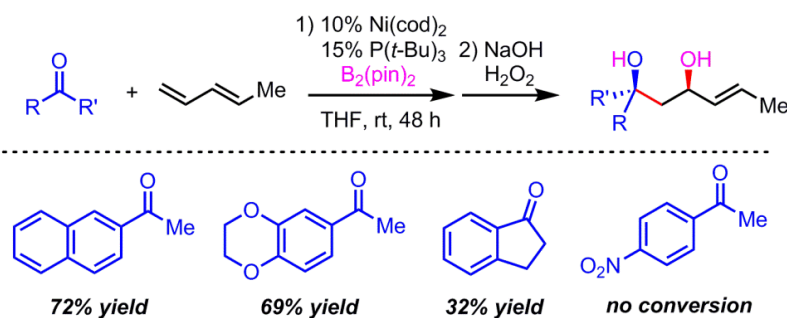
Under the optimized reaction conditions, a number of different substrates (both ketones and unsaturated hydrocarbons) were examined for the coupling reactions of ketones and dienes. In general, aromatic ketones that are derived from acetophenone were compatible with these reaction conditions to furnish the corresponding tertiary alcohols in good yield (Scheme 4.21).

Scheme 4.21 Survey of Acetophenone Derivatives for Borylative Ketone–Diene Coupling



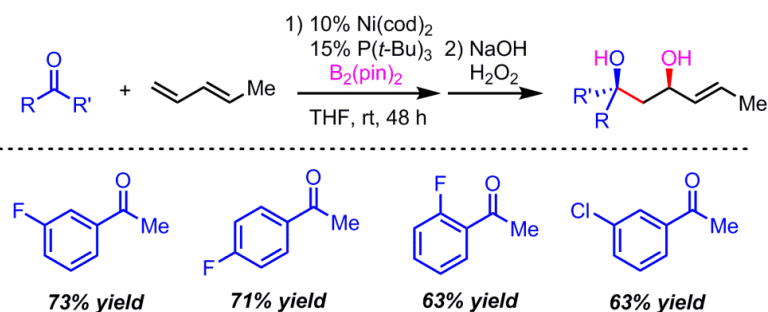
The more sterically-encumbered ketones (i.e. 2'-acetonaphthone, 6-acetyl-1,4-benzodioxane) were also competent reaction partners in the coupling reactions (Scheme 4.22). The borylative coupling reaction of 1-indanone and pentadiene afforded the 1,3 diol in moderate yield (32% yield). However, when 4'-nitroacetophenone was employed as a ketone electrophile, the reaction did not give the corresponding product.

Scheme 4.22 Survey of Aromatic Ketones for Borylative Ketone–Diene Coupling



Several halogenated acetophenone derivatives were also examined for this coupling process (Scheme 4.23). All of the fluorinated acetophenones turned out to be competent coupling partners in this process, no matter where the fluorine atom is substituted (63–73% yield). Also, the reaction with 3'-chloroacetophenone afforded the corresponding diol product in 63% yield.

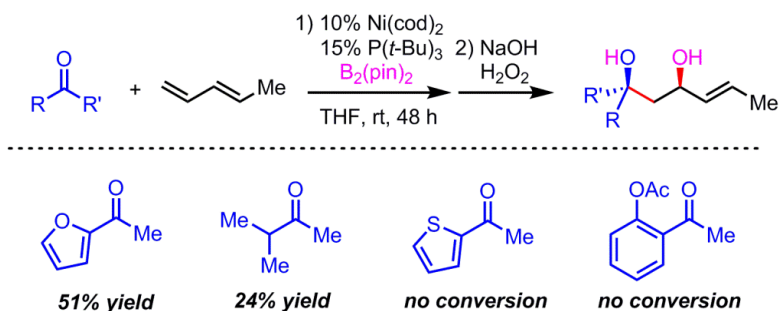
Scheme 4.23 Survey of Halogenated Aromatic Ketones for Borylative Ketone–Diene Coupling



Additionally, the reactivities of some heteroaromatic ketones toward this coupling reaction was examined (Scheme 4.24). The borylative coupling of 2-acetylfuran and pentadiene furnished the desired tertiary alcohol in 51% yield. However, the same reaction

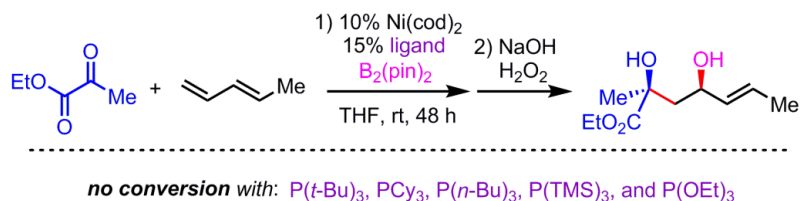
with 2-acetylthiophene did not afford the expected product. An aliphatic ketone, 3-methyl-2-butanone, participated in the multicomponent coupling to give the diol product in moderate yield (24% yield). It was observed that the borylative coupling reaction with 2'-acetoxyacetophenone did not proceed to produce the 1,3 diol.

Scheme 4.24 Survey of Various Ketones for Borylative Ketone–Diene Coupling



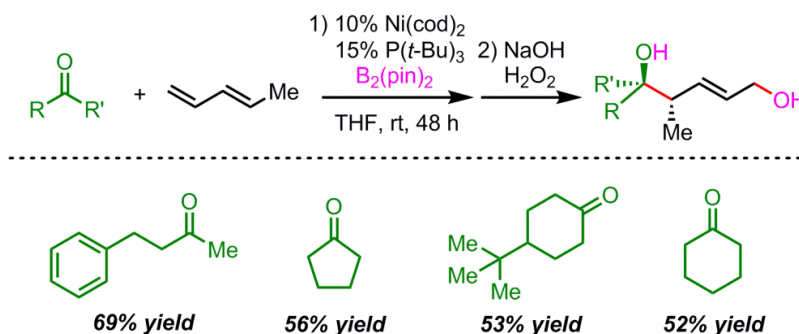
Also, we were interested in whether pyruvates would participate in this process to afford more functionalized products (Scheme 4.25). When ethyl pyruvate was employed as an electrophile, however, the desired products were not formed. For this coupling, a number of phosphine ligands were examined as listed in Scheme 4.25; however, none of those phosphine ligands were able to promote the borylative pyruvate–diene coupling reactions.

Scheme 4.25 Attempted Experiments for Borylative Pyruvate–Diene Coupling



Several aliphatic ketones were also employed in the borylative multicomponent coupling with ketones (Scheme 4.26). All of the aliphatic ketones that are listed in Scheme 4.26 participated in this borylative coupling with reasonable efficiency (52–69% yield). Notably, the products from these aliphatic ketones were regioisomeric to those from other aromatic ketones. In other words, a new carbon–carbon bond was formed between the carbonyl carbon and the *substituted* carbon of the diene. Furthermore, the products were 1,5 diols, instead of 1,3 diols that were produced from the aromatic ketones.

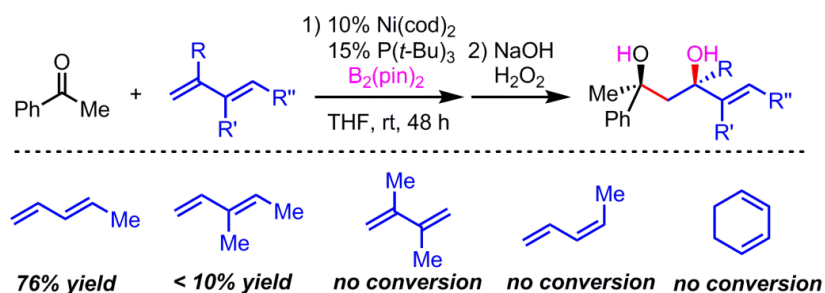
Scheme 4.26 Survey of Aliphatic Ketones for 1,5-Diol Synthesis



4.3.1.3.2. Survey of Unsaturated Hydrocarbons

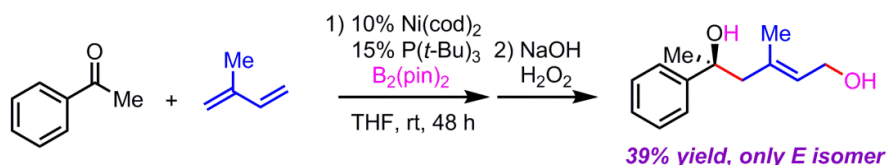
We also examined various dienes for the borylative multicomponent coupling reaction involving ketone electrophiles. The reaction with *trans*-piperylene exhibited great reactivity and selectivity to afford the 1,3-diol in 75% yield. However, when 3-methyl-1,3-pentadiene was employed in the coupling reaction, the corresponding product was formed in less than 10% yield. The reactions with other substituted dienes or 1,3-cyclohexadiene did not show any conversion in this coupling process.

Scheme 4.27 Survey of Dienes for Borylative Ketone–Diene Coupling



Finally, we investigated the reactivity of isoprene toward this borylative multicomponent coupling reaction (Scheme 4.28). The reaction of isoprene and acetophenone in the presence of the nickel catalyst furnished the coupling product in 39% yield. In contrast to *trans*-piperylene (see Scheme 4.27), however, the coupling with isoprene afforded a 1,5 diol as a reaction product; this is regioisomeric to the 1,3 diol product that was prepared from the reaction with pentadiene.

Scheme 4.28 Borylative Coupling of Acetophenone and Isoprene



4.3.1.3.3. Summary of Substrate Scope

As described in Table 4.3, acetophenone and its derivatives exhibited excellent selectivities and reactivities toward the borylative multicomponent reactions. Acetophenone and 4'-methylacetophenone afforded the corresponding products in high yield and with

>20:1 diastereoselectivity when they were subjected to the optimized reaction conditions (Table 4.3, entries 1 and 2). Fluoro functional groups were tolerated in the ketone electrophile, as shown in entries 3 and 4.

Table 4.3 Borylative Ketone–Diene Coupling with Acetophenone Derivatives

entry	ketone	diene	product	yield	dr
1				76%	> 20:1
2				79%	> 20:1
3				73%	> 20:1
4				71%	> 20:1

Aromatic ketones containing either electron-neutral or electron-withdrawing groups are processed in a similar manner as acetophenone (Table 4.4). The reaction with 2'-acetonaphthone afforded the desired tertiary alcohol in 72% yield, and >20:1 *syn:anti* diastereoselectivity was observed (entry 1). When an electron-withdrawing group (e.g. trifluoromethyl group) was substituted in the aromatic ring, neither reactivity nor selectivity decreased in the coupling reaction (entry 2). As for the halogen substitutions, both fluoro and chloro groups are tolerated in the ketone–diene coupling reaction (entries 3 and 4).

Table 4.4 Borylative Ketone–Diene Coupling with Methyl Ketones

entry	ketone	diene	product	yield	dr
1				72%	> 20:1
2				63%	> 20:1
3				70%	> 20:1
4				63%	> 20:1

Furthermore, aromatic ketones possessing electron-donating groups are also competent reaction partners for this process (Table 4.5). The reactions with 6-acetyl-1,4-benzodioxane and 4'-methoxyacetophenone furnished the corresponding reaction products in 69% and 52% yield, respectively (entries 1 and 2). In both cases, a 1,3-*syn*-diol was a major product with >20:1 diastereomeric ratio. In addition, 2-acetylfuran and 3-methyl-2-butanone were coupled with pentadiene and B₂(pin)₂ to afford the 1,3 diols with high selectivity (entries 3 and 4).

Table 4.5 Borylative Ketone–Piperylene Coupling Reactions

entry	ketone	diene	product	yield	dr
1				69%	> 20:1
2				52%	> 20:1
3				51%	> 20:1
4				24%	> 20:1

Whereas aromatic methyl ketones were found to react with good yield and selectivity regardless of substitution, the efficiency and selectivity of reactions of aliphatic ketones was much more sensitive to substrate structure. For example, 4-phenyl-2-butanone (Table 4.6, entry 1) underwent smooth coupling with pentadiene but, in contrast to reactions of aromatic ketones, was converted to the derived 1,5-diol in a manner similar to that observed for reactions of benzaldehyde. On the other hand, we observed that when the more hindered substrate 3-methyl-2-butanone (Table 4.5, entry 4) was subjected to the diene-carbonyl coupling reaction, the 1,3-diol, similar to those produced from aryl ketones, was the predominant reaction product.

Table 4.6 Borylative Ketone–Diene Coupling Reactions

entry	ketone	diene	product	yield	dr
1				69%	7:1
2				56%	only E
3				53%	> 20:1
4				52%	only E

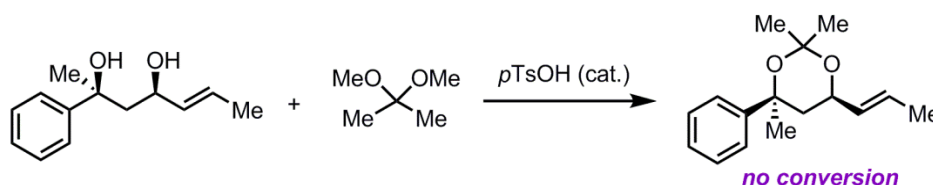
Suspecting that the steric encumbrance surrounding the reacting carbonyl determines the regiochemical outcome, we examined constrained cyclic ketones and found that, consistent with the correlation, these also deliver the 1,5-diol product (Table 4.6, entries 2–4). It should be noted that the product of entry 3 appears to arise by preferred equatorial attachment of the diene to the carbonyl carbon of the substrate.

4.3.1.4. Product Transformation

The stereochemical outcome of the ketone–diene coupling reactions (*i.e.* 1,3-*syn* hydroxyl group relationship) was determined by 2D NMR analysis (NOESY analysis) of an acetone that was derived from a coupling product. We first attempted to protect a 1,3 diol

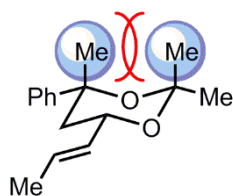
with benzylidene acetal in the presence of acid catalyst; but the 1,3 diol was not converted to the desired ketal (Scheme 4.29).

Scheme 4.29 Attempts to Protect the Coupling Product with Acetonide



We reasoned that the steric hindrance between the two methyl groups in the most stable chair form of the acetonide might prevent the formation of the desired cyclic ketal (Figure 4.3). This 1,3-diaxial interaction would become significantly more problematic in the acetonide 6-membered ring due to the decreased bond lengths (*i.e.* C–O bond vs C–C bond), compared to an all-carbon cyclohexane ring.

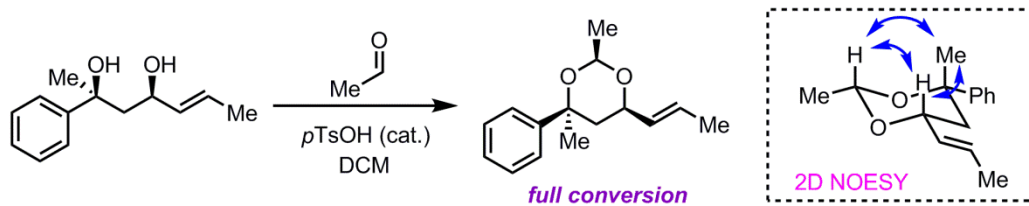
Figure 4.3 Rationale for the Observed Reactivity of the Diol



Thus, we employed another method to prepare a cyclic acetal from the coupling product (1,3-diol). When the 1,3-diol was reacted with acetaldehyde in the presence of a catalytic amount of tosic acid, an acetal was afforded in full conversion (Scheme 4.30). Then, we conducted 2D NOESY analysis of the prepared acetal to gather information on

stereochemical relationship of the coupling product, as shown in the box below. The through-space correlation data revealed that the two hydroxyl groups of the product have *syn* relationship.

Scheme 4.30 Acetal Analysis for Relative Configurations

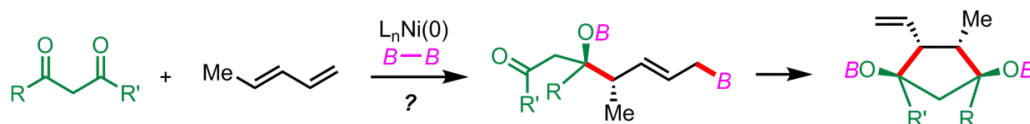


4.3.2. Ni-Catalyzed Borylative Coupling of Bisketones and Dienes⁵⁸

4.3.2.1. Project Goals

During the investigations on the borylative ketone–diene coupling reactions, we were inquisitive about whether these processes would also apply to bisketone electrophiles (*i.e.* a molecule containing two ketone moieties). As described in Scheme 4.31, the bis-electrophiles (e.g. bisketones) could not only participate in the multicomponent coupling process, but also engage in the subsequent allylation reaction with the intermediate allylic boronate.

Scheme 4.31 Borylative Coupling Reactions with Bis-Electrophiles

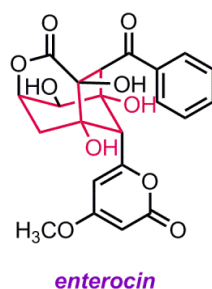


The expected product from this borylative bisketone–diene coupling reaction can be applied to the synthesis of natural products with challenging structural motifs. One such synthetic target would be enterocin,⁵⁹ which is illustrated in Figure 4.4.⁶⁰

⁵⁸ This project was originally initiated by Mr. Zhiyong Yu (a Ph.D. student in the Morken group).

⁵⁹ (a) Aymerich, T.; Holo, H.; Håvarstein, L. S.; Hugas, M.; Garriga, M.; Nes, I. F., "Biochemical and Genetic Characterization of Enterocin a from *Enterococcus Faecium*, a New Antilisterial Bacteriocin in the Pediocin Family of Bacteriocins," *Applied and Environmental Microbiology* **1996**, *62*, 1676-1682. (b) Casaus, P.; Nilsen, T.; Cintas, L. M.; Nes, I. F.; Hernández, P. E.; Holo, H., "Enterocin B, a New Bacteriocin from *Enterococcus Faecium* T136 Which Can Act Synergistically with Enterocin A," *Microbiology* **1997**, *143*, 2287-2294.

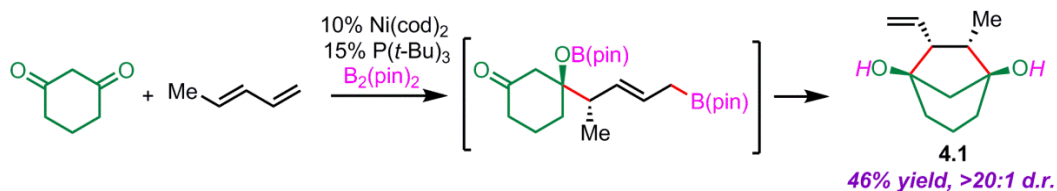
Figure 4.4 Potential Synthetic Target for Borylative Bisketone–Diene Coupling



4.3.2.2. Project Descriptions

To initiate studies in borylative bisketone–diene coupling reactions, 1,3-cyclohexanedione was treated with *trans*-piperylene and $B_2(\text{pin})_2$ in the presence of $Ni(\text{cod})_2$ and $P(t\text{-Bu})_3$ (Scheme 4.32). To our great pleasure, the reaction with the bisketone proceeded well to furnish a bicyclic diol product (**4.1**) with good efficiency and excellent selectivity (46% yield, >20:1 dr). The reaction product (**4.1**) features four contiguous stereogenic centers, [3.2.1] bicyclic system, 1,3-*syn*-diol, and a terminal alkene. This cascade reaction sequence provides a product that is particularly well suited for the polyketide natural products.

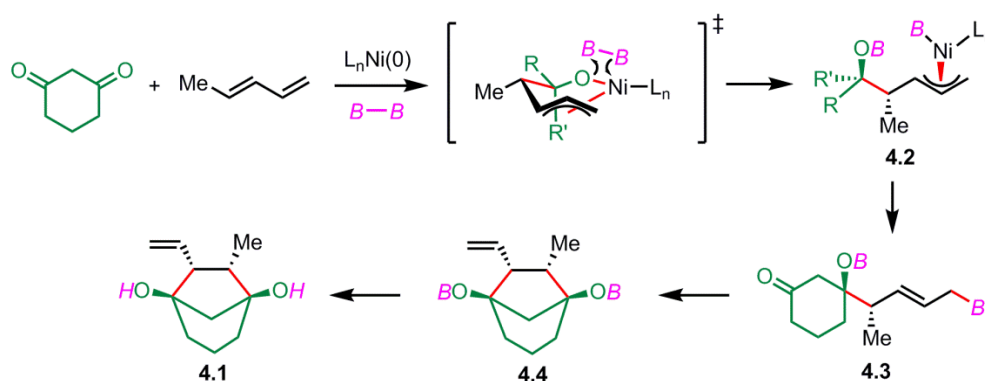
Scheme 4.32 Intramolecular Allylation with Bisketone–Diene Coupling



⁶⁰ For enzymatic total synthesis of enterocin, see: Cheng, Q.; Xiang, L.; Izumikawa, M.; Meluzzi, D.; Moore, B. S., "Enzymatic Total Synthesis of Enterocin Polyketides," *Nature Chemical Biology* **2007**, *3*, 557-558.

The proposed reaction pathway for this tandem process is described in Scheme 4.33. In the first step of this process, the dione would undergo the borylative ketone–diene coupling reaction with trans-piperylene and $B_2(\text{pin})_2$ to give complex **4.2** through a similar transition state that was described in the borylative aldehyde–diene coupling. Then, reductive elimination of the nickel– π -allyl complex (**4.2**) will afford compound **4.3**.

Scheme 4.33 Proposed Reaction Pathway for Borylative Bisketone–Diene Coupling



In the second step of this sequence, the intermediate allylboronate (**4.3**) would undergo an intramolecular allylation with the remaining ketone to afford compound **4.4**. Then, an acidic work-up will furnish the bicyclic diol as a product (**4.1**). This one-pot cascade reaction sequence directly provides a structurally, functionally, and stereochemically enriched product whose synthesis would otherwise require multiple steps.⁶¹

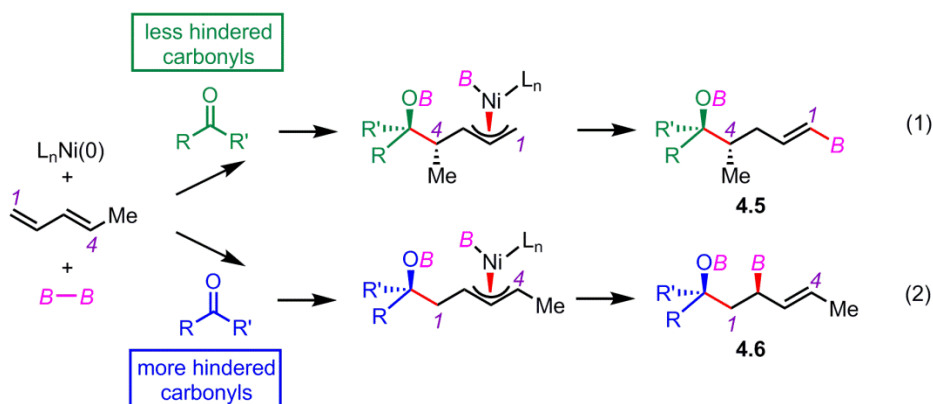
⁶¹ This concept of employing bis-electrophiles in a tandem reaction sequence has also been applied to other diboration projects in the Morken group. For an example, see: Ferris, G. E.; Hong, K.; Roundtree, I. A.; Morken, J. P., "A Catalytic Enantioselective Tandem Allylation Strategy for Rapid Terpene Construction: Application to the Synthesis of Pumilaside Aglycon," *Journal of the American Chemical Society* **2013**, *135*, 2501-2504.

4.4. Mechanistic Considerations

4.4.1. Observed Product Selectivity

As mentioned in the previous sections, the reaction of acetophenone followed a different regiochemical course compared to the analogous reaction with benzaldehyde in the borylative multicomponent reaction. As described in Scheme 4.34 (eq 1), when benzaldehyde is subjected to the multicomponent reaction conditions, 1,5-bisboronate **4.5** is produced. In contrast, when acetophenone is treated with diene and $B_2(\text{pin})_2$, the 1,3-diol (**4.6**) predominates (Scheme 4.34, eq 2).

Scheme 4.34 Observed Effects of Substrate Sterics on Product Selectivity



Not only is the hydroxyl-positioning different between the two products, but the diene is also incorporated into the product with opposite connectivity (*i.e.* C4 vs C1 in compounds **4.5** and **4.6**) in the case of the ketone relative to the aldehyde electrophile.

4.4.2. Proposed Reaction Pathways

Diene-carbonyl coupling reactions have been extensively studied by Tamaru and Mori, both of whom executed these transformations under reducing conditions with silane, organozinc reductants, and organoborane reductants.^{62, 63} These processes are thought to occur by conversion of the diene and aldehyde to metallacyclic intermediates. The identity of this intermediate was secured by Ogoshi and Kurosawa who isolated such structures from stoichiometric reactions between Ni(cod)₂, PCy₃, a 1,3-diene, and benzaldehyde.⁶⁴

Considering the similar reaction conditions, it is considered likely that such mechanisms also operate in the borylative carbonyl–diene coupling reactions and these can be used to understand the regiochemical course of the coupling processes with hindered and non-hindered carbonyl substrates. As described in Scheme 4.35, with less hindered

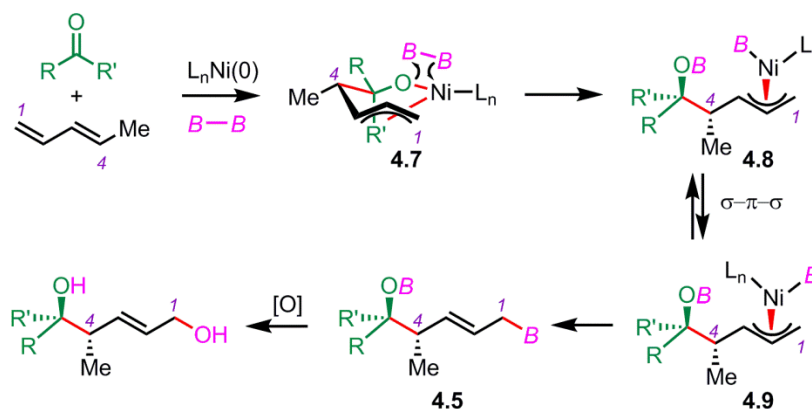
⁶² For selected examples, see: (a) Kimura, M.; Ezo, A.; Shibata, K.; Tamaru, Y., "Novel and Highly Regio- and Stereoselective Nickel-Catalyzed Homoallylation of Benzaldehyde with 1,3-Dienes," *Journal of the American Chemical Society* **1998**, *120*, 4033-4034. (b) Takimoto, M.; Hiraga, Y.; Sato, Y.; Mori, M., "Nickel-Catalyzed Regio- and Stereoselective Synthesis of Homoallylic Alcohol Derivatives from Dienes and Aldehydes," *Tetrahedron Letters* **1998**, *39*, 4543-4546. (c) Sato, Y.; Takanashi, T.; Hoshiba, M.; Mori, M., "Nickel(0)-Catalyzed Diene-Aldehyde Cyclization," *Tetrahedron Letters* **1998**, *39*, 5579-5582.

⁶³ For selected ketone–diene couplings, see: (a) Sato, Y.; Takimoto, M.; Hayashi, K.; Katsuhara, T.; Takagi, K.; Mori, M., "Novel Stereoselective Cyclization via π -Allylnickel Complex Generated from 1,3-Diene and Hydride Nickel Complex," *Journal of the American Chemical Society* **1994**, *116*, 9771-9772. (b) Sato, Y.; Takimoto, M.; Mori, M., "Remarkable Regio-Controlled Effect of 1,3-Diene as a Ligand on Nickel-Promoted Cyclization," *Tetrahedron Letters* **1996**, *37*, 887-890. (c) Kimura, M.; Fujimatsu, H.; Ezo, A.; Shibata, K.; Shimizu, M.; Matsumoto, S.; Tamaru, Y., "Nickel-Catalyzed Homoallylation of Aldehydes and Ketones with 1,3-Dienes and Complementary Promotion by Diethylzinc or Triethylborane," *Angewandte Chemie International Edition* **1999**, *38*, 397-400.

⁶⁴ Ogoshi, S.; Ikeda, H.; Kurosawa, H., "Formation of an Aza-Nickelacycle by Reaction of an Imine and an Alkyne with Nickel(0): Oxidative Cyclization, Insertion, and Reductive Elimination," *Angewandte Chemie* **2007**, *119*, 5018-5020.

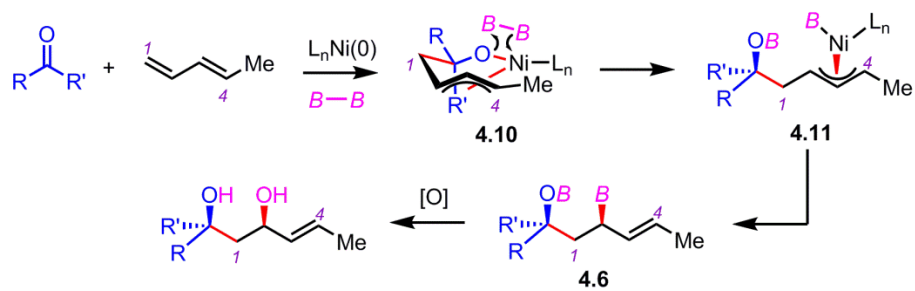
electrophiles, reaction with pentadiene may occur to give a nickellacycle (**4.7**). Subsequent σ -bond metathesis with $B_2(\text{pin})_2$ would then deliver π -allyl **4.8**. This nickel- π -allyl complex (**4.8**) may engage in π - σ - π isomerization to give Ni-complex **4.9**. Then, reductive elimination of π -allyl **4.9** would afford the 1,5-bisboronate (**4.5**).

Scheme 4.35 Proposed Reaction Mechanism for Less Hindered Carbonyls



With more hindered carbonyls, it is tenable that steric effects retard C–C bond formation with the substituted terminus of the diene (C4) and, instead, the less hindered end of the diene (C1) adds to the carbonyl (Scheme 4.36). This new C–C bond formation that is promoted by a nickel catalyst would lead to formation of a nickellacycle (**4.10**). Subsequent σ -bond metathesis delivers a π -allyl **4.11**, which undergoes reductive elimination to furnish the 1,3-bisboronic ester (**4.6**). It is conceivable that, with a substituted π -allyl, the π - σ - π isomerization is retarded relative to reductive elimination, and the geometry of the initial σ -bond metathesis product dictates the regiochemical outcome of the reaction.

Scheme 4.36 Proposed Reaction Mechanism for More Hindered Carbonyls



4.5. Conclusions and Outlook

Borylative ketone–diene coupling reactions can be accomplished in high yields and with excellent levels of diastereocontrol. Importantly, this reaction is compatible with both aryl–alkyl ketones as well as dialkyl ketones. Also of note, this reaction occurs in a predictable fashion, yet with regioselection that is distinct from related aldehyde–diene coupling reactions.

The reaction products from these coupling processes, which possess tertiary alcohol functionality and an allylic alcohol moiety, are particularly well suited for the preparation of polyketide natural products. Especially, bicyclic products that are constructed from the borylative diketone–diene coupling process feature two tertiary alcohol functionalities with four contiguous stereocenters. A facile tandem route to such structures provides an efficient synthetic method for structurally and stereochemically complex chiral molecules in natural products.

4.6. Experimental Section

4.6.1. General Information

All reactions were performed in oven- or flame-dried glassware fitted with rubber septa under a positive pressure of nitrogen, unless otherwise stated. Air- and moisture-sensitive liquids were transferred via syringe or stainless steel cannula. Organic solvents were concentrated by rotary evaporation at various temperatures, unless otherwise noted. All work-up and purification procedures were carried out with reagent grade solvents under typical bench-top conditions. Analytical thin-layer chromatography (TLC) was performed using glass plates, which are pre-coated with silica gel 60 F254 (0.25 mm thickness) impregnated with a fluorescent indicator (254 nm). TLC plates were visualized by exposure to UV (ultraviolet) light, and then were stained with phosphomolybdic acid (PMA) in ethanol, potassium permanganate (KMnO₄) in water, or cerium(IV) sulfate and ammonium molybdate in sulfuric acid (CAM). Liquid chromatography was performed using forced flow (flash chromatography)⁶⁵ on silica gel (porosity = 60 Å, particle size = 40-63 μm) purchased from Silicycle. Medium pressure gradient chromatography was performed on a Teledyne Isco CombiFlash automated flash chromatography system with a 200-780 nm UV-vis variable wavelength detector.

⁶⁵ Still, W. C.; Kahn, M.; Mitra, A., "Rapid Chromatographic Technique for Preparative Separations with Moderate Resolution," *The Journal of Organic Chemistry* **1978**, *43*, 2923-2925.

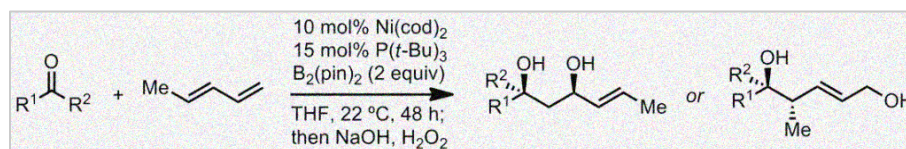
Tetrahydrofuran (THF), dichloromethane, and diethyl ether were purified using a Pure Solv MD-4 solvent purification system from Innovative Technology Inc. Bis(pinacolato)diboron [B₂(pin)₂] was obtained from AllyChem Co., Ltd. and recrystallized from pentane prior to use. Aldehydes were purchased from Aldrich and distilled or recrystallized prior to use. Bis(1,5-cyclooctadiene)nickel(0) [Ni(cod)₂] and tricyclohexylphosphine (PCy₃) were purchased from Strem Chemicals, Inc. Piperylene (1,3-pentadiene) and 3-methyl-1,3-pentadiene were purchased from ChemSampCo. All other reagents were purchased from Sigma Aldrich, Acros, Strem, Alfa Aesar, Fisher, or TCI America and used without further purification.

Proton nuclear magnetic resonance (¹H NMR) spectra were recorded on either a Varian Gemini-400 (400 MHz), or a Varian Inova-500 (500 MHz) spectrometer. Proton chemical shifts are reported in ppm (parts per million, δ scale) downfield from tetramethylsilane and are referenced to residual protium in the NMR solvent as the internal standard (CHCl₃: 7.26 ppm). Data are reported as follows: chemical shift, integration, multiplicity (s = singlet, d = doublet, t = triplet, q = quartet, br = broad, m = multiplet), coupling constants (Hz), and assignment. ¹³C NMR spectra were recorded on either a Varian Gemini-400 (100 MHz), or a Varian Inova-500 (125 MHz) spectrometer with complete proton decoupling. Carbon chemical shifts are reported in ppm (parts per million, δ scale) downfield from tetramethylsilane and are referenced to the NMR solvent resonance as the internal standard (CDCl₃: 77.16 ppm). Infrared (IR) spectra were recorded on a Bruker alpha spectrophotometer, ν_{\max} cm⁻¹. Bands are characterized as broad (br), strong (s), medium (m),

and weak (w). High resolution mass spectrometry (HRMS) was performed at the Mass Spectrometry Facility, Boston College. Melting points were determined with a Thomas-Hoover Unimelt capillary melting point apparatus and were uncorrected.

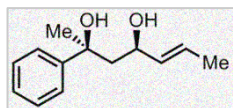
4.6.2. Experimental Procedures

4.6.2.1. General Procedure for Borylative Ketone–Diene Coupling



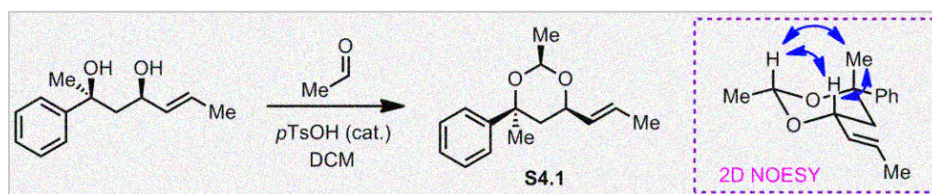
An oven-dried 20 mL scintillation vial, equipped with a magnetic stir-bar, was charged with Ni(cod)₂ (0.05 mmol, 0.10 equiv), P(*t*-Bu)₃ (0.075 mmol, 0.15 equiv), and THF (2.5 mL, 0.2 M) in a dry box under an argon atmosphere. After stirring for 5 min, the ketone (0.5 mmol, 1.0 equiv), *trans*-1,3-pentadiene (1.0 mmol, 2.0 equiv), and B₂(pin)₂ (1.0 mmol, 2.0 equiv) were added sequentially. The vial was sealed with a polypropylene cap and removed from the dry box. The reaction mixture was then allowed to stir at ambient temperature for 48 h. After this time, the mixture was cooled to 0 °C (ice-water bath), and 2 mL of 3 M NaOH and 1.5 mL of 30% H₂O₂ were added dropwise with caution. The mixture was then allowed to stir at ambient temperature for 10 h. The resulting solution was cooled to 0 °C and quenched by the addition of 2 mL of saturated aqueous Na₂S₂O₃. The two-phase mixture was extracted with ethyl acetate (3 × 20 mL), and the combined organic layers were dried over anhydrous Na₂SO₄. The drying agent was removed by filtration and the solvent was evaporated *in vacuo*. The crude material was purified by silica gel chromatography (hexanes/EtOAc) to afford the title compounds.

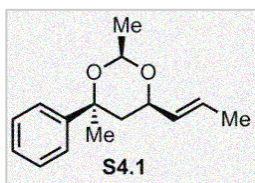
4.6.2.2. Characterization Data and Proof of Stereochemistry



(2*S,4*R**,*E*)-2-phenylhept-5-ene-2,4-diol.** The reaction was performed according to the general procedure with 13.8 mg (0.05 mmol) of Ni(cod)₂, 15.2 mg (0.075 mmol) of P(*t*-Bu)₃, 60.1 mg (0.5 mmol) of acetophenone, 68.1 mg (1.0 mmol) of *trans*-1,3-pentadiene, and 253.9 mg (1.0 mmol) of B₂(pin)₂ in THF (2.5 mL) for 48 h, followed by oxidation, to afford the title compound as a colorless oil (78.2 mg, 76% yield). R_f = 0.32 (1:1 hexanes:Et₂O); ¹H NMR (500 MHz, CDCl₃): δ 7.46 (2H, d, *J* = 7.5 Hz, aromatic), 7.34 (2H, t, *J* = 7.0 Hz, aromatic), 7.23 (1H, t, *J* = 7.0 Hz, aromatic), 5.68 (1H, dq, *J* = 15.5 Hz, 6.5 Hz, CH₃CHCH), 5.47 (1H, dd, *J* = 15.5 Hz, 7.0 Hz, CH₃CHCH), 4.52 (1H, br t, *J* = 7.5 Hz, CH₃CHCHCH), 3.66 (1H, br s, OH), 2.89 (1H, br s, OH), 1.97 (1H, dd, *J* = 15.0 Hz, 10.0 Hz, ArCCH_aH_b), 1.85 (1H, dd, *J* = 15.0 Hz, 3.0 Hz, ArCCH_aH_b), 1.67 (3H, s, ArCCH₃), 1.66 (3H, d, *J* = 6.0 Hz, CHCHCH₃); ¹³C NMR (125 MHz, CDCl₃): δ 149.2, 133.9, 128.4, 127.1, 126.8, 124.5, 74.8, 71.0, 49.5, 28.3, 17.7; IR (neat): 3328 (br), 2973 (w), 2915 (w), 1446 (m), 1375 (m), 1211 (m), 1099 (m), 1065 (s), 964 (s), 842 (m), 761 (s), 698 (s), 565 (m) cm⁻¹; HRMS (ESI+) calculated for C₁₃H₁₅ [M-2H₂O+H]⁺: 171.1174, found: 171.1182.

Proof of Stereochemistry. The relative configuration was assigned as *syn* (C₂-C₄) by analysis of the spectral data, after conversion of the title compound into **S4.1** as shown below.





(2S*,4S*,6R*)-2,4-dimethyl-4-phenyl-6-((E)-prop-1-en-1-yl)-1,3-dio-

xane (S4.1). A flame-dried 10 mL round-bottom flask, equipped with a magnetic stir-bar, was charged with the diol (59.8 mg, 0.29 mmol, 1 equiv), acetaldehyde (25.5 mg, 0.58 mmol, 2 equiv), *p*-

toluenesulfonic acid (2.9 mg, 0.015 mmol, 0.05 equiv), and dichloromethane (1.5 mL, 0.2 M).

After stirring at ambient temperature for 6 h, a saturated aqueous NaHCO₃ solution was

added. The reaction mixture was extracted with diethyl ether (3 × 10 mL) and the organic

layer was washed with brine. The combined organic layers were dried over anhydrous

Na₂SO₄. The drying agent was removed by filtration and the solvent was evaporated *in vacuo*.

The crude product was purified by silica gel chromatography to afford **S4.1** as a colorless oil.

R_f = 0.23 (9:1 hexanes:Et₂O); ¹H NMR (500 MHz, CDCl₃): δ 7.46 (2H, d, *J* = 8.5 Hz, aromatic),

7.34 (2H, t, *J* = 8.5 Hz, aromatic), 7.24 (1H, t, *J* = 8.5 Hz, aromatic), 5.79 (1H, dq, *J* = 15.5 Hz, 6.5

Hz, CH₃CHCH), 5.49 (1H, dd, *J* = 15.5 Hz, 7.0 Hz, CH₃CHCH), 5.25 (1H, q, *J* = 5.0 Hz,

CH₃CHO), 4.37-4.33 (1H, m, CH₃CHCHCHO), 1.83 (1H, dd, *J* = 13.5 Hz, 3.0 Hz, ArCCH_aH_b),

1.77 (1H, dd, *J* = 14.0 Hz, *J* = 11.5 Hz, ArCCH_aH_b), 1.71 (3H, d, *J* = 6.0 Hz, CHCHCH₃), 1.63

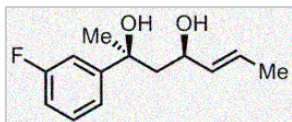
(3H, s, ArCCH₃), 1.44 (3H, d, *J* = 5.0 Hz, OCHCH₃); ¹³C NMR (125 MHz, CDCl₃): δ 148.9, 131.2,

128.5, 128.3, 126.8, 124.1, 92.3, 74.6, 73.6, 42.0, 23.2, 21.8, 17.9; IR (neat): 2980 (w), 2934 (w),

2852 (w), 1495 (w), 1447 (m), 1405 (w), 1378 (w), 1173 (m), 1121 (s), 1042 (w), 969 (s), 937 (w),

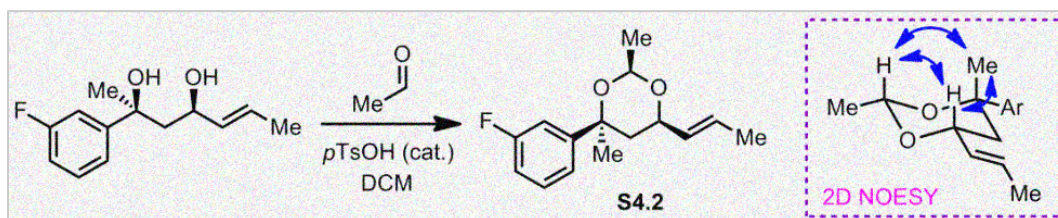
763 (m), 676 (s), 544 (w) cm⁻¹; HRMS (ESI+) calculated for C₁₅H₂₄NO₂ [M+NH₄]⁺: 250.1807,

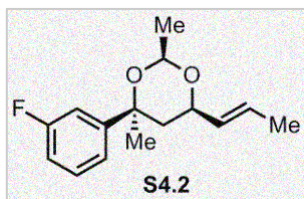
found: 250.1806.



(2S*,4R*,E)-2-(3-fluorophenyl)hept-5-ene-2,4-diol. The reaction was performed according to the general procedure with 13.8 mg (0.05 mmol) of Ni(cod)₂, 15.2 mg (0.075 mmol) of P(*t*-Bu)₃, 69.1 mg (0.5 mmol) of 3'-fluoroacetophenone, 68.1 mg (1.0 mmol) of *trans*-1,3-pentadiene, and 253.9 mg (1.0 mmol) of B₂(pin)₂ in THF (2.5 mL) for 48 h, followed by oxidation, to afford the title compound as a colorless oil (81.8 mg, 73% yield). *R*_f = 0.27 (1:1 hexanes:Et₂O); ¹H NMR (500 MHz, CDCl₃): δ 7.31-7.26 (1H, m, aromatic), 7.22-7.19 (2H, m, aromatic), 6.94-6.89 (1H, m, aromatic), 5.69 (1H, dq, *J* = 15.5 Hz, 6.5 Hz, CH₃CHCH), 5.46 (1H, dd, *J* = 15.0 Hz, 7.0 Hz, CH₃CHCH), 4.53 (1H, br t, *J* = 8.0 Hz, CH₃CHCHCH), 3.93 (1H, br s, OH), 2.58 (1H, br s, OH), 1.93 (1H, dd, *J* = 14.0 Hz, 9.5 Hz, ArCCH_aH_b), 1.83 (1H, dd, *J* = 14.5 Hz, 3.0 Hz, ArCCH_aH_b), 1.67 (3H, d, *J* = 6.5 Hz, CHCHCH₃), 1.65 (3H, s, ArCCH₃); ¹³C NMR (125 MHz, CDCl₃): δ 163.0 (d, ¹*J*_{CF} = 244.4 Hz), 152.1, 133.7, 129.7, 127.4, 120.2, 113.5 (d, ²*J*_{CF} = 20.7 Hz), 111.9 (d, ²*J*_{CF} = 22.5 Hz), 74.4, 71.2, 49.2, 28.3, 17.7; IR (neat): 3239 (br), 2940 (m), 2879 (m), 1614 (m), 1589 (s), 1485 (m), 1439 (s), 1377 (m), 1272 (m), 1252 (m), 1178 (m), 966 (s), 786 (m), 699 (s) cm⁻¹; HRMS (ESI⁺) calculated for C₁₃H₂₁FNO₂ [M+NH₄]⁺: 242.1556, found: 242.1565.

Proof of Stereochemistry. The relative configuration was assigned as *syn* (C₂-C₄) by analysis of the spectral data, after conversion of the title compound into **S4.2** as shown below.





(2S*,4S*,6R*)-4-(3-fluorophenyl)-2,4-dimethyl-6-((E)-prop-1-en-1-yl)-1,3-dioxane (S4.2). The acetonide (S4.2) was prepared in the same method as described for acetonide S4.1. $R_f = 0.23$ (9:1

hexanes:Et₂O); ¹H NMR (500 MHz, CDCl₃): δ 7.31-7.27 (1H, m,

aromatic), 7.22-7.17 (2H, m, aromatic), 6.94-6.90 (1H, m, aromatic), 5.79 (1H, dq, $J = 15.5$ Hz,

6.0 Hz, CH₃CHCH), 5.36 (1H, dd, $J = 15.5$ Hz, 8.5 Hz, CH₃CHCH), 5.33 (1H, q, $J = 5.0$ Hz,

CH₃CHO), 4.36-4.32 (1H, m, CH₃CHCHCHO), 1.81 (1H, dd, $J = 13.0$ Hz, 2.5 Hz, ArCCH_aH_b),

1.74 (1H, dd, overlapped ArCCH_aH_b), 1.71 (3H, d, $J = 6.5$ Hz, CHCHCH₃), 1.61 (3H, s,

ArCCH₃), 1.44 (3H, d, $J = 5.0$ Hz, OCHCH₃); ¹³C NMR (125 MHz, CDCl₃): δ 163.0 (d, ¹J_{CF} =

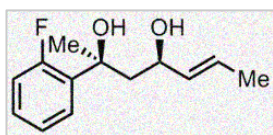
244.4 Hz), 151.7, 131.0, 129.7, 128.7, 119.6, 113.6 (d, ²J_{CF} = 21.1 Hz), 111.5 (d, ²J_{CF} = 23.1 Hz),

92.4, 74.4, 73.5, 41.9, 23.2, 21.7, 17.9; IR (neat): 2989 (w), 2939 (w), 2873 (w), 1618 (w), 1589 (m),

1484 (w), 1437 (w), 1271 (m), 1156 (s), 1109 (s), 1040 (w), 968 (s), 899 (m), 864 (m), 784 (s), 744

(s), 482 (w) cm⁻¹; HRMS (ESI+) calculated for C₁₅H₂₃FNO₂ [M+NH₄]⁺: 268.1713, found:

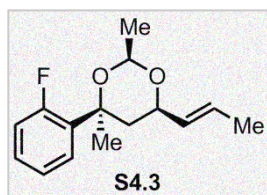
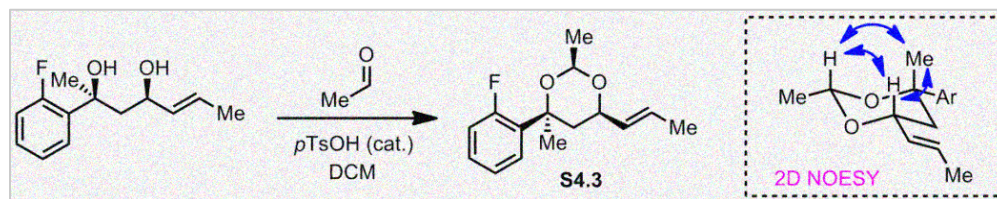
268.1708.



(**2S*,4R*,E**)-2-(2-fluorophenyl)hept-5-ene-2,4-diol. The reaction was performed according to the general procedure with 13.8 mg (0.05 mmol) of Ni(cod)₂, 15.2 mg (0.075 mmol) of P(*t*-Bu)₃, 69.1 mg

(0.5 mmol) of 2'-fluoroacetophenone, 68.1 mg (1.0 mmol) of *trans*-1,3-pentadiene, and 253.9 mg (1.0 mmol) of B₂(pin)₂ in THF (2.5 mL) for 48 h, followed by oxidation, to afford the title compound as a colorless oil (70.9 mg, 63% yield). R_f = 0.31 (1:1 hexanes:Et₂O); ¹H NMR (500 MHz, CDCl₃): δ 7.67 (1H, t, *J* = 8.0 Hz, aromatic), 7.24-7.20 (1H, m, aromatic), 7.14 (1H, t, *J* = 8.0 Hz, aromatic), 7.00 (1H, dd, *J* = 12.0 Hz, 8.0 Hz, aromatic), 5.68 (1H, dq, *J* = 15.5 Hz, 7.0 Hz, CH₃CHCH), 5.45 (1H, dd, *J* = 15.0 Hz, 7.0 Hz, CH₃CHCH), 4.55 (1H, br t, *J* = 7.5 Hz, CH₃CHCHCH), 3.99 (1H, br s, OH), 2.47 (1H, br s, OH), 2.17 (1H, dd, *J* = 14.5 Hz, 3.0 Hz, ArCCH_aH_b), 1.99 (1H, dd, *J* = 15.0 Hz, 10.0 Hz, ArCCH_aH_b), 1.70 (3H, s, ArCCH₃), 1.65 (3H, d, *J* = 6.5 Hz, CHCHCH₃); ¹³C NMR (125 MHz, CDCl₃): δ 159.5 (d, ¹J_{CF} = 243.7 Hz), 135.6, 135.5, 133.7, 128.6, 127.1 (d, ²J_{CF} = 21.6 Hz), 124.2, 116.0 (d, ²J_{CF} = 24.0 Hz), 73.6, 71.1, 46.5, 27.5, 17.7; IR (neat): 3340 (br), 2972 (w), 2917 (w), 1614 (w), 1485 (m), 1448 (s), 1376 (w), 1214 (s), 1066 (m), 1037 (w), 965 (m), 818 (m), 757 (s), 447 (w) cm⁻¹; HRMS (ESI+) calculated for C₁₃H₁₄F [M-2H₂O+H]⁺: 189.1079, found: 189.1074.

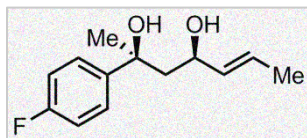
Proof of Stereochemistry. The relative configuration was assigned as *syn* (C₂-C₄) by analysis of the spectral data, after conversion of the title compound into **S4.3** as shown below.



(2*S**,4*S**,6*R**)-4-(2-fluorophenyl)-2,4-dimethyl-6-((*E*)-prop-1-en-1-yl)-1,3-dioxane (**S4.3**). The acetonide (**S4.3**) was prepared in the

same method as described for acetonide **S4.1**. $R_f = 0.33$ (9:1 hexanes:Et₂O); ¹H NMR (500 MHz, CDCl₃): δ 7.69 (1H, t, $J = 8.0$ Hz,

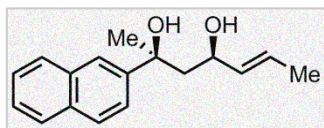
aromatic), 7.23-7.19 (1H, m, aromatic), 7.13 (1H, t, $J = 7.5$ Hz, aromatic), 6.98 (1H, dd, $J = 12.0$ Hz, 8.0 Hz, aromatic), 5.78 (1H, dq, $J = 15.0$ Hz, 6.5 Hz, CH₃CHCH), 5.46 (1H, dd, $J = 15.5$ Hz, 7.0 Hz, CH₃CHCH), 5.26 (1H, q, $J = 5.0$ Hz, CH₃CHO), 4.37-4.33 (1H, m, CH₃CHCHCHO), 2.21 (1H, dd, $J = 13.5$ Hz, 2.5 Hz, ArCCH_aH_b), 1.71 (1H, dd, overlapped, ArCCH_aH_b), 1.69 (3H, d, $J = 6.5$ Hz, CHCHCH₃), 1.69 (3H, s, ArCCH₃), 1.45 (3H, d, $J = 5.0$ Hz, OCHCH₃); ¹³C NMR (125 MHz, CDCl₃): δ 159.4 (d, $^1J_{CF} = 245.5$ Hz), 135.5, 135.4, 131.1, 128.4 (d, $^2J_{CF} = 22.2$ Hz), 126.4, 124.1, 115.9 (d, $^2J_{CF} = 23.2$ Hz), 91.9, 73.5, 73.2, 40.0, 21.8, 21.7, 17.9; IR (neat): 3089 (w), 2991 (w), 2876 (w), 1678 (w), 1616 (w), 1581 (m), 1488 (s), 1449 (w), 1125 (s), 1110 (s), 1069 (w), 1037 (m), 971 (s), 879 (w), 804 (m), 758 (s), 498 (w) cm⁻¹; HRMS (ESI+) calculated for C₁₅H₂₃FNO₂ [M+NH₄]⁺: 268.1713, found: 268.1722.

**(2S*,4R*,E)-2-(4-fluorophenyl)hept-5-ene-2,4-diol.**

The

reaction was performed according to the general procedure with 13.8 mg (0.05 mmol) of Ni(cod)₂, 15.2 mg (0.075 mmol) of P(*t*-Bu)₃, 69.1 mg (0.5 mmol) of 4'-fluoroacetophenone, 68.1 mg (1.0 mmol) of *trans*-1,3-pentadiene, and 253.9 mg (1.0 mmol) of B₂(pin)₂ in THF (2.5 mL) for 48 h, followed by oxidation, to afford the title compound as a colorless oil (79.3 mg, 71% yield). R_f = 0.23 (1:1 hexanes:Et₂O); ¹H NMR (500 MHz, CDCl₃): δ 7.43-7.41 (2H, m, aromatic), 7.02-6.98 (2H, m, aromatic), 5.68 (1H, dq, *J* = 15.0 Hz, 6.5 Hz, CH₃CHCH), 5.46 (1H, dd, *J* = 15.5 Hz, 7.0 Hz, CH₃CHCH), 4.52 (1H, br t, *J* = 7.5 Hz, CH₃CHCHCH), 3.88 (1H, br s, OH), 2.71 (1H, br s, OH), 1.92 (1H, dd, *J* = 15.0 Hz, 10.5 Hz, ArCCH_aH_b), 1.81 (1H, dd, *J* = 14.5 Hz, 2.5 Hz, ArCCH_aH_b), 1.66 (3H, d, *J* = 6.0 Hz, CHCHCH₃), 1.65 (3H, s, ArCCH₃); ¹³C NMR (125 MHz, CDCl₃): δ 161.7 (d, ¹J_{CF} = 244.4 Hz), 145.0, 133.8, 127.3, 126.3, 114.9 (d, ²J_{CF} = 21.2 Hz), 74.4, 71.2, 49.5, 28.3, 17.7; IR (neat): 3324 (br), 2941 (m), 2876 (m), 1602 (w), 1510 (s), 1420 (w), 1375 (w), 1223 (s), 1160 (m), 1090 (m), 1074 (w), 967 (m), 849 (m), 836 (s), 814 (w), 563 (w) cm⁻¹; HRMS (ESI+) calculated for C₁₃H₁₄F [M-2H₂O+H]⁺: 189.1080, found: 180.1083.

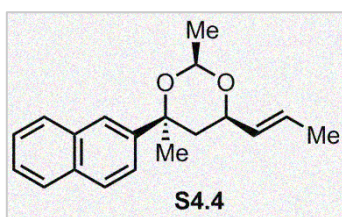
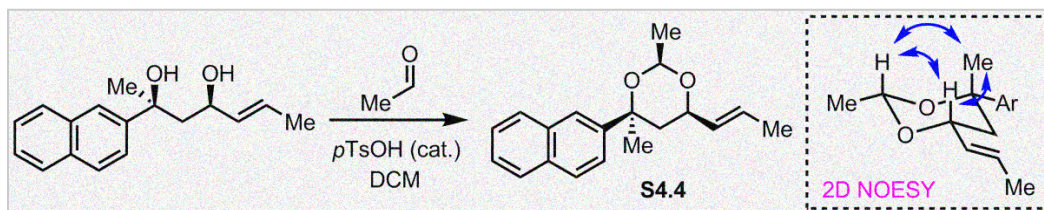
Stereochemistry. The relative configuration was assigned as *syn* (C₂-C₄) by analogy.



(2S*,4R*,E)-2-(naphthalen-2-yl)hept-5-ene-2,4-diol. The

reaction was performed according to the general procedure with 13.8 mg (0.05 mmol) of Ni(cod)₂, 15.2 mg (0.075 mmol) of P(*t*-Bu)₃, 85.1 mg (0.5 mmol) of 2'-acetonaphthone, 68.1 mg (1.0 mmol) of *trans*-1,3-pentadiene, and 253.9 mg (1.0 mmol) of B₂(pin)₂ in THF (2.5 mL) for 48 h, followed by oxidation, to afford the title compound (92.4 mg, 72% yield). R_f = 0.24 (1:1 hexanes:Et₂O); ¹H NMR (500 MHz, CDCl₃): δ 7.95 (1H, s, aromatic), 7.85-7.81 (3H, m, aromatic), 7.56 (1H, dd, *J* = 8.5 Hz, 2.0 Hz, aromatic), 7.49-7.44 (2H, m, aromatic), 5.70 (1H, dq, *J* = 15.5 Hz, 6.5 Hz, CH₃CHCH), 5.50 (1H, dd, *J* = 15.5 Hz, 7.0 Hz, CH₃CHCH), 4.58 (1H, br t, *J* = 9.0 Hz, CH₃CHCHCH), 3.71 (1H, br s, OH), 2.64 (1H, br s, OH), 2.06 (1H, dd, *J* = 14.5 Hz, 10.0 Hz, ArCCH_aH_b), 1.97 (1H, dd, *J* = 15.0 Hz, 3.5 Hz, ArCCH_aH_b), 1.76 (3H, s, ArCCH₃), 1.67 (3H, d, *J* = 6.5 Hz, CHCHCH₃); ¹³C NMR (125 MHz, CDCl₃): δ 146.5, 133.9, 133.4, 132.4, 128.4, 128.1, 127.6, 127.3, 126.2, 125.8, 123.5, 122.8, 74.9, 71.2, 49.3, 28.5, 17.7; IR (neat): 3325 (br), 3022 (w), 2938 (w), 2853 (w), 1600 (w), 1506 (w), 1450 (m), 1435 (m), 1420 (m), 1376 (m), 1186 (m), 1128 (s), 965 (m), 922 (w), 902 (w), 860 (s), 820 (s), 747 (s), 479 (m) cm⁻¹; HRMS (ESI+) calculated for C₁₇H₁₇O [M-2H₂O+H]⁺: 237.1279, found: 237.1283.

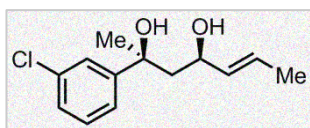
Proof of Stereochemistry. The relative configuration was assigned as *syn* (C₂-C₄) by analysis of the spectral data, after conversion of the title compound into **S4.4** as shown below.



(2*S*^{*},4*S*^{*},6*R*^{*})-2,4-dimethyl-4-(naphthalen-2-yl)-6-((*E*)-prop-1-en-1-yl)-1,3-dioxane (**S4.4**). The acetonide (**S4.4**) was prepared in the same method as described for acetonide **S4.1**.

$R_f = 0.22$ (9:1 hexanes:Et₂O); ¹H NMR (500 MHz, CDCl₃):

δ 7.93 (1H, s, aromatic), 7.86-7.82 (3H, m, aromatic), 7.59 (1H, dd, $J = 8.5$ Hz, 2.0 Hz, aromatic), 7.49-7.44 (2H, m, aromatic), 5.83 (1H, dq, $J = 15.0$ Hz, 6.5 Hz, CH₃CHCH), 5.52 (1H, dd, $J = 15.5$ Hz, 7.0 Hz, CH₃CHCH), 5.32 (1H, q, $J = 5.0$ Hz, CH₃CHO), 4.44-4.40 (1H, m, CH₃CHCHCHO), 1.94 (1H, dd, $J = 13.5$ Hz, 2.5 Hz, ArCCH_aH_b), 1.86 (1H, dd, $J = 13.0$ Hz, $J = 11.5$ Hz, ArCCH_aH_b), 1.73 (3H, d, overlapped, CHCHCH₃), 1.72 (3H, s, ArCCH₃), 1.51 (3H, d, $J = 5.0$ Hz, OCHCH₃); ¹³C NMR (125 MHz, CDCl₃): δ 146.2, 133.3, 132.5, 131.2, 128.6, 128.4, 128.0, 127.6, 126.0, 125.8, 123.0, 122.4, 92.4, 74.8, 73.6, 42.0, 23.2, 21.8, 18.0; IR (neat): 2987 (w), 2936 (w), 2917 (w), 2869 (w), 1405 (m), 1378 (m), 1163 (m), 1128 (s), 1108 (s), 1040 (w), 966 (s), 935 (m), 856 (m), 817 (m), 746 (s), 663 (w), 652 (w), 478 (s) cm⁻¹; HRMS (ESI⁺) calculated for C₁₉H₂₆NO₂ [M+NH₄]⁺: 300.1963, found: 300.1953.

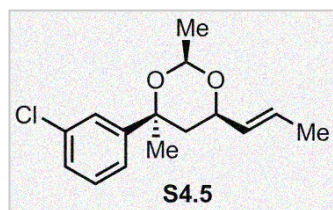
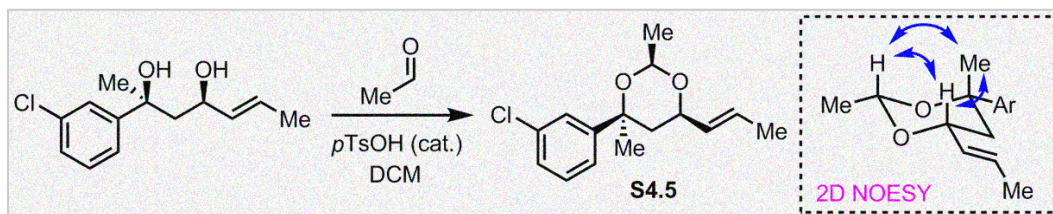
**(2S*,4R*,E)-2-(3-chlorophenyl)hept-5-ene-2,4-diol.**

The

reaction was performed according to the general procedure with 13.8 mg (0.05 mmol) of Ni(cod)₂, 15.2 mg (0.075 mmol) of

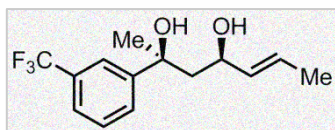
P(*t*-Bu)₃, 77.3 mg (0.5 mmol) of 3'-chloroacetophenone, 68.1 mg (1.0 mmol) of *trans*-1,3-pentadiene, and 253.9 mg (1.0 mmol) of B₂(pin)₂ in THF (2.5 mL) for 48 h, followed by oxidation, to afford the title compound as a colorless oil (75.5 mg, 63% yield). R_f = 0.33 (1:1 hexanes:Et₂O); ¹H NMR (500 MHz, CDCl₃): δ 7.47 (1H, t, *J* = 2.0 Hz, aromatic), 7.33 (1H, dt, *J* = 8.0 Hz, 2.0 Hz, aromatic), 7.26 (1H, t, *J* = 8.0 Hz, aromatic), 7.20 (1H, d, *J* = 8.0 Hz, aromatic), 5.69 (1H, dq, *J* = 15.5 Hz, 6.5 Hz, CH₃CHCH), 5.46 (1H, dd, *J* = 15.5 Hz, 7.0 Hz, CH₃CHCH), 4.53 (1H, br t, *J* = 8.5 Hz, CH₃CHCHCH), 3.94 (1H, br s, OH), 2.50 (1H, br s, OH), 1.93 (1H, dd, *J* = 15.0 Hz, 10.0 Hz, ArCCH_aH_b), 1.83 (1H, dd, *J* = 15.0 Hz, 3.0 Hz, ArCCH_aH_b), 1.67 (3H, d, *J* = 6.5 Hz, CHCHCH₃), 1.64 (3H, s, ArCCH₃); ¹³C NMR (125 MHz, CDCl₃): δ 151.4, 134.3, 133.7, 129.6, 127.4, 126.8, 125.1, 122.8, 74.4, 71.1, 49.1, 28.2, 17.7; IR (neat): 3320 (br), 2977 (m), 2897 (m), 1596 (w), 1571 (w), 1421 (s), 1376 (w), 1212 (m), 1142 (w), 1112 (w), 1080 (m), 965 (s), 894 (w), 850 (w), 785 (s), 699 (s), 495 (w), 406 (w) cm⁻¹; HRMS (ESI+) calculated for C₁₃H₁₄Cl [M-2H₂O+H]⁺: 205.0784, found: 205.0784.

Proof of Stereochemistry. The relative configuration was assigned as *syn* (C₂-C₄) by analysis of the spectral data, after conversion of the title compound into **S4.5** as shown below.



(2S*,4S*,6R*)-4-(3-chlorophenyl)-2,4-dimethyl-6-((E)-prop-1-en-1-yl)-1,3-dioxane (S4.5). The acetonide (S4.5) was prepared in the same method as described for acetonide S4.1. $R_f = 0.28$ (9:1 hexanes:Et₂O); ¹H NMR (500 MHz, CDCl₃): δ 7.46 (1H, t, $J =$

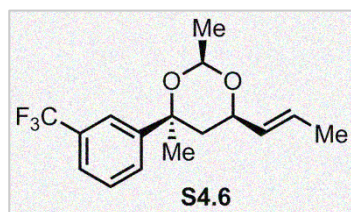
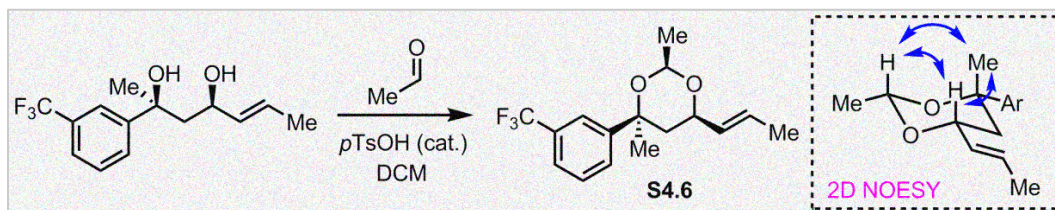
1.5 Hz, aromatic), 7.31 (1H, d, $J = 7.5$ Hz, aromatic), 7.26 (1H, t, $J = 8.0$ Hz, aromatic), 7.21 (1H, d, $J = 7.5$ Hz, aromatic), 5.79 (1H, dq, $J = 15.5$ Hz, 7.0 Hz, CH₃CHCH), 5.48 (1H, dd, $J = 15.5$ Hz, 7.0 Hz, CH₃CHCH), 5.22 (1H, q, $J = 5.0$ Hz, CH₃CHO), 4.35-4.31 (1H, m, CH₃CHCHCHO), 1.80 (1H, dd, $J = 13.5$ Hz, 2.5 Hz, ArCCH_aH_b), 1.71 (1H, dd, overlapped, ArCCH_aH_b), 1.70 (3H, d, $J = 6.5$ Hz, CHCHCH₃), 1.61 (3H, s, ArCCH₃), 1.44 (3H, d, $J = 5.0$ Hz, OCHCH₃); ¹³C NMR (125 MHz, CDCl₃): δ 151.0, 134.3, 131.0, 129.6, 128.7, 127.0, 124.6, 122.3, 92.4, 74.4, 73.5, 41.9, 23.3, 21.7, 17.9; IR (neat): 2990 (w), 2938 (w), 2918 (w), 2876 (w), 1597 (w), 1572 (w), 1474 (w), 1419 (m), 1407 (m), 1223 (w), 1173 (s), 1124 (s), 1081 (w), 971 (s), 879 (w), 847 (w), 785 (m), 697 (s), 610 (w) cm⁻¹; HRMS (ESI⁺) calculated for C₁₅H₂₃ClNO₂ [M+NH₄]⁺: 284.1417, found: 284.1410.



(2S*,4R*,E)-2-(3-(trifluoromethyl)phenyl)hept-5-ene-2,4-diol.

The reaction was performed according to the general procedure with 13.8 mg (0.05 mmol) of Ni(cod)₂, 15.2 mg (0.075 mmol) of P(*t*-Bu)₃, 94.1 mg (0.5 mmol) of 3'-(trifluoromethyl)-acetophenone, 68.1 mg (1.0 mmol) of *trans*-1,3-pentadiene, and 253.9 mg (1.0 mmol) of B₂(pin)₂ in THF (2.5 mL) for 48 h, followed by oxidation, to afford the title compound as a colorless oil (96.3 mg, 70% yield). R_f = 0.27 (1:1 hexanes:Et₂O); ¹H NMR (500 MHz, CDCl₃): δ 7.75 (1H, s, aromatic), 7.64 (1H, d, *J* = 8.0 Hz, aromatic), 7.49 (1H, d, *J* = 7.5 Hz, aromatic), 7.44 (1H, t, *J* = 7.5 Hz, aromatic), 5.69 (1H, dq, *J* = 15.5 Hz, 6.5 Hz, CH₃CHCH), 5.46 (1H, dd, *J* = 15.5 Hz, 7.0 Hz, CH₃CHCH), 4.56 (1H, br t, *J* = 8.0 Hz, CH₃CHCHCH), 4.19 (1H, br s, OH), 2.50 (1H, br s, OH), 1.94 (1H, dd, *J* = 14.5 Hz, 10.0 Hz, ArCCH_aH_b), 1.85 (1H, dd, *J* = 15.0 Hz, 3.0 Hz, ArCCH_aH_b), 1.68 (3H, s, ArCCH₃), 1.66 (3H, d, *J* = 6.5 Hz, CHCHCH₃); ¹³C NMR (125 MHz, CDCl₃): δ 150.3, 133.6, 130.6 (q, ²J_{CF} = 31.8 Hz), 128.7, 128.1, 127.7, 124.0 (q, ¹J_{CF} = 272.1 Hz), 123.6 (q, ³J_{CF} = 3.6 Hz), 121.6 (q, ³J_{CF} = 3.6 Hz), 74.4, 71.3, 49.2, 28.2, 17.7; IR (neat): 3333 (br), 2976 (m), 2919 (m), 1438 (w), 1377 (w), 1328 (s), 1207 (w), 1164 (s), 1122 (s), 1072 (m), 966 (w), 899 (w), 852 (w), 804 (w), 730 (w), 704 (m), 657 (w) cm⁻¹; HRMS (ESI⁺) calculated for C₁₃H₂₁FNO₂ [M+NH₄]⁺: 292.1524, found: 292.1525.

Proof of Stereochemistry. The relative configuration was assigned as *syn* (C₂-C₄) by analysis of the spectral data, after conversion of the title compound into **S4.6** as shown below.

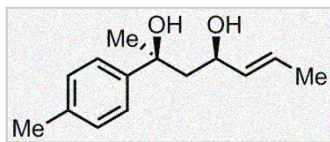


(2S*,4S*,6R*)-2,4-dimethyl-6-((E)-prop-1-en-1-yl)-4-(3-(trifluoromethyl)phenyl)-1,3-dioxane (S4.6). The acetonide (S4.6)

was prepared in the same method as described for acetonide

S4.1. $R_f = 0.23$ (9:1 hexanes:Et₂O); ¹H NMR (500 MHz, CDCl₃):

δ 7.72 (1H, s, aromatic), 7.64 (1H, d, $J = 7.5$ Hz, aromatic), 7.50 (1H, d, $J = 7.5$ Hz, aromatic), 7.45 (1H, t, $J = 7.5$ Hz, aromatic), 5.80 (1H, dq, $J = 15.0$ Hz, 6.5 Hz, CH₃CHCH), 5.48 (1H, dd, $J = 15.5$ Hz, 7.0 Hz, CH₃CHCH), 5.25 (1H, q, $J = 5.0$ Hz, CH₃CHO), 4.38-4.35 (1H, m, CH₃CHCHCHO), 1.85 (1H, dd, $J = 13.5$ Hz, 2.5 Hz, ArCCH_aH_b), 1.72 (1H, dd, overlapped, ArCCH_aH_b), 1.71 (3H, d, $J = 6.5$ Hz, CHCHCH₃), 1.64 (3H, s, ArCCH₃), 1.45 (3H, d, $J = 5.0$ Hz, OCHCH₃); ¹³C NMR (125 MHz, CDCl₃): δ 149.9, 130.9, 130.6 (q, ² $J_{CF} = 31.8$ Hz), 128.8 (2 C's), 127.6, 124.4 (q, ¹ $J_{CF} = 272.5$ Hz), 123.7 (q, ³ $J_{CF} = 3.6$ Hz), 121.1 (q, ³ $J_{CF} = 3.6$ Hz), 92.4, 74.4, 73.4, 41.8, 23.3, 21.7, 18.0; IR (neat): 2990 (w), 2940 (w), 2921 (w), 2878 (w), 1440 (w), 1333 (s), 1287 (w), 1220 (w), 1165 (s), 1125 (s), 1072 (m), 971 (m), 804 (w), 703 (m), 656 (w), 611 (w), 546 (w) cm⁻¹; HRMS (ESI⁺) calculated for C₁₆H₂₃F₃NO₂ [M+NH₄]⁺: 318.1681, found: 318.1694.



(2S*,4R*,E)-2-(p-tolyl)hept-5-ene-2,4-diol. The reaction was

performed according to the general procedure with 13.8 mg

(0.05 mmol) of Ni(cod)₂, 15.2 mg (0.075 mmol) of P(*t*-Bu)₃, 67.1

mg (0.5 mmol) of 4'-methylacetophenone, 68.1 mg (1.0 mmol) of *trans*-1,3-pentadiene, and

253.9 mg (1.0 mmol) of B₂(pin)₂ in THF (2.5 mL) for 48 h, followed by oxidation, to afford the

title compound as a colorless oil (86.9 mg, 79% yield). R_f = 0.26 (1:1 hexanes:Et₂O); ¹H NMR

(500 MHz, CDCl₃): δ 7.35 (2H, d, *J* = 8.5 Hz, aromatic), 7.15 (2H, d, *J* = 8.5 Hz, aromatic), 5.69

(1H, dq, *J* = 15.5 Hz, 6.5 Hz, CH₃CHCH), 5.48 (1H, dd, *J* = 15.0 Hz, 7.0 Hz, CH₃CHCH), 4.52

(1H, br t, *J* = 7.5 Hz, CH₃CHCHCH), 3.32 (1H, br s, OH), 2.71 (1H, br s, OH), 2.33 (3H, s,

ArCH₃), 1.96 (1H, dd, *J* = 15.0 Hz, 10.5 Hz, ArCCH_aH_b), 1.85 (1H, dd, *J* = 15.0 Hz, 3.0 Hz,

ArCCH_aH_b), 1.67 (3H, d, *J* = 6.0 Hz, CHCHCH₃), 1.66 (3H, s, ArCCH₃); ¹³C NMR (125 MHz,

CDCl₃): δ 146.3, 136.4, 134.0, 129.1, 127.0, 124.4, 74.8, 71.0, 49.6, 28.4, 21.1, 17.7; IR (neat): 3331

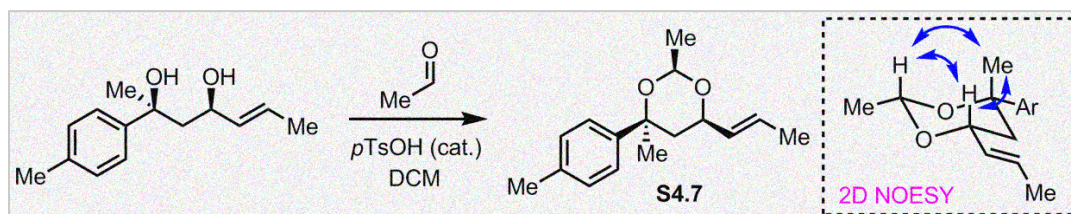
(br), 2973 (m), 2917 (m), 2883 (w), 1514 (w), 1450 (m), 1420 (m), 1375 (m), 1218 (m), 1207 (m),

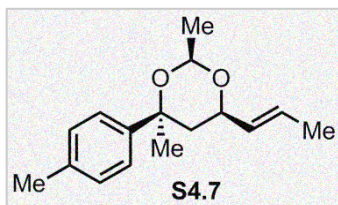
1135 (m), 1094 (s), 1074 (s), 1043 (m), 1020 (w), 965 (s), 846 (s), 817 (s), 723 (w), 565 (s), 504 (w)

cm⁻¹; HRMS (ESI⁺) calculated for C₁₄H₁₇ [M-2H₂O+H]⁺: 185.1330, found: 185.1336.

Proof of Stereochemistry. The relative configuration was assigned as *syn* (C₂-C₄) by analysis

of the spectral data, after conversion of the title compound into **S4.7** as shown below.





(2S*,4S*,6R*)-2,4-dimethyl-6-((E)-prop-1-en-1-yl)-4-(p-tolyl)-

1,3-dioxane (S4.7). The acetonide (S4.7) was prepared in the

same method as described for acetonide S4.1. $R_f = 0.22$ (9:1

hexanes:Et₂O); ¹H NMR (500 MHz, CDCl₃): δ 7.34 (2H, d, $J =$

8.5 Hz, aromatic), 7.15 (2H, d, $J = 8.5$ Hz, aromatic), 5.78 (1H, dq, $J = 15.0$ Hz, 6.0 Hz,

CH₃CHCH), 5.48 (1H, dd, $J = 15.5$ Hz, 7.0 Hz, CH₃CHCH), 5.23 (1H, q, $J = 5.0$ Hz, CH₃CHO),

4.36-4.32 (1H, m, CH₃CHCHCHO), 2.33 (3H, s, ArCH₃), 1.80 (1H, dd, $J = 13.5$ Hz, 3.0 Hz,

ArCCH_aH_b), 1.75 (1H, dd, overlapped, ArCCH_aH_b), 1.70 (3H, d, $J = 6.5$ Hz, CHCHCH₃), 1.61

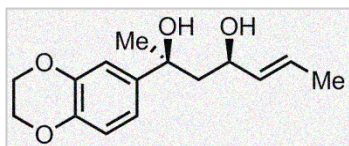
(3H, s, ArCCH₃), 1.43 (3H, d, $J = 5.5$ Hz, OCHCH₃); ¹³C NMR (125 MHz, CDCl₃): δ 146.1, 136.3,

131.3, 129.0, 128.5, 124.0, 92.3, 74.5, 73.6, 42.1, 23.2, 21.8, 21.1, 18.0; IR (neat): 3024 (w), 2990

(m), 2937 (m), 2919 (m), 2869 (w), 1515 (w), 1450 (w), 1406 (m), 1377 (w), 1172 (s), 1115 (s), 969

(s), 875 (w), 837 (w), 817 (m), 721 (w), 560 (w), 460 (w) cm⁻¹; HRMS (ESI+) calculated for

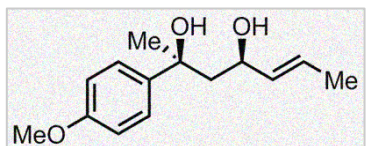
C₁₆H₂₆NO₂ [M+NH₄]⁺: 264.1963, found: 264.1953.



(2*S**,4*R**,*E*)-2-(2,3-dihydrobenzo[*b*][1,4]dioxin-6-yl)hept-5-ene-2,4-diol. The reaction was performed according to the general procedure with 13.8 mg (0.05 mmol) of Ni(cod)₂, 15.2

mg (0.075 mmol) of P(*t*-Bu)₃, 89.1 mg (0.5 mmol) of 1,4-benzodioxan-6-yl methyl ketone, 68.1 mg (1.0 mmol) of *trans*-1,3-pentadiene, and 253.9 mg (1.0 mmol) of B₂(pin)₂ in THF (2.5 mL) for 48 h, followed by oxidation, to afford the title compound as a colorless oil (90.9 mg, 69% yield). *R*_f = 0.28 (1:2 hexanes:Et₂O); ¹H NMR (500 MHz, CDCl₃): δ 6.98 (1H, s, aromatic), 6.91 (1H, d, *J* = 9.0 Hz, aromatic), 6.82 (1H, d, *J* = 8.5 Hz, aromatic), 5.67 (1H, dq, *J* = 15.5 Hz, 6.5 Hz, CH₃CHCH), 5.46 (1H, dd, *J* = 15.0 Hz, 7.0 Hz, CH₃CHCH), 4.49 (1H, br t, *J* = 8.5 Hz, CH₃CHCHCH), 4.25 (4H, s, ArOCH₂CH₂), 3.38 (1H, br s, OH), 2.80 (1H, br s, OH), 1.93 (1H, dd, *J* = 15.0 Hz, 10.0 Hz, ArCCH_aH_b), 1.80 (1H, dd, *J* = 15.0 Hz, 2.5 Hz, ArCCH_aH_b), 1.67 (3H, d, *J* = 6.0 Hz, CHCHCH₃), 1.63 (3H, s, ArCCH₃); ¹³C NMR (125 MHz, CDCl₃): δ 143.2, 142.8, 142.3, 133.9, 127.0, 117.6, 117.0, 113.8, 74.5, 71.0, 64.5 (2 C's), 49.5, 28.3, 17.8; IR (neat): 3412 (br), 2996 (m), 2930 (w), 2854 (w), 1590 (w), 1505 (s), 1460 (w), 1424 (m), 1377 (m), 1309 (m), 1285 (s), 1258 (m), 1175 (w), 1126 (m), 1100 (w), 1068 (s), 949 (w), 887 (w), 642 (w), 496 (w) cm⁻¹; HRMS (ESI+) calculated for C₁₅H₁₇O₂ [M-2H₂O+H]⁺: 229.1228, found: 229.1228.

Stereochemistry. The relative configuration was assigned as *syn* (C₂-C₄) by analogy.



(2S*,4R*,E)-2-(4-methoxyphenyl)hept-5-ene-2,4-diol. The

reaction was performed according to the general procedure

with 13.8 mg (0.05 mmol) of Ni(cod)₂, 15.2 mg (0.075 mmol)

of P(*t*-Bu)₃, 75.1 mg (0.5 mmol) of 4'-methoxyacetophenone, 68.1 mg (1.0 mmol) of *trans*-1,3-

pentadiene, and 253.9 mg (1.0 mmol) of B₂(pin)₂ in THF (2.5 mL) for 48 h, followed by

oxidation, to afford the title compound as a colorless oil (61.3 mg, 52% yield). R_f = 0.31 (1:2

hexanes:Et₂O); ¹H NMR (500 MHz, CDCl₃): δ 7.38 (2H, d, *J* = 9.0 Hz, aromatic), 6.87 (2H, d, *J* =

9.0 Hz, aromatic), 5.69 (1H, dq, *J* = 15.0 Hz, 6.5 Hz, CH₃CHCH), 5.48 (1H, dd, *J* = 15.5 Hz, 7.0

Hz, CH₃CHCH), 4.51 (1H, br t, *J* = 7.5 Hz, CH₃CHCHCH), 3.80 (3H, s, ArOCH₃), 3.35 (1H, br

s, OH), 2.72 (1H, br s, OH), 1.96 (1H, dd, *J* = 14.5 Hz, 10.0 Hz, ArCCH_aH_b), 1.83 (1H, dd, *J* =

15.0 Hz, 3.0 Hz, ArCCH_aH_b), 1.68 (3H, d, *J* = 6.5 Hz, CHCHCH₃), 1.66 (3H, s, ArCCH₃); ¹³C

NMR (125 MHz, CDCl₃): δ 158.5, 141.5, 134.0, 127.0, 125.7, 113.7, 74.6, 71.1, 55.4, 49.7, 28.4,

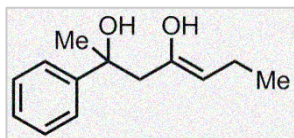
17.8; IR (neat): 3372 (br), 2938 (w), 2916 (w), 2854 (w), 1611 (w), 1512 (s), 1459 (w), 1442 (w),

1416 (w), 1302 (m), 1249 (s), 1215 (w), 1179 (s), 1094 (m), 1074 (w), 1035 (m), 966 (m), 847 (m),

832 (m), 802 (w), 491 (w) cm⁻¹; HRMS (ESI+) calculated for C₁₄H₁₉O₂ [M-H₂O+H]⁺: 219.1385,

found: 219.1386.

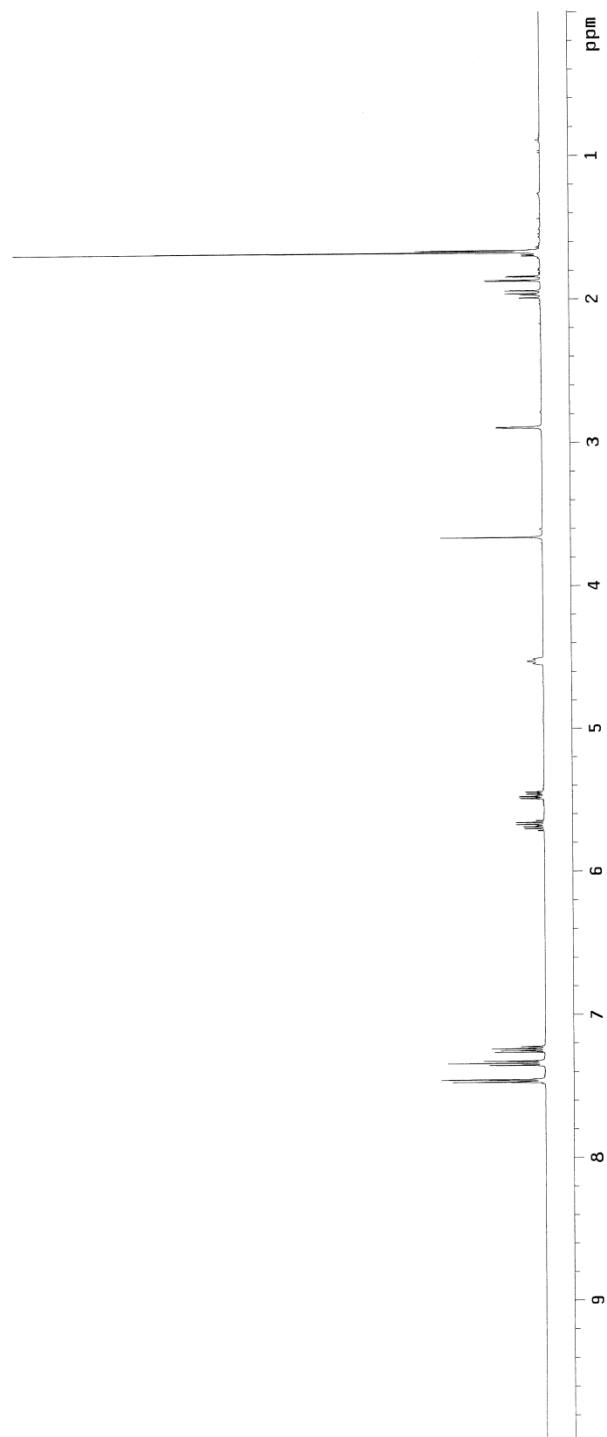
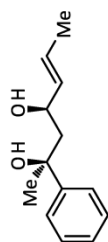
Stereochemistry. The relative configuration was assigned as *syn* (C₂-C₄) by analogy.

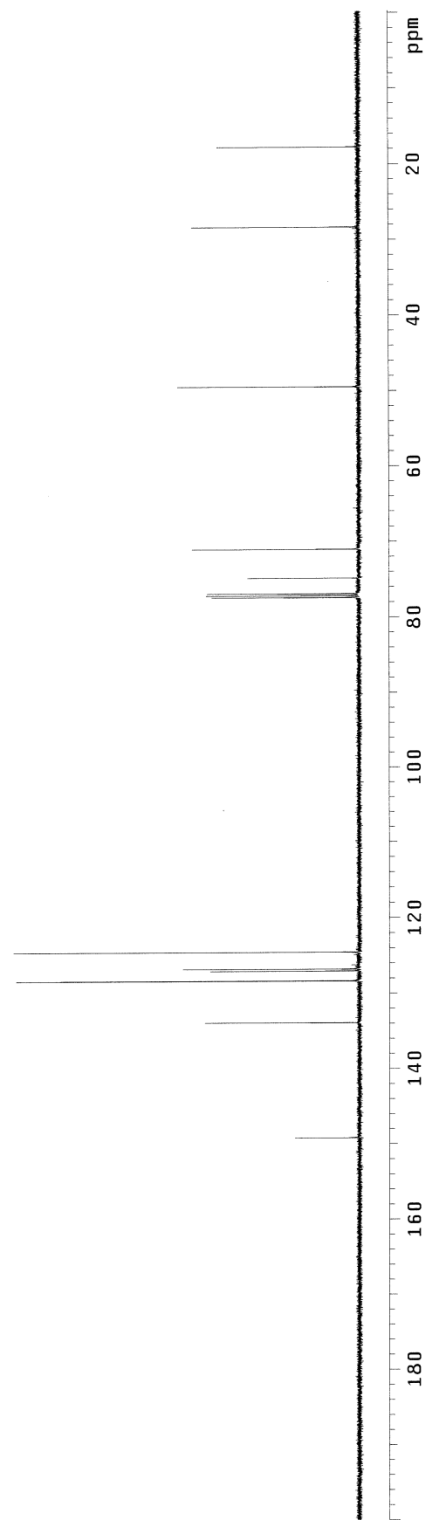
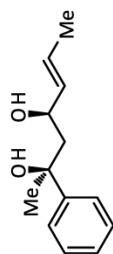


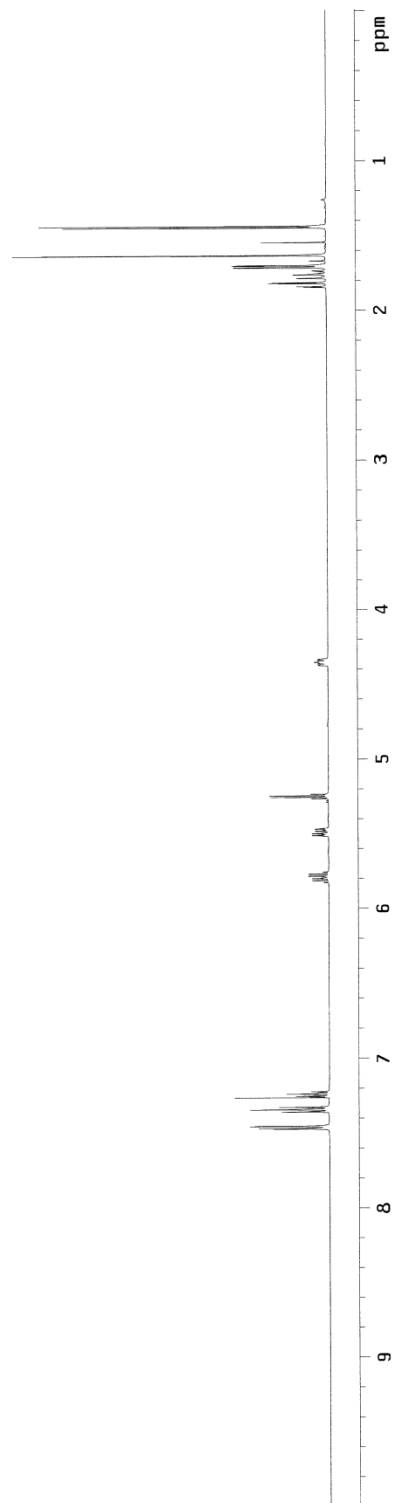
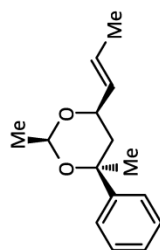
(E)-3-methyl-5-phenylhex-2-ene-1,5-diol. The reaction was performed according to the general procedure with 13.8 mg (0.05 mmol) of Ni(cod)₂, 15.2 mg (0.075 mmol) of P(*t*-Bu)₃, 60.1 mg (0.5 mmol) of acetophenone, 68.1 mg (1.0 mmol) of isoprene, and 253.9 mg (1.0 mmol) of B₂(pin)₂ in THF (2.5 mL) for 48 h, followed by oxidation, to afford the title compound as a colorless oil (40.1 mg, 39% yield). *R*_f = 0.28 (1:2 hexanes:EtOAc); ¹H NMR (500 MHz, CDCl₃): δ 7.45 (2H, d, *J* = 7.0 Hz, aromatic), 7.34 (2H, d, *J* = 7.0 Hz, aromatic), 7.24 (1H, t, *J* = 7.0 Hz, aromatic), 5.34 (1H, t, *J* = 7.5 Hz, CHCH₂OH), 3.97 (2H, s, CHCH₂OH), 2.60 (2H, d, *J* = 8.0 Hz, ArCCH₂), 1.95 (1H, br s, OH), 1.64 (3H, s, OHCH₂CHCCH₃), 1.57 (3H, s, ArCCH₃); ¹³C NMR (100 MHz, CDCl₃): δ 147.9, 139.1, 128.3, 126.8, 124.9, 120.4, 74.7, 68.8, 42.1, 30.0, 14.1; IR (neat): 3357 (br), 2965 (m), 2846 (m), 2792 (w), 1494 (w), 1446 (s), 1373 (m), 1286 (w), 1218 (w), 1068 (m), 1028 (m), 1013 (m), 950 (w), 880 (w), 764 (s), 700 (s), 623 (w), 555 (w) cm⁻¹; HRMS (ESI+) calculated for C₁₃H₂₂NO₂ [M+NH₄]⁺: 224.1650, found: 224.1645.

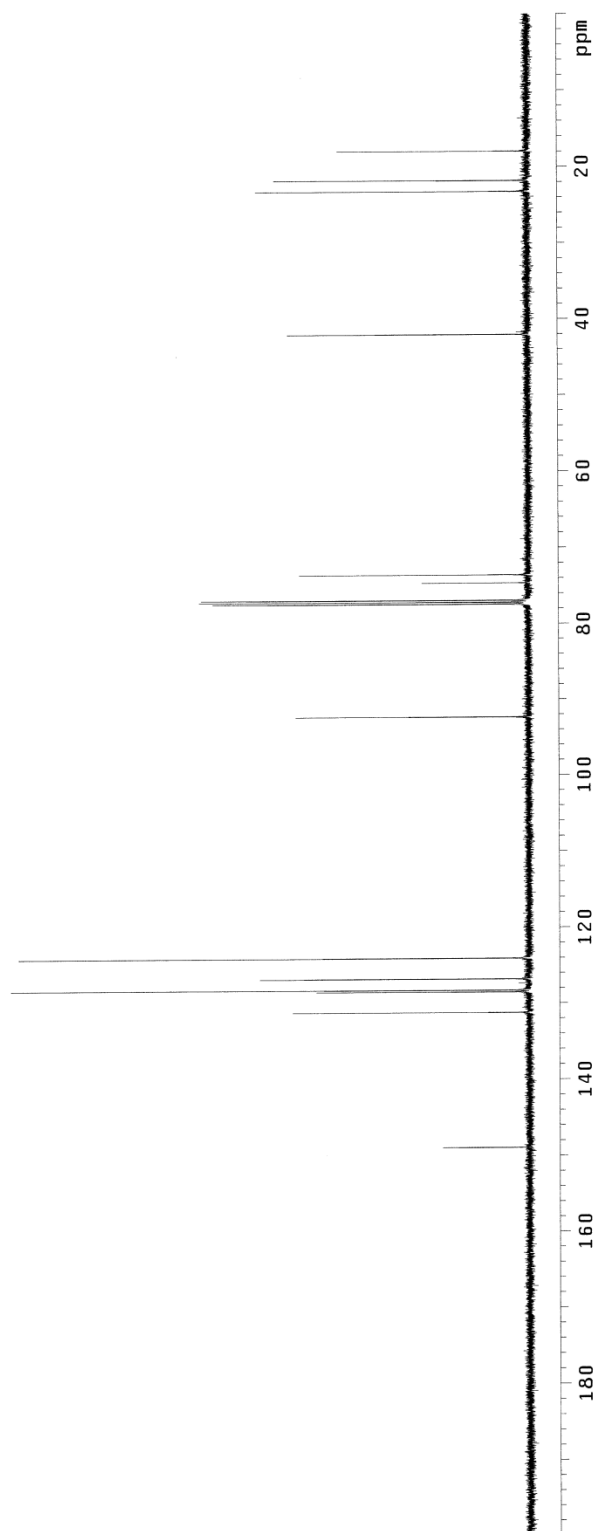
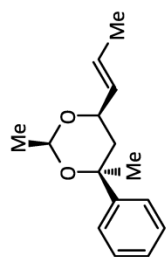
Stereochemistry. The alkene configuration was assigned as (*E*) by NOESY analysis.

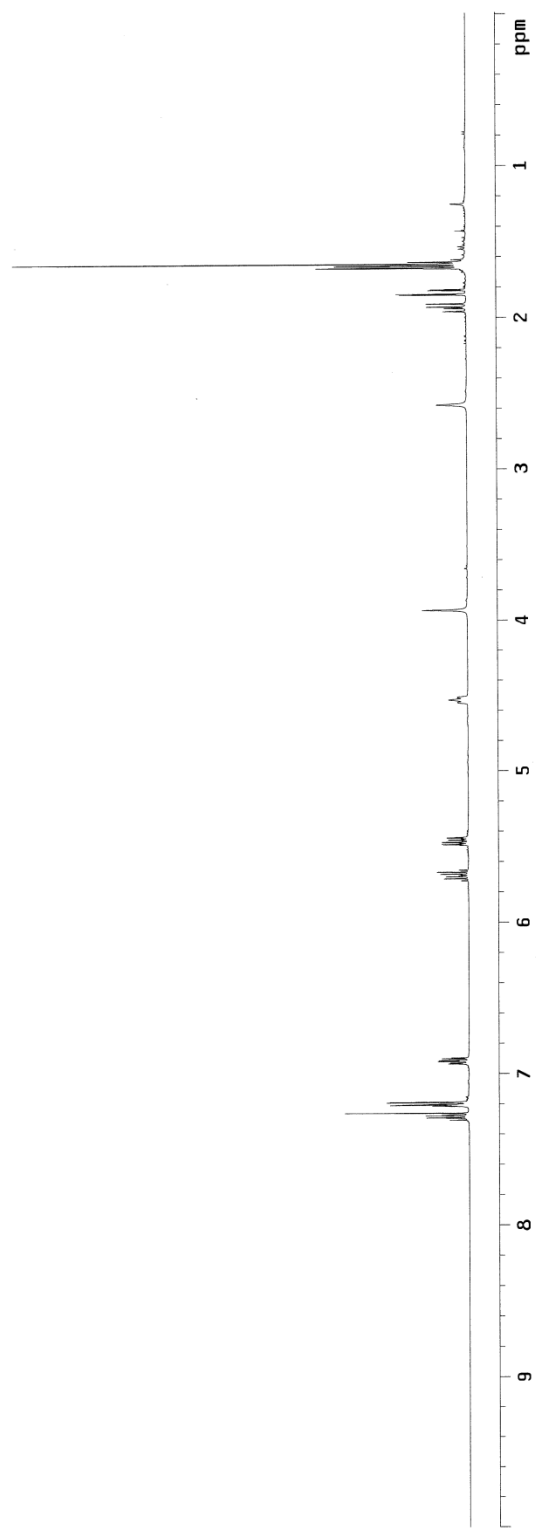
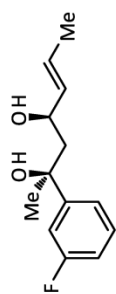
4.6.3. Representative Spectral Data

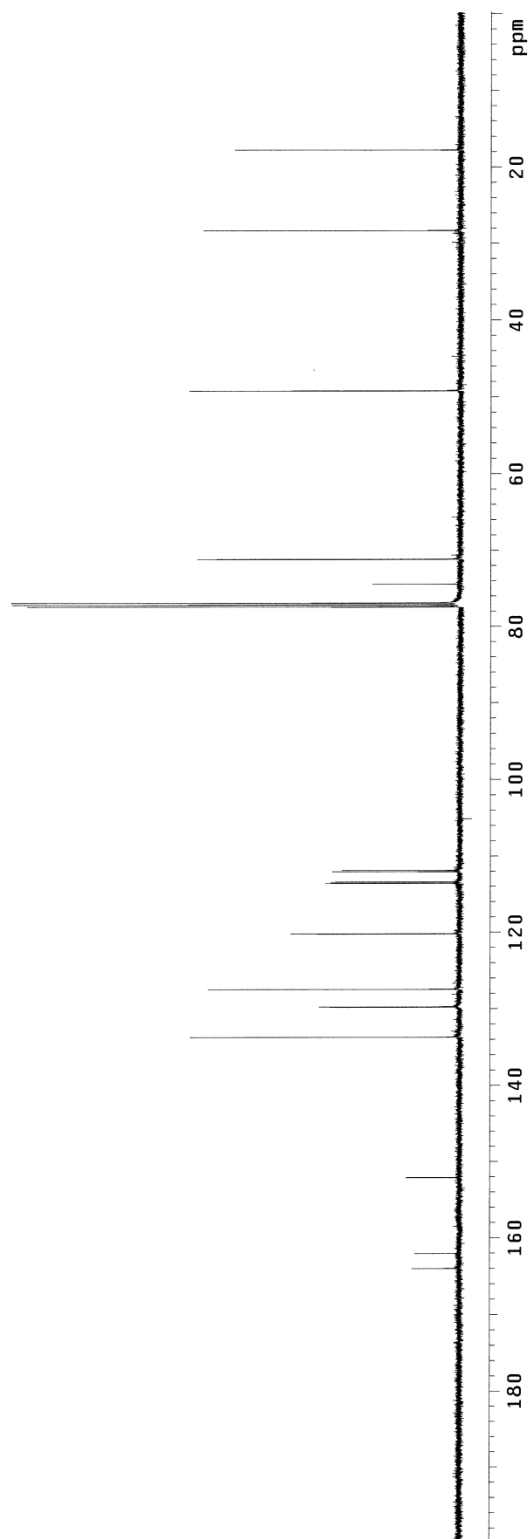
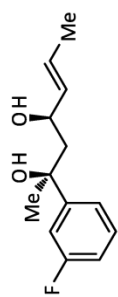


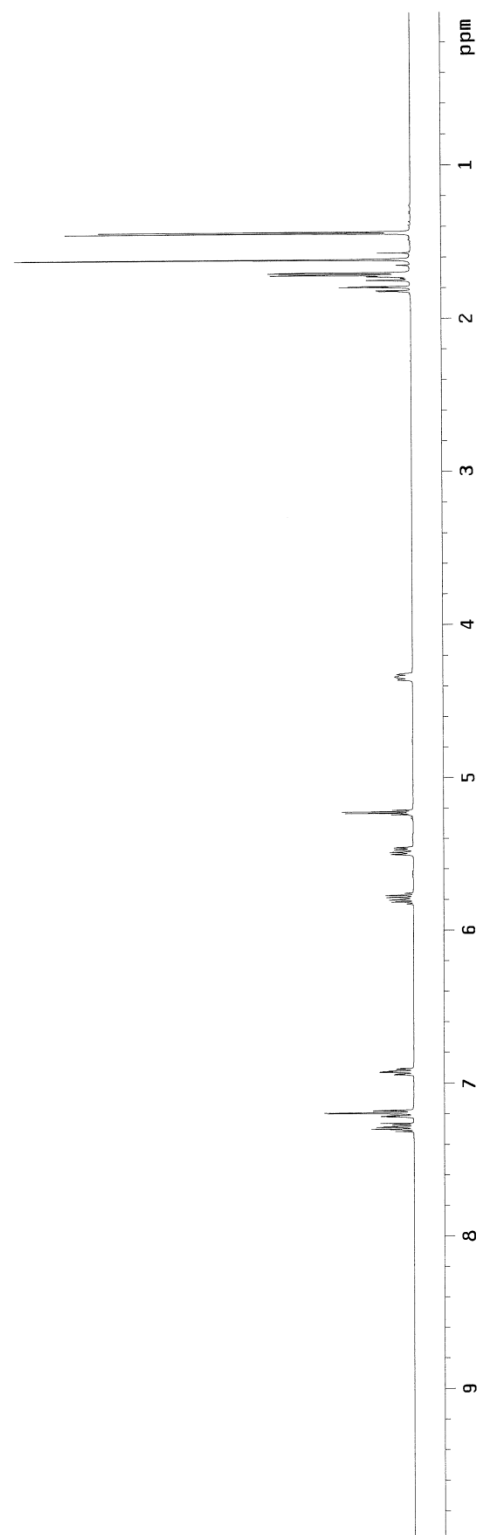
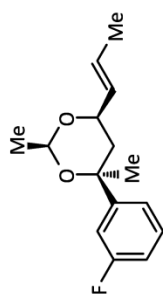


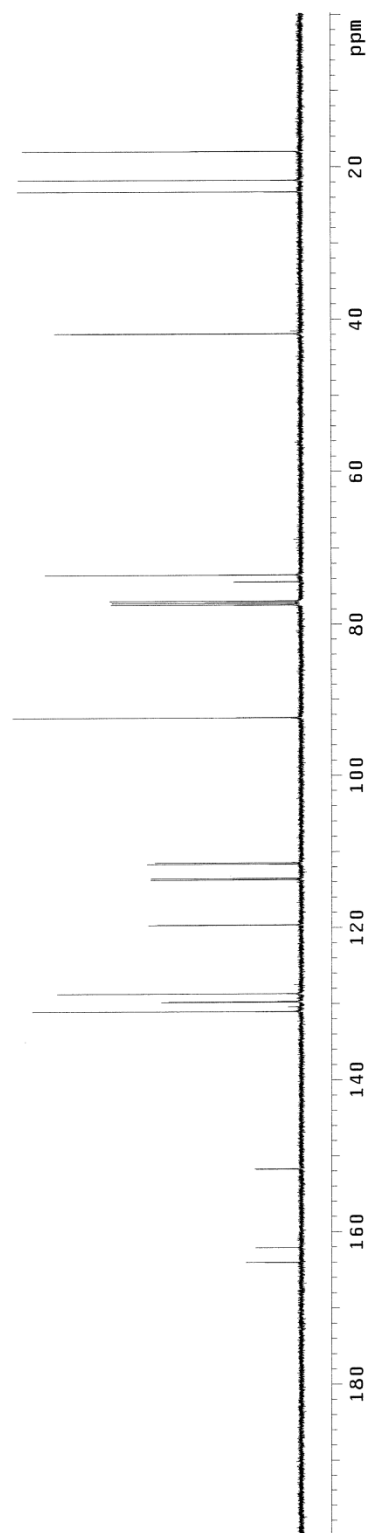
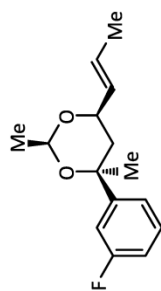


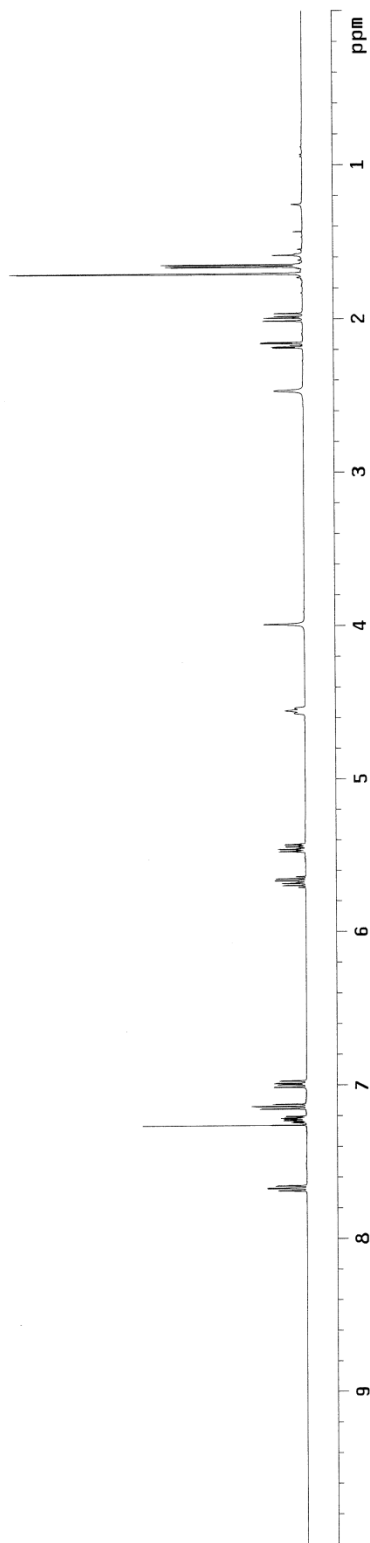
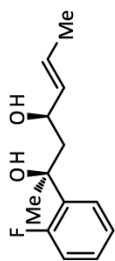


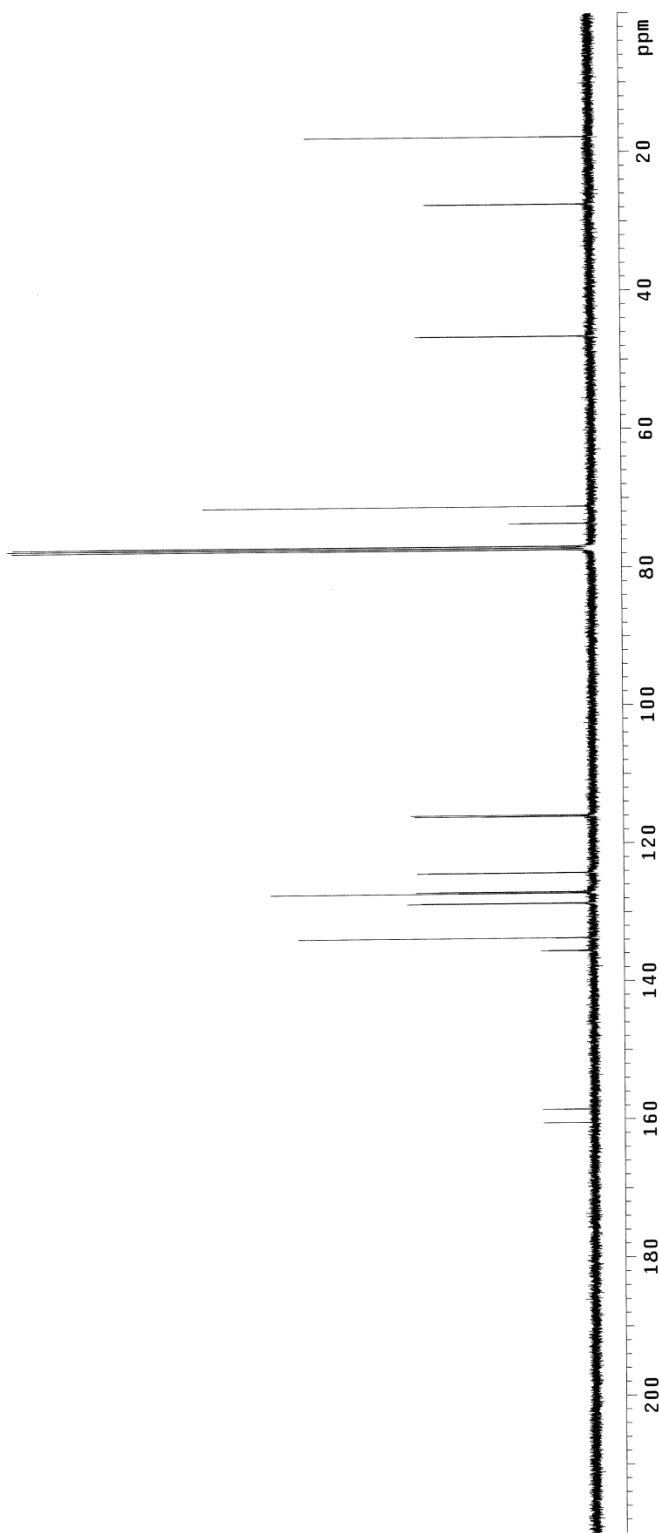
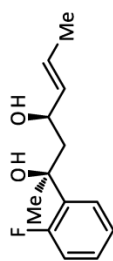


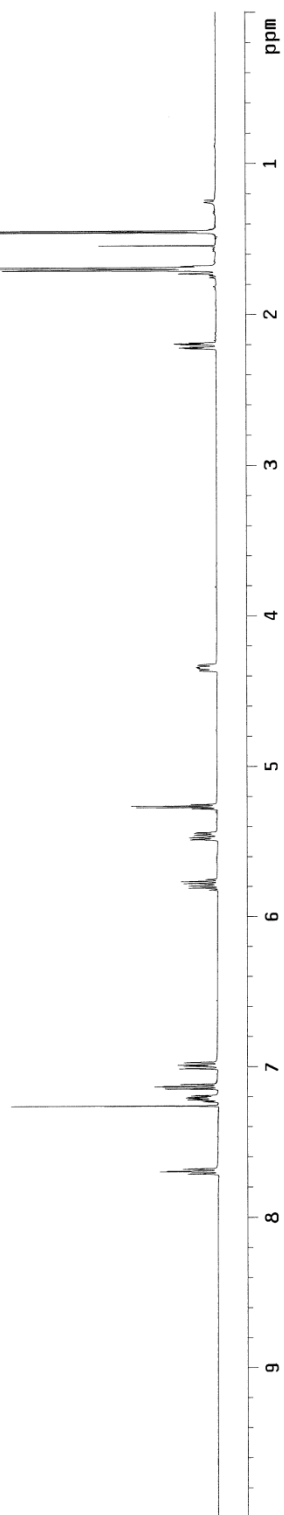
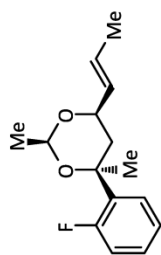


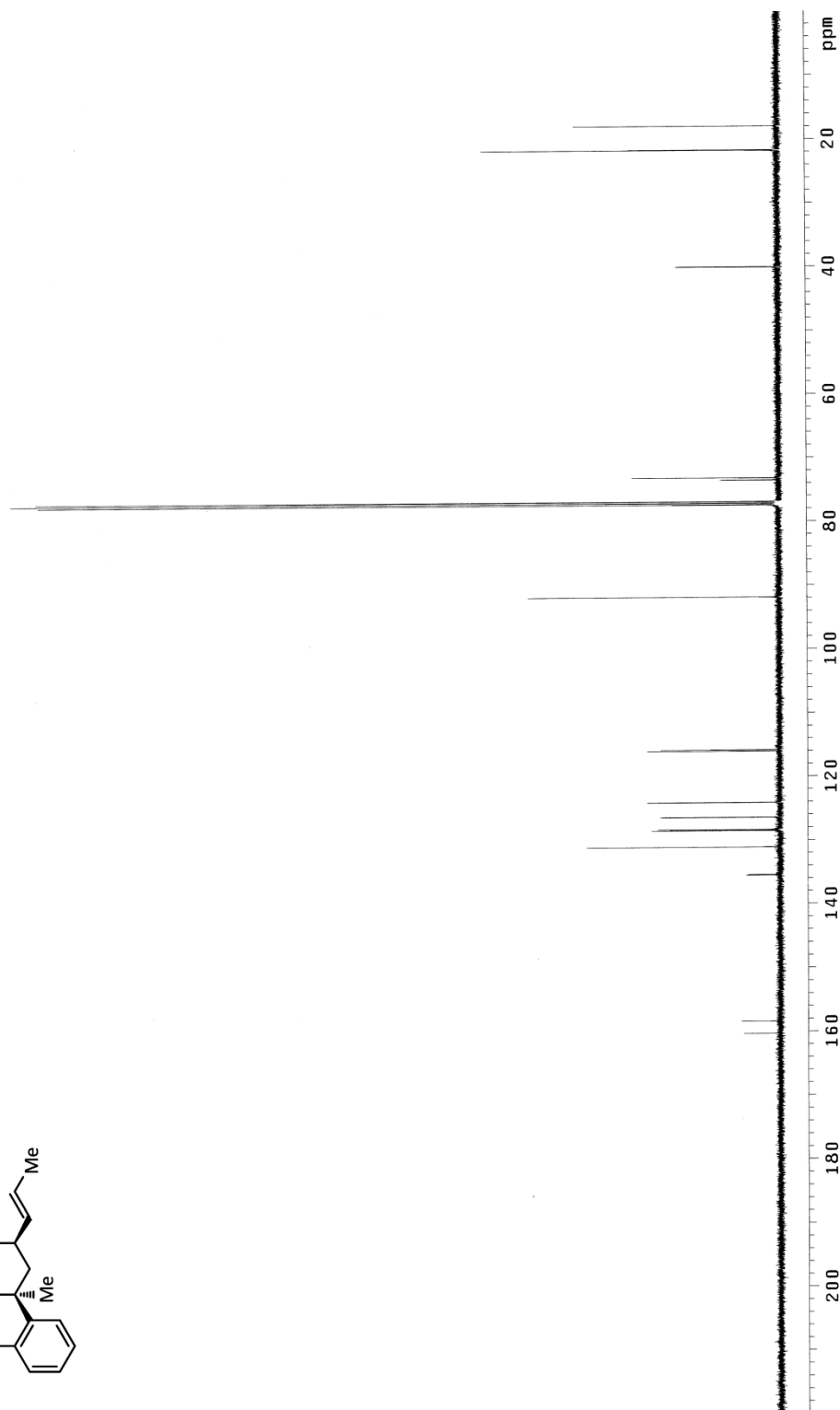
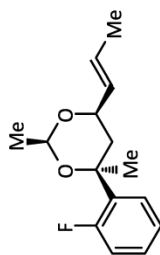


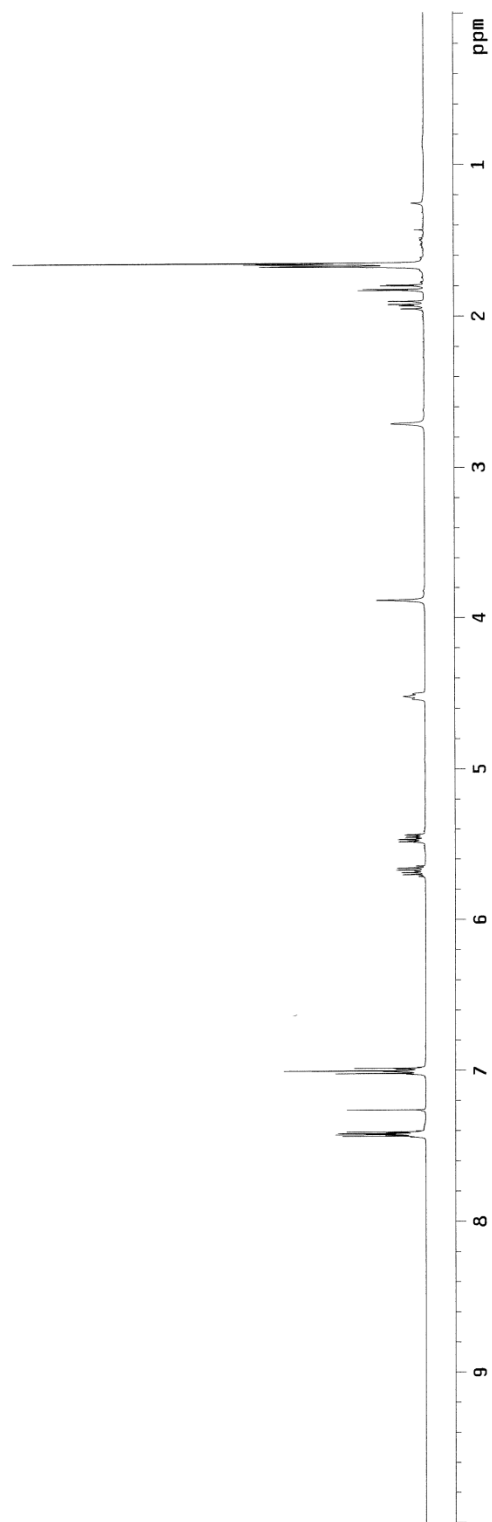
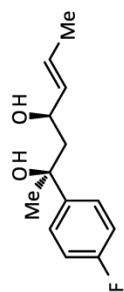


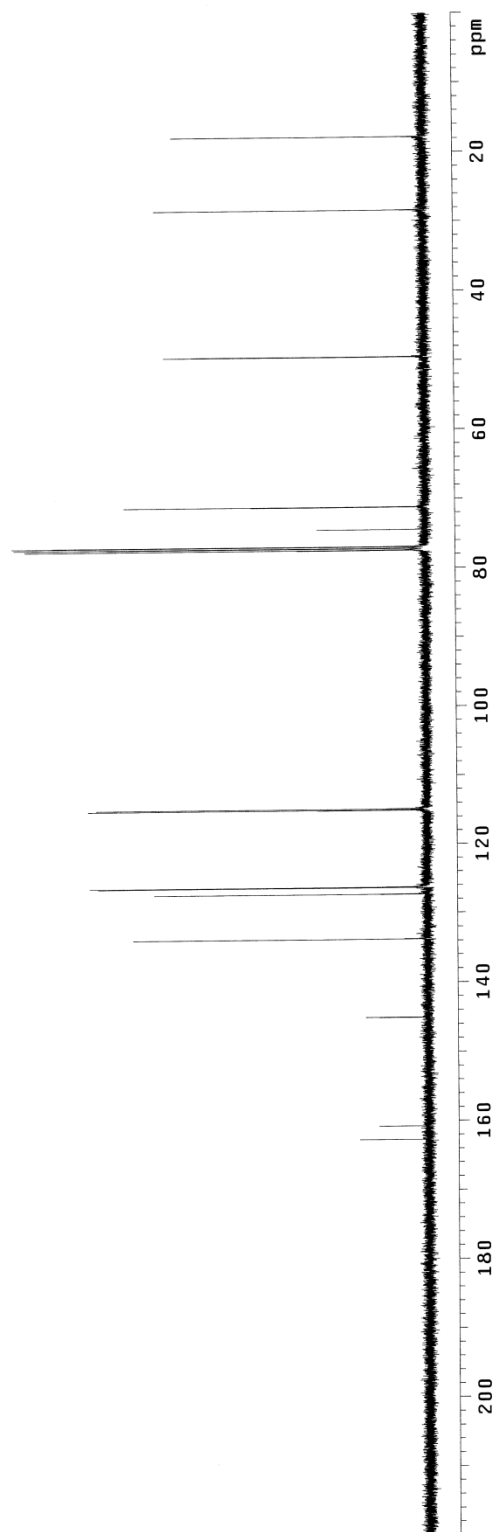
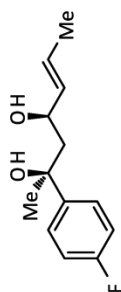


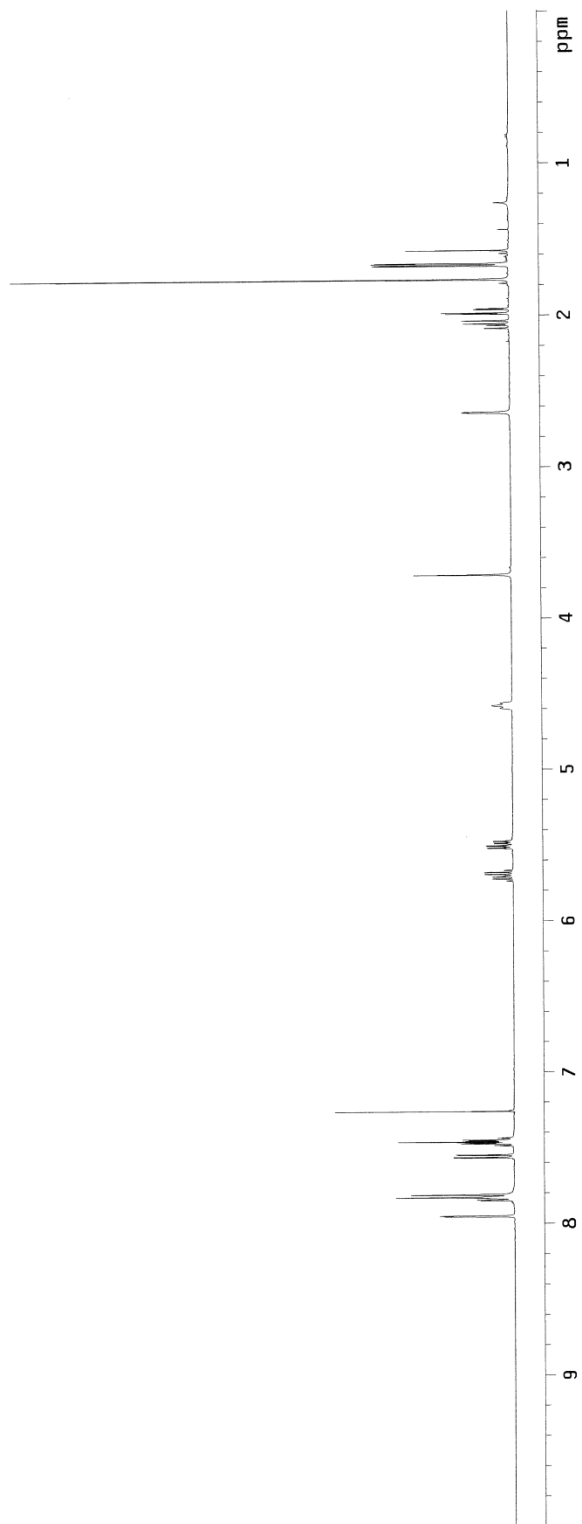
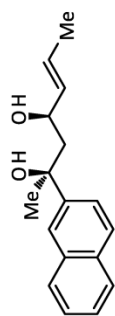


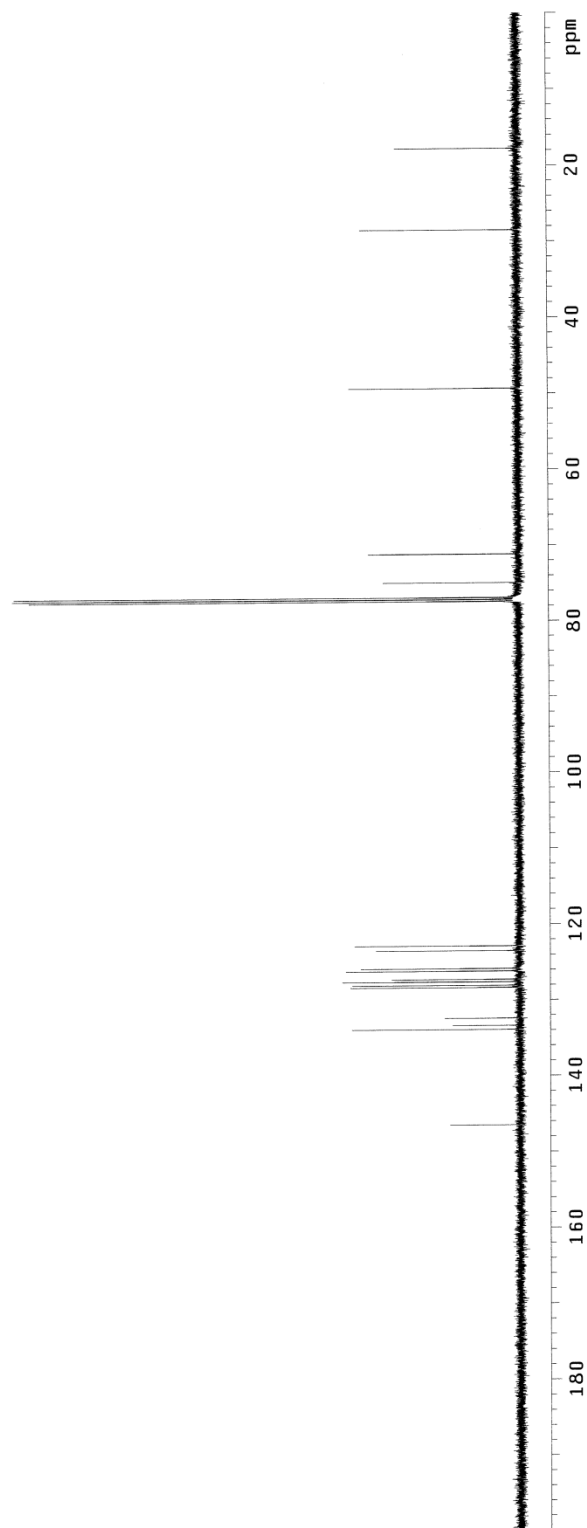
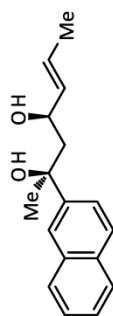


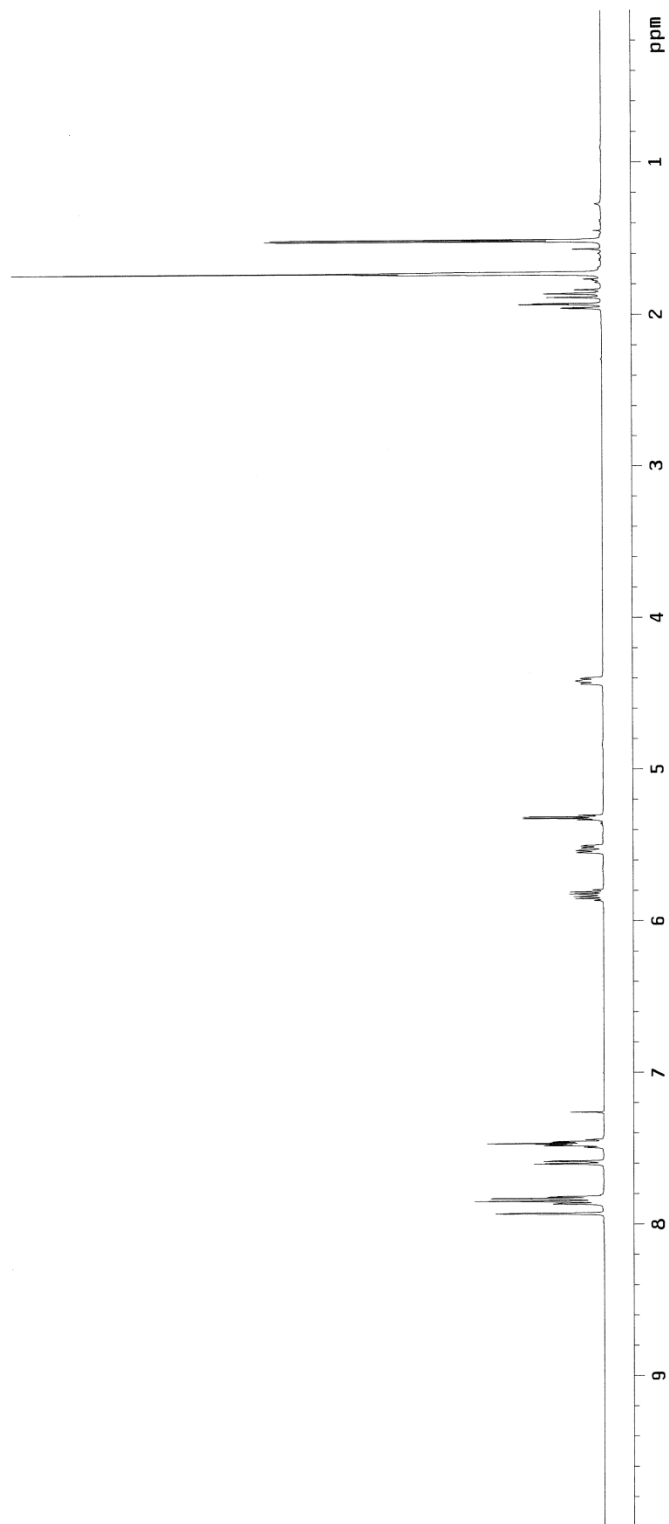
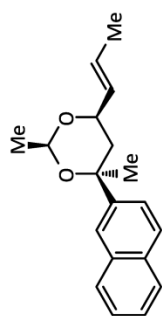


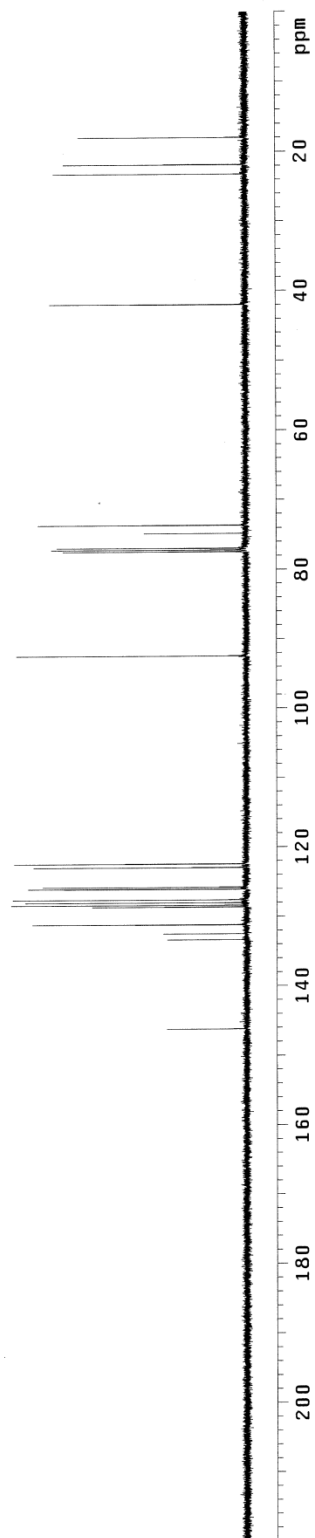
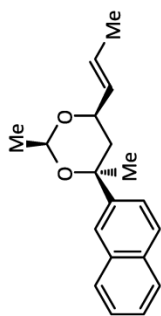


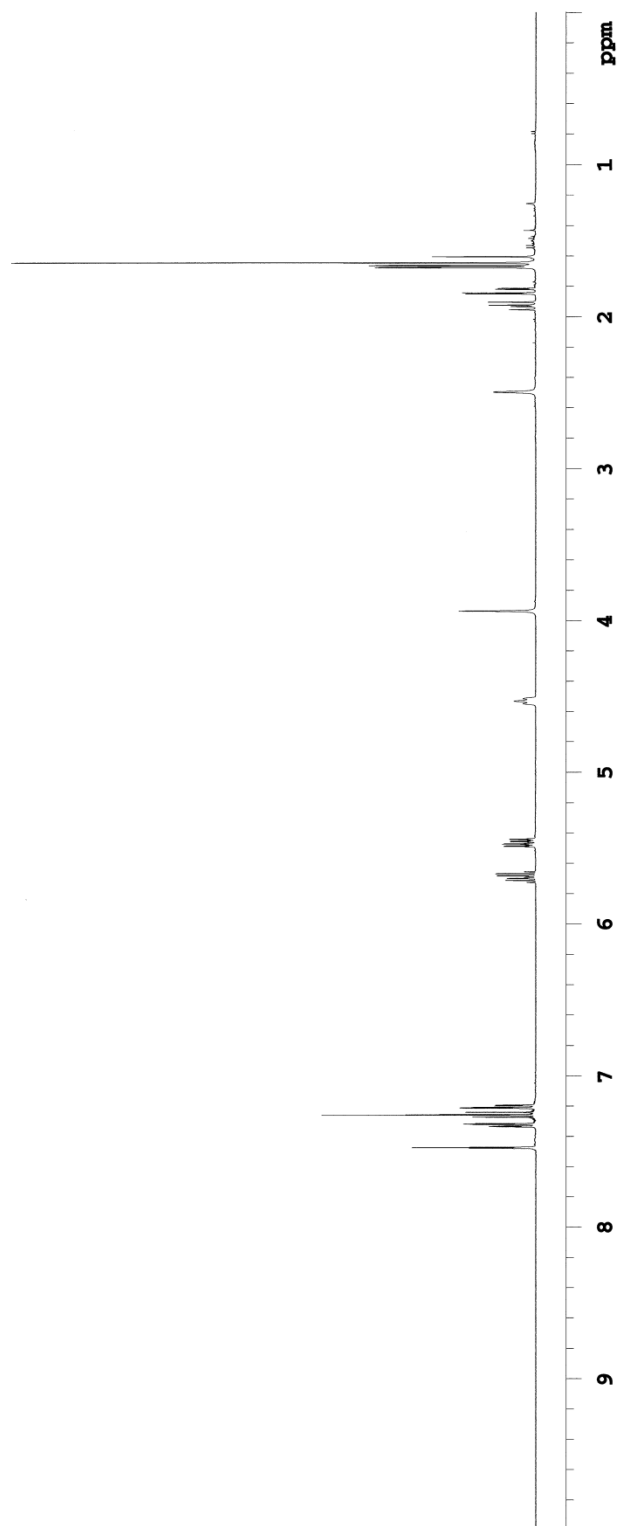
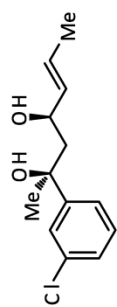


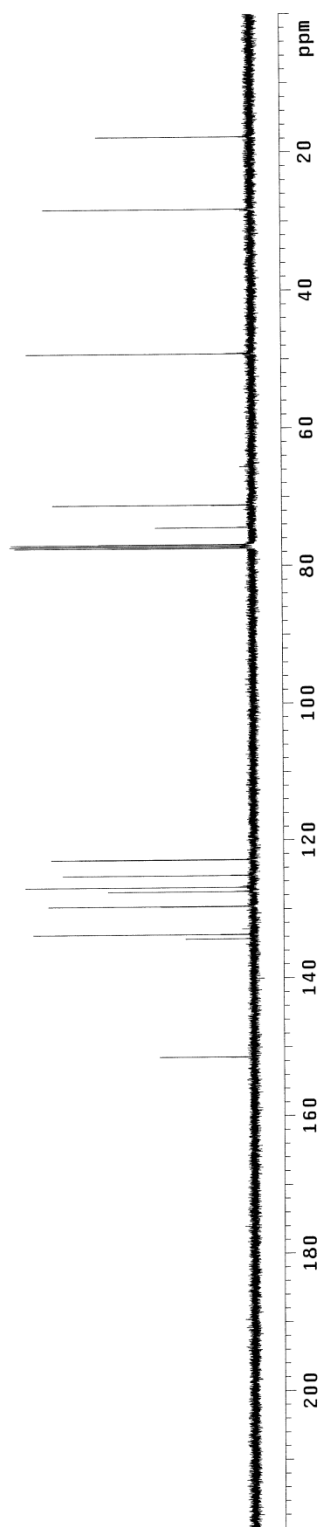
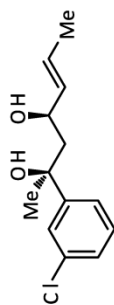


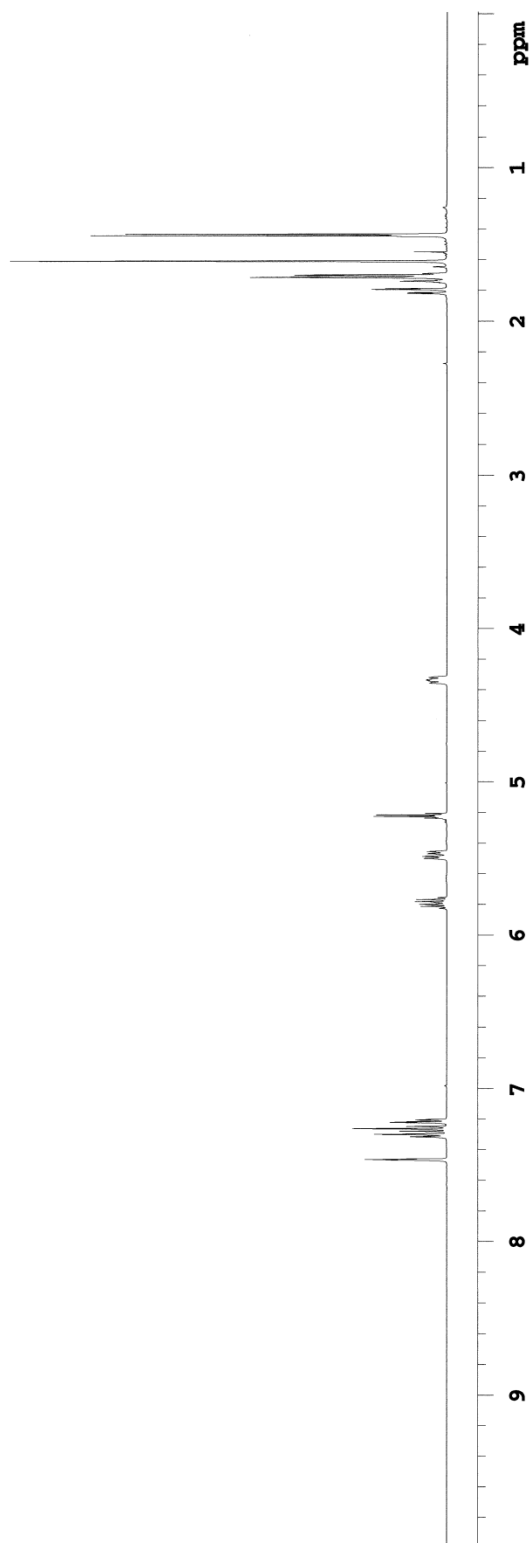
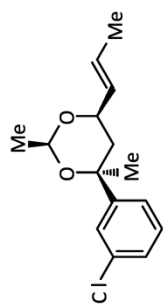


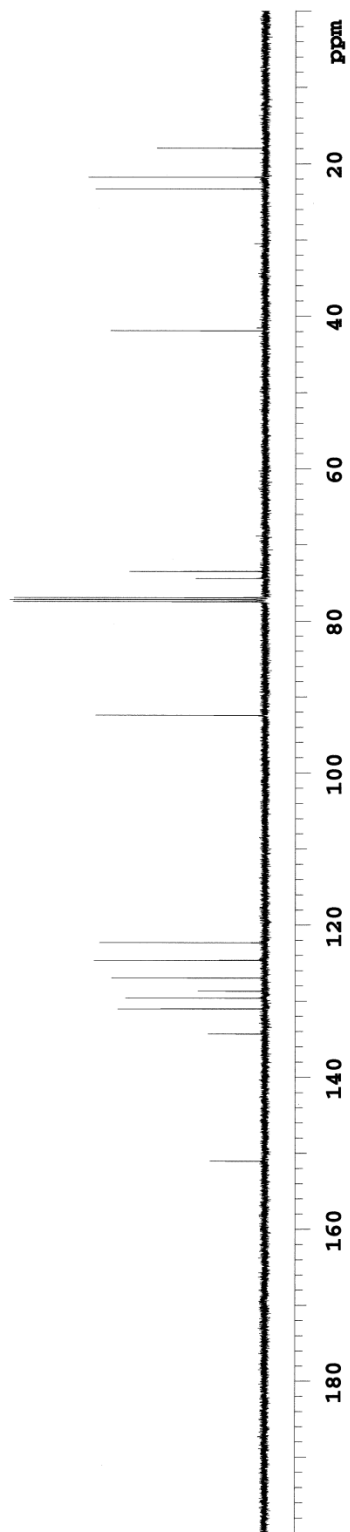
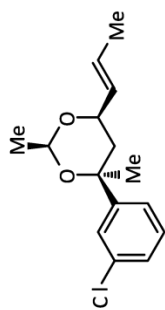


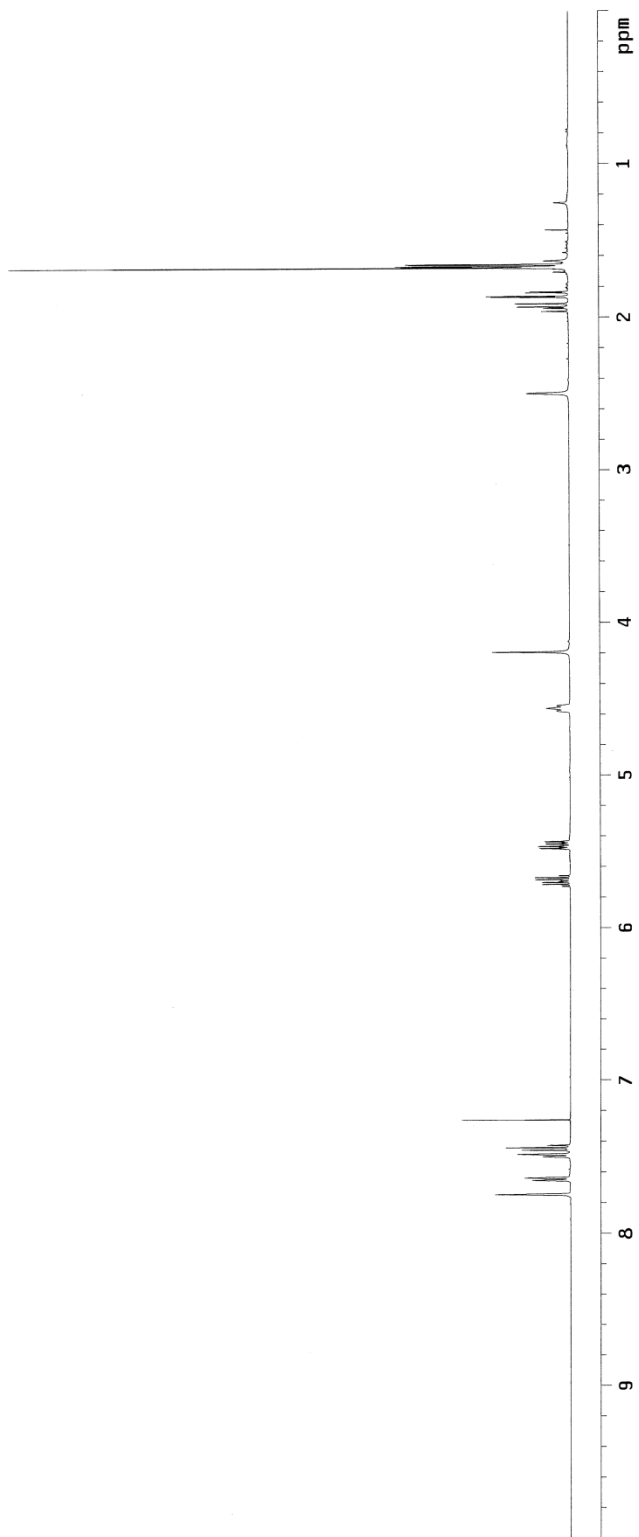
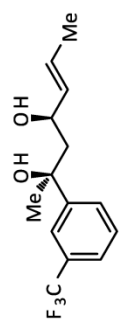


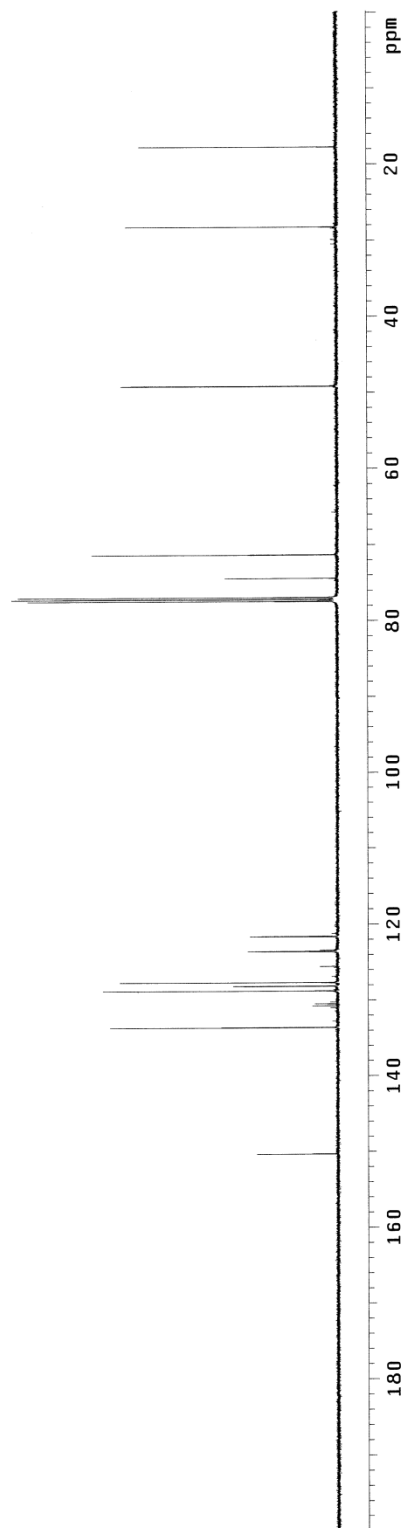
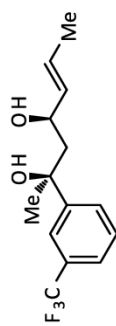


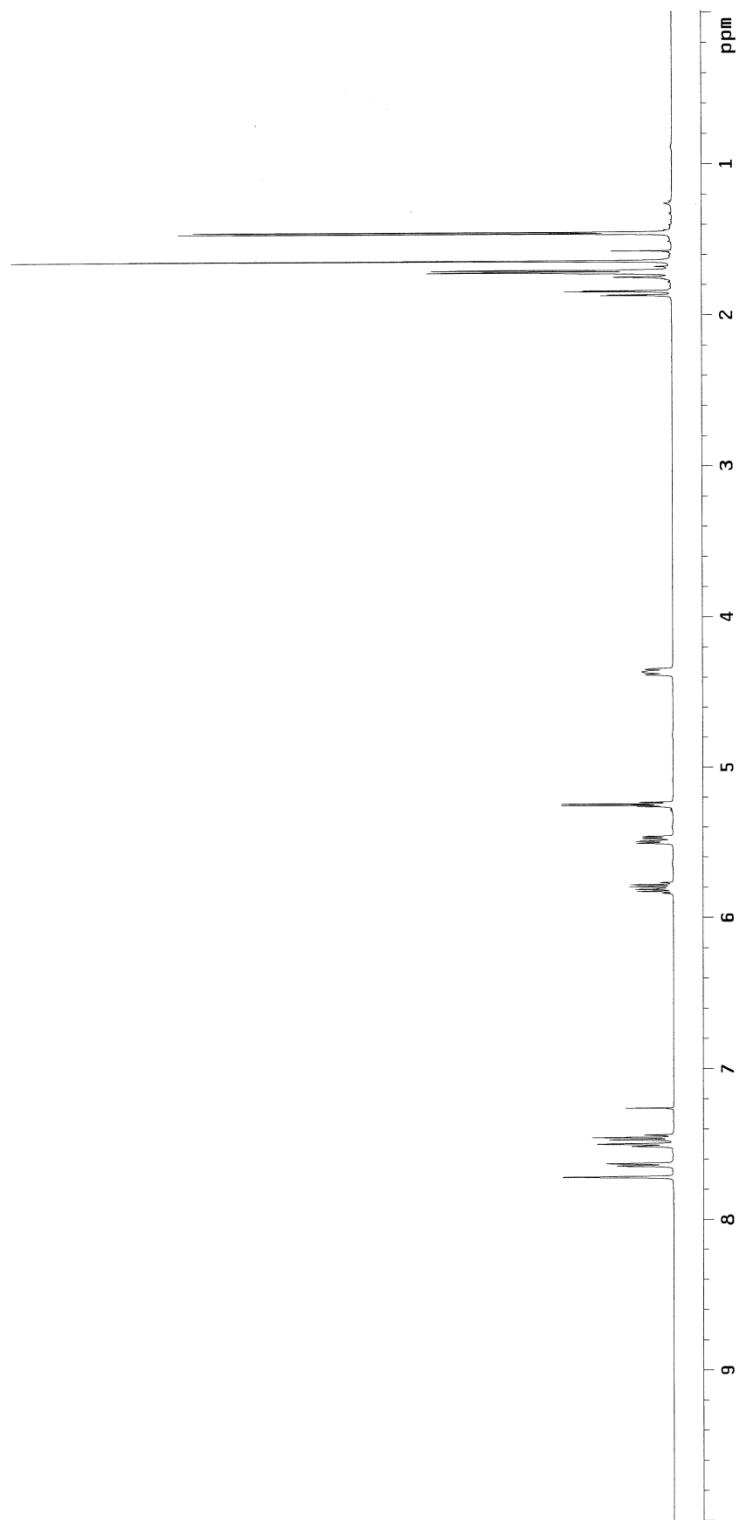
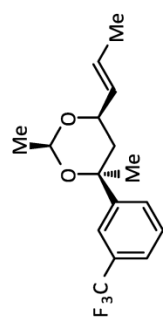


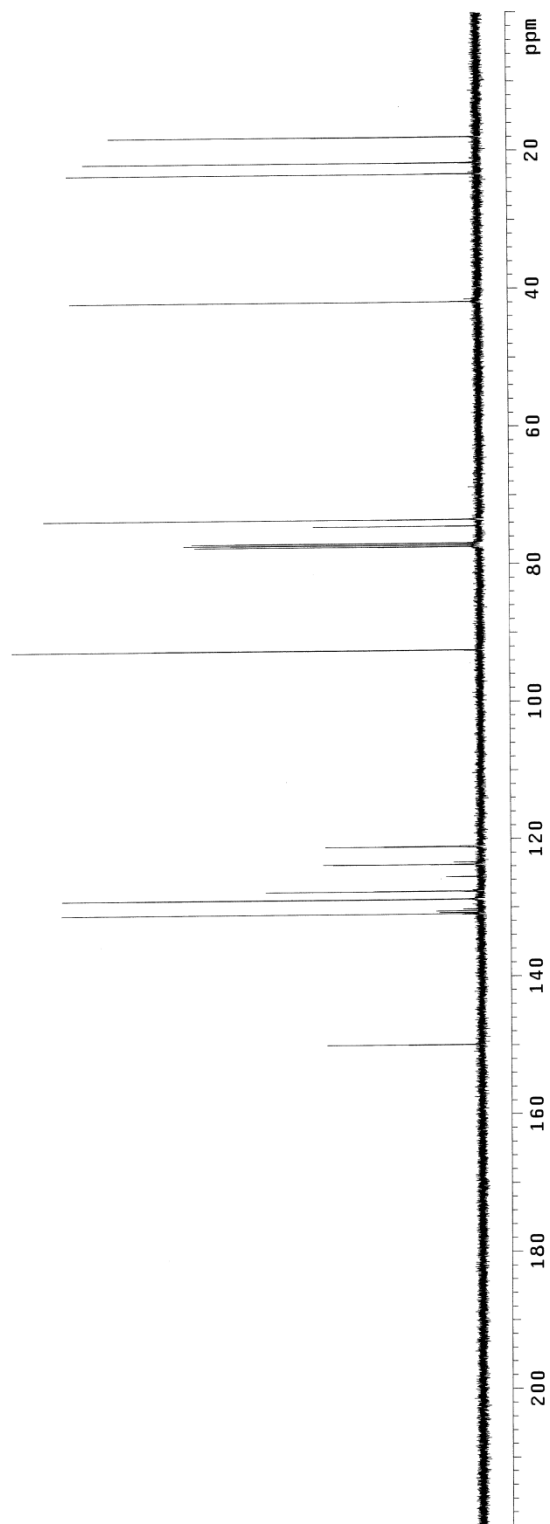
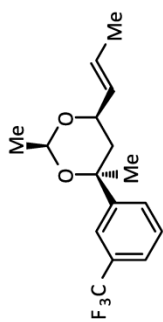


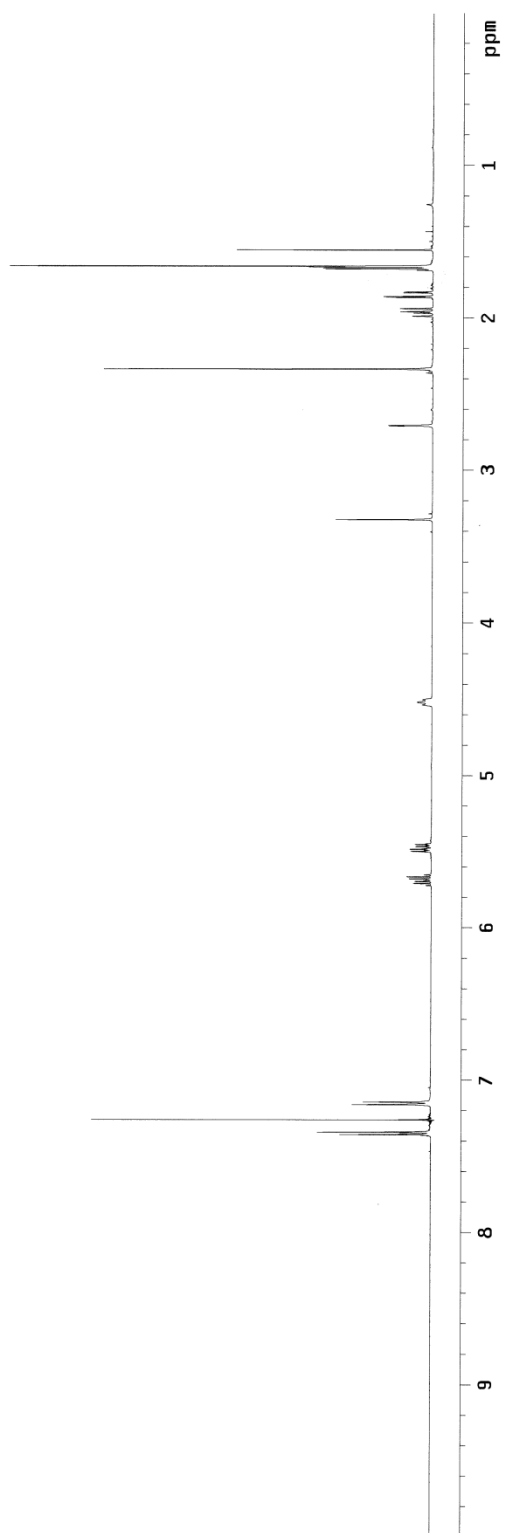
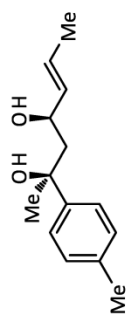


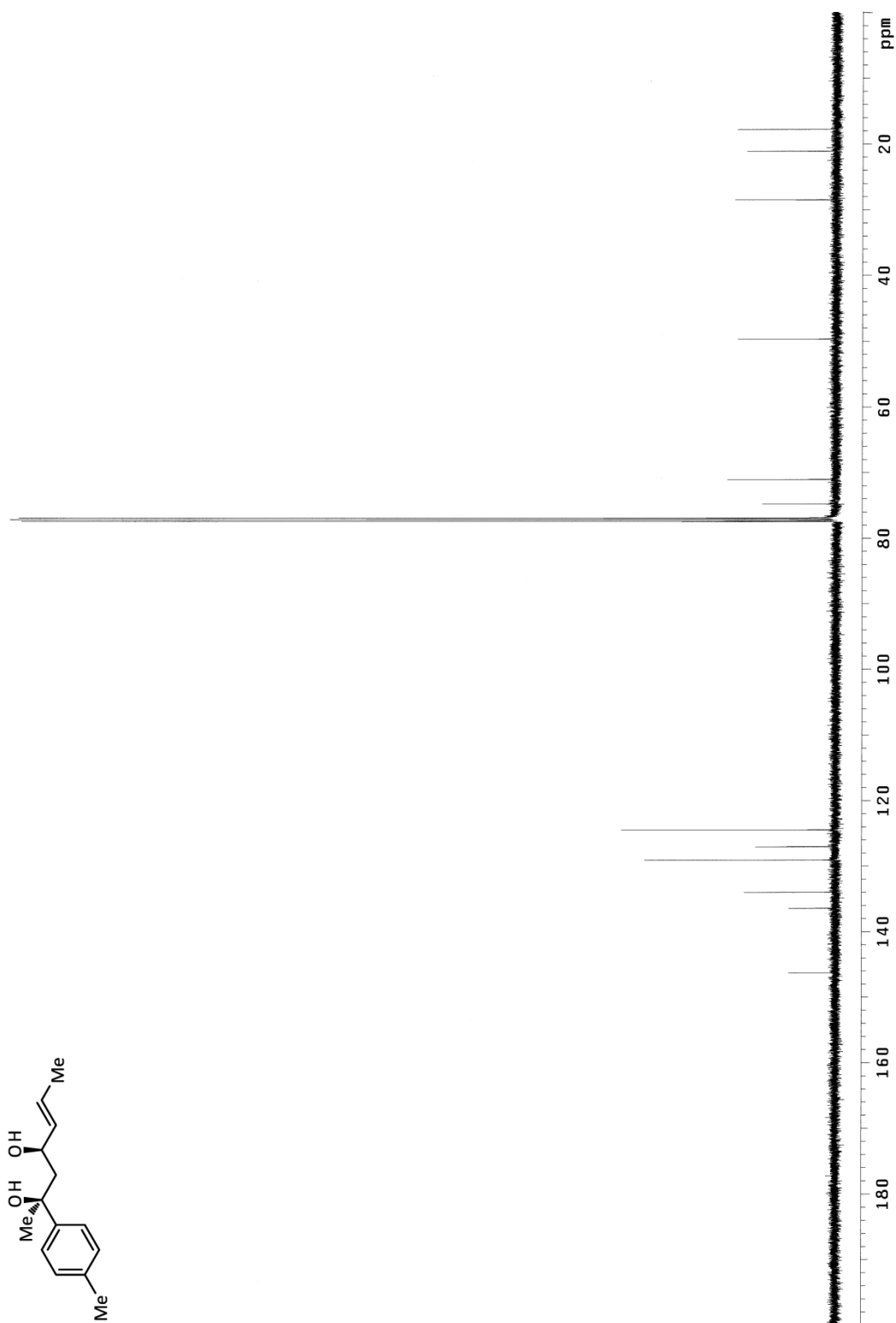


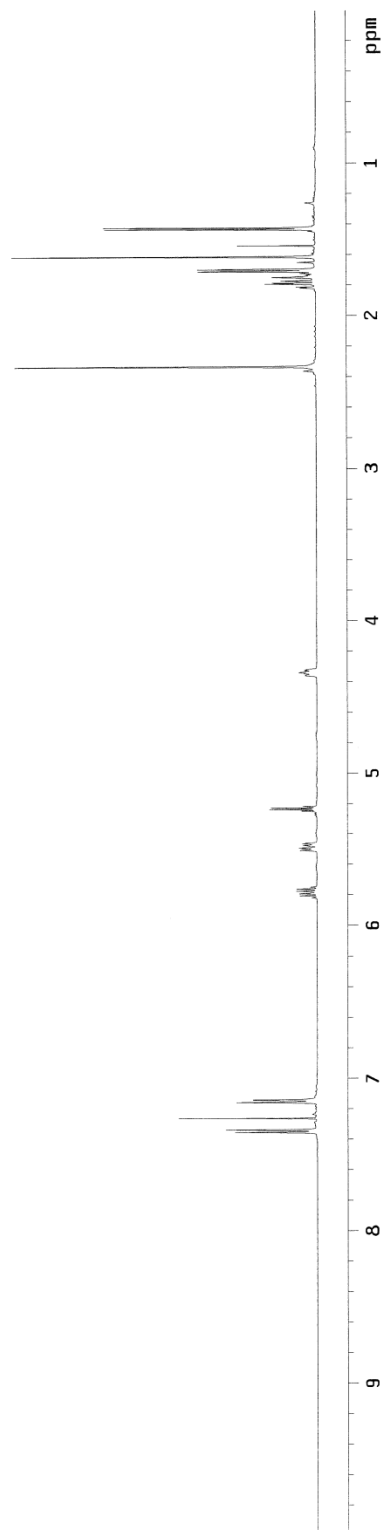
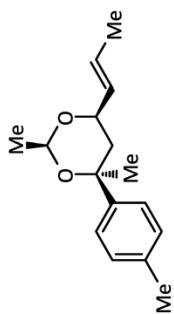


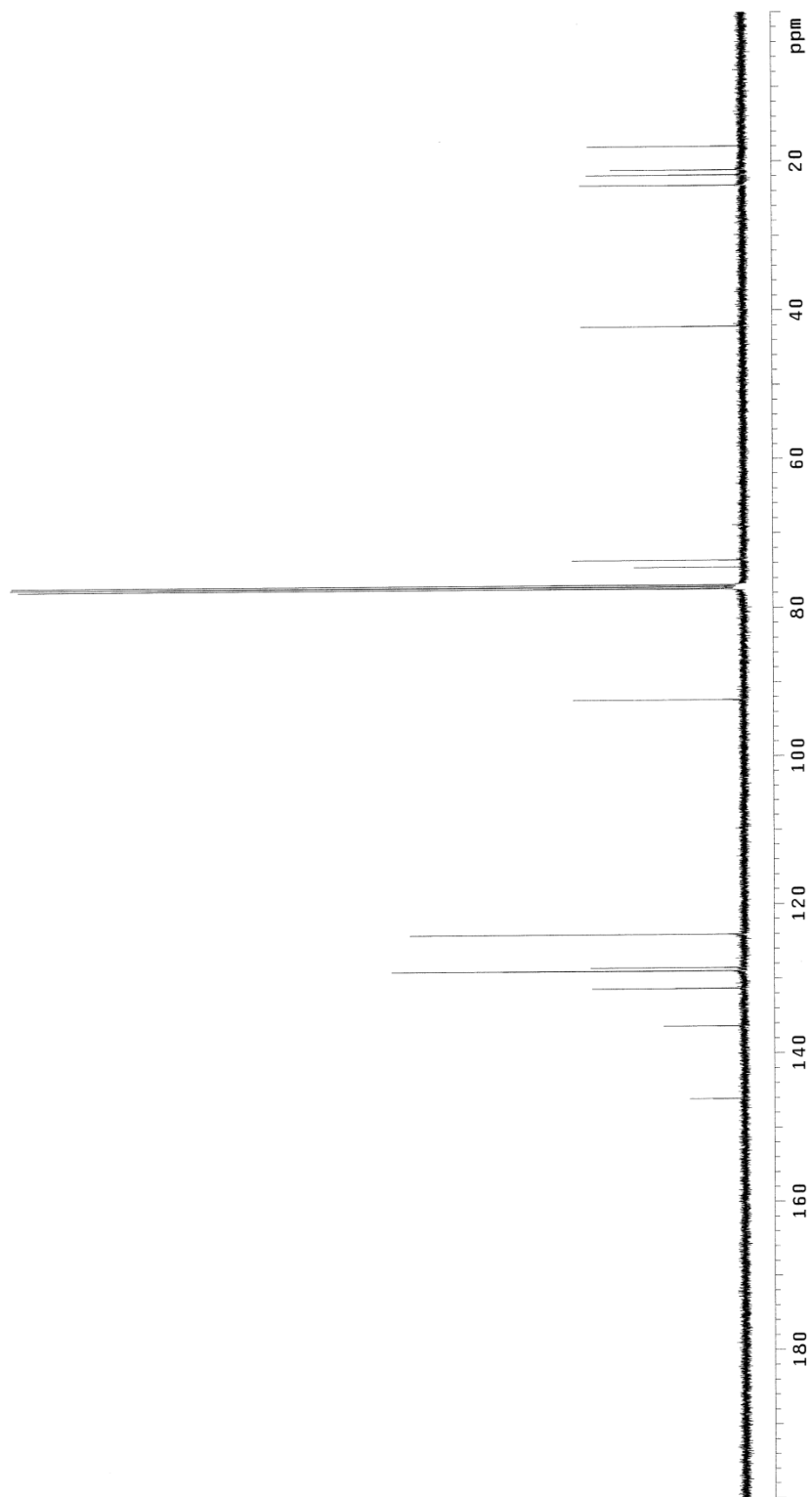
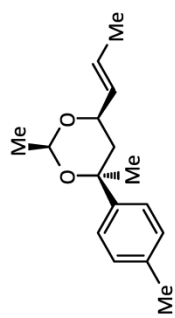


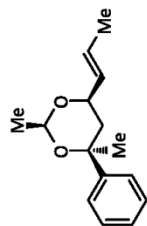
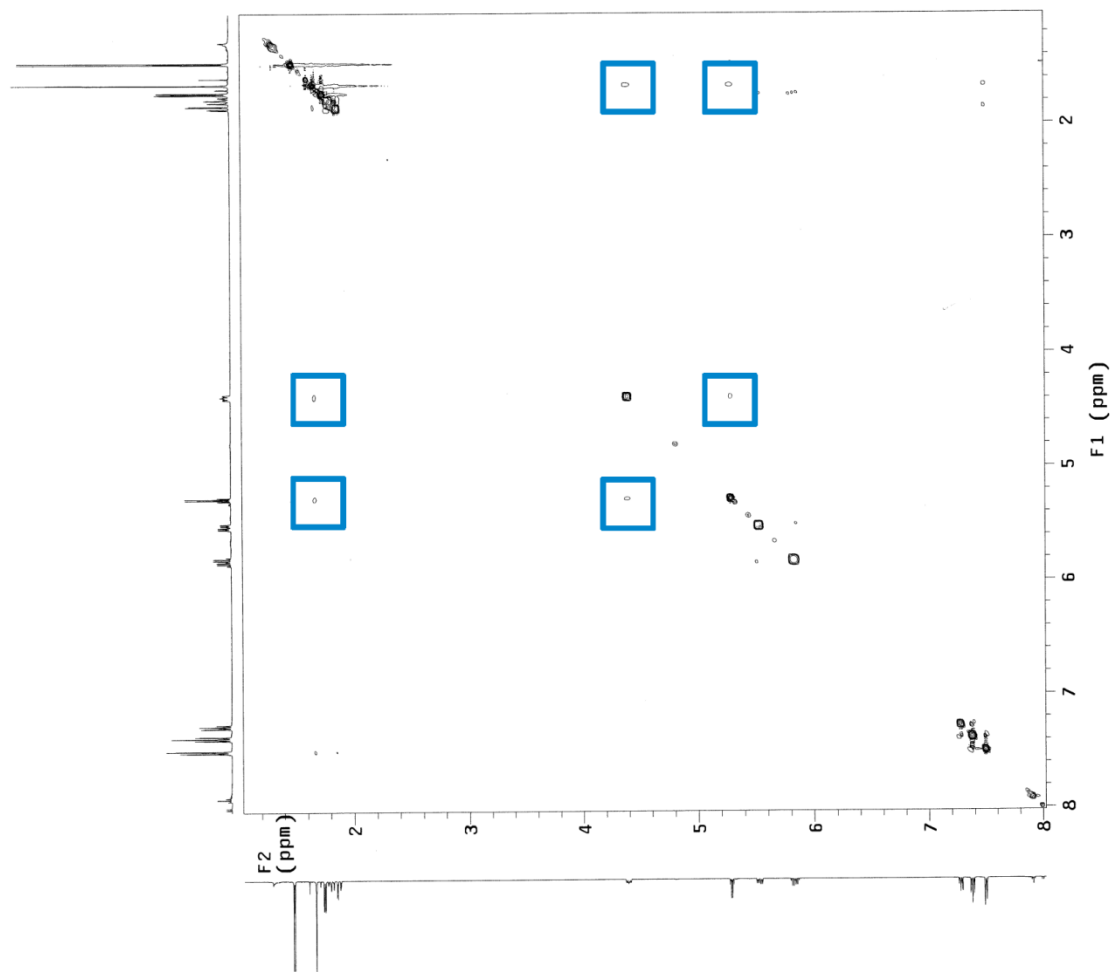


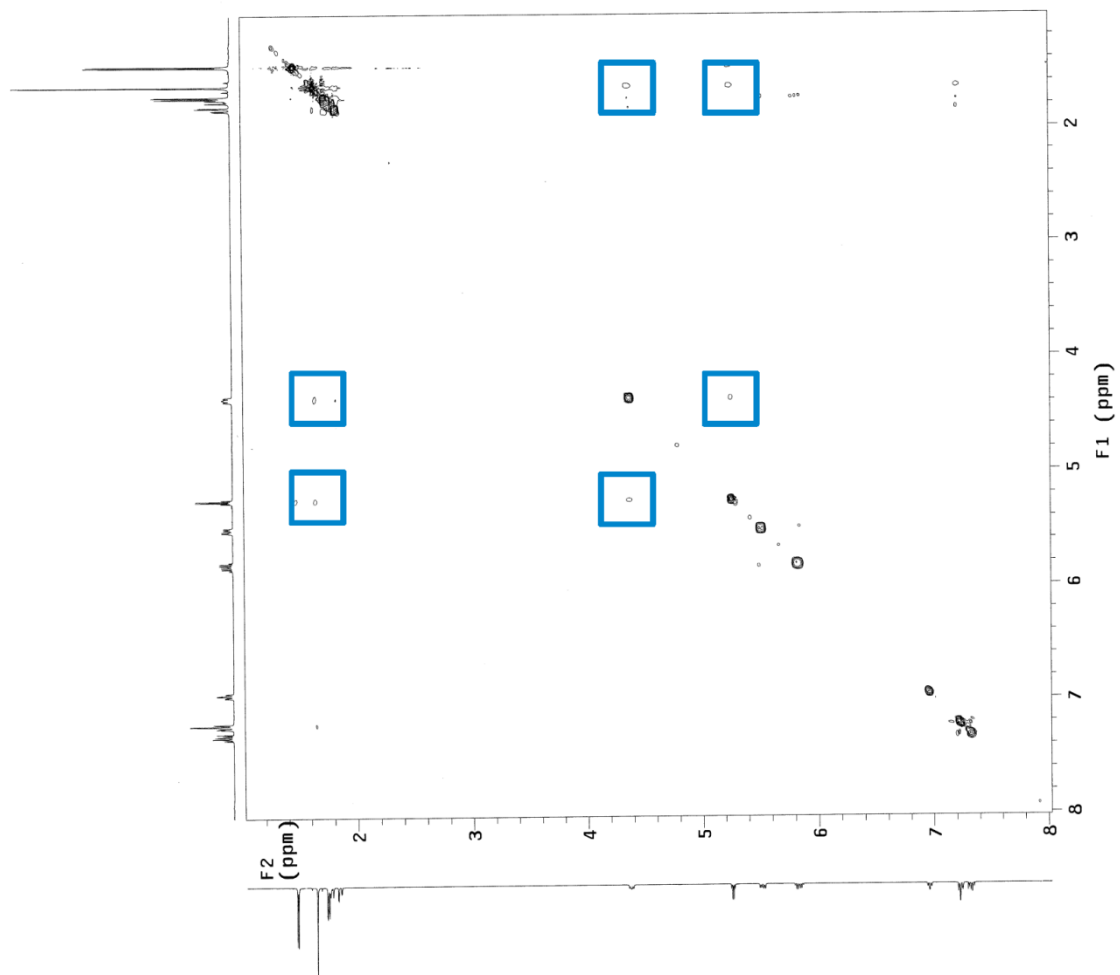


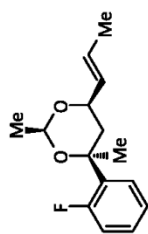
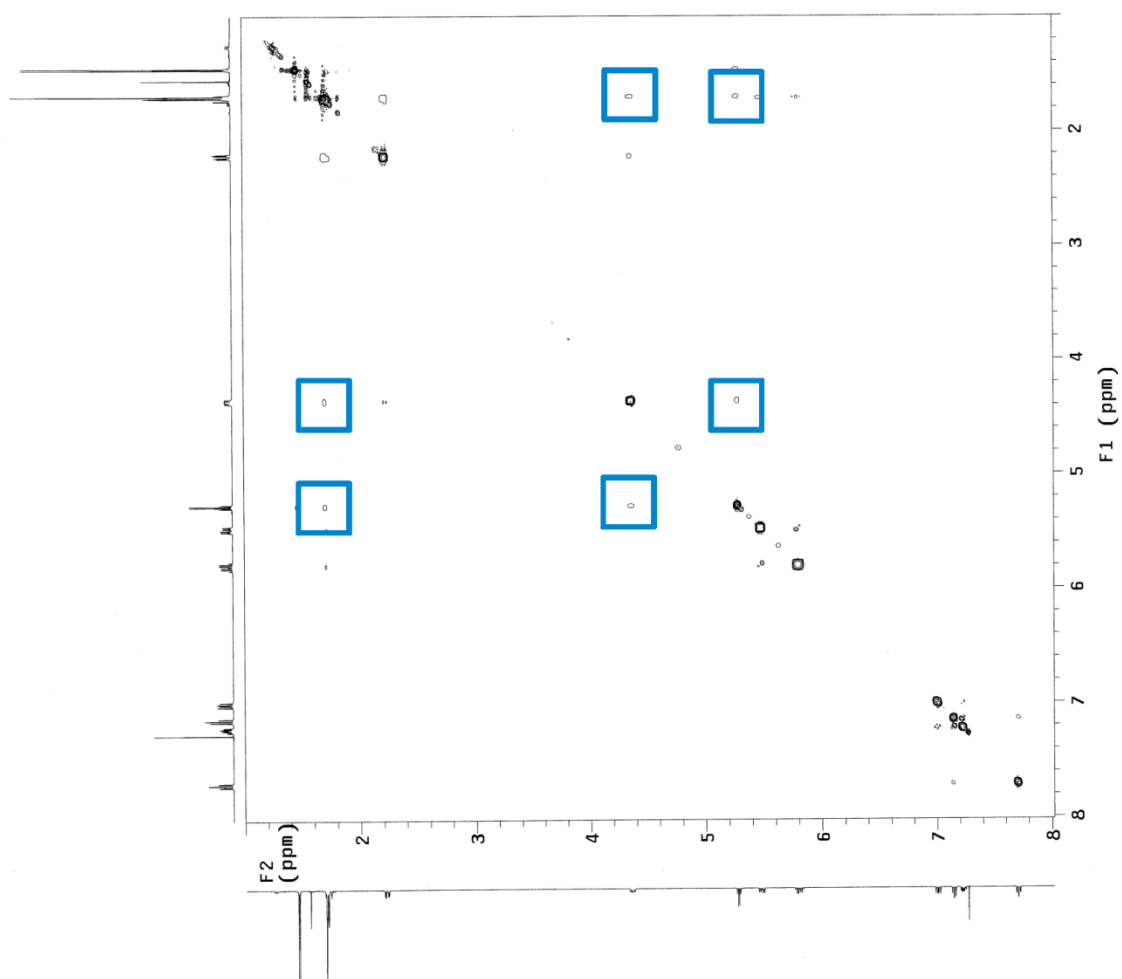


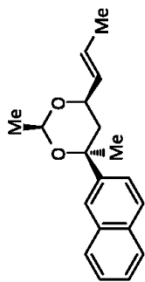
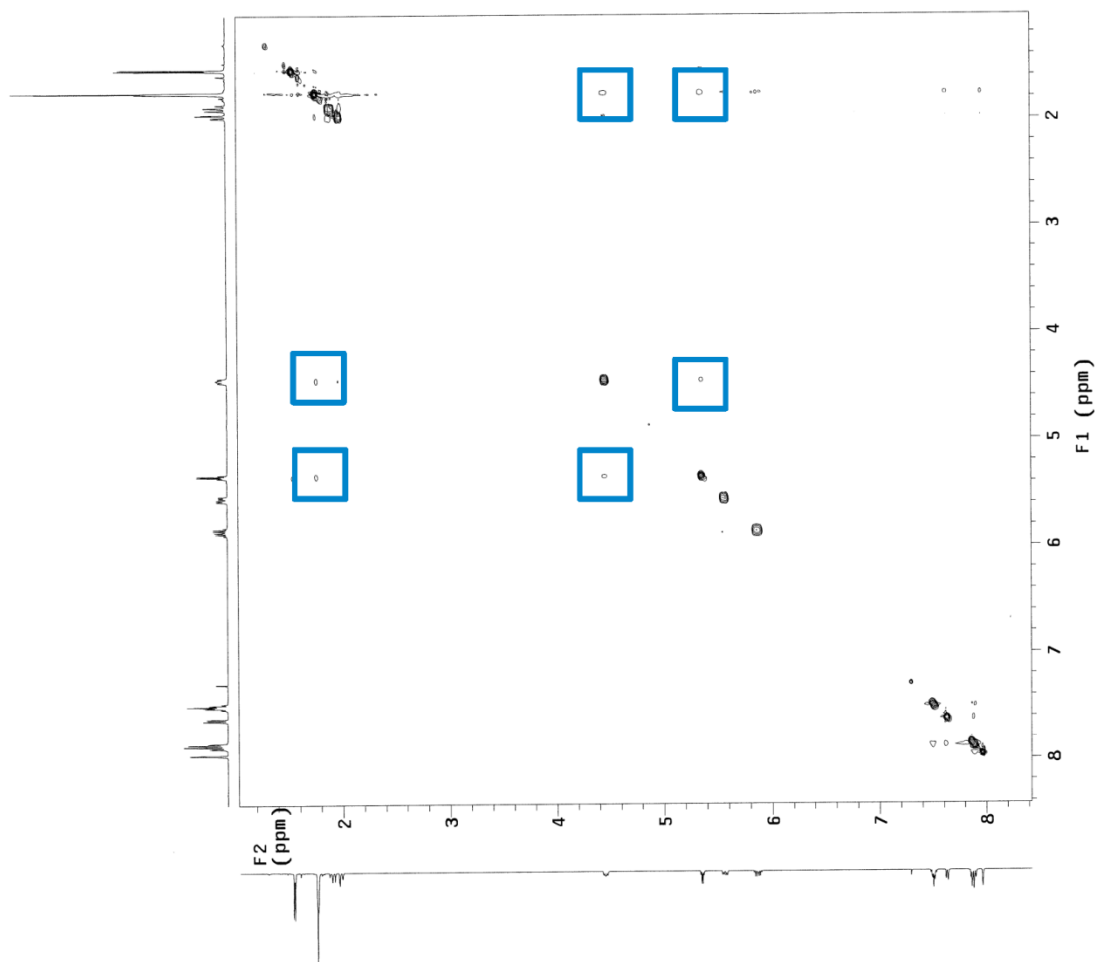


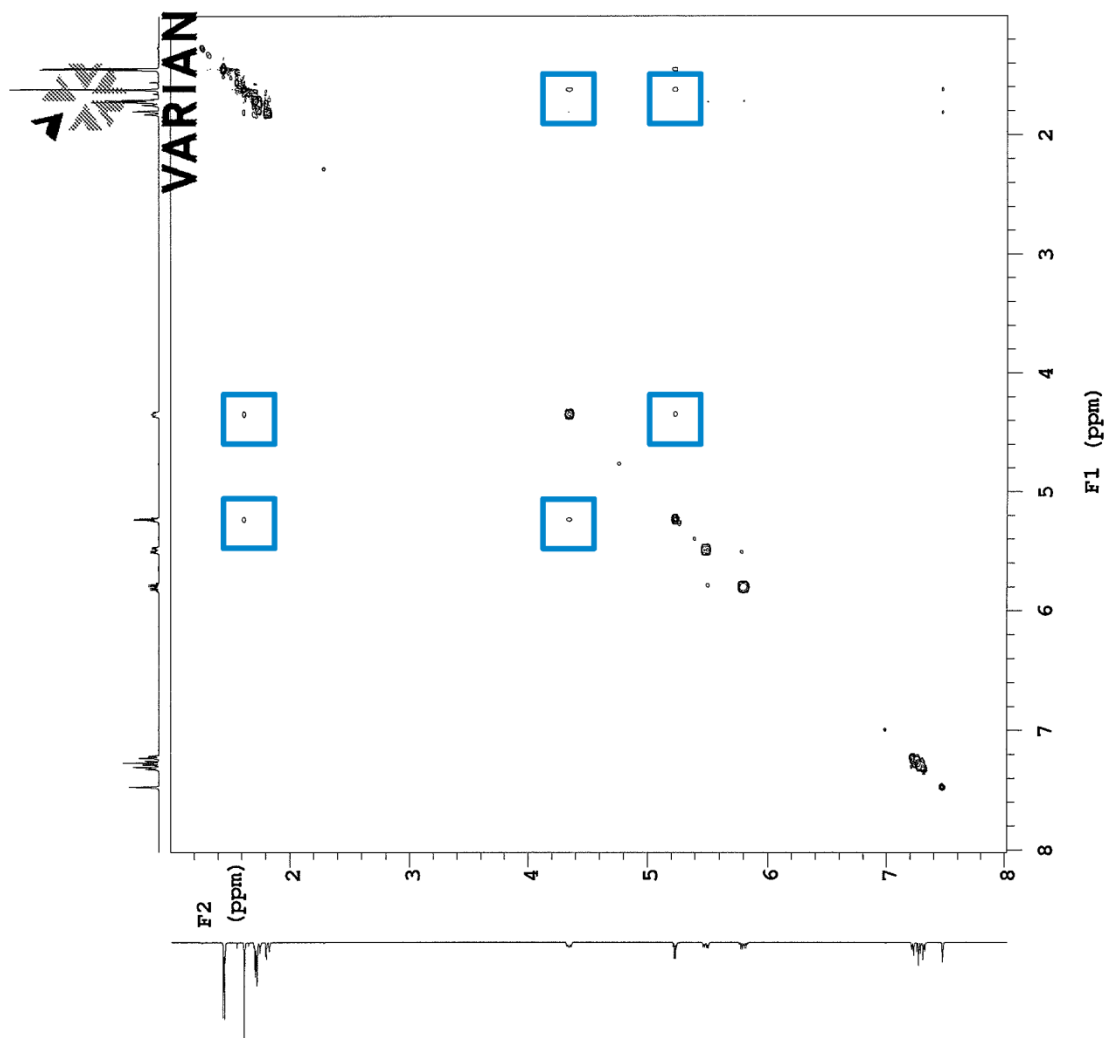


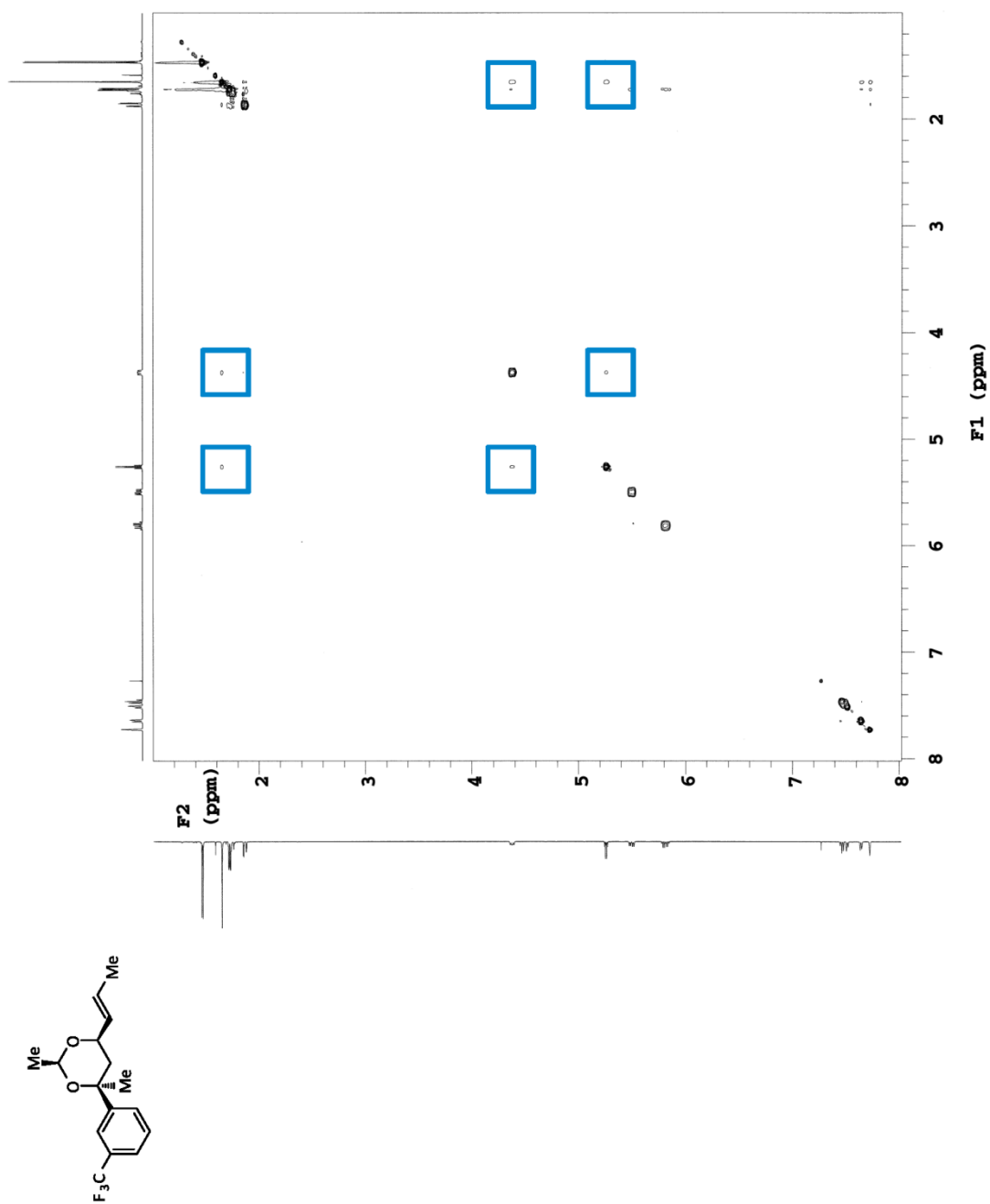


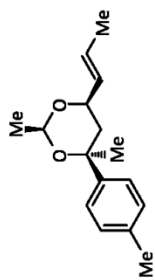
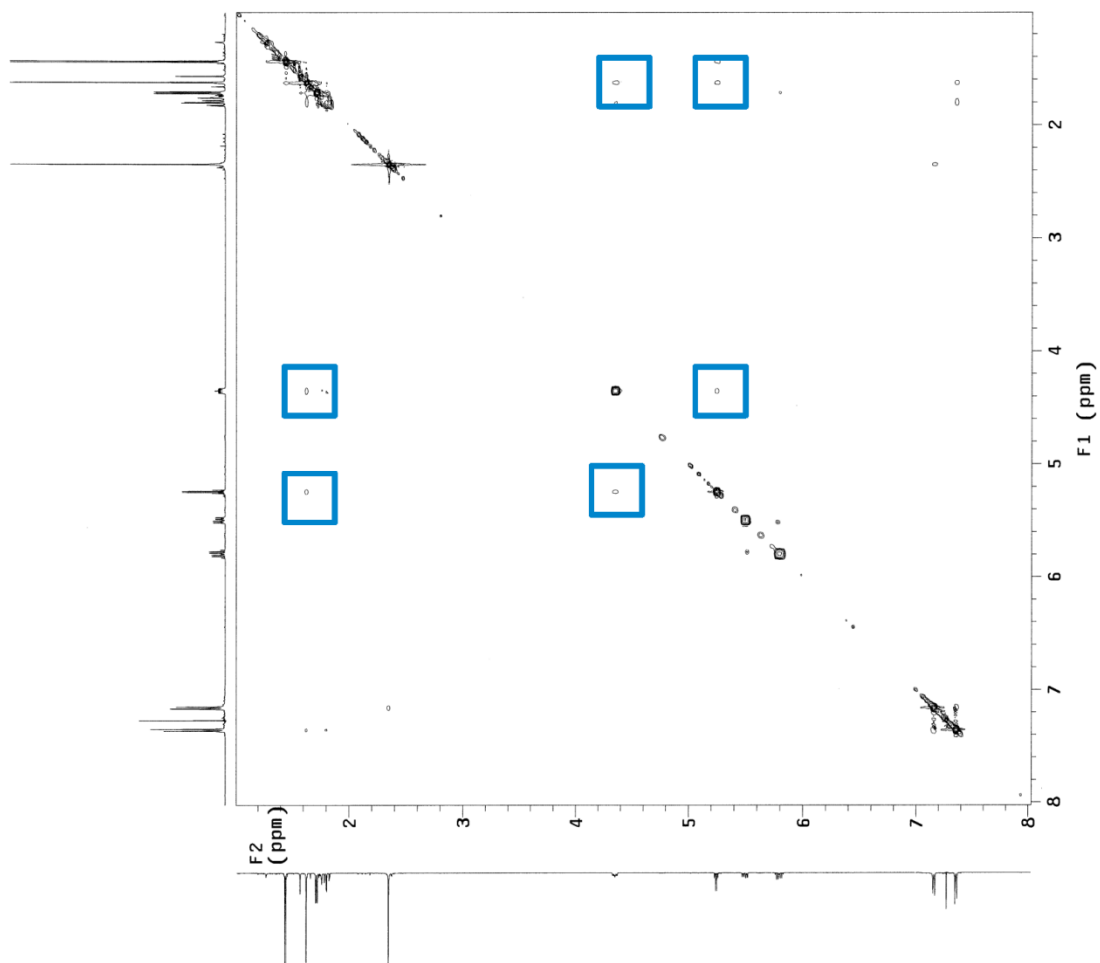


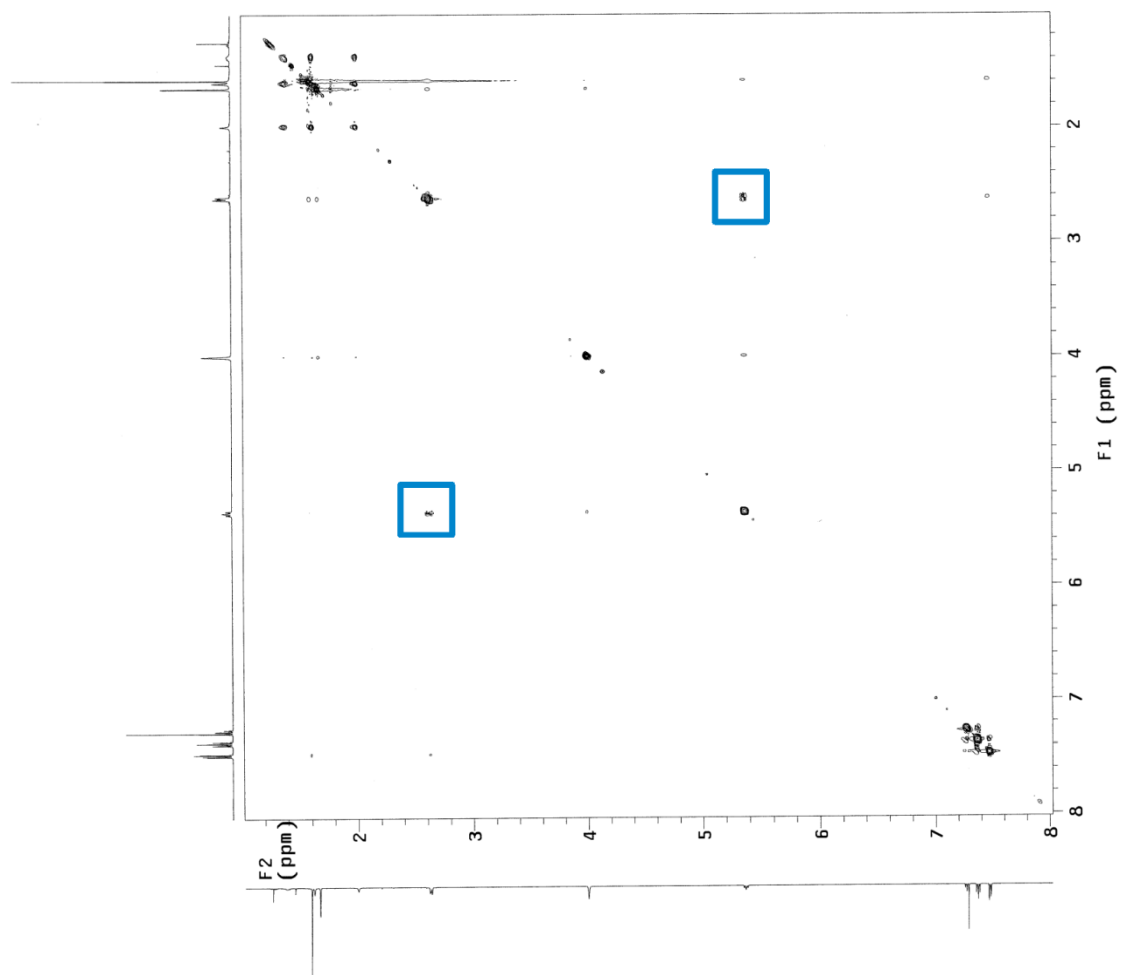
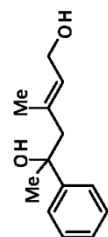












Chapter 5. Site-Selective Functionalization of a Bowl-Shaped Polycyclic Aromatic Hydrocarbon (PAH)

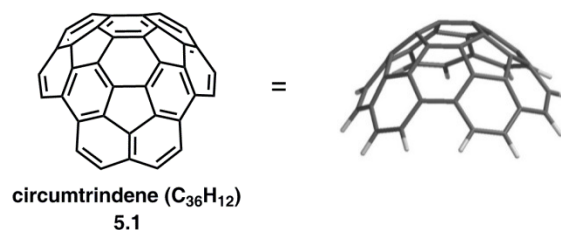
5.1. Introduction to Circumtrindene (C₃₆H₁₂)

Open geodesic polycyclic aromatic hydrocarbons (PAHs), which map onto the surfaces of fullerenes, represent a unique class of non-planar π -conjugated molecules.^{1,2} Circumtrindene (5.1, Figure 5.1), one of the largest known open geodesic polyarenes, exhibits fullerene-like reactivity at the interior carbon atoms, while it still possesses the reactivity of a planar polycyclic aromatic hydrocarbon (PAH) at the edge carbons. Among various chemical modification methods for such polyarenes, covalent functionalization plays an important role in altering their chemical and physical properties, as demonstrated in the chemistry of fullerenes, carbon nanotubes, and their fragments.^{3,4,5}

¹ For reviews, see: (a) Tsefrikas, V. M.; Scott, L. T., "Geodesic Polyarenes by Flash Vacuum Pyrolysis," *Chemical Reviews* **2006**, *106*, 4868-4884. (b) Wu, Y.-T.; Siegel, J. S., "Aromatic Molecular-Bowl Hydrocarbons: Synthetic Derivatives, Their Structures, and Physical Properties," *Chemical Reviews* **2006**, *106*, 4843-4867.

² (a) Kawase, T.; Kurata, H., "Ball-, Bowl-, and Belt-Shaped Conjugated Systems and Their Complexing Abilities: Exploration of the Concave-Convex π - π Interaction," *Chemical Reviews* **2006**, *106*, 5250-5273. (b) Sygula, A., "Chemistry on a Half-Shell: Synthesis and Derivatization of Buckybowls," *European Journal of Organic Chemistry* **2011**, *2011*, 1611-1625.

³ For fullerene functionalizations, see: (a) Maggini, M.; Scorrano, G.; Prato, M., "Addition of Azomethine Ylides to C₆₀: Synthesis, Characterization, and Functionalization of Fullerene Pyrrolidines," *Journal of the American Chemical Society* **1993**, *115*, 9798-9799. (b) Diederich, F.; Thilgen, C., "Covalent Fullerene Chemistry," *Science* **1996**, *271*, 317-324.

Figure 5.1 Circumtrindene ($C_{36}H_{12}$)

In Sections 5.4 and 5.5 of this chapter, synthetic methods to functionalize a fullerene fragment, circumtrindene, via site-selective covalent bond formation are described (Scheme 5.1). The Bingel–Hirsch⁶ and Prato^{3a, 7} reactions — traditional methods for fullerene functionalization — of circumtrindene afford circumtrindene derivatives with one of the interior C–C bonds modified. On the other hand, one of the most common classes of aromatic reactions, electrophilic substitution, leads to functionalization on the rim of circumtrindene. This peripheral functionalization was utilized to extend the π system of the

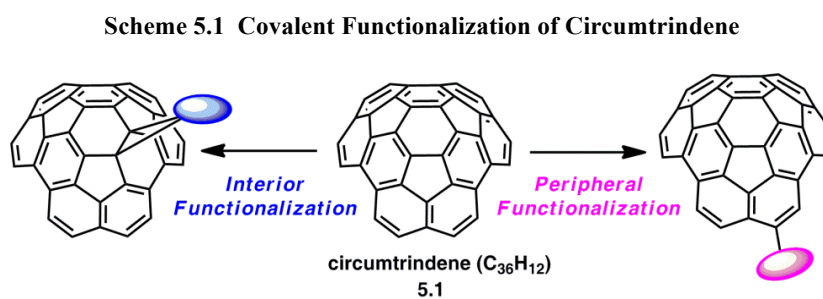
⁴ (a) Thilgen, C.; Herrmann, A.; Diederich, F., "The Covalent Chemistry of Higher Fullerenes: C_{70} and Beyond," *Angewandte Chemie International Edition* **1997**, *36*, 2268-2280. (b) Guldi, D. M.; Prato, M., "Excited-State Properties of C_{60} Fullerene Derivatives," *Accounts of Chemical Research* **2000**, *33*, 695-703.

⁵ For carbon nanotube functionalizations, see: (a) Hirsch, A., "Functionalization of Single-Walled Carbon Nanotubes," *Angewandte Chemie International Edition* **2002**, *41*, 1853-1859. (b) Dyke, C. A.; Tour, J. M., "Covalent Functionalization of Single-Walled Carbon Nanotubes for Materials Applications," *The Journal of Physical Chemistry A* **2004**, *108*, 11151-11159. (c) Banerjee, S.; Hemraj-Benny, T.; Wong, S. S., "Covalent Surface Chemistry of Single-Walled Carbon Nanotubes," *Advanced Materials* **2005**, *17*, 17-29.

⁶ (a) Bingel, C., "Cyclopropanierung Von Fullerenen," *Chemische Berichte* **1993**, *126*, 1957-1959. (b) Camps, X.; Hirsch, A., "Efficient Cyclopropanation of C_{60} Starting from Malonates," *Journal of the Chemical Society, Perkin Transactions 1* **1997**, 1595-1596.

⁷ (a) Prato, M.; Maggini, M., "Fulleropyrrolidines: A Family of Full-Fledged Fullerene Derivatives," *Accounts of Chemical Research* **1998**, *31*, 519-526. (b) Prato, M.; Da Ros, T.; Maggini, M.; Guldi, D. M.; Pasimeni, L. In *Current Trends in Organic Synthesis*; Springer, 1999. (c) Tagmatarchis, N.; Prato, M., "The Addition of Azomethine Ylides to [60]Fullerene Leading to Fulleropyrrolidines," *Synlett* **2003**, *2003*, 0768-0779.

polyarene with subsequent coupling reactions and to explore the magnetic and stereoelectronic environment of the concave/convex space around the compound. For both classes of functionalization, theoretical investigations (NBO analysis, GIAO method, electrostatic potentials, etc.) are conducted to support the experimental results.



Furthermore, circumtrindene can be also functionalized via noncovalent bond formation. Noncovalent functionalization can be achieved by reduction of circumtrindene or by metal(I) complexation of circumtrindene. This method will be presented in Section 5.5 of this chapter.

5.2. Background

5.2.1. Nonplanar Polycyclic Aromatic Hydrocarbons (PAHs)

Investigations into the structures and properties of geodesic polyarenes, which began with the synthesis of corannulene (**5.2**, C₂₀H₁₀) in 1966,^{8, 9, 10} were greatly stimulated by the discovery of buckminsterfullerene C₆₀ (**5.3**) in 1985 (Figure 5.2).¹¹ Whereas fullerenes comprising complete three-dimensional polyhedra are classified as “closed” geodesic polyarenes, subunits of fullerenes that lack one or more of the rings but remain curved are regarded as “open” geodesic polyarenes. The fullerenes constitute one family of geodesic polyarenes, and bowl-shaped polycyclic aromatic hydrocarbons (PAHs) constitute another.

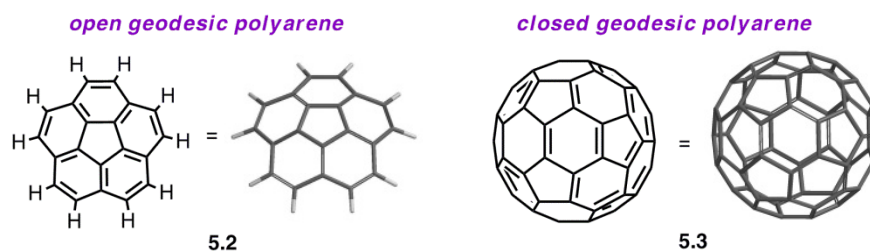
⁸ For the original synthesis, see: (a) Barth, W. E.; Lawton, R. G., "Dibenzo[ghi,mno]Fluoranthene," *Journal of the American Chemical Society* **1966**, *88*, 380-381. (b) Lawton, R. G.; Barth, W. E., "Synthesis of Corannulene," *Journal of the American Chemical Society* **1971**, *93*, 1730-1745.

⁹ For improved syntheses, see: (a) Scott, L. T.; Hashemi, M. M.; Meyer, D. T.; Warren, H. B., "Corannulene. A Convenient New Synthesis," *Journal of the American Chemical Society* **1991**, *113*, 7082-7084. (b) Scott, L. T.; Hashemi, M. M.; Bratcher, M. S., "Corannulene Bowl-to-Bowl Inversion Is Rapid at Room Temperature," *Journal of the American Chemical Society* **1992**, *114*, 1920-1921. (c) Borchardt, A.; Fuchicello, A.; Kilway, K. V.; Baldrige, K. K.; Siegel, J. S., "Synthesis and Dynamics of the Corannulene Nucleus," *Journal of the American Chemical Society* **1992**, *114*, 1921-1923.

¹⁰ (a) Zimmermann, G.; Nuechter, U.; Hagen, S.; Nuechter, M., "Synthesis and Hydroxyolysis of Bis-Trimethylsilyl Substituted 3-(4H-Cyclopenta[def]Phenanthrylidene)-1,4-Pentadiyne. A New Route to Corannulene," *Tetrahedron Letters* **1994**, *35*, 4747-4750. (b) Liu, C. Z.; Rabideau, P. W., "Corannulene Synthesis via the Pyrolysis of Silyl Vinyl Ethers," *Tetrahedron Letters* **1996**, *37*, 3437-3440.

¹¹ Kroto, H. W.; Heath, J. R.; O'Brien, S. C.; Curl, R. F.; Smalley, R. E., "C₆₀: Buckminsterfullerene," *Nature* **1985**, *318*, 162-163.

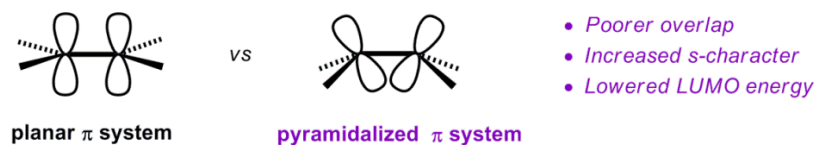
Figure 5.2 Prototypical Open and Closed Geodesic Polyarenes



Both open and closed geodesic polyarenes are characterized by curved π systems composed of pyramidalized carbon atoms (Figure 5.3).¹² Pyramidalization has several consequences. The less parallel the alignment of π -orbitals, the poorer will be their overlap, which will lead to weaker π bonds. Weakening a π bond tends to raise the energy of the bonding π molecular orbitals (MOs) and lower the antibonding π^* MOs. Another important consequence of pyramidalization is the mixing of s-orbital character with the p-orbital that makes up the π system. This lowers the energy of each atomic orbital and thereby lowers the energy of all the derived π MOs, including both the HOMO (highest occupied molecular orbital) and LUMO (lowest unoccupied molecular orbital).¹³ While this lowering of the HOMO offsets the tendency of the HOMO to rise as a consequence of poorer π overlap, the lowering of the LUMO due to the hybridization change amplifies the lowering imposed by the weaker π bond. A major consequence of curvature, therefore, is a substantial lowering of the energy of the LUMO with relatively little change in the HOMO.

¹² Scott, L. T.; Bronstein, H. E.; Preda, D. V.; Ansems, R. B.; Bratcher, M. S.; Hagen, S., "Geodesic Polyarenes with Exposed Concave Surfaces," *Pure and Applied Chemistry* **1999**, *71*, 209-220.

¹³ Fleming, I. *Molecular Orbitals and Organic Chemical Reactions*; Reference Edition; Wiley: Hoboken N.J., 2010.

Figure 5.3 Planar vs Pyramidalized π System.

The degree of the pyramidalization for these types of molecules can be measured quantitatively by π -orbital axis vector (POAV) angles.¹⁴ Figure 5.4 shows the POAV angles for some nonplanar aromatic compounds that have the same patterns of pentagons and hexagons as those found in fullerene- C_{60} . The POAV angles of C_{60} (5.3),¹⁵ corannulene (5.2),¹⁶ and diindenochrysene (5.4)¹⁷ are 11.6° ($101.6^\circ - 90^\circ = 11.6^\circ$ pyramidalization), 8.3° , and 9.0° , respectively.^{18, 19} The distortion of the π system in the open geodesic polyarenes (5.2 and 5.4)

¹⁴ (a) Haddon, R. C., "Rehybridization And π -Orbital Overlap in Nonplanar Conjugated Organic Molecules: π -Orbital Axis Vector (POAV) Analysis and Three-Dimensional Hückel Molecular Orbital (3D-HMO) Theory," *Journal of the American Chemical Society* **1987**, *109*, 1676-1685. (b) Haddon, R., "Pyramidalization: Geometrical Interpretation of the Pi-Orbital Axis Vector in Three Dimensions," *Journal of Physical Chemistry* **1987**, *91*, 3719-3720. (c) Haddon, R., "Measure of Nonplanarity in Conjugated Organic Molecules: Which Structurally Characterized Molecule Displays the Highest Degree of Pyramidalization?," *Journal of the American Chemical Society* **1990**, *112*, 3385-3389.

¹⁵ (a) Haddon, R. C., "Chemistry of the Fullerenes: The Manifestation of Strain in a Class of Continuous Aromatic Molecules," *Science* **1993**, *261*, 1545-1550. (b) Haddon, R. C., " C_{60} : Sphere or Polyhedron?," *Journal of the American Chemical Society* **1997**, *119*, 1797-1798.

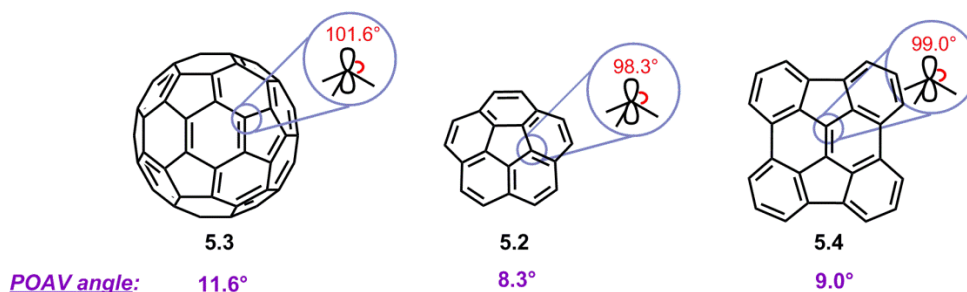
¹⁶ Petrukhina, M. A.; Andreini, K. W.; Mack, J.; Scott, L. T., "X-Ray Quality Geometries of Geodesic Polyarenes from Theoretical Calculations: What Levels of Theory Are Reliable?," *The Journal of Organic Chemistry* **2005**, *70*, 5713-5716.

¹⁷ Bronstein, H. E.; Choi, N.; Scott, L. T., "Practical Synthesis of an Open Geodesic Polyarene with a Fullerene-Type 6:6-Double Bond at the Center: Diindeno[1,2,3,4-defg; 1',2',3',4'-mnop]Chrysene," *Journal of the American Chemical Society* **2002**, *124*, 8870-8875.

¹⁸ For related studies, see: (a) Scott, L., " π -Orbital Conjugation and Rehybridization Bridged Annulenes and Deformed Molecules in General: π -Orbital Axis Vector Analysis," **1986**. (b) Haddon, R. C., " π -Electrons in Three Dimensions," *Accounts of Chemical Research* **1988**, *21*, 243-249.

is much less severe than that in C_{60} , as indicated by their π -orbital axis vector (POAV) angles. Furthermore, it is known that the barrier for bowl-to-bowl inversion in corannulene (10.2 kcal/mol at $-64\text{ }^{\circ}\text{C}$)^{9b} is low enough that its inversion is rapid even at room temperature. The inversion barrier of diindenochoyrene (5.4) was calculated to be 6.7 kcal/mol at ambient temperature (B3LYP/6-311G**).²⁰

Figure 5.4 POAV Angles of C_{60} -Fullerene, Corannulene, and Diindenochoyrene



5.2.2. Preparation of Nonplanar PAHs

Considerable effort has been made in a number of research groups to prepare fullerenes as well as fullerene fragments and to illuminate their chemical/physical properties.^{1, 21} Several laboratories, including our laboratory, have been particularly

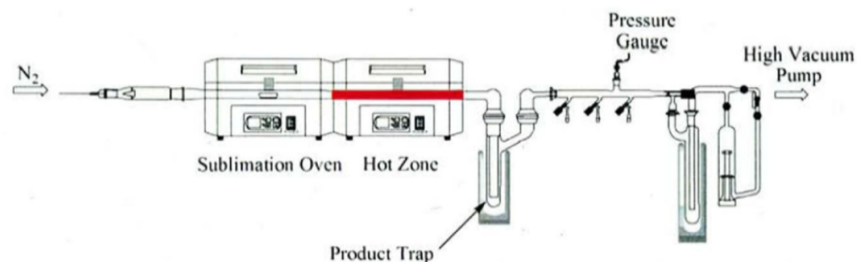
¹⁹ (a) Bühl, M.; Hirsch, A., "Spherical Aromaticity of Fullerenes," *Chemical Reviews* **2001**, *101*, 1153-1183. (b) Haddon, R., "Comment on the Relationship of the Pyramidalization Angle at a Conjugated Carbon Atom to the Sigma Bond Angles," *Journal of Physical Chemistry A* **2001**, *105*, 4164-4165.

²⁰ Scott, L. T.; Petrukhina, M. A. *Fragments of Fullerenes and Carbon Nanotubes Designed Synthesis, Unusual Reactions, and Coordination Chemistry*; John Wiley & Sons: Hoboken NJ, 2012.

²¹ (a) Haley, M. M.; Tykwinski, R. R. *Carbon-Rich Compounds: From Molecules to Materials*; Wiley-VCH; John Wiley : Weinheim Chichester, 2006. (b) Hirsch, A.; Brettreich, M.; Hirsch, A. *Fullerenes Chemistry and Reactions*; Wiley-VCH: Weinheim, 2005.

interested in synthesizing geodesic polyarenes using a flash vacuum pyrolysis (FVP) method (Figure 5.5).^{1a} An FVP experiment involves a succinct exposure of the precursor sublimed into a hot zone under vacuum and the succeeding capture of the products in a cold trap.²² The abnormally high temperatures (ca. 1100 °C) in FVP enable reactants to overcome high activation energies by providing sufficient thermal energy. Moreover, these exceptionally high temperatures favor intramolecular reactions over intermolecular ones by enhancing the effect of the entropic term in the Gibbs free energies equation ($\Delta G^\ddagger = \Delta H^\ddagger - T\Delta S^\ddagger$).

Figure 5.5 Flash Vacuum Pyrolysis Apparatus



The FVP approach takes advantage of the fact that the normal out-of-plane deformation of simple planar polyarenes becomes greatly amplified under conditions of flash vacuum pyrolysis. The initial synthesis of a $C_{36}H_{12}$ bucky bowl, circumtrindene (**5.1**), was accomplished by the FVP method.²³ Moreover, FVP is employed to prepare numerous

²² Brown, R. F., "Are Flash Pyrolytic Reactions Useful?," *Pure and Applied Chemistry* **1990**, 62, 1981-1986.

²³ Scott, L. T.; Bratcher, M. S.; Hagen, S., "Synthesis and Characterization of a $C_{36}H_{12}$ Fullerene Subunit," *Journal of the American Chemical Society* **1996**, 118, 8743-8744.

other highly-curved polyarenes, including corannulene (5.2),^{9a} fullerene-C₆₀ (5.3),²⁴ dibenzo[*a,g*]corannulene (5.5, C₂₈H₁₄),²⁵ hemifullerene-C₃ (5.6, C₃₀H₁₂),²⁶ triphenyleno[1,12-*bcd*:4,5-*b'c'd'*:8,9-*b''c''d''*]trithiophene (5.7, C₁₈H₆S₃);²⁷ some of the structures of these molecules are shown in Figure 5.6. However, the synthesis of these strained polynuclear aromatic hydrocarbons is not limited to FVP. Non-pyrolytic methods to access fullerene fragments were first developed by the Siegel group;²⁸ then, several other non-pyrolytic methods were reported by our and other laboratories.^{29, 30, 31}

²⁴ (a) Scott, L. T.; Boorum, M. M.; McMahon, B. J.; Hagen, S.; Mack, J.; Blank, J.; Wegner, H.; de Meijere, A., "A Rational Chemical Synthesis of C₆₀," *Science* **2002**, *295*, 1500-1503. (b) Scott, L. T., "Methods for the Chemical Synthesis of Fullerenes," *Angewandte Chemie International Edition* **2004**, *43*, 4994-5007.

²⁵ Reisch, H. A.; Bratcher, M. S.; Scott, L. T., "Imposing Curvature on a Polyarene by Intramolecular Palladium-Catalyzed Arylation Reactions: A Simple Synthesis of Dibenzo[*a,g*]Corannulene," *Organic Letters* **2000**, *2*, 1427-1430.

²⁶ (a) Abdourazak, A. H.; Marcinow, Z.; Sygula, A.; Sygula, R.; Rabideau, P. W., "Buckybowls 2. Toward the Total Synthesis of Buckminsterfullerene (C₆₀): Benz[5,6]-as-indaceno[3,2,1,8,7-mnopqr]indeno[4,3,2,1-cdef]chrysene," *Journal of the American Chemical Society* **1995**, *117*, 6410-6411. (b) Hagen, S.; Bratcher, M. S.; Erickson, M. S.; Zimmermann, G.; Scott, L. T., "Novel Syntheses of Three C₃₀H₁₂ Bowl-Shaped Polycyclic Aromatic Hydrocarbons," *Angewandte Chemie International Edition* **1997**, *36*, 406-408.

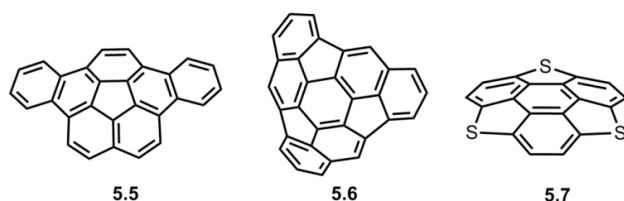
²⁷ Imamura, K.; Takimiya, K.; Otsubo, T.; Aso, Y., "Triphenyleno[1,12-*bcd*:4,5-*b'c'd'*:8,9-*b''c''d''*] Trithiophene: The First Bowl-Shaped Heteroaromatic," *Chemical Communications* **1999**, 1859-1860.

²⁸ Seiders, T. J.; Elliott, E. L.; Grube, G. H.; Siegel, J. S., "Synthesis of Corannulene and Alkyl Derivatives of Corannulene," *Journal of the American Chemical Society* **1999**, *121*, 7804-7813.

²⁹ For selected examples, see: (a) Sygula, A.; Xu, G.; Marcinow, Z.; Rabideau, P. W., "Buckybowls'—Introducing Curvature by Solution Phase Synthesis," *Tetrahedron* **2001**, *57*, 3637-3644. (b) Marcinow, Z.; Grove, D. I.; Rabideau, P. W., "Synthesis of a New C₃₂H₁₂ Bowl-Shaped Aromatic Hydrocarbon: Acenaphtho [3,2,1,8-*Ijklm*]Diindeno[4,3,2,1-cdef:1',2',3',4'-*pqra*]Triphenylene," *The Journal of Organic Chemistry* **2002**, *67*, 3537-3539.

³⁰ (a) Sygula, A.; Karlen, S. D.; Sygula, R.; Rabideau, P. W., "Formation of the Corannulene Core by Nickel-Mediated Intramolecular Coupling of Benzyl and Benzylidene Bromides: A Versatile Synthesis of Dimethyl 1,2-Corannulene Dicarboxylate," *Organic Letters* **2002**, *4*, 3135-3137. (b) Steinberg, B. D.; Jackson, E. A.; Filatov, A. S.; Wakamiya, A.; Petrukhina, M. A.; Scott, L. T., "Aromatic π -Systems More Curved Than

Figure 5.6 Selected Examples of Geodesic Polyarenes Synthesized by FVP



5.2.3. Functionalization of Nonplanar PAHs

In addition to the preparation of these molecules, the functionalization of such nonplanar PAHs — via both covalent and noncovalent bonding — has attracted significant attention in recent years. The functionalization of fullerenes^{32, 33} has been extensively explored following the development of bulk preparation methods for fullerenes in 1990.^{34, 35}

C₆₀. The Complete Family of All Indenocorannulenes Synthesized by Iterative Microwave-Assisted Intramolecular Arylations," *Journal of the American Chemical Society* **2009**, *131*, 10537-10545.

³¹ For sumanene synthesis, see: (a) Sakurai, H.; Daiko, T.; Hirao, T., "A Synthesis of Sumanene, a Fullerene Fragment," *Science* **2003**, *301*, 1878-1878. (b) Higashibayashi, S.; Sakurai, H., "Asymmetric Synthesis of a Chiral Buckybowl, Trimethylsumanene," *Journal of the American Chemical Society* **2008**, *130*, 8592-8593. (c) Amaya, T.; Nakata, T.; Hirao, T., "Synthesis of Highly Strained π -Bowls from Sumanene," *Journal of the American Chemical Society* **2009**, *131*, 10810-10811.

³² For selected early examples, see: (a) Taylor, R.; Walton, D. R., "The Chemistry of Fullerenes," **1993**. (b) Hirsch, A.; Lamparth, I.; Groesser, T.; Karfunkel, H. R., "Regiochemistry of Multiple Additions to the Fullerene Core: Synthesis of a T_h-Symmetric Hexakis Adduct of C₆₀ with Bis(Ethoxycarbonyl)methylene," *Journal of the American Chemical Society* **1994**, *116*, 9385-9386.

³³ (a) Avent, A. G.; Darwish, A. D.; Heimbach, D. K.; Kroto, H. W.; Meidine, M. F.; Parsons, J. P.; Remars, C.; Roers, R.; Ohashi, O.; Taylor, R., "Formation of Hydrides of Fullerene-C₆₀ and Fullerene-C₇₀," *Journal of the Chemical Society, Perkin Transactions 2* **1994**, 15-22. (b) Chiang, L. Y.; Bhonsle, J.; Wang, L.; Shu, S.; Chang, T.; Hwu, J. R., "Efficient One-Flask Synthesis of Water-Soluble [60]Fullerenols," *Tetrahedron* **1996**, *52*, 4963-4972. (c) Diederich, F., "Covalent Fullerene Chemistry," *Pure and Applied Chemistry* **1997**, *69*, 395-400.

³⁴ For selected recent examples, see: (a) Nakamura, Y.; Kato, S. I., "Exohedral Functionalization of Fullerenes and Supramolecular Chemistry," *The Chemical Record* **2011**, *11*, 77-94. (b) Itami, K., "Molecular Catalysis for Fullerene Functionalization," *The Chemical Record* **2011**, *11*, 226-235.

Within 10 years, various covalent functionalization sequences were investigated and are now widely used for the construction of multifunctional architectures with C₆₀ as an integral building unit. Representative synthetic reactions of fullerene-C₆₀ (5.3) include cyclopropanation,⁶ [3+2] cycloaddition,⁷ [4+2] cycloaddition,³⁶ nucleophilic addition,³⁷ and radical addition reactions.³⁸

The two earliest and most widely used reactions, the Bingel–Hirsch reaction and the Prato reaction, are illustrated in Scheme 5.2 and Scheme 5.3. The Bingel–Hirsch reaction⁶ affords a cyclopropanated fullerene (5.8), and the Prato reaction⁷ gives a [3+2] cycloaddition adduct (5.9). In conjunction with covalent functionalization, numerous noncovalent functionalization methods have also been investigated. In particular, the host-guest

³⁵ (a) Zhu, S.-E.; Cheng, X.; Li, Y.-J.; Mai, C.-K.; Huang, Y.-S.; Wang, G.-W.; Peng, R.-F.; Jin, B.; Chu, S.-J., "Study on the Thermal Reactions of [60]Fullerene with Amino Acids and Amino Acid Esters," *Organic & Biomolecular Chemistry* **2012**, *10*, 8720-8729. (b) Kanbur, Y.; Küçükyavuz, Z., "Synthesis and Characterization of Surface Modified Fullerene," *Fullerenes, Nanotubes and Carbon Nanostructures* **2012**, *20*, 119-126.

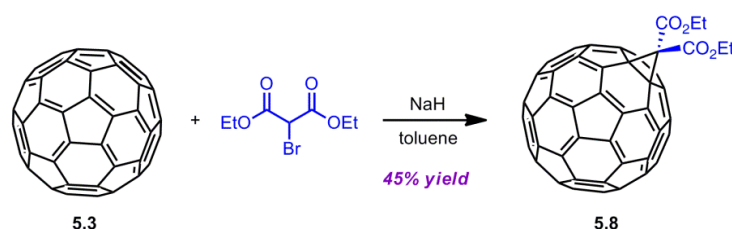
³⁶ Nakamura, Y.; O-kawa, K.; Matsumoto, M.; Nishimura, J., "Separation and Characterization of [60]Fullerene Bisadducts Modified by 4,5-Dimethoxy-O-Quinodimethane," *Tetrahedron* **2000**, *56*, 5429-5434.

³⁷ (a) Anderson, H. L.; Faust, R.; Rubin, Y.; Diederich, F., "Fullerene–Acetylene Hybrids: On the Way to Synthetic Molecular Carbon Allotropes," *Angewandte Chemie International Edition in English* **1994**, *33*, 1366-1368. (b) Komatsu, K.; Murata, Y.; Takimoto, N.; Mori, S.; Sugita, N.; Wan, T. S., "Synthesis and Properties of the First Acetylene Derivatives of C₆₀," *The Journal of Organic Chemistry* **1994**, *59*, 6101-6102.

³⁸ Morton, J. R.; Preston, K. F.; Krusic, P. J.; Hill, S. A.; Wasserman, E., "The Dimerization of Fullerene RC₆₀ Radicals [R = Alkyl]," *Journal of the American Chemical Society* **1992**, *114*, 5454-5455.

chemistry, which involves trapping small molecules (e.g. H₂ or H₂O)^{39, 40} inside the fullerenes, is of significant importance in fullerene chemistry.^{41, 42}

Scheme 5.2 Bingel–Hirsch Reaction of C₆₀-Fullerene

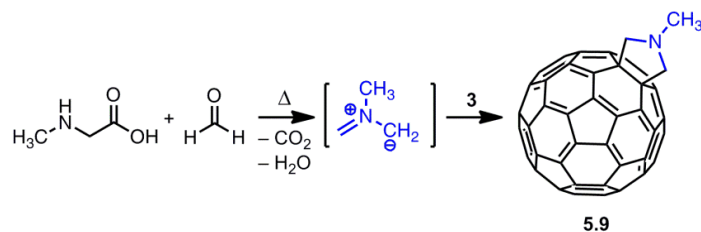


³⁹ For H₂ trapping, see: (a) Komatsu, K.; Murata, M.; Murata, Y., "Encapsulation of Molecular Hydrogen in Fullerene C₆₀ by Organic Synthesis," *Science* **2005**, 307, 238-240. (b) Murata, M.; Murata, Y.; Komatsu, K., "Synthesis and Properties of Endohedral C₆₀ Encapsulating Molecular Hydrogen," *Journal of the American Chemical Society* **2006**, 128, 8024-8033.

⁴⁰ (a) Turro, N. J.; Martí, A. A.; Chen, J. Y.-C.; Jockusch, S.; Lawler, R. G.; Ruzzi, M.; Sartori, E.; Chuang, S.-C.; Komatsu, K.; Murata, Y., "Demonstration of a Chemical Transformation inside a Fullerene. The Reversible Conversion of the Allotropes of H₂@C₆₀," *Journal of the American Chemical Society* **2008**, 130, 10506-10507. (b) Murata, M.; Maeda, S.; Morinaka, Y.; Murata, Y.; Komatsu, K., "Synthesis and Reaction of Fullerene C₇₀ Encapsulating Two Molecules of H₂," *Journal of the American Chemical Society* **2008**, 130, 15800-15801.

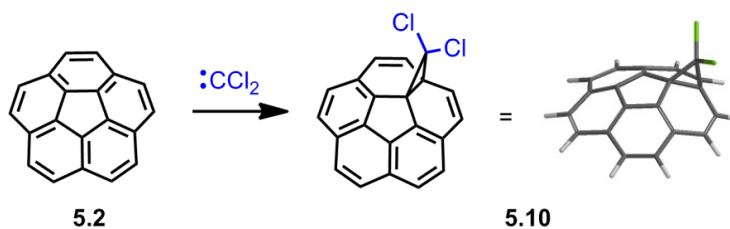
⁴¹ (a) Kurotobi, K.; Murata, Y., "A Single Molecule of Water Encapsulated in Fullerene C₆₀," *Science* **2011**, 333, 613-616. (b) Beduz, C.; Carravetta, M.; Chen, J. Y.-C.; Concistrè, M.; Denning, M.; Frunzi, M.; Horsewill, A. J.; Johannessen, O. G.; Lawler, R.; Lei, X., "Quantum Rotation of Ortho and Para-Water Encapsulated in a Fullerene Cage," *Proceedings of the National Academy of Sciences* **2012**, 109, 12894-12898.

⁴² (a) Li, Y.; Chen, J. Y.-C.; Lei, X.; Lawler, R. G.; Murata, Y.; Komatsu, K.; Turro, N. J., "Comparison of Nuclear Spin Relaxation of H₂O@C₆₀ and H₂@C₆₀ and Their Nitroxide Derivatives," *The Journal of Physical Chemistry Letters* **2012**, 3, 1165-1168. (b) Bucher, D., "Orientational Relaxation of Water Trapped inside C₆₀ Fullerenes," *Chemical Physics Letters* **2012**, 534, 38-42.

Scheme 5.3 Prato Reaction of C₆₀-Fullerene

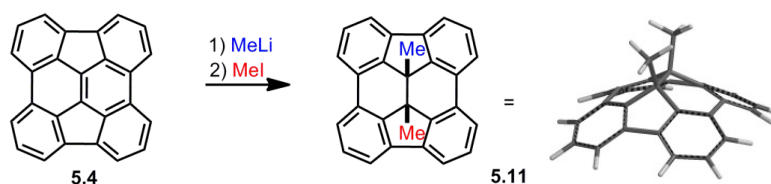
Covalent functionalization involving interior carbon atoms of some open geodesic polyarenes has been investigated by our laboratory.¹² Well-known curved PAHs, corannulene (5.2) and diindeno[1,1-b]chrysene (5.4), have shown fullerene-type reactivities towards carbenes (Scheme 5.4) and nucleophiles (Scheme 5.5). Dichlorocarbene adds to corannulene (5.2) to afford the cyclopropanated product (5.10).⁴³ When 5.4 is reacted with an excess of methyllithium and quenched with methyl iodide, the 1,2-addition product (5.11) is formed.

Scheme 5.4 Carbene Addition to Corannulene



⁴³ Preda, D. V.; Scott, L. T., "Addition of Dihalocarbenes to Corannulene. A Fullerene-Type Reaction," *Tetrahedron Letters* **2000**, *41*, 9633-9637.

Scheme 5.5 Dimethylation of Diindenochrysene



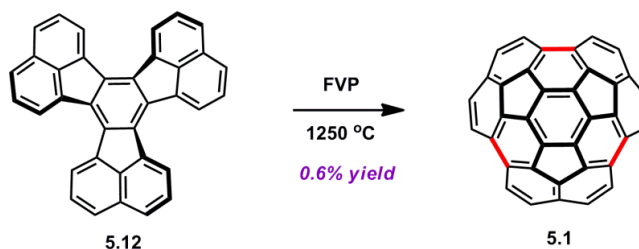
While there are ample examples of covalent chemistry for fullerenes (i.e. closed geodesic polyarenes), covalent functionalization of open geodesic polyarenes other than corannulene is rarely reported.¹² Particularly, conformationally-locked “true” fullerene fragments have never been explored in this regard. As implied in fullerene chemistry, chemical derivatization of buckybowls is expected to play an important role; it would change the electronic, magnetic, mechanical, and chemical properties of the material. In such functionalization reactions, site-selectivity often becomes an issue, since there are multiple places that the reaction can occur. Presented in the following sections (Sections 5.4–5.6) are our efforts toward developments of site-selective functionalization for circumtrindene (5.1), which is one of the most highly-curved fullerene fragments and is composed of 60% of the C₆₀ ball, via covalent bond formation.

5.3. Synthesis of Circumtrindene

5.3.1. Circumtrindene from Decacyclene

In 1996, our laboratory reported that flash vacuum pyrolysis of decacyclene (**5.12**) produces the $C_{36}H_{12}$ bowl, circumtrindene (**5.1**, Scheme 5.6).²³ It was the first synthesis of a fullerene fragment containing more than thirty carbons; it comprises 60% of fullerene C_{60} . For this reaction, temperatures in the range of 1200–1300 °C were required, and the yield was only less than 1%. Also, it was found that the FVP reaction did not produce circumtrindene at a lower temperature, 1100 °C.

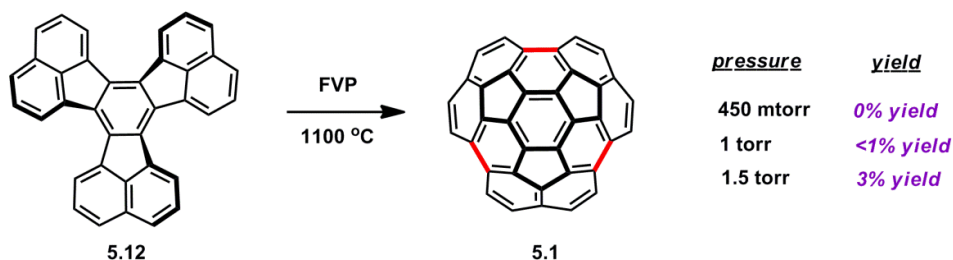
Scheme 5.6 Synthesis of Circumtrindene with FVP



Since the maximum temperature of the oven in our lab was 1100 °C at the time when I started this project, we decided to modify other reaction variables to find a way to access circumtrindene at 1100 °C. The following variables were examined: the pressure, a source of radical generator, and the rate of nitrogen flow. The use of radical generator (by introducing hexane vapor) or modification of the rate of the nitrogen flow was not effective. However, it

turned out that the reaction is sensitive to the strength of the vacuum applied to the system (*i.e.* the pressure of the system); at 1100°C, decacyclene (**5.12**) was converted into circumtrindene (**5.1**) in 3% yield at a raised pressure, 1.5 torr (Scheme 5.7).

Scheme 5.7 Pyrolysis of Circumtrindene at 1100 °C at Different Pressures



With this method, we were able to prepare the starting material for functionalizations of circumtrindene. But, obviously, this approach is not one of the best methods in terms of efficiency and productivity. Furthermore, decacyclene was not a commercially available chemical any more. Both the inefficiency of the method and the unavailability of the starting material (decacyclene) made us think about alternative methods to access circumtrindene, which are presented in the following sections.

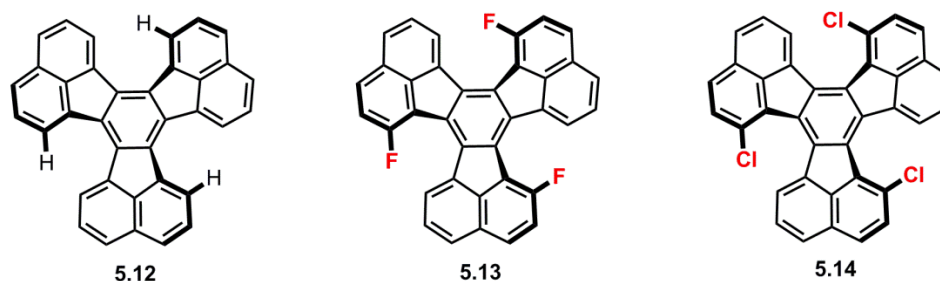
5.3.2. Circumtrindene from Decacyclene Derivatives

5.3.2.1. Synthesis of Halogenated Decacyclenes

We envisioned that the incorporation of substituents capable of generating radicals in the fjord regions might work better for the pyrolysis (Figure 5.7); we planned to synthesize both fluorinated (**5.13**) and chlorinated decacyclenes (**5.14**). These high-

temperature pyrolytic reactions are known to be a radical process in general. Therefore, chlorinated decacyclene is expected to be a better starting material for the cyclization reaction due to the smaller bond dissociation energy of the C–Cl bond than the C–H bond.

Figure 5.7 Incorporation of Halogens in the Fjord Regions

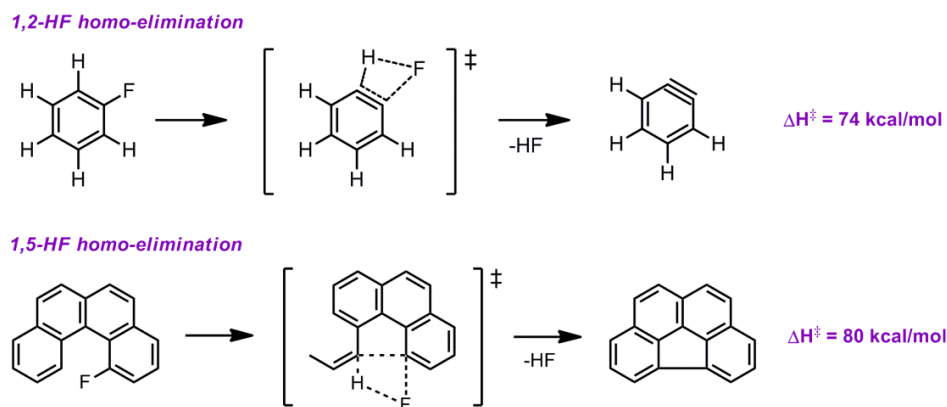


Regarding the fluorinated decacyclene, it has been reported that the activation energy of HF homo-elimination is in the range of 74–80 kcal under FVP conditions for similar aromatic compounds (Scheme 5.8).^{44,45} According to these studies, the fluorinated aromatic compounds do not go through free radical intermediates; the HF is eliminated in a concerted fashion. Therefore, despite the higher bond dissociation energy of HF bond, the FVP of trifluorodecacyclene (**5.13**) is expected to afford circumtrindene in a more efficient way than decacyclene (**5.12**).

⁴⁴ (a) Amsharov, K. Y.; Kabdulov, M. A.; Jansen, M., "Homo-Elimination of HF—an Efficient Approach for Intramolecular Aryl–Aryl Coupling," *Chemistry—A European Journal* **2010**, *16*, 5868–5871. (b) Kabdulov, M. A.; Amsharov, K. Y.; Jansen, M., "A Step toward Direct Fullerene Synthesis: C₆₀ Fullerene Precursors with Fluorine in Key Positions," *Tetrahedron* **2010**, *66*, 8587–8593.

⁴⁵ (a) Amsharov, K. Y.; Kabdulov, M. A.; Jansen, M., "Facile Bucky-Bowl Synthesis by Regiospecific Cove-Region Closure by HF Elimination," *Angewandte Chemie* **2012**, *124*, 4672–4675. (b) Amsharov, K. Y.; Merz, P., "Intramolecular Aryl–Aryl Coupling of Fluoroarenes through Al₂O₃-Mediated HF Elimination," *The Journal of Organic Chemistry* **2012**, *77*, 5445–5448.

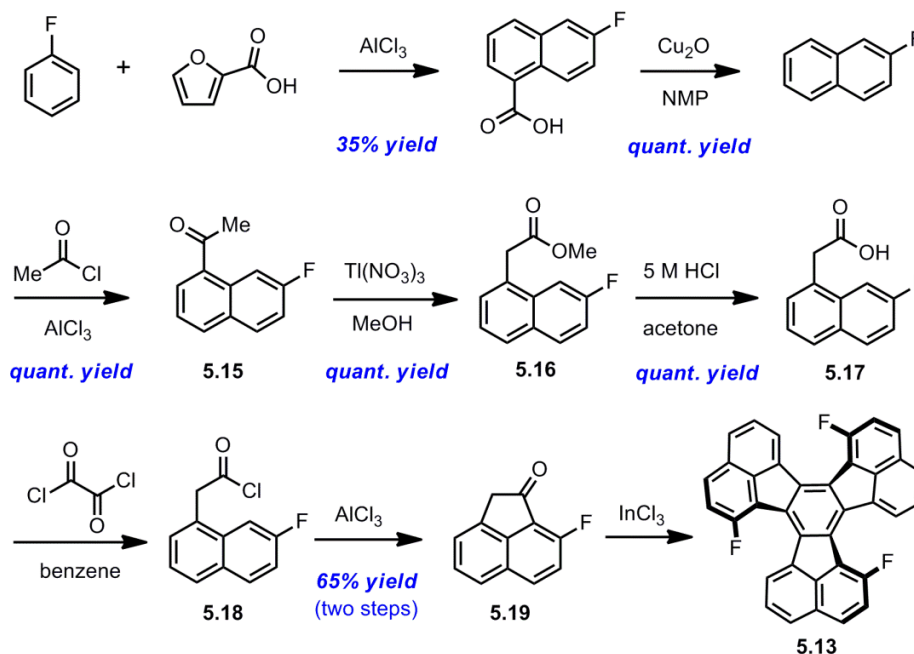
Scheme 5.8 HF Homo-Elimination



The synthetic route to trifluorodecacyclene (**5.13**) is described in Scheme 5.9. The reaction sequence begins with an AlCl_3 -mediated coupling reaction between fluorobenzene and 2-furanoic acid.⁴⁶ Then, a decarboxylation reaction was performed with Cu_2O and NMP to afford 2-fluoronaphthalene. Then, compound **5.15** was synthesized by a Friedel–Crafts acylation with 2-fluoronaphthalene, and the resulting ketone **5.15** was transformed to an ester **5.16** with thallium(III) nitrate and methanol. An acidic hydrolysis and subsequent chlorination afforded the acid chloride (**5.18**), and an intramolecular Friedel–Crafts acylation gave a cyclic ketone **5.19**.

⁴⁶ Krülle, T. M.; Barba, O.; Davis, S. H.; Dawson, G.; Procter, M. J.; Staroske, T.; Thomas, G. H., "A Simple Route to 6- and 7-Fluoro-Substituted Naphthalene-1-Carboxylic Acids," *Tetrahedron Letters* **2007**, *48*, 1537-1540.

Scheme 5.9 Synthetic Route to Trifluorodecacyclene



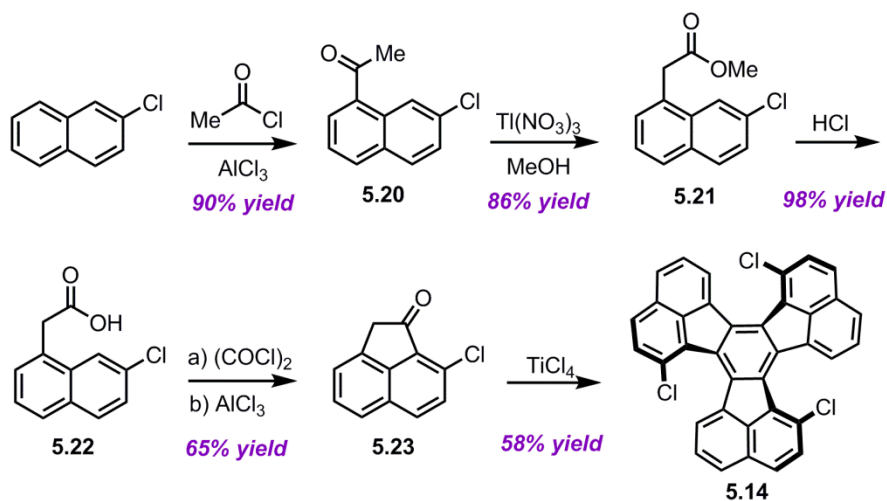
The last step toward the trifluorodecacyclene (5.13) is a Lewis-acid promoted cyclotrimerization reaction.⁴⁷ Extensive optimization experiments were conducted with a variety of Lewis acids for this step. The Lewis acids that were tried for this reaction include TiCl_4 , InCl_3 , AlCl_3 , $\text{BF}_3\text{-OEt}$, ZrCl_2 , BCl_3 , GaCl_2 , CeCl_3 , $\text{Cu}(\text{OTf})_2$, etc. Among these and other Brønsted acids that were surveyed for this step, indium(III) chloride and titanium(IV)

⁴⁷ (a) Amick, A. W.; Griswold, K. S.; Scott, L. T., "Synthesis and Aldol Cyclotrimerization of 4,7-Di-*Tert*-Butylacenaphthenone," *Canadian Journal of Chemistry* **2006**, *84*, 1268-1272. (b) Amick, A. W.; Scott, L. T., "Trisannulated Benzene Derivatives by Acid Catalyzed Aldol Cyclotrimerizations of Cyclic Ketones. Methodology Development and Mechanistic Insight," *The Journal of Organic Chemistry* **2007**, *72*, 3412-3418.

chloride gave the best results.⁴⁸ Even though the desired product (5.13) was formed by this route, the insolubility of the compound rendered its purification very challenging.

The trichlorinated decacyclene (5.14) was prepared by a multistep synthetic route that is illustrated in Scheme 5.10. A Friedel–Crafts acylation of 2-chloronaphthalene at $-78\text{ }^{\circ}\text{C}$ gave the desired ketone (5.20) in 90% yield. Oxidative rearrangement of 5.20 with thallium(III) nitrate and methanol afforded the corresponding ester (5.21) in 86% yield. Hydrolysis of the ester (5.21) to the corresponding carboxylic acid (5.22), conversion of the acid into an acyl chloride, and an intramolecular Friedel–Crafts acylation produced 8-chloroacenaphthenone (5.23) on a multigram scale. Finally, a trimerization of 5.23 with TiCl_4 produced 8-chloroacenaphthenone (5.23) on a multigram scale.

Scheme 5.10 Synthetic Route to Trichlorodecacyclene



⁴⁸ For a detailed experimental procedure for this step, please refer to Section 5.8.2.20.

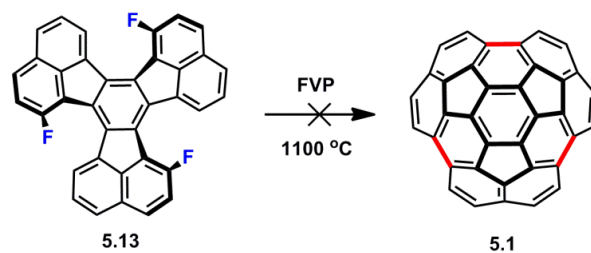
Cyclotrimerization of 8-chloroacenaphthenone **5.23** to the C₃-symmetric trichlorodecacyclene (**5.14**) was accomplished by triple aldol condensation of the chloro ketone (**5.23**). After extensive optimization of reaction parameters (Lewis acid, solvent, temperature, and concentration), the best conditions were found to involve addition of the chloro ketone (**5.23**) as a dilute solution in 1,2-dichlorobenzene (0.06 M) to an equal volume of boiling 1,2-dichlorobenzene (bp = 180 °C) that contains 6 molar equivalent of TiCl₄. In lower boiling solvents, the trimerization proceeds only very slowly and gives numerous byproducts.

5.3.2.2. Pyrolysis of Halogenated Decacyclenes

With both halogenated decacyclenes (**5.13** and **5.14**) in hand, we conducted FVP reactions of these compounds under various reaction conditions. When the fluorinated decacyclene (**5.13**) was subjected to the pyrolysis reaction at 1100 °C, the reaction did not yield any desired product, decacyclene (Scheme 5.11). Only a small portion of the starting material (~10%) was recovered unreacted, and most of the starting material was decomposed in the hot oven during the course of the reaction.⁴⁹ The HF elimination, which was reported by the Jansen group (Scheme 5.8),⁴⁴ does not seem to be operative in our system.

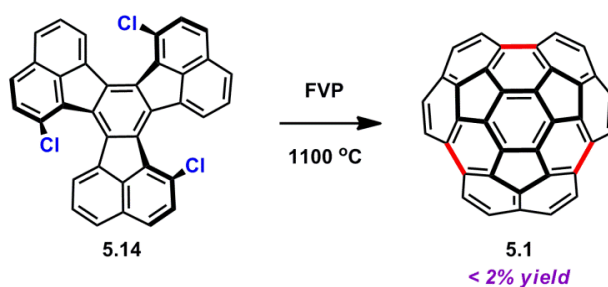
⁴⁹ For a detailed experimental procedure for this step, please refer to Section 5.8.2.1.

Scheme 5.11 Pyrolysis of Trifluorodecacyclene



The pyrolysis reaction with trichlorodecacyclene was also conducted at 1100 °C. In the crude reaction mixture, the desired product (5.1) was formed in less than 2% yield. Most of the starting materials was decomposed and produced black tar in the pyrolysis tube. In this case, none of the starting material was recovered at the end of the reaction.

Scheme 5.12 Pyrolysis of Trichlorodecacyclene



These unsuccessful results lead us to think about another approach to the problem of this project. In particular, we wanted to address the problems related to the insolubility of the halogenated and non-halogenated decacyclenes in organic solvents. In other words, if we can install any solubilizing groups on the decacyclene systems, those compounds that are soluble in organic solvents would be much better candidates for the precursor to the pyrolysis. These efforts are described in the following sections.

5.3.2.3. Pyrolysis of *t*-Butylated Decacyclenes

As mentioned above, one of the difficulties encountered in this project was the insolubility of the polyaromatic compounds in common/noncommon organic solvents. For instance, decacyclene is barely soluble in dichloromethane or chloroform and essentially insoluble in hexanes. When decacyclene is halogenated, the degree of insolubility substantially increases. The insolubility originates from the intermolecular forces between the molecules; the strong attraction between the molecules prevents them from being solvated in solvents. When molecules are halogenated, the halogenated molecules become more polar. Consequently, the intermolecular forces substantially increase, and the molecules are more strongly attracted to each other due to the polar–polar interactions.

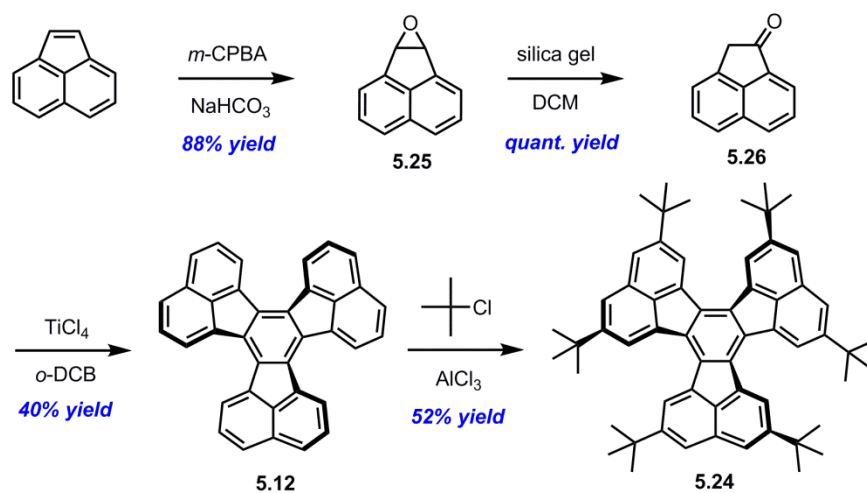
One of the well-known solubilizing groups for polycyclic aromatic hydrocarbons is a *tert*-butyl group. Installation of *t*-butyl groups tends to break the stacking of the flat aromatic compounds with the three-dimensional framework. Also, it was found in our laboratory that compounds with *tert*-butyl groups tend to be sublimed more easily than non-*t*-butylated compounds, and the *tert*-butyl groups come off from the aromatic system under the pyrolysis conditions. For these reasons, we planned to synthesize *tert*-butylated decacyclene **5.24** (Figure 5.8).

Figure 5.8 Decacyclene with Solubilizing Group



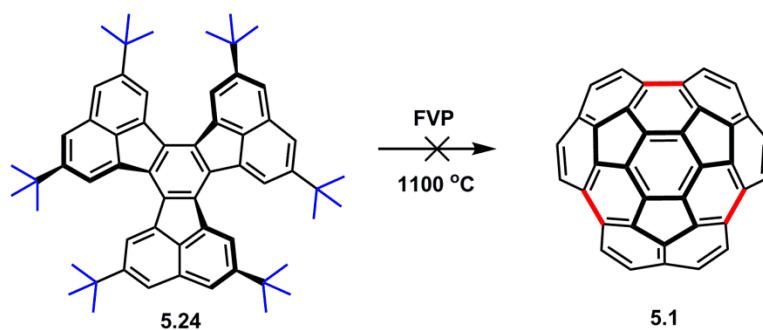
The synthetic route to hexa-*t*-butyl decacyclene is described in Scheme 5.13. Acenaphthylene can be transformed to an epoxide **5.25** with *m*-CPBA (*meta*-chloro peroxybenzoic acid) under basic conditions. The resulting epoxide (**5.25**) was treated with silica gel in dichloromethane to be converted into a ketone **5.26**. The silica gel solution was acidic enough to perform this transformation, and this method was operationally very convenient by eliminating a purification step. Decacyclene (**5.12**) can be prepared from this cyclic ketone (**5.26**) with triple aldol condensation in the presence of TiCl_4 . Finally, the hexa-*tert*-butylated decacyclene (**5.24**) was synthesized by Friedel–Crafts alkylation of decacyclene in 52% yield.⁵⁰ As expected, compound **5.24** was very soluble in organic solvents; consequently, it made the handling and purification of the compound effortless.

⁵⁰ For a detailed experimental procedure for this step, please refer to Section 5.8.2.20.

Scheme 5.13 Synthesis of Hexa-*t*-butyldecacyclene

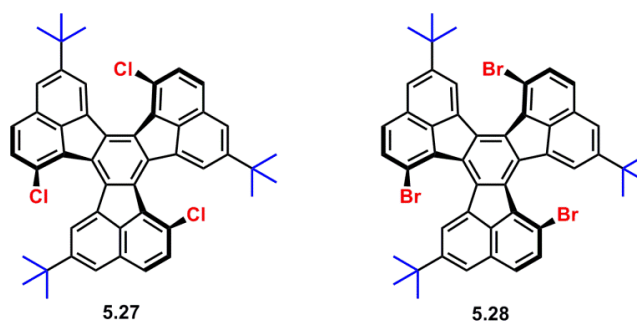
The hexa-*t*-butyldecacyclene (**5.24**), which was prepared by the multistep synthesis, was subjected to the FVP reaction (Scheme 5.14).⁵¹ However, unfortunately, the reaction did not afford the desired product, circumtrindene (**5.1**). The *t*-butyl groups were all lost during the pyrolysis reaction, as we hoped. However, only unwanted byproducts with incomplete cyclization were afforded in this process. In other words, the majority of the reaction product was the singly-closed or doubly-closed decacyclenes. This partially-completed cyclization might indicate that the C–H bonds of the decacyclene are not reactive enough towards the radical-involving pyrolytic reactions.

⁵¹ For a detailed experimental procedure for this step, please refer to Section 5.8.2.1.

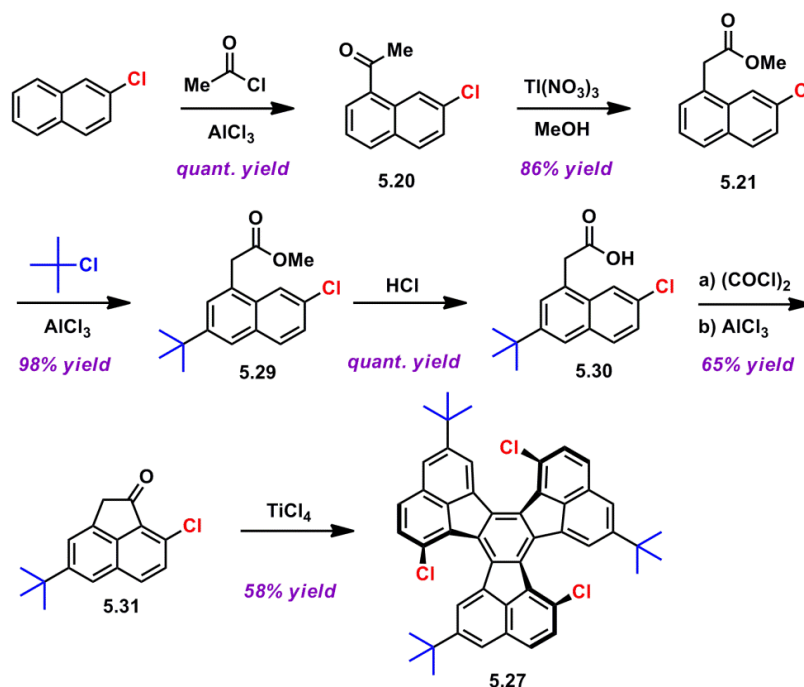
Scheme 5.14 Pyrolysis of Hexa-*t*-butyldecacyclene

5.3.2.4. Pyrolysis of *t*-Butylated and Halogenated Decacyclenes

After having observed the low reactivity of the *t*-butylated decacyclene (5.24, Scheme 5.14), we planned to prepare other types of precursors to circumtrindene. In order to handle both the reactivity and the solubility of the starting material, it was aimed to install both halogen atoms and *tert*-butyl groups on decacyclene. More specifically, the syntheses of tri-*t*-butyl-trichlorodecacyclene (5.27) and tri-*t*-butyl-tribromodecacyclene (5.28) were envisaged (Figure 5.9).

Figure 5.9 *Tert*-Butylated and Halogenated Decacyclenes

As shown in Scheme 5.15, the synthesis of tri-*t*-butyl-trichlorodecacyclene (5.27) commenced with Friedel–Crafts acylation to afford a chlorinated ketone 5.20. Then, an oxidative rearrangement with thallium(III) nitrate gave an ester 5.21. The *t*-butyl group was installed on this ester (5.21) by Friedel–Crafts alkylation in 98% yield. The *t*-butylated ester (5.29) was converted to a carboxylic acid (5.30) by acidic hydrolysis in quantitative yield. Then, the cyclic ketone (5.31) was prepared from the acid (5.30) by chlorination and subsequent intramolecular Friedel–Crafts acylation (65% yield for two steps). The last step of the synthesis is titanium(IV)-mediated triple aldol condensation; this reaction gave tri-*t*-butyl-trichlorodecacyclene (5.27) in 58% yield. As far as the solubility of the molecule is concerned, the chlorinated trimer (5.27) was pleasingly soluble in organic solvents.

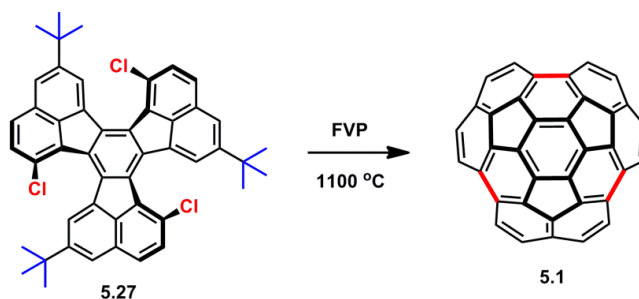
Scheme 5.15 Synthesis of *tert*-Butylated Trichlorodecacyclene

Furthermore, synthesis of tri-*t*-butyl-tribromodecacyclene (5.28) was also attempted. The synthetic route to tri-*t*-butyl-tribromodecacyclene (5.28) is similar to that of tri-*t*-butyl-trichlorodecacyclene (5.27) in Scheme 5.15. Also, the yields of each step were comparable except for the last aldol condensation reaction. In the case of tri-*t*-butyl-tribromodecacyclene (5.28), the last trimerization reaction with the corresponding cyclic ketone did not afford the desired product (5.28) at all. It was thought that the steric hindrance of the fjord region of decacyclene became too cumbersome due to the presence of a bromine atom.

When the tri-*t*-butylated and tri-chlorinated decacyclene (5.27) was subjected to the FVP experiment, it was observed a trace amount of the desired product (5.1) was formed (Scheme 5.16). In the crude reaction mixture, some incomplete cyclization products were

observed. It is expected that better results could be obtained by optimizing the reaction conditions further.

Scheme 5.16 Pyrolysis of *tert*-Butylated Trichlorodecacyclene

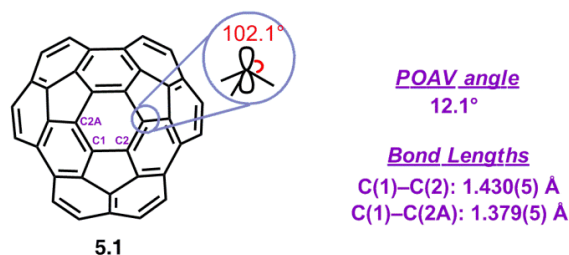


5.3.3. Properties of Circumtrindene

In agreement with DFT calculations, an X-ray crystal structure of circumtrindene (5.1) has confirmed that the carbon atoms comprising the top of the dome are distorted from planarity even more than the carbon atoms in C₆₀; the distortion in circumtrindene (POAV angle of circumtrindene = 12.1°, Figure 5.10)⁵² is slightly more significant than in C₆₀-fullerene (POAV angle of C₆₀-fullerene = 11.6°). It is worth noting that the greatest POAV angle in circumtrindene is located in the [6,6]-bond (*i.e.* the double bond at the junctions of two hexagons) in the interior π system.

⁵² The POAV angle at the largest curved point of the molecule is considered.

Figure 5.10 POAV Angle and Bond Lengths of Circumtrindene



Moreover, the X-ray structure of circumtrindene (5.1) reveals that the double bonds of this aromatic system are not equivalent. The bond lengths vary depending on their locations (Figure 5.10), which is also observed in fullerenes.⁵³ The double bonds that are located between two six-membered rings (1.379 Å) are shorter than those between a 6-membered ring and a 5-membered ring (1.430 Å). Therefore, the double bonds of the central hexagon in circumtrindene are not the same as those in benzene (C₆H₆). In other words, the central hexagon in circumtrindene can be seen as a “cyclohexatriene,” rather than as a benzene ring.

The NMR signals for the twelve hydrogen atoms on the rim of circumtrindene (5.1) fall in the aromatic region of the spectrum (7.58 and 7.20 ppm); however, the ring currents within the molecule provide substantially less deshielding than one sees in large, planar or

⁵³ The X-ray structure of fullerene-C₆₀ shows that the [6,6] bond of C₆₀ is 1.355 Å and the [6,5] bond is 1.467 Å. For more details, see: Buhl, M.; Hirsch, A., “Spherical Aromaticity of Fullerenes,” *Chemical Reviews* **2001**, *101*, 1153-1183.

less strongly curved PAHs.⁵⁴ Clearly, the great curvature of the molecule, which is implied by the large POAV angle, has an impact on the NMR resonances of the compound.

⁵⁴ A proton NMR (¹H NMR) of Corannulene (C₂₄H₁₂) has a single resonance at 7.82 ppm. For more information, see: Filatov, A. S.; Jackson, E. A.; Scott, L. T.; Petrukhina, M. A., "Foregoing Rigidity to Achieve Greater Intimacy," *Angewandte Chemie International Edition* **2009**, *48*, 8473-8476.

5.4. Interior Functionalization of Circumtrindene

As seen in the vast chemical literature on polycyclic aromatic hydrocarbons (PAHs), chemical reactions of PAHs typically proceed at carbon atoms on the rims of the molecules. Covalent chemistry at “interior” carbon atoms of planar PAHs has never been observed when edge carbon atoms exist in the same molecule. On the other hand, fullerenes do not possess any edge carbons; therefore, any reactions on fullerenes inevitably lead to bond formation at interior carbon atoms, irrespective of the reaction type: oxidation, reduction, halogenation, electrophilic addition, nucleophilic addition, cycloaddition, hydrogenation, or some other reactions.^{32, 33}

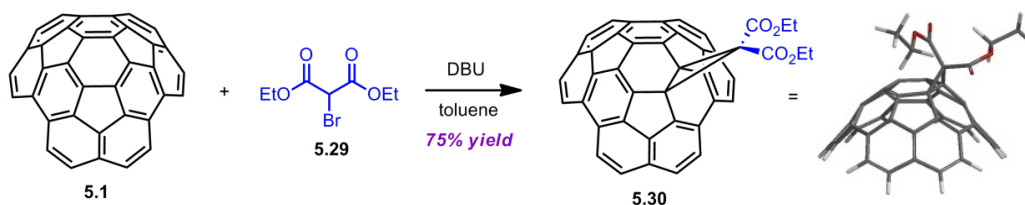
5.4.1. Bingel–Hirsch Reaction

As described in the previous section, the Bingel–Hirsch reaction is a nucleophilic addition reaction to fullerenes that produces 3-membered rings (Scheme 5.2); it is considered one of the most valuable preparative methods applicable to fullerenes, since it changes both the solubility and the electrochemical behavior of fullerenes.

Considering the similarity between circumtrindene and fullerene-C₆₀ in terms of the curvature of the π system, we conjectured the Bingel reaction might occur with circumtrindene (5.1) in the same manner as that with fullerene-C₆₀ (5.3). To our great pleasure, the cyclopropanation of circumtrindene proceeded to afford the desired

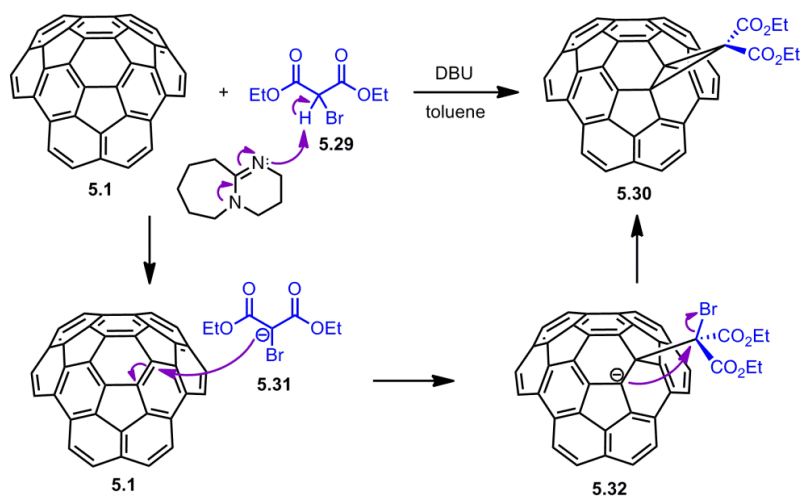
cyclopropanated circumtrindene (**5.30**) in a good yield and with great site-selectivity (Scheme 5.17). The reaction was carried out with circumtrindene (**5.1**), ethyl bromomalonate (**5.29**), and DBU (1,8-diazabicyclo[5.4.0]undec-7-ene) as a base in toluene at ambient temperature for 2 h.

Scheme 5.17 Bingel–Hirsch Reaction of Circumtrindene



Based on the mechanistic studies on the Bingel reaction of fullerenes, the mechanism of the Bingel reaction of circumtrindene was proposed, as described in Scheme 5.18. The deprotonated bromomalonate that is generated from bromomalonate (**5.29**) with DBU as a base functions as a nucleophile; it attacks the double bond of circumtrindene and ultimately generates a cyclopropanated circumtrindene (**5.30**). Notably, this cyclopropanation reaction exclusively occurs at a [6,6]-bond (*i.e.* a double bond at the junctions of two 6-membered rings) of circumtrindene. Furthermore, the reaction occurs only on the convex face of the molecule; no reactivity toward nucleophiles was observed on the concave side of circumtrindene.

Scheme 5.18 Proposed Mechanism for the Bingel–Hirsch Reaction of Circumtrindene



In the Bingel reaction of circumtrindene, as observed in C_{60} -fullerene chemistry, the double bond at the juncture of two six-membered rings reacts with the nucleophilic reagent. Unlike C_{60} -fullerene, however, there are three distinct sets of [6,6]-bonds in circumtrindene; it is noteworthy that the reaction is site-selective for the [6,6]-bond at the point of greatest curvature on the convex surface (*i.e.* the bond with the greatest POAV angle, see Figure 5.10). Also, as stated above, the [6,6]-bonds are shorter than the [6,5]-bonds; the greater reactivity at the [6,6]-bonds over [6,5]-bonds supports the abovementioned perspective of seeing the hexagon as a cyclohexatriene, rather than as a benzene ring. Similar site-selectivity for the most pyramidalized [6,6]-bonds of fullerene- C_{70} has also been observed.⁵⁵

⁵⁵ Kraszewska, A.; Diederich, F.; Thilgen, C., "Higher Fullerenes: Chirality and Covalent Adducts," *Chemistry of Nanocarbons* **2010**, 129-171.

As described in the preceding section, the curved π system tends to render the LUMO energy lower due to the poorer overlap and increased *s*-character in the π molecular orbitals. The great reactivity of both fullerenes and circumtrindene towards a nucleophile can be rationalized by such lowered LUMO energies. In the initial nucleophilic attack to the π system (see Scheme 5.19), the nucleophile seeks the site with the largest LUMO coefficient. DFT studies were conducted for calculation of the LUMO orbitals in circumtrindene, and the results are described in the subsequent section.

Furthermore, we observed that the reaction proceeded with excellent facial selectivity; the cyclopropane ring was formed exclusively on the convex face of circumtrindene. Besides the steric hindrance of the molecule on the concave face, it is speculated that the different electron densities of the two faces might also play a role in determining the facial selectivity. Due to the curvature of the π system, the convex face would have less electron density than the concave face, which would render the convex side more favorable for a nucleophilic attack.

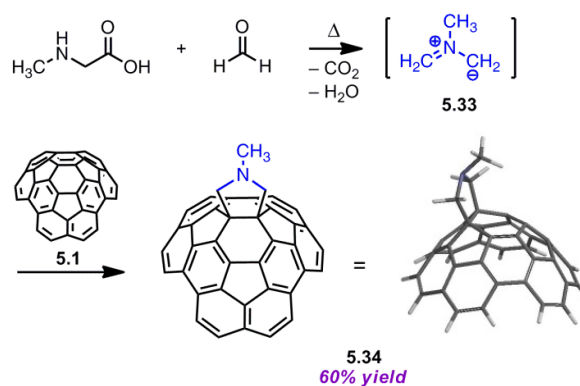
5.4.2. Prato Reaction

Another major class of fullerene chemistry is cycloaddition reactions to the π system. Especially, 1,3-dipolar reagents readily add to the [6,6]-bond of fullerene- C_{60} , which acts as a good dipolarophile. Among such [3+2] cycloadditions, the reaction with azomethine ylides is beneficial because it leads to versatile pyrrolidine derivatives of C_{60} . The sources of the ylide can be iminium salts, aziridines, oxazolidines or silylated iminium compounds. In 1993,

Prato and coworkers developed a protocol for the process, which is now often carried out.^{3a} In the first step an amino acid (e.g. *N*-methylglycine) is reacted with an aldehyde or ketone, and a subsequent addition of fullerene-C₆₀ (5.3) provides a fullerene-pyrrolidine derivative (5.9), as illustrated in Scheme 5.3.

In light of the great electrophilicity of circumtrindene in the Bingel reaction, it came as no surprise that circumtrindene can act as a good dipolarophile in a [3+2] cycloaddition reaction as well. The azomethine ylide (5.33), generated *in situ* from *N*-methylglycine and formaldehyde, adds to the interior [6,6]-bond of circumtrindene in refluxing benzene to give the pyrrolidine derivative (5.34, Scheme 5.19).⁵⁶ As observed in the Bingel reaction, the 1,3-dipolar reacts with the double bond that has the greatest POAV angle in the molecule.

Scheme 5.19 Prato Reaction of Circumtrindene



⁵⁶ Ansems, R. B. M., "Circumtrindene: Synthesis and Property Exploration," *Boston College Dissertations and Theses* **2004**, AAI3135958.

Considering the frontier molecular orbitals involved in [3+2]-cycloaddition processes, the dominant interaction would be the one between the HOMO of the 1,3-dipole and the LUMO of dipolarophile. In the Prato reaction in Scheme 5.19, the electron rich ylide will seek out the carbon atoms of circumtrindene with the highest LUMO coefficient. In addition, the Prato reaction of circumtrindene also shows complete facial selectivity, as seen in the Bingel reaction in the previous section.

5.4.3. Computational Studies

5.4.3.1. Frontier Molecular Orbital (FMO) Analysis

From both of the reactions in the interior functionalization (*i.e.* Bingel reaction and Prato reaction), complete site-selectivity was observed in terms of the type of the double bond and the face of the molecule. As noted above, the distorted π system caused by the molecule's curvature lowers the LUMO energy (see Figure 5.3). It is also to be expected that the electron density is not equal for the two different faces of circumtrindene due to the curvature.⁵⁷ Our experimental results are consistent with these hypotheses; theoretical studies of this section will provide more insight about these phenomena.

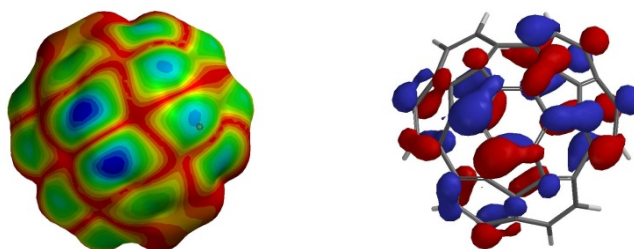
In the fullerene-type functionalization reactions reported here, circumtrindene functions as an electrophile towards the nucleophile (deprotonated bromomalonate for the

⁵⁷ Klärner, F.-G.; Panitzky, J.; Preda, D.; Scott, L. T., "Modeling of Supramolecular Properties of Molecular Tweezers, Clips, and Bowls," *Molecular Modeling Annual* **2000**, *6*, 318-327.

Bingel reaction) and the dipolar (azomethine ylide for the Prato reaction). In consequence, the frontier molecular orbital of circumtrindene that controls these interior functionalizations should be the LUMO of the compound. The LUMO of circumtrindene was calculated at the B3LPY/6-31G* level of theory, using the curved geometry obtained at the same level of theory optimization.

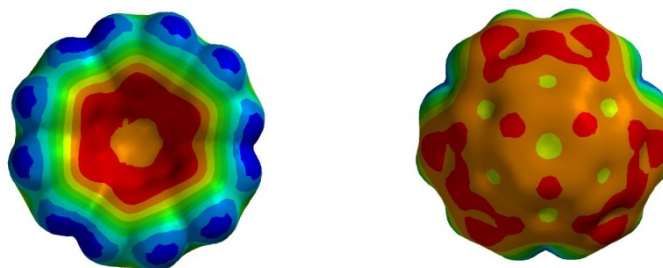
The calculated LUMO for circumtrindene is doubly degenerate; one of the LUMO orbital maps for circumtrindene is illustrated in Figure 5.11.⁵⁸ The antibonding LUMO has its largest coefficients at the interior [6,6]-bond with the greatest pyramidalization, which is consistent with the experimental results.

⁵⁸ (a) Calculated at B3LYP/6-31G**. (b) All the calculations are done by Gaussian 09, Revision C.01, M. J. Frisch, G. W. Trucks, H. B. Schlegel, G. E. Scuseria, M. A. Robb, J. R. Cheeseman, G. Scalmani, V. Barone, B. Mennucci, G. A. Petersson, H. Nakatsuji, M. Caricato, X. Li, H. P. Hratchian, A. F. Izmaylov, J. Bloino, G. Zheng, J. L. Sonnenberg, M. Hada, M. Ehara, K. Toyota, R. Fukuda, J. Hasegawa, M. Ishida, T. Nakajima, Y. Honda, O. Kitao, H. Nakai, T. Vreven, J. A. Montgomery, Jr., J. E. Peralta, F. Ogliaro, M. Bearpark, J. J. Heyd, E. Brothers, K. N. Kudin, V. N. Staroverov, T. Keith, R. Kobayashi, J. Normand, K. Raghavachari, A. Rendell, J. C. Burant, S. S. Iyengar, J. Tomasi, M. Cossi, N. Rega, J. M. Millam, M. Klene, J. E. Knox, J. B. Cross, V. Bakken, C. Adamo, J. Jaramillo, R. Gomperts, R. E. Stratmann, O. Yazyev, A. J. Austin, R. Cammi, C. Pomelli, J. W. Ochterski, R. L. Martin, K. Morokuma, V. G. Zakrzewski, G. A. Voth, P. Salvador, J. J. Dannenberg, S. Dapprich, A. D. Daniels, O. Farkas, J. B. Foresman, J. V. Ortiz, J. Cioslowski, and D. J. Fox, Gaussian, Inc., Wallingford CT, 2010.

Figure 5.11 LUMO Orbital Map of Circumtrindene (B3LYP/6-31G*)⁵⁹

5.4.3.2. Electrostatic Potential (ESP) Analysis

The exclusive facial selectivity of the interior functionalization reactions, whereby the reactions occur on the convex face, implies that the electron deficiency would be greater on the convex face than the concave face. In agreement with the experimental data, the results of density functional calculations (B3LYP/6-31G*) suggest that the outer surface should be electrophilic resembling that of C₆₀, and the inside surface is predicted to be relatively nucleophilic (Figure 5.12).

Figure 5.12 Electrostatic Potentials on the Surfaces of Circumtrindene (B3LYP/6-31G*)

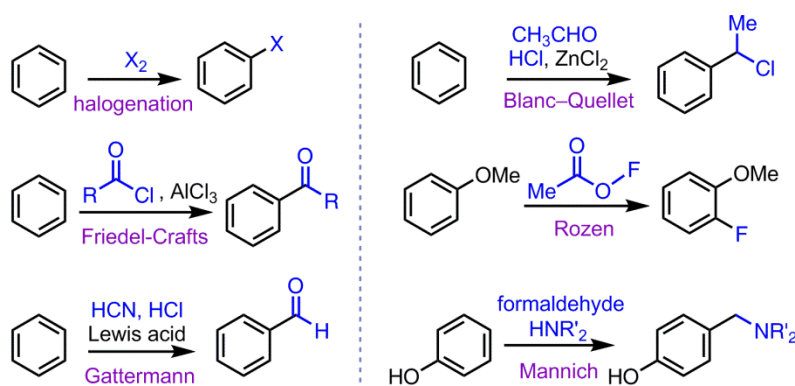
⁵⁹ The darkest blue areas correspond to the largest LUMO coefficients.

Both the stereoelectronic factor and the electrostatic factor of circumtrindene have a crucial impact on the reactivity and selectivity for the circumtrindene chemistry. Those aspects were examined by computational methods, and the results were consistent with the experimental data.

5.5. Peripheral Functionalization of Circumtrindene

Since the isolation of the first polycyclic aromatic compounds, a tremendous range of chemical reactions on these polycyclic aromatic hydrocarbons (PAHs) has been developed for more than 100 years.⁶⁰ Most of their chemistry involves chemical modification on the edge carbons and has been used to functionalize the existing polyarenes and/or to extend them to larger PAHs. One of the most common class of aromatic reactions is electrophilic aromatic substitution reactions (Scheme 5.20); but, free radical, nucleophilic addition, reduction and oxidation reactions are also possible. To synthesize larger PAHs that are not available in nature or to make existing ones in more rational ways, functionalization reactions can be followed by functional group interconversion and coupling reactions.

Scheme 5.20 Selected Electrophilic Aromatic Substitution Reactions

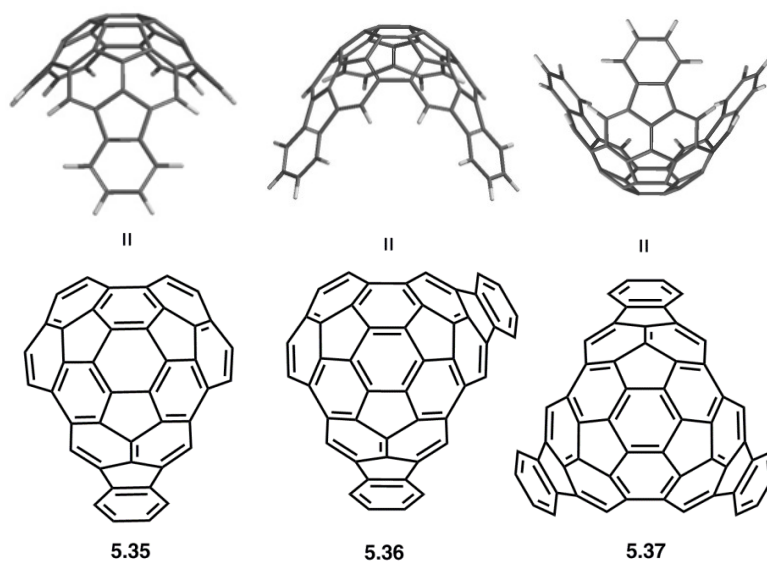


⁶⁰ (a) Harvey, R. G. *Polycyclic Aromatic Hydrocarbons*; Wiley-VCH: New York, 1997. (b) Clar, E.; Schoental, R. *Polycyclic Hydrocarbons ... With a Chapter on Carcinogenesis by Regina Schoental. With Plates.*; Academic Press; Springer-Verlag: Berlin: London & New York, 1964.

5.5.1. Ring Extension Process

The synthesis of bowl-shaped geodesic polyarenes is non-trivial due to the substantial strain energy of such molecules. In this regard, it is generally easier to construct deeper bowls from already existing curved molecules, rather than making them from planar building blocks. Circumtrindene (5.1) has a curvature comparable to C₆₀-fullerene and that has much of the strain already built in, which is needed to synthesize deeper bowls. Circumtrindene (5.1) represents 60% of the network of sp² carbons that constitute C₆₀-fullerene. To go to 70%, 80%, and 90% of C₆₀, the number of carbon atoms added in each step would be six, as in monoindeno-substituted circumtrindene (5.35, Figure 5.13), diindeno-substituted circumtrindene (5.36), and triindeno-substituted circumtrindene (5.37). In this regard, we have envisioned that circumtrindene can be used as a building block for deeper bowls by a peripheral functionalization method with standard aromatic chemistry.

Figure 5.13 Monoindeno, Diindeno, and Triindeno Substituted Circumtrindene

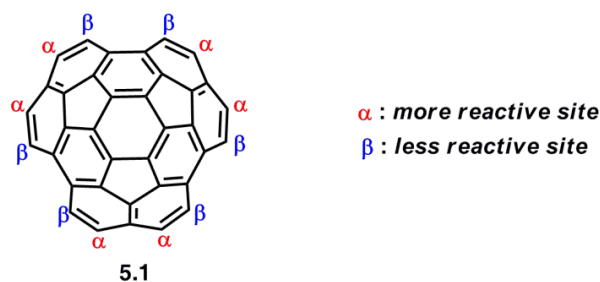


As demonstrated by DFT calculations, the curvature of the π system alters the stereoelectronic and electrostatic environments on both faces of the π molecule (see Figures 5.11 and 5.12). In this regard, we were interested in whether such peripheral functionalization reactions would allow us to explore the magnetic environment of the two different faces of circumtrindene. In other words, it might be possible to probe the different magnetic environments experimentally if a suitable substituent could be placed on the rim of circumtrindene that hangs over both the concave and the convex faces without restraints. With such experiments, we will understand better the effect of curvature on the distortion of the magnetic environments of the π system.

To achieve the aforementioned goal, a reasonable first step would be functionalizing the π -position of circumtrindene with a group that is suitable for subsequent coupling

reactions. Bromination is one of the most common aromatic reactions, which is easily done on many PAHs; moreover, the brominated PAHs can be used in several different coupling reactions. Since the α -positions of circumtrindene are inherently more reactive than the more crowded β -positions (Figure 5.14), the site-selectivity between those two carbon atoms is not expected to be a problem.

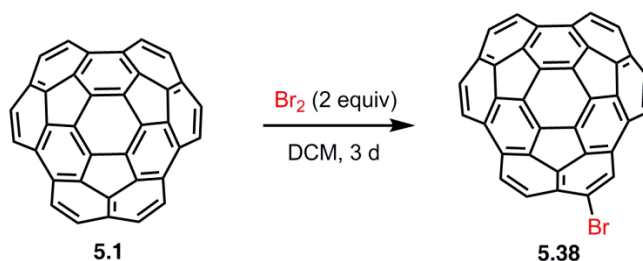
Figure 5.14 Two Different Rim Carbon Atoms on Circumtrindene



However, it is also possible for interior carbon atoms of circumtrindene to be brominated. It has been known that fullerenes undergo bromine addition with elemental bromine in chlorinated solvents at room temperature.⁶¹ To avoid the unwanted bromination on the interior carbon atoms, the reaction conditions were carefully optimized. In a reasonably dilute solution and with two equivalents of bromine, selective mono-bromination on the α -carbon of circumtrindene has been achieved to afford a mono-brominated circumtrindene **5.38** in a quantitative yield (Scheme 5.21).⁵⁶

⁶¹ Hirsch, A. *The Chemistry of the Fullerenes*; G. Thieme Verlag: Stuttgart ; New York, 1994.

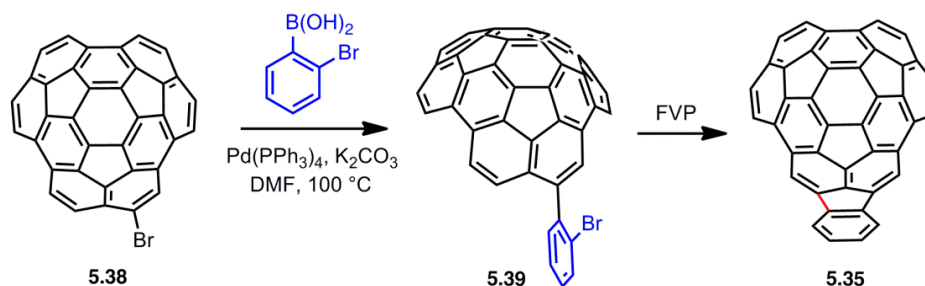
Scheme 5.21 Site-Selective Peripheral Monobromination of Circumtrindene



With bromocircumtrindene (5.38) in hand, a Suzuki coupling reaction was carried out with a commercially available boronic acid (Scheme 5.22). The reaction proceeds smoothly with 2-bromophenylboronic acid in the presence of a Pd(0) catalyst and a base to furnish the aryl substituted circumtrindene (5.39). The Suzuki reaction proceeds reasonably well, despite the possibility of the product undergoing a subsequent Suzuki coupling with the bromine of the phenyl group. The next step of the sequence, a ring closure to indenocircumtrindene (5.35), was accomplished by FVP.⁵⁶ The bromine in the *ortho*-position of the phenyl group is presumably lost by homolytic bond cleavage, and the resulting aryl radical then cyclizes. However, the reaction also generates a significant amount of circumtrindene by loss of the phenyl group during the FVP process.⁶²

⁶² We have observed similar phenyl loss processes in other FVP reactions involving phenyl substituted substrates. Detailed mechanistic studies on these phenyl-loss processes are currently on-going in our laboratory.

Scheme 5.22 Suzuki Coupling and Ring Closing Reactions toward Indenocircumtrindene



Since FVP reactions are typically a low-yielding process, which is mostly caused by decomposition of the starting material and products under harsh conditions, solution phase chemistry was also tried for this ring closing reaction. However, attempts to close the substituted circumtrindene (5.39) to indenocircumtrindene (5.35) by Heck-type cyclization were not successful. It has been observed that the Heck-type cyclization works nicely with planar PAHs and even on slightly curved PAHs, such as corannulene. Nonetheless, when it was applied to the indenocircumtrindene synthesis, the reaction did not give any ring-closed products. Oxidative addition of Pd(0) into one of the strained C–C bonds on the rim of circumtrindene might be competing with the desired cyclization,⁶³ but we have not characterized any of the decomposition products from this reaction.

⁶³ Alvarez, C. M.; Angelici, R. J.; Sygula, A.; Sygula, R.; Rabideau, P. W., "η⁶-Corannulene Buckybowl Complexes of Iridium, Including Ring-to-Ring Migration," *Organometallics* **2003**, *22*, 624-626.

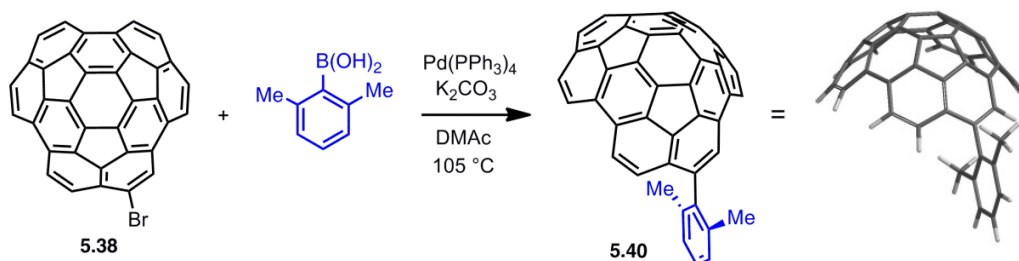
5.5.2. Computational Studies

5.5.2.1. Magnetic Environment

In planar PAHs, in which the π orbitals are perpendicular to the σ bonds, the electrons are distributed equally on both faces of the aromatic system. However, when curvature is built into the molecules, by which π bonds are pyramidalized, an increased electron density on the concave lobes results. One of the highly curved molecules, circumtrindene, is expected to have this property. We envisioned that NMR (nuclear magnetic resonance) experiments will provide qualitative data points regarding the electron density of circumtrindene, considering the shielding and deshielding effect by electron densities in the NMRs.

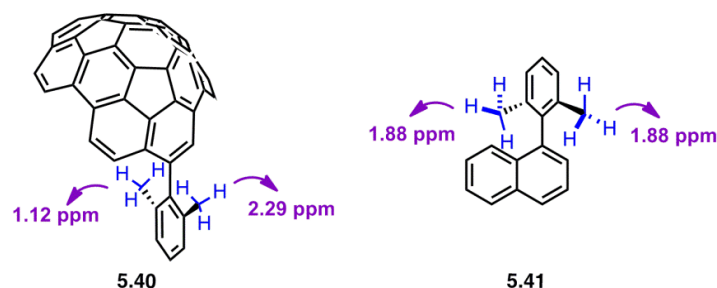
To probe the ring current of each face, a circumtrindene derivative, which possesses a group that can hang over both the concave and convex side of circumtrindene, was designed. This can be accomplished by substituting the bromo group of bromocircumtrindene (**5.38**) with a 2,6-dimethyl substituted phenyl group (Scheme 5.23). The Suzuki coupling was again employed; compound **5.38** underwent the coupling reaction with 2,6-dimethylphenyl boronic acid in the presence of a palladium catalyst [Pd(PPh₃)₄] and potassium carbonate (K₂CO₃) to furnish the corresponding product (**5.40**) in 60% yield.⁵⁶

Scheme 5.23 Suzuki Coupling of Brominated Circumtrindene



In the proton NMR spectrum of compound **5.40**, there are two distinct peaks for the two methyl groups at 2.29 and 1.12 ppm. Considering the different electron densities on each face of circumtrindene, we speculated that the resonance of the methyl group over the concave side is shifted upfield (1.12 ppm), whereas that over the convex side is shifted downfield (2.29 ppm). The difference in chemical shifts between the two singlets is 1.17 ppm.

Since the walls of circumtrindene consist of three naphthalene units, a 2,6-dimethylphenyl substituted naphthalene (**5.41**, Figure 5.15) was synthesized as a reference. The naphthalene units of circumtrindene are arched, but the naphthyl group of compound **5.41** is planar; therefore, it will be a good comparison for shielding and de-shielding effects that are affected by the curvature of the π system. As anticipated, the proton NMR spectrum of the reference compound (**5.41**) indicated that the methyl peaks are magnetically equivalent showing a single peak at 1.88 ppm (Figure 5.15). A comparison between the NMR spectra of compounds **5.40** and **5.41** revealed that the signal of the methyl group, which hangs over the concave side of circumtrindene, is shifted upfield by 0.76 ppm, and downfield by 0.41 ppm for the methyl group hanging over the convex side.

Figure 5.15 Chemical Shifts of *ortho*-Methyl Groups in Compounds 5.40 and 5.41

To confirm the assignments of the two methyl NMR signals in compound 5.40, computational studies on the NMR chemical shifts were conducted (GIAO method). The calculation results showed a good agreement between the experimentally-obtained chemical shifts and the calculated ones for both compound 5.40 and the reference compound (5.41, Table 5.1). The data indicated that the resonance of the methyl group over the concave face is shifted upfield by 0.76 ppm, and the methyl group over the convex face is shifted downfield by 0.41 ppm. These data validate a striking difference in the magnetic environments over the two different faces — convex and concave — of circumtrindene, which is caused by the curved π system.

Table 5.1 Calculated and Experimentally-Obtained NMR Chemical Shifts

Compounds	δ_{exp} (ppm)	δ_{calc} (ppm)
1-(2,6-dimethylphenyl)naphthalene (5.41)	1.88	1.94
1-(2,6-dimethylphenyl)circumtrindene (5.40-endo)	1.12	1.13
1-(2,6-dimethylphenyl)circumtrindene (5.40-exo)	2.29	2.32

5.5.2.2. Stereoelectronic Environment

5.5.2.2.1. Introduction to Natural Bond Orbital (NBO)

NBOs (natural bond orbitals) were originally developed to investigate hybridization and covalency effects of polyatomic wavefunctions.⁶⁴ A natural bond orbital is a calculated bonding orbital with maximum electron density, and it represents a *localized* electron correlation treatment. In contrast to the NBOs, the Hartree-Fock (HF) molecular orbitals (MOs), which are used in the traditional correlated methods, are highly *delocalized* over the entire molecular system.⁶⁵ The property of delocalization in the Hartree-Fock (HF) molecular orbitals (MOs) leads to exponential scaling behavior in computer time with an increasing number of electrons. Because the HF-MOs are calculated over the entire molecular system, the electron correlations can become “unphysical” or “unrealistic” in the Hartree-Fock (HF) molecular orbital (MO) description.

On the other hand, the natural bond orbitals NBOs were constructed to allow for interpretation of chemical phenomena in terms of the language of chemists (*e.g.* transition state structures, bond breaking during reactions, etc.). Since natural bond orbitals (NBOs)

⁶⁴ (a) Foster, J. P.; Weinhold, F., "Natural Hybrid Orbitals," *Journal of the American Chemical Society* **1980**, *102*, 7211-7218. (b) Weinhold, F.; Landis, C. R. *Valency and Bonding: A Natural Bond Orbital Donor-Acceptor Perspective*; Cambridge University Press: Cambridge UK ; New York, 2005.

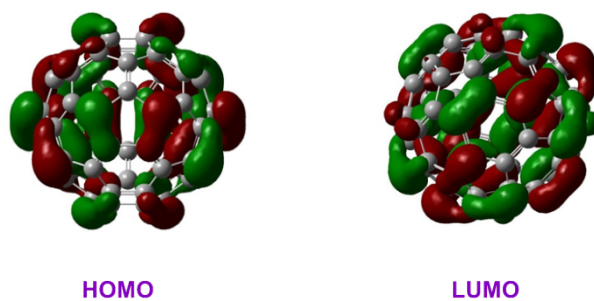
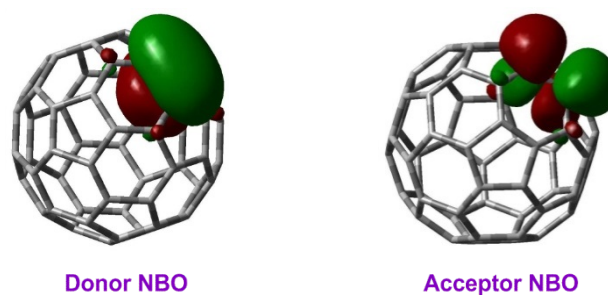
⁶⁵ Flocke, N.; Bartlett, R. J., "Localized Correlation Treatment Using Natural Bond Orbitals," *Chemical Physics Letters* **2003**, *367*, 80-89.

closely describe the picture of *localized* bonds and lone pairs as basic units of molecular structure, they are often referred as a “chemist’s basis set.”⁶⁶

To demonstrate the localization/delocalization concept of these theories, we calculated molecular orbitals of fullerene-C₆₀ with both HF-MO and NBO methods (Figures 5.16 and 5.17).⁶⁷ In the canonical molecular orbitals (MOs) of fullerene, the HOMO and LUMO orbitals are delocalized over the entire molecule (Figure 5.16). And, the description of these MOs often seems to be less chemically intuitive. However, the NBOs of fullerene-C₆₀ clearly show where the electrons exist and where the antibonding orbital is located in terms of a specific bond (Figure 5.17); they often deliver chemically more meaningful messages. In other words, the NBOs represent the molecular system in a chemically intuitive way, agreeing with the picture of local structures that chemists assign to the distribution of electrons in molecules.

⁶⁶ Reed, A. E.; Curtiss, L. A.; Weinhold, F., "Intermolecular Interactions from a Natural Bond Orbital, Donor-Acceptor Viewpoint," *Chemical Reviews* **1988**, *88*, 899-926.

⁶⁷ Calculated at B3LYP/6-31G*.

Figure 5.16 Canonical Molecular Orbitals of Fullerene-C₆₀Figure 5.17 Natural Bond Orbitals of Fullerene-C₆₀

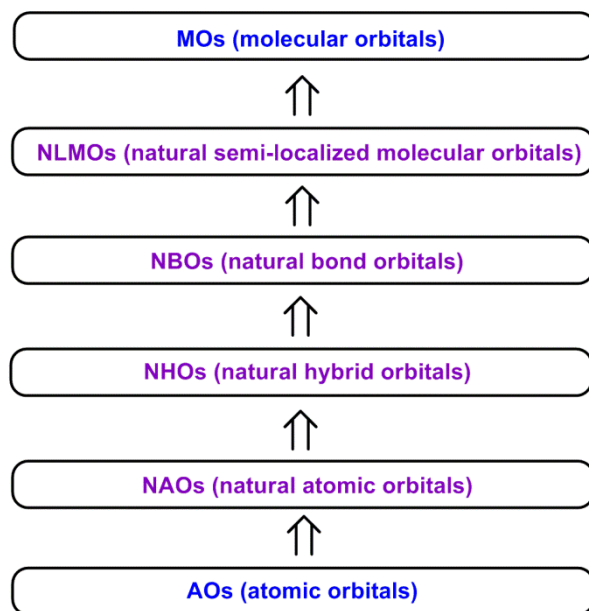
In quantum chemistry, NBOs are obtained through a series of block-diagonalizations of the one-electron density matrix and can be grouped into five sets of orbitals: core electrons (CR), lone-pairs (LP), bonds (BD), antibonds (BD*), and Rydberg orbitals (RY*).⁶⁸ The NBOs are orthogonal; the overlap between the orbitals is zero. Also, they are highly localized in space, transferable from one similar molecular structure to the next. In addition, NBOs divide themselves into an occupied orbital set [*i.e.* core electrons (CR), lone-pairs (LP), and bonds] and a virtual orbital set [*i.e.* antibonds (BD*) and Rydberg orbitals (RY*)]. Each

⁶⁸ Weinhold, F.; Landis, C. R. *Discovering Chemistry with Natural Bond Orbitals*; Wiley: Hoboken, N.J., 2012.

valence bonding orbital NBO σ must be paired with a corresponding valence antibonding NBO σ^* to complete the span of the valence space.

The NBO for a localized σ bond between two atoms is generated from directed orthogonal hybrids, natural hybrid orbitals (NHOs). The NBOs are one of a sequence of natural localized orbital sets, and the hierarchy of the orbitals is illustrated in Figure 5.18.⁶⁹ The natural localized orbital sets include natural atomic orbitals (NAOs), natural hybrid orbitals (NHOs), natural bond orbitals (NBOs), and natural semi-localized molecular orbitals (NLMOs). These natural orbital sets are intermediates between bases atomic orbitals (AOs) and canonical molecular orbitals (MOs).

Figure 5.18 Hierarchy of Orbitals



⁶⁹ Weinhold, F.; Landis, C. R., "Natural Bond Orbitals and Extensions of Localized Bonding Concepts," *Chemistry Education Research and Practice* **2001**, 2, 91-104.

The concept of natural orbitals was first introduced by Löwdin in 1955 to describe the unique set of orthonormal one-electron functions that are intrinsic to the N-electron wavefunction.⁷⁰ Even though the idea of using localized orbitals in electron correlation treatments is as old as the field,⁷¹ practical methods for research have developed and implemented in recent years.^{72,73} The NBO analysis is considered one of the best methods for research with localized electrons correlation treatments.

The use of NBOs has been a great means to investigate atomic charges, bond order, charge transfer, spectroscopic description, and many others. In particular, we were interested in *the second-order perturbation theory of NBO donor-acceptor interactions*. Natural bond orbital (NBO) analysis stresses the role of intermolecular orbital interactions in the complex. This is carried out by considering all possible interactions between filled donor NBOs and empty acceptor NBOs and estimating their energetic importance by second-order perturbation theory. For each donor NBO and acceptor NBO, the stabilization energy associated with electron delocalization between donor and acceptor is estimated. For this

⁷⁰ Löwdin, P.-O., "Quantum Theory of Many-Particle Systems. I. Physical Interpretations by Means of Density Matrices, Natural Spin-Orbitals, and Convergence Problems in the Method of Configurational Interaction," *Physical Review* **1955**, *97*, 1474-1489.

⁷¹ Nesbet, R. K. In *Advances in Chemical Physics*; John Wiley & Sons, Inc., 2007.

⁷² (a) Haser, M.; Almlöf, J., "Laplace Transform Techniques in Møller–Plesset Perturbation Theory," *The Journal of Chemical Physics* **1992**, *96*, 489-494. (b) Maslen, P. E.; Head-Gordon, M., "Non-Iterative Local Second Order Møller–Plesset Theory," *Chemical Physics Letters* **1998**, *283*, 102-108.

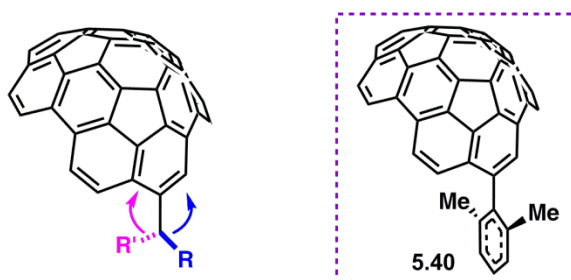
⁷³ (a) Scuseria, G. E.; Ayala, P. Y., "Linear Scaling Coupled Cluster and Perturbation Theories in the Atomic Orbital Basis," *The Journal of Chemical Physics* **1999**, *111*, 8330-8343. (b) Schutz, M.; Werner, H.-J., "Low-Order Scaling Local Electron Correlation Methods. IV. Linear Scaling Local Coupled-Cluster (LCCSD)," *The Journal of Chemical Physics* **2001**, *114*, 661-681.

project, the stabilization energy was calculated for a circumtrindene derivative, as presented in the succeeding section.

5.5.2.2. NBO Analysis of Circumtrindene

To understand better the difference in nature between the convex face and concave face of circumtrindene, the stereoelectronic effect of this nonplanar aromatic system was investigated by the NBO analysis.⁷⁴ We conjectured that the curvature of the molecule would create different hyperconjugative environments on the two faces of the π system. In consequence, the interactions between the two donors (R and R' in Figure 5.19) and the acceptor (the π system of circumtrindene) would be different (Figure 5.19). Those interactions can be quantitatively examined by an NBO analysis. More specifically, we planned to calculate those energies from the phenyl-substituted circumtrindene (**5.40**), which was also chemically synthesized.

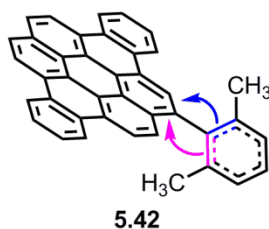
Figure 5.19 Consequence of the Curvature



⁷⁴ For the NBO analysis, the NBO 5.0 program, which is implemented in Gaussian 09, was used.

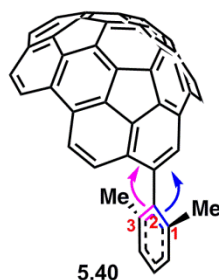
Due to the structural resemblance between compound **5.42** and the phenyl-substituted circumtrindene (**5.40**), we chose the phenyl-substituted dibenzo[*a,j*]coronene (**5.42**) as a reference compound (Figure 5.20). In contrast to **5.40**, the π system of compound **5.42** is planar; therefore, the two π faces of the molecule are equivalent. The NBO calculation of the donor/acceptor interactions for compound **5.42** revealed that there is no difference for these two interactions, as we anticipated. The same NBO energy, 1.79 kcal/mol, was obtained for both interactions that are indicated in Figure 5.20.

Figure 5.20 Reference System for NBO Analysis



On the other hand, the NBO analysis of compound **5.40** suggested that there is difference between two π faces of **5.40** in terms of the strength of hyperconjugation. While the NBO energy for C1–C2 bond donation was 2.14 kcal/mol, the NBO energy for C2–C3 bond donation was 1.62 kcal/mol (Figure 5.21). The calculation results suggest that the hyperconjugation energy for the interaction between the donor and the convex face is greater. In other words, the donor–accepter interaction is more favored on the convex face of circumtrindene than the concave face of the molecule.

Figure 5.21 NBO Analysis for Hyperconjugation



During the studies on this project, a number of computational methods were employed to aid and rationalize the experimental results. The theoretical investigations enabled us to examine feasible, but difficult to be proved by experiments, properties/reactivities of our system in a quantitative way. As far as the properties of circumtrindene is concerned, the computational results suggested that the curvature of the π system created different environments on the two faces of circumtrindene; the differentiated environments include stereoelectronic, electrostatic, magnetic, and hyperconjugative environments.

5.6. Noncovalent Functionalization of Circumtrindene

5.6.1. Reduction with Lithium Metal

Reduction of corannulene (5.2) with lithium metal to give a tetraanion of corannulene (5.43) was first reported by Rabinovitz and Scott.⁷⁵ More recently, the X-ray crystal structure of $2\text{Cor}^{4-}/8\text{Li}^{+}$ was reported by the Petrukhina group in 2011 (Scheme 5.24).⁷⁶ It has been known that planar sp^2 π -systems can serve as key anode components in lithium-ion batteries.⁷⁷ More recently, nonplanar carbon allotropes, such as fullerenes and nanotubes, are also being examined as prospective anode materials for energy storage.⁷⁸ For example, the anode material made from corannulene (5.2) showed a high reversible lithium capacity.⁷⁹

⁷⁵ Ayalon, A.; Rabinovitz, M.; Cheng, P. C.; Scott, L. T., "Corannulene Tetraanion: A Novel Species with Concentric Anionic Rings," *Angewandte Chemie International Edition* **1992**, *31*, 1636-1637.

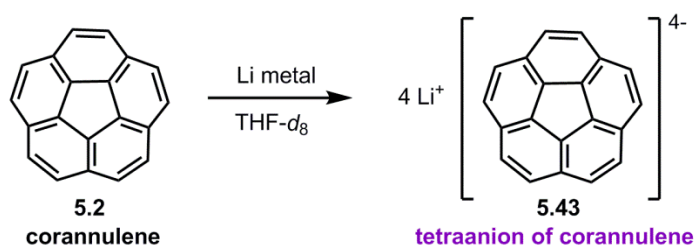
⁷⁶ (a) Zabula, A. V.; Filatov, A. S.; Spisak, S. N.; Rogachev, A. Y.; Petrukhina, M. A., "A Main Group Metal Sandwich: Five Lithium Cations Jammed between Two Corannulene Tetraanion Decks," *Science* **2011**, *333*, 1008-1011. (b) Filatov, A. S.; Petrukhina, M. A., "Probing the Binding Sites and Coordination Limits of Buckybowls in a Solvent-Free Environment: Experimental and Theoretical Assessment," *Coordination Chemistry Reviews* **2010**, *254*, 2234-2246.

⁷⁷ (a) Tarascon, J. M.; Armand, M., "Issues and Challenges Facing Rechargeable Lithium Batteries," *Nature* **2001**, *414*, 359-367. (b) Armand, M.; Tarascon, J. M., "Building Better Batteries," *Nature* **2008**, *451*, 652-657.

⁷⁸ (a) Lee, S. W.; Yabuuchi, N.; Gallant, B. M.; Chen, S.; Kim, B.-S.; Hammond, P. T.; Shao-Horn, Y., "High-Power Lithium Batteries from Functionalized Carbon-Nanotube Electrodes," *Nature Nanotechnology* **2010**, *5*, 531-537. (b) Lahiri, I.; Oh, S.-W.; Hwang, J. Y.; Cho, S.; Sun, Y.-K.; Banerjee, R.; Choi, W., "High Capacity and Excellent Stability of Lithium Ion Battery Anode Using Interface-Controlled Binder-Free Multiwall Carbon Nanotubes Grown on Copper," *ACS Nano* **2010**, *4*, 3440-3446.

⁷⁹ (a) Sandi, G.; Gerald, R.; Scanlon, L.; Johnson, C.; Klingler, R.; Rathke, J., "Molecular Orbital and Li-7 Nmr Investigation of the Influence of Curved Lattices in Lithium Intercalated Carbon Anodes," *Journal*

Scheme 5.24 Reduction of Corannulene

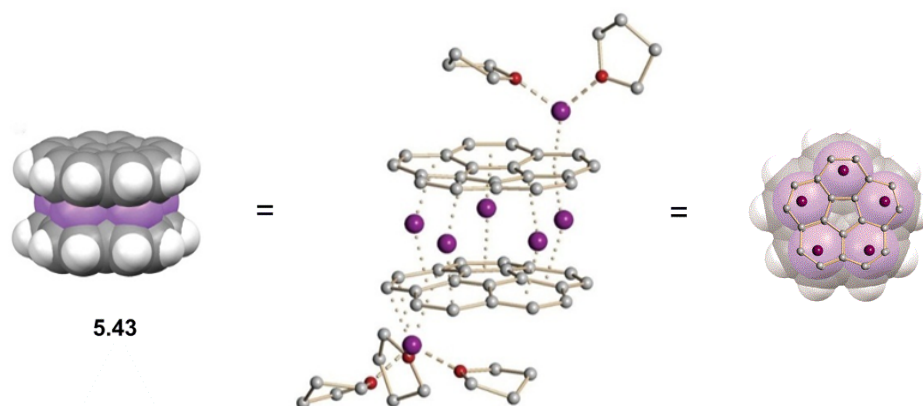


The lowest unoccupied molecular orbital (LUMO) of corannulene is doubly degenerate and thus can accept up to four extra electrons, which would form a stable tetraanion **5.43** at the highest reduction level.⁸⁰ In this work, the lithium salt (**5.43**) was crystallized by slow diffusion of hexane vapor into a THF solution of the product at 15 °C. The X-ray analysis revealed a sandwich-type arrangement for complex **5.43** (Figure 5.22). The five lithium cations were found between the two anionic corannulene molecules and were in the solid state. The two more lithium ions were bound to the external surface of this sandwich-like structure; one of them was on the top, and the other one was on the bottom. The remaining one lithium cation was found to be solvent-separated (not shown in Figure 5.22).

of New Materials for Electrochemical Systems **2000**, 3, 13-20. (b) Gerald II, R. E.; Johnson, C. S.; Rathke, J. W.; Klingler, R. J.; Sandí, G.; Scanlon, L. G., "⁷Li NMR Study of Intercalated Lithium in Curved Carbon Lattices," *Journal of Power Sources* **2000**, 89, 237-243.

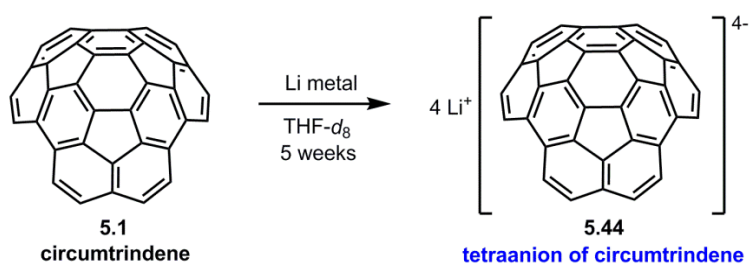
⁸⁰ (a) Ayalon, A.; Rabinovitz, M.; Cheng, P.-C.; Scott, L. T., "Corannulene Tetraanion: A Novel Species with Concentric Anionic Rings," *Angewandte Chemie International Edition* **1992**, 31, 1636-1637. (b) Rabideau, P. W.; Marcinow, Z.; Sygula, R.; Sygula, A., "Concerning the Structure of the Corannulene Tetraanion," *Tetrahedron Letters* **1993**, 34, 6351-6354. (c) Baumgarten, M.; Gherghel, L.; Wagner, M.; Weitz, A.; Rabinovitz, M.; Cheng, P.-C.; Scott, L. T., "Corannulene Reduction: Spectroscopic Detection of All Anionic Oxidation States," *Journal of the American Chemical Society* **1995**, 117, 6254-6257.

Figure 5.22 X-Ray Structure of Corannulene Tetraanion



Considering resemblance between circumtrindene (5.1) and corannulene (5.2) in terms of the nonplanar π system and the molecular orbital system, we speculated that circumtrindene also could be reduced with lithium metal in a similar fashion. To our pleasure, we observed that a tetraanion of circumtrindene (5.44) was formed when circumtrindene was treated with Li metal for five weeks (Scheme 5.25).⁸¹

Scheme 5.25 Reduction of Circumtrindene



⁸¹ This investigation was conducted in collaboration with the Professor Petrukhina's group at the University at Albany.

The lowest unoccupied molecular orbital (LUMO) of circumtrindene is also doubly degenerate, as in the corannulene case; thus, circumtrindene can accept up to four extra electrons at the highest reduction level, which was observed experimentally. The proton NMR analysis indicated that the circumtrindene tetraanion (**5.44**) has two distinct sets of hydrogens; two doublets at 6.5 and 5.5 ppm were observed. As anticipated, the two doublets in naked circumtrindene (**5.1**) at 7.6 and 7.2 ppm were shifted upfield when circumtrindene was reduced with lithium.

5.6.2. Complexation with Silver Ion

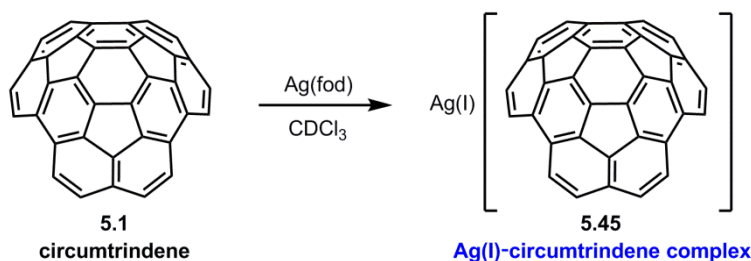
In recent years, cation- π complexes of aromatic compounds have received a significant amount of attention in chemical sciences.⁸² These complexes are believed to involve protein folding, neurological signaling, the functioning of ion channels and other biological activities.⁸³ As demonstrated in the previous section, the concave face of circumtrindene showed the more negative electrostatic potential (see Figure 5.12). Thus, we were interested in whether cation- π complexation would be favored inside circumtrindene

⁸² (a) Dougherty, D. A., "Cation- π Interactions in Chemistry and Biology: A New View of Benzene, Phe, Tyr, and Trp," *Science* **1996**, 271, 163-168. (b) Ma, J. C.; Dougherty, D. A., "The Cation- π Interaction," *Chemical Reviews* **1997**, 97, 1303-1324.

⁸³ (a) Gallivan, J. P.; Dougherty, D. A., "Cation- π Interactions in Structural Biology," *Proceedings of the National Academy of Sciences* **1999**, 96, 9459-9464. (b) Meyer, E. A.; Castellano, R. K.; Diederich, F., "Interactions with Aromatic Rings in Chemical and Biological Recognition," *Angewandte Chemie International Edition* **2003**, 42, 1210-1250.

(5.1) rather than outside. The first experimental evidence for silver(I)–circumtrindene complexation was reported by our laboratory (Scheme 5.26).^{84, 85}

Scheme 5.26 Preparation of Ag(I)–Circumtrindene Complex



Among the monoatomic +1 ions, silver(I) stands out because it shows particularly strong affinity for the electron-rich faces of aromatic hydrocarbons.⁸⁶ Thus, Ag(fod) was employed for the complexation agent in this experiment, and Yb(fod)₃ was added to assist NMR analyses of the complexation reaction. In the proton NMR spectra for the experiment described in Scheme 5.26, both doublets of circumtrindene (5.1) were shifted downfield in the presence of Ag(fod)·Yb(fod)₃, which was expected for the formation of complex 5.45. This experimental result was also supported by DFT calculations.

⁸⁴ Ansems, R.; Scott, L. T., "Cation- π Complexes of a Bowl-Shaped Polycyclic Aromatic Hydrocarbon," *Journal of Physical Organic Chemistry* **2004**, 17, 819-823.

⁸⁵ For related studies, see: (a) Dunbar, R. C., "Binding of Transition-Metal Ions to Curved Π Surfaces: Corannulene and Coronene," *The Journal of Physical Chemistry A* **2002**, 106, 9809-9819. (b) Jemmis, E. D.; Parameswaran, P.; Anoop, A., "Effect of Metal Complexation on Ring Opening of Bowl-Shaped Hydrocarbons: Theoretical Study," *International Journal Of Quantum Chemistry* **2003**, 95, 810-815.

⁸⁶ Munakata, M.; Wu, L. P.; Ning, G. L., "A New Type of Multilayer System–Silver(I) Complexes of Polycyclic Aromatic Compounds," *Coordination Chemistry Reviews* **2000**, 198, 171-203.

5.7. Conclusions and Outlook

Bowl-shaped geodesic polyarenes can be considered the missing links between the “classic” flat PAHs and the spheroidal fullerenes. The present study has shown that open geodesic polyarenes can feature chemistry inherent to both classes of aromatics. The curved π system induces unequal environments on the two faces of circumtrindene, significant strain energy to the molecule, and non-identical bond lengths.

Along with the electronic effects, the stereoelectronic effect (*i.e.* the lowered LUMO energy and the specific distribution of the LUMO coefficient) enabled the site-selective interior functionalization with fullerene-type chemistry. On the other hand, the edge carbons, which are not present in fullerenes, still possess reactivity of common planar PAHs. Peripheral functionalization was conducted on those edge carbons, by which the π system is extended towards a larger bowl and the magnetic environments of the two different faces were examined. In addition to these covalent functionalization reactions, noncovalent functionalization processes of circumtrindene have also been demonstrated by reduction with lithium metal and complexation with silver ion.

Computational studies for each functionalization method not only support the experimental data but also provide deeper insights into this curved aromatic system. In this project, the computational results suggest that the curvature of the π system creates unequal

environments on the two faces of circumtrindene, including stereoelectronic, electrostatic, magnetic, and hyperconjugative environments.

Considering the chemistry and application of fullerenes and related compounds,⁸⁷ understanding of the properties and chemistry of fullerene fragments like circumtrindene is expected to contribute to practical applications such as electronic devices, fuel cells, and biologically-active materials.

⁸⁷ (a) Prato, M. In *Fullerenes and Related Structures*; Hirsch, A., Ed.; Springer Berlin Heidelberg, 1999; Vol. 199. (b) Langa, F.; Nierengarten, J.-F.; Royal Society of Chemistry (Grande-Bretagne) *Fullerenes Principles and Applications*; Royal Society of Chemistry: Cambridge, 2007. (c) Akasaka, T.; Wudl, F.; Nagase, S. *Chemistry of Nanocarbons*; Wiley: Chichester West Sussex, 2010.

5.8. Experimental Section

5.8.1. General Information

All reactions were performed in oven- or flame-dried glassware fitted with rubber septa under a positive pressure of nitrogen, unless otherwise stated. Air- and moisture-sensitive liquids were transferred via syringe or stainless steel cannula. Organic solvents were concentrated by rotary evaporation at various temperatures, unless otherwise noted. All work-up and purification procedures were carried out with reagent grade solvents under typical bench-top conditions. Analytical thin-layer chromatography (TLC) was performed using glass plates, which are pre-coated with silica gel 60 F254 (0.25 mm thickness) impregnated with a fluorescent indicator (254 nm). TLC plates were visualized by exposure to UV (ultraviolet) light, and then were stained with phosphomolybdic acid (PMA) in ethanol, potassium permanganate (KMnO₄) in water, or cerium(IV) sulfate and ammonium molybdate in sulfuric acid (CAM). Liquid chromatography was performed using forced flow (flash chromatography)⁸⁸ on silica gel (porosity = 60 Å, particle size = 32-63 μm) purchased from Sorbent Technologies. Medium pressure gradient chromatography was performed on a Teledyne Isco CombiFlash automated flash chromatography system with a 200-780 nm UV-vis variable wavelength detector.

⁸⁸ Still, W. C.; Kahn, M.; Mitra, A., "Rapid Chromatographic Technique for Preparative Separations with Moderate Resolution," *The Journal of Organic Chemistry* **1978**, *43*, 2923-2925.

All commercially available chemicals and solvents were purchased from Sigma Aldrich, Acros, Strem, Alfa Aesar, Fisher, or TCI America and were used without purification with the following exceptions. Tetrahydrofuran (THF), methylene chloride (CH_2Cl_2), toluene, *N,N*-dimethylacetamide (DMAc), 1,2-dichlorobenzene (*o*-DCB), and carbon disulfide (CS_2) were dried and purified using a solvent purification system from Innovative Technology Inc.

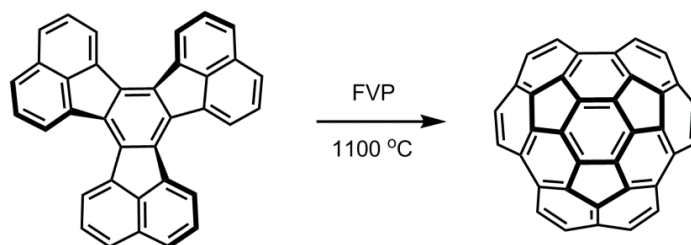
Proton nuclear magnetic resonance (^1H NMR) spectra were recorded on either a Varian INOVA 500 (500 MHz) or a Varian VNMR 500 (500 MHz) at 23 °C unless specified otherwise. Proton chemical shifts are reported in ppm (parts per million, δ scale) downfield from tetramethylsilane and are referenced to residual protium in the NMR solvent as the internal standard (CHCl_3 : 7.26 ppm, C_6H_6 : 7.16 ppm). Data are reported as follows: chemical shift, integration, multiplicity (s = singlet, d = doublet, t = triplet, q = quartet, qn = quintet, br = broad, and m = multiplet), coupling constant (*J*) in hertz (Hz), and assignment. Carbon nuclear magnetic resonance (^{13}C NMR) spectra were recorded on either a Varian INOVA 500 (125 MHz) or a Varian VNMR 500 (125 MHz) with complete proton decoupling at 23 °C unless otherwise stated. Carbon chemical shifts are reported in ppm (parts per million, δ scale) downfield from tetramethylsilane and are referenced to the NMR solvent resonance as the internal standard (CDCl_3 : 77.16 ppm, C_6D_6 : 128.06 ppm).

Melting points were determined with a Thomas-Hoover Unimelt capillary melting point apparatus and were uncorrected. Infrared (IR) spectra were recorded on a Bruker FT-

IR Alpha (ATR Mode) spectrophotometer, ν_{\max} cm^{-1} . Data are represented as follows: frequency of absorption (cm^{-1}) and intensity of absorption (s = strong, m = medium, w = weak, and br = broad). Low resolution mass spectrometric analyses were performed using a Thermo Electron Corporation Finnigan Trace GC Ultra gas chromatograph unit connected to a Thermo Electron Corporation Finnigan Trace DSQ mass spectrometer with direct inlet capabilities. High-resolution mass spectra (HRMS) were obtained by the Boston College Mass Spectrometry Center using various TOF instruments.

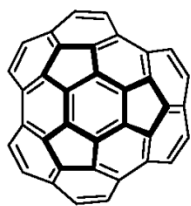
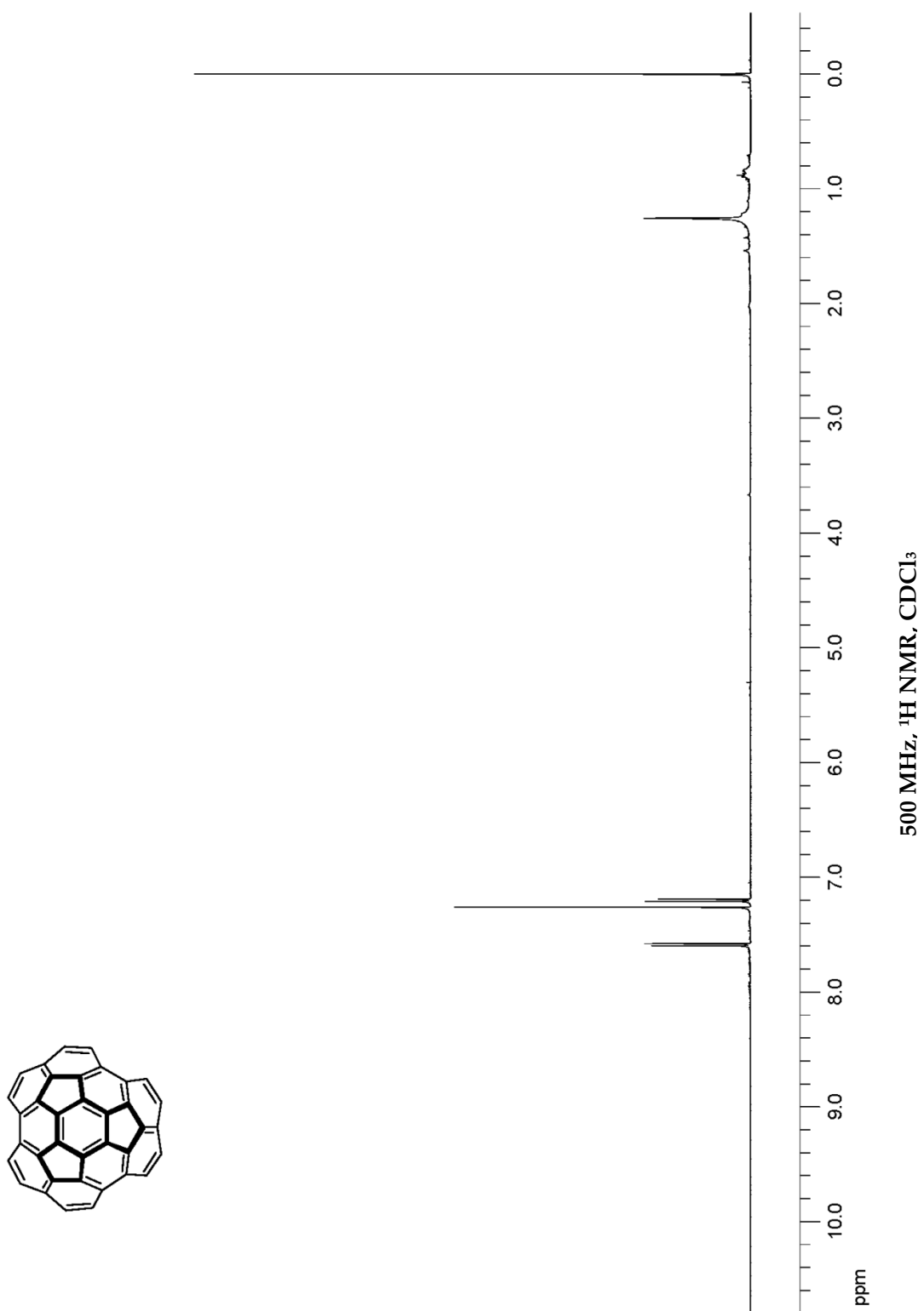
5.8.2. Experimental and Spectral Data

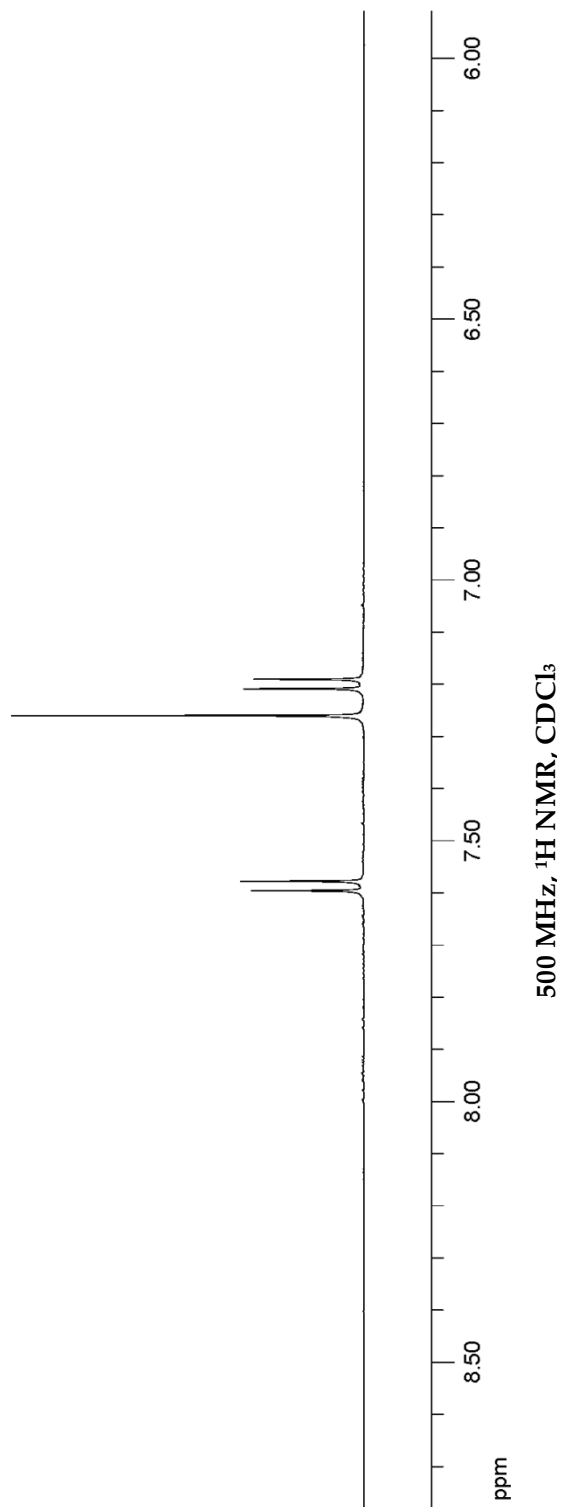
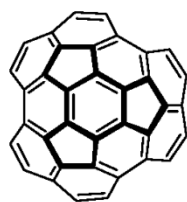
5.8.2.1. Circumtrindene

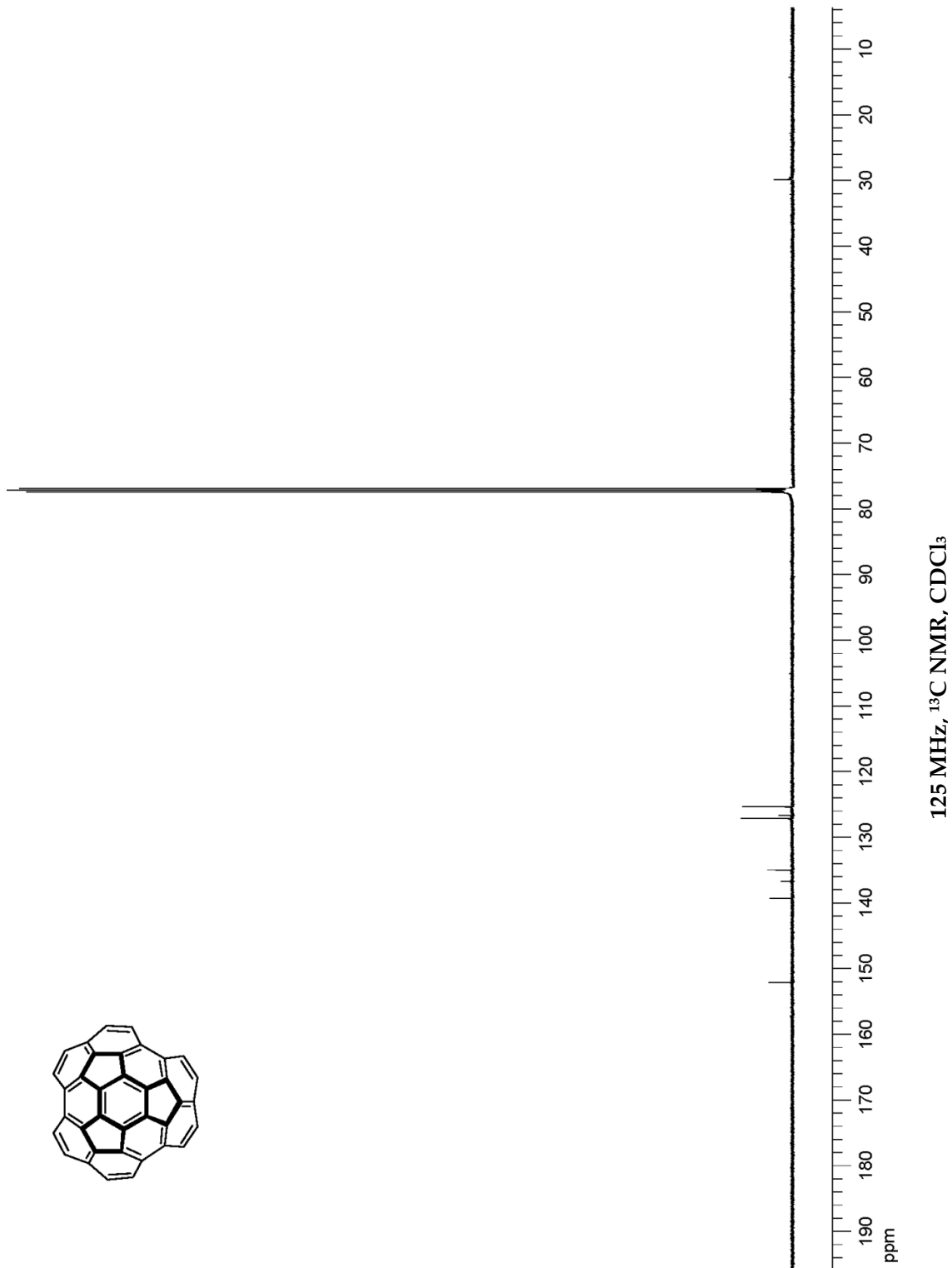


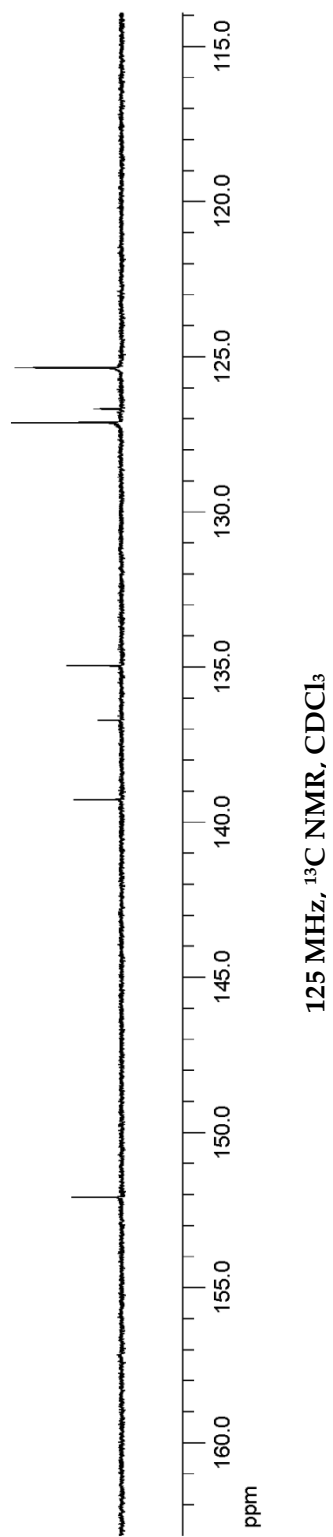
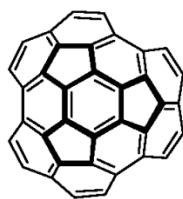
The apparatus for the flash vacuum pyrolysis (FVP) has been described in Figure 5.5. The reaction was performed with 200 mg (0.44 mmol) of decacyclene, which was placed in a sample boat in a supplemental heating oven. On one side of the FVP apparatus, the system was connected to a nitrogen gas reservoir through a capillary inlet tube made out of a section of GC capillary. On the other side of the oven, the pyrolysis tube was connected to a high-capacity vacuum pump through a cold trap filled with liquid nitrogen. The supplemental oven was heated to 300 °C, and the reaction oven was heated to 1100 °C. The pressure of the system was equilibrated to 1.5 torr. As soon as both of the ovens reached the desired temperatures, the sample boat was moved into the center of the supplemental oven. After 2 hours of reaction time, it was observed that all the starting material was sublimed leaving a black tar on the sample boat. Then, the ovens were shut off, and the liquid nitrogen traps were removed. After allowing some time for the system to reach equilibration, the apparatus was open to the atmosphere. The crude product was collected by rinsing both the quartz

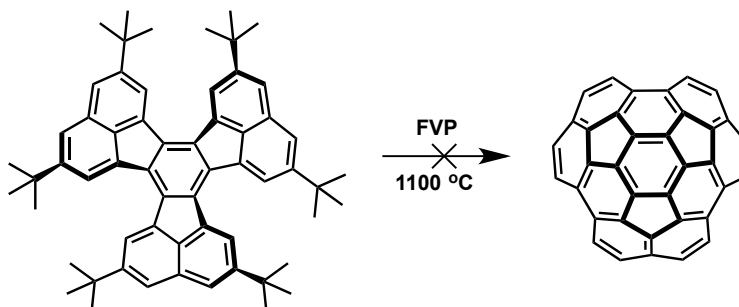
tube and the glass trap with dichloromethane (~500 mL). The crude material was purified by column chromatography on silica gel (hexanes/DCM) to afford circumtrindene in 3% yield (6 mg). $R_f = 0.28$ (5:1 hexane:DCM). $^1\text{H NMR}$ (500 MHz, CDCl_3): δ 7.59 (d, $J = 9.5$ Hz, 6H), 7.20 (d, $J = 9.5$ Hz, 6H). $^{13}\text{C NMR}$ (125 MHz, CDCl_3): δ 152.1, 139.3, 136.7, 135.0, 127.1, 126.7, 125.4. The characterization data were in agreement with literature values.²³





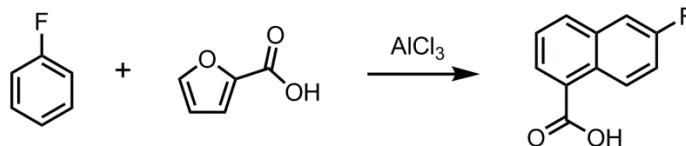




5.8.2.2. Attempted Synthesis of Circumtrindene from C₆₀H₆₆

The FVP reaction was performed with 100 mg (0.13 mmol) of 2,5,8,11,14,17-hexa-*tert*-butyldecacycylene, which was placed in a sample boat in a supplemental heating oven. On one side of the FVP apparatus, the system was connected to a nitrogen gas reservoir through a capillary inlet tube made out of a section of GC capillary. On the other side of the oven, the pyrolysis tube was connected to a high-capacity vacuum pump through a cold trap filled with liquid nitrogen. The supplemental oven was heated to 200 °C, and the reaction oven was heated to 1100 °C. The pressure of the system was equilibrated to 0.5 torr. As soon as both of the ovens reached the desired temperatures, the sample boat was moved into the center of the supplemental oven. After 2 hours of reaction time, it was observed that all the starting material was sublimed leaving a black tar on the sample boat. The crude product was collected by rinsing both the quartz tube and the glass trap with dichloromethane (~500 mL). The mass spectrum of the crude material did not show the desired product peak ($m/z = 444.09$).

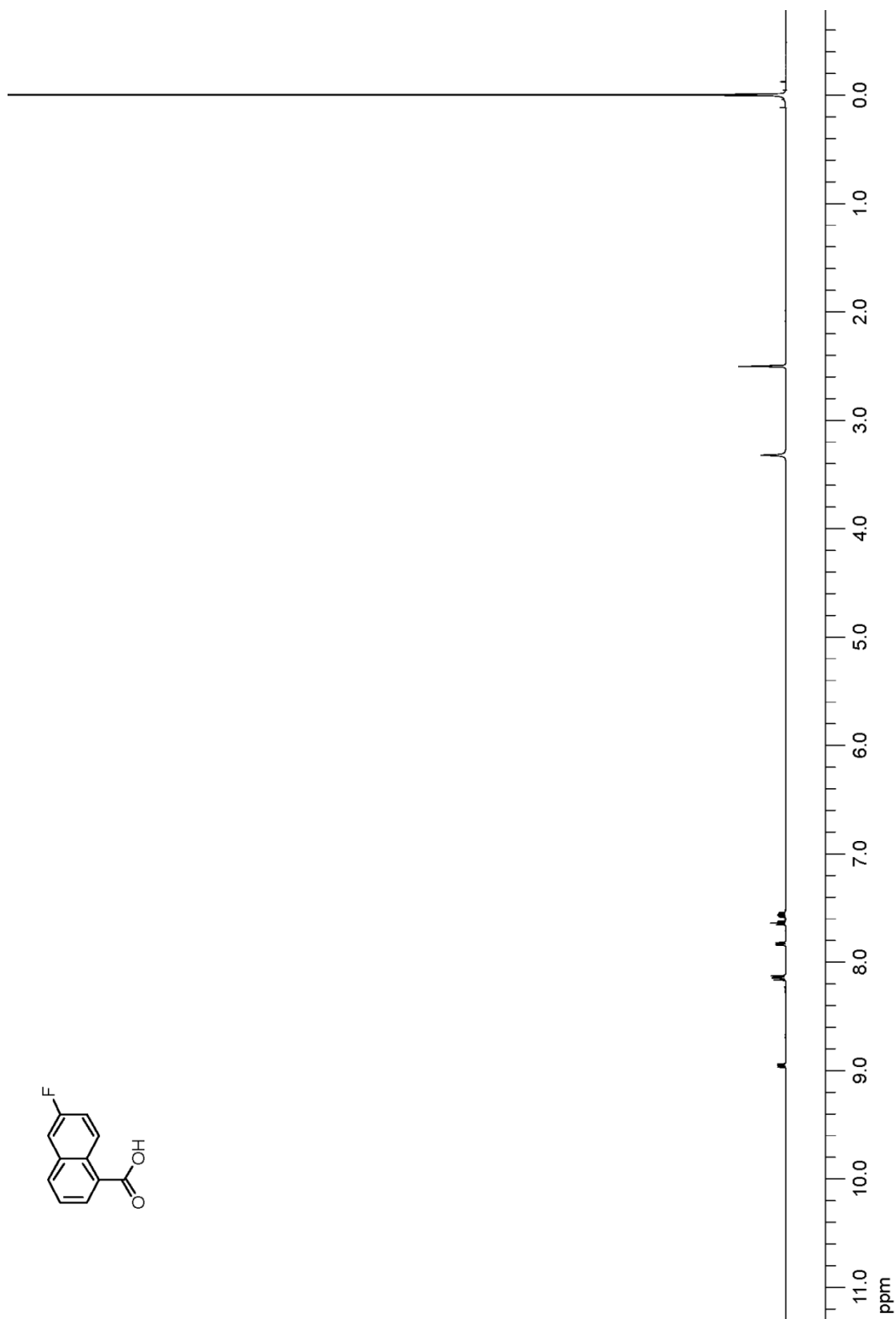
5.8.2.3. 6-Fluoro-1-naphthoic acid

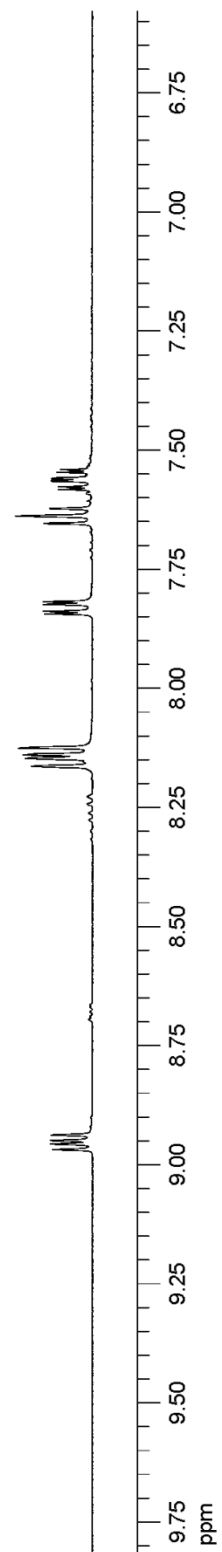
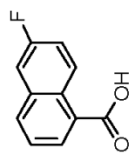


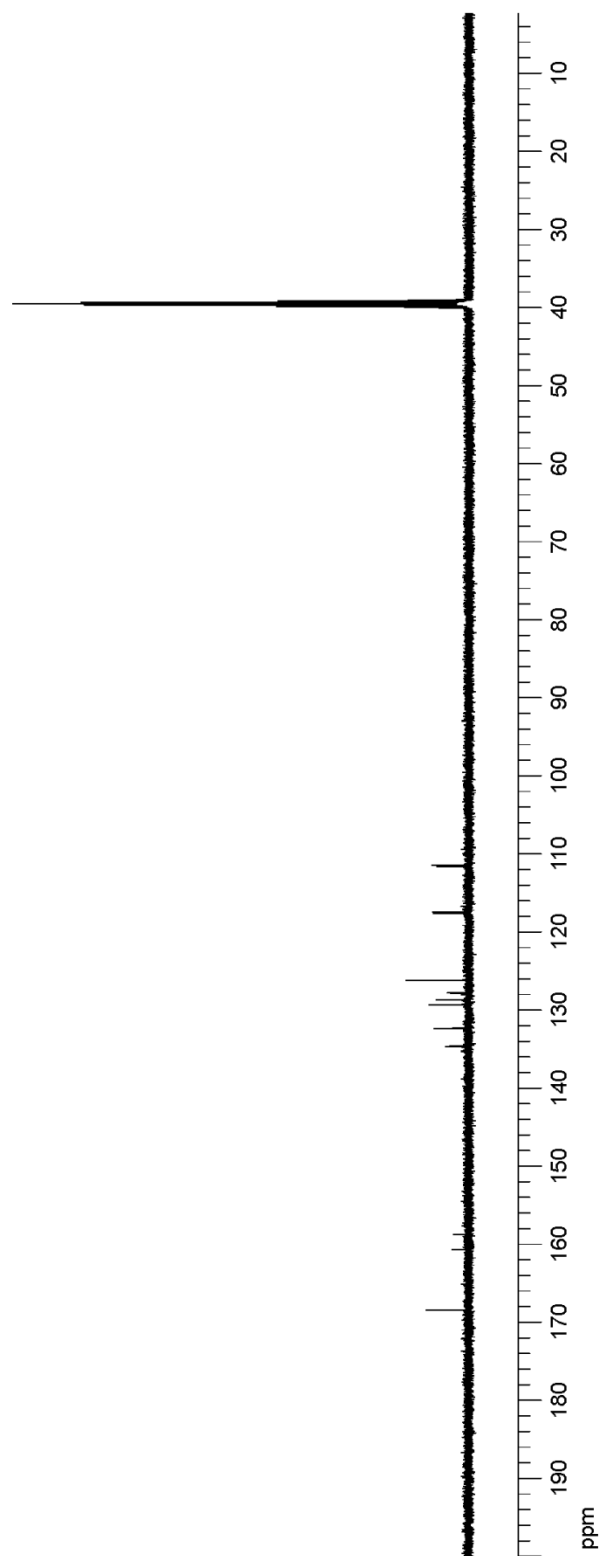
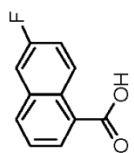
To an oven-dried round-bottomed flask, 274 g (2.86 mmol) of fluorobenzene and 40 g (3.57 mmol) of furan-2-carboxylic acid were added, and the mixture was cooled to 0 °C. Then, 105 g (7.85 mmol) of aluminum chloride was carefully added to the mixture. After 30 min of stirring, the reaction mixture was heated to 75 °C and kept at this temperature for 48 h. After this time, the mixture was poured to a 2 N HCl solution (~2 L) and extracted with ether. The ether layers were combined and washed with water. Then, the washed ether layers were extracted with saturated NaHCO₃ solution. The resulting basic solution was acidified with concentrated HCl solution and extracted again with EtOAc. The combined organic layers were dried over anhydrous sodium sulfate (Na₂SO₄). The drying agent was removed by filtration, and the solvent was removed *in vacuo*. The resulting solid was stirred in toluene for 10 h. After this time, the mixture was filtered to afford 6-fluoro-1-naphthoic acid as an off-white solid in 42% yield (227 g). ¹H NMR (500 MHz, DMSO-*d*₆): δ 8.95 (dd, *J* = 9.5, 6.0 Hz, 1H), 8.16 (d, *J* = 8.5 Hz, 1H), 8.13 (d, *J* = 7.5 Hz, 1H), 7.83 (dd, *J* = 10, 3.0 Hz, 1H), 7.64 (t, *J* = 7.5 Hz, 1H), 7.56 (td, *J* = 9.0, 3.0 Hz, 1H). ¹³C NMR (125 MHz, DMSO-*d*₆): δ 168.4, 159.7 (d, *J* = 245.2 Hz), 134.6 (d, *J* = 9.3 Hz), 132.3 (d, *J* = 5.2 Hz), 129.3, 129.2, 128.6 (d, *J* = 8.9 Hz), 127.8 (d,

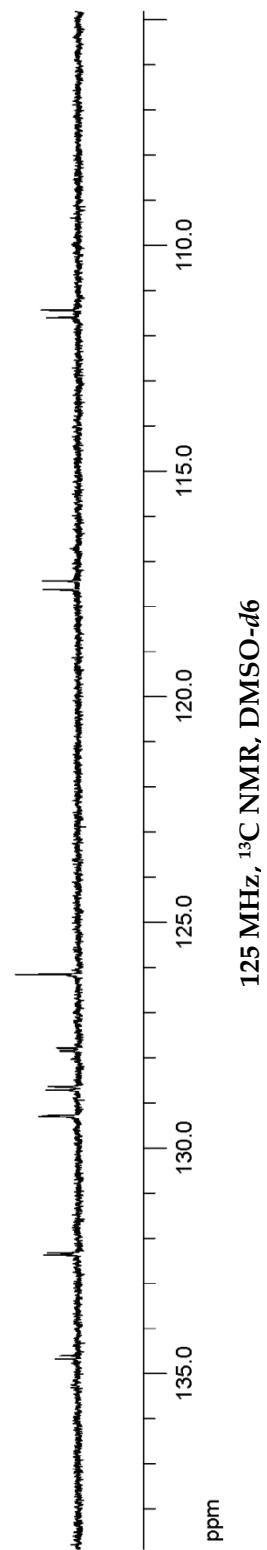
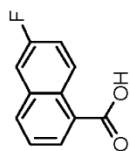
$J = 7.8$ Hz), 126.1, 117.5 (d, $J = 24.6$ Hz), 111.5 (d, $J = 20.0$ Hz). The proton NMR data were in agreement with literature values. 46⁸⁹

⁸⁹ Tagat, J. R.; McCombie, S. W.; Nazareno, D. V.; Boyle, C. D.; Kozlowski, J. A.; Chackalamannil, S.; Josien, H.; Wang, Y.; Zhou, G., "Synthesis of Mono- and Difluoronaphthoic Acids," *The Journal of Organic Chemistry* **2002**, *67*, 1171-1177.

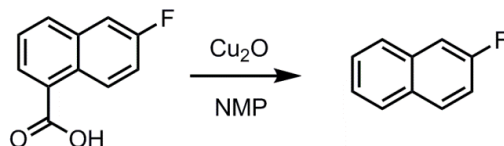


500 MHz, ¹H NMR, DMSO-d₆



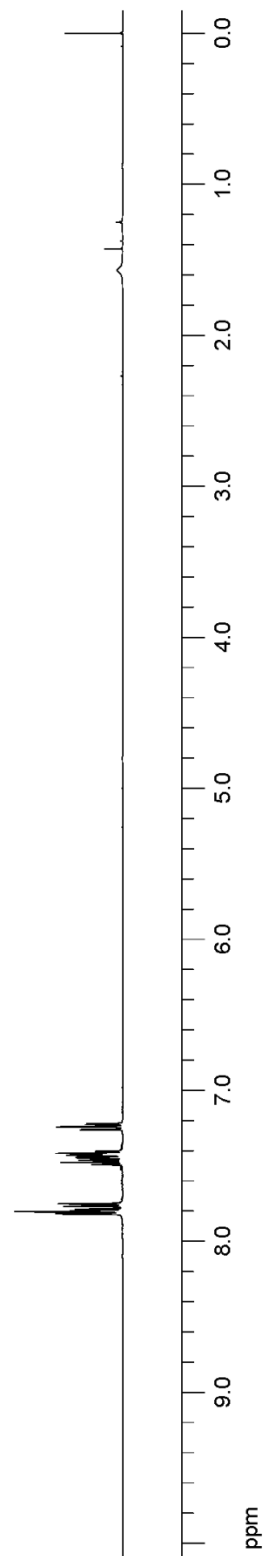
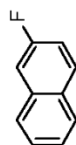


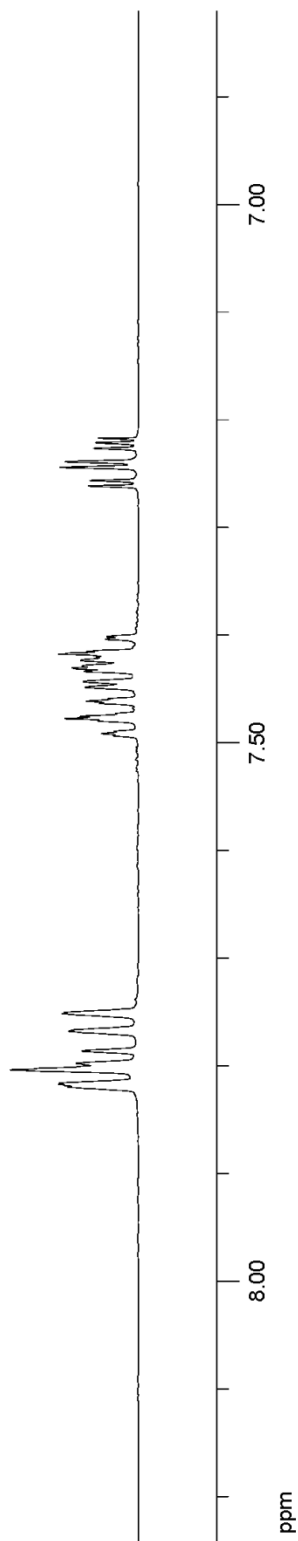
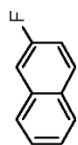
5.8.2.4. 2-Fluoronaphthalene

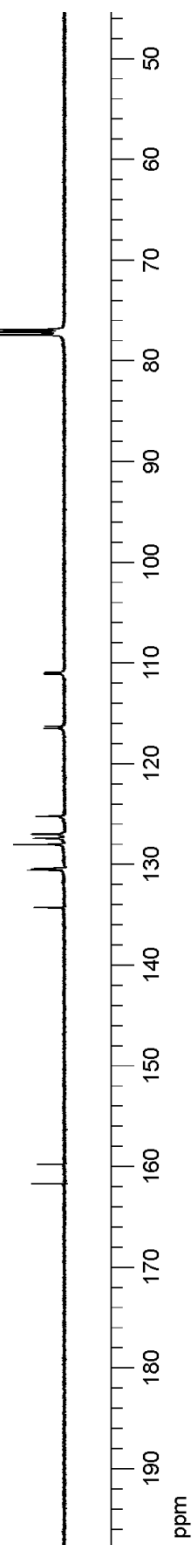
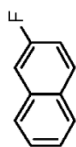


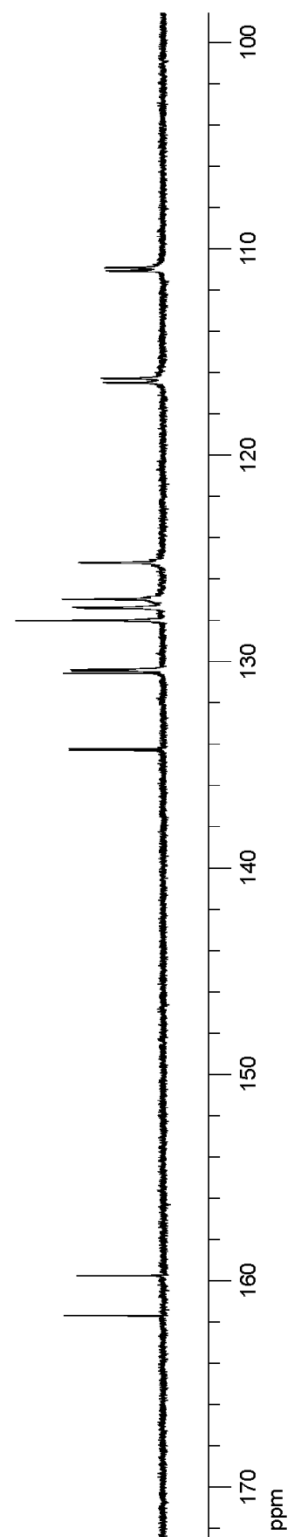
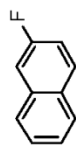
To an oven-dried round-bottomed flask, 1.0 g (5.3 mmol) of 6-fluoro-1-naphthoic acid, 75 mg (0.5 mmol) of cuprous oxide, and 190 mg (1.0 mmol) of 1,10-phenanthroline were added. The reaction flask was purged with alternating cycles of vacuum and nitrogen (3 cycles). Then, 7.9 mL (0.67 M) of NMP and 2.6 mL (2.0 M) of quinolone were added to the reaction mixture using a syringe. The resulting mixture was heated to 170 °C and stirred at this temperature for 18 h. After this time, the mixture was poured into aqueous HCl solution and extracted with diethyl ether. The combined organic layers were washed with brine and dried over anhydrous Na_2SO_4 . The drying agent was removed by filtration, and the solvent was removed *in vacuo*. The resulting solid was further purified by recrystallization to give 2-fluoronaphthalene as a white solid in 95% yield (734 mg). mp = 59–60 °C. ^1H NMR (500 MHz, CDCl_3): δ 7.82-7.77 (m, 2H), 7.75 (d, J = 8.0 Hz, 1H), 7.48-7.41 (m, 3H), 7.24 (ddd, J = 11.0, 8.5, 2.5 Hz, 1H). ^{13}C NMR (125 MHz, CDCl_3): δ 160.1 (d, J = 244.0 Hz), 134.3 (d, J = 9.4 Hz), 130.6, 130.4 (d, J = 9.6 Hz), 128.0, 127.4 (d, J = 5.4 Hz), 127.0, 125.2, 116.4 (d, J = 25.0 Hz), 111.0 (d, J = 20.3 Hz). The characterization data were in agreement with literature values.⁹⁰

⁹⁰ Ye, Y.; Sanford, M. S., "Mild Copper-Mediated Fluorination of Aryl Stannanes and Aryl Trifluoroborates," *Journal of the American Chemical Society* **2013**, *135*, 4648-4651.

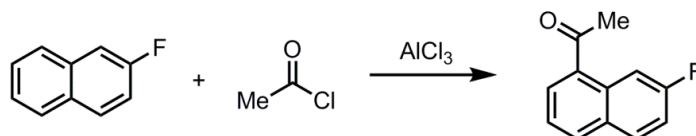
500 MHz, ¹H NMR, CDCl₃

500 MHz, ¹H NMR, CDCl₃

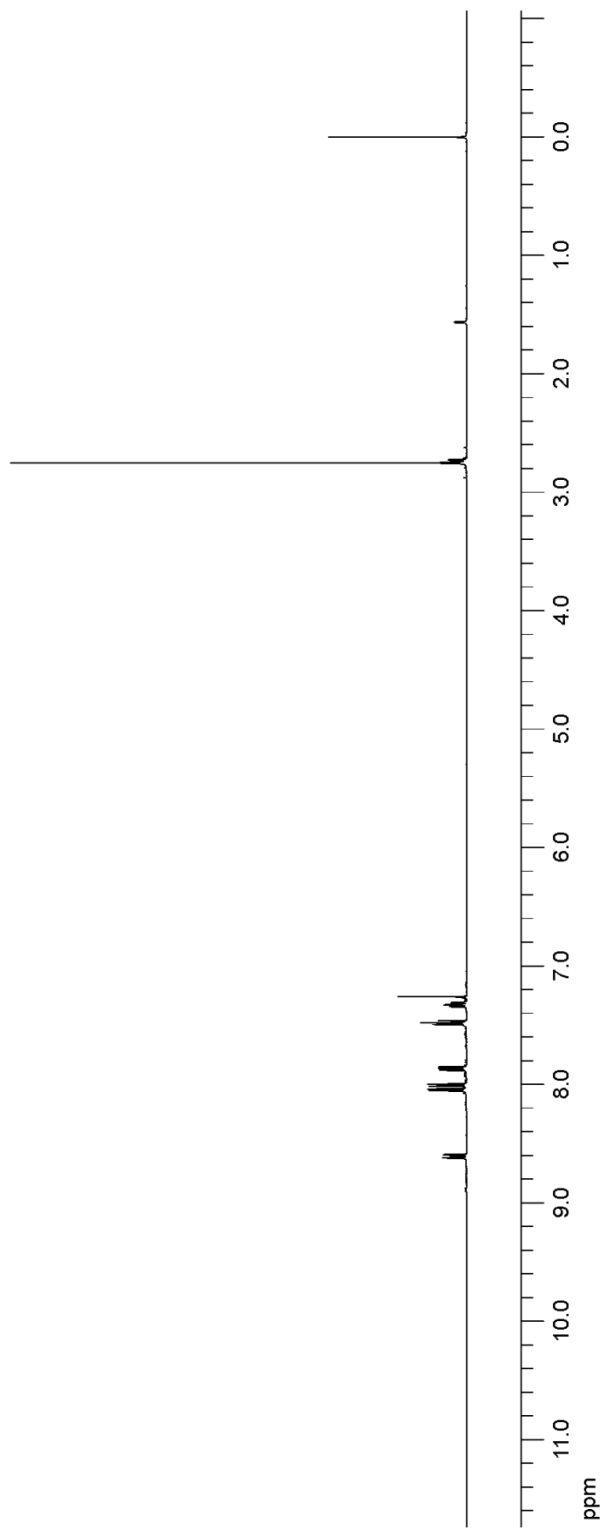
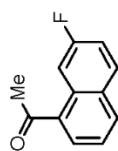
125 MHz, ^{13}C NMR, CDCl_3

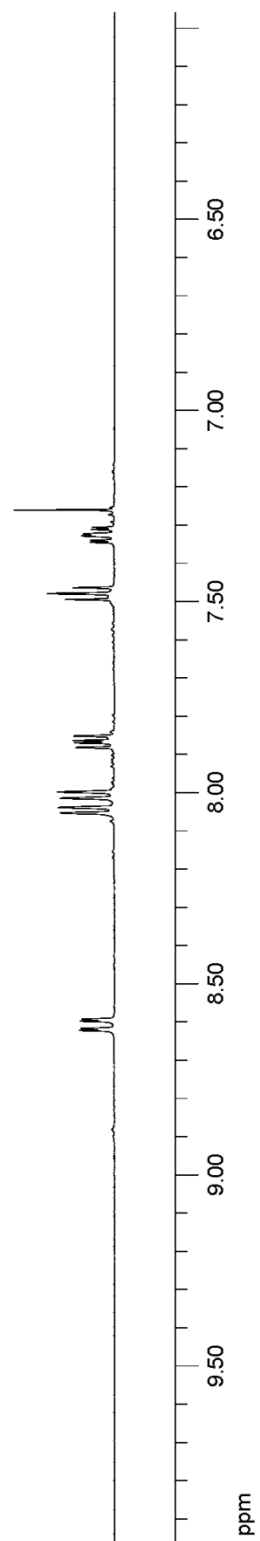
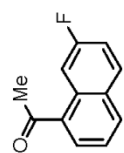


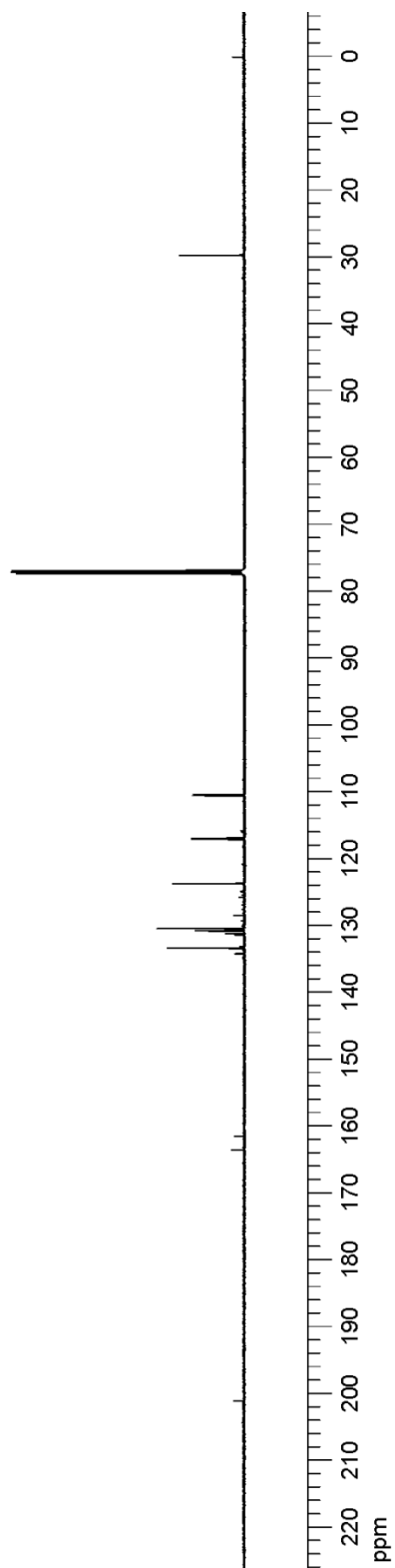
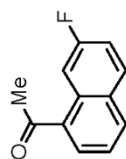
5.8.2.5. 1-(7-Fluoronaphthalen-1-yl)ethan-1-one



To an oven-dried round-bottomed flask, 2-fluoronaphthalene (6.4 g, 44 mmol) was dissolved in dichloromethane (73 mL, 0.60 M). The resulting solution was cooled to $-10\text{ }^{\circ}\text{C}$, and then aluminum chloride (18 g, 130 mmol) was added to the solution. The resulting mixture was then cooled to $-78\text{ }^{\circ}\text{C}$. At this temperature, acetyl chloride (7.1 g, 90 mmol) was added, and the reaction mixture was stirred at the same temperature for 10 h. The reaction was then quenched with a dilute HCl solution, and the resulting solution was extracted with dichloromethane. The combined organic layers were washed with brine and dried over anhydrous Na_2SO_4 . The drying agent was removed by filtration, and the solvent was removed *in vacuo*. The crude material was purified by column chromatography on silica gel to give 1-(7-fluoronaphthalen-1-yl)ethan-1-one as a white solid (90% yield, 7.5 g). ^1H NMR (500 MHz, CDCl_3): δ 8.61 (d, $J = 12.5$ Hz, 1H), 8.07 (d, $J = 7.0$ Hz, 1H), 8.03 (d, $J = 8.0$ Hz, 1H), 7.89 (dd, $J = 9.0, 6.0$ Hz, 1H), 7.51 (t, $J = 7.5$ Hz, 2H), 7.35 (td, $J = 8.5, 2.0$ Hz, 1H), 2.78 (s, 3H). ^{13}C NMR (125 MHz, CDCl_3): δ 201.2, 162.6 (d, $J = 247.0$ Hz), 134.2 (d, $J = 6.0$ Hz), 133.4, 131.5 (d, $J = 10.7$ Hz), 130.8 (d, $J = 9.4$ Hz), 130.5, 128.5, 123.7, 117.1 (d, $J = 24.1$ Hz), 110.5 (d, $J = 25.6$ Hz), 30.0. HRMS (DART) calculated for $\text{C}_{12}\text{H}_{10}\text{FO}$ $[\text{M}+\text{H}]^+$: 189.0718, found: 189.0716. The characterization data were in agreement with literature values.⁴⁶

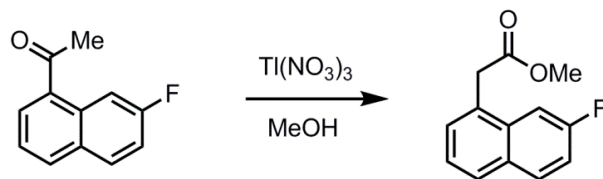
500 MHz, $^1\text{H NMR}$, CDCl_3

500 MHz, ¹H NMR, CDCl₃



125 MHz, ^{13}C NMR, CDCl_3

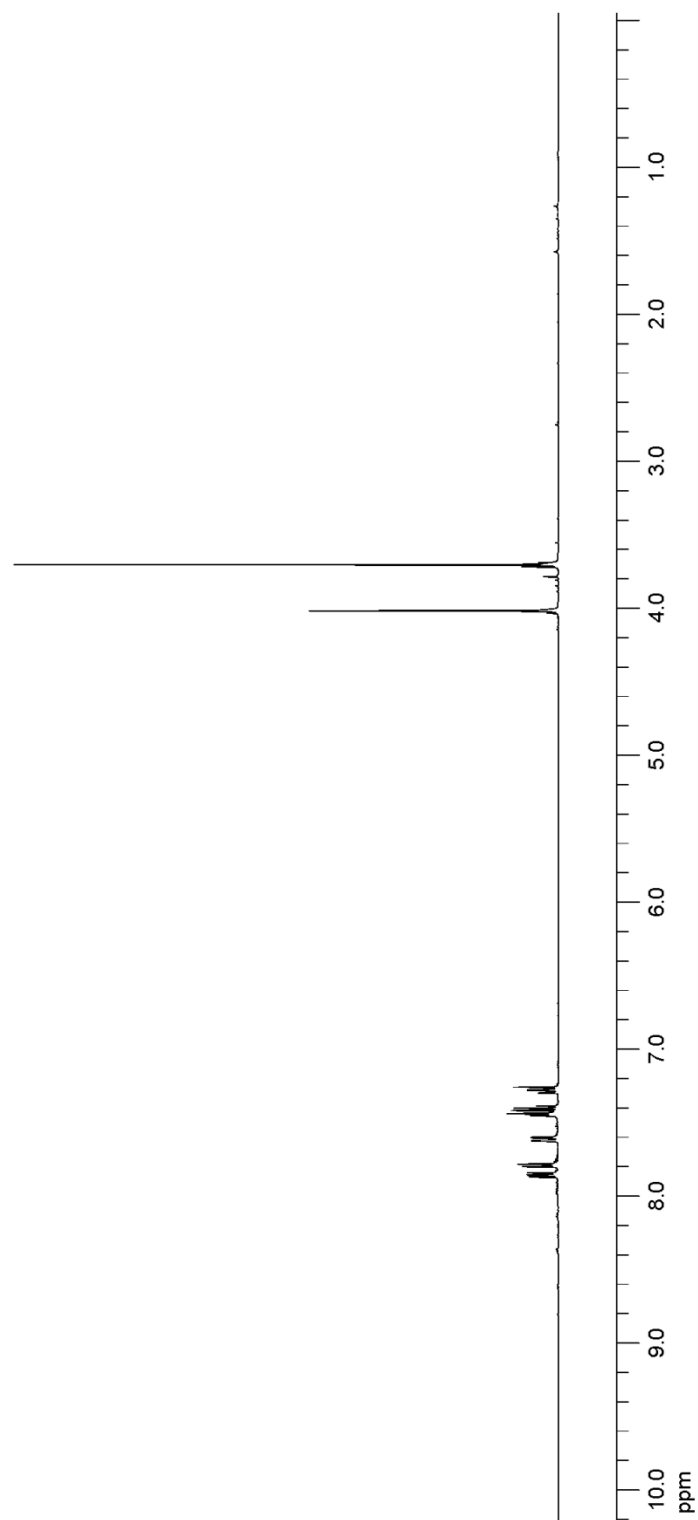
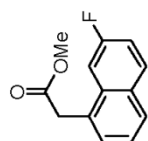
5.8.2.6. Methyl 2-(7-fluoronaphthalen-1-yl)acetate

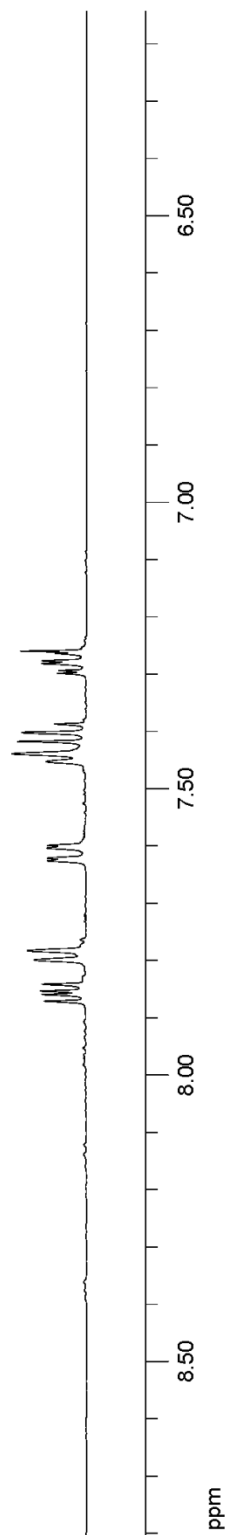
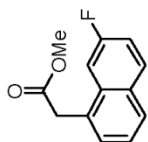


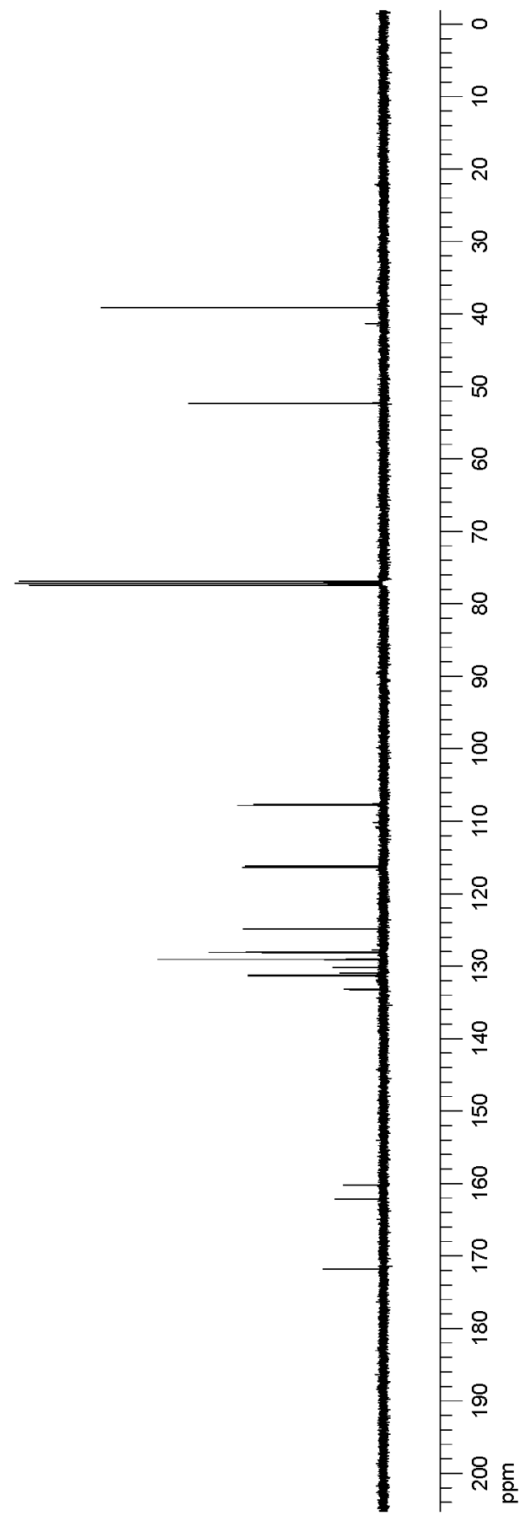
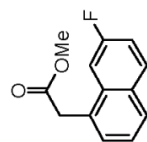
In a flame-dried round-bottomed flask, 2.4 g (5.3 mmol) of thallium(III) nitrate (TTN), 21 mL (0.25 M) of methanol, 11 mL (0.5 M) of perchloric acid (70%), and 11 mL (0.5 M) of dichloromethane were placed. Then, 1.0 g (5.3 mmol) of the starting material, 1-(7-fluoronaphthalen-1-yl)ethan-1-one, was slowly added to the reaction mixture. The resulting mixture was stirred at ambient temperature for 10 h. After this time, the resulting thallium(I) was removed by vacuum filtration, and the reaction mixture was diluted in water. The organic layer was separated from the aqueous layer, and the remaining aqueous layer was extracted with dichloromethane. The combined organic layers were washed with brine and dried with anhydrous Na_2SO_4 . The drying agent was removed by filtration, and the solvent was evaporated *in vacuo*. The crude material was purified by column chromatography on silica gel (hexanes/EtOAc) to afford the title compound as a yellow oil in quantitative yield (1.2 g). ^1H NMR (500 MHz, CDCl_3): δ 7.86 (dd, $J = 9.0, 5.5$ Hz, 1H), 7.79 (d, $J = 8.0$ Hz, 1H), 7.61 (dd, $J = 11.5, 2.5$ Hz, 1H), 7.44 (d, $J = 6.5$ Hz, 1H), 7.40 (t, $J = 8.0$ Hz, 1H), 7.28 (td, $J = 8.0, 2.5$ Hz, 1H), 4.02 (s, 2H), 3.70 (s, 3H). ^{13}C NMR (125 MHz, CDCl_3): δ 171.8, 161.2 (d, $J = 246.1$ Hz), 133.2, 131.3 (d, $J = 9.4$ Hz), 131.0, 130.2 (d, $J = 5.7$ Hz), 129.1, 128.1, 124.9 (d, $J = 2.9$ Hz),

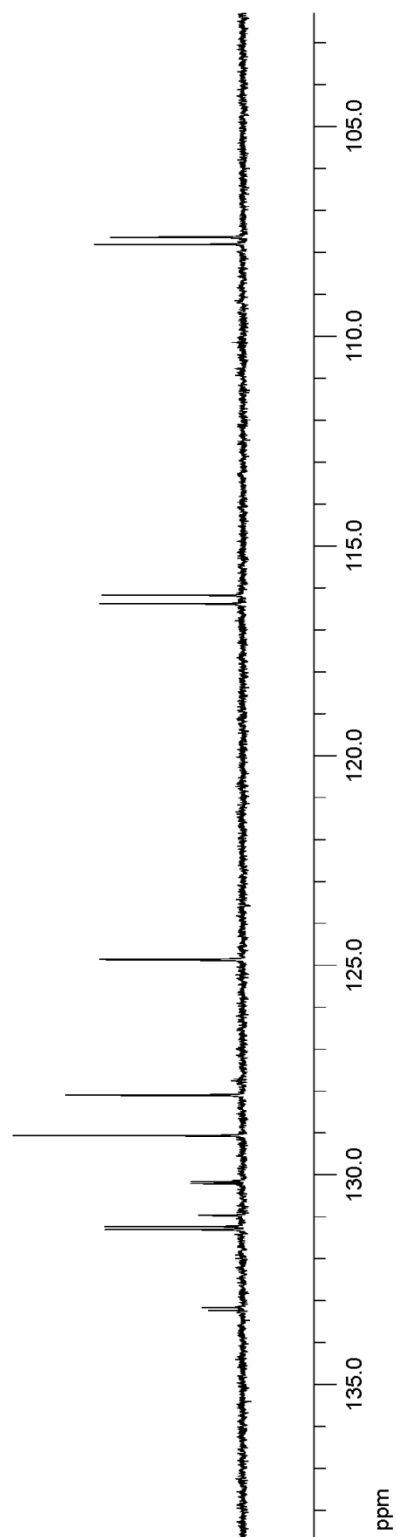
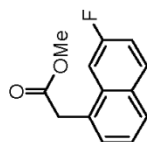
116.3 (d, $J = 25.6$ Hz), 107.7 (d, $J = 22.0$ Hz), 52.3, 39.1. HRMS (DART) calculated for $C_{13}H_{12}FO_2$

$[M+H]^+$: 219.0815, found: 219.0821.

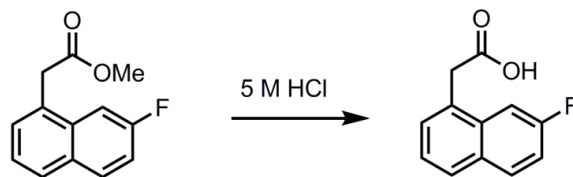
500 MHz, ¹H NMR, CDCl₃

500 MHz, ¹H NMR, CDCl₃

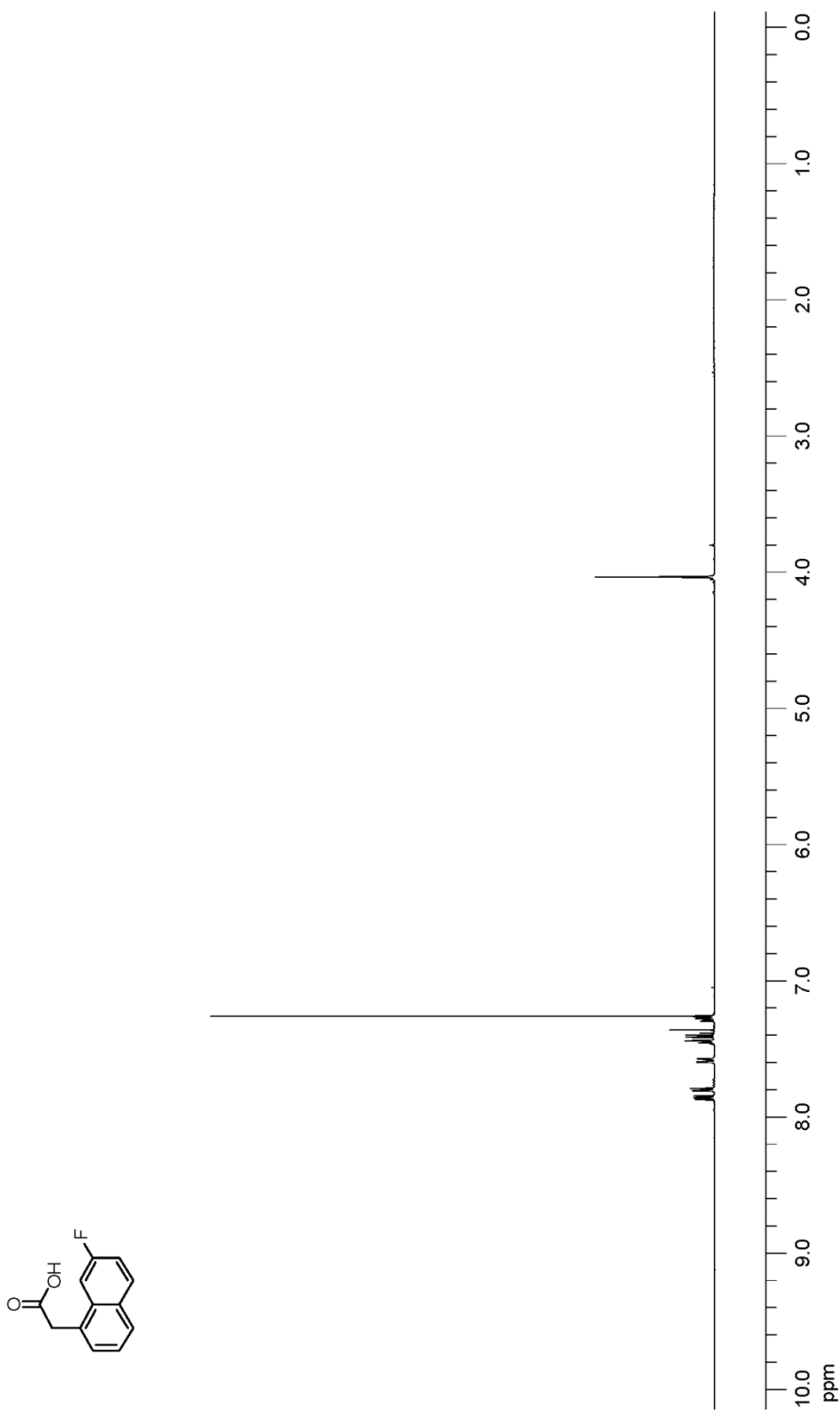


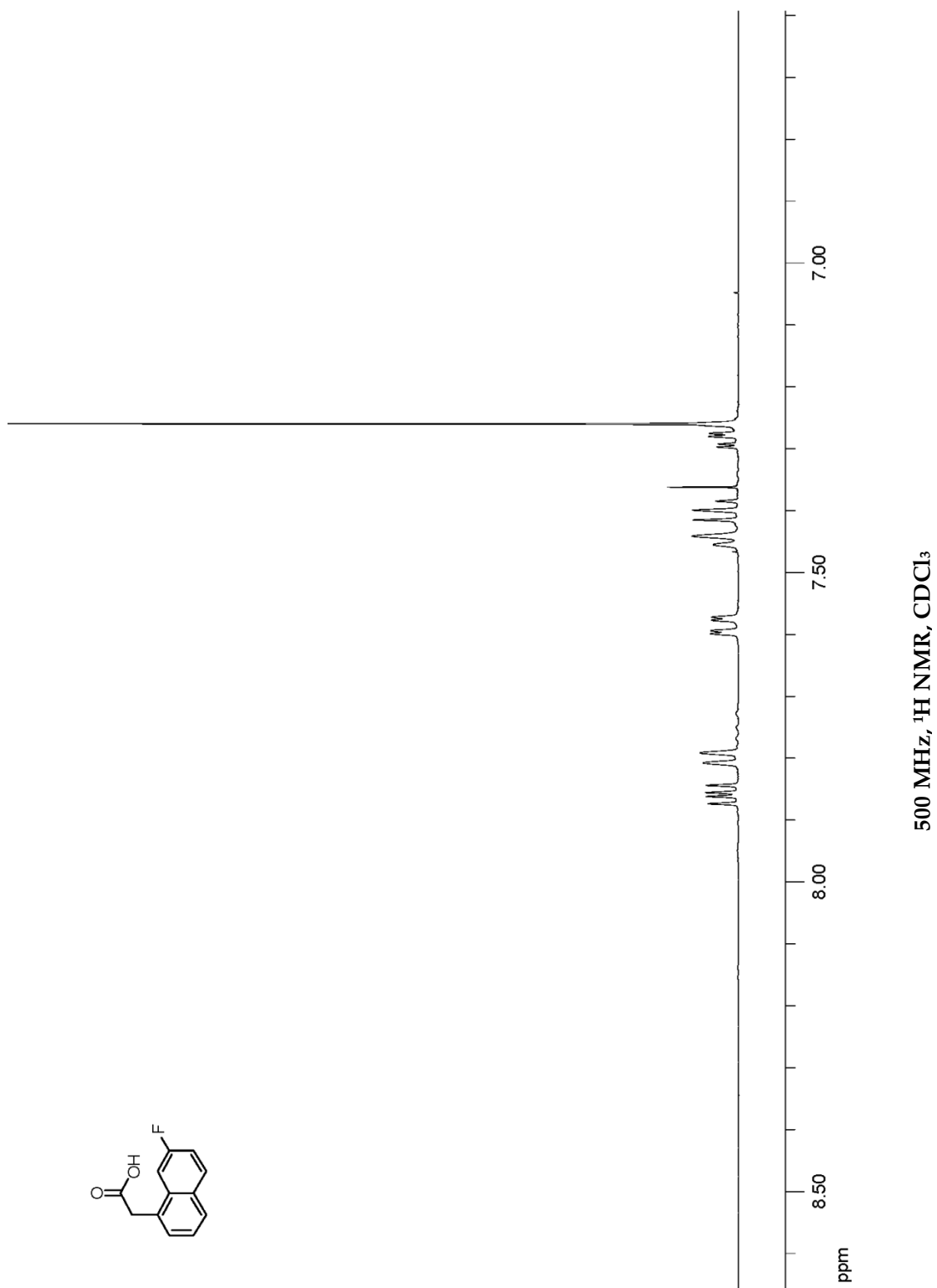
125 MHz, ¹³C NMR, CDCl₃

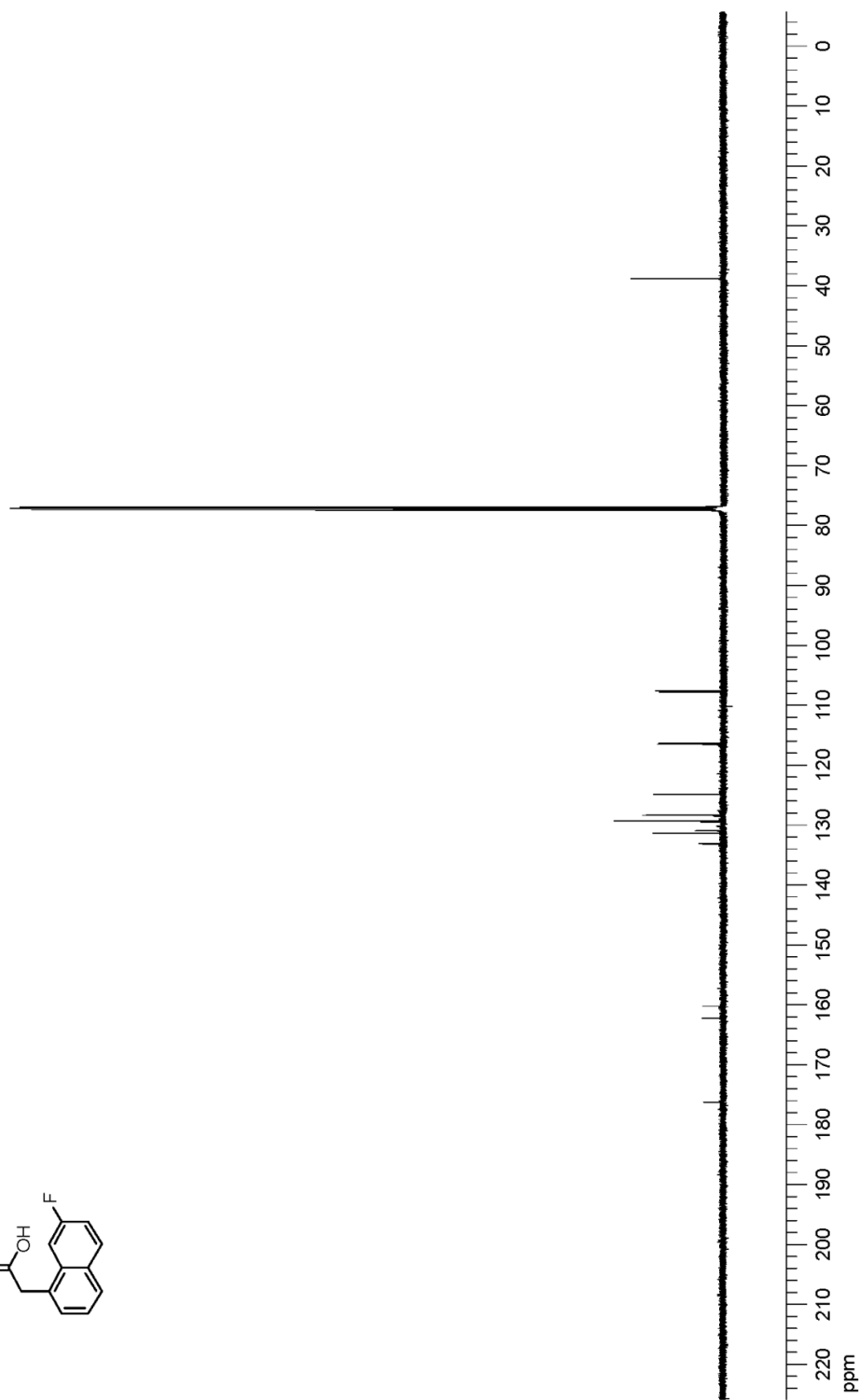
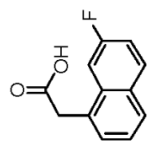
5.8.2.7. 2-(7-Fluoronaphthalen-1-yl)acetic acid

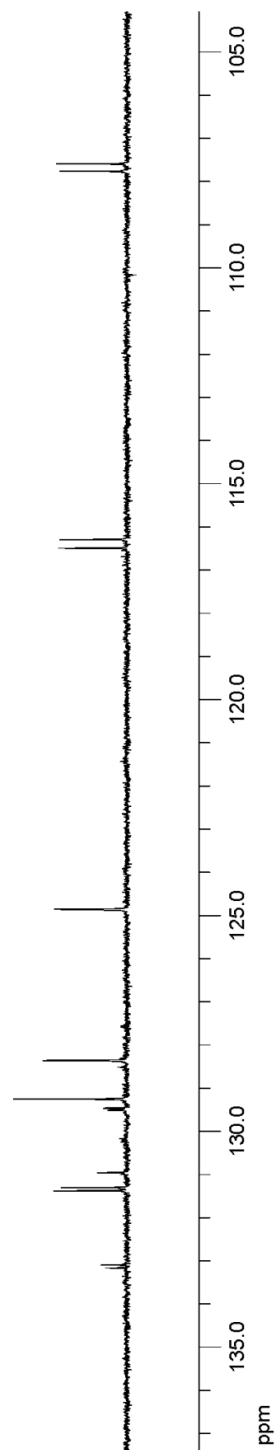
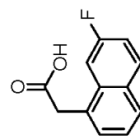


In a round-bottomed flask, 1.1 g (5.04 mmol) of methyl 2-(7-fluoronaphthalen-1-yl)acetate was dissolved in 5 M HCl (93 mL, 0.054 M) and acetone (93 mL, 0.054 M). Then, a reflux condenser was placed on the flask, and the mixture was heated at reflux for 5 h. After this time, the reaction mixture was cooled to room temperature, and the organic solvents (acetone and methanol) were evaporated *in vacuo*. The aqueous residue was extracted with dichloromethane, and the solvent was removed to give the crude product. The crude material was dissolved in a dilute NaOH solution, and the solution was washed with benzene. Upon slow addition of 5 M HCl to this basic solution with cooling, the title compound was precipitated out of the solution. The purified product, 2-(7-fluoronaphthalen-1-yl)acetic acid, was obtained by vacuum filtration as an off-white solid in quantitative yield (1.1 g). ¹H NMR (500 MHz, CDCl₃): δ 7.86 (dd, *J* = 9.5, 6.0 Hz, 1H), 7.80 (d, *J* = 8.0 Hz, 1H), 7.58 (dd, *J* = 11.0, 2.5 Hz, 1H), 7.45 (d, *J* = 7.0 Hz, 1H), 7.40 (t, *J* = 8.0 Hz, 1H), 7.28 (td, *J* = 8.0, 2.5 Hz, 1H), 4.03 (s, 2H). ¹³C NMR (125 MHz, CDCl₃): δ 176.3, 161.2 (d, *J* = 247.0 Hz), 133.1 (d, *J* = 8.5 Hz), 131.4 (d, *J* = 8.5 Hz), 131.0, 129.5, 129.3, 128.4, 124.9 (d, *J* = 2.9 Hz), 116.4 (d, *J* = 25.6 Hz), 107.7 (d, *J* = 21.9 Hz), 38.8.

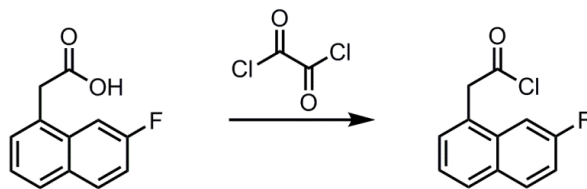
500 MHz, $^1\text{H NMR}$, CDCl_3



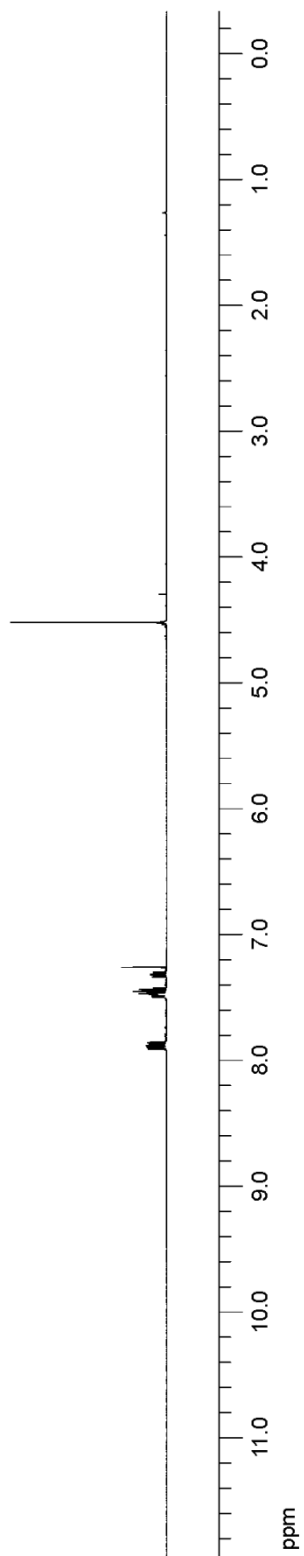
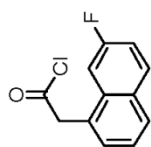
125 MHz, ¹³C NMR, CDCl₃

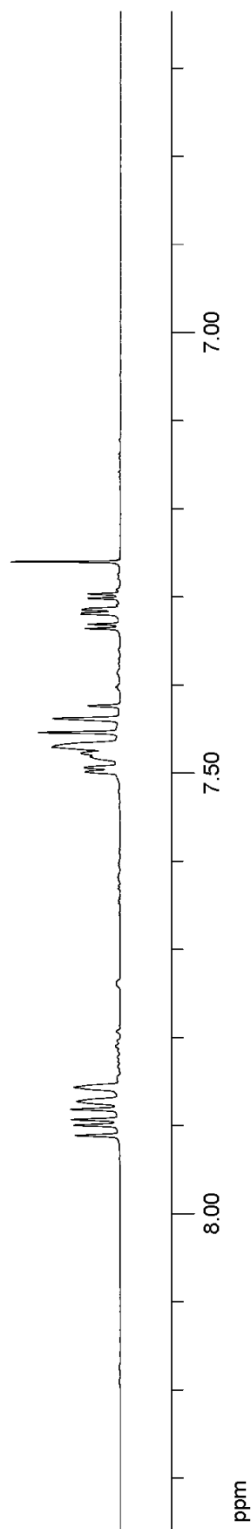
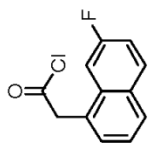
125 MHz, ¹³C NMR, CDCl₃

5.8.2.8. 2-(7-Fluoronaphthalen-1-yl)acetyl chloride



In an oven-dried round-bottomed flask, 7.1 g (35 mmol) of 2-(7-fluoronaphthalen-1-yl)acetic acid was dissolved in 42 mL (0.80 M) of benzene. While stirring, 14.5 mL (173 mmol) of oxalyl chloride was added to the mixture. Then, the resulting solution was heated at reflux for 5 h. After this time, the reaction mixture was cooled to room temperature, and the volatiles were removed under reduced pressure to afford 2-(7-fluoronaphthalen-1-yl)acetyl chloride as a yellow solid. Purification was not performed for this compound, and it was immediately used as a starting material for the next step (see Section 5.8.2.9). ¹H NMR (500 MHz, CDCl₃): δ 7.89 (dd, *J* = 9.0, 6.0 Hz, 1H), 7.87 (d, *J* = 8.0 Hz, 1H), 7.49 (dd, *J* = 8.5, 2.5 Hz, 1H), 7.47 (d, *J* = 6.0 Hz, 1H), 7.44 (t, *J* = 7.5 Hz, 1H), 7.32 (td, *J* = 8.0, 2.5 Hz, 1H), 4.52 (s, 2H).

500 MHz, ¹H NMR, CDCl₃

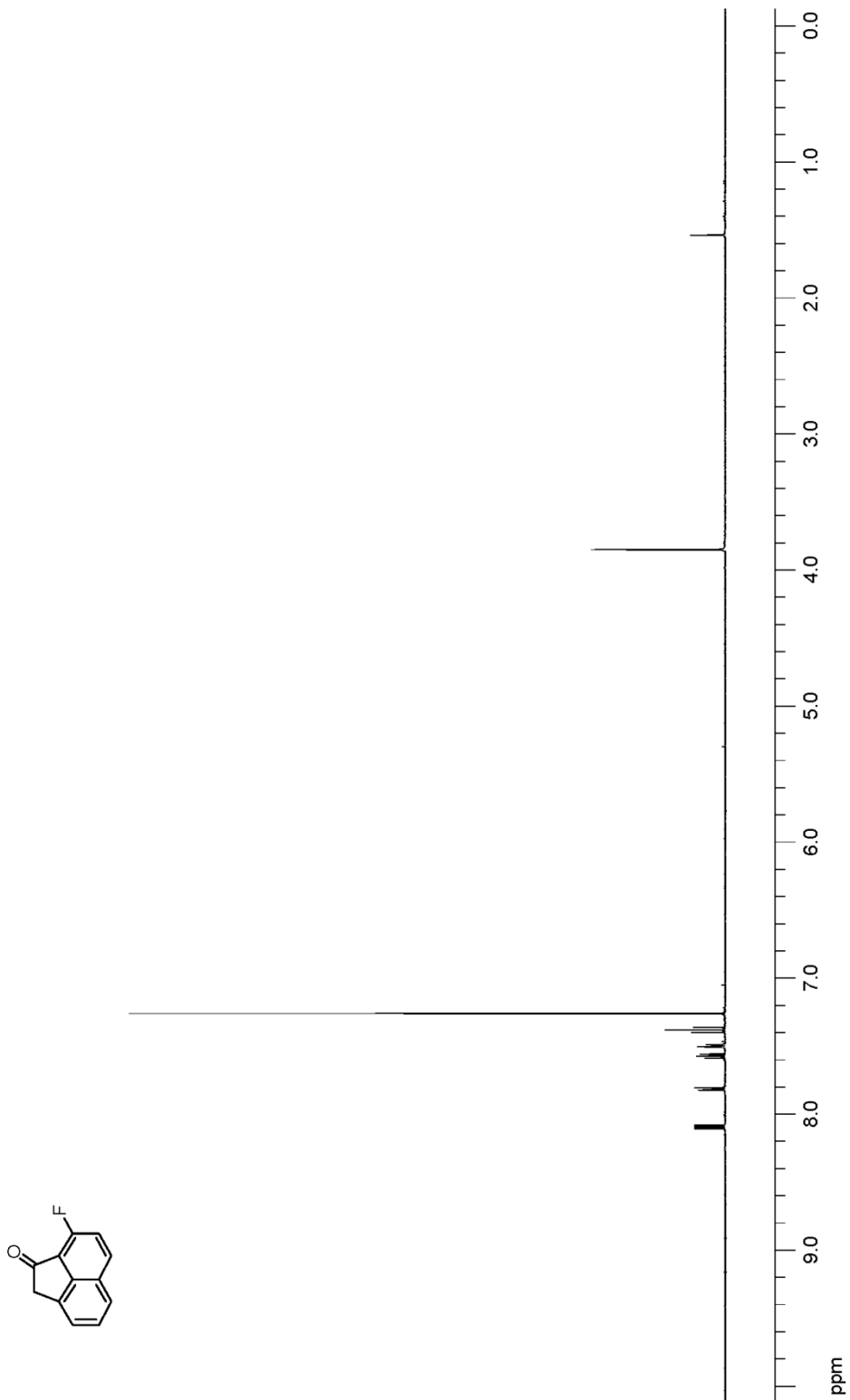


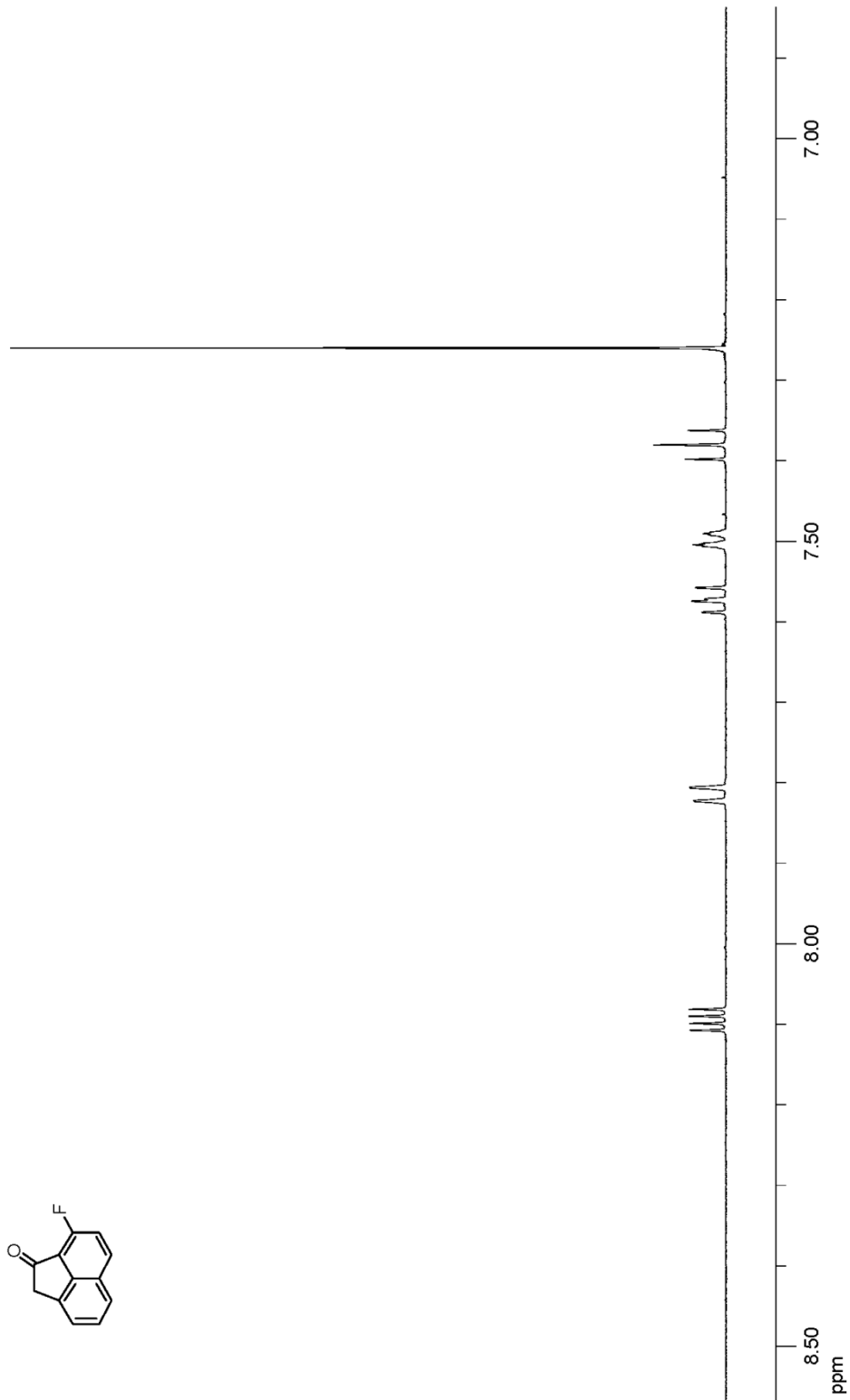
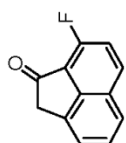
500 MHz, ¹H NMR, CDCl₃

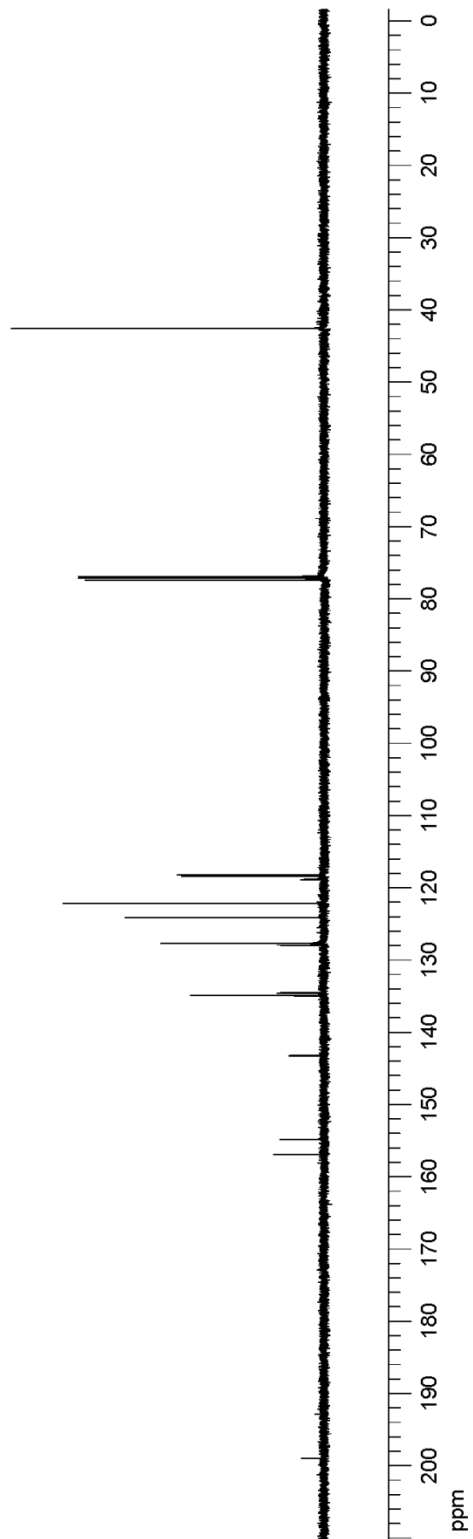
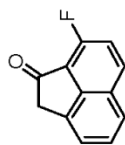
5.8.2.9. 8-Fluoroacenaphthylen-1(2H)-one

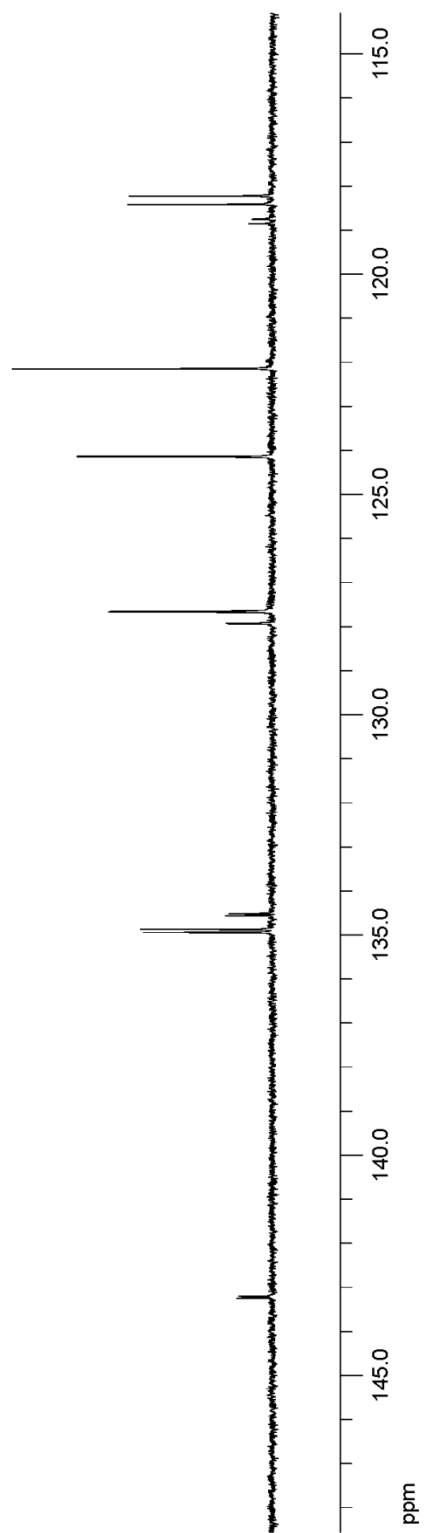
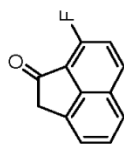


In a flame-dried round-bottomed flask, 2-(7-fluoronaphthalen-1-yl)acetyl chloride (7.8 g, 35 mmol) was dissolved in dichloromethane (350 mL, 0.1 M). The resulting solution was cooled to 0 °C in an ice-bath, and then aluminum chloride (9.3 g, 70 mmol) was added to the solution. After the reaction mixture was stirred at 0 °C for 6 h, it was warmed to room temperature. Then, the mixture was stirred at ambient temperature for 12 h. The reaction was quenched with a dilute HCl solution, and the resulting solution was extracted with dichloromethane. The solvent was removed *in vacuo* to afford the title compound. The crude material was further purified by column chromatography on silica gel (65% yield, 4.2 g, an off-white solid). ¹H NMR (500 MHz, CDCl₃): δ 8.11 (dd, *J* = 9.0, 4.0 Hz, 1H), 7.84 (d, *J* = 8.0 Hz, 1H), 7.60 (t, *J* = 8.5 Hz, 1H), 7.52 (d, *J* = 8.0 Hz, 1H), 7.40 (t, *J* = 9.5 Hz, 1H), 3.85 (s, 2H). ¹³C NMR (125 MHz, CDCl₃): δ 199.0, 155.9 (d, *J* = 267.1 Hz), 143.2 (d, *J* = 4.8 Hz), 134.9 (d, *J* = 7.7 Hz), 134.5 (d, *J* = 5.7 Hz), 128.0, 127.7 (d, *J* = 2.9 Hz), 124.1, 122.2, 118.8 (d, *J* = 13.3 Hz), 118.3 (d, *J* = 23.9 Hz), 42.6. HRMS (DART) calculated for C₁₂H₈FO [M+H]⁺: 187.0559, found: 187.0562.

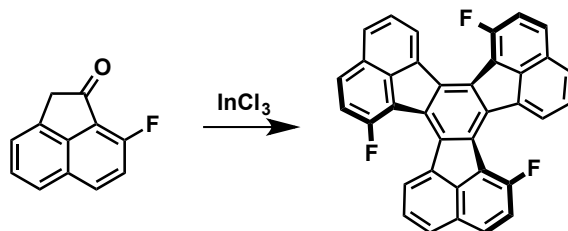


500 MHz, ^1H NMR, CDCl_3

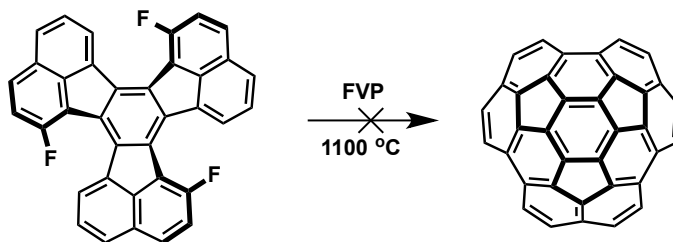
125 MHz, ^{13}C NMR, CDCl_3

125 MHz, ^{13}C NMR, CDCl_3

5.8.2.10. 1,7,13-trifluorodecacyclene

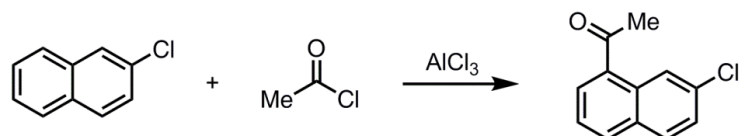


An oven-dried round-bottomed flask, equipped with a magnetic stir-bar, was charged with 1.5 g (6.6 mmol) of indium(III) chloride and 20 mL (0.055 M) of 1,2-dichloroethane. The mixture was heated to reflux under an inert atmosphere of nitrogen. After the reflux point was reached, 200 mg (1.1 mmol) of 8-fluoroacenaphthylen-1(2H)-one, which was dissolved in 4.4 mL (0.25 M) of 1,2-dichloroethane, was added dropwise with a syringe over 30 min. Then, the reaction mixture was refluxed under nitrogen for 24 h. After this time, the reaction mixture was cooled to room temperature and poured into a solution of 10% HCl and ice. The resulting heterogeneous mixture was extracted with dichloromethane, and the combined organic layers were dried with anhydrous sodium sulfate. The drying agent was removed by vacuum filtration, and the solvent was evaporated under reduced pressure to obtain a crude product. The mass spectrum of the crude material indicated that the desired product ($m/z = 504.51$) was formed as a minor product. Due to the low solubility of the product and the low efficiency of the process, further purification of the crude product was not successful.

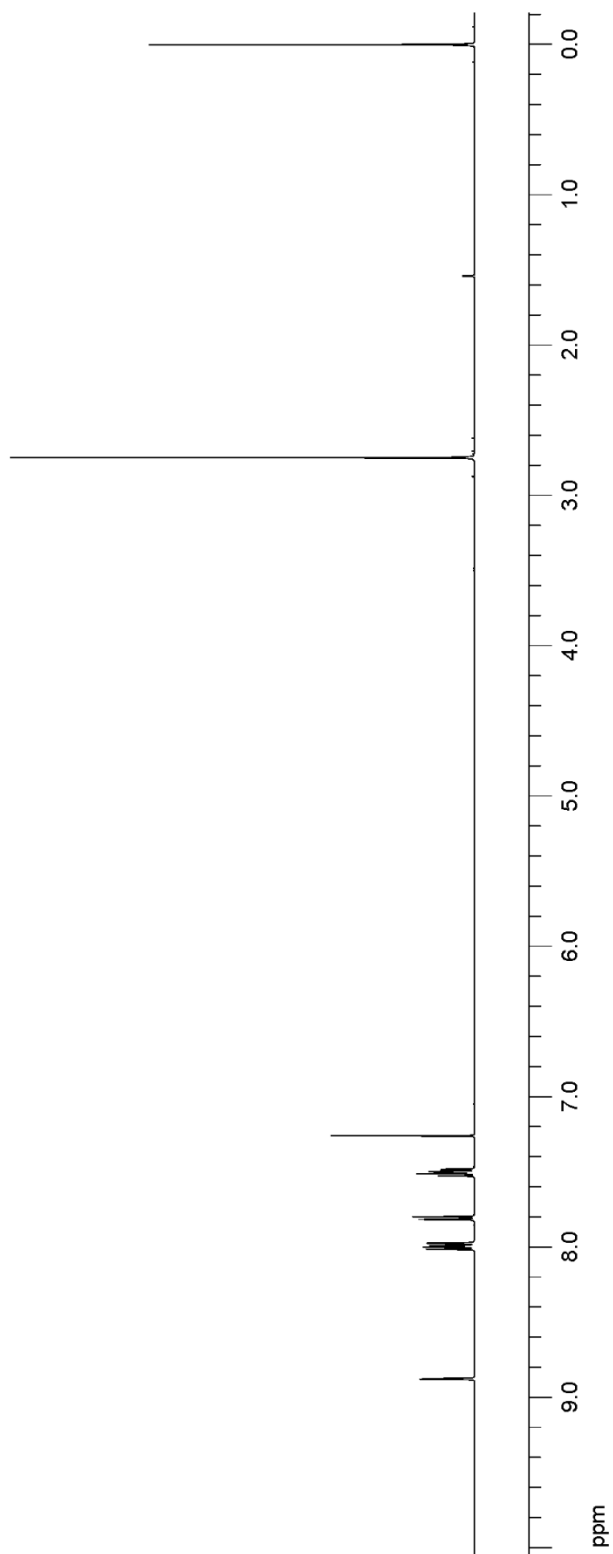
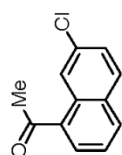
5.8.2.11. Attempted Synthesis of Circumtrindene from $C_{36}H_{15}F_3$ 

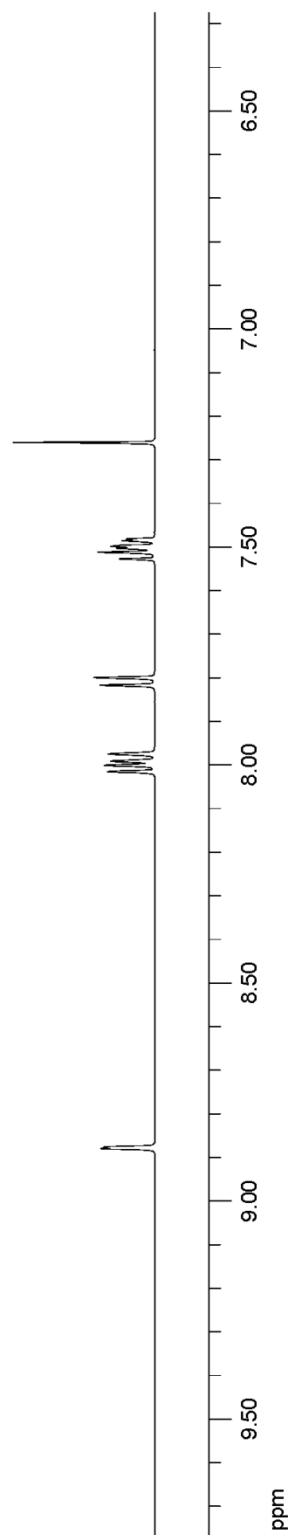
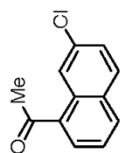
The FVP reaction was performed with 100 mg (0.20 mmol) of 1,7,13-trifluorodecacyclene (subjected as a crude material), which was placed in a sample boat in a supplemental heating oven. On one side of the FVP apparatus, the system was connected to a nitrogen gas reservoir through a capillary inlet tube made out of a section of GC capillary. On the other side of the oven, the pyrolysis tube was connected to a high-capacity vacuum pump through a cold trap filled with liquid nitrogen. The supplemental oven was heated to 300 °C, and the reaction oven was heated to 1100 °C. The pressure of the system was equilibrated to 0.5 torr. As soon as both of the ovens reached the desired temperatures, the sample boat was moved into the center of the supplemental oven. After 6 hours of reaction time, it was observed that all the starting material was sublimed leaving a black tar on the sample boat. The crude product was collected by rinsing both the quartz tube and the glass trap with dichloromethane (~500 mL). The mass spectrum of the crude material did not show the desired product peak ($m/z = 444.09$).

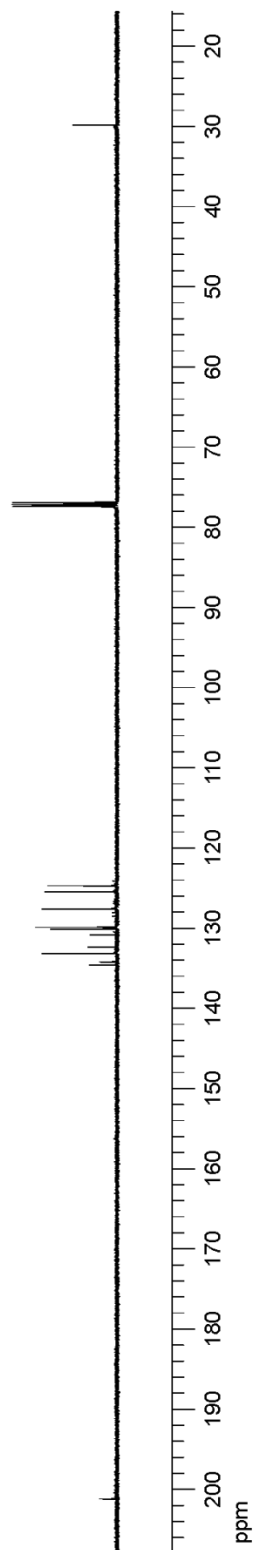
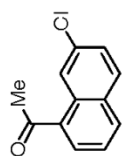
5.8.2.12. 1-(7-Chloronaphthalen-1-yl)ethan-1-one



To an oven-dried round-bottomed flask, 2-chloronaphthalene (7.2 g, 44 mmol) was dissolved in dichloromethane (73 mL, 0.6 M). The resulting solution was cooled to $-10\text{ }^{\circ}\text{C}$, and then aluminum chloride (18 g, 133 mmol) was added to the solution. The resulting mixture was then cooled to $-78\text{ }^{\circ}\text{C}$. At this temperature, acetyl chloride (7.1 g, 90 mmol) was added, and the reaction mixture was stirred at the same temperature for 10 h. The reaction was quenched with a dilute HCl solution, and the resulting solution was extracted with dichloromethane. The solvent was removed *in vacuo* to afford the title compound. The crude material was purified by column chromatography on silica gel (90% yield, 8.0 g, white solid). ^1H NMR (500 MHz, CDCl_3): δ 8.88 (d, $J = 2.0$ Hz, 1H), 8.01 (d, $J = 7.5$ Hz, 1H), 7.89 (d, $J = 8.0$ Hz, 1H), 7.80 (d, $J = 8.5$ Hz, 1H), 7.51 (t, $J = 8.0$ Hz, 1H), 7.49 (d, $J = 7.5$ Hz, 1H), 2.75 (s, 3H). ^{13}C NMR (125 MHz, CDCl_3): δ 201.1, 134.5, 134.1, 133.1, 132.2, 130.8, 130.0, 129.8, 127.5, 125.4, 124.6, 29.8. The characterization data were in agreement with literature values.⁵⁶

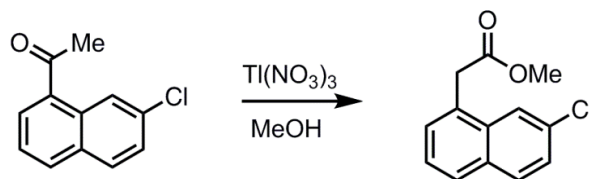
500 MHz, $^1\text{H NMR}$, CDCl_3

500 MHz, ^1H NMR, CDCl_3

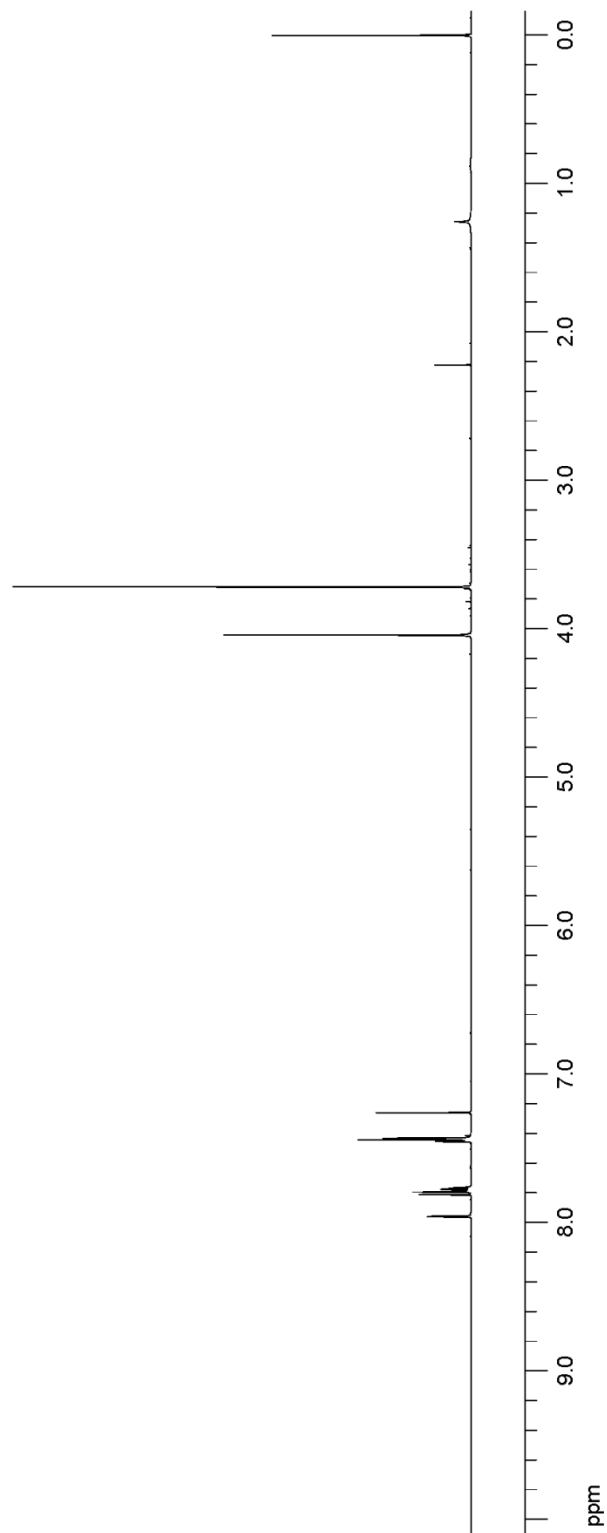
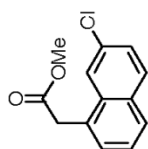


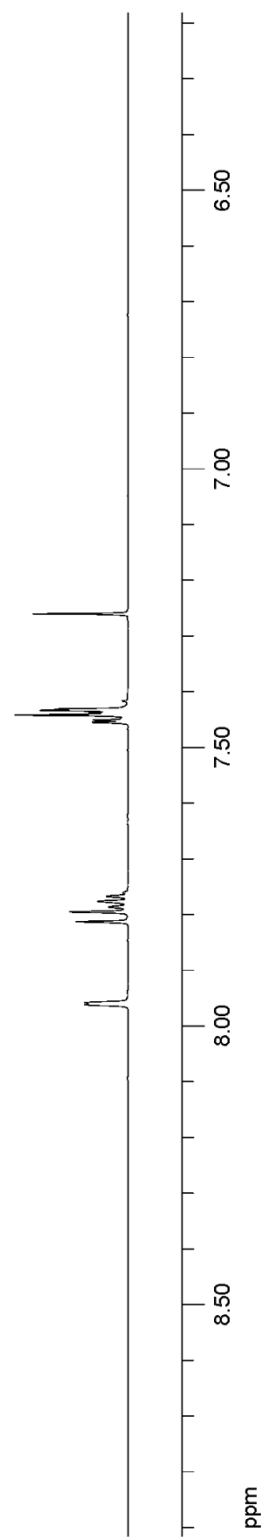
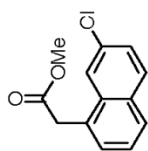
125 MHz, ^{13}C NMR, CDCl_3

5.8.2.13. Methyl 2-(7-chloronaphthalen-1-yl)acetate

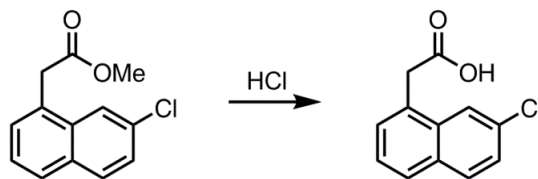


In a flame-dried round-bottomed flask, 2.4 g (5.3 mmol) of thallium(III) nitrate (TTN), methanol (21 mL, 0.25 M), perchloric acid (11 mL, 0.5 M), and dichloromethane (11 mL, 0.5 M) were placed. Then, 1.1 g (5.3 mmol) of the starting material, 1-(7-chloronaphthalen-1-yl)ethan-1-one, was slowly added to the reaction mixture. The mixture was then stirred at ambient temperature for 10 h. After this time, the resulting thallium(I) was removed by vacuum filtration, and the filtered reaction mixture was diluted in water. The organic layer of the mixture was separated from the aqueous layer, and the remaining aqueous layer was extracted with dichloromethane. The combined organic layers were washed with brine and dried with anhydrous Na₂SO₄. The drying agent was removed by filtration, and the solvent was evaporated *in vacuo*. The crude material was purified by column chromatography on silica gel (hexanes/EtOAc) to afford methyl 2-(7-chloronaphthalen-1-yl)acetate as a dark yellow oil in quantitative yield (1.2 g). ¹H NMR (500 MHz, CDCl₃): δ 7.96 (d, *J* = 1.5 Hz, 1H), 7.80 (d, *J* = 8.5 Hz, 1H), 7.78 (m, 1H), 7.45–7.43 (m, 3H), 4.04 (s, 2H), 3.72 (s, 3H). The characterization data were in agreement with literature values.⁵⁶

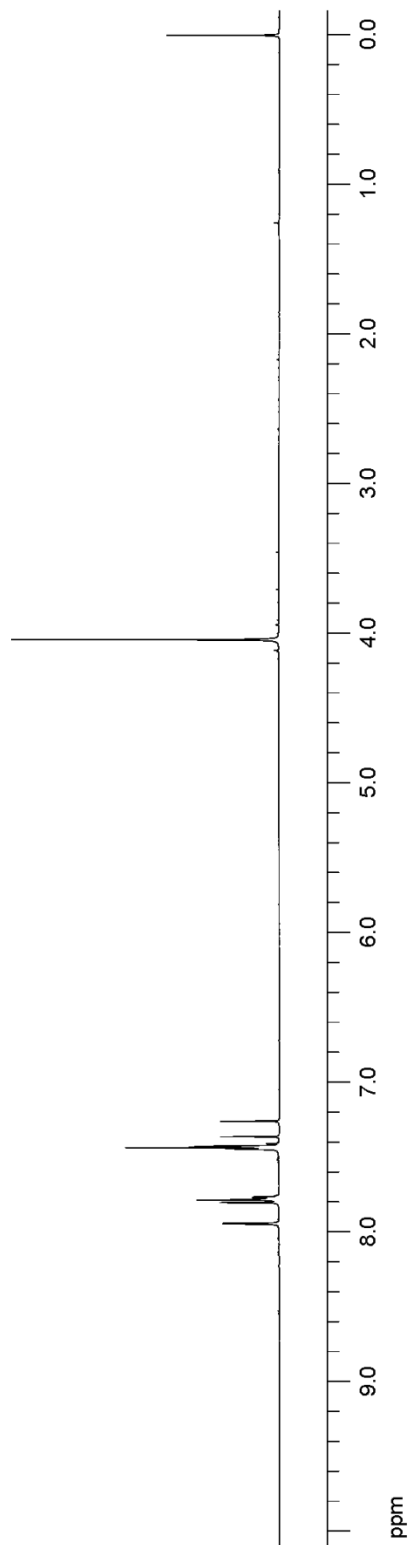
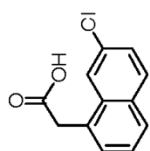
500 MHz, ¹H NMR, CDCl₃

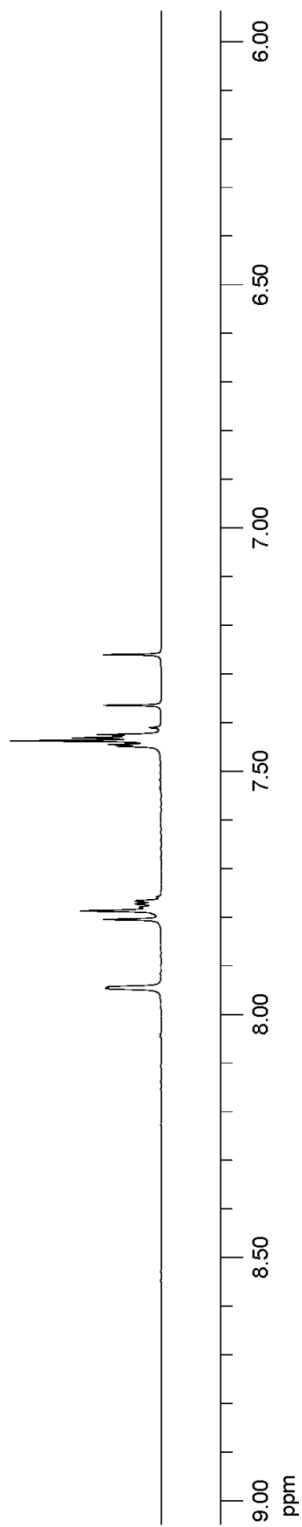
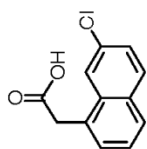
500 MHz, ¹H NMR, CDCl₃

5.8.2.14. 2-(7-Chloronaphthalen-1-yl)acetic acid

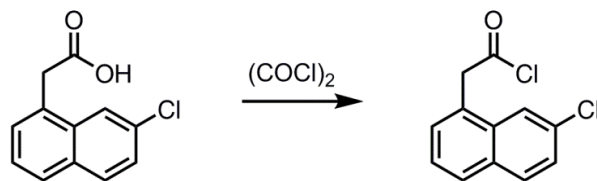


In a round-bottomed flask, 1.2 g (5.0 mmol) of methyl 2-(7-chloronaphthalen-1-yl)acetate was dissolved in 5 M HCl (93 mL, 0.054 M) and acetone (93 mL, 0.054 M). A reflux condenser was placed on the flask, and the mixture was refluxed for 5 h. After this time, the reaction mixture was cooled to room temperature, and the organic solvents (acetone and methanol) were evaporated *in vacuo*. The aqueous residue was extracted with dichloromethane, and the solvent was removed to give the crude product. The crude material was dissolved in a dilute NaOH solution, and the solution was washed with benzene. Upon slow addition of 5 M HCl to this basic solution with cooling, the title compound was precipitated out of the solution. The product, 2-(7-chloronaphthalen-1-yl)acetic acid, was obtained by vacuum filtration as an off-white solid in quantitative yield (1.1 g). ¹H NMR (500 MHz, CDCl₃): δ 7.94 (d, *J* = 1.5 Hz, 1H), 7.80 (d, *J* = 9.0 Hz, 1H), 7.78–7.76 (m, 1H), 7.45–7.42 (m, 3H), 4.04 (s, 2H). The characterization data were in agreement with literature values.⁵⁶

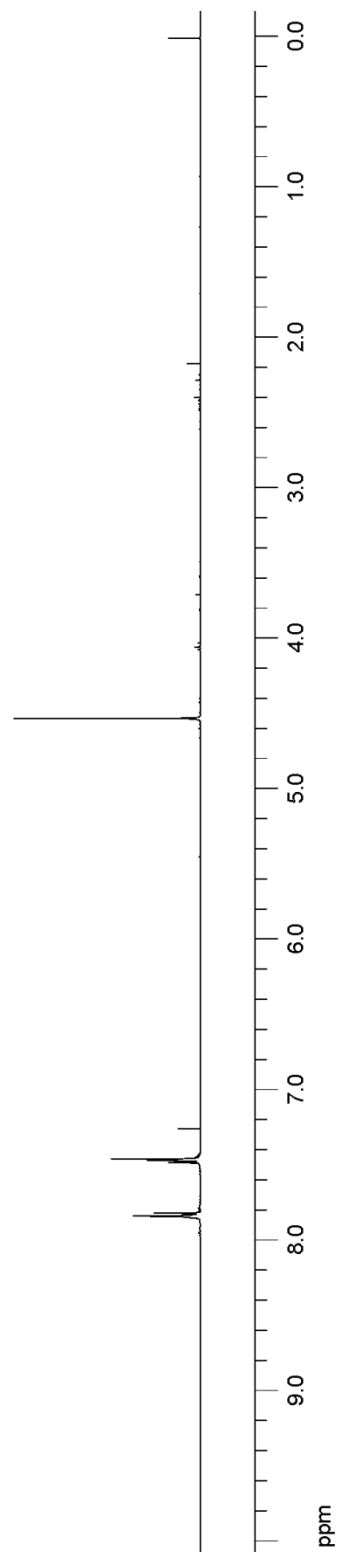
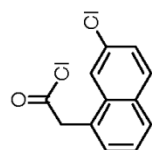
500 MHz, ¹H NMR, CDCl₃

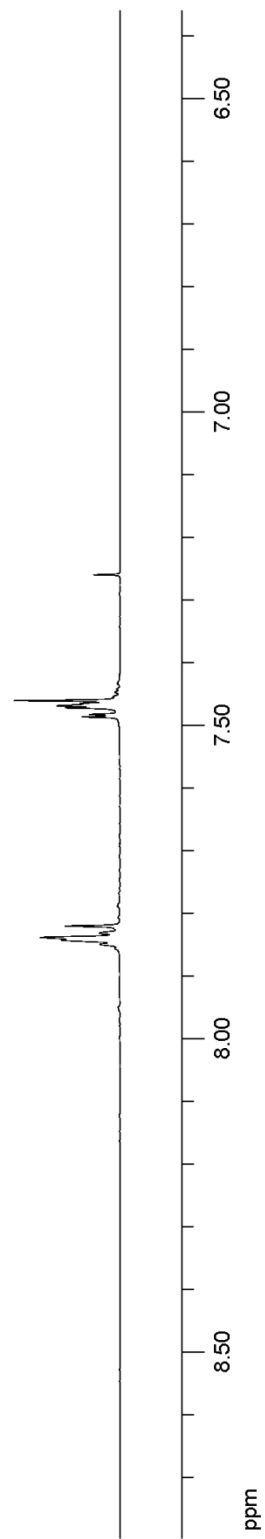
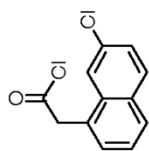
500 MHz, ^1H NMR, CDCl_3

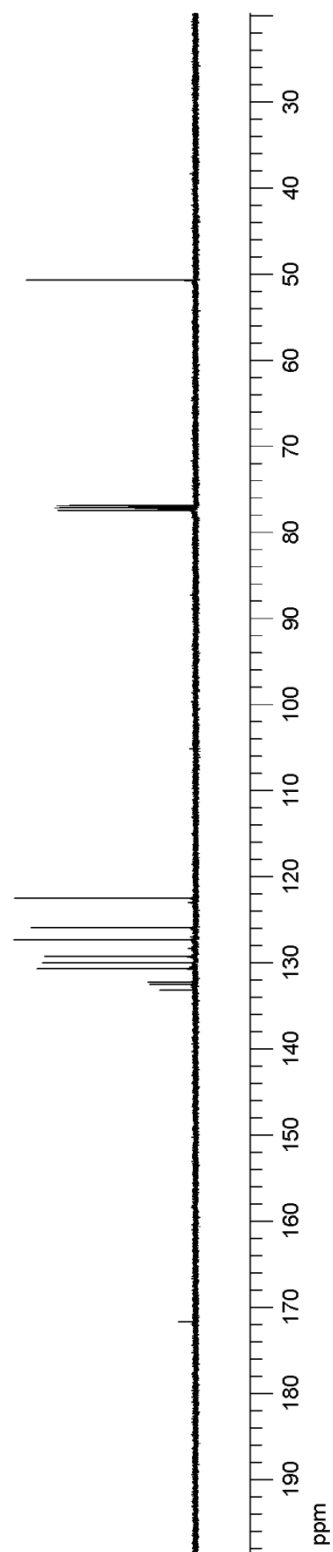
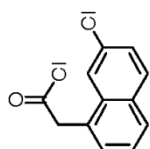
5.8.2.15. 2-(7-Chloronaphthalen-1-yl)acetyl chloride



To an oven-dried round-bottomed flask, 7.7 g (35 mmol) of 2-(7-chloronaphthalen-1-yl)acetic acid was dissolved in 42 mL (0.8 M) of benzene. To this solution, 14.5 mL (173 mmol) of oxalyl chloride was added, and the reaction mixture was heated at reflux for 5 h. After this time, the volatiles (the solvent and oxalyl chloride) were removed under reduced pressure to afford 2-(7-chloronaphthalen-1-yl)acetyl chloride as a yellow solid. Purification was not performed for this compound, and it was directly used as a starting material for the next step (see Section 5.8.2.16). ¹H NMR (500 MHz, CDCl₃): δ 7.84–7.83 (m, 2H), 7.82 (s, 1H), 7.48–7.46 (m, 3H), 4.53 (s, 2H). ¹³C NMR (125 MHz, CDCl₃): δ 171.6, 133.1, 132.4, 132.1, 130.6, 129.8, 129.1, 127.2, 127.1, 125.8, 122.4, 50.6.

500 MHz, ¹H NMR, CDCl₃

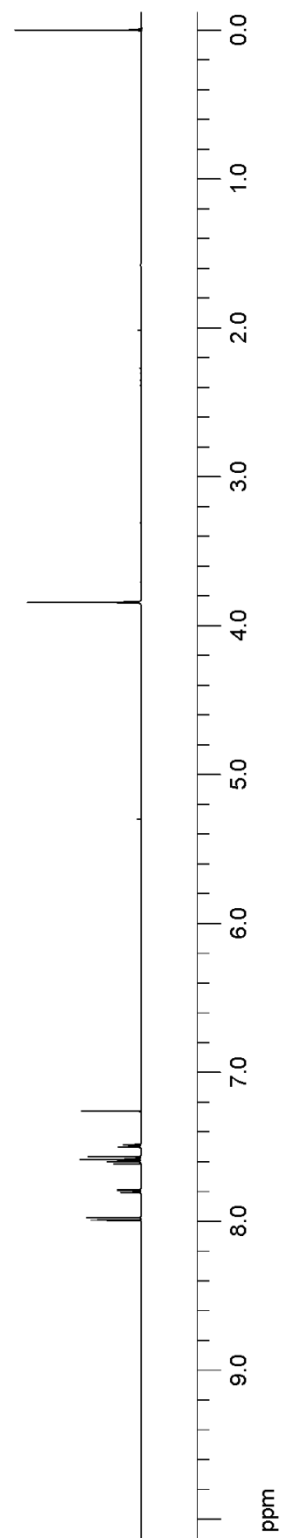
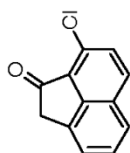
500 MHz, ¹H NMR, CDCl₃

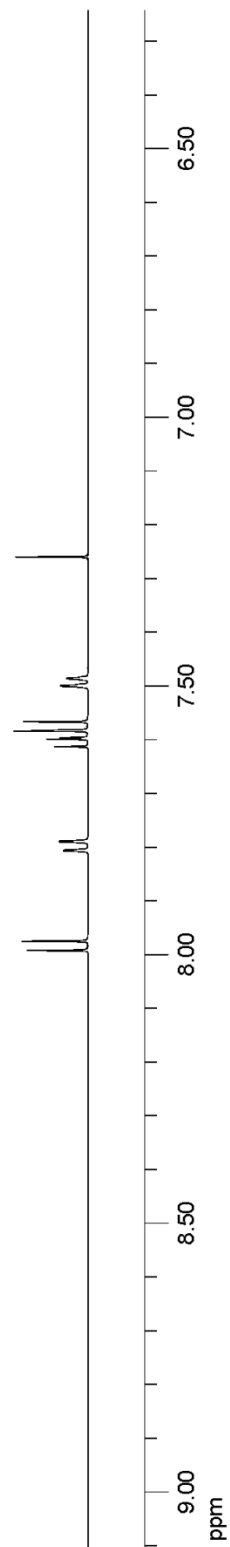
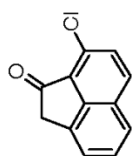
125 MHz, ¹³C NMR, CDCl₃

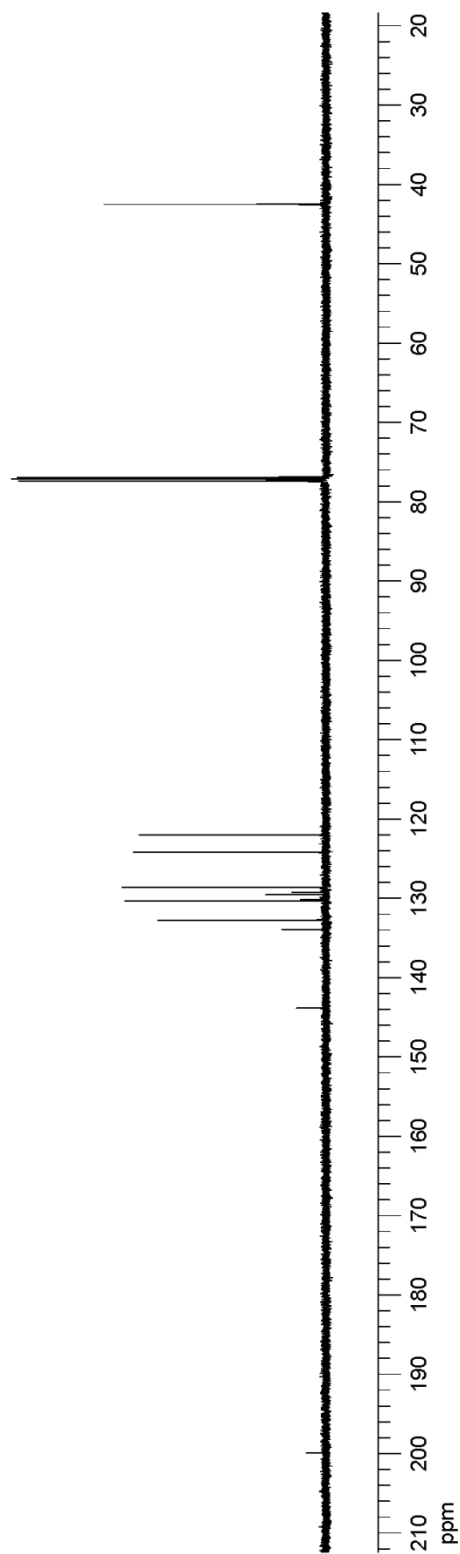
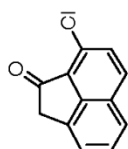
5.8.2.16. 8-Chloroacenaphthylen-1(2H)-one



In a flame-dried round-bottomed flask, 2-(7-chloronaphthalen-1-yl)acetyl chloride (7.1 g, 35 mmol) was dissolved in dichloromethane (350 mL, 0.1 M). The resulting solution was cooled to 0 °C in an ice-bath, and then aluminum chloride (9.3 g, 70 mmol) was added to the mixture. After the reaction mixture was stirred at 0 °C for 6 h, it was warmed to room temperature. Then, the mixture was stirred at ambient temperature for 12 h. The reaction was quenched with a dilute HCl solution, and the resulting solution was extracted with dichloromethane. The solvent was removed *in vacuo* to afford the crude product. The crude material was purified by column chromatography on silica gel to give 8-chloroacenaphthylen-1(2H)-one as an off-white solid (65% yield over two steps, 4.6 g). ¹H NMR (500 MHz, CDCl₃): δ 7.98 (d, *J* = 8.5 Hz, 1H), 7.80 (d, *J* = 8.5 Hz, 1H), 7.60 (d, *J* = 8.5 Hz, 1H), 7.58 (t, *J* = 7.5 Hz, 1H), 7.49 (d, *J* = 7.0 Hz, 1H), 3.84 (s, 2H). ¹³C NMR (125 MHz, CDCl₃): δ 199.8, 143.7, 133.8, 132.6, 130.2, 130.0, 129.4, 129.1, 128.4, 124.0, 121.9, 42.4. The characterization data were in agreement with literature values.⁵⁶

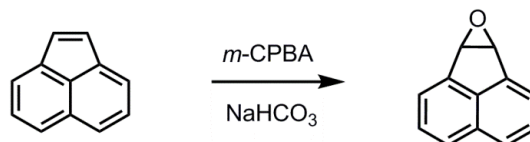
500 MHz, $^1\text{H NMR}$, CDCl_3

500 MHz, $^1\text{H NMR}$, CDCl_3



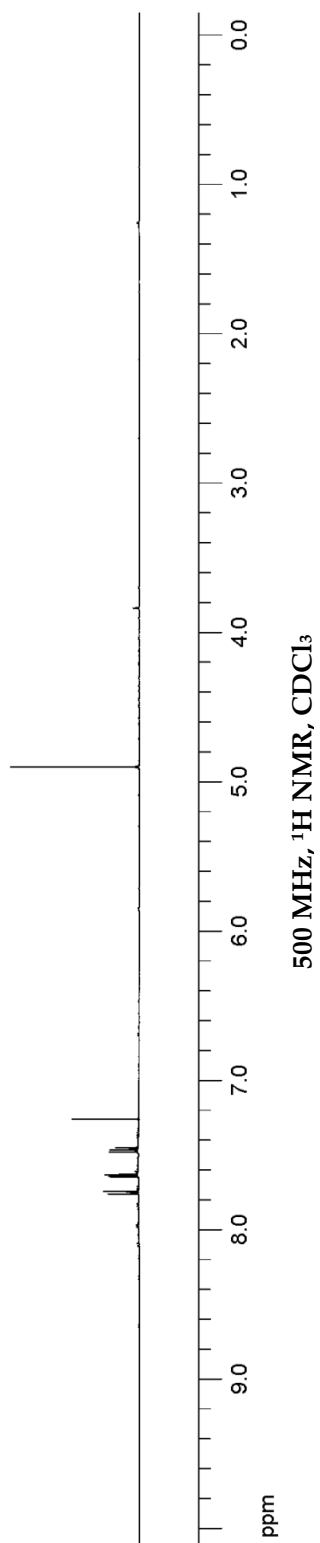
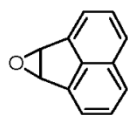
125 MHz, ^{13}C NMR, CDCl_3

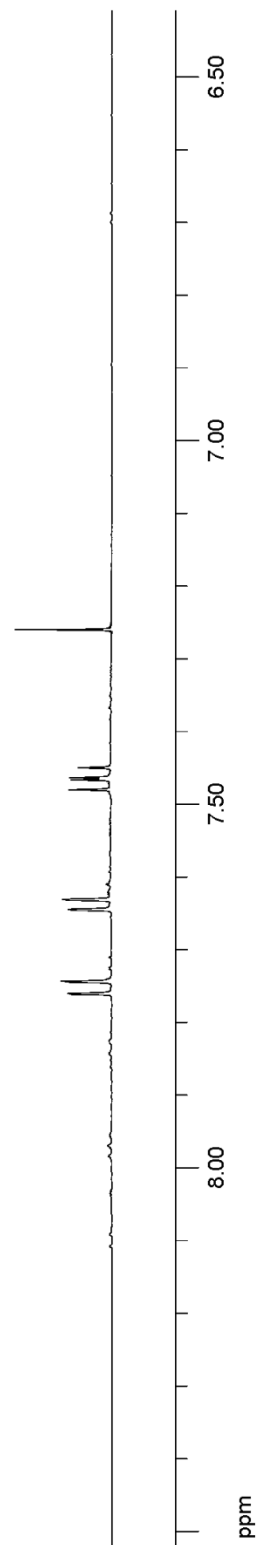
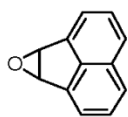
5.8.2.17. 6b,7a-Dihydroacenaphtho[1,2-b]oxirene



In an oven-dried round-bottomed flask, 6.1 g (40 mmol) of acenaphthylene was dissolved in a solution of *m*-chloroperoxybenzoic acid (13.8 g, 80 mmol), dichloromethane (100 mL, 0.4 M) and saturated aqueous sodium bicarbonate (100 mL, 0.4 M). Then, the reaction mixture was stirred vigorously at ambient temperature for 2 h. After this time, the organic layer was separated, and the remaining aqueous layer was extracted with dichloromethane twice. The combined organic layer was washed with saturated NaHCO₃ solution and dried over anhydrous Na₂SO₄. The drying agent was removed by filtration, and the solvent was evaporated under reduced pressure to give 6b,7a-dihydroacenaphtho[1,2-b]oxirene as a white solid in 88% yield (5.9 g). ¹H NMR (500 MHz, CDCl₃): δ 7.75 (d, *J* = 8.5 Hz, 1H), 7.64 (d, *J* = 7.0 Hz, 1H), 7.46 (dd, *J* = 8.5, 7.0 Hz, 1H), 4.90 (s, 3H). The spectral data were consistent with literature values.⁹¹

⁹¹ Imuta, M.; Ziffer, H., "Convenient Method for the Preparation of Reactive Oxiranes by Direct Epoxidation," *The Journal of Organic Chemistry* **1979**, *44*, 1351-1352.



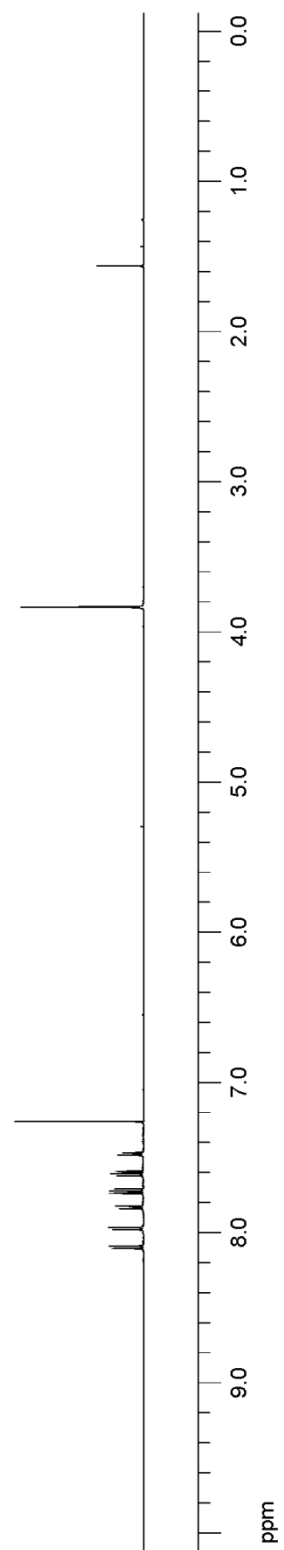
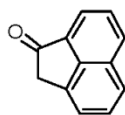


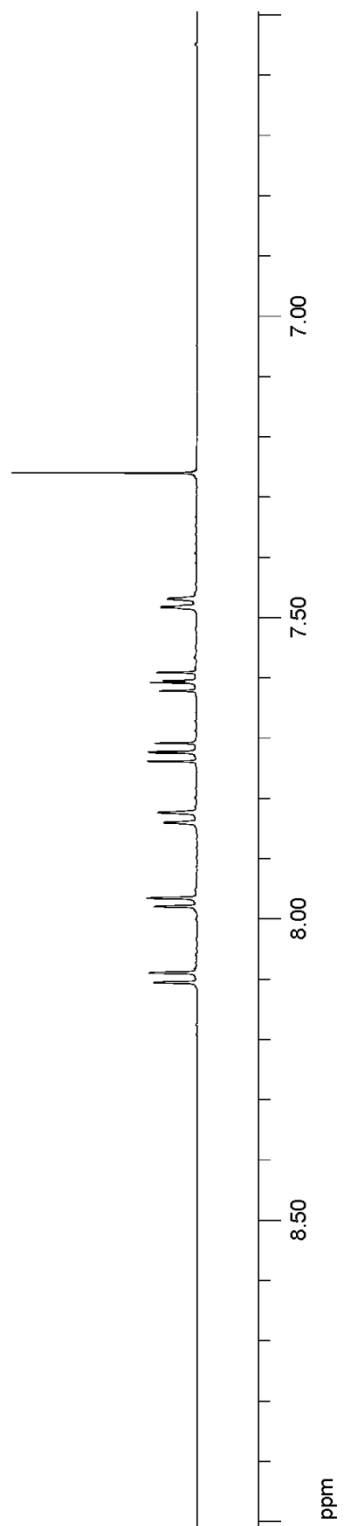
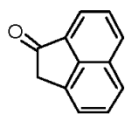
5.8.2.18. 1-Acenaphthone



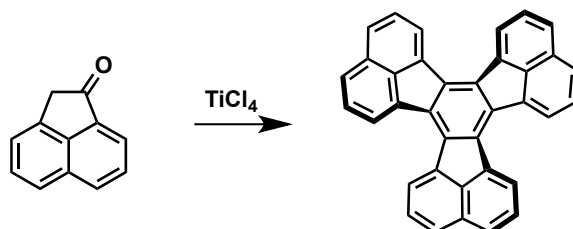
In a round-bottomed flask, 6b,7a-dihydroacenaphtho[1,2-b]oxirene (6.0 g, 36 mmol) was dissolved in dichloromethane (360 mL, 0.1 M). Then, around 100 g of silica gel was added to the solution. The reaction mixture was stirred at ambient temperature for 4 h. After this time, silica gel was removed by vacuum filtration. The solvent was evaporated under reduced pressure to give the crude product. The crude material was recrystallized from hexanes to give 1-acenaphthone as a white solid (quantitative yield, 6.0 g). mp = 82–83 °C. ^1H NMR (500 MHz, CDCl_3): δ 8.10 (d, J = 8.0 Hz, 1H), 7.97 (d, J = 6.5 Hz, 1H), 7.83 (d, J = 9.0 Hz, 1H), 7.72 (dd, J = 8.0, 7.0 Hz, 1H), 7.60 (dd, J = 8.5, 7.0 Hz, 1H), 7.48 (d, J = 7.0 Hz, 1H), 3.83 (s, 3H). The characterization data were in agreement with literature values.⁹²

⁹² Yang, G.; Zhang, Q.; Miao, H.; Tong, X.; Xu, J., "Selective Organocatalytic Oxygenation of Hydrocarbons by Dioxxygen Using Anthraquinones and *N*-Hydroxyphthalimide," *Organic Letters* **2004**, *7*, 263-266.

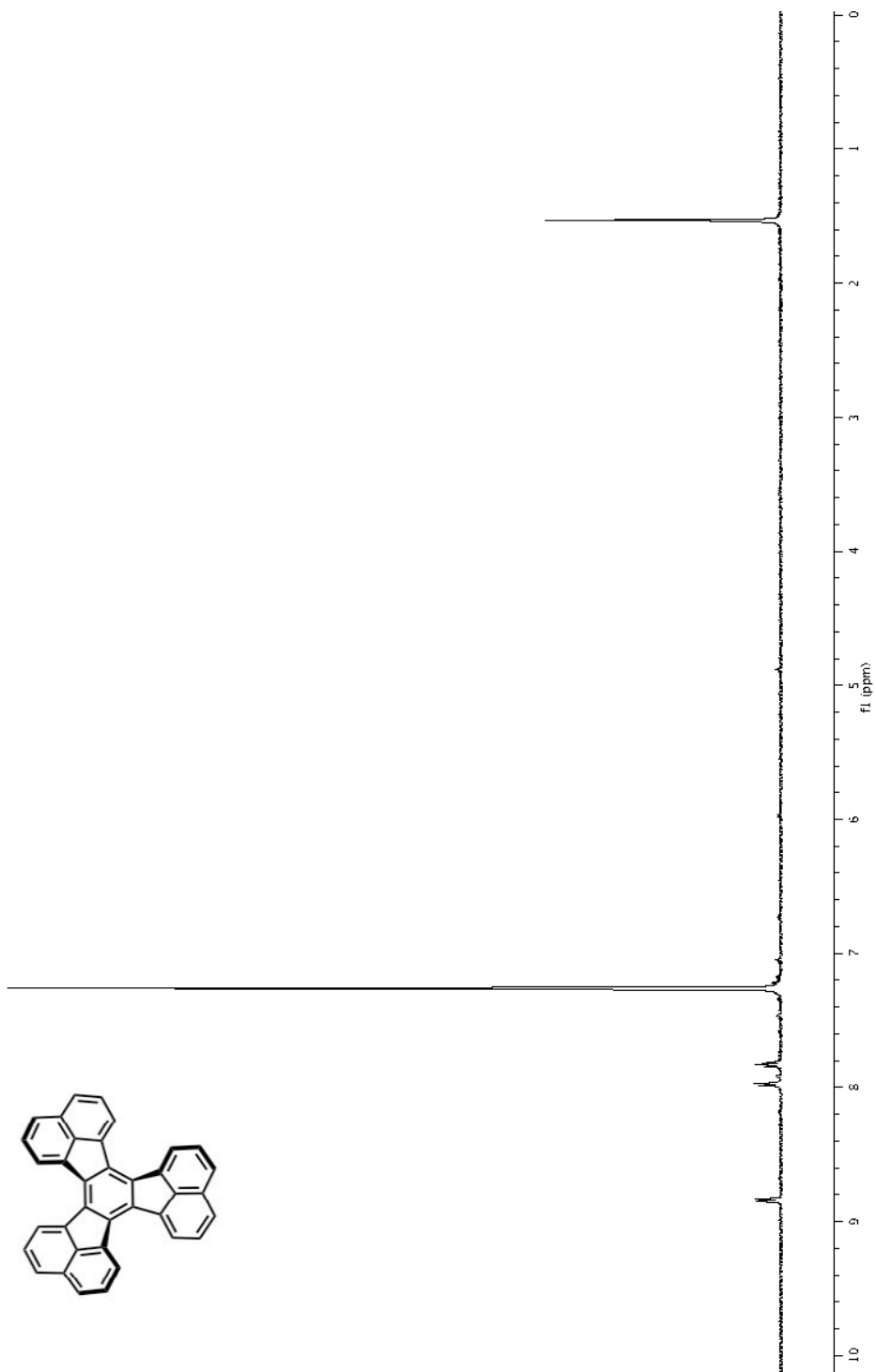


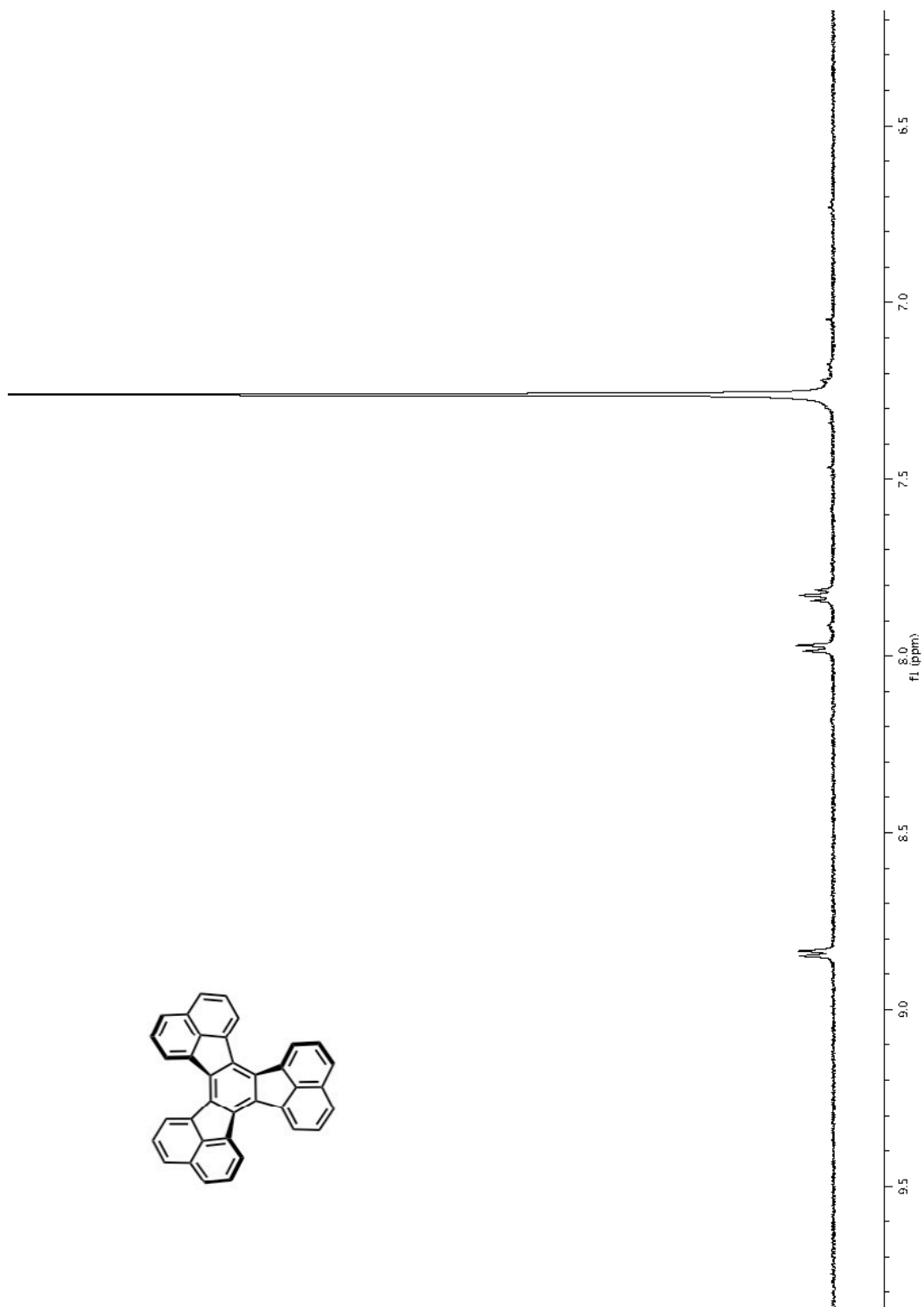
500 MHz, ^1H NMR, CDCl_3

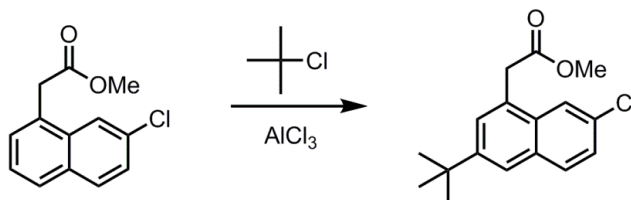
5.8.2.19. Decacyclene



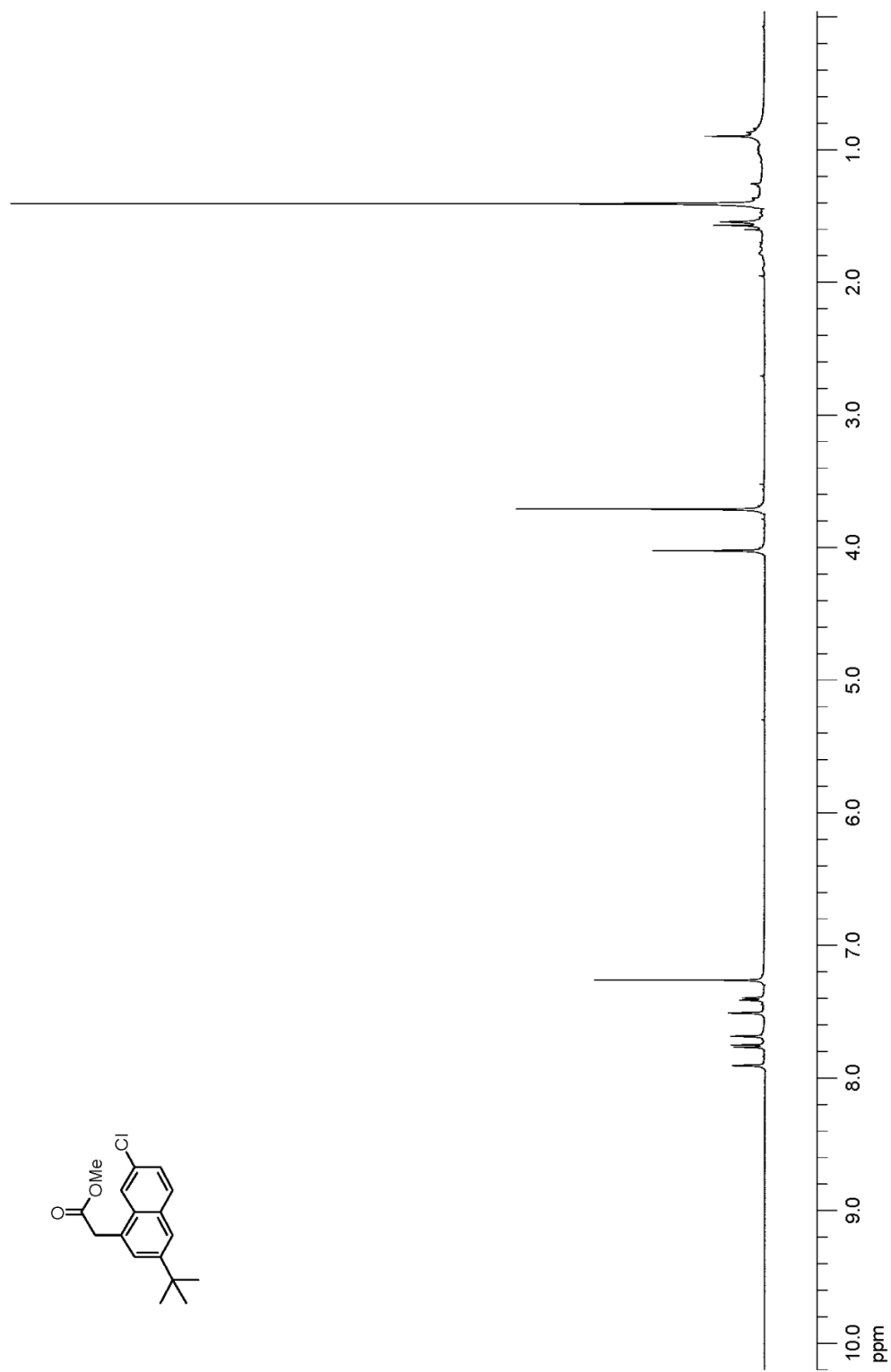
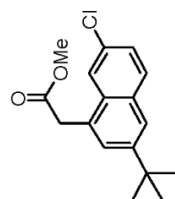
An oven-dried round-bottomed flask, equipped with a magnetic stir-bar, was charged with 0.40 mL (0.66 g, 3.6 mmol) of titanium(IV) chloride and 11 mL (0.055 M) of *o*-DCB. The mixture was heated to reflux under an inert atmosphere of nitrogen. After the reflux point was reached, 100 mg (0.60 mmol) of 1-acenaphthenone, which was dissolved in 2.4 mL (0.25 M) of *o*-DCB, was added dropwise with a syringe over 30 min. Then, the reaction mixture was refluxed under nitrogen for 14 h. After this time, the reaction mixture was cooled to room temperature and poured into a solution of 10% HCl and ice. The resulting heterogeneous mixture was extracted with dichloromethane, and the combined organic layers were dried with anhydrous sodium sulfate. The drying agent was removed by vacuum filtration, and the solvent was evaporated under reduced pressure. The crude material was purified by column chromatography on neutral alumina with hexanes/DCM to afford decacyclene as a brown solid in 40% yield (36 mg). ^1H NMR (500 MHz, CDCl_3): δ 8.84 (d, $J = 7.2$, 6H), 7.98 (d, $J = 8.0$ Hz, 6H), 7.83 (t, $J = 7.6$ Hz, 6H). The characterization data were in agreement with literature values.^{47b}

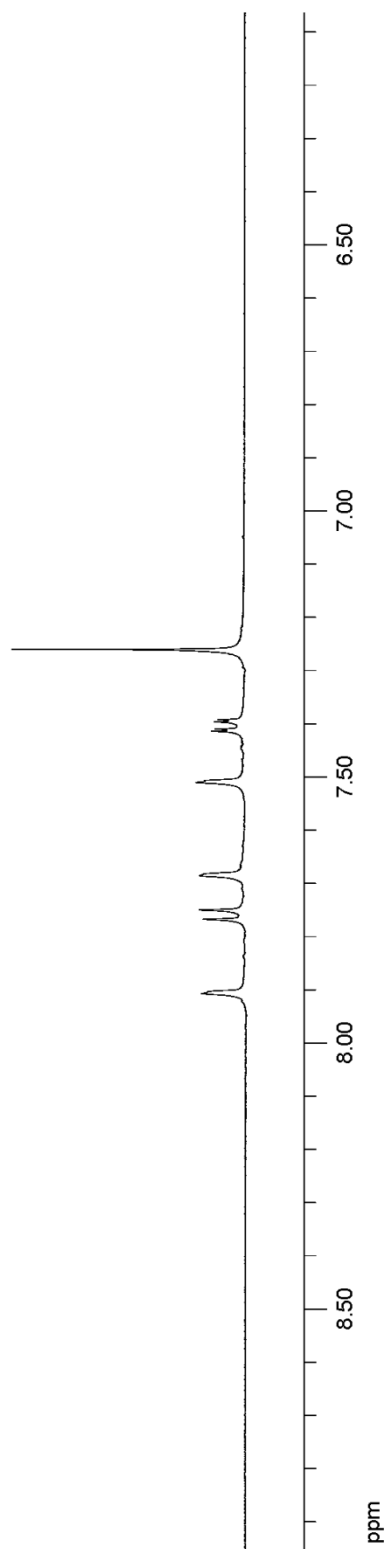
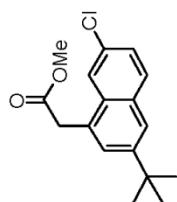


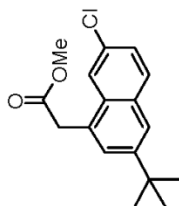
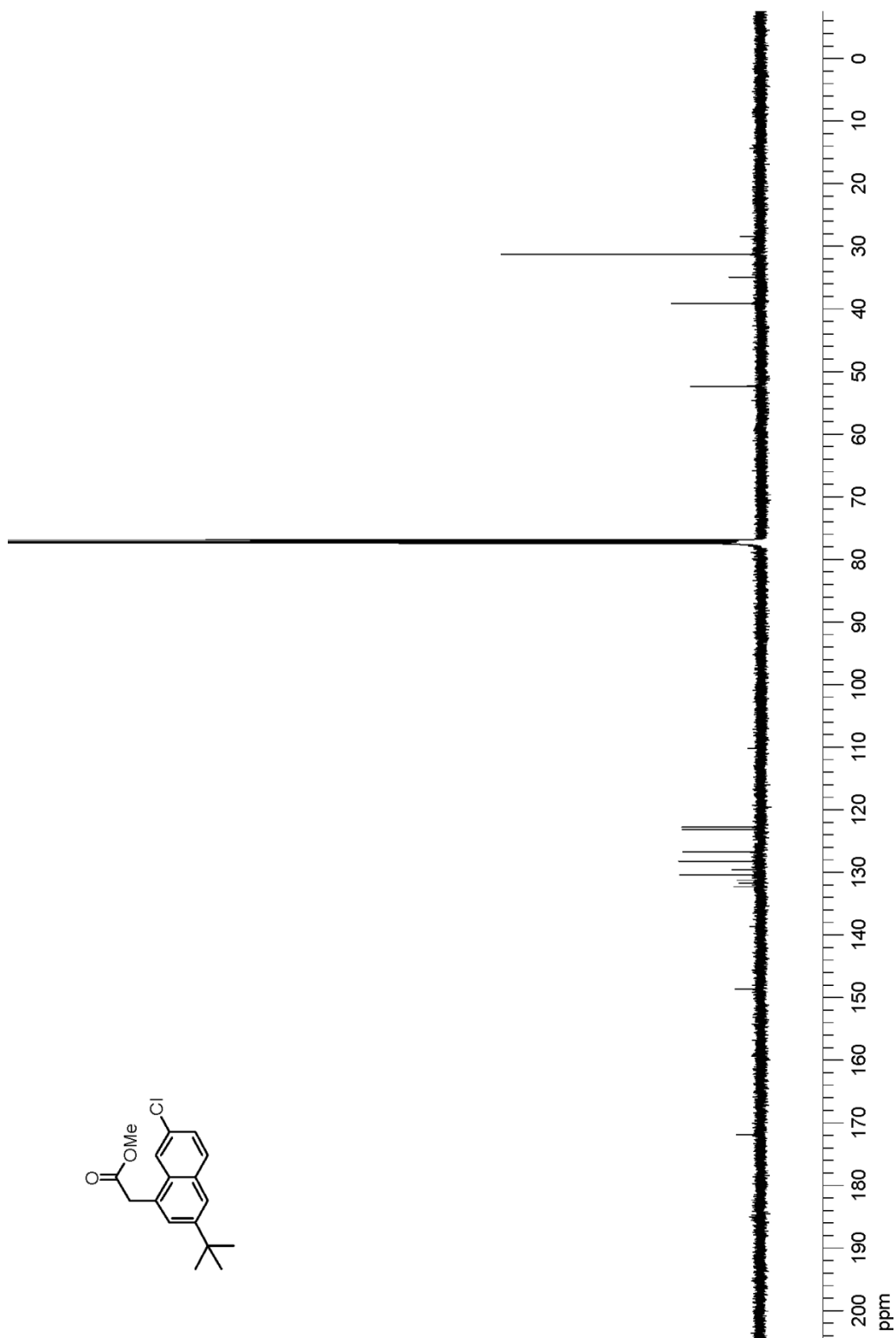
500 MHz, ^1H NMR, CDCl_3

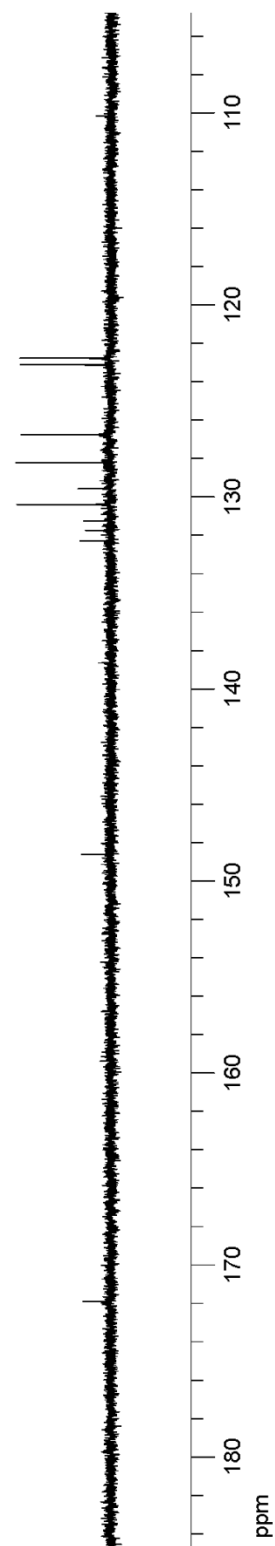
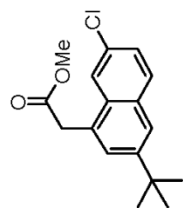
5.8.2.20. Methyl 2-(3-(*tert*-butyl)-7-chloronaphthalen-1-yl)acetate

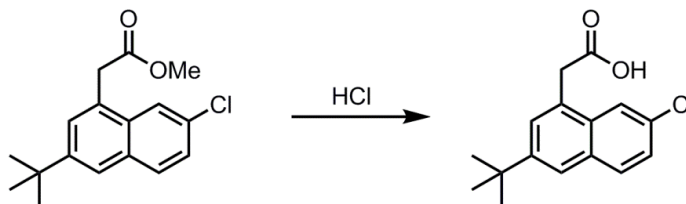
In a flame-dried round-bottomed flask, equipped with a magnetic stir-bar, 1.0 g (4.3 mmol) of methyl 2-(7-chloronaphthalen-1-yl)acetate was dissolved in 107 mL (0.04 M) of dichloromethane and 4.7 mL (3.9 g, 43 mmol) of *t*-butyl chloride. To this solution, 1.3 g (9.5 mmol) of anhydrous aluminum chloride was carefully added. Then, the reaction mixture was stirred at ambient temperature for 2 h. After this time, the mixture was filtered through a short pad of silica gel with DCM/hexane (1:1) as an eluent. The organic solvent was evaporated under reduced pressure to give the title compound. This material was further purified by column chromatography on silica gel with hexanes/EtOAc to afford methyl 2-(3-(*tert*-butyl)-7-chloronaphthalen-1-yl)acetate as a yellow oil in 98% yield (1.2 g). ¹H NMR (500 MHz, CDCl₃): δ 7.91 (s, 1H), 7.76 (d, *J* = 8.5 Hz, 1H), 7.68 (s, 1H), 7.51 (s, 1H), 7.40 (dd, *J* = 8.5, 2.0 Hz, 1H), 4.02 (s, 2H), 3.71 (s, 3H), 1.40 (s, 9H). ¹³C NMR (125 MHz, CDCl₃): δ 171.9, 148.6, 132.3, 131.7, 131.3, 130.4, 129.6, 128.2, 126.8, 123.1, 122.8, 52.4, 39.1, 34.9, 31.3. HRMS (DART) calculated for C₁₇H₂₀ClO₂ [M+H]⁺: 291.1161, found: 291.1152.



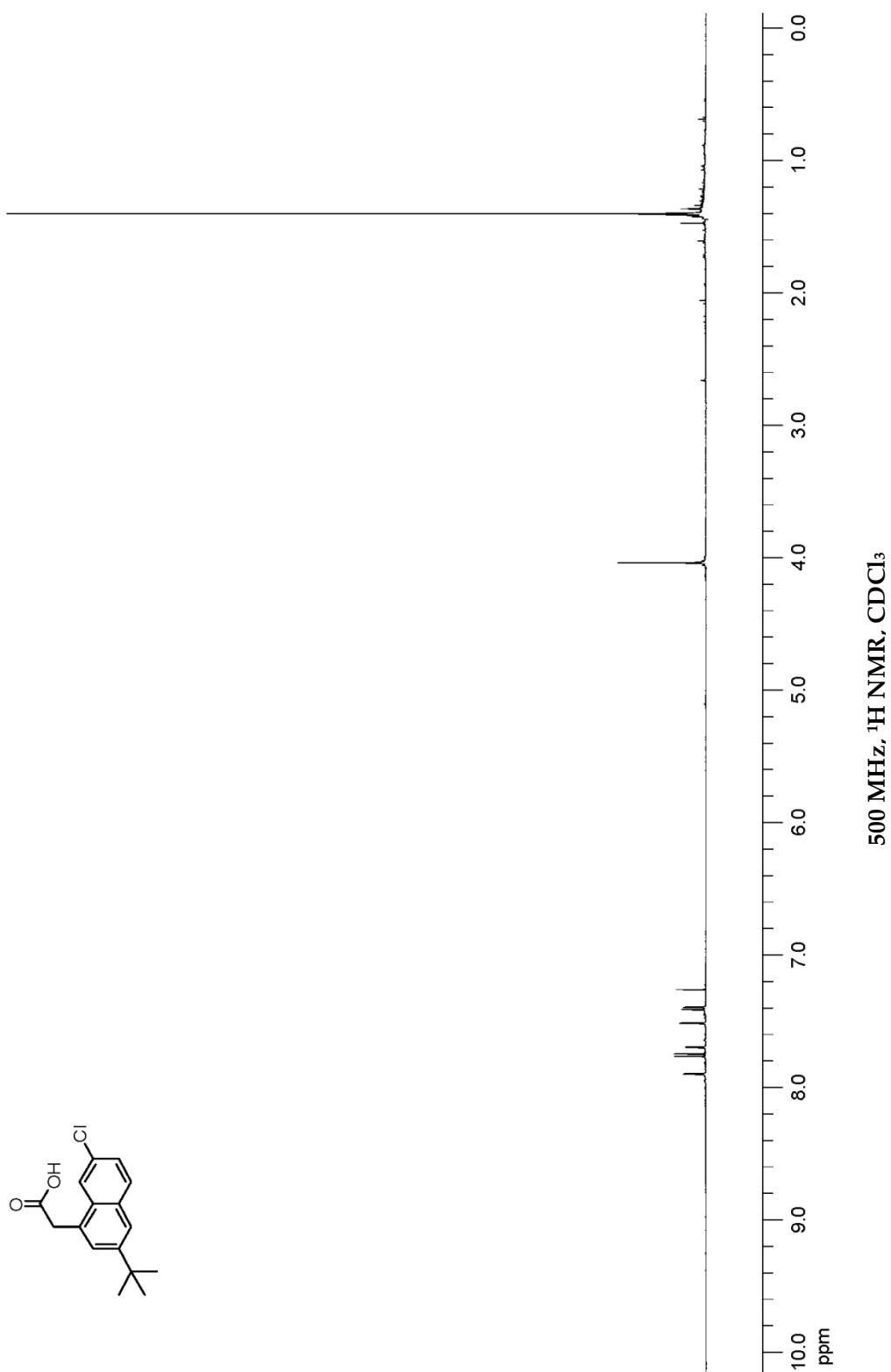
500 MHz, ¹H NMR, CDCl₃

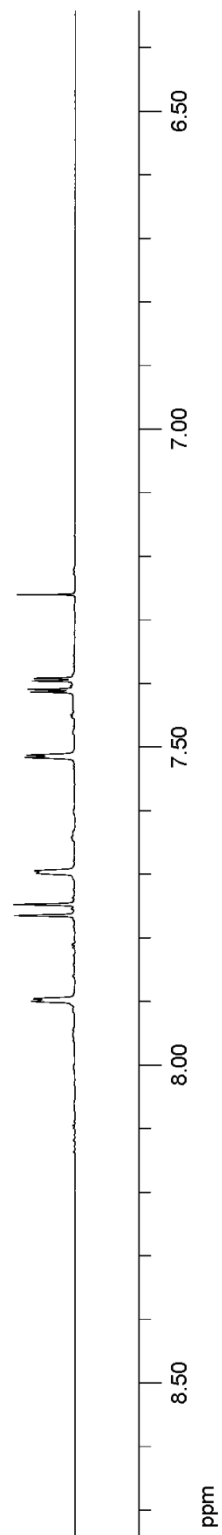
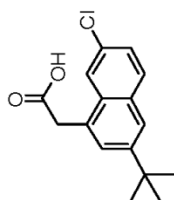
125 MHz, ^{13}C NMR, CDCl_3

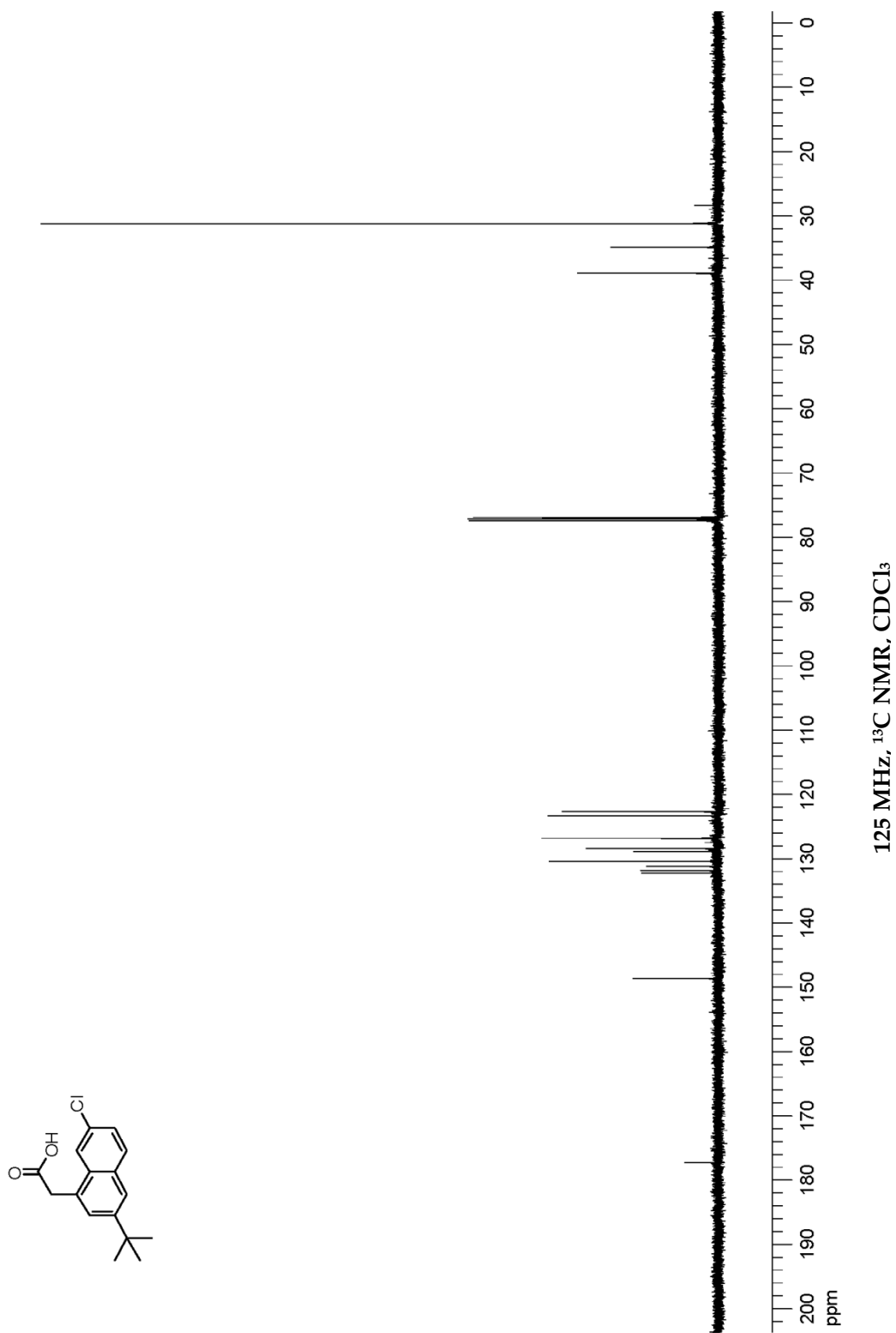
125 MHz, ¹³C NMR, CDCl₃

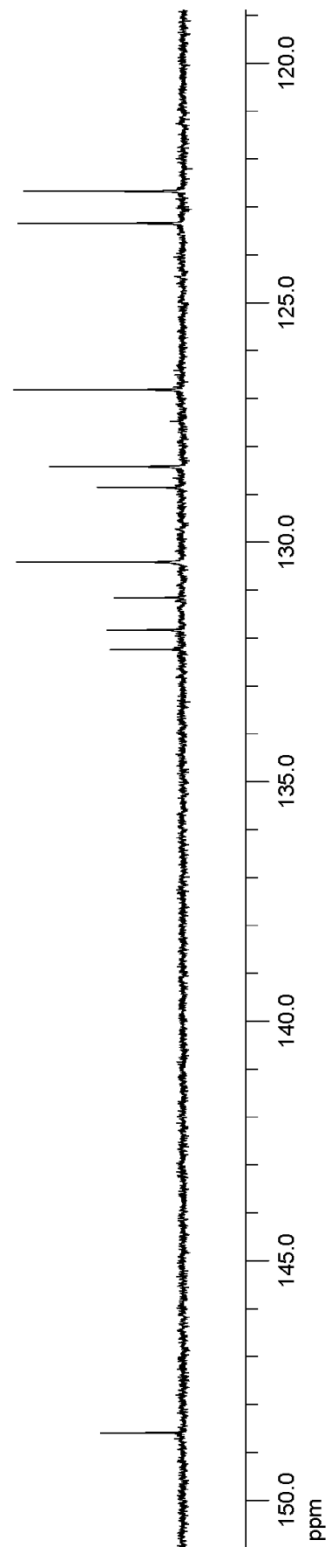
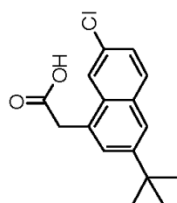
5.8.2.21. 2-(3-(*tert*-Butyl)-7-chloronaphthalen-1-yl)acetic acid

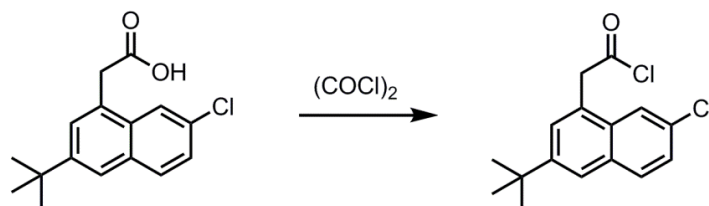
In a round-bottomed flask, 1.5 g (5.0 mmol) of methyl 2-(3-(*tert*-butyl)-7-chloronaphthalen-1-yl)acetate was dissolved in 5 M HCl (93 mL, 0.054 M) and acetone (93 mL, 0.054 M). A reflux condenser was placed on the top of the flask, and the mixture was refluxed for 5 h. After this time, the reaction mixture was cooled to room temperature, and the solvents (acetone and methanol) were evaporated *in vacuo*. The aqueous residue was extracted with dichloromethane, and the solvent was removed to give the crude product. The crude material was dissolved in a dilute NaOH solution, and the resulting solution was washed with benzene. Upon slow addition of 5 M HCl to this basic solution with cooling, the title compound was precipitated out of the solution. The desired product, 2-(3-(*tert*-Butyl)-7-chloronaphthalen-1-yl)acetic acid, was obtained by vacuum filtration as an off-white solid in quantitative yield (1.4 g). ¹H NMR (500 MHz, CDCl₃): δ 7.79 (d, *J* = 2.0 Hz, 1H), 7.76 (d, *J* = 9.0 Hz, 1H), 7.70 (d, *J* = 2.0 Hz, 1H), 7.51 (d, *J* = 2.0 Hz, 1H), 7.40 (dd, *J* = 9.0, 2.0 Hz, 1H), 4.04 (s, 2H), 1.41 (s, 9H). ¹³C NMR (125 MHz, CDCl₃): δ 177.3, 148.6, 132.3, 131.8, 131.2, 130.4, 128.9, 128.4, 126.8, 123.4, 122.7, 38.9, 34.9, 31.3.



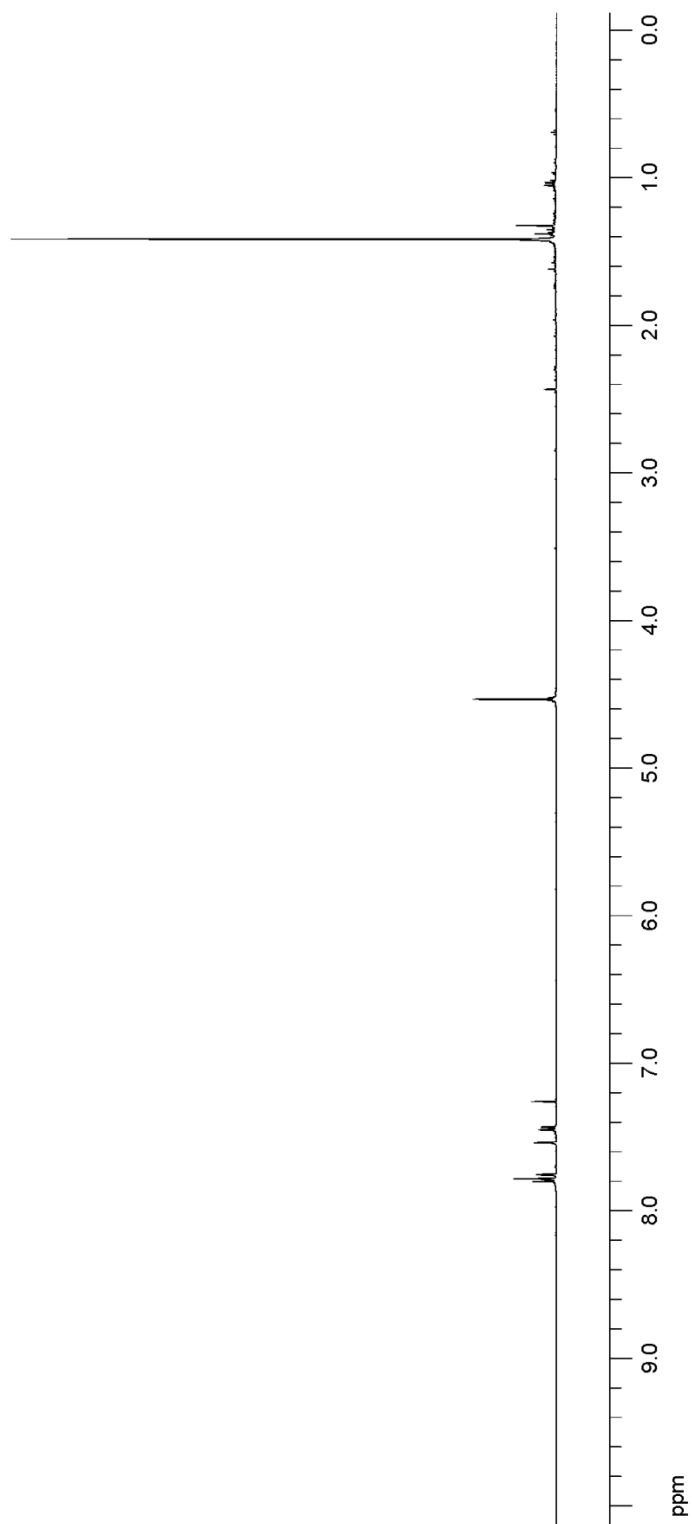
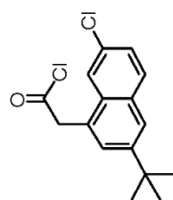
500 MHz, ¹H NMR, CDCl₃

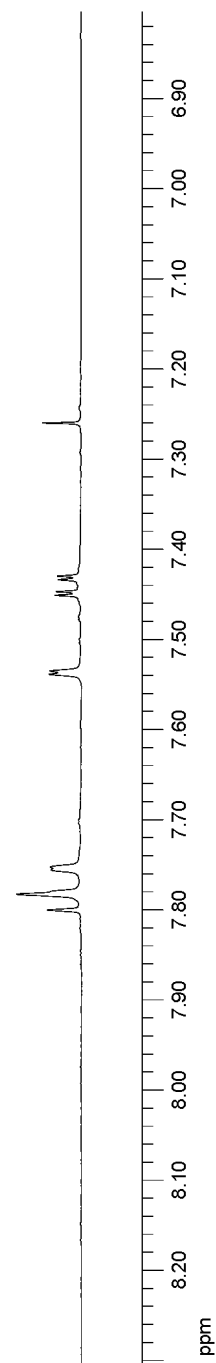
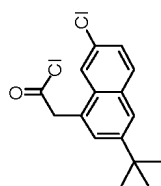


125 MHz, ¹³C NMR, CDCl₃

5.8.2.22. 2-(3-(*tert*-Butyl)-7-chloronaphthalen-1-yl)acetyl chloride

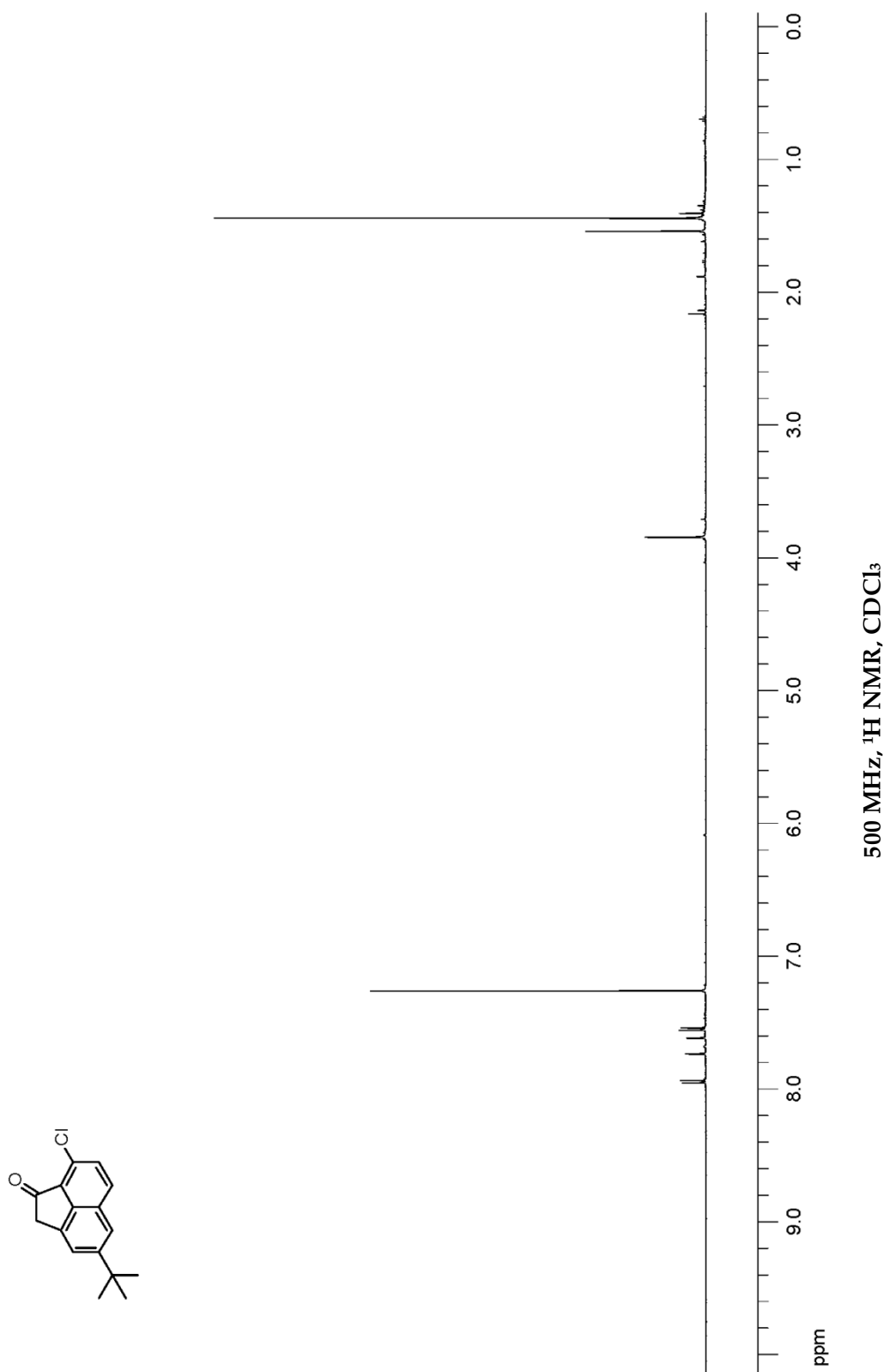
To an oven-dried round-bottomed flask, 7.7 g (35 mmol) of 2-(3-(*tert*-butyl)-7-chloronaphthalen-1-yl)acetic acid and 42 mL (0.8 M) of benzene were placed. While stirring, 14.5 mL (173 mmol) of oxalyl chloride was added to this mixture. Then, the resulting solution was heated at reflux for 5 h. After this time, the volatiles (the solvent and oxalyl chloride) were removed under reduced pressure to afford 2-(3-(*tert*-butyl)-7-chloronaphthalen-1-yl)acetyl chloride as a yellow solid. Purification was not performed for this compound, and the product was directly used as a starting material for the next step (see Section 5.8.2.23). ^1H NMR (500 MHz, CDCl_3): δ 7.79 (d, $J = 9.0$ Hz, 1H), 7.78 (s, 2H), 7.75 (d, $J = 1.5$ Hz, 1H), 7.54 (d, $J = 1.5$ Hz, 1H), 7.44 (dd, $J = 9.0, 2.0$ Hz, 1H), 4.53 (s, 2H), 1.41 (s, 9H).

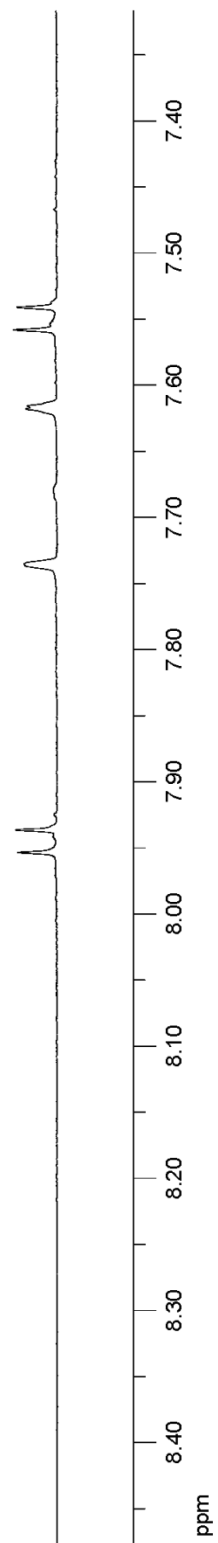
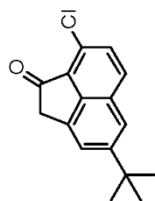


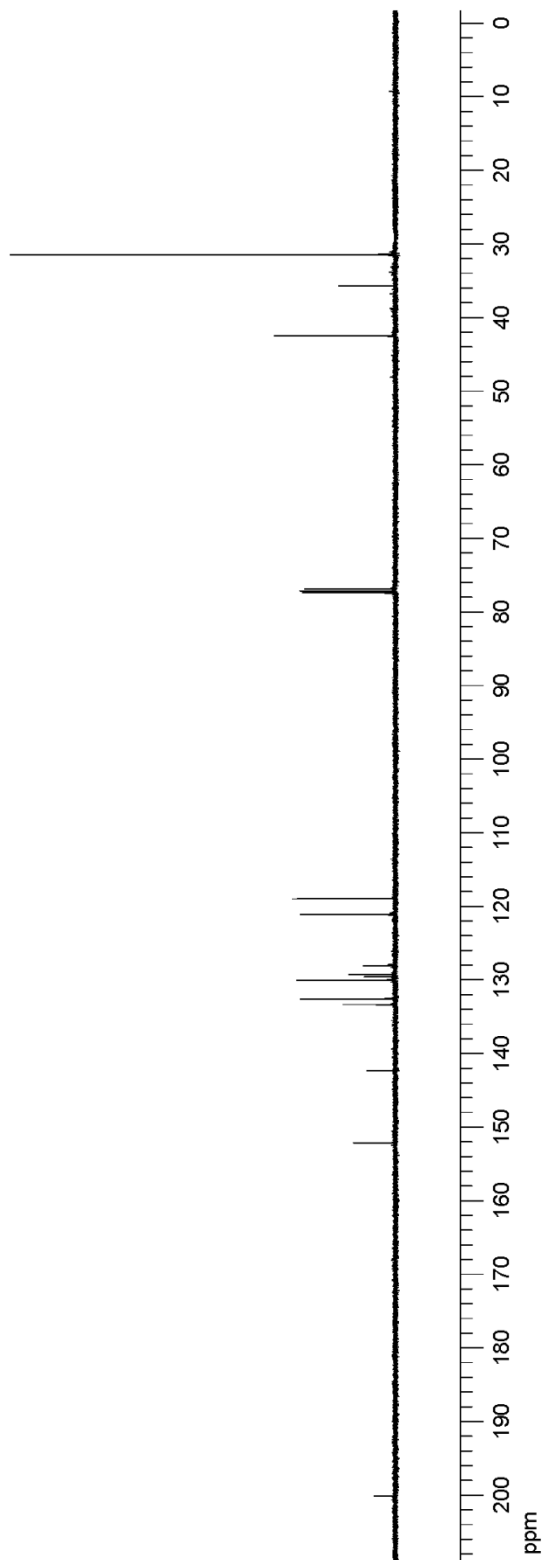
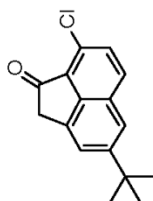
500 MHz, ¹H NMR, CDCl₃

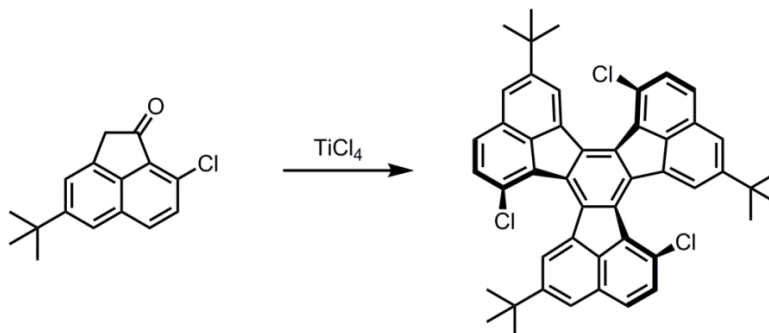
5.8.2.23. 4-(*tert*-Butyl)-8-chloroacenaphthylen-1(2H)-one

In a flame-dried round-bottomed flask, 2-(3-(*tert*-butyl)-7-chloronaphthalen-1-yl)acetyl chloride (2.1 g, 8 mmol) was dissolved in dichloromethane (80 mL, 0.1 M). The resulting solution was cooled to 0 °C in an ice-bath, and then aluminum chloride (2.1 g, 16 mmol) was added to the mixture. After the reaction mixture was stirred at 0 °C for 6 h, it was warmed to room temperature. Then, the mixture was stirred at ambient temperature for 12 h. The reaction was quenched with a dilute HCl solution, and the resulting solution was extracted with dichloromethane. The solvent was removed *in vacuo* to afford the crude product. The crude material was purified by column chromatography on silica gel with hexanes/ether to give 8-chloroacenaphthylen-1(2H)-one as an off-white solid (65% yield over two steps, 1.3 g). $R_f = 0.25$ (9:1 hexanes:ether). ¹H NMR (500 MHz, CDCl₃): δ 7.92 (d, $J = 8.5$ Hz, 1H), 7.74 (s, 1H), 7.62 (s, 1H), 7.50 (d, $J = 8.0$ Hz, 1H), 3.85 (s, 2H), 1.44 (s, 9H). ¹³C NMR (125 MHz, CDCl₃): δ 200.2, 152.1, 142.4, 133.4, 132.6, 130.0, 129.6, 129.3, 128.1, 121.1, 119.0, 42.5, 35.7, 31.4. HRMS (DART) calculated for C₁₆H₁₆ClO [M+H]⁺: 259.0882, found: 259.0890.



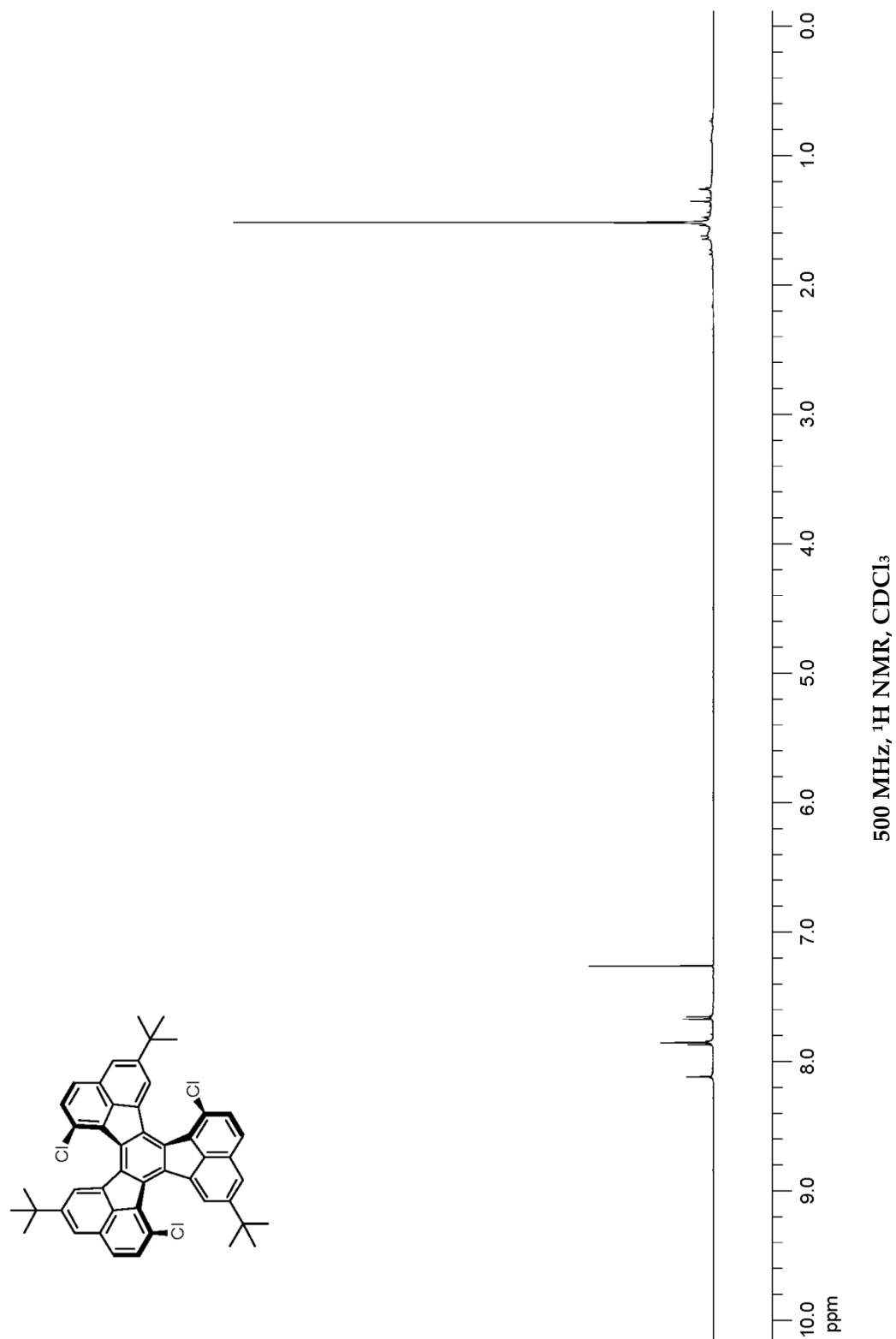
500 MHz, ¹H NMR, CDCl₃

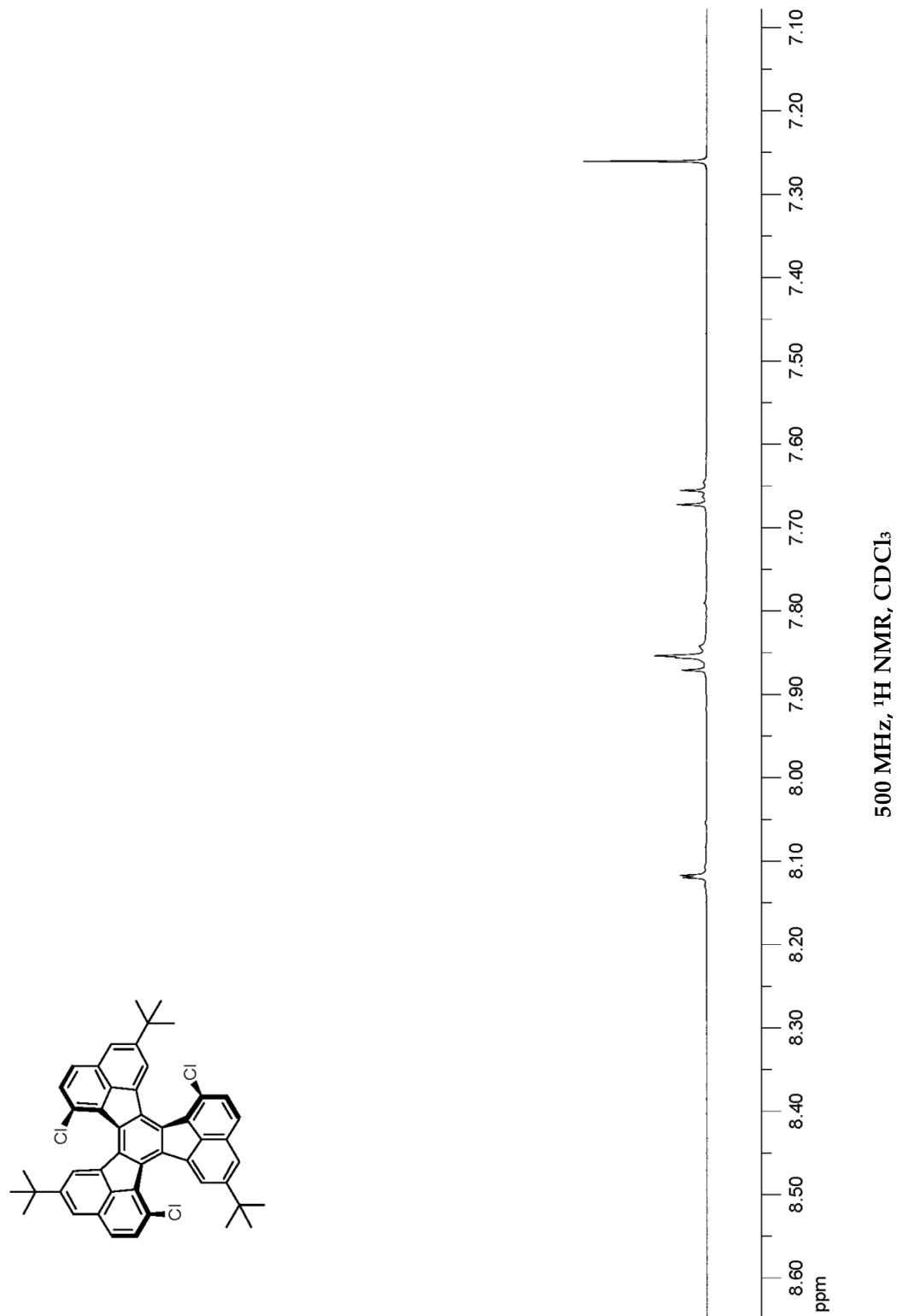
125 MHz, ^{13}C NMR, CDCl_3

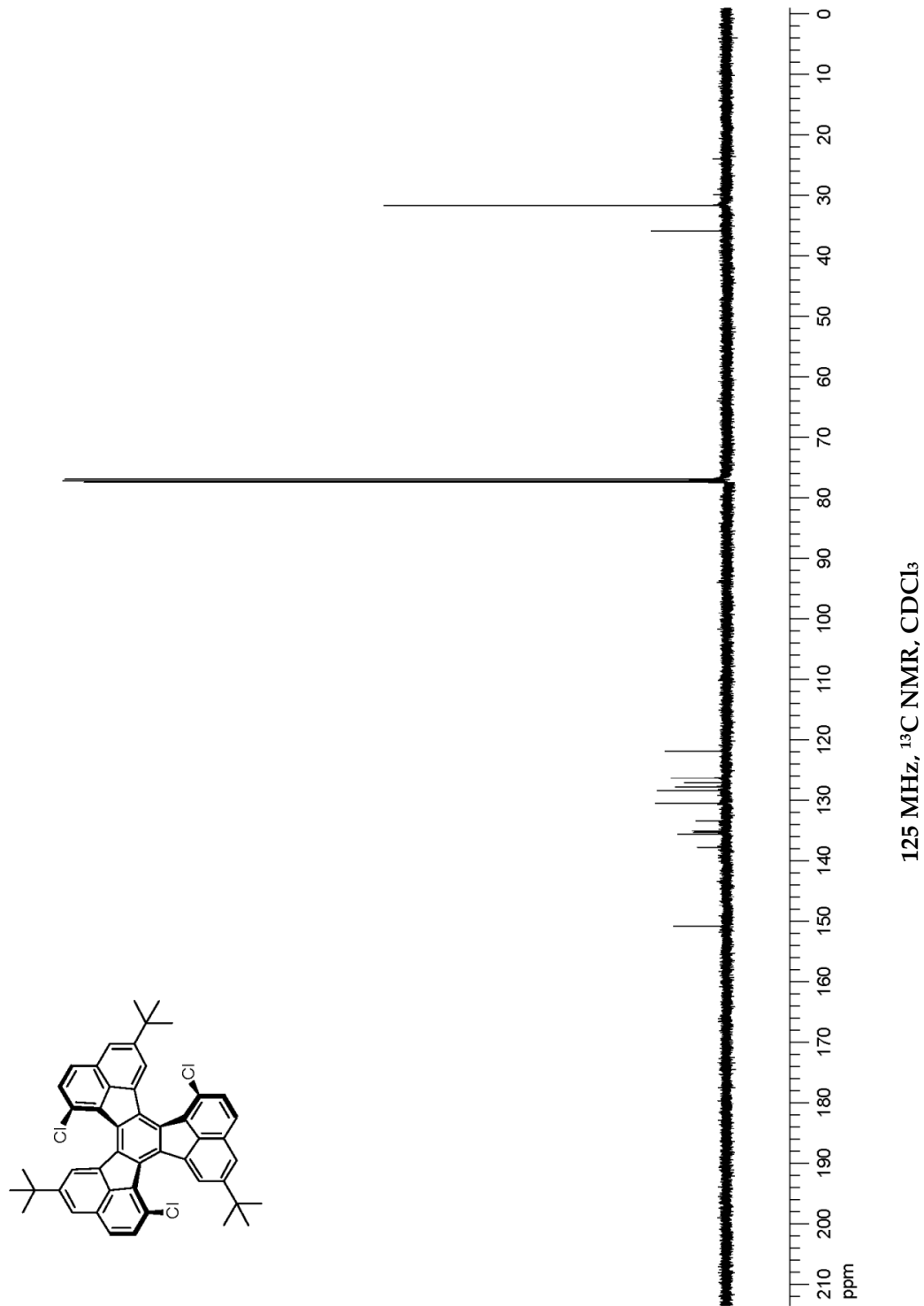
5.8.2.24. 5,11,17-tri-*tert*-butyl-1,7,13-trichlorodecacyclene

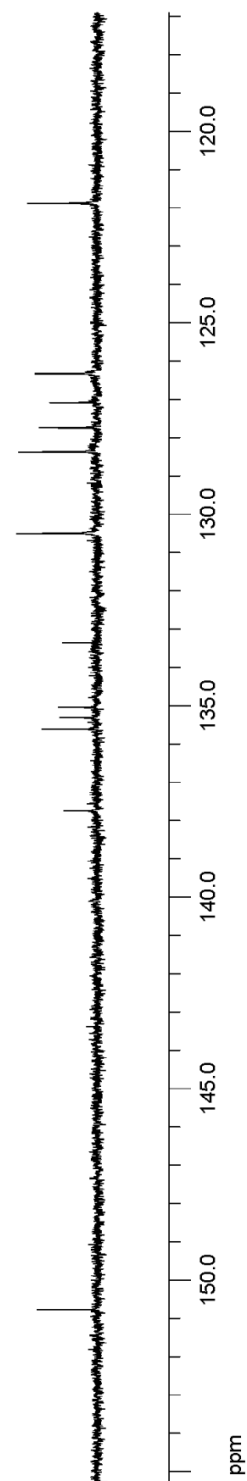
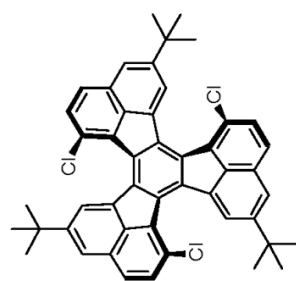
An oven-dried round-bottomed flask, equipped with a magnetic stir-bar, was charged with 0.66 mL (1.1 g, 6.0 mmol) of titanium(IV) chloride and 18 mL (0.055 M) of 1,2-dichloroethane. The mixture was heated to reflux under an inert atmosphere of nitrogen. After the reflux point was reached, 259 mg (1.0 mmol) of 4-(*tert*-butyl)-8-chloroacenaphthylen-1(2H)-one, which was dissolved in 4 mL (0.25 M) of 1,2-dichloroethane, was added dropwise with a syringe over 30 min. Then, the reaction mixture was refluxed under nitrogen for 18 h. After this time, the reaction mixture was cooled to room temperature and poured into a solution of 10% HCl and ice. The resulting heterogeneous mixture was extracted with dichloromethane, and the combined organic layers were dried with anhydrous sodium sulfate. The drying agent was removed by vacuum filtration, and the solvent was evaporated under reduced pressure. The crude material was purified by column chromatography on silica gel with hexanes/DCM to afford 5,11,17-tri-*tert*-butyl-1,7,13-trichlorodecacyclene as a red solid in 58% yield (416 mg). ^1H NMR (500 MHz, CDCl_3): δ 8.12 (s, 3H), 7.86 (d, $J = 8.5$ Hz, 3H), 7.85 (s, 3H), 7.66 (d, $J = 8.5$ Hz, 3H), 1.52 (s, 27H). ^{13}C

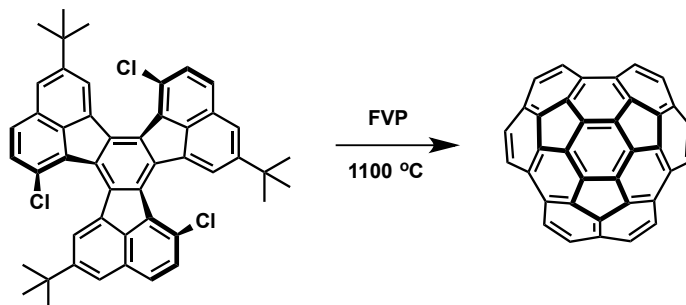
NMR (125 MHz, CDCl₃): δ 150.8, 137.8, 135.6, 135.3, 135.1, 133.4, 130.5, 128.4, 127.8, 127.1, 126.3, 121.9, 35.9, 31.7. HRMS (DART) calculated for C₄₈H₄₀Cl₃ [M+H]⁺: 721.2235, found: 721.2196.





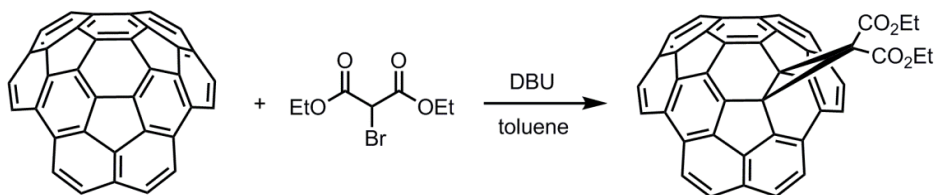




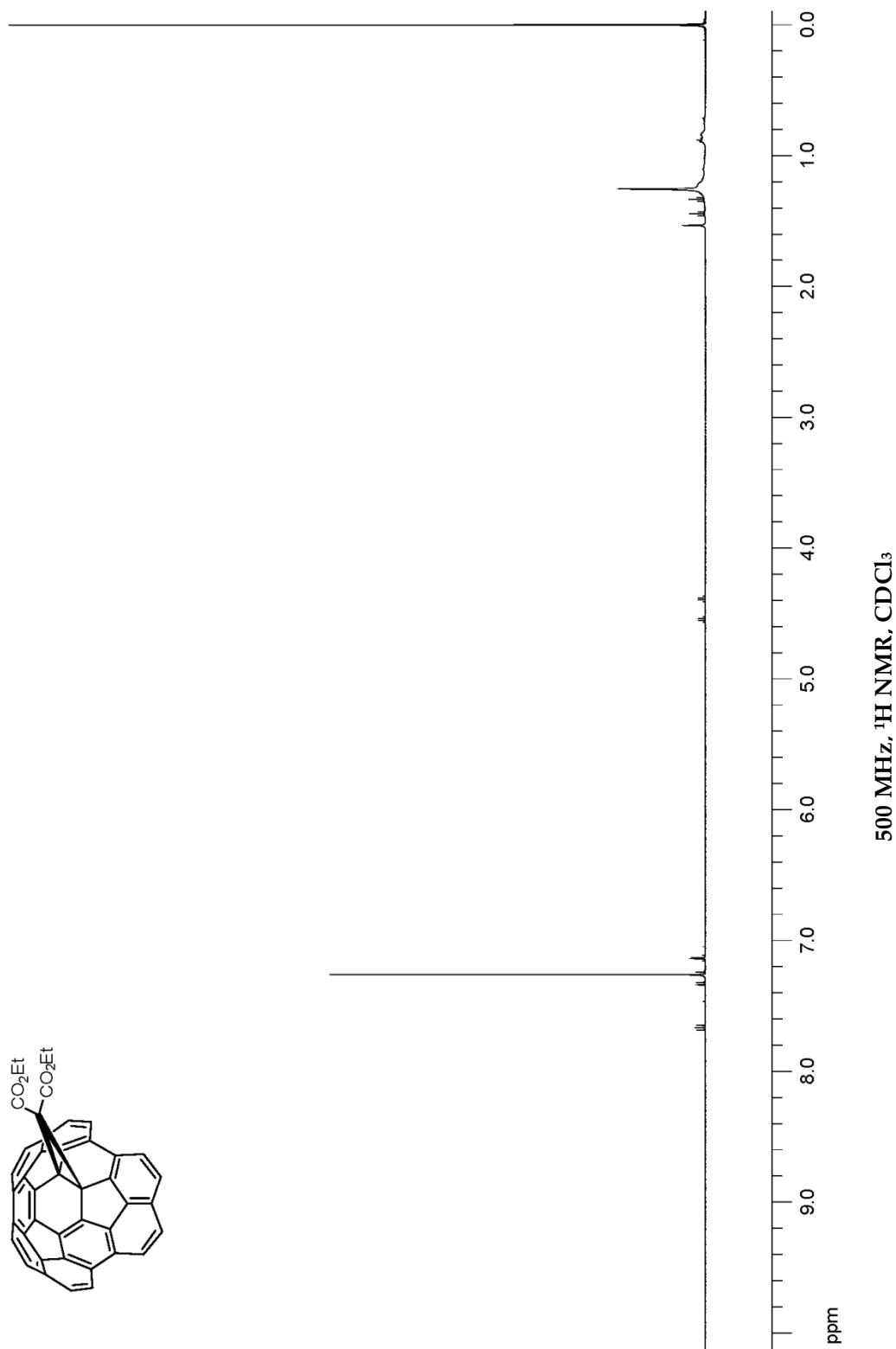
5.8.2.25. Circumtrindene from $C_{48}H_{39}Cl_3$ 

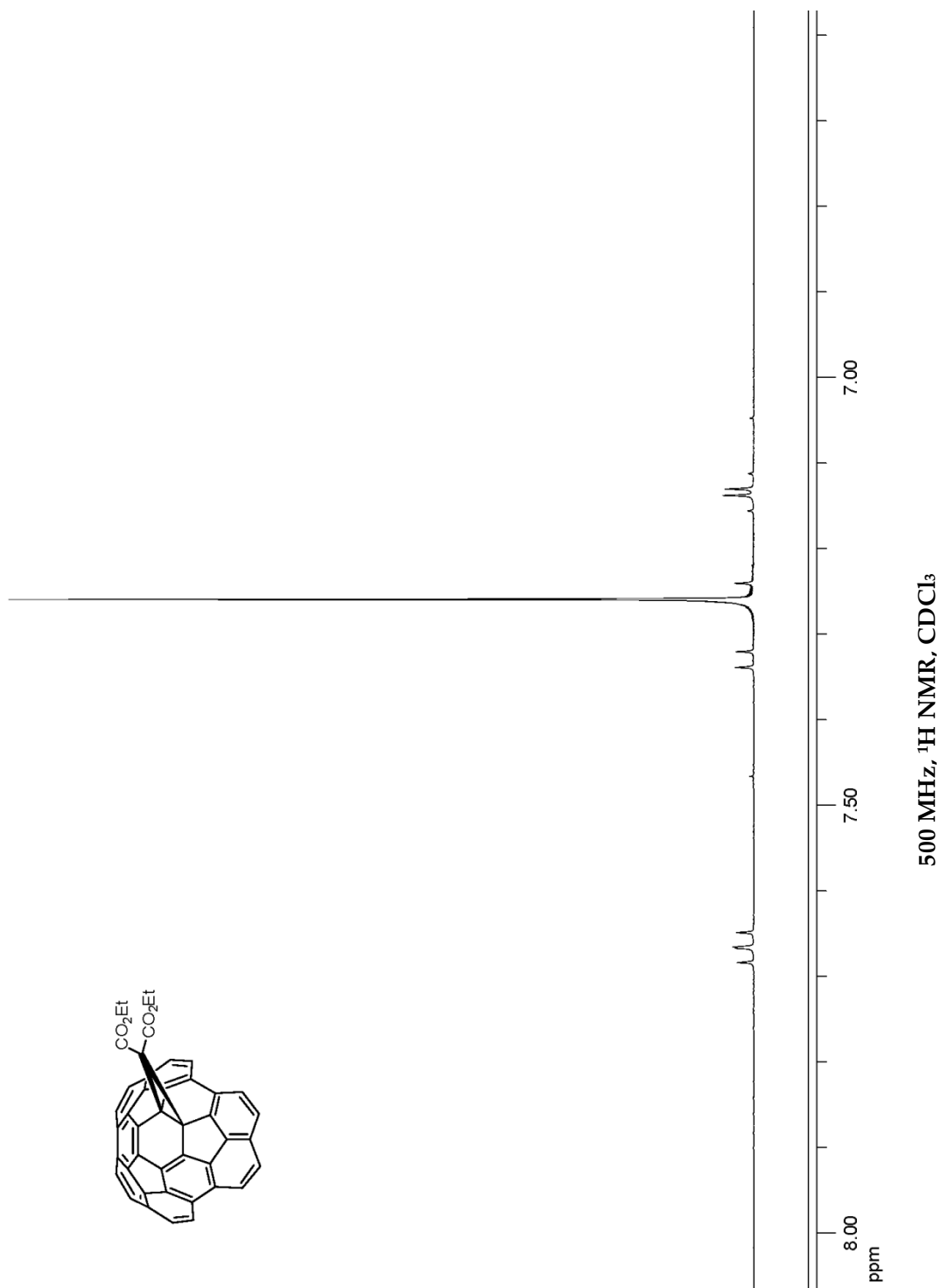
The FVP reaction was performed with 100 mg (0.14 mmol) of 5,11,17-tri-*tert*-butyl-1,7,13-trichlorodecacyclene, which was placed in a sample boat in a supplemental heating oven. On one side of the FVP apparatus, the system was connected to a nitrogen gas reservoir through a capillary inlet tube made out of a section of GC capillary. On the other side of the oven, the pyrolysis tube was connected to a high-capacity vacuum pump through a cold trap filled with liquid nitrogen. The supplemental oven was heated to 200 °C, and the reaction oven was heated to 1100 °C. The pressure of the system was equilibrated to 0.5 torr. As soon as both of the ovens reached the desired temperatures, the sample boat was moved into the center of the supplemental oven. After 2 hours of reaction time, it was observed that all the starting material was sublimed leaving a black tar on the sample boat. The crude product was collected by rinsing both the quartz tube and the glass trap with dichloromethane (~500 mL). The mass spectrum of the crude material indicated that the desired product ($m/z = 444.09$) was formed as a minor product. Due to the low efficiency of the reaction and the excessive amount of byproducts, further purification of the crude product was not successful.

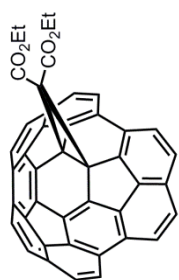
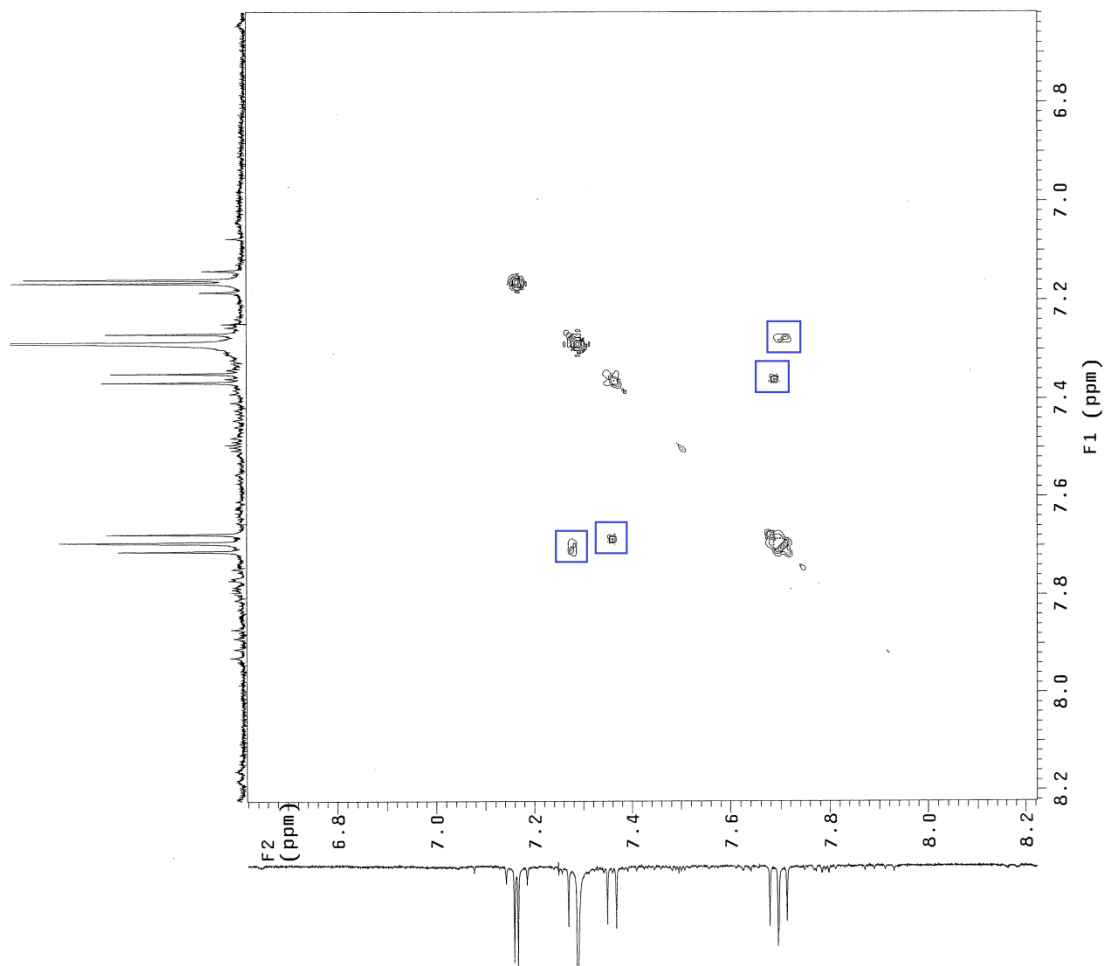
5.8.2.26. 12d,12e-(bis(ethoxycarbonyl)methylene-bridged)circumtrindene



An oven-dried round-bottomed flask, equipped with a magnetic stir-bar, was charged with 4.2 mg (0.0095 mmol) of circumtrindene, 23 mg (0.095 mmol) of ethyl bromo malonates, 14 mg (0.095 mmol) of DBU, and 1.9 mL (0.005 M) of toluene. The reaction mixture was stirred at ambient temperature for 2 h under an inert atmosphere of nitrogen. After this time, the reaction was quenched with trifluoroacetic acid (72 μ L, 0.95 mmol), and the organic solvent was evaporated under reduced pressure. The crude material was purified by column chromatography on silica gel with hexanes/ether as an eluent to afford 12d,12e-(bis(ethoxycarbonyl)methylene-bridged)circumtrindene as a yellow solid in 75% yield (4.3 mg). R_f = 0.26 (1:1 hexane:ether). ^1H NMR (500 MHz, CDCl_3): δ 7.68 (d, J = 9.0 Hz, 2H), 7.66 (d, J = 8.5 Hz, 2H), 7.33 (d, J = 9.0 Hz, 2H), 7.25 (d, J = 9.0 Hz, 2H), 7.15 (d, J = 9.0 Hz, 2H), 7.12 (d, J = 9.0 Hz, 2H), 4.55 (q, J = 7.0 Hz, 2H), 4.39 (q, J = 7.0 Hz, 2H), 1.45 (t, J = 7.0 Hz, 3H), 1.34 (t, J = 7.0 Hz, 3H). HRMS (MALDI) calculated for $\text{C}_{43}\text{H}_{22}\text{O}_4$ $[\text{M}]^+$: 602.1513, found: 602.1515.







Chapter 6. Intermolecular Oxidative Coupling of Arenes and Unactivated Alkenes Leading to π -Conjugated Cyclic Trimers

6.1. Introduction

6.1.1. Oxidative Coupling of Unactivated Arenes

Carbon-carbon bond forming reactions between aromatic compounds are fundamentally important reactions in organic, medicinal, and materials chemistry. Such transformations have been achieved by chemical,¹ photochemical,² or electrochemical methods.³ Notably, the remarkable developments in transition metal catalysis during the last few decades provided various powerful methods for aryl-aryl bond formation.⁴

¹ (a) Bringmann, G.; Walter, R.; Weirich, R., "The Directed Synthesis of Biaryl Compounds: Modern Concepts and Strategies," *Angewandte Chemie International Edition* **1990**, *29*, 977-991. (b) Stanforth, S. P., "Catalytic Cross-Coupling Reactions in Biaryl Synthesis," *Tetrahedron* **1998**, *54*, 263-303.

² (a) Grimshaw, J.; De Silva, A., "Photochemistry and Photocyclization of Aryl Halides," *Chemical Society Reviews* **1981**, *10*, 181-203. (b) Davidson, R. S.; Goodin, J. W.; Kemp, G., "The Photochemistry of Aryl Halides and Related Compounds," *Advances in Physical Organic Chemistry* **1984**, *20*, 191-233. (c) Pagni, R. M.; Sigman, M. E., "The Photochemistry of PAHs and PCBs in Water and on Solids," *Handbook of Environmental Chemistry* **1999**, 139-180.

³ (a) Watson, M. D.; Fechtenkötter, A.; Müllen, K., "Big Is Beautiful—"Aromaticity" Revisited from the Viewpoint of Macromolecular and Supramolecular Benzene Chemistry," *Chemical Reviews* **2001**, *101*, 1267-1300. (b) Sainsbury, M., "Modern Methods of Aryl-Aryl Bond Formation," *Tetrahedron* **1980**, *36*, 3327-3359. (c) Speight, J. G.; Kovacic, P.; Koch, F. W., "Synthesis and Properties of Polyphenyls and Polyphenylenes," *Journal of Macromolecular Science, Part C* **1971**, *5*, 295-386.

⁴ (a) Alberico, D.; Scott, M. E.; Lautens, M., "Aryl-Aryl Bond Formation by Transition-Metal-Catalyzed Direct Arylation," *Chemical Reviews* **2007**, *107*, 174-238. (b) Hassan, J.; Sevignon, M.; Gozzi, C.;

Among various methods for aryl–aryl coupling, the chemical method for such transformations has a long history going back to the nineteenth century. The Pschorr reaction (reported in 1896) is one of the oldest coupling reactions; it is an intramolecular aryl–aryl bond forming reaction with aryl radicals that are generated from the reduction of aryl diazonium salts.⁵ Another well-known classic reaction is the Ullmann coupling (reductive coupling), which involves two aryl halides and finely divided copper forming biaryl compounds.^{6,7} With regard to the construction of polycyclic aromatic compounds, however, the Scholl reaction (oxidative coupling) is the most widely employed.

6.1.2. Scholl Oxidation

The Scholl reaction (or Scholl oxidation) is one of the oldest C–C bond forming reactions in organic chemistry, which involves dehydrogenative condensation between

Schulz, E.; Lemaire, M., "Aryl–Aryl Bond Formation One Century after the Discovery of the Ullmann Reaction," *Chemical Reviews* **2002**, *102*, 1359-1470. (c) Ackermann, L. *Modern Arylation Methods*; Wiley Online Library, 2009.

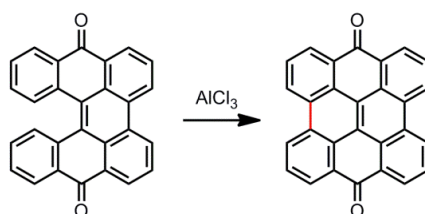
⁵ (a) Pschorr, R., "Neue Synthese Des Phenanthrens Und Seiner Derivate," *Berichte der Deutschen Chemischen Gesellschaft* **1896**, *29*, 496-501. (b) Meille, V.; Schulz, E.; Lemaire, M.; Faure, R.; Vrinat, M., "An Efficient Synthesis of Pure 4,6-Dimethyldibenzothiophene," *Tetrahedron* **1996**, *52*, 3953-3960.

⁶ (a) Ullmann, F.; Bielecki, J., "Ueber Synthesen in Der Biphenylreihe," *Berichte der Deutschen Chemischen Gesellschaft* **1901**, *34*, 2174-2185. (b) Fanta, P. E., "The Ullmann Synthesis of Biaryls," *Synthesis* **1974**, *1974*, 9-21. (c) Fanta, P. E., "The Ullmann Synthesis of Biaryls, 1945-1963," *Chemical Reviews* **1964**, *64*, 613-632.

⁷ (a) Matsumoto, H.; Inaba, S.; Rieke, R. D., "Activated Metallic Nickel as a Reagent for the Dehalogenative Coupling of Halobenzenes," *The Journal of Organic Chemistry* **1983**, *48*, 840-843. (b) Brown, E.; Robin, J.-P.; Dhal, R., "Syntheses Totales Et Etudes De Lignanes Biologiquement Actifs—I : Application De La Reaction D'ullmann a La Synthese De Biaryles Precurseurs De Lignanes Bisbenzocyclooctadienes," *Tetrahedron* **1982**, *38*, 2569-2579. (c) De Lera, A. R.; Suau, R.; Castedo, L., "Synthetic Approaches to Cularines. Ii. Ullmann Condensation," *Journal of Heterocyclic Chemistry* **1987**, *24*, 313-319.

aromatic compounds. The first reaction reported by Scholl was the synthesis of *meso*-naphthodianthrone from helianthron with aluminum chloride (Scheme 6.1).^{8,9} Balaban and Nenitzescu defined the Scholl reaction as *the elimination of two aryl-bound hydrogens accompanied by the formation of an aryl–aryl bond under the influence of Friedel–Crafts catalysts*.¹⁰ This Scholl-type process has been heavily used in the synthesis of large polyaromatic hydrocarbon systems.¹¹

Scheme 6.1 Scholl Reaction (Original Report by Scholl)



While most of the well-known cross-coupling reactions require pre-functionalized coupling components (*e.g.* aryl halides), the Scholl-type reactions avoid the necessity of the pre-functionalization of coupling components. Moreover, not many palladium catalyzed coupling reactions participate in a cascade reaction sequence; however, the Scholl-type

⁸ Scholl, R.; Mansfeld, J., "Meso-Benzdianthron (Helianthron), Meso-Naphthodianthron, Und Ein Neuer Weg Zum Flavanthron," *Berichte der Deutschen Chemischen Gesellschaft* **1910**, 43, 1734-1746.

⁹ For a representative review, see: Kovacic, P.; Jones, M. B., "Dehydro Coupling of Aromatic Nuclei by Catalyst-Oxidant Systems: Poly(*p*-Phenylene)," *Chemical Reviews* **1987**, 87, 357-379.

¹⁰ Balaban, A.; Nenitzescu, C. In *Friedel-Crafts and Related Reactions*; Olah, G. A., Ed.; Wiley: New York, 1964; Vol. 2, Part 2, pp. 979-1047.

¹¹ (a) Mueller, M.; Kübel, C.; Muellen, K., "Giant Polycyclic Aromatic Hydrocarbons," *Chemistry—A European Journal* **1998**, 4, 2099-2109. (b) Wu, J.; Pisula, W.; Mullen, K., "Graphenes as Potential Material for Electronics," *Chemical Reviews* **2007**, 107, 718-747.

reactions are known to be involved in such domino reactions. For example, the Müllen group has demonstrated that 126 carbon–carbon bonds can be formed in one step by the cascade Scholl oxidation.¹²

Even though this class of reaction has a very long history and has been developed by a number of research groups in various contexts, the name of “Scholl reaction” has not been widely used in the literature.¹⁰ In the following sections, this underappreciated area in organic chemistry — the Scholl and Scholl-type oxidation reactions — will be briefly introduced. The reactions are categorized according to the oxidants that are employed in the processes.

¹² Simpson, C. D.; Mattersteig, G.; Martin, K.; Gherghel, L.; Bauer, R. E.; Räder, H. J.; Müllen, K., "Nanosized Molecular Propellers by Cyclodehydrogenation of Polyphenylene Dendrimers," *Journal of the American Chemical Society* **2004**, *126*, 3139-3147.

6.2. Background

6.2.1. Aluminum- or Copper/Aluminum-Mediated Scholl Oxidation

After the original report by Scholl (Scheme 6.1), he recognized numerous ring systems can undergo this process to afford various polycyclic aromatic compounds.^{13,14} One of these examples is depicted in Scheme 6.2; benzanthrone (7*H*-Benz[*d,e*]anthracen-7-one) was prepared from 1-benzoylnaphthalene in the presence of aluminum chloride.¹⁵ This Scholl reaction with aluminum chloride leading to polycyclic aromatic systems has been further developed by several other investigators including Baddeley.¹⁶

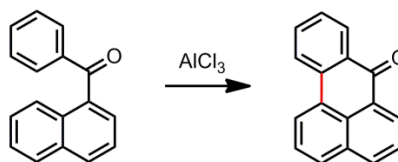
¹³ (a) Scholl, R.; Seer, C.; Weitzenböck, R., "Perylen, Ein Hoch Kondensierter Aromatischer Kohlenwasserstoff C₂₀H₁₂," *Berichte der Deutschen Chemischen Gesellschaft* **1910**, 43, 2202-2209. (b) Scholl, R.; Seer, C., "Abspaltung Aromatisch Gebundenen Wasserstoffes Unter Verknüpfung Aromatischer Kerne Durch Aluminiumchlorid, 6. Mitteilung: Versuche Mit Phenol-Äthern Und Mit Diphenyl-Methan," *Berichte der deutschen chemischen Gesellschaft (A and B Series)* **1922**, 55, 330-341. (c) Scholl, R.; Neumann, H., "Abspaltung Aromatisch Gebundenen Wasserstoffes Unter Verknüpfung Aromatischer Kerne Durch Aluminiumchlorid. 4. Mitteilung: Über Den Ringschluß Bei Zweifach Benzoylierten Naphthalinen," *Berichte der deutschen Chemischen Gesellschaft (A and B Series)* **1922**, 55, 118-126.

¹⁴ (a) Scholl, R.; Meyer, H. K.; Winkler, W., "Die Tautomerie Der Anthrachinon-1,5-Dicarbonsäure-Chloride Und Der Aufbau Von Ringgebilden Der Hetero-Coerdianthren-Reihe. Mit Einem Beitrag Zur Stereochemie Schwer Verseifbarer Ester," *Justus Liebigs Annalen der Chemie* **1932**, 494, 201-224. (b) Scholl, R.; Meyer, K., "Die Aromatischen Grundkohlenwasserstoffe Des Anth-Anthrone, Anth-Dianthrone (2,3,4,5-Dibenz-Coronenchinone-(1.6)), Pyranthrone Bzw. Amphi-Isopyranthrone, Violanthrone, Iso-Violanthrone, 1,2,3,7,8,9-Dinaphthocoronenchinone-(4.10) Und Das Dibenz-Rubicon," *Berichte der Deutschen Chemischen Gesellschaft (A and B Series)* **1934**, 67, 1229-1235.

¹⁵ Scholl, R.; Seer, C., "Abspaltung Aromatisch Gebundenen Wasserstoffes Und Verknüpfung Aromatischer Kerne Durch Aluminiumchlorid," *Justus Liebigs Annalen der Chemie* **1912**, 394, 111-177.

¹⁶ a) Baddeley, G.; Kenner, J., "64. The Meta-Alkylation of Aromatic Hydrocarbons by the Friedel-Crafts Reaction," *Journal of the Chemical Society (Resumed)* **1935**, 303-309. (b) Baddeley, G., "141. The Action of Aluminium Chloride on Some Phenol Homologues," *Journal of the Chemical Society (Resumed)* **1943**, 527-

Scheme 6.2 Aluminum-Mediated Intramolecular Oxidation



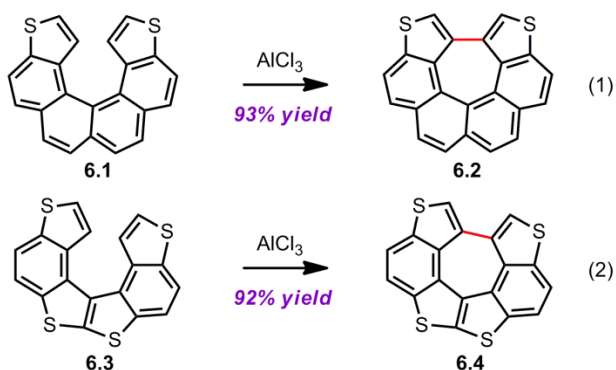
Wynberg and co-workers have demonstrated that the Scholl oxidation with AlCl_3 can cyclize heterohelicenes to furnish dehydrohelicenes (Scheme 6.3).^{17, 18} Heterohelicene **6.1** was mixed with AlCl_3 and NaCl at $140\text{ }^\circ\text{C}$ to afford dehydrohelicenes **6.2** in 93% yield (Scheme 6.3, eq 1). Another dehydrohelicene containing thiophene moieties (**6.4**) was obtained from compound **6.3** under the same Scholl oxidation condition in 92% yield (Scheme 6.3, eq 2).

531. (c) Baddeley, G., "205. Hydrogen Chloride-Aluminium Chloride as an Agent of Isomerisation," *Journal of the Chemical Society (Resumed)* **1950**, 994-997.

¹⁷ (a) Dopper, J.; Oudman, D.; Wynberg, H., "Dehydrogenation of Heterohelicenes by a Scholl Type Reaction. Dehydrohelicenes," *The Journal of Organic Chemistry* **1975**, *40*, 3398-3401. (b) Wynberg, H.; Groen, M. B.; Schadenberg, H., "Synthesis and Resolution of Some Heterohelicenes," *The Journal of Organic Chemistry* **1971**, *36*, 2797-2809.

¹⁸ For related studies on helicene chemistry, see: (a) Randić, M.; Gimarc, B. M.; Nikolić, S.; Trinajstić, N., "On the Aromatic Stabilities of Thiophene Analogues of Helicenes," *Journal of Molecular Structure: THEOCHEM* **1988**, *181*, 111-140. (b) Rajca, A.; Miyasaka, M.; Xiao, S.; Boratyński, P. J.; Pink, M.; Rajca, S., "Intramolecular Cyclization of Thiophene-Based[7]Helicenes to Quasi-[8]Circulenes," *The Journal of Organic Chemistry* **2009**, *74*, 9105-9111. (c) Shen, Y.; Chen, C., "Helicenes: Synthesis and Applications," *Chemical Reviews* **2012**, *112*, 1463-1535.

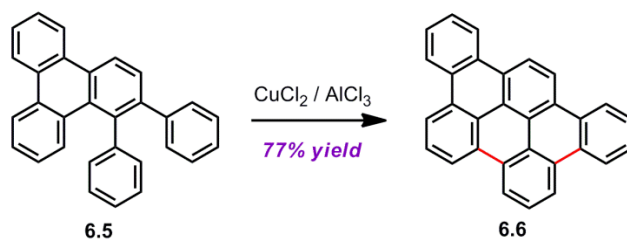
Scheme 6.3 Preparation of Dehydrohelicenes



The Scholl-type oxidation reactions with copper-aluminum oxidants have been extensively examined by Müllen and co-workers.^{12, 19} Under these milder Lewis acid oxidation conditions, large polycyclic aromatic hydrocarbons (PAHs) have been prepared. Diphenyltriphenylene **6.5** has been transformed into the desired product, tribenzo[*b,n,pqr*]perylene **6.6**, at room temperature in the presence of copper(II) chloride and aluminum chloride (77% yield, Scheme 6.4).^{19a}

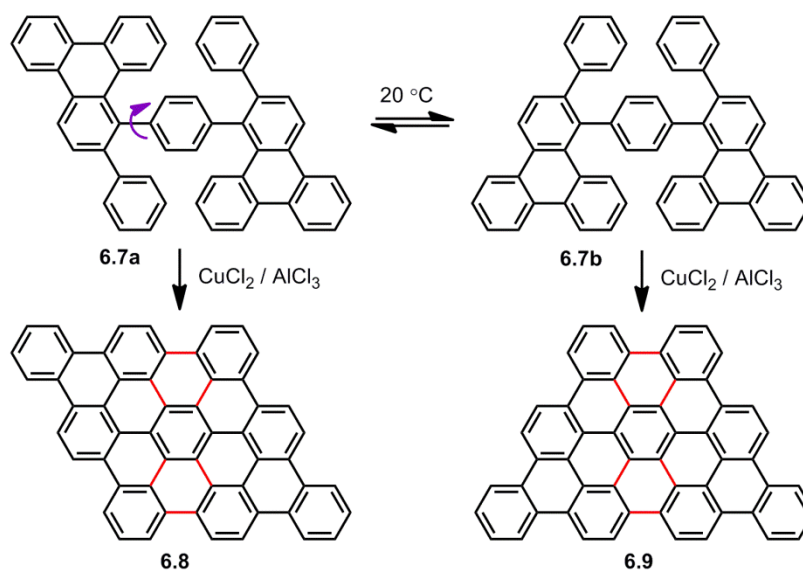
¹⁹ (a) Müller, M.; Mauermann-Düll, H.; Wagner, M.; Enkelmann, V.; Müllen, K., "A Cycloaddition-Cyclodehydrogenation Route from Stilbenoids to Extended Aromatic Hydrocarbons," *Angewandte Chemie International Edition* **1995**, *34*, 1583-1586. (b) Kubel, C.; Eckhardt, K.; Enkelmann, V.; Wegner, G.; Mullen, K., "Synthesis and Crystal Packing of Large Polycyclic Aromatic Hydrocarbons: Hexabenzob[*bc,ef,hi,kl,no,qr*]Coronene and Dibenzob[*fg,ij*]Phenanthro[9,10,1,2,3-*pqrst*]Pentaphene," *Journal of Materials Chemistry* **2000**, *10*, 879-886.

Scheme 6.4 Copper/Aluminum-Mediated Intramolecular Oxidation



However, when multiple conformations exist for a certain compound, this process tends to produce mixtures of products (Scheme 6.5).^{19a} For instance, there are two conformations (**6.7a** and **6.7b**) for the *para*-phenylene-bridged oligophenylene. Under the Scholl oxidation conditions, new six C–C bonds are formed from both of the conformers of the starting material, which leads to a mixture of compounds **6.8** and **6.9**. For the selective formation of one product over the other one, it is required to install substituents on specific positions that could render the molecule prefer a certain geometrical conformation.

Scheme 6.5 Various Planar Conformations of Oligophenylene



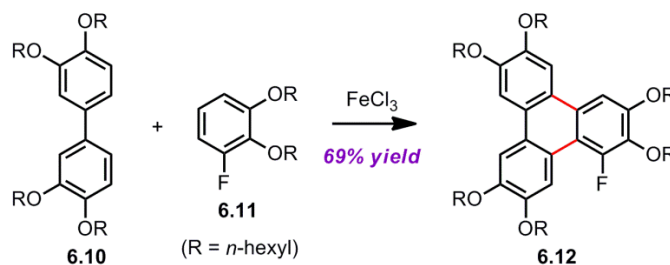
6.2.2. Iron-Mediated Scholl Oxidation

The Bushby group reported that iron(III)-mediated intermolecular Scholl oxidation can afford a triphenylene derivative (Scheme 6.6).²⁰ When tetrahexyloxybiphenyl **6.10** is mixed with 1-fluoro-2,3-dihexyloxybenzene (**6.11**) in the presence of iron(III) chloride (ferric chloride), the desired product (**6.12**) is afforded in 69% yield. With use of this method, the authors were able to install a fluorine atom at the alpha position, and the fluorinated product (**6.12**) was a valuable material for their studies on chiral discogens.²¹

²⁰ Boden, N.; Bushby, R. J.; Cammidge, A. N.; Duckworth, S.; Headdock, G., " α -Halogenation of Triphenylene-Based Discotic Liquid Crystals: Towards a Chiral Nucleus," *Journal of Materials Chemistry* **1997**, 7, 601-605.

²¹ (a) Malthete, J.; Jacques, J.; Tinh, N. H.; Destrade, C., "Macroscopic Evidence of Molecular Chirality in Columnar Mesophases," *Nature* **1982**, 298, 46-48. (b) van Nostrum, C. F.; Bosman, A. W.; Gelinck, G. H.; Schouten, P. G.; Warman, J. M.; Kentgens, A. P.; Devillers, M. A.; Meijerink, A.; Picken, S. J.;

Scheme 6.6 Iron-Mediated Intermolecular Oxidation

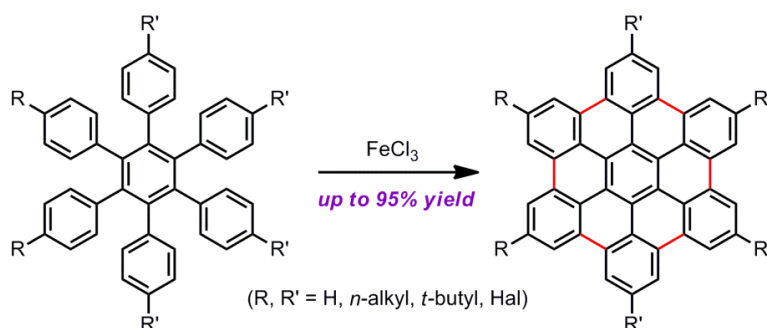


The Scholl reaction with iron(III) has also been applied to prepare hexabenzocoronene (HBC) derivatives (Scheme 6.7).²² Various alkyl-substituted hexa-*peri*-hexabenzocoronene derivatives were prepared from the corresponding hexaphenyl benzenes under the ferric-mediated Scholl conditions in good yields (up to 95% yield). The resulting alkylated PAHs can form liquid crystalline discotic mesophases, and the materials exhibit exceptionally broad temperature ranges. In addition, the halogenated hexabenzocoronenes (HBCs), which have also been synthesized by this method, can become convenient intermediates for further functionalizations.

Sohling, U., "Supramolecular Structure, Physical Properties, and Langmuir-Blodgett Film Formation of an Optically Active Liquid-Crystalline Phthalocyanine," *Chemistry—A European Journal* **1995**, *1*, 171-182.

²² Ito, S.; Wehmeier, M.; Brand, J. D.; Kübel, C.; Epsch, R.; Rabe, J. P.; Müllen, K., "Synthesis and Self-Assembly of Functionalized Hexa-*peri*-Hexabenzocoronenes," *Chemistry—A European Journal* **2000**, *6*, 4327-4342.

Scheme 6.7 Iron-Mediated Intramolecular Oxidation



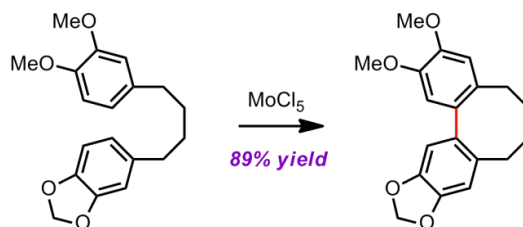
6.2.3. Molybdenum-Mediated Scholl Oxidation

Another possible oxidant for the Scholl-type reactions in the synthesis of PAHs is molybdenum(V). It is known that molybdenum pentachloride (MoCl_5) is an inexpensive yet effective reagent for the dehydrodimerization of alkoxy-substituted aromatic substrates, which leads to formation of novel structures in supramolecular chemistry.²³ The Waldvogel group has demonstrated the intramolecular Scholl reaction can be promoted by molybdenum(V) chloride to afford the desired eight-membered ring system in 89% yield (Scheme 6.8).²⁴

²³ (a) Waldvogel, S. R.; Fröhlich, R.; Schalley, C. A., "First Artificial Receptor for Caffeine—a New Concept for the Complexation of Alkylated Oxopurines," *Angewandte Chemie International Edition* **2000**, *39*, 2472-2475. (b) Waldvogel, S. R.; Wartini, A. R.; Rasmussen, P. H.; Rebek Jr, J., "A Triphenylene Scaffold with C_{3v} -Symmetry and Nanoscale Dimensions," *Tetrahedron Letters* **1999**, *40*, 3515-3518.

²⁴ Kramer, B.; Fröhlich, R.; Waldvogel, Siegfried R., "Oxidative Coupling Reactions Mediated by MoCl_5 Leading to 2,2'-Cyclolignans: The Specific Role of HCl," *European Journal of Organic Chemistry* **2003**, *2003*, 3549-3554.

Scheme 6.8 Molybdenum-Mediated Intramolecular Oxidation



The same group has also reported the intermolecular oxidative coupling reactions mediated with molybdenum pentachloride (MoCl₅). A representative example of such processes would be the conversion of 4-iodoveratrole to the corresponding dehydro-dimer (81% yield, Scheme 6.9).²⁵ It is particularly interesting that iodine is tolerated under these oxidative conditions; more commonly, deiodinated products are obtained under similar oxidative conditions.²⁶ Additionally, some other examples of intermolecular oxidation reactions with MoCl₅ have been reported by Kovacic^{27, 28} and Kumar.²⁹

²⁵ Waldvogel, S. R.; Aits, E.; Holst, C.; Frohlich, R., "Dehydromerization of Iodobenzenes to Iodinated Biaryls," *Chemical Communications* **2002**, 1278-1279.

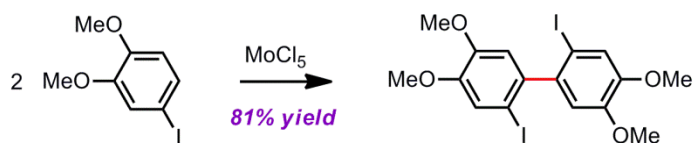
²⁶ Boden, N.; Bushby, R. J.; Lu, Z.; Headdock, G., "Synthesis of Dibromotetraalkoxybiphenyls Using Ferric Chloride," *Tetrahedron Letters* **2000**, *41*, 10117-10120.

²⁷ Kovacic, P.; Lange, R. M., "Polymerization of Benzene to *p*-Polyphenyl by Molybdenum Pentachloride," *The Journal of Organic Chemistry* **1963**, *28*, 968-972.

²⁸ For related studies, see: Kovacic, P.; Lange, R. M., "Reactions of Molybdenum Pentachloride and Vanadium Tetrachloride with Alkyl- and Halobenzenes," *The Journal of Organic Chemistry* **1965**, *30*, 4251-4254.

²⁹ Kumar, S.; Manickam, M., "Oxidative Trimerization of O-Dialkoxybenzenes Tohexaalkoxytriphenylenes: Molybdenum(V) Chloride as a Novel Reagent," *Chemical Communications* **1997**, 1615-1666.

Scheme 6.9 Molybdenum-Mediated Intermolecular Oxidation



6.2.4. Antimony-Mediated Scholl Oxidation

The Scholl-type oxidation reactions involving antimony(V) pentachloride (SbCl₅)^{30,31} have been demonstrated by several research groups. The Kochi group has been particularly interested in a masked form of SbCl₅ as trialkyloxonium hexachloroantimonate(V) salts.³² In the presence of this antimony(V) reagent, 1-methoxynaphthalene was readily oxidized to the corresponding dehydrogenated dimer³³ in quantitative yield (Scheme 6.10).³⁴ In this study,

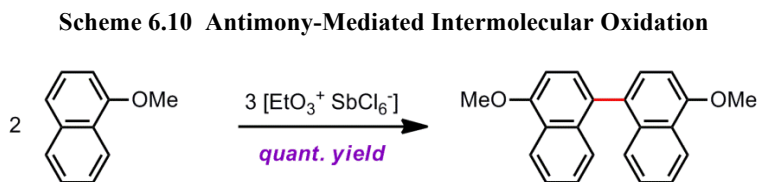
³⁰ (a) Bell, F. A.; Ledwith, A.; Sherrington, D. C., "Cation-Radicals: Tris-(*p*-Bromophenyl)Amminium Perchlorate and Hexachloroantimonate," *Journal of the Chemical Society C: Organic* **1969**, 2719-2720. (b) Cowell, G. W.; Ledwith, A.; White, A. C.; Woods, H. J., "Electron-Transfer Oxidation of Organic Compounds with Hexachloroantimonate [SbCl₆]⁻ Ion," *Journal of the Chemical Society B: Physical Organic* **1970**, 227-231. (c) Lopez, L.; Troisi, L., "Electron-Transfer Chain Isomerization of Epoxides Induced by One-Electron Oxidizing Agents," *Tetrahedron Letters* **1989**, 30, 3097-3100.

³¹ (a) Kovacic, P.; Sparks, A. K., "Reaction of Antimony Pentachloride with Monoalkylbenzenes1," *The Journal of Organic Chemistry* **1963**, 28, 972-974. (b) Kovacic, P.; Hsu, L. C., "Polymerization of Aromatic Nuclei. VIII. Molecular Weight Control in Benzene Polymerization," *Journal of Polymer Science Part A-1: Polymer Chemistry* **1966**, 4, 5-28.

³² (a) Meerwein, H.; Battenberg, E.; Gold, H., "Über Tertiäre Oxoniumsalze, Ii," *Journal für Praktische Chemie* **1939**, 154, 83-156. (b) Böttger, G.; Geisler, A.; Fröhlich, R.; Würthwein, E.-U., "Trifluoromethanesulfonic Anhydride Induced Cleavage of a Bis(Iminomethane) Compound: A New Access to a 1,3-Diaryl-2-Azaallenium Triflate and a N-((Trifluoromethyl)Sulfonyl)Methanimine. Synthesis, Structures, and Quantum Chemical Calculations," *The Journal of Organic Chemistry* **1997**, 62, 6407-6411.

³³ Radner, F., "Iodine Cyanide Promoted Iodination of Aromatic Compounds. A Simple Synthesis of 1-Iodopyrene," *Acta Chemica Scandinavica* **1989**, 43, 481-484.

the effectiveness of the Sb(V) reagent, $[\text{Et}_3\text{O}\cdot\text{SbCl}_6]$, was demonstrated by several other examples.



The Swager group has reported the cascade intra- and intermolecular oxidation reactions mediated by antimony(V) pentachloride (Scheme 6.11).^{35,36} When 1.5 equiv of SbCl_5 was added to a DCM solution of the bis(biaryl)acetylene, the cyclized and dimerized product was afforded in 43% yield. The authors speculated that the mechanism of this reaction involves one-electron oxidation of the acetylene forming radical cationic intermediates. Computational investigations with PM3-level calculations revealed that

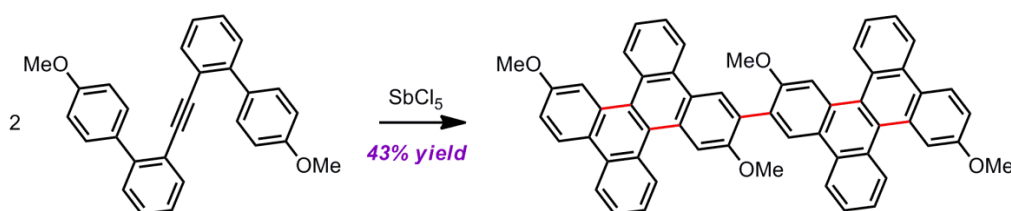
³⁴ Rathore, R.; Kumar, A.; Lindeman, S.; Kochi, J., "Preparation and Structures of Crystalline Aromatic Cation-Radical Salts. Triethyloxonium Hexachloroantimonate as a Novel (One-Electron) Oxidant," *The Journal of Organic Chemistry* **1998**, 63, 5847-5856.

³⁵ (a) Yamaguchi, S.; Swager, T. M., "Oxidative Cyclization of Bis(Biaryl)Acetylenes: Synthesis and Photophysics of Dibenzo[*g,p*]Chrysene-Based Fluorescent Polymers," *Journal of the American Chemical Society* **2001**, 123, 12087-12088. (b) Rose, A.; Tovar, J. D.; Yamaguchi, S.; Nesterov, E. E.; Zhu, Z.; Swager, T. M., "Energy Migration in Conjugated Polymers: The Role of Molecular Structure," *Philosophical Transactions of the Royal Society A: Mathematical, Physical and Engineering Sciences* **2007**, 365, 1589-1606.

³⁶ For related studies, see: (a) Yang, J.-S.; Swager, T. M., "Porous Shape Persistent Fluorescent Polymer Films: An Approach to TNT Sensory Materials," *Journal of the American Chemical Society* **1998**, 120, 5321-5322. (b) Yang, J.-S.; Swager, T. M., "Fluorescent Porous Polymer Films as TNT Chemosensors: Electronic and Structural Effects," *Journal of the American Chemical Society* **1998**, 120, 11864-11873. (c) Zhu, Z.; Swager, T. M., "Conjugated Polymer Liquid Crystal Solutions: Control of Conformation and Alignment," *Journal of the American Chemical Society* **2002**, 124, 9670-9671.

HOMO of the starting material is located at the central acetylene moiety, which suggests that the initial oxidation happens at the triple bond.

Scheme 6.11 Antimony-Mediated Cyclization and Dimerization



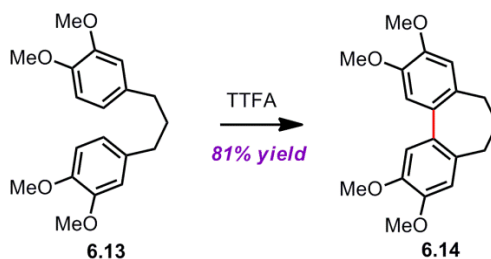
6.2.5. Thallium-Mediated Scholl Oxidation

It has been observed that a thallium(III) reagent can transform a variety of aromatic compounds into dehydrogenated coupling products in both intra- and intermolecular fashions. As shown in Scheme 6.12, the McKillop group has demonstrated that 1,3-bis(3,4-dimethoxyphenyl)propane (**6.13**) can be converted into the corresponding bridged biphenyl (**6.14**) in the presence of thallium(III) trifluoroacetate (TTFA) in trifluoroacetic acid (81% yield).³⁷ Several applications of this method in other polycyclic aromatic systems are presented in this and other accounts.^{38,39}

³⁷ McKillop, A.; Turrell, A. G.; Taylor, E. C., "Thallium in Organic Synthesis. 46. Oxidative Coupling of Aromatic Compounds Using Thallium(III) Trifluoroacetate. Synthesis of Biaryls," *The Journal of Organic Chemistry* **1977**, *42*, 764-765.

³⁸ (a) Taylor, E. C.; Jagdmann Jr, G. E.; McKillop, A., "Thallium in Organic Synthesis. 56. A Novel Oxidative Intramolecular Cyclization/Rearrangement of 5-Norbornene-Trans-2,3-Dicarboxylic Acid with Thallium (III) Trifluoroacetate (TTFA)," *The Journal of Organic Chemistry* **1980**, *45*, 3373-3375. (b) Taylor, E. C.; Conley, R. A.; Johnson, D. K.; McKillop, A.; Ford, M. E., "Thallium in Organic Synthesis. 57. Reaction of Chalcones and Chalcone Ketals with Thallium(III) Trinitrate," *The Journal of Organic Chemistry* **1980**, *45*, 3433-3436.

Scheme 6.12 Thallium-Mediated Intramolecular Oxidation

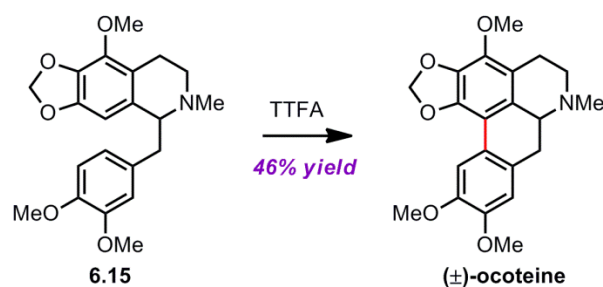


McKillop and co-workers have also employed this method to synthesize racemic ocoteine (Scheme 6.13).⁴⁰ The desired product, (±)-ocoteine, was obtained from a tetrahydroisoquinoline **6.15** under the TTFA oxidation conditions (46% yield). The TTFA method considerably improved this process, compared to the result of the same cyclization that was conducted under the Pschorr reaction conditions (11% yield).⁴¹

³⁹ (a) Taylor, E. C.; Andrade, J. G.; Rall, G. J.; Steliou, K.; Jagdmann Jr, G. E.; McKillop, A., "Thallium in Organic Synthesis. 60. 2,6-Diaryl-3,7-dioxabicyclo[3.3.0]octane-4,8-dione Lignans by Oxidative Dimerization of 4-Alkoxybenzoic Acids with Thallium(III) Trifluoroacetate or Cobalt(III) Trifluoride," *The Journal of Organic Chemistry* **1981**, *46*, 3078-3081. (b) Taylor, E. C.; Andrade, J. G.; Rall, G. J.; Turchi, I. J.; Steliou, K.; Jagdmann Jr, G. E.; McKillop, A., "Thallium in Organic Synthesis. 61. Intramolecular Capture of Radical Cations from Thallium(III) Trifluoroacetate Oxidation of Arylalkanoic Acids and Arylalkanoic Alcohols. New Routes to Oxygen Heterocycles," *Journal of the American Chemical Society* **1981**, *103*, 6856-6863.

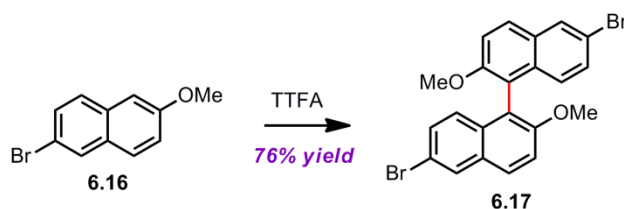
⁴⁰ (a) Taylor, E. C.; Andrade, J. G.; McKillop, A., "Thallium in Organic Synthesis. Synthesis of (+/-)-Ocoteine by Non-Phenolic Coupling with Thallium Tris(trifluoroacetate) (TTFA)," *Journal of the Chemical Society, Chemical Communications* **1977**, 538-539. (b) Taylor, E. C.; Andrade, J. G.; Rall, G. J. H.; McKillop, A., "Thallium in Organic Synthesis. 59. Alkaloid Synthesis Via Intramolecular Nonphenolic Oxidative Coupling. Preparation of (±)-Ocoteine, (±)-Acetoxyocoxylonine, (±)-3-Methoxy-N-Acetylnornantenine, (±)-Neolitsine, (±)-Kreysigine, (±)-O-Methylkreysigine, and (±)-Multifloramine," *Journal of the American Chemical Society* **1980**, *102*, 6513-6519.

⁴¹ Govindachari, T.; Pai, B.; Shanmugasundaram, G., "Synthesis of (±) Thalimine (Ocoteine)," *Tetrahedron* **1964**, *20*, 2895-2901.

Scheme 6.13 Synthesis of (\pm)-Ocoteine

An example of the intermolecular Scholl-type reactions mediated by thallium(III) is illustrated in Scheme 6.14, which is also examined by the McKillop group.⁴² Upon treatment with TTFA, 2-methoxy-6-bromonaphthalene (**6.16**) was dimerized to the dehydrogenated coupling product (**6.17**) in 76% yield. Notably, the bromine atoms are tolerated and unaffected under the TTFA oxidation conditions. The authors postulated that this process is initiated by one-electron transfer from the aromatic substrate to the Tl(III) reagent (i.e. one-electron oxidation), which would result in generation of the corresponding aryl radical cation.

Scheme 6.14 Thallium-Mediated Intermolecular Oxidation

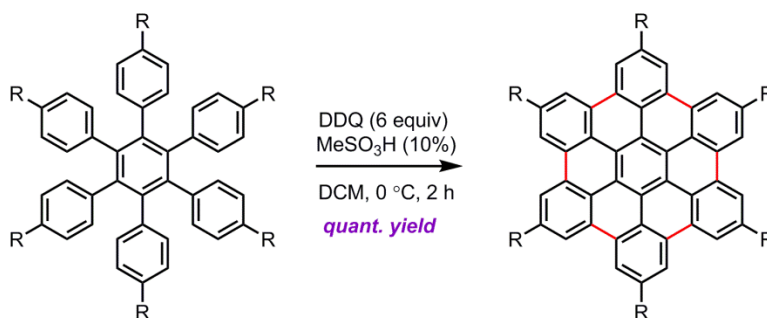


⁴² McKillop, A.; Turrell, A. G.; Young, D. W.; Taylor, E. C., "Thallium in Organic Synthesis. 58. Regiospecific Intermolecular Oxidative Dehydrodimerization of Aromatic Compounds to Biaryls Using Thallium(III) Trifluoroacetate," *Journal of the American Chemical Society* **1980**, *102*, 6504-6512.

6.2.6. DDQ/Acid-Mediated Scholl Oxidation

The oxidative C-C bond forming reactions involving non-metallic reagents have been demonstrated by the Rathore group (Scheme 6.15).⁴³ In this process, the DDQ/methanesulfonic acid system promotes new six intramolecular carbon-carbon bond formations leading to a hexa-*peri*-hexabenzocoronene (HBC) in an excellent yield. For the experiment, a 0.01 M solution of hexaarylbenzene in a mixture of dichloromethane and methanesulfonic acid was treated with DDQ for 2 h to obtain the desired product. After the reaction was completed, the identity of DDQ-H₂ was confirmed by NMR and melting point analysis. Moreover, they pointed out that DDQ can be regenerated from DDQ-H₂ by simple oxidation with concentrated nitric acid or N₂O₄.⁴⁴

Scheme 6.15 Rathore's Hexabenzocoronene Synthesis

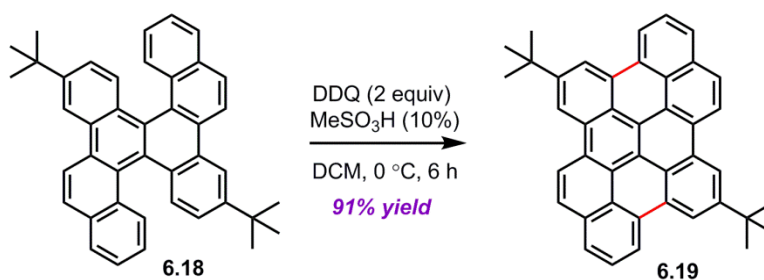


⁴³ Zhai, L.; Shukla, R.; Rathore, R., "Oxidative C-C Bond Formation (Scholl Reaction) with DDQ as an Efficient and Easily Recyclable Oxidant," *Organic Letters* **2009**, *11*, 3474-3477.

⁴⁴ (a) Scott, J. W.; Parrish, D. R.; Bizzarro, F. T., "A Rapid and Mild Process for the Oxidation of 2,3-Dichloro-5,6-Dicyanobenzoquinone (DDQ) from 2,3-Dichloro-5,6-Dicyanohydroquinone (DDHQ)," *Organic Preparations and Procedures International* **1977**, *9*, 91-94. (b) Newman, M. S.; Khanna, V. K., "Oxidation of 2,3-dichloro-5,6-Dicyanohydroquinone to 2,3-Dichloro-5,6-Dicyanobenzoquinone," *Organic Preparations and Procedures International* **1985**, *17*, 422-423.

Chen and Liu demonstrated that a dibenzochrysene derivative **6.18** can be transformed to a planar polycyclic aromatic hydrocarbon **6.19** (Scheme 6.16)⁴⁵ Compound **6.18** possesses two non-planar fjord regions, which are transformed to closed ring systems under the DDQ/methanesulfonic acid system in 91% yield. The DDQ/MSA system provided a new synthetic method toward large polycyclic aromatic hydrocarbons with low Clar sextets.

Scheme 6.16 Chen & Liu's Fjord Region Oxidation



The DDQ/acid oxidation system is known to oxidize various aromatic donors with oxidation potential as high as 1.7 V to the corresponding cation radicals;⁴³ this system has been applied for the preparation of several polycyclic hydrocarbons, including hexabenzocoronenes. In addition, the DDQ/H⁺ procedure eliminates the problems with chlorination of the aromatic compounds and the use of an excessive amount of oxidants, which are usually related with more commonly used Scholl oxidants such as FeCl₃, MoCl₅, or SbCl₅.

⁴⁵ Chen, T.-A.; Liu, R.-S., "Synthesis of Large Polycyclic Aromatic Hydrocarbons from Bis(Biaryl) Acetylenes: Large Planar PAHs with Low π -Sextets," *Organic Letters* **2011**, *13*, 4644-4647.

6.2.7. Summary

Representative, yet not comprehensive, examples of the Scholl-type reactions have been presented.^{46, 47} As observed in the literature precedents, it is unquestionable that a variety of metal-based oxidants can promote the Scholl-type oxidation reactions for preparation of diverse polycyclic aromatic compounds. According to the mechanistic perspectives that are presented in some of these studies, it is speculated that this type of coupling reactions might proceed by one-electron oxidation of the aromatic compounds, thereby involving radical cation intermediates.

⁴⁶ For lead(IV)-mediated oxidations, see: (a) Aylward, J., "Boron Trifluoride–Lead Tetra-Acetate: The Oxidation of Some Benzenoid Compounds," *Journal of the Chemical Society B: Physical Organic* **1967**, 1268-1270. (b) de Vos, D.; Boschman, F.; Wolters, J.; van der Gen, A., "Aromatic Lead(IV) Compounds Iv the Plumbylation of Halogen- and Alkyl-Substituted Aromatic Ethers," *Recueil des Travaux Chimiques des Pays-Bas* **1973**, 92, 467-470. (c) Norman, R.; Thomas, C.; Willson, J., "Reactions of Lead Tetra-Acetate. Part XXI. Acyloxylaton, Plumbylation, and Oxidative Dimerisation of Some Benzenoid Compounds in the Presence of Trifluoro- or Trichloro-Acetic Acid," *Journal of Chemical Society B* **1971**, 518-529.

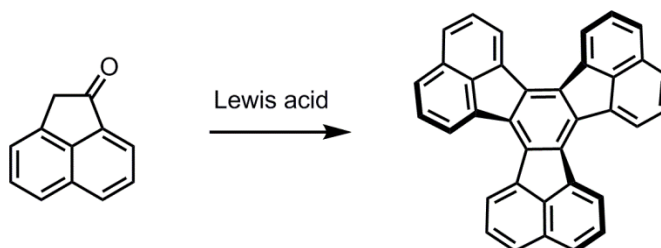
⁴⁷ For oxidations with hypervalent iodine(III) reagents, see: (a) Takada, T.; Arisawa, M.; Gyoten, M.; Hamada, R.; Tohma, H.; Kita, Y., "Oxidative Biaryl Coupling Reaction of Phenol Ether Derivatives Using a Hypervalent Iodine(III) Reagent," *The Journal of Organic Chemistry* **1998**, 63, 7698-7706. (b) Tohma, H.; Morioka, H.; Takizawa, S.; Arisawa, M.; Kita, Y., "Efficient Oxidative Biaryl Coupling Reaction of Phenol Ether Derivatives Using Hypervalent Iodine(III) Reagents," *Tetrahedron* **2001**, 57, 345-352. (c) Tohma, H.; Iwata, M.; Maegawa, T.; Kita, Y., "Novel and Efficient Oxidative Biaryl Coupling Reaction of Alkylarenes Using a Hypervalent Iodine(III) Reagent," *Tetrahedron Letters* **2002**, 43, 9241-9244.

6.3. Method Development

6.3.1. Project Goals

During the investigations on circumtrindene, we have conducted triple aldol condensation reactions to obtain the FVP precursors to circumtrindene (Scheme 6.17). These reactions usually require harsh reaction conditions and are conducted in high-boiling organic solvents. Moreover, the precursors to the aldol condensation usually require multiple synthetic steps to install the ketone functionality. So far, very few synthetic methods to access the carbon skeletons (*i.e.* triply-annulated central benzene rings) that are required for circumtrindene precursors have been reported. In this regard, we were interested in developing a new methodology to construct a central benzene ring by intermolecular trimerization of simple hydrocarbons.

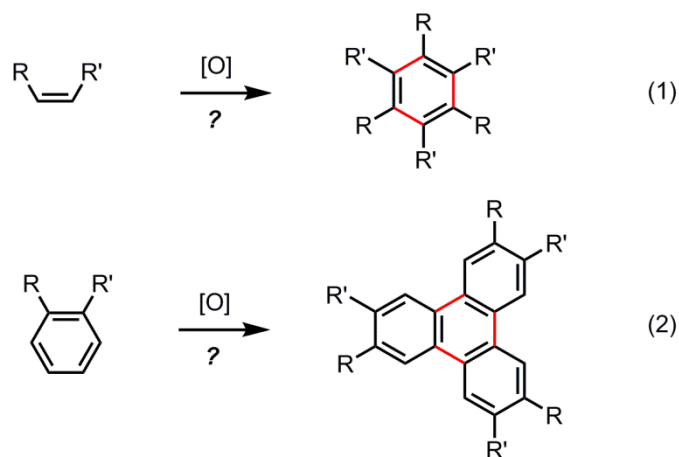
Scheme 6.17 Triple Aldol Condensation Reaction



We envisioned that alkenes could be trimerized to give the central benzene system under suitable oxidative reaction conditions (Scheme 6.18, eq 1). Under the commonly-used Scholl oxidation conditions, alkenes have never been oxidized or cyclized. Notably, this

method eliminates the necessity to functionalize the substrate (*e.g.* preparing ketones); simple hydrocarbons would be directly oxidized to form new C–C bonds. In addition to alkenes, aromatic rings could undergo similar cyclooxidative processes to give the triphenylene cores (Scheme 6.18, eq 2). Even though it is known that aromatic compounds undergo cyclotrimerization reactions under Scholl-type oxidation conditions, the cyclotrimerization reaction has never been carried out with non-metallic Scholl reagents.

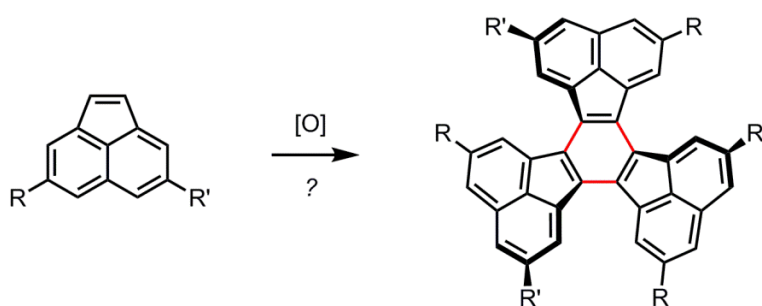
Scheme 6.18 Oxidative Coupling toward Triply-Annulated Benzene Rings



Considering our projects in polycyclic aromatic hydrocarbon (PAH) synthesis, we were particularly interested in cyclic alkenes, such as acenaphthylene. As shown in Scheme 6.19, acenaphthylene is a monomer of trimeric decacyclene systems. And, as described previously, decacyclene and its derivatives are common FVP precursors toward nonplanar

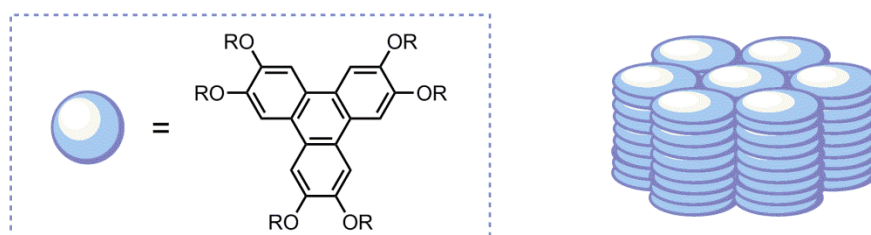
PAHs.⁴⁸ Moreover, the fact that decacycene is no longer commercially available at this point renders the development of this method more appealing.

Scheme 6.19 Trimerization of Acenaphthylene Derivatives



Additionally, the corresponding products from the reaction with aromatic compounds possess a triphenylene carbon framework (see eq 2 in Scheme 6.18). This triphenylene skeleton is often used as the core structure for discotic liquid crystals as depicted in Figure 6.1.

Figure 6.1 Triphenylene Core in Discotic Liquid Crystals

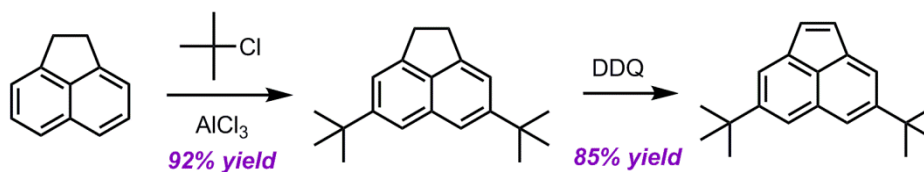


⁴⁸ For more details, see Section 5.3 of this thesis.

6.3.2. Reaction Optimization

Initial investigations involved oxidation reactions toward a *tert*-butylated decacyclene. We chose the *tert*-butylated system because the *tertiary* butyl groups will increase the solubility of the resulting polyaromatic product. The starting material for the trimerization, 4,7-di-*tert*-butylacenaphthylene, was prepared as described in Scheme 6.20.⁴⁹ A Friedel-Crafts alkylation was carried out with acenaphthene and *tert*-butyl chloride to give 4,7-di-*tert*-butylacenaphthylene in 92% yield. Then, DDQ oxidation of the *tert*-butylated acenaphthene under reflux conditions afforded the desired product, 4,7-di-*tert*-butylacenaphthylene, in 85% yield.

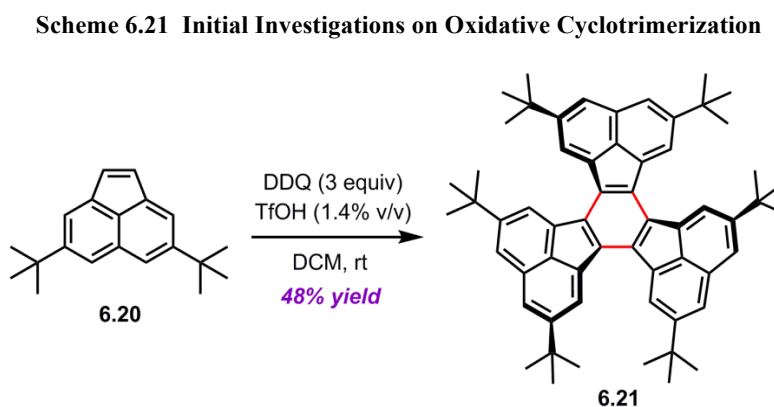
Scheme 6.20 Synthesis of *Tert*-butylated Acenaphthylene



The initial experiments were carried out with 1 equivalent of 4,7-di-*tert*-butylacenaphthylene (**6.20**), 3 equivalents of DDQ, and 3 equivalents (1.4% v/v) of trifluoromethanesulfonic acid in dichloromethane at ambient temperature. To our great pleasure, the desired product (2,5,8,11,14,17-hexa-*tert*-butyldecacyclene, **6.21**) was afforded from 4,7-di-*tert*-butylacenaphthylene (**6.20**) under the oxidation conditions in good yield

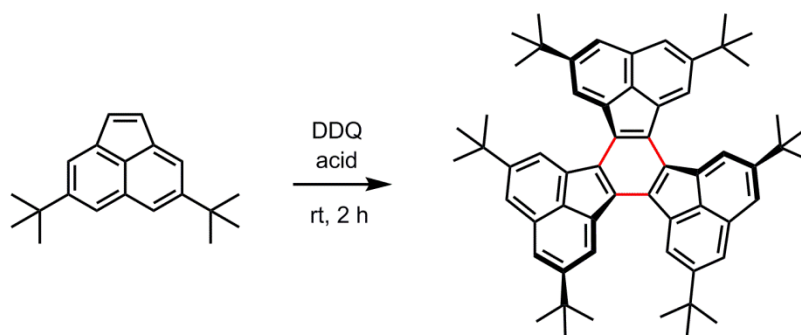
⁴⁹ Adapted from: Amick, A. W.; Griswold, K. S.; Scott, L. T., "Synthesis and Aldol Cyclotrimerization of 4,7-Di-*Tert*-Butylacenaphthenone," *Canadian Journal of Chemistry* **2006**, *84*, 1268-1272.

(Scheme 6.21). The product was soluble enough in common organic solvents to be purified and to be fully characterized.



To improve the efficiency of this process, a series of optimization experiment for reaction parameters (reagents, temperature, and concentration) was conducted. As far as the acid is concerned, the reaction proceeded most effectively with trifluoromethanesulfonic acid to afford the desired trimer in 48% yield (entry 1, Table 6.1). When methanesulfonic acid was used instead, the yield of the reaction was less than 10% (entry 2). We examined other Brønsted acids, such as trifluoroacetic acid and $\text{HBF}_4 \cdot \text{OEt}_2$, but the reactions with these acids did not afford any desired product (entries 3–4).

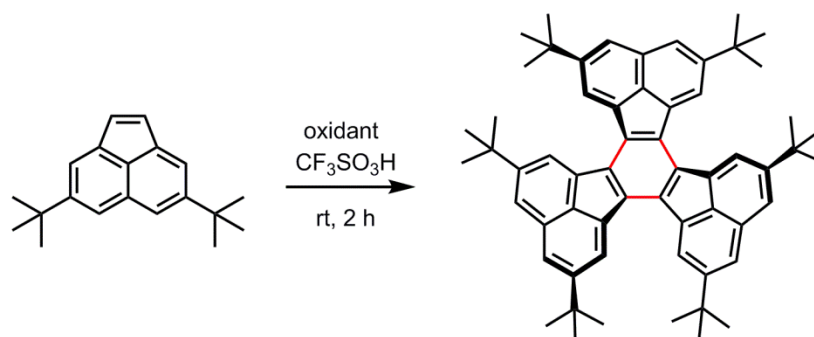
Table 6.1 Screen of Acids for Oxidative Cyclotrimerization



entry	acid	yield (%)
1	CF ₃ SO ₃ H	48%
2	CH ₃ SO ₃ H	<10%
3	TFA	no conversion
4	HBF ₄ -OEt ₂	no conversion

We also surveyed several oxidants for the oxidative cyclotrimerization process; the reaction outcome was heavily dependent on the oxidant used in this process. When DDQ (2,3-dichloro-5,6-dicyano-1,4-benzoquinone) was employed as an oxidant, the desired product was afforded as a major reaction product (entry 1, Table 6.2). However, other kinds of oxidants, such as 1,4-benzoquinone, tetrachloro-*p*-benzoquinone, or tetrachloro-*o*-benzoquinone, did not furnish the desired product (entries 2–4).

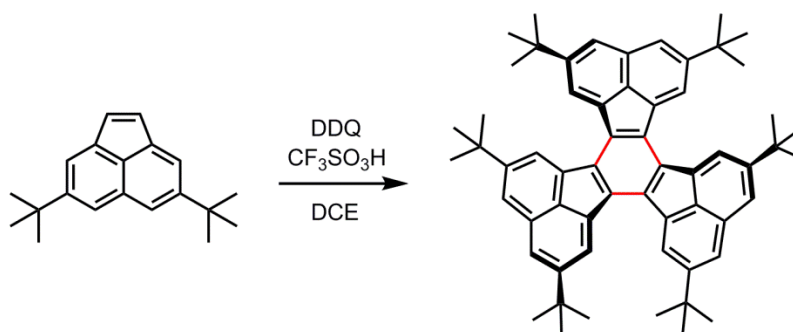
Table 6.2 Screen of Oxidants for Oxidative Cyclotrimerization



entry	oxidant	yield (%)
1	DDQ	48%
2	1,4-benzoquinone	no conversion
3	tetrachloro- <i>p</i> -benzoquinone	no conversion
4	tetrachloro- <i>o</i> -benzoquinone	no conversion

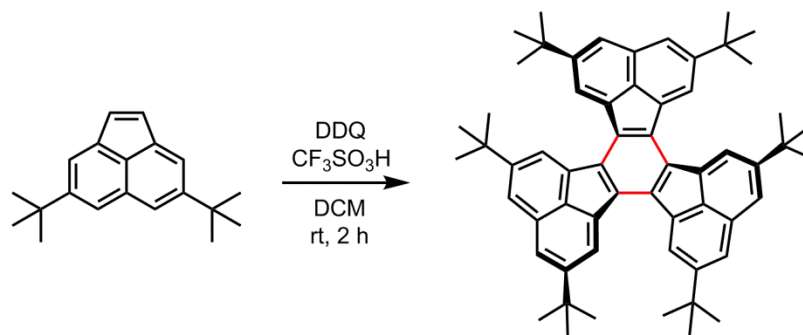
When optimizing the reaction conditions, we observed the efficiency of the reaction changed depending on the temperature of the reaction mixtures (Table 6.3). The trimerization reaction at 0°C afforded the desired product in 32% yield (entry 1). At ambient temperature, the yield of the oxidative coupling reaction was improved to 48% (entry 2). At a more elevated temperature, 80 °C, however, the desired product was formed in only less than 10% yield (entry 3). We speculated that side products from polymerization processes are generated faster at an elevated temperature.

Table 6.3 Effect of Temperature on Oxidative Cyclotrimerization



entry	temperature	yield (%)
1	0 °C	32%
2	room temperature	48%
3	80 °C	<10%

The effects of the concentration of the substrate as well as the reagents on the efficiency of the reaction were examined, as described in Table 6.4. When 3 equivalents of DDQ and 3 equivalents (1.4% v/v) of triflic acid were employed, the reaction having 0.02 M concentration (with regard to the substrate) afforded the desired product in 48% yield (entry 1, Table 6.4). When a more concentrated condition (0.10 M) was used, the efficiency of the reaction did not change significantly giving the trimer in 40% yield (entry 2). However, the yield of the reaction was more dependent on the concentration of the reagents (both the oxidant and the acid). When 1 equivalent of DDQ and 1 equivalent (0.46% v/v) of triflic acid were employed, the reaction with 0.02 M substrate concentration furnished the product in an improved yield, 68% yield (entry 3). The cyclized trimeric product was not afforded when 7 equivalents of DDQ and triflic acid were employed in the reaction mixture of 0.02 M concentration (entry 4).

Table 6.4 Influence of Concentrations on Oxidative Cyclotrimerization

entry	DCM	DDQ	CF ₃ SO ₃ H	yield (%)
1	0.02 M	3.0 equiv	3.0 equiv	48%
2	0.10 M	3.0 equiv	3.0 equiv	40%
3	0.02 M	1.0 equiv	1.0 equiv	68%
4	0.02 M	7.0 equiv	7.0 equiv	no conversion

After a series of experiments with various reaction parameters, as shown above, the optimal set of reaction conditions was found to include 1.0 equiv (0.46% v/v) of trifluoromethanesulfonic acid, 1.0 equiv of DDQ, 0.02 M of substrate concentration, and ambient temperature.

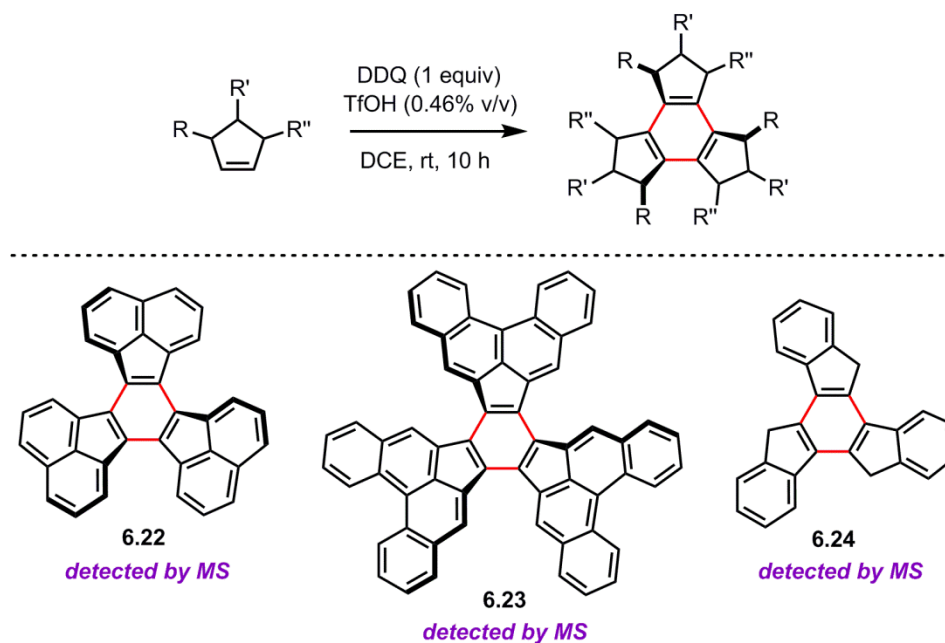
6.3.3. Substrate Scope

6.3.3.1. Survey of Unsaturated Hydrocarbons

After observing an efficient conversion of 4,7-di-*tert*-butylacenaphthene (**6.20**) to 2,5,8,11,14,17-hexa-*tert*-butyldecaacyclene (**6.21**) under the DDQ/TfOH condition, we wanted to expand the scope of alkene substrates. A number of cyclic alkenes were examined using the optimized conditions from Table 6.4 (1.0 equiv DDQ, 0.46% v/v TfOH, 0.02 M substrate

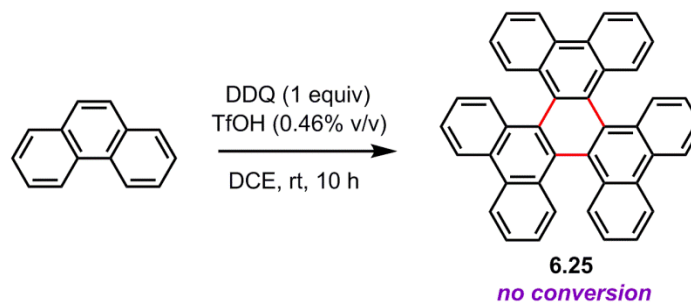
concentration); some of the examples are shown in Scheme 6.22. When acenaphthylene (without *tert*-butyl groups) was subjected to the oxidative reaction, the product (6.22) was detected by mass spectrometry (LRMS). We were particularly interested in this substrate (acenaphthylene) because the corresponding product (decacyclene, 6.22) is not commercially available anymore. Thus, we conducted extensive optimization experiments for several reaction parameters including solvents, oxidants, acids, concentrations, and temperature. Also, various purification procedures were employed to isolate the product (6.22) from reaction mixture. However, the insolubility of the product (decacyclene) in most organic solvents, together with the formation of other insoluble byproducts, rendered the isolation/purification of the product very challenging. In addition, we also examined the oxidative trimerization reactions with benz[*a*]acephenanthrylene and indene to see whether they would afford the corresponding products (6.23 or 6.24); the desired products were detected by mass spectrometry but were not isolated.

Scheme 6.22 Oxidative Cyclotrimerization of Cyclic Alkenes



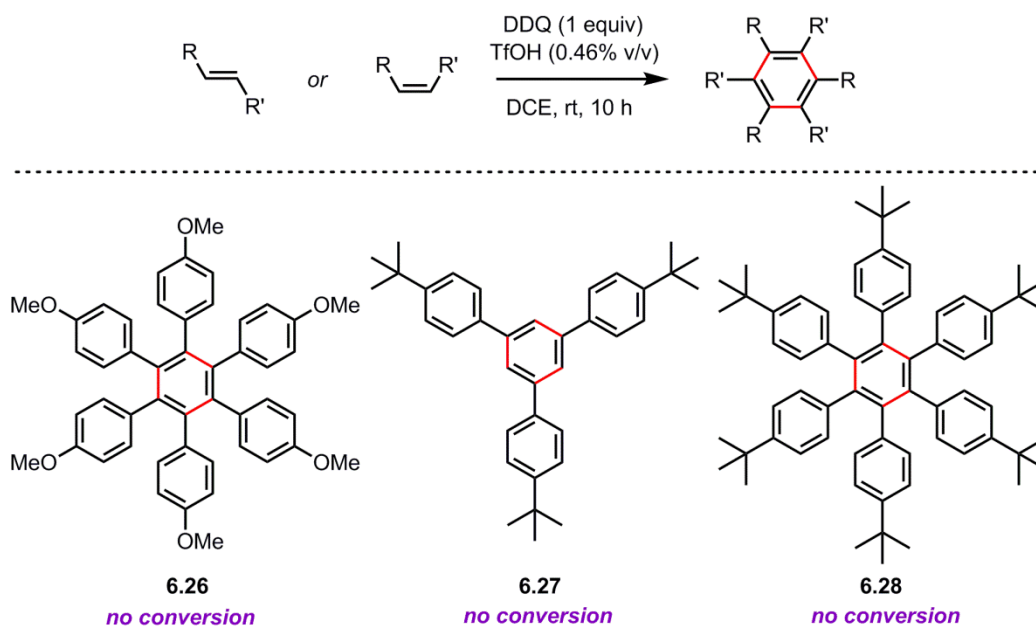
Another cyclic alkene, phenanthrene, was examined to see whether it would undergo a similar oxidative cyclization process under the DDQ/acid system. Unfortunately, we observed that phenanthrene was not converted to the corresponding product (**6.25**) in the presence of DDQ and trifluoromethanesulfonic acid (Scheme 6.23).

Scheme 6.23 Oxidative Cyclotrimerization of Phenanthrene



In addition to cyclic alkenes, several acyclic alkenes were also examined for the intermolecular oxidative coupling reactions. As shown in Scheme 6.24, none of the acyclic alkenes examined afforded the desired products (**6.26**, **6.27** or **6.28**) in the oxidation reaction with DDQ and triflic acid. We speculated that the problem with these alkenes was mainly related to the competition with rapid polymerization processes, which are facile under acidic conditions.

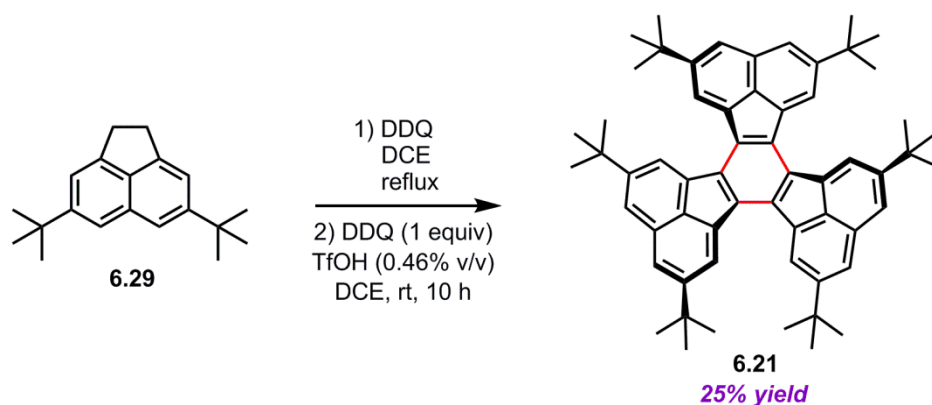
Scheme 6.24 Oxidative Cyclotrimerization of Acyclic Alkenes



As described in Scheme 6.20 above, the precursor (4,7-di-*tert*-butylacenaphthylene) to a trimer **6.21** (2,5,8,11,14,17-hexa-*tert*-butyldecacyclene) was prepared by DDQ oxidation of **6.29** (4,7-di-*tert*-butylacenaphthene). For a more convenient experimental procedure, we examined the possibility for a one-pot operation of sequential DDQ oxidation and

DDQ/TfOH cyclotrimerization. When 4,7-di-*tert*-butylacenaphthene (**6.29**) was subjected to the DDQ oxidation and then to the oxidative cyclotrimerization reaction without isolating the intermediate (4,7-di-*tert*-butylacenaphthylene), the desired trimeric product (**6.21**) was formed in a reduced yield (25% yield). We conducted several optimization experiments (temperature, time, and concentration) to improve the efficiency of this procedure, but the yield from the one-pot process was never better than that (68% yield) from the experiments with two separate operations.

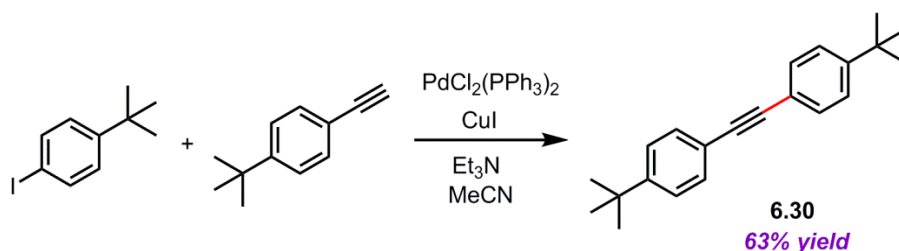
Scheme 6.25 One-pot Operation for DDQ Oxidation and Oxidative Cyclotrimerization



Another type of unsaturated hydrocarbons, an alkyne, was examined. For the ease of isolation of the coupling product, we decided to employ *tert*-butylated alkynes as a starting material. The di-*tert*-butylated alkyne (**6.30**) was synthesized by the Sonogashira coupling of

4-*tert*-butylphenylacetylene and 4-*tert*-butyliodobenzene in the presence of a palladium catalyst in 63% yield (Scheme 6.26).⁵⁰

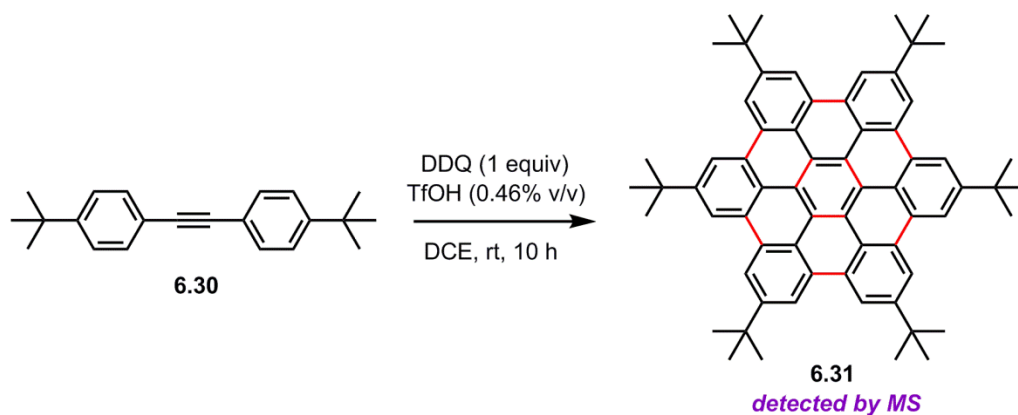
Scheme 6.26 Sonogashira Coupling of 4-*tert*-Butylphenylacetylene



The oxidative cyclotrimerization of bis(4-*tert*-butylphenyl)acetylene (**6.30**) was expected to give a trimer **6.31** by intermolecular coupling of alkynes followed by intramolecular oxidative coupling reactions (Scheme 6.27). When bis(4-*tert*-butylphenyl)acetylene (**6.30**) was subjected to the standard DDQ/TfOH oxidation reaction, the desired product (**6.31**) was detected by mass spectrometry but not isolated.

⁵⁰ Adapted from: Busacca, C. A.; Farber, E.; DeYoung, J.; Campbell, S.; Gonnella, N. C.; Grinberg, N.; Haddad, N.; Lee, H.; Ma, S.; Reeves, D.; Shen, S.; Senanayake, C. H., "Ambient Temperature Hydrophosphination of Internal, Unactivated Alkynes and Allenyl Phosphineoxides with Phosphine Borane Complexes," *Organic Letters* **2009**, *11*, 5594-5597.

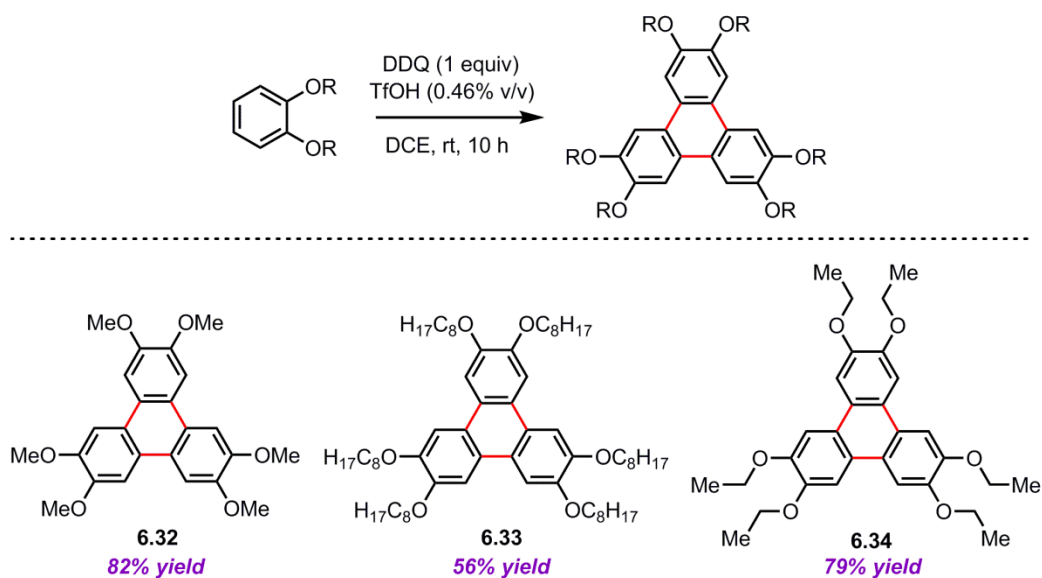
Scheme 6.27 Oxidative Cyclotrimerization of Alkyne



6.3.3.2. Survey of Aromatic Compounds

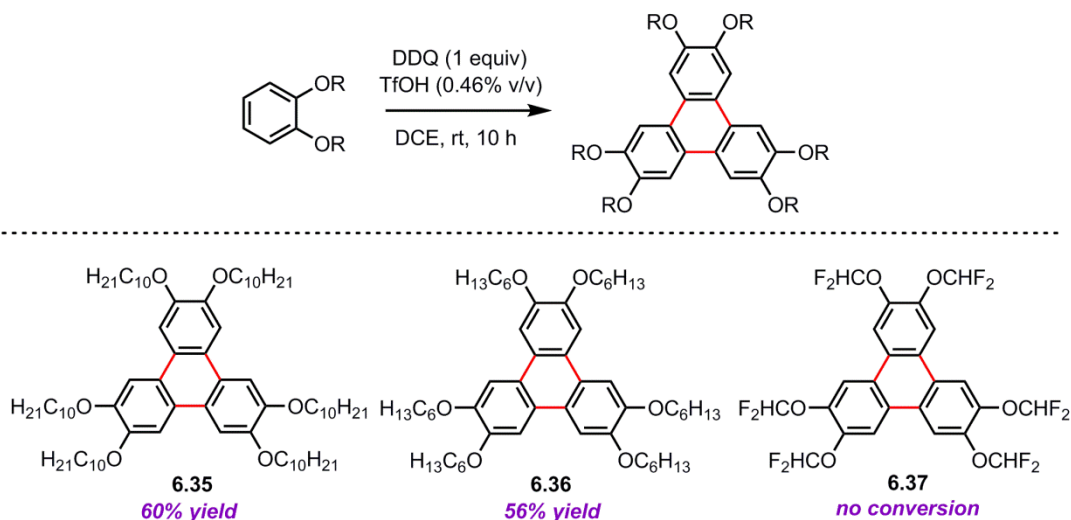
We examined a number of aromatic compounds for the oxidative cyclotrimerization reactions; coupling reactions of these compounds would lead to construction of the triphenylene carbon skeleton. When veratrole (1,2-dimethoxybenzene) was subjected to the DDQ/acid oxidation reaction, the corresponding trimer (**6.32**) was afforded in 82% yield (Scheme 6.28). A similar substrate with longer alkyl chains was also a competent substrate for this coupling reaction; the reaction with 1,2-bis(octyloxy)benzene furnished the desired product (**6.33**) in 56% yield. Additionally, when 1,2-diethoxybenzene was subjected to the DDQ/triflic acid oxidation reaction, the corresponding coupling product (**6.34**) was formed in good yield (79% yield).

Scheme 6.28 Oxidative Cyclotrimerization of Veratrole Derivatives



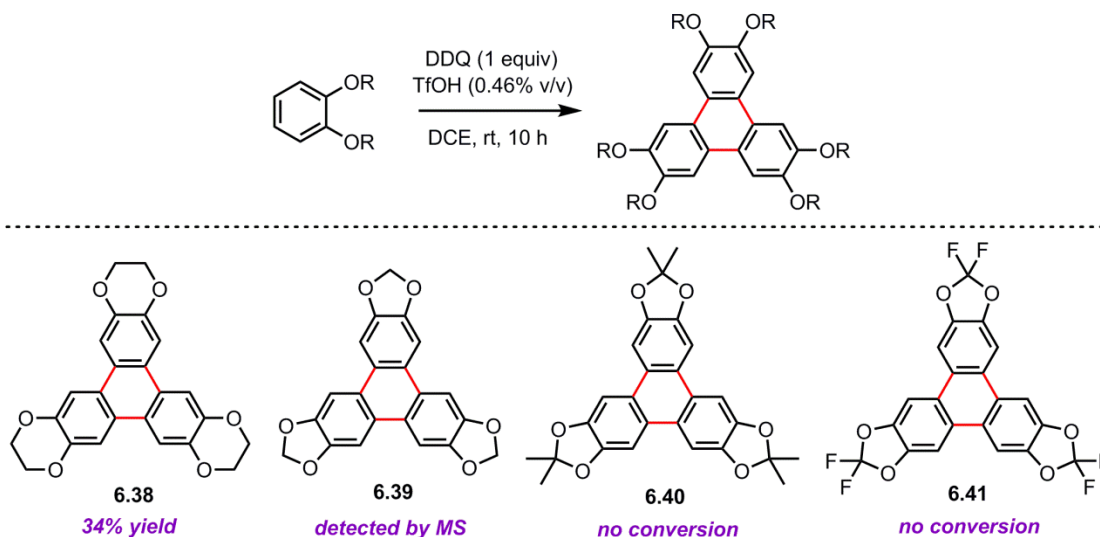
Some aromatic compounds containing alkoxy or fluoroalkoxy groups were examined (Scheme 6.29). When 1,2-bis(decyloxy)benzene was subjected to the DDQ/acid oxidation reaction, the desired trimer (**6.35**) was furnished in good yield (60% yield). The reaction with 1,2-bis(hexyloxy)benzene afforded the corresponding trimerized product (**6.36**) in 56% yield. However, installing fluorine atoms in the alkyl chain significantly decreased the reactivity of the aromatic compound; the reaction with 1,2-bis(difluoromethoxy)benzene did not produce the desired product (**6.37**) under the DDQ/triflic acid oxidation condition.

Scheme 6.29 Oxidative Cyclotrimerization of Dialkoxy/Difluoroalkoxy Benzenes



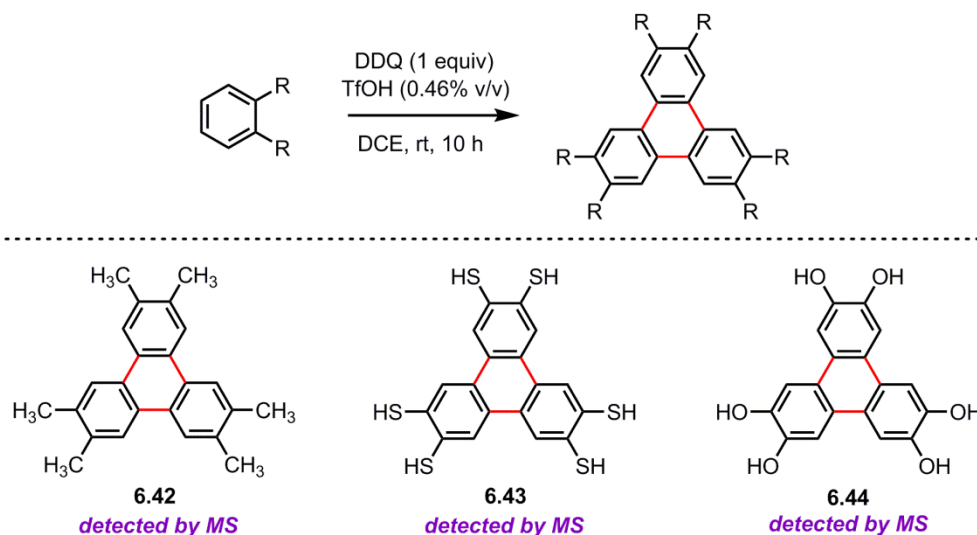
We investigated the reactivity of several benzodioxole derivatives toward the oxidative cyclotrimerization reactions with DDQ and trifluoromethanesulfonic acid (Scheme 6.30). When 1,4-benzodioxane was subjected to the DDQ/acid oxidation reaction, the corresponding trimer (**6.38**) was afforded in 34% yield. The reaction with 1,3-benzodioxole under the standard DDQ/TfOH condition furnished the desired product (**6.39**) as a major product. This cyclic trimer (**6.39**) was identified by mass spectrometry but was not isolated. When 2,2-dimethyl-1,3-benzodioxole was subjected to the oxidative coupling reaction, no desired product (**6.40**) was formed; we speculated that the substituted dioxole ring could be opened under the acidic conditions. We also employed 2,2-difluoro-1,3-benzodioxole as a starting material in the oxidative cyclotrimerization reaction; however, the corresponding trimer (**6.41**) was not afforded under the standard DDQ/acid condition.

Scheme 6.30 Oxidative Cyclotrimerization of Benzodioxoles



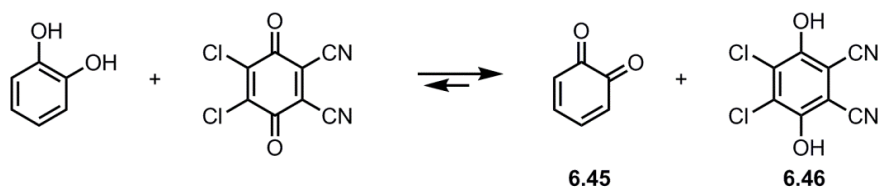
Other *ortho*-disubstituted benzenes were examined for the intermolecular oxidative coupling reactions. When *ortho*-xylene was reacted with DDQ and triflic acid, the desired product (**6.42**) was formed as a minor product (Scheme 6.31). This cyclic product was detected by mass spectrometry but not isolated. Also, we observed that the oxidative cyclotrimerization reaction of 1,2-benzenedithiol furnished the corresponding trimer (**6.43**). When catechol was subjected to the standard DDQ/triflic acid condition, the desired cyclic trimer (**6.44**) was formed but only as a minor product. We made substantial efforts to isolate these compounds from their reaction mixtures; however, the low efficiency and the insolubility of those compounds made the purification process problematic.

Scheme 6.31 Oxidative Cyclotrimerization of Disubstituted Benzenes



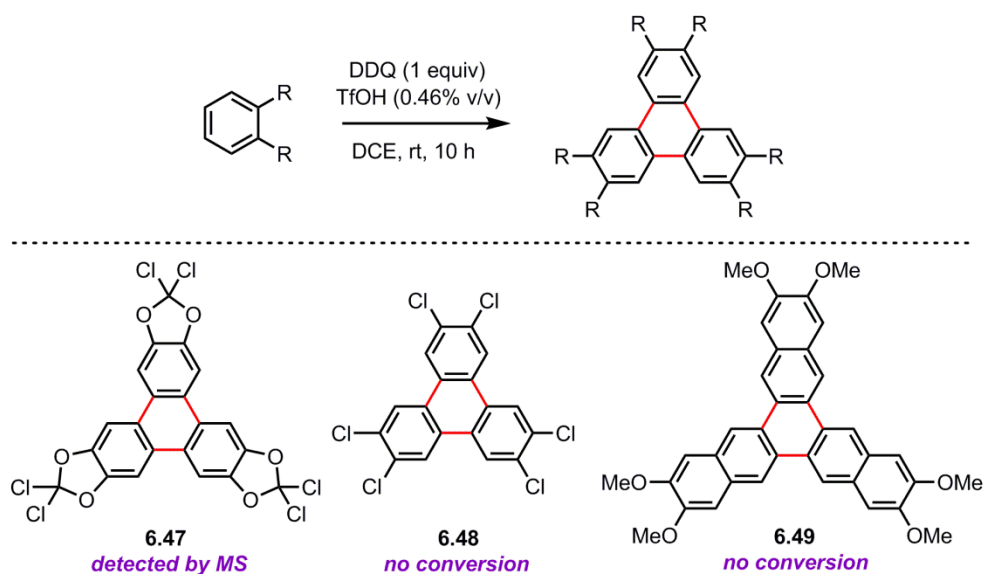
In retrospect, the low efficiency of the oxidative coupling of catechol leading to **6.44** should not have been an unexpected outcome. It would be reasonable to assume that catechol might undergo another oxidation process, which competes with the desired oxidative cyclization pathway. A plausible oxidation route for catechol is described in Scheme 6.32. When catechol reacts with DDQ, it can be oxidized to *ortho*-quinone (**6.45**) generating DDQ-H₂ (**6.46**).

Scheme 6.32 Possible Oxidation Route for Catechol



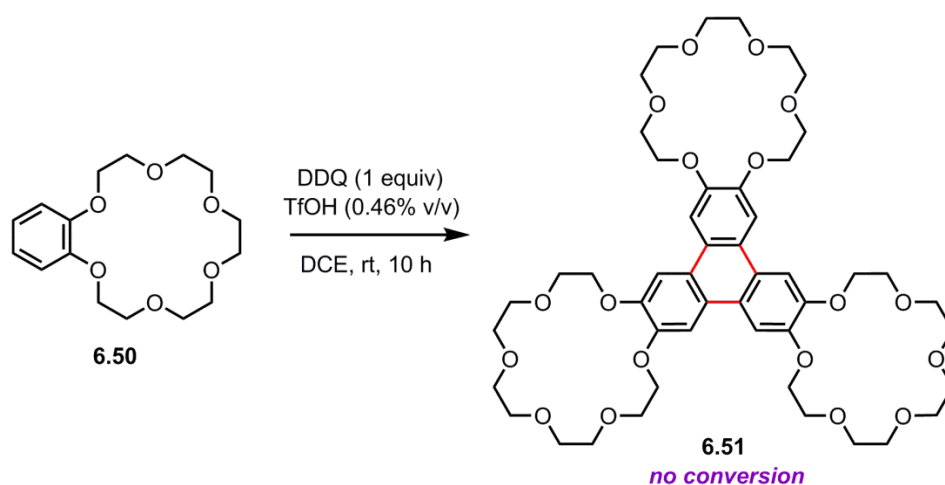
In addition, some chlorinated aromatic compounds were also examined for the intermolecular oxidative coupling reaction. When 2,2-dichloro-1,3-benzodioxole was subjected to the DDQ/H⁺ oxidation reaction, the desired cyclic trimer (6.47) was detected by mass spectrometry (Scheme 6.33). On the other hand, the oxidation reaction with *ortho*-dichlorobenzene (*o*-DCB) did not furnish the corresponding product (6.48). When 2,3-dimethoxynaphthalene was reacted with DDQ and trifluoromethanesulfonic acid, the desired cyclic trimer (6.49) was not observed. According to the analysis with mass spectrometry, the major product of the reaction with 2,3-dimethoxynaphthalene was a linear trimer, not a cyclized trimer.

Scheme 6.33 Oxidative Cyclotrimerization of Aromatic Compounds



One of our interests in this project was to investigate the reactivity of crown ethers⁵¹ toward the DDQ/acid-mediated oxidative cyclotrimerization reaction. Considering their capability of complexation with metal ions, coupling products containing crown ethers would have unique properties in their cyclic forms. When benzo-18-crown-6 (**6.50**) was subjected to the oxidative cyclization reaction, however, the desired trimer (**6.51**) was not formed (Scheme 6.34). We observed that the reaction mixture was turned into a heterogeneous solution containing insoluble polymeric materials.

Scheme 6.34 Oxidative Cyclotrimerization of Benzo-18-crown-6



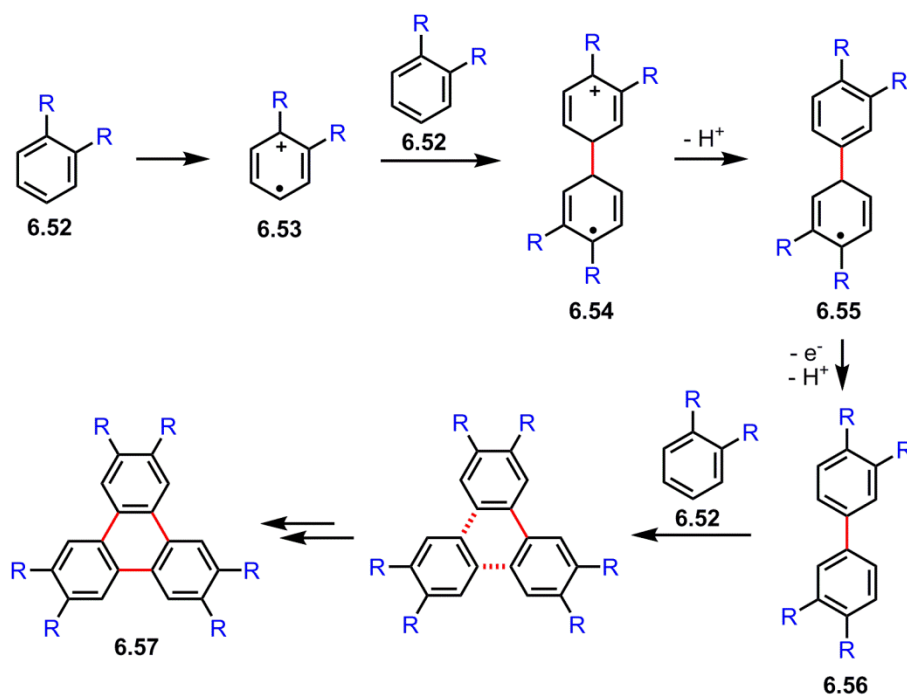
⁵¹ (a) Pedersen, C. J., "Cyclic Polyethers and Their Complexes with Metal Salts," *Journal of the American Chemical Society* **1967**, *89*, 7017-7036. (b) Pedersen, C. J., "Cyclic Polyethers and Their Complexes with Metal Salts," *Journal of the American Chemical Society* **1967**, *89*, 2495-2496. (c) Pedersen, C. J.; Frensdorff, H., "Macrocyclic Polyethers and Their Complexes," *Angewandte Chemie International Edition* **1972**, *11*, 16-25.

6.4. Mechanistic Considerations

There are two possible mechanistic pathways for this type of processes (*i.e.* Scholl-type oxidation): an electron transfer mechanism and a proton transfer mechanism. There has been a debate on which mechanistic pathway is operating for this type of process, and several theoretical investigations have been reported.⁵² During the investigation on the oxidative cyclotrimerization reactions, we also considered these two mechanisms for possible reaction pathways. If an electron transfer mechanism is operative (Scheme 6.35), a monomer **6.52** will lose one electron to generate a radical cation **6.53**. Then, a coupling between the radical cation (**6.53**) with another monomer (**6.52**) will lead to the formation of a dimeric radical cation **6.54**. A loss of a proton from **6.54** will give a dimeric radical **6.55**. Then, the radical intermediate (**6.55**) will lose an electron and a proton to afford a neutral dimer (**6.56**). With the intermediate dimer (**6.56**) and another monomer (**6.52**), a similar process involving radical cations will proceed to afford the observed trimer (**6.57**).

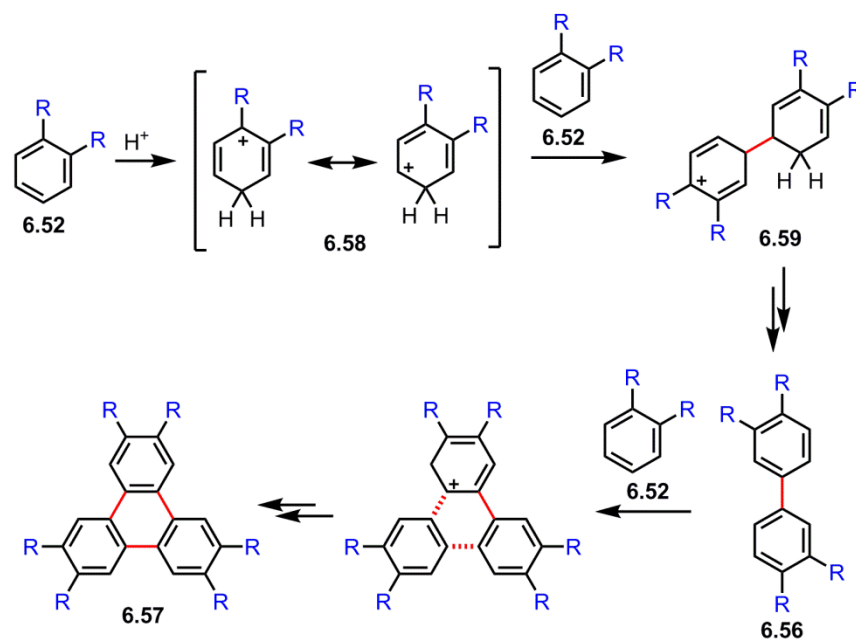
⁵² (a) Rempala, P.; Kroulík, J.; King, B. T., "A Slippery Slope: Mechanistic Analysis of the Intramolecular Scholl Reaction of Hexaphenylbenzene," *Journal of the American Chemical Society* **2004**, *126*, 15002-15003. (b) Rempala, P.; Kroulík, J.; King, B. T., "Investigation of the Mechanism of the Intramolecular Scholl Reaction of Contiguous Phenylbenzenes," *The Journal of Organic Chemistry* **2006**, *71*, 5067-5081. (c) Zhai, L.; Shukla, R.; Wadumethrige, S. H.; Rathore, R., "Probing the Arenium-Ion (Protontransfer) Versus the Cation-Radical (Electron Transfer) Mechanism of Scholl Reaction Using DDQ as Oxidant," *The Journal of Organic Chemistry* **2010**, *75*, 4748-4760.

Scheme 6.35 Electron Transfer Mechanism for Oxidative Cyclotrimerization



If a proton transfer mechanism is operative for this process, however, the reaction would involve different types of intermediates (Scheme 6.36). If a proton transfer mechanism is operative, a monomer **6.52** will be protonated to generate a cation **6.58**. Then, a coupling between the cation (**6.58**) and another monomer (**6.52**) will lead to the formation of a dimeric cation **6.59**. A neutral dimer (**6.56**) can be generated from the cation (**6.59**) via a loss of a proton and H_2 . Then, a coupling between the dimer (**6.56**) and another monomer (**6.52**) will afford the observed trimer (**6.57**) by a similar process involving intermediate cations.

Scheme 6.36 Proton Transfer Mechanism for Oxidative Cyclotrimerization



The two different mechanistic pathways (*i.e.* electron transfer vs proton transfer mechanisms) obviously involve different types of reaction intermediates (*i.e.* radical cations vs cations). However, as far as the products are concerned, the reactions following either of the reaction mechanistic pathways will furnish the same final products from the reactions with the symmetrical disubstituted benzenes surveyed in this chapter. Thus, we could not determine which reaction pathway is more plausible for the oxidative cyclotrimerization process at this point based on the experimental results. More details on the reaction mechanism for this process are discussed in the next chapter of this thesis.

6.5. Conclusions and Outlook

The intermolecular oxidative cyclotrimerization reactions of alkenes and aromatic compounds with DDQ and trifluoromethanesulfonic acid are presented. The Scholl-type oxidation reactions involving alkenes have never been demonstrated. Moreover, the DDQ/acid system has never been used for the intermolecular oxidative cyclization reactions. This convenient non-metallic reagent system (DDQ/TfOH) is advantageous over the metal-based Scholl-type oxidants because it eliminates the possibility of halogenation of aromatic compounds and the reduced oxidant (*i.e.* DDQ-H₂) can be reoxidized.

6.6. Experimental Section

6.6.1. General Information

All reactions were performed in oven- or flame-dried glassware fitted with rubber septa under a positive pressure of nitrogen, unless otherwise stated. Air- and moisture-sensitive liquids were transferred via syringe or stainless steel cannula. Organic solvents were concentrated by rotary evaporation at various temperatures, unless otherwise noted. All work-up and purification procedures were carried out with reagent grade solvents under typical bench-top conditions. Analytical thin-layer chromatography (TLC) was performed using glass plates, which are pre-coated with silica gel 60 F254 (0.25 mm thickness) impregnated with a fluorescent indicator (254 nm). TLC plates were visualized by exposure to UV (ultraviolet) light, and then were stained with phosphomolybdic acid (PMA) in ethanol, potassium permanganate (KMnO₄) in water, or cerium(IV) sulfate and ammonium molybdate in sulfuric acid (CAM). Liquid chromatography was performed using forced flow (flash chromatography)⁵³ on silica gel (porosity = 60 Å, particle size = 32-63 μm) purchased from Sorbent Technologies. Medium pressure gradient chromatography was performed on a Teledyne Isco CombiFlash automated flash chromatography system with a 200-780 nm UV-vis variable wavelength detector.

⁵³ Still, W. C.; Kahn, M.; Mitra, A., "Rapid Chromatographic Technique for Preparative Separations with Moderate Resolution," *The Journal of Organic Chemistry* **1978**, *43*, 2923-2925.

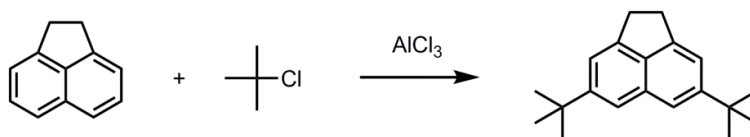
All commercially available chemicals and solvents were purchased from Sigma Aldrich, Acros, Strem, Alfa Aesar, Fisher, or TCI America and were used without purification with the following exceptions. Tetrahydrofuran (THF), methylene chloride (CH_2Cl_2), toluene, *N,N*-dimethylacetamide (DMAc), 1,2-dichlorobenzene (*o*-DCB), and carbon disulfide (CS_2) were dried and purified using a solvent purification system from Innovative Technology Inc.

Proton nuclear magnetic resonance (^1H NMR) spectra were recorded on either a Varian INOVA 500 (500 MHz) or a Varian VNMR 500 (500 MHz) at 23 °C unless specified otherwise. Proton chemical shifts are reported in ppm (parts per million, δ scale) downfield from tetramethylsilane and are referenced to residual protium in the NMR solvent as the internal standard (CHCl_3 : 7.26 ppm, C_6H_6 : 7.16 ppm). Data are reported as follows: chemical shift, integration, multiplicity (s = singlet, d = doublet, t = triplet, q = quartet, qn = quintet, br = broad, and m = multiplet), coupling constant (*J*) in hertz (Hz), and assignment. Carbon nuclear magnetic resonance (^{13}C NMR) spectra were recorded on either a Varian INOVA 500 (125 MHz) or a Varian VNMR 500 (125 MHz) with complete proton decoupling at 23 °C unless otherwise stated. Carbon chemical shifts are reported in ppm (parts per million, δ scale) downfield from tetramethylsilane and are referenced to the NMR solvent resonance as the internal standard (CDCl_3 : 77.16 ppm, C_6D_6 : 128.06 ppm).

Melting points were determined with a Thomas-Hoover Unimelt capillary melting point apparatus and were uncorrected. Infrared (IR) spectra were recorded on a Bruker FT-

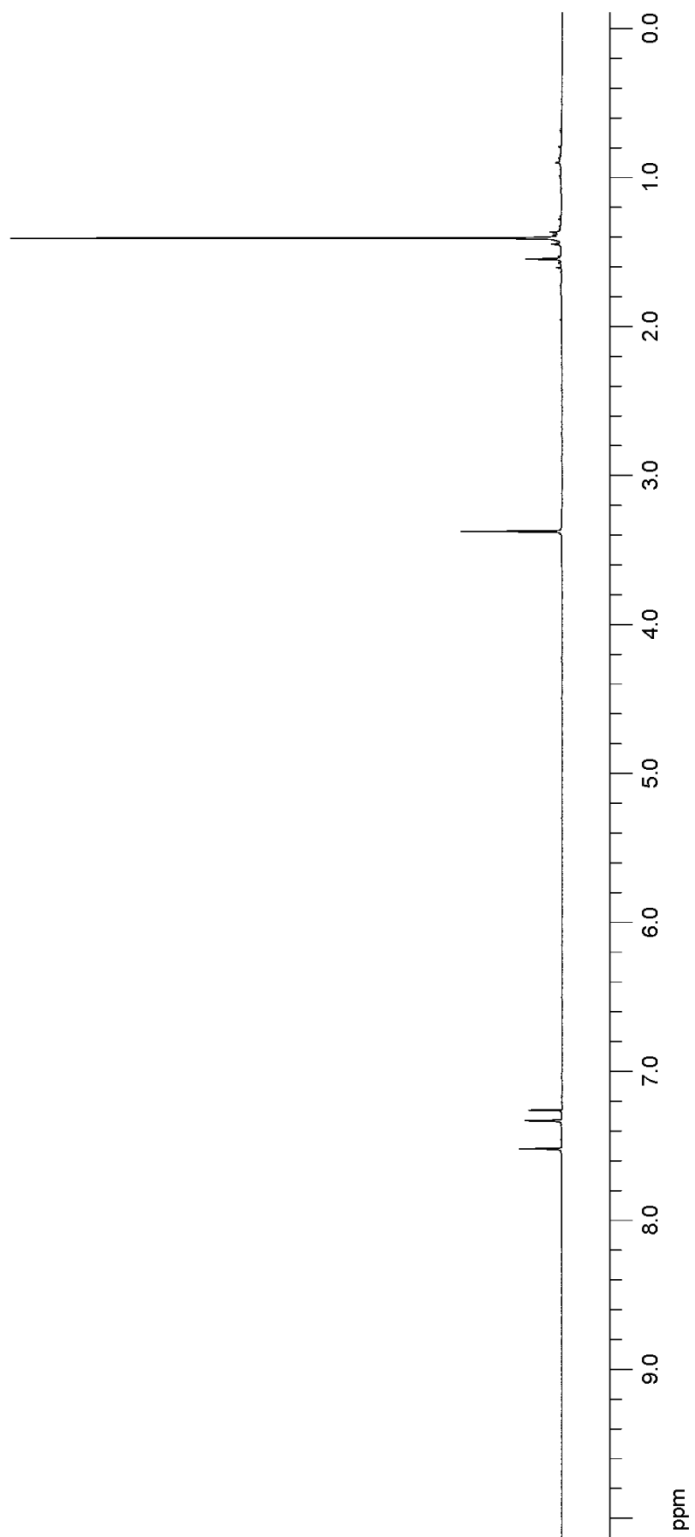
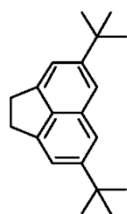
IR Alpha (ATR Mode) spectrophotometer, ν_{\max} cm^{-1} . Data are represented as follows: frequency of absorption (cm^{-1}) and intensity of absorption (s = strong, m = medium, w = weak, and br = broad). Low resolution mass spectrometric analyses were performed using a Thermo Electron Corporation Finnigan Trace GC Ultra gas chromatograph unit connected to a Thermo Electron Corporation Finnigan Trace DSQ mass spectrometer with direct inlet capabilities. High-resolution mass spectra (HRMS) were obtained by the Boston College Mass Spectrometry Center using various TOF instruments.

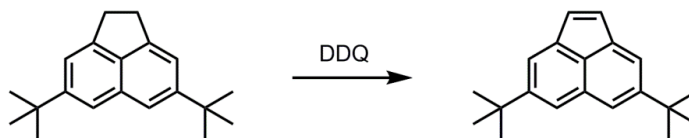
6.6.2. Experimental and Spectral Data

6.6.2.1. 4,7-Di-*tert*-butylacenaphthene

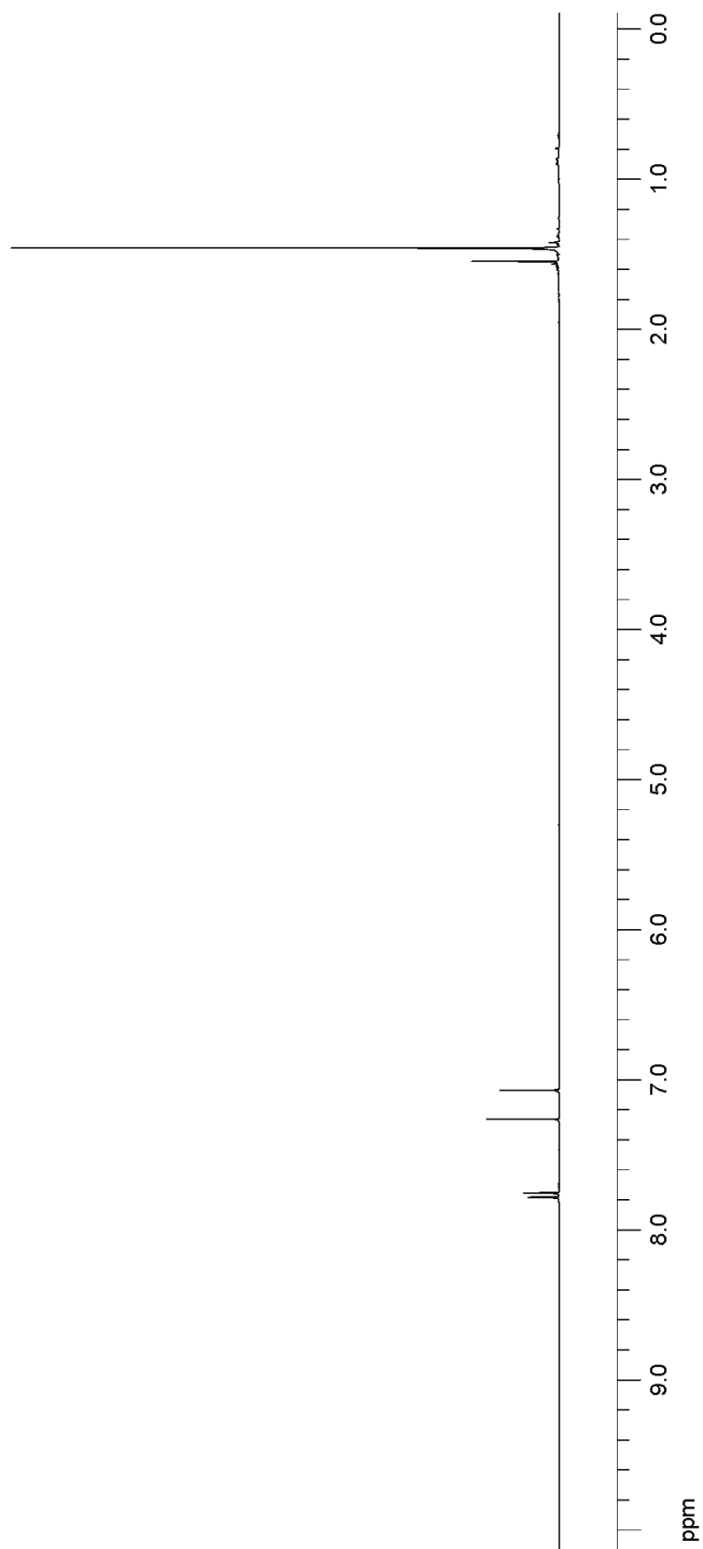
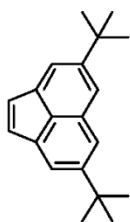
In an oven-dried round-bottomed flask, 5.0 g (32 mmol) of acenaphthene was dissolved in 800 mL (0.04 M) of dichloromethane and 36 mL (30 g, 320 mmol) of *t*-butyl chloride. Then, 5.1 g (38 mmol) of anhydrous aluminum chloride was added to this solution. The reaction mixture was stirred at ambient temperature for 2 h. After this time, the mixture was filtered through a short column of silica gel with DCM/hexane (1:1) as an eluent. The organic solvent was evaporated under reduced pressure to give the title compound. The crude material was purified by recrystallization with ethanol/DCM to afford 4,7-di-*tert*-butylacenaphthene in 92% yield (7.8 g, colorless solid). ¹H NMR (500 MHz, CDCl₃): δ 7.55 (s, 2H), 7.36 (s, 2H), 3.41 (s, 4H), 1.44 (s, 18H). HRMS (DART) calculated for C₂₀H₂₇ [M+H]⁺: 267.2113, found: 267.2113. The characterization data were in agreement with literature values.⁵⁴

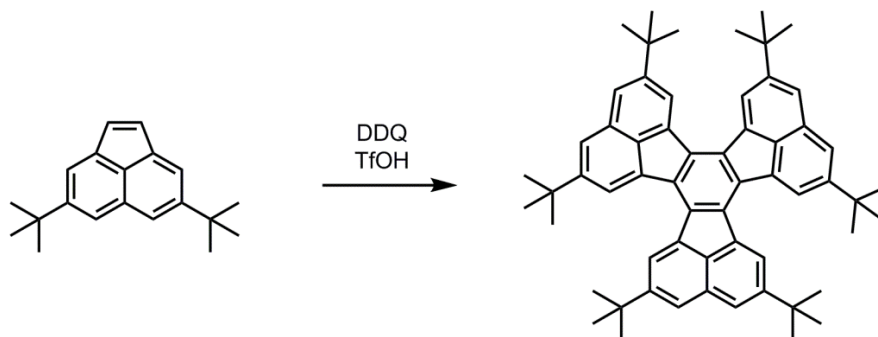
⁵⁴ Amick, A. W.; Griswold, K. S.; Scott, L. T., "Synthesis and Aldol Cyclotrimerization of 4,7-Di-*Tert*-Butylacenaphthenone," *Canadian Journal of Chemistry* **2006**, *84*, 1268-1272.

500 MHz, ^1H NMR, CDCl_3

6.6.2.2. 4,7-Di-*tert*-butylacenaphthylene

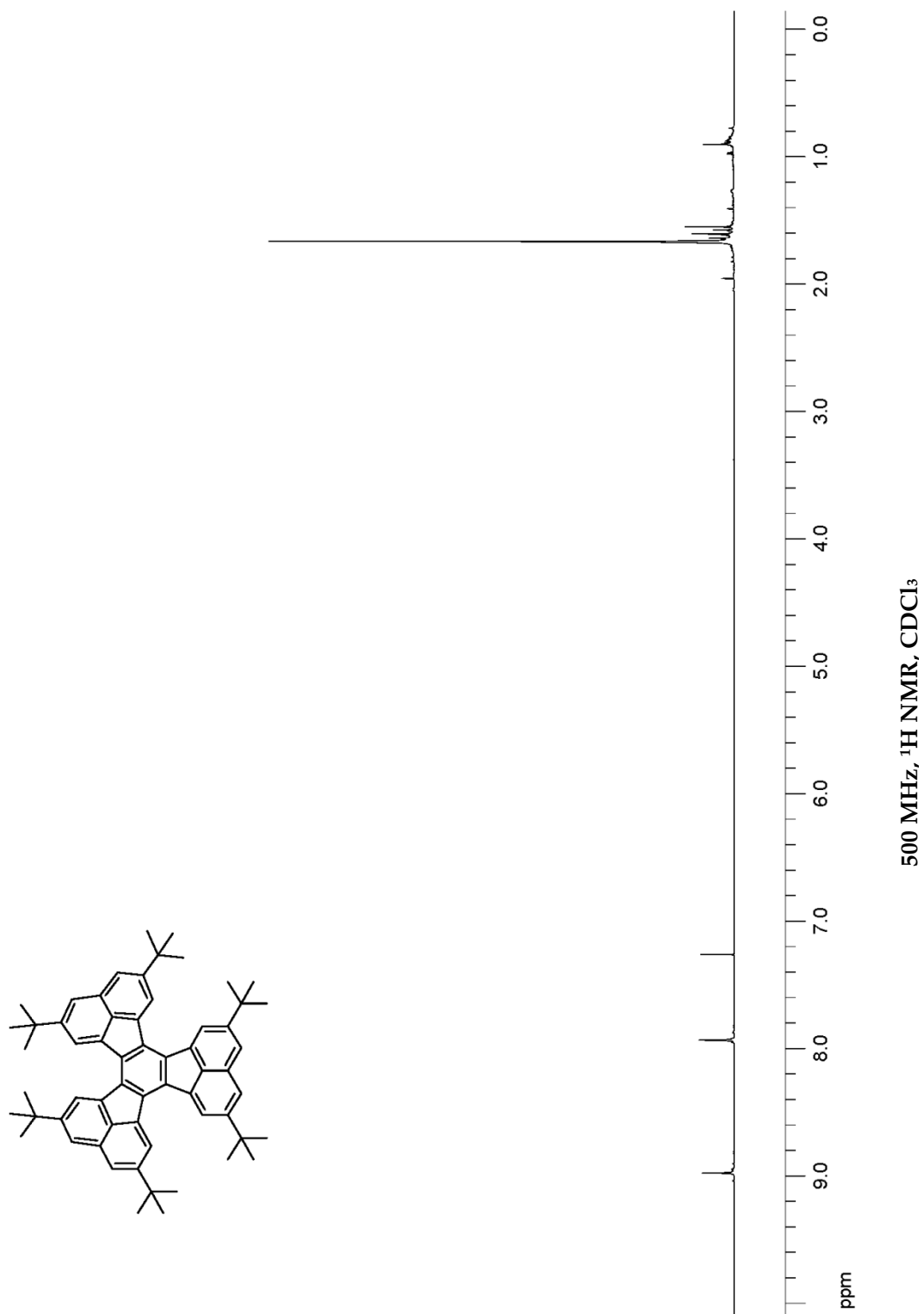
In an oven-dried round-bottomed flask, 7.8 g (32 mmol) of 4,7-di-*tert*-butylacenaphthene and 6.1 g (27 mmol) of DDQ were dissolved in 90 mL (0.2 M) of benzene. Then, the reaction mixture was heated to reflux for 2 h. After this time, the mixture was cooled to room temperature, and the organic solvent was removed *in vacuo*. The crude material was purified by silica gel column chromatography with hexanes/DCM as an eluent to afford 4,7-di-*tert*-butylacenaphthylene as a yellow solid in 85% yield (7.2 g). $^1\text{H NMR}$ (500 MHz, CDCl_3): δ 7.78 (s, 2H), 7.75 (s, 2H), 7.06 (s, 2H), 1.45 (s, 18H). HRMS (DART) calculated for $\text{C}_{20}\text{H}_{25}$ $[\text{M}+\text{H}]^+$: 265.1950, found: 265.1956. The characterization data were in agreement with literature values.⁵⁴

500 MHz, $^1\text{H NMR}$, CDCl_3

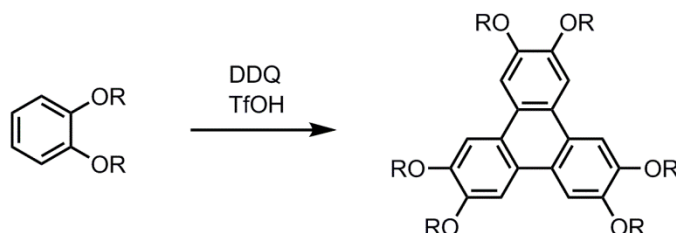
6.6.2.3. 2,5,8,11,14,17-Hexa-*tert*-butyldecacyclene

An oven-dried round-bottomed flask, equipped with a magnetic stir-bar, was charged with 50 mg (0.19 mmol) of 4,7-di-*tert*-butylacenaphthylene, 43 mg (0.19 mmol) of DDQ, 16.7 μ L (0.46% v/v, 0.19 mmol) of trifluoromethanesulfonic acid, and 9.5 mL (0.02 M) of dichloromethane. The reaction mixture was then allowed to stir at ambient temperature for 2 h. After this time, methanol (0.02M) was added, and the solution was then allowed to stir at ambient temperature for an additional hour. Then, the organic solvent was removed under reduced pressure. The crude material was purified by column chromatography on silica gel with hexanes/DCM to give 2,5,8,11,14,17-hexa-*tert*-butyldecacyclene as a red solid in 67% yield (100 mg). ^1H NMR (500 MHz, CDCl_3): δ 8.97 (s, 6H), 7.93 (s, 6H), 1.66 (s, 18H). HRMS (DART) calculated for $\text{C}_{60}\text{H}_{67}$ $[\text{M}+\text{H}]^+$: 787.5213, found: 787.5243. The characterization data were in agreement with literature values.^{54, 55}

⁵⁵ Kubo, T.; Yamamoto, K.; Nakasuji, K.; Takui, T.; Murata, I., "4,7,11,14,18,21-Hexa-*t*-Butyltribenzodecacyclenyl Radical: A Six-Stage Amphoteric Redox System," *Bulletin of the Chemical Society of Japan* **2001**, 74, 1999-2009.

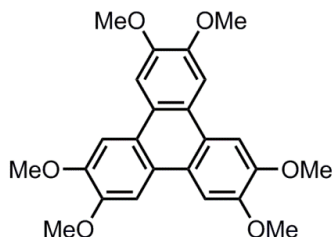


6.6.2.4. Representative Procedure for Oxidative Coupling



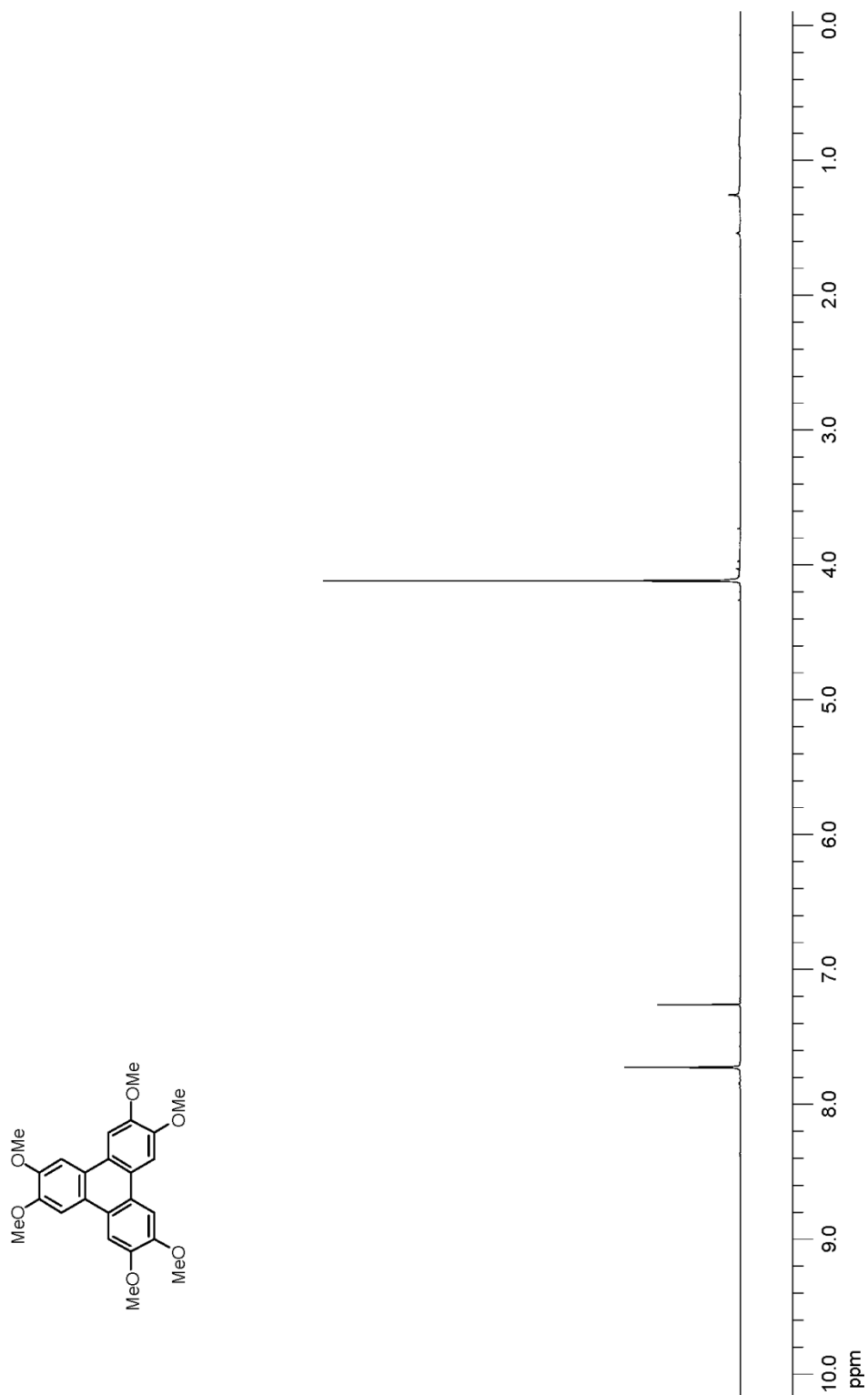
An oven-dried 20 mL scintillation vial, equipped with a magnetic stir-bar, was charged with the starting material (1.0 equiv), DDQ (1.0 equiv), trifluoromethanesulfonic acid (1.4% v/v, 3.0 equiv), and 1,2-dichloroethane (0.05 M). The reaction mixture was then allowed to stir at ambient temperature for 10 h. After this time, methanol (0.05M) was added, and the solution was then allowed to stir at ambient temperature for an additional hour. Upon addition of the methanol, some solids were precipitated out of the solution. Then, the solvent was removed from the heterogeneous mixture under reduced pressure. The crude material was purified by either recrystallization (methanol/DCM) or silica-gel column chromatography (hexanes/DCM) to give the title compounds.

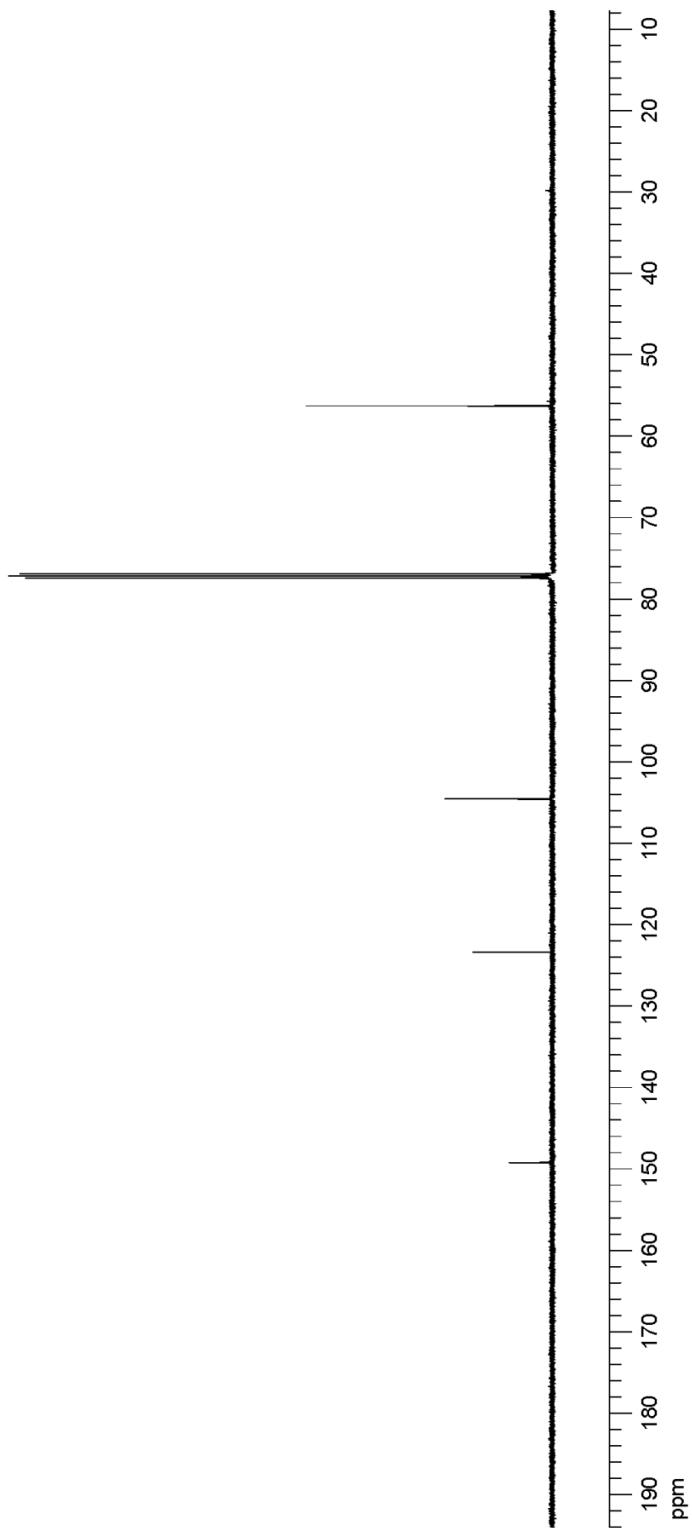
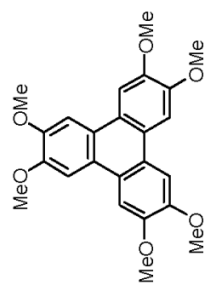
6.6.2.5. 2,3,6,7,10,11-Hexamethoxytriphenylene



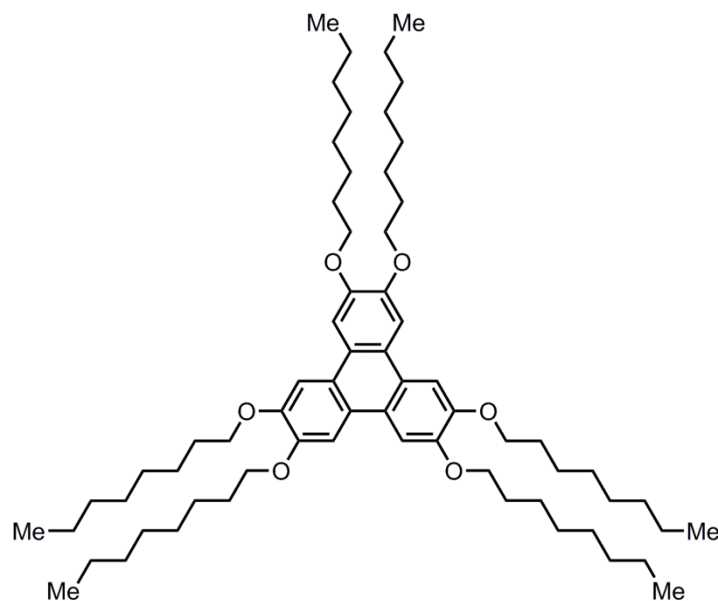
The general procedure described in Section 6.6.2.4 was followed on 0.10 mmol scale (14 mg) to obtain 2,3,6,7,10,11-hexamethoxytriphenylene as a white solid in 82% yield (33 mg). ^1H NMR (500 MHz, CDCl_3): δ 7.73 (s, 6H), 4.12 (s, 18H). ^{13}C NMR (125 MHz, CDCl_3): δ 149.2, 123.4, 104.5, 56.3. HRMS (DART) calculated for $\text{C}_{24}\text{H}_{25}\text{O}_6$ $[\text{M}+\text{H}]^+$: 409.1663, found: 409.1651. The characterization data were in agreement with literature values.⁵⁶

⁵⁶ (a) Percec, V.; Imam, M. R.; Peterca, M.; Wilson, D. A.; Graf, R.; Spiess, H. W.; Balagurusamy, V. S. K.; Heiney, P. A., "Self-Assembly of Dendronized Triphenylenes into Helical Pyramidal Columns and Chiral Spheres," *Journal of the American Chemical Society* **2009**, *131*, 7662-7677. (b) Bhalla, V.; Singh, H.; Kumar, M., "Facile Cyclization of Terphenyl to Triphenylene: A New Chemodosimeter for Fluoride Ions," *Organic Letters* **2009**, *12*, 628-631.

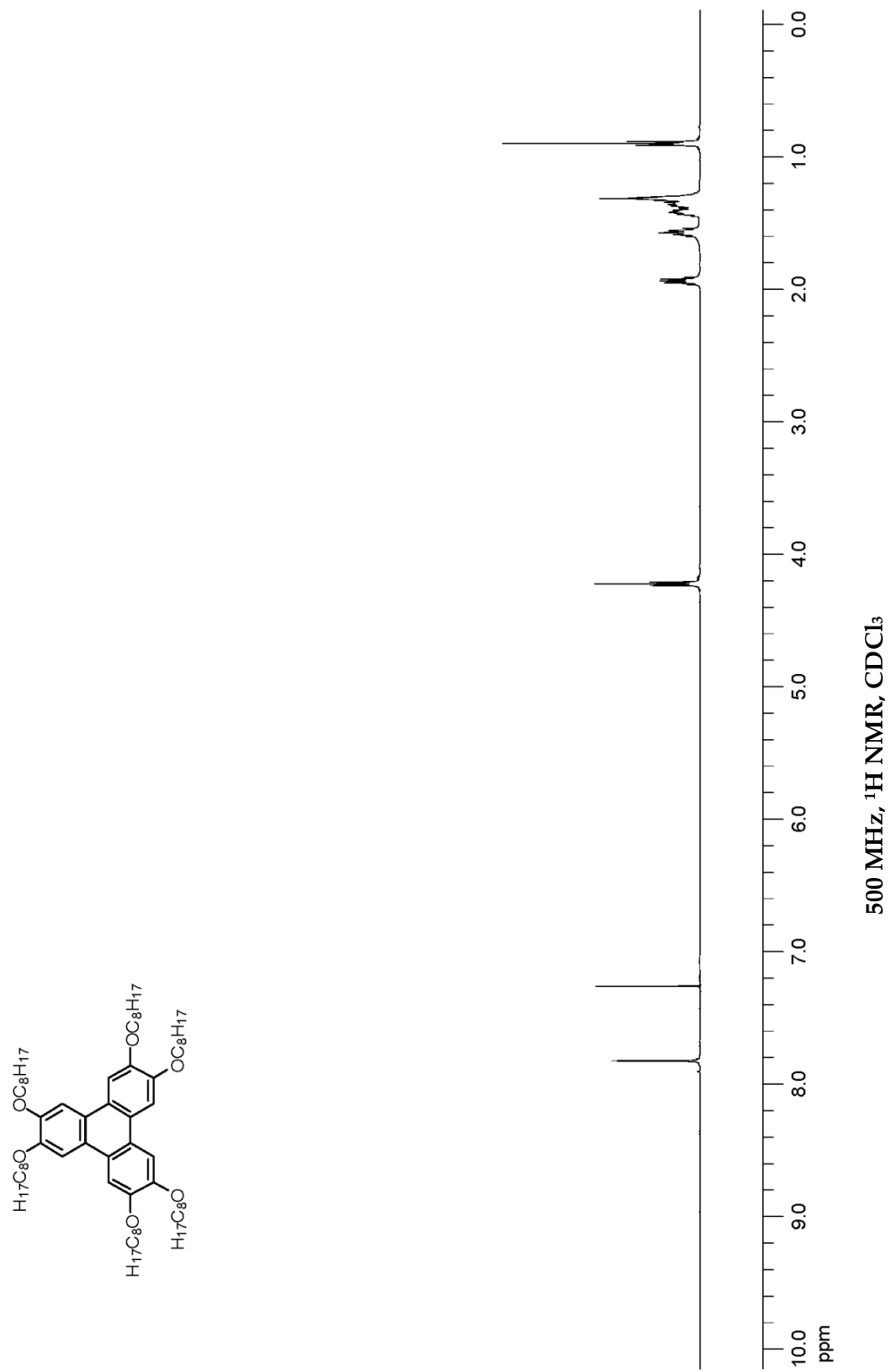
500 MHz, $^1\text{H NMR}$, CDCl_3

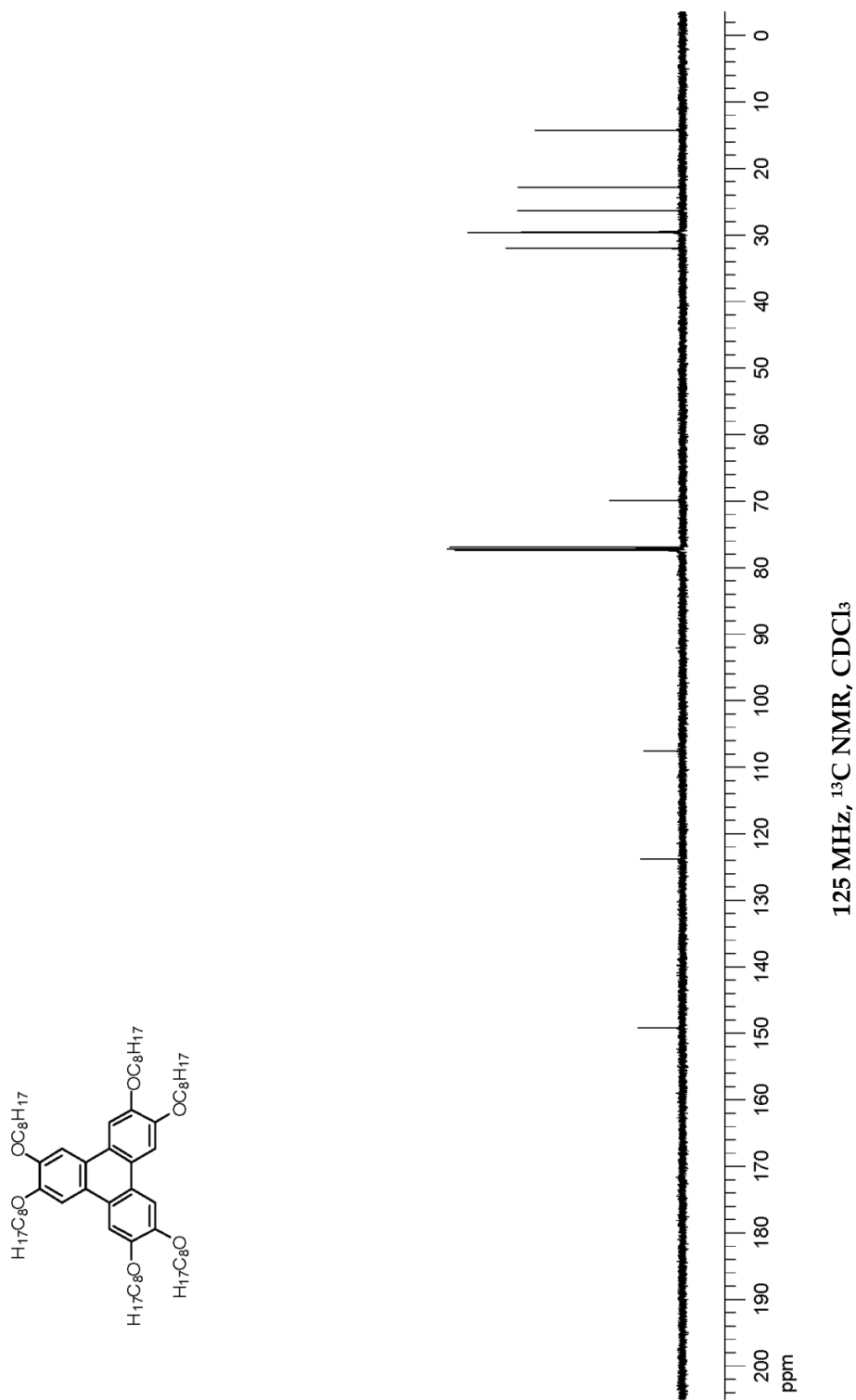
125 MHz, ^{13}C NMR, CDCl₃

6.6.2.6. 2,3,6,7,10,11-Hexakis(octyloxy)triphenylene

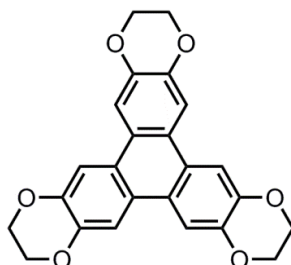


The general procedure described in Section 6.6.2.4 was followed on 0.10 mmol scale (33 mg) to obtain 2,3,6,7,10,11-hexakis(octyloxy)triphenylene as a white solid in 82% yield (81 mg). ^1H NMR (500 MHz, CDCl_3): δ 7.82 (s, 6H), 4.22 (t, $J = 7.0$ Hz, 12H), 1.94 (qn, $J = 7.0$ Hz, 12H), 1.57 (qn, $J = 7.5$ Hz, 12H), 1.43–1.31 (m, 48H), 0.90 (t, $J = 6.5$ Hz, 18H). ^{13}C NMR (125 MHz, CDCl_3): δ 149.2, 123.8, 107.6, 69.9, 32.0, 29.6, 29.5, 26.4, 22.8, 14.3. HRMS (DART) calculated for $\text{C}_{66}\text{H}_{109}\text{O}_6$ $[\text{M}+\text{H}]^+$: 997.8247, found: 997.8224.



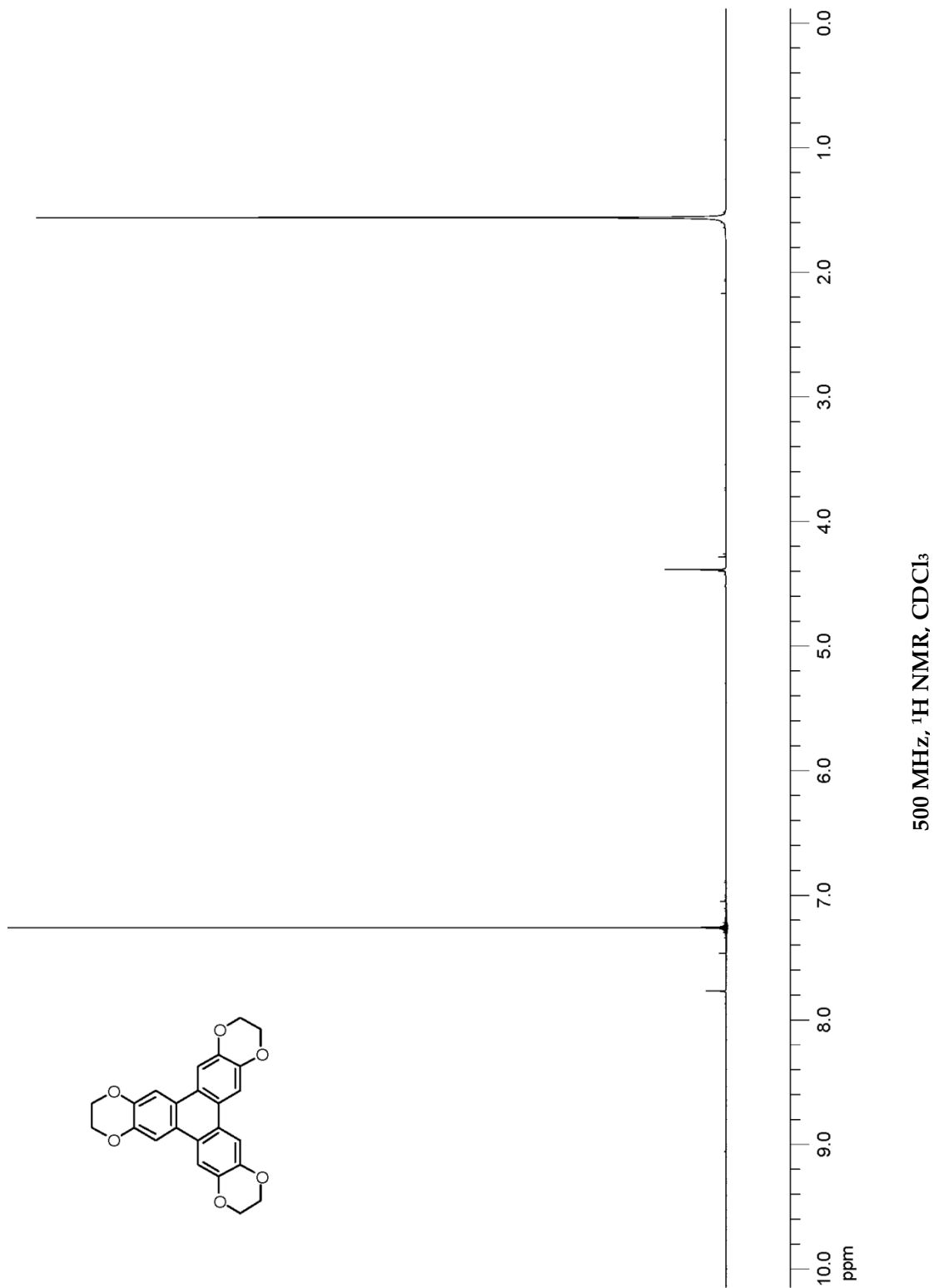


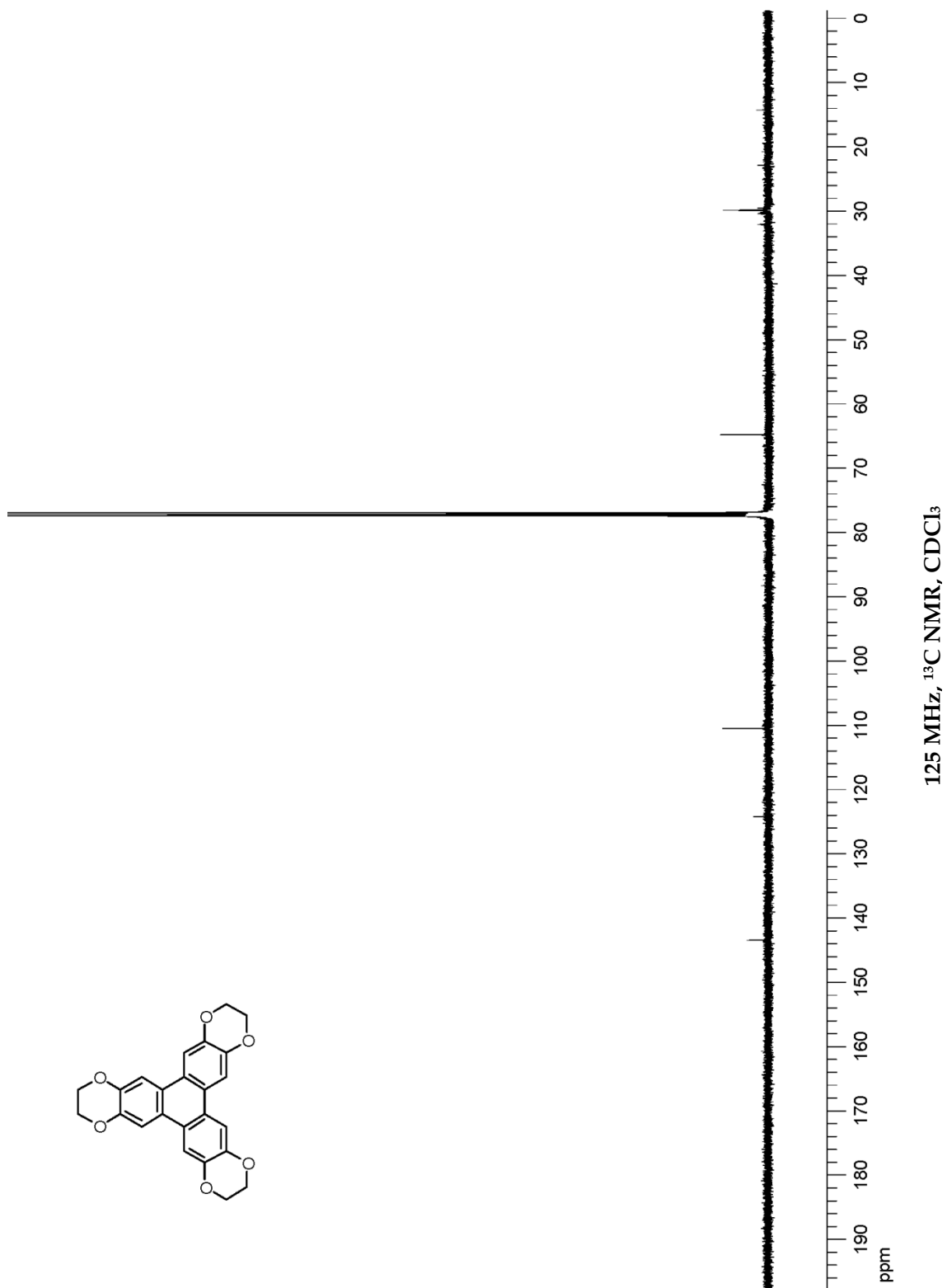
6.6.2.7. 2,3,8,9,14,15-Hexahydrotriphenyleno[2,3-b:6,7-b':10,11-b'']tris-([1,4]dioxine)



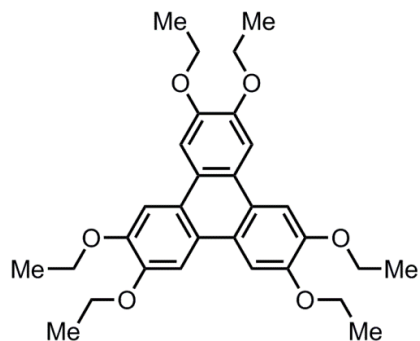
The general procedure described in Section 6.6.2.4 was followed on 0.10 mmol scale (14 mg) to obtain 2,3,8,9,14,15-hexahydrotriphenyleno[2,3-b:6,7-b':10,11-b'']tris-([1,4]dioxine) as a white solid in 34% yield (14 mg). ^1H NMR (500 MHz, CDCl_3): δ 7.79 (s, 6H), 4.38 (s, 12H). ^{13}C NMR (125 MHz, CDCl_3): δ 143.5, 124.2, 110.5, 64.8. HRMS (DART) calculated for $\text{C}_{24}\text{H}_{19}\text{O}_6$ $[\text{M}+\text{H}]^+$: 403.1182, found: 403.1170. The spectral data were in agreement with literature values.⁵⁷

⁵⁷ Naarmann, H.; Hanack, M.; Mattmer, R., "A High Yield Easy Method for the Preparation of Alkoxy-Substituted Triphenylenes," *Synthesis* **1994**, 1994, 477-478.

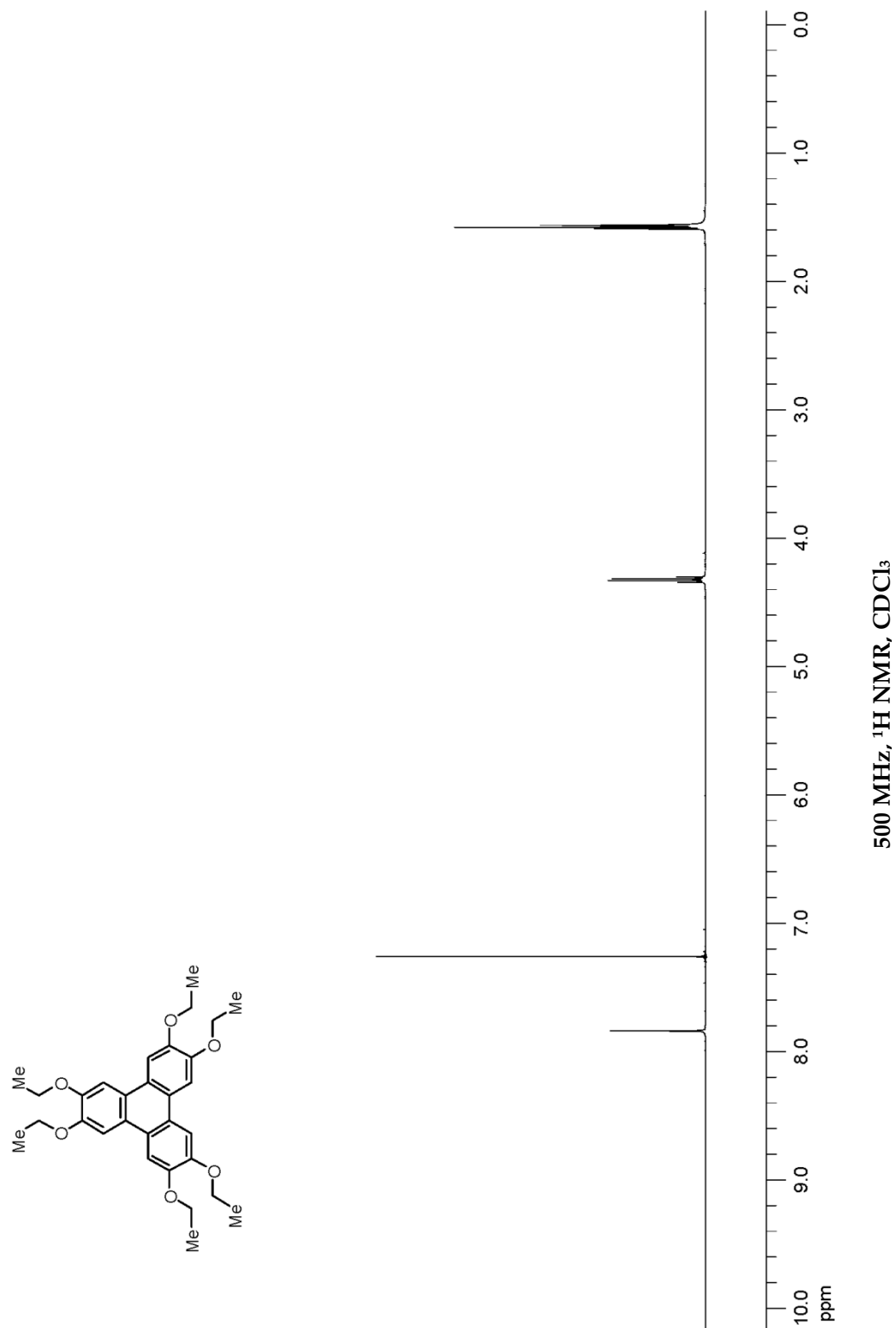


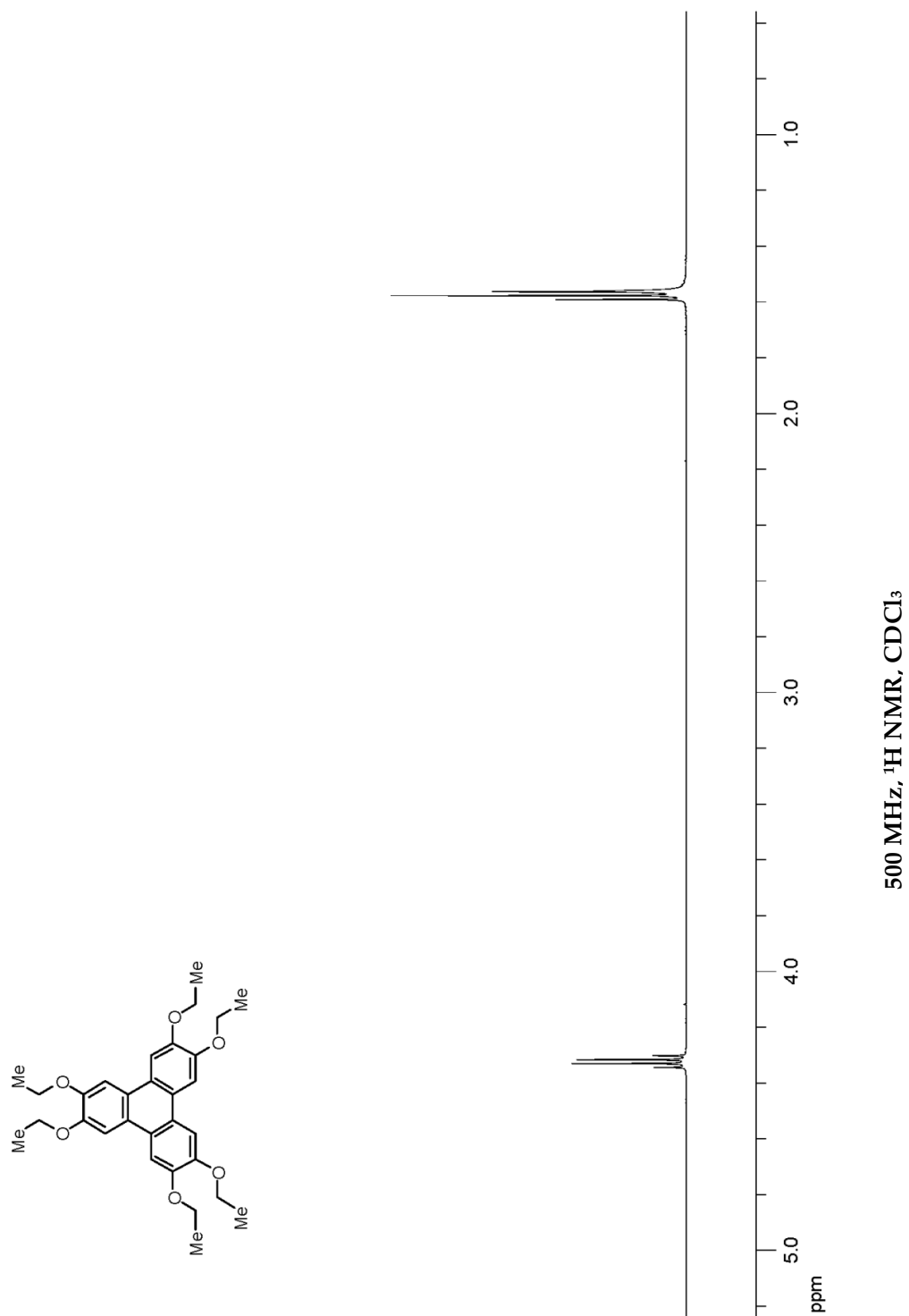


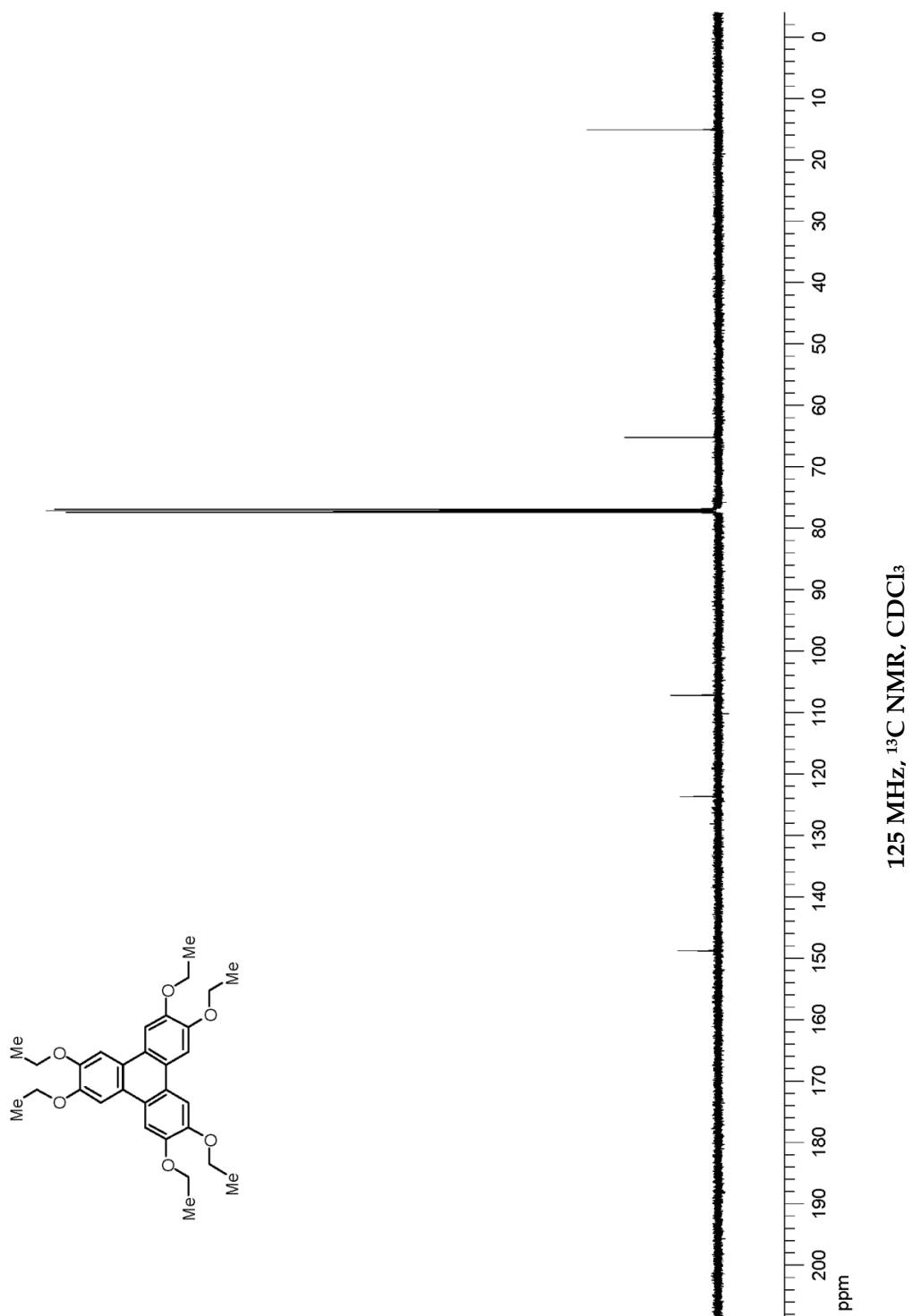
6.6.2.8. 2,3,6,7,10,11-Hexaethoxytriphenylene



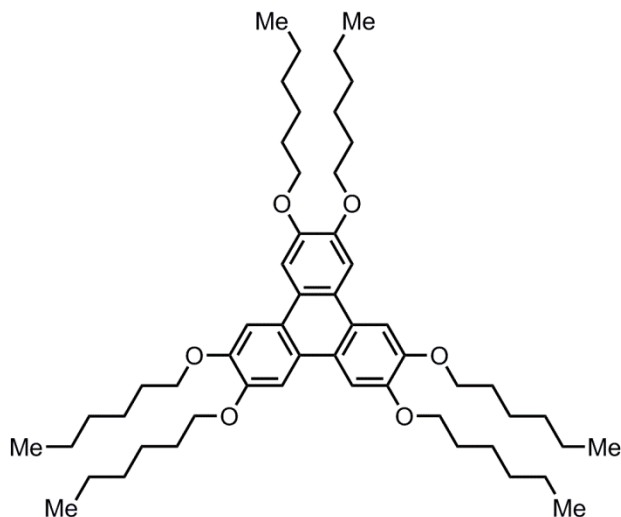
The general procedure described in Section 6.6.2.4 was followed on 0.10 mmol scale (17 mg) to obtain 2,3,6,7,10,11-hexaethoxytriphenylene as a white solid in 79% yield (39 mg). ^1H NMR (500 MHz, CDCl_3): δ 7.84 (s, 6H), 4.32 (q, $J = 7.0$ Hz, 12H), 1.58 (t, $J = 7.0$ Hz, 18H). ^{13}C NMR (125 MHz, CDCl_3): δ 148.8, 123.7, 107.2, 65.2, 15.1. HRMS (DART) calculated for $\text{C}_{30}\text{H}_{37}\text{O}_6$ $[\text{M}+\text{H}]^+$: 493.2590, found: 493.2574.





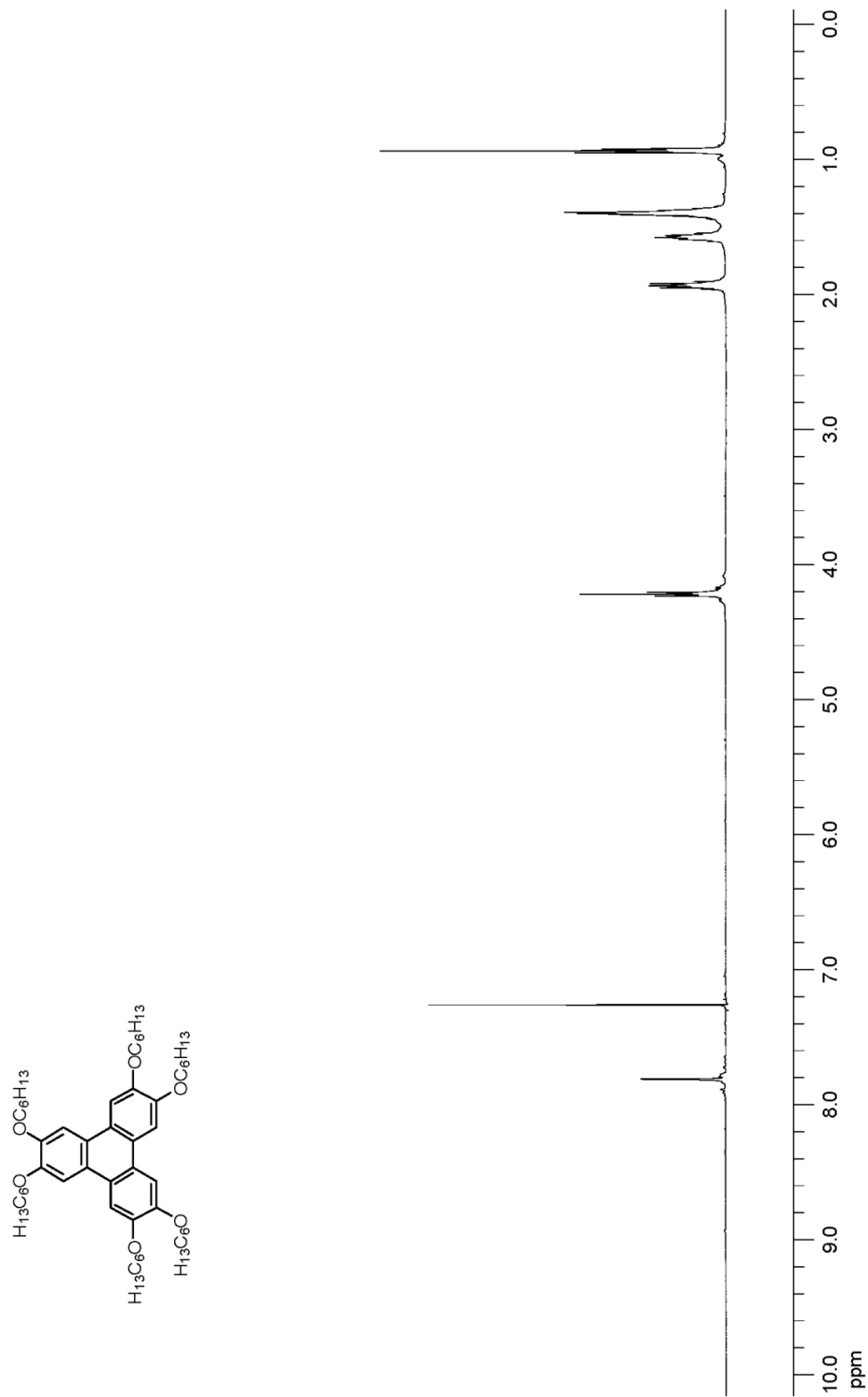


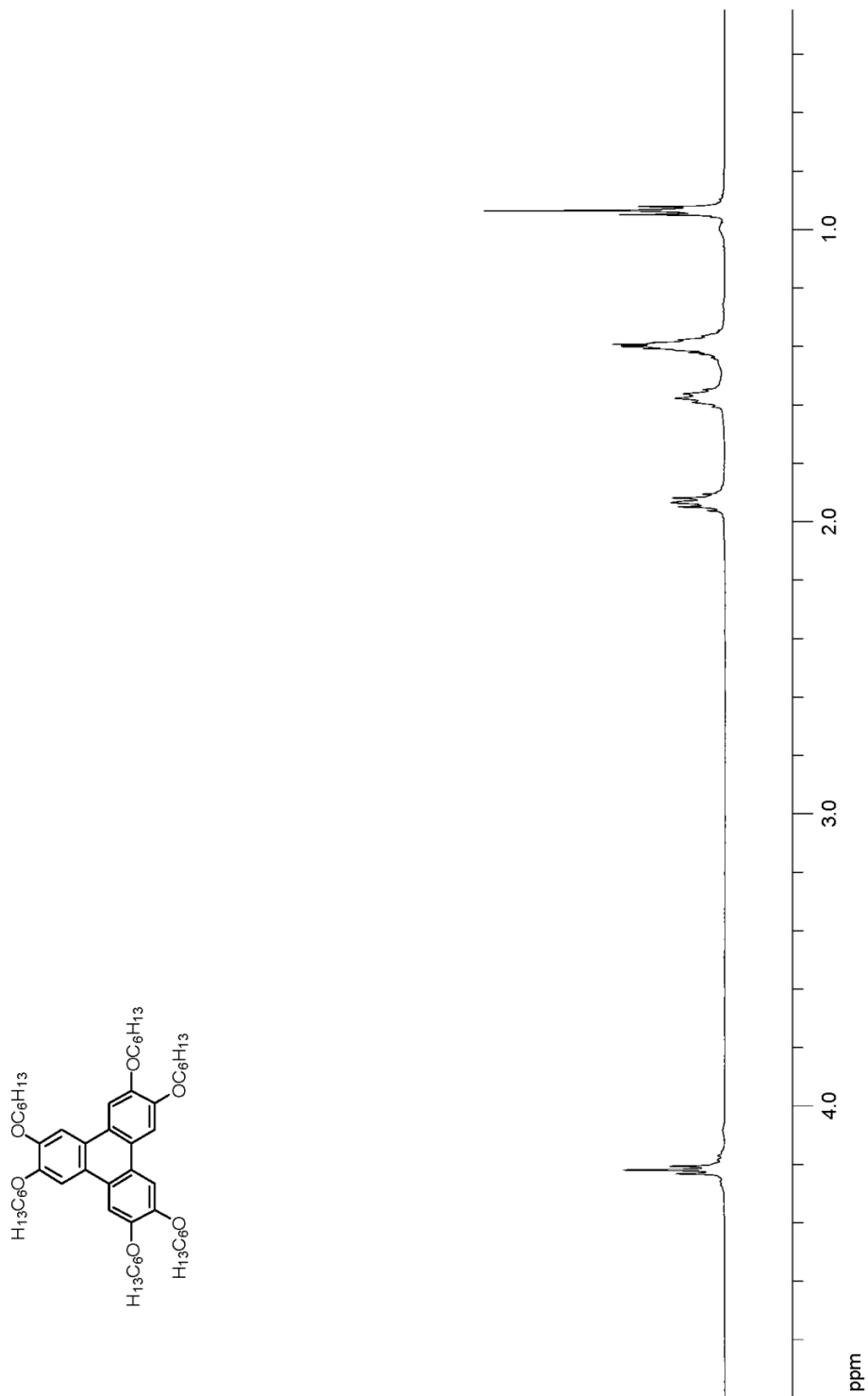
6.6.2.9. 2,3,6,7,10,11-Hexakis(hexyloxy)triphenylene

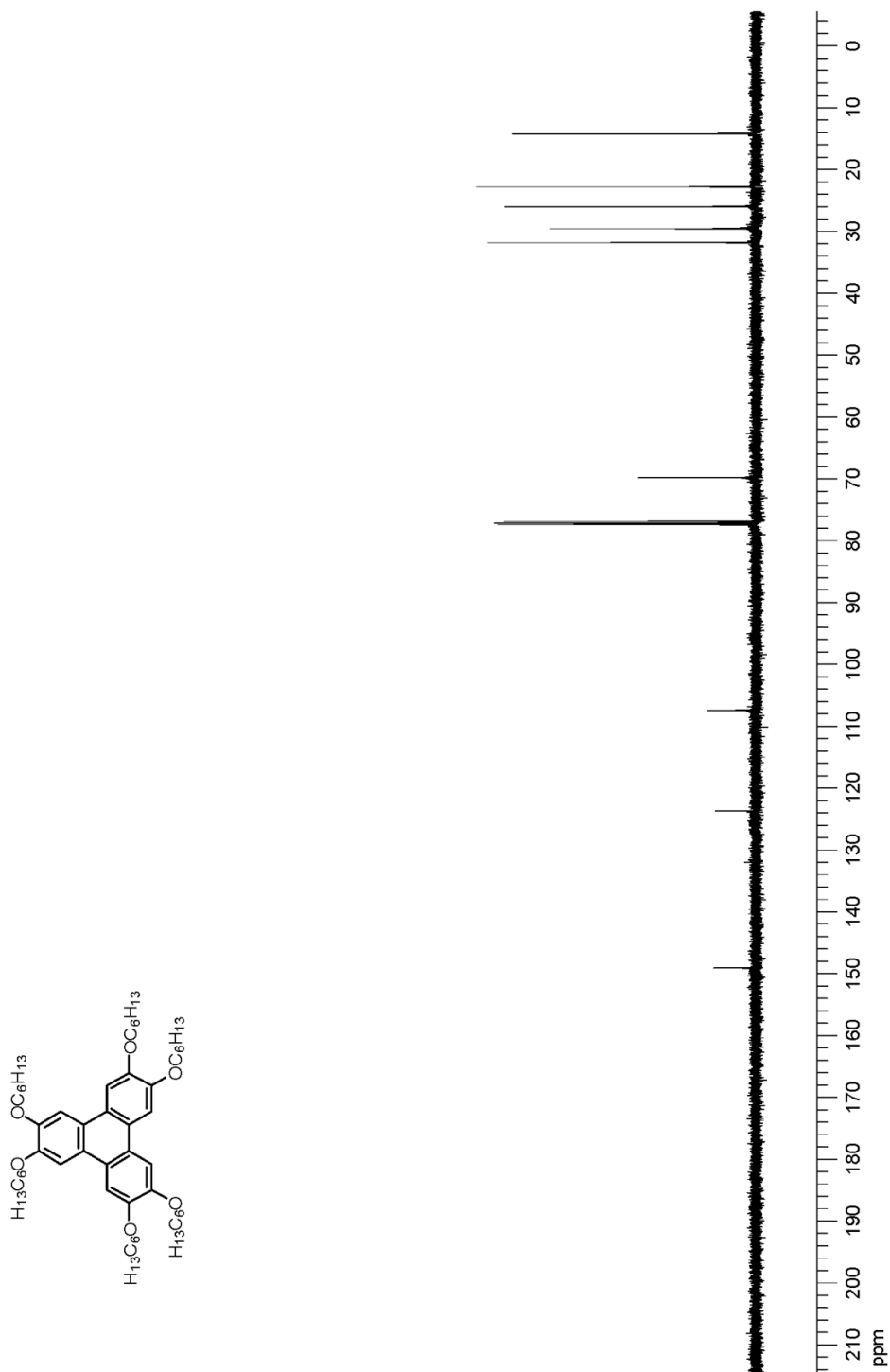


The general procedure described in Section 6.6.2.4 was followed on 0.10 mmol scale (28 mg) to obtain 2,3,6,7,10,11-hexakis(hexyloxy)triphenylene as a white solid in 56% yield (46 mg). ^1H NMR (500 MHz, CDCl_3): δ 7.81 (s, 6H), 4.22 (t, $J = 6.5$ Hz, 12H), 1.94 (qn, $J = 7.0$ Hz, 12H), 1.58 (qn, $J = 7.5$ Hz, 12H), 1.41–1.38 (m, 24H), 0.94 (t, $J = 7.0$ Hz, 18H). ^{13}C NMR (125 MHz, CDCl_3): δ 149.1, 123.7, 107.4, 69.8, 31.8, 29.6, 26.0, 22.8, 14.2. HRMS (DART) calculated for $\text{C}_{54}\text{H}_{85}\text{O}_6$ $[\text{M}+\text{H}]^+$: 829.6373, found: 829.6346. The proton NMR data were in agreement with literature values.⁵⁸

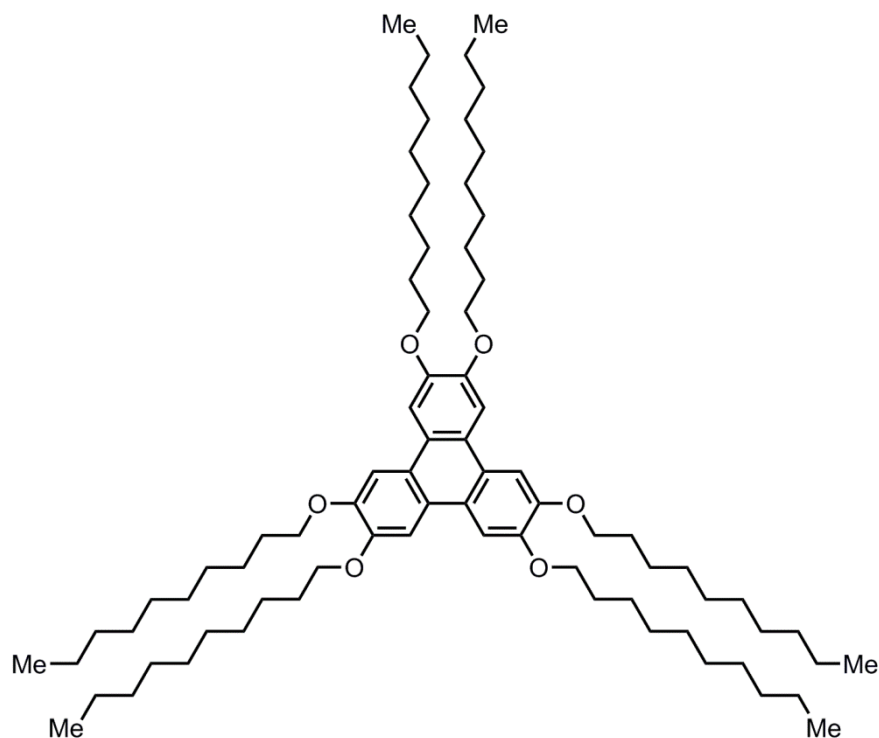
⁵⁸ (a) Zhao, B.; Liu, B.; Png, R. Q.; Zhang, K.; Lim, K. A.; Luo, J.; Shao, J.; Ho, P. K. H.; Chi, C.; Wu, J., "New Discotic Mesogens Based on Triphenylene-Fused Triazatruxenes: Synthesis, Physical Properties, and Self-Assembly," *Chemistry of Materials* **2009**, 22, 435-449. (b) Cooke, G.; Sage, V.; Richomme, T., "Synthesis of Hexa-Alkyloxytriphenylenes Using FeCl_3 Supported on Alumina," *Synthetic Communications* **1999**, 29, 1767-1771.



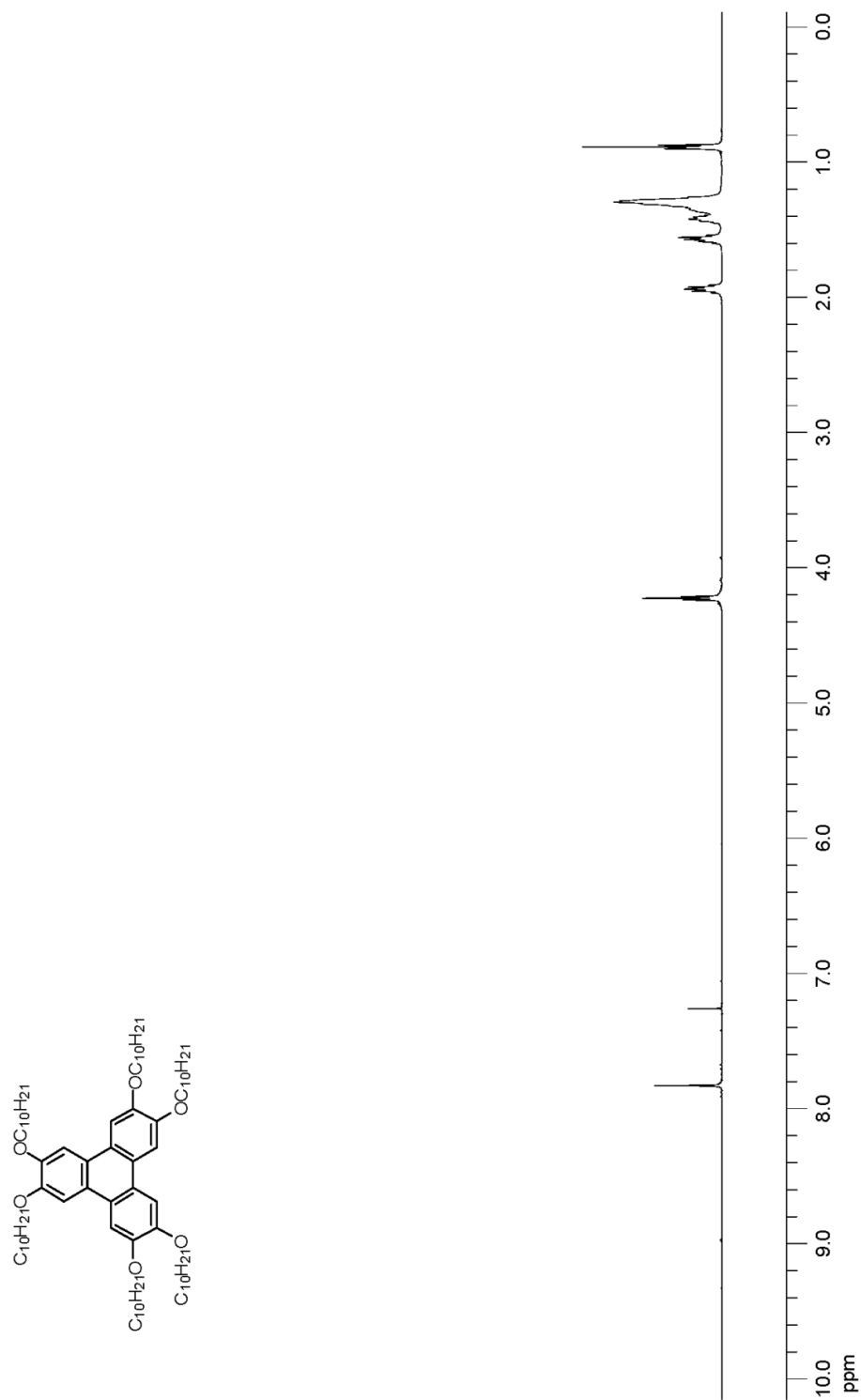


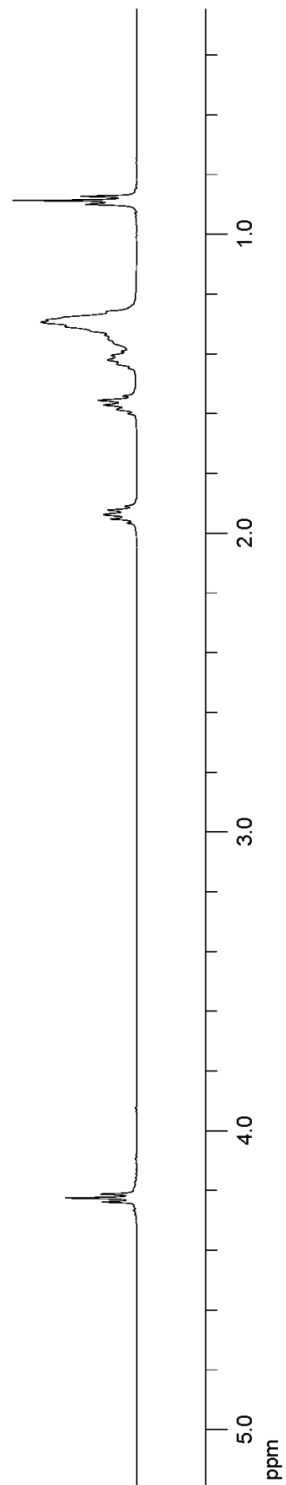
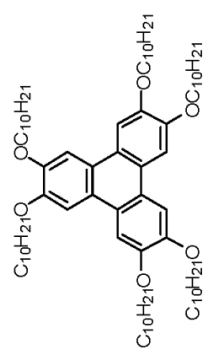
125 MHz, ^{13}C NMR, CDCl_3

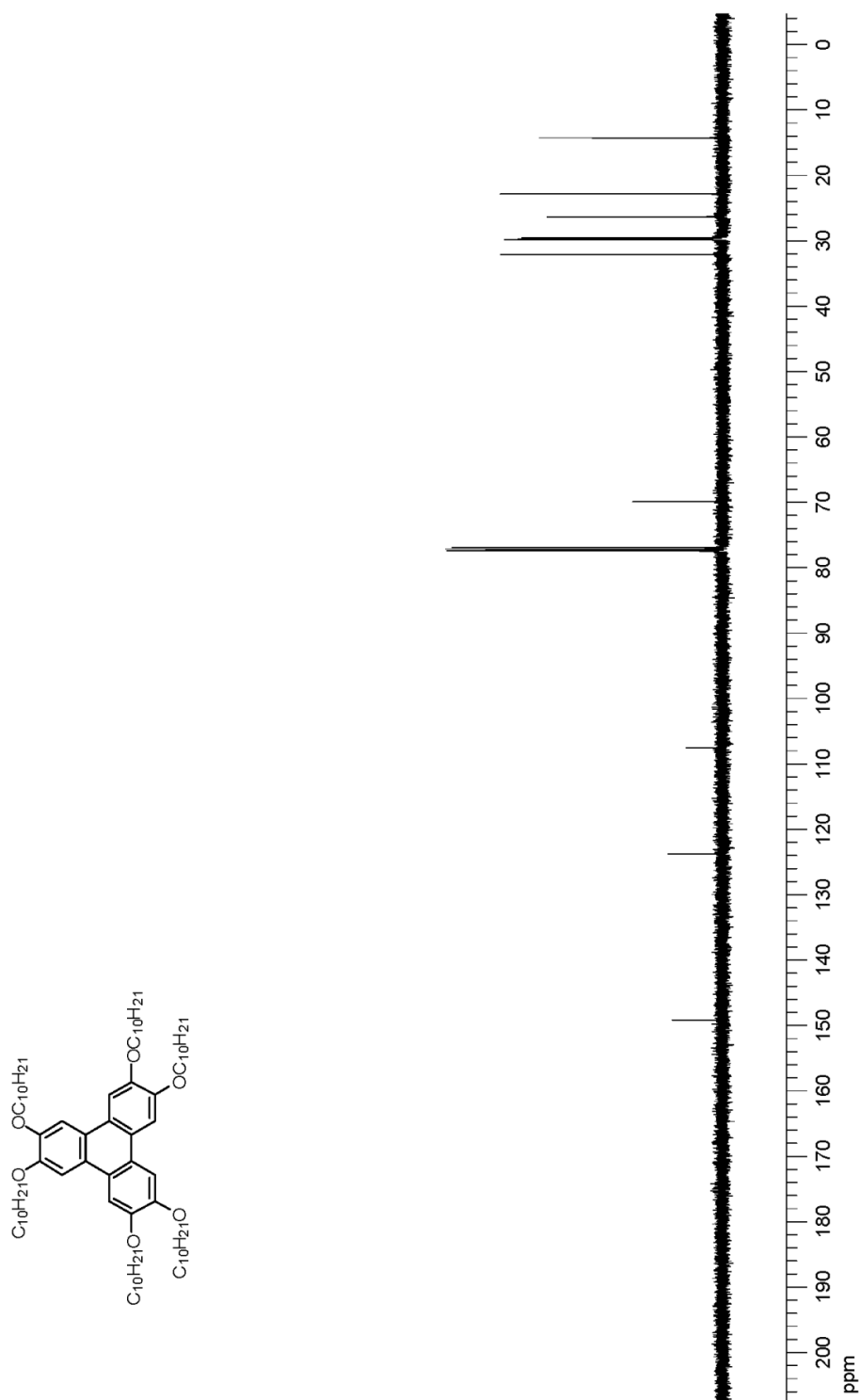
6.6.2.10. 2,3,6,7,10,11-Hexakis(decyloxy)triphenylene



The general procedure described in Section 6.6.2.4 was followed on 0.10 mmol scale (39 mg) to obtain 2,3,6,7,10,11-hexakis(decyloxy)triphenylene as a white solid in 60% yield (66 mg). ^1H NMR (500 MHz, CDCl_3): δ 7.83 (s, 6H), 4.23 (t, $J = 6.5$ Hz, 12H), 1.94 (qn, $J = 7.0$ Hz, 12H), 1.60 (qn, $J = 7.5$ Hz, 12H), 1.44–1.26 (m, 72H), 0.89 (t, $J = 6.5$ Hz, 18H). ^{13}C NMR (125 MHz, CDCl_3): δ 149.1, 123.8, 107.6, 69.9, 32.1, 30.0, 29.8, 29.7, 29.6, 29.5, 26.4, 22.9, 14.3. HRMS (DART) calculated for $\text{C}_{78}\text{H}_{133}\text{O}_6$ $[\text{M}+\text{H}]^+$: 1166.0144, found: 1166.0102. The proton NMR data were in agreement with literature values.⁵⁷

500 MHz, ^1H NMR, CDCl_3

500 MHz, ¹H NMR, CDCl₃



Chapter 7. Regioselective Synthesis of Star-Shaped Polycyclic Aromatic Compounds: Evidence for a Radical Cation Mechanism

7.1. Introduction

7.1.1. Conjugated Aromatic Systems in Materials Science

Conjugated materials have attracted significant interests in material sciences due to their utilities in various types of devices.¹ Throughout the history of organic semiconductors and electronics, conjugated polymers have been the main types of the materials in those fields. Some examples of such conjugated polymers include electrochromics,² sensors,³ lasers,⁴ organic solar cells,^{5,6} organic field effect transistors (OFETs),⁷ and organic light

¹ Kanibolotsky, A. L.; Perepichka, I. F.; Skabara, P. J., "Star-Shaped π -Conjugated Oligomers and Their Applications in Organic Electronics and Photonics," *Chemical Society Reviews* **2010**, *39*, 2695-2728.

² (a) Beaujuge, P. M.; Reynolds, J. R., "Color Control in π -Conjugated Organic Polymers for Use in Electrochromic Devices," *Chemical Reviews* **2010**, *110*, 268-320. (b) Mortimer, R. J.; Dyer, A. L.; Reynolds, J. R., "Electrochromic Organic and Polymeric Materials for Display Applications," *Displays* **2006**, *27*, 2-18. (c) Sonmez, G., "Polymeric Electrochromics," *Chemical Communications* **2005**, 5251-5259.

³ (a) McQuade, D. T.; Pullen, A. E.; Swager, T. M., "Conjugated Polymer-Based Chemical Sensors," *Chemical Reviews* **2000**, *100*, 2537-2574. (b) Bobacka, J.; Ivaska, A.; Lewenstam, A., "Potentiometric Ion Sensors Based on Conducting Polymers," *Electroanalysis* **2003**, *15*, 366-374.

⁴ Samuel, I. D. W.; Turnbull, G. A., "Organic Semiconductor Lasers," *Chemical Reviews* **2007**, *107*, 1272-1295.

⁵ (a) Chen, J.; Cao, Y., "Development of Novel Conjugated Donor Polymers for High-Efficiency Bulk-Heterojunction Photovoltaic Devices," *Accounts of Chemical Research* **2009**, *42*, 1709-1718. (b) Günes, S.; Neugebauer, H.; Sariciftci, N. S., "Conjugated Polymer-Based Organic Solar Cells," *Chemical Reviews* **2007**, *107*, 1324-1338. (c) Cheng, Y.-J.; Yang, S.-H.; Hsu, C.-S., "Synthesis of Conjugated Polymers for Organic

emitting diodes (OLEDs).⁸ In many cases, however, shorter conjugated molecules (*e.g.* conjugated oligomers) often exhibit substantial improvements in terms of efficiency and performance in the devices, mainly because those oligomers possess well-defined energy levels and better solubilities than polymeric materials.¹

There are several kinds of conjugated oligomers (Figure 7.1): linear oligomers,^{9,10} star-shaped oligomers,^{11,12} dendritic oligomers,^{13,14} and HBC (hexabenzocoronene) based

Solar Cell Applications," *Chemical Reviews* **2009**, *109*, 5868-5923. (d) Helgesen, M.; Sondergaard, R.; Krebs, F. C., "Advanced Materials and Processes for Polymer Solar Cell Devices," *Journal of Materials Chemistry* **2010**, *20*, 36-60.

⁶ (a) Dennler, G.; Scharber, M. C.; Brabec, C. J., "Polymer-Fullerene Bulk-Heterojunction Solar Cells," *Advanced Materials* **2009**, *21*, 1323-1338. (b) Coakley, K. M.; McGehee, M. D., "Conjugated Polymer Photovoltaic Cells," *Chemistry of Materials* **2004**, *16*, 4533-4542. (c) Bundgaard, E.; Krebs, F. C., "Low Band Gap Polymers for Organic Photovoltaics," *Solar Energy Materials and Solar Cells* **2007**, *91*, 954-985.

⁷ (a) Grobert, N., "Carbon Nanotubes – Becoming Clean," *Materials Today* **2007**, *10*, 28-35. (b) Allard, S.; Forster, M.; Souharce, B.; Thiem, H.; Scherf, U., "Organic Semiconductors for Solution-Processable Field-Effect Transistors (OFETs)," *Angewandte Chemie International Edition* **2008**, *47*, 4070-4098.

⁸ (a) Kamtekar, K. T.; Monkman, A. P.; Bryce, M. R., "Recent Advances in White Organic Light-Emitting Materials and Devices (Woleds)," *Advanced Materials* **2010**, *22*, 572-582. (b) Grimsdale, A. C.; Leok Chan, K.; Martin, R. E.; Jokisz, P. G.; Holmes, A. B., "Synthesis of Light-Emitting Conjugated Polymers for Applications in Electroluminescent Devices," *Chemical Reviews* **2009**, *109*, 897-1091. (c) Perepichka, I. F.; Perepichka, D. F.; Meng, H.; Wudl, F., "Light-Emitting Polythiophenes," *Advanced Materials* **2005**, *17*, 2281-2305.

⁹ (a) Roncali, J., "Molecular Bulk Heterojunctions: An Emerging Approach to Organic Solar Cells," *Accounts of Chemical Research* **2009**, *42*, 1719-1730. (b) Mishra, A.; Ma, C.-Q.; Bäuerle, P., "Functional Oligothiophenes: Molecular Design for Multidimensional Nanoarchitectures and Their Applications†," *Chemical Reviews* **2009**, *109*, 1141-1276. (c) Tang, C. W., "Two-Layer Organic Photovoltaic Cell," *Applied Physics Letters* **1986**, *48*, 183-185.

¹⁰ (a) Segura, J. L.; Martin, N.; Guldi, D. M., "Materials for Organic Solar Cells: The C₆₀/[Small Pi]-Conjugated Oligomer Approach," *Chemical Society Reviews* **2005**, *34*, 31-47. (b) McNeill, C. R.; Clifton-Smith, M. J.; Quinton, J. S.; King, B. V.; Hotta, S.; Dastoor, P. C., "The Photovoltaic Properties of Phenyl-Capped Thiophene Oligomers," *Current Applied Physics* **2004**, *4*, 335-338. (c) Schulze, K.; Urich, C.; Schüppel, R.; Leo, K.; Pfeiffer, M.; Brier, E.; Reinold, E.; Bäuerle, P., "Efficient Vacuum-Deposited Organic Solar Cells Based on a New Low-Bandgap Oligothiophene and Fullerene C₆₀," *Advanced Materials* **2006**, *18*, 2872-2875.

oligomers.¹⁵ These π -conjugated oligomers have advantages in their synthesis, purification, structure identification, and energy definition compared to the corresponding polymers.

¹¹ (a) Wu, G.; Zhao, G.; He, C.; Zhang, J.; He, Q.; Chen, X.; Li, Y., "Synthesis and Photovoltaic Properties of a Star-Shaped Molecule with Triphenylamine as Core and Benzo[1,2,5]Thiadiazol Vinylene as Arms," *Solar Energy Materials and Solar Cells* **2009**, *93*, 108-113. (b) Roquet, S.; Cravino, A.; Leriche, P.; Alévêque, O.; Frère, P.; Roncali, J., "Triphenylamine-Thienylenevinylene Hybrid Systems with Internal Charge Transfer as Donor Materials for Heterojunction Solar Cells," *Journal of the American Chemical Society* **2006**, *128*, 3459-3466. (c) Cremer, J.; Bauerle, P., "Star-Shaped Perylene-Oligothiophene-Triphenylamine Hybrid Systems for Photovoltaic Applications," *Journal of Materials Chemistry* **2006**, *16*, 874-884.

¹² (a) Cremer, J.; Mena-Osteritz, E.; Pschierer, N. G.; Mullen, K.; Bauerle, P., "Dye-Functionalized Head-to-Tail Coupled Oligo(3-Hexylthiophenes)-Perylene-Oligothiophene Dyads for Photovoltaic Applications," *Organic & Biomolecular Chemistry* **2005**, *3*, 985-995. (b) Ziessel, R.; Ulrich, G.; Harriman, A., "The Chemistry of Bodipy: A New El Dorado for Fluorescence Tools," *New Journal of Chemistry* **2007**, *31*, 496-501. (c) Rousseau, T.; Cravino, A.; Bura, T.; Ulrich, G.; Ziessel, R.; Roncali, J., "Multi-Donor Molecular Bulk Heterojunction Solar Cells: Improving Conversion Efficiency by Synergistic Dye Combinations," *Journal of Materials Chemistry* **2009**, *19*, 2298-2300.

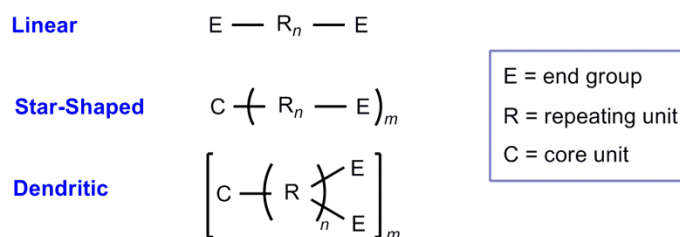
¹³ (a) Kopidakis, N.; Mitchell, W. J.; van de Lagemaat, J.; Ginley, D. S.; Rumbles, G.; Shaheen, S. E.; Rance, W. L., "Bulk Heterojunction Organic Photovoltaic Devices Based on Phenyl-Cored Thiophene Dendrimers," *Applied Physics Letters* **2006**, *89*, 103524-103523. (b) Ma, C.-Q.; Mena-Osteritz, E.; Debaerdemaeker, T.; Wienk, M. M.; Janssen, R. A. J.; Bäuerle, P., "Functionalized 3D Oligothiophene Dendrons and Dendrimers—Novel Macromolecules for Organic Electronics," *Angewandte Chemie International Edition* **2007**, *46*, 1679-1683. (c) Ma, C.-Q.; Fonrodona, M.; Schikora, M. C.; Wienk, M. M.; Janssen, R. A. J.; Bäuerle, P., "Solution-Processed Bulk-Heterojunction Solar Cells Based on Monodisperse Dendritic Oligothiophenes," *Advanced Functional Materials* **2008**, *18*, 3323-3331.

¹⁴ (a) Mishra, A.; Ma, C. Q.; Janssen, R. A.; Bäuerle, P., "Shape-Persistent Oligothiophene-Ethynylene-Based Dendrimers: Synthesis, Spectroscopy and Electrochemical Characterization," *Chemistry—A European Journal* **2009**, *15*, 13521-13534. (b) Mastalerz, M.; Fischer, V.; Ma, C.-Q.; Janssen, R. A. J.; Bäuerle, P., "Conjugated Oligothiophenyl Dendrimers Based on a Pyrazino[2,3-g]Quinoxaline Core," *Organic Letters* **2009**, *11*, 4500-4503.

¹⁵ (a) Wu, J.; Pisula, W.; Müllen, K., "Graphenes as Potential Material for Electronics," *Chemical Reviews* **2007**, *107*, 718-747. (b) Wong, W. W. H.; Jones, D. J.; Yan, C.; Watkins, S. E.; King, S.; Haque, S. A.; Wen, X.; Ghiggino, K. P.; Holmes, A. B., "Synthesis, Photophysical, and Device Properties of Novel Dendrimers Based on a Fluorene-Hexabenzocoronene (FHBC) Core," *Organic Letters* **2009**, *11*, 975-978. (c) Wong, W. W. H.; Ma, C.-Q.; Pisula, W.; Yan, C.; Feng, X.; Jones, D. J.; Müllen, K.; Janssen, R. A. J.; Bäuerle, P.; Holmes, A. B., "Self-Assembling Thiophene Dendrimers with a Hexa-Peri-Hexabenzocoronene Core—Synthesis, Characterization and Performance in Bulk Heterojunction Solar Cells," *Chemistry of Materials* **2009**, *22*, 457-466.

Hence, there has been a growing interest in these materials.¹⁶ In particular, star-shaped conjugated oligomers stand out among those oligomers due to their unique physical/chemical properties and flexibility with regard to their synthesis.¹⁷

Figure 7.1 Structure Types of Conjugated Oligomers



7.1.2. Star-Shaped Conjugated Oligomers

Star-shaped conjugated molecules possess a common central unit with three or more conjugated arms radiating from the core. These compounds are known to be amenable to solution-phase processes for amorphous thin film formation¹⁸ and to have enhanced

¹⁶ Tang, W.; Hai, J.; Dai, Y.; Huang, Z.; Lu, B.; Yuan, F.; Tang, J.; Zhang, F., "Recent Development of Conjugated Oligomers for High-Efficiency Bulk-Heterojunction Solar Cells," *Solar Energy Materials and Solar Cells* **2010**, *94*, 1963-1979.

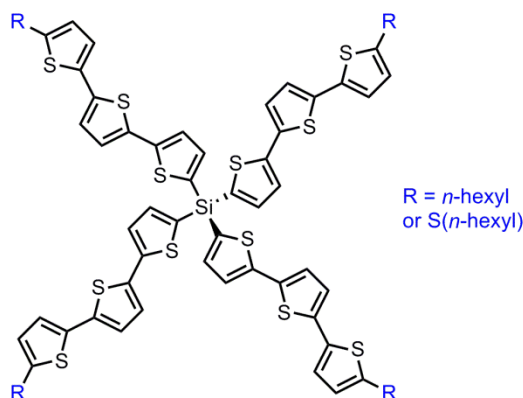
¹⁷ Lai, W. Y.; He, Q. Y.; Zhu, R.; Huang, W., "Kinked Star-Shaped Fluorene/Triazatruxene Co-Oligomer Hybrids with Enhanced Functional Properties for High-Performance, Solution-Processed, Blue Organic Light-Emitting Diodes," *Advanced Functional Materials* **2008**, *18*, 265-276.

¹⁸ (a) Ponomarenko, S. A.; Kirchmeyer, S.; Elschner, A.; Huisman, B. H.; Karbach, A.; Drechsler, D., "Star-Shaped Oligothiophenes for Solution-Processible Organic Field-Effect Transistors," *Advanced Functional Materials* **2003**, *13*, 591-596. (b) Sonntag, M.; Kreger, K.; Hanft, D.; Strohrriegl, P.; Setayesh, S.; de Leeuw, D., "Novel Star-Shaped Triphenylamine-Based Molecular Glasses and Their Use in Ofets," *Chemistry of Materials* **2005**, *17*, 3031-3039. (c) Zhou, X.-H.; Yan, J.-C.; Pei, J., "Synthesis and Relationships between the Structures and Properties of Monodisperse Star-Shaped Oligofluorenes," *Organic Letters* **2003**, *5*, 3543-3546.

luminescent properties.¹⁹ The electronic and physical properties of these oligomers are varied depending on the conjugated arms and the core structures.

One of the first star-shaped oligomers was prepared with a silicon core and four branches of conjugated oligothiophene chains (Figure 7.2).²⁰ The ends of the branches were capped with *n*-hexyl or *n*-hexylthio groups to increase the solubility of the molecules and to stabilize the radical cations with their electron-donating abilities. This star-shaped oligomer showed 17–19 nm red-shifted absorption band in comparison with that of the corresponding linear oligomer.

Figure 7.2 Star-Shaped Oligomers with a Silicon Core

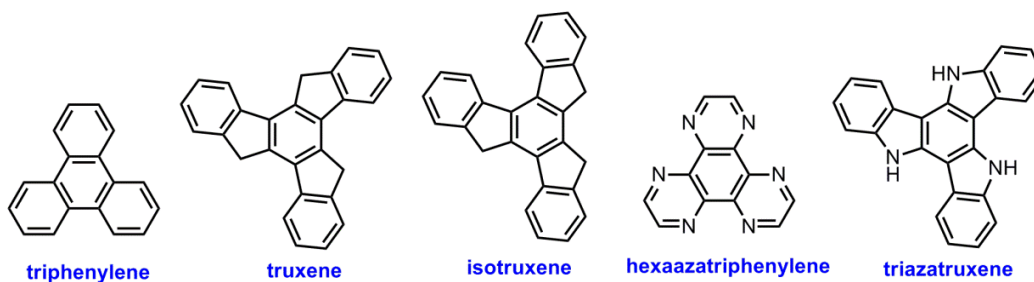


¹⁹ (a) Yamaguchi, Y.; Ochi, T.; Miyamura, S.; Tanaka, T.; Kobayashi, S.; Wakamiya, T.; Matsubara, Y.; Yoshida, Z.-i., "Rigid Molecular Architectures That Comprise a 1,3,5-Trisubstituted Benzene Core and Three Oligoaryleneethynylene Arms: Light-Emitting Characteristics and π Conjugation between the Arms," *Journal of the American Chemical Society* **2006**, *128*, 4504-4505. (b) Kanibolotsky, A. L.; Berridge, R.; Skabara, P. J.; Perepichka, I. F.; Bradley, D. D. C.; Koeberg, M., "Synthesis and Properties of Monodisperse Oligofluorene-Functionalized Truxenes: Highly Fluorescent Star-Shaped Architectures," *Journal of the American Chemical Society* **2004**, *126*, 13695-13702.

²⁰ Roquet, S.; de Bettignies, R.; Leriche, P.; Cravino, A.; Roncali, J., "Three-Dimensional Tetra(Oligothieryl)Silanes as Donor Material for Organic Solar Cells," *Journal of Materials Chemistry* **2006**, *16*, 3040-3045.

Possible moieties for the core structure of star-shaped oligomers include single atoms (*e.g.* B, C⁺, N, Si, etc.), a benzene ring, azine rings (*e.g.* pyridine, pyrimidine, pyrazine, 1,3,5-triazine, etc.), and polycyclic rings (Figure 7.3, *e.g.* triphenylene, truxene, isotruxene, hexaazatriphenylene, triazatruxene, etc.).²¹ Among these, star-shaped oligomers bearing polyaromatic cores are the most relevant to our studies; thus, they will be briefly introduced in the following sections.

Figure 7.3 Polycyclic Ring Cores of Star-Shaped Oligomers



²¹ Detert, H.; Lehmann, M.; Meier, H., "Star-Shaped Conjugated Systems," *Materials* **2010**, 3, 3218-3330.

7.2. Background

7.2.1. Star-Shaped Oligomers with a Triphenylene Core

One of the classic methods for the triphenylene synthesis is the oxidative dehydrogenation reaction of benzene, as shown in Scheme 7.1. Several oxidants can be employed for this process; iron(III) chloride is one of the most common reagents for the trimerization (Scheme 7.1, eq 1).²² In addition, molybdenum(V) chloride²³ or vanadium(V) chloride²⁴ can also participate in this process as an oxidant. Furthermore, Sato and co-workers demonstrated that photocyclization (with UV light) of *ortho*-terphenyl can afford triphenylene in the presence of iodine (Scheme 7.1, eq 2).²⁵

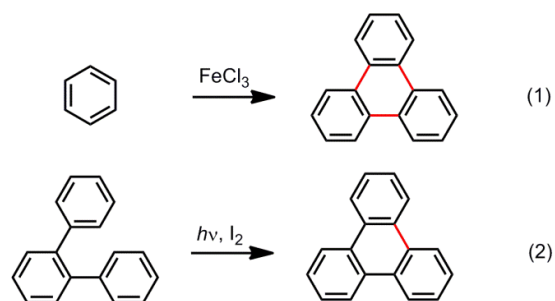
²² Pérez, D.; Guitián, E., "Selected Strategies for the Synthesis of Triphenylenes," *Chemical Society Reviews* **2004**, 33, 274-283.

²³ Kumar, S.; Manickam, M., "Oxidative Trimerization of O-Dialkoxybenzenes to Hexaalkoxytriphenylenes: Molybdenum(V) Chloride as a Novel Reagent," *Chemical Communications* **1997**, 1615-1666.

²⁴ Kumar, S.; Varshney, S. K., "Synthesis of Triphenylene and Dibenzopyrene Derivatives: Vanadium Oxytrichloride a Novel Reagent," *Synthesis* **2001**, 2001, 0305-0311.

²⁵ Sato, T.; Shimada, S.; Hata, K., "A New Route to Polycondensed Aromatics: Photolytic Formation of Triphenylene and Dibenzo[*fg,op*]Naphthacene Ring Systems," *Bulletin of the Chemical Society of Japan* **1971**, 44, 2484-2490

Scheme 7.1 Synthesis of Triphenylene by Oxidative Dehydrogenation



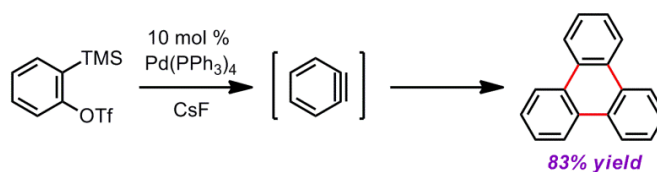
Transition-metal (TM) catalyzed reactions also have been developed to prepare the triphenylene skeleton from benzyne. Pérez and Guitián have shown that triphenylene can be synthesized by the cyclotrimerization of benzyne, which is generated from 2-(trimethylsilyl)phenyl triflate in situ, in the presence of a palladium(0) catalyst and cesium fluoride (83% yield, Scheme 7.2).²⁶ This catalytic method has been applied to the synthesis of various substituted triphenylenes.^{27,28}

²⁶ Peña, D.; Escudero, S.; Pérez, D.; Guitián, E.; Castedo, L., "Efficient Palladium-Catalyzed Cyclotrimerization of Arynes: Synthesis of Triphenylenes," *Angewandte Chemie International Edition* **1998**, *37*, 2659-2661.

²⁷ (a) Peña, D.; Pérez, D.; Guitián, E.; Castedo, L., "Synthesis of Hexabenzotriphenylene and Other Strained Polycyclic Aromatic Hydrocarbons by Palladium-Catalyzed Cyclotrimerization of Arynes," *Organic Letters* **1999**, *1*, 1555-1557. (b) Peña, D.; Cobas, A.; Pérez, D.; Guitián, E.; Castedo, L., "Kinetic Control in the Palladium-Catalyzed Synthesis of C_2 -Symmetric Hexabenzotriphenylene. A Conformational Study," *Organic Letters* **2000**, *2*, 1629-1632. (c) Peña, D.; Pérez, D.; Guitián, E.; Castedo, L., "Selective Palladium-Catalyzed Cocyclotrimerization of Arynes with Dimethyl Acetylenedicarboxylate: A Versatile Method for the Synthesis of Polycyclic Aromatic Hydrocarbons," *The Journal of Organic Chemistry* **2000**, *65*, 6944-6950

²⁸ (a) Peña, D.; Cobas, A.; Pérez, D.; Guitián, E.; Castedo, L., "Dibenzo[a,o]Phenanthro[3,4-s]Pycene, a Configurationally Stable Double Helicene: Synthesis and Determination of Its Conformation by Nmr and Giau Calculations," *Organic Letters* **2003**, *5*, 1863-1866. (b) Iglesias, B.; Cobas, A.; Pérez, D.; Guitián, E.; Vollhardt, K. P. C., "Tris(Benzocyclobutadieno)Triphenylene and Its Lower Biphenylene Homologues by Palladium-Catalyzed Cyclizations of 2,3-Didehydrobiphenylene," *Organic Letters* **2004**, *6*, 3557-3560. (c)

Scheme 7.2 Trimerization of Benzyne

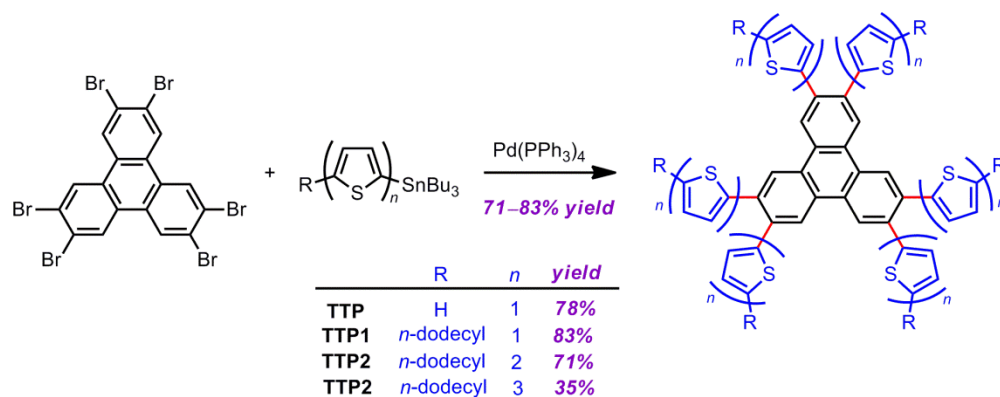


The synthetic route for the functionalized triphenylenes, which was reported by the Chi group, is shown in Scheme 7.3.²⁹ A series of triphenylenes that are derivatized with thiophene (**TTP**, **TTP1**, **TTP2**, and **TTP3**) are synthesized by six-fold Stille coupling reactions from hexabromotriphenylene in good yields. The crystal structure of **TTP** revealed that the molecules are stacked in a one-dimensional columnar structure. In the structure of **TTP1**, however, the molecules are further self-assembled into three-dimensional packed structures, due to the presence of weak interactions (for example, π - π , C-H \cdots S, and C-H \cdots π interactions). It is also observed that the absorptions of compounds **TTP2** and **TTP3** are red shifted by 36 nm and 66 nm, along with the increase in conjugation.

Romero, C.; Peña, D.; Pérez, D.; Guitián, E., "Synthesis of Extended Triphenylenes by Palladium-Catalyzed [2+2+2] Cycloaddition of Triphenylnes," *Chemistry—A European Journal* **2006**, *12*, 5677-5684.

²⁹ Luo, J.; Zhao, B.; On Chan, H. S.; Chi, C., "Synthesis, Physical Properties and Self-Assembly of Star-Shaped Oligothiophenes-Substituted and Fused Triphenylenes," *Journal of Materials Chemistry* **2010**, *20*, 1932-1941.

Scheme 7.3 Preparation of Functionalized Triphenylenes



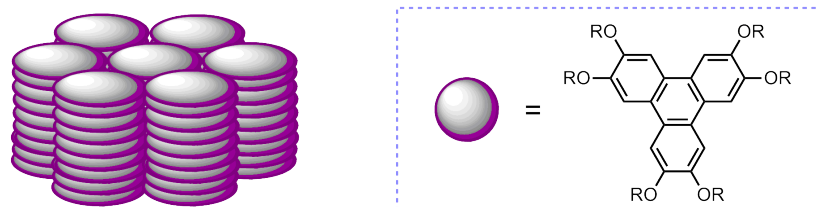
The ordered self-assembling properties render these star-shaped oligomers good candidates for columnar liquid crystal materials. Indeed, triphenylenes are often found at the core of various discotic liquid crystals.^{30,31} As illustrated in Figure 7.4, one triphenylene unit consists of a single disc in the liquid crystalline columns.³² The peripheral long alkyl (R) chains of triphenylenes help the molecules to stay in solution. One of the most popular applications of these crystals would be liquid crystal displays (LCDs).

³⁰ (a) Boden, N.; Bushby, R.; Clements, J., "Mechanism of Quasi-One-Dimensional Electronic Conductivity in Discotic Liquid Crystals," *The Journal of Chemical Physics* **1993**, *98*, 5920-5931. (b) Chandrasekhar, S., "Discotic Liquid Crystals. A Brief Review," *Liquid Crystals* **1993**, *14*, 3-14. (c) Yamamura, K.; Ono, S.; Ogoshi, H.; Masuda, H.; Kuroda, Y., "Chiral Liquid Crystal Mesogens. Synthesis and Determination of Absolute Configuration of Mesogens with 4,4'-Biphenanthryl Cores," *Synlett* **2002**, 1889, 18-19.

³¹ (a) Wright, P. T.; Gillies, I.; Kilburn, J. D., "A Modified Procedure for the Synthesis of C₃-Symmetric 'Mixed-Tail' Triphenylenes," *Synthesis* **1997**, 1997, 1007-1009. (b) Kumar, S.; Manickam, M., "Oxidative Trimerization of *o*-Dialkoxybenzenes Tohexaalkoxytriphenylenes: Molybdenum(V) Chloride as a Novel Reagent," *Chemical Communications*. **1997**, 1615-1666.

³² Sergeyev, S.; Pisula, W.; Geerts, Y. H., "Discotic Liquid Crystals: A New Generation of Organic Semiconductors," *Chemical Society Reviews* **2007**, *36*, 1902-1929.

Figure 7.4 Discotic Liquid Crystals



7.2.2. Star-Shaped Oligomers with a Truxene Core

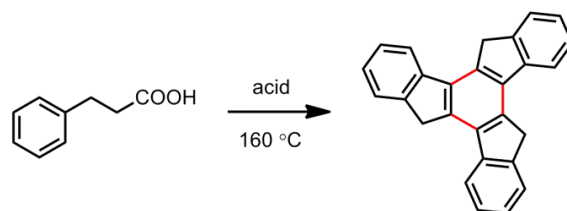
Among various polycyclic aromatic hydrocarbons (PAHs), fluorene (or 9*H*-fluorene, C₁₃H₁₀) is one of the most common units that are used in organic light-emitting diodes (OLEDs).³³ Truxenes are C₃-symmetric molecules, which consist of three overlapping fluorene units, and are known to be one of the most compelling PAHs for organic optoelectronic materials.³⁴ A classical method for the truxene synthesis is depicted in Scheme 7.4; 3-phenylpropanoic acid can be trimerized to truxene at 160 °C under acidic conditions.³⁵

³³ Xie, L.-H.; Liang, J.; Song, J.; Yin, C.-R.; Huang, W., "Spirocyclic Aromatic Hydrocarbons (SAHs) and Their Synthetic Methodologies," *Current Organic Chemistry* **2010**, *14*, 2169-2195.

³⁴ Chen, J.-H.; Wang, S.-A.; Liu, Y.-H.; Wong, K.-T., "Synthesis and Properties of Novel C₃-Symmetric Coplanar Chromophores," *Organic Letters* **2011**, *13*, 4168-4171.

³⁵ (a) Kipping, F. S., "Xxix. The Formation of the Hydrocarbon "Truxene" from Phenylpropionic Acid, and from Hydrindone," *Journal of the Chemical Society, Transactions* **1894**, *65*, 269-290. (b) Yuan, M.-S.; Fang, Q.; Liu, Z.-Q.; Guo, J.-P.; Chen, H.-Y.; Yu, W.-T.; Xue, G.; Liu, D.-S., "Acceptor or Donor (Diaryl B or N) Substituted Octupolar Truxene: Synthesis, Structure, and Charge-Transfer-Enhanced Fluorescence," *The Journal of Organic Chemistry* **2006**, *71*, 7858-7861.

Scheme 7.4 Synthesis of Truxene

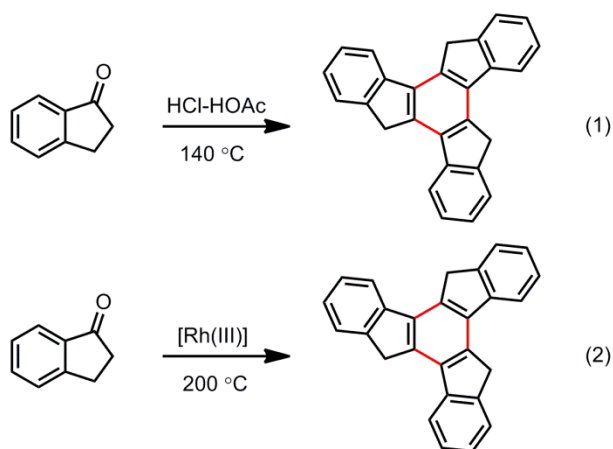


Another synthetic route to truxene, which was reported by the Scott group, employs 1-indanone as a starting material (Scheme 7.5, eq 1).³⁶ In the presence of a Brønsted acid (or Lewis acid), truxene can be prepared from 1-indanone via triple aldol condensation reactions. In addition, 1-indanone can be transformed to truxene in the presence of a catalytic amount of rhodium(III) complex, as demonstrated by the Naota group (Scheme 7.5, eq 2).³⁷

³⁶ (a) Amick, A. W.; Scott, L. T., "Trisannulated Benzene Derivatives by Acid Catalyzed Aldol Cyclotrimerizations of Cyclic Ketones. Methodology Development and Mechanistic Insight," *The Journal of Organic Chemistry* **2007**, *72*, 3412-3418. (b) Amick, A. W.; Griswold, K. S.; Scott, L. T., "Synthesis and Aldol Cyclotrimerization of 4,7-Di-*Tert*-Butylacenaphthenone," *Canadian Journal of Chemistry* **2006**, *84*, 1268-1272. (c) Dehmlow, E. V.; Kelle, T., "Synthesis of New Truxene Derivatives: Possible Precursors of Fullerene Partial Structures?," *Synthetic Communications* **1997**, *27*, 2021-2031.

³⁷ (a) Terai, H.; Takaya, H.; Naota, T., "Rhodium-Catalyzed Direct Aldol Condensation of Ketones: A Facile Synthesis of Fused Aromatic Compounds," *Tetrahedron Letters* **2006**, *47*, 1705-1708. (b) Rybinskaya, M. I.; Kudinov, A. R.; Kaganovich, V. S., "A New Preparative Route to Cationic Arene Complexes of Ruthenium(II), Rhodium(III) and Iridium(III)," *Journal of Organometallic Chemistry* **1983**, *246*, 279-285.

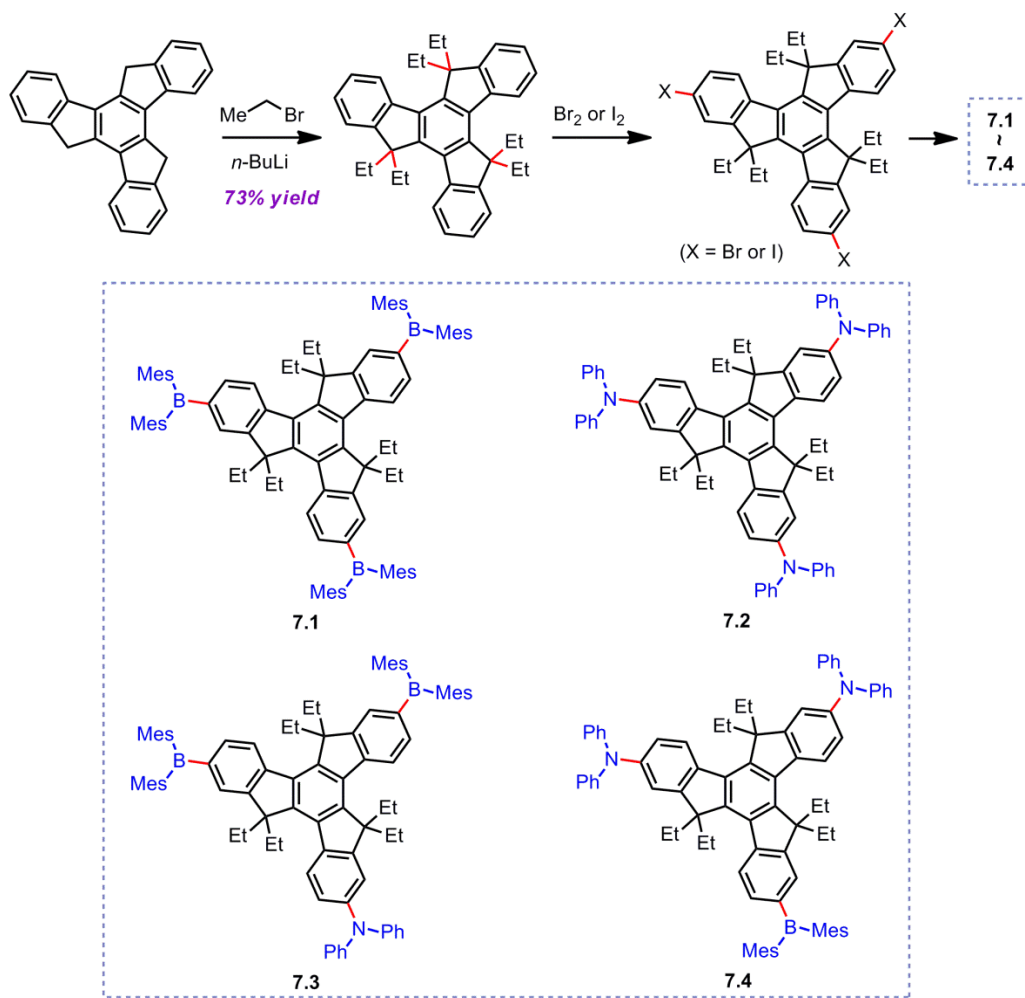
Scheme 7.5 Synthesis of Truxene from 1-Indanone



Some derivatives of truxenes have been synthesized by the Fang group to demonstrate both inter- and intramolecular donor-acceptor interactions (Scheme 7.6).^{35b, 38} The targeted molecules (7.1 to 7.4) are synthesized by alkylations and subsequent halogenations of truxene. Compound 7.1 is an acceptor-substituted truxene, and compound 7.2 is a donor-substituted truxene; these two compounds were used to examine intermolecular donor-acceptor interactions.

³⁸ Yuan, M.-S.; Liu, Z.-Q.; Fang, Q., "Donor-and-Acceptor Substituted Truxenes as Multifunctional Fluorescent Probes," *The Journal of Organic Chemistry* **2007**, *72*, 7915-7922.

Scheme 7.6 Preparation of Functionalized Truxenes

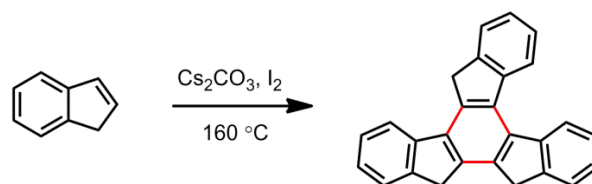


On the other hand, compounds 7.3 and 7.4 possess both donor and acceptor substituents; hence, the intramolecular donor–acceptor interactions were examined with these two compounds. These studies employed UV-Vis spectroscopy to analyze the properties of these compounds (7.1 to 7.4), and the spectral data were interpreted based on the expected donor–acceptor interactions of the substituents on the truxene derivatives.

7.2.3. Star-Shaped Oligomers with an Isotruxene Core

Isotruxene, an isomer of truxene, can be synthesized by the cyclotrimerization of 1*H*-indene in the presence of cesium carbonate and iodine (Scheme 7.7).³⁹ There are additional reports on the synthesis of isotruxenes and the examination of their properties.^{40, 41} Notably, it has been observed that isotruxenes showed similar absorption and fluorescence spectra as those of truxenes in these studies. However, a difference between truxenes and isotruxenes was found in their two-photon absorption cross sections; the cross section of isotruxene-cored compounds was larger than that of truxene derivatives.^{40c}

Scheme 7.7 Synthesis of Isotruxene



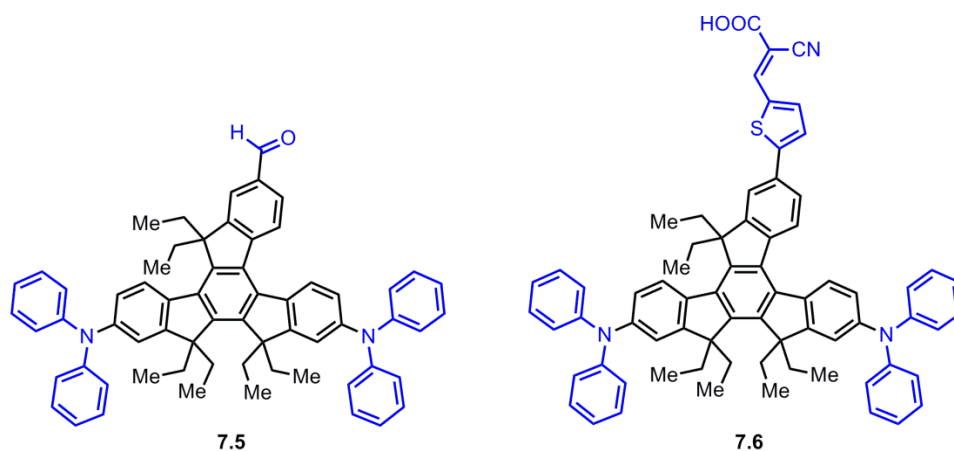
³⁹ Yang, J.-S.; Lee, Y.-R.; Yan, J.-L.; Lu, M.-C., "Synthesis and Properties of a Fluorene-Capped Isotruxene: A New Unsymmetrical Star-Shaped π -System," *Organic Letters* **2006**, *8*, 5813-5816.

⁴⁰ (a) Yang, J.-S.; Huang, H.-H.; Lin, S.-H., "Facile Multistep Synthesis of Isotruxene and Isotruxenone⁺," *The Journal of Organic Chemistry* **2009**, *74*, 3974-3977. (b) Yang, J.-S.; Huang, H.-H.; Ho, J.-H., "Electronic Properties of Star-Shaped Oligofluorenes Containing an Isotruxene Core: Interplay of Para and Ortho Conjugation Effects in Phenylene-Based π Systems," *The Journal of Physical Chemistry B* **2008**, *112*, 8871-8878. (c) Fujitsuka, M.; Cho, D. W.; Huang, H.-H.; Yang, J.-S.; Majima, T., "Structural Relaxation in the Singlet Excited State of Star-Shaped Oligofluorenes Having a Truxene or Isotruxene as a Core," *The Journal of Physical Chemistry B* **2011**, *115*, 13502-13507.

⁴¹ (a) Yang, J.-S.; Huang, H.-H.; Liu, Y.-H.; Peng, S.-M., "Synthesis and Electronic Properties of Isotruxene-Derived Star-Shaped Ladder-Type Oligophenylenes: Bandgap Tuning with Two-Dimensional Conjugation," *Organic Letters* **2009**, *11*, 4942-4945. (b) Huang, H.-H.; Prabhakar, C.; Tang, K.-C.; Chou, P.-T.; Huang, G.-J.; Yang, J.-S., "Ortho-Branched Ladder-Type Oligophenylenes with Two-Dimensionally Π -Conjugated Electronic Properties," *Journal of the American Chemical Society* **2011**, *133*, 8028-8039.

Figure 7.5 illustrates some of the isotruxene derivatives that were synthesized by the Yang group.⁴² Compound 7.5 was prepared from a dibromo-isotruxene derivative in two steps (*i.e.* a formylation followed by Buchwald–Hartwig cross coupling reactions). A thiophene-based isotruxene derivative 7.6 was prepared from the same starting material but in five steps. Their studies revealed that both of the compounds (7.5 and 7.6) can function as organic dye sensitizers and can be applied in dye-sensitized solar cell (DSSC) devices.

Figure 7.5 Functionalized Isotruxenes



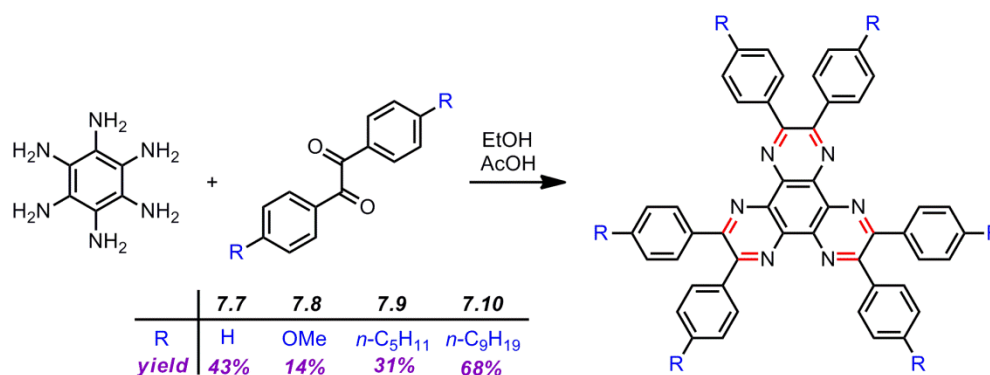
7.2.4. Star-Shaped Oligomers with a Hexaazatriphenylene (HAT) Core

After a number of organic semiconductors have been prepared with various polycyclic aromatic hydrocarbons (PAHs), interests have been extended to a class of *N*-hetero-PAHs. Generally, these *N*-hetero-PAHs are synthesized by the condensation of

⁴² Lin, S.-H.; Hsu, Y.-C.; Lin, J. T.; Lin, C.-K.; Yang, J.-S., "Isotruxene-Derived Cone-Shaped Organic Dyes for Dye-Sensitized Solar Cells," *The Journal of Organic Chemistry* **2010**, *75*, 7877-7886.

aromatic amines with 1,2-diketones.⁴³ The Praefcke group has synthesized six-armed *N*-hetero-triphenylenes by the three-fold condensation starting from benzene-1,2,3,4,5,6-hexamine and various 1,2-diketones (compounds **7.7** to **7.10**, Scheme 7.8).⁴⁴

Scheme 7.8 Preparation of Hexaazatriphenylene Derivatives



The properties of these hexaazatriphenylene derivatives have been explored by several research groups in various contexts. Lehn and co-workers reported that compound **7.7** can be utilized for the formation of supramolecular architectures of nanometric size in combination with bis-bipyridyl and a copper cation.⁴⁵ In addition, the Bushby group

⁴³ (a) Slepko, A. D.; Hegmann, F. A.; Tykwinski, R. R.; Kamada, K.; Ohta, K.; Marsden, J. A.; Spitler, E. L.; Miller, J. J.; Haley, M. M., "Two-Photon Absorption in Two-Dimensional Conjugated Quadrupolar Chromophores," *Optics Letters* **2006**, *31*, 3315-3317. (b) Aumiller, W. D.; Dalton, C. R.; Czarnik, A. W., "Preparatively Useful Oxidation Reactions of Hexamethylhexaazatriphenylene," *The Journal of Organic Chemistry* **1995**, *60*, 728-729.

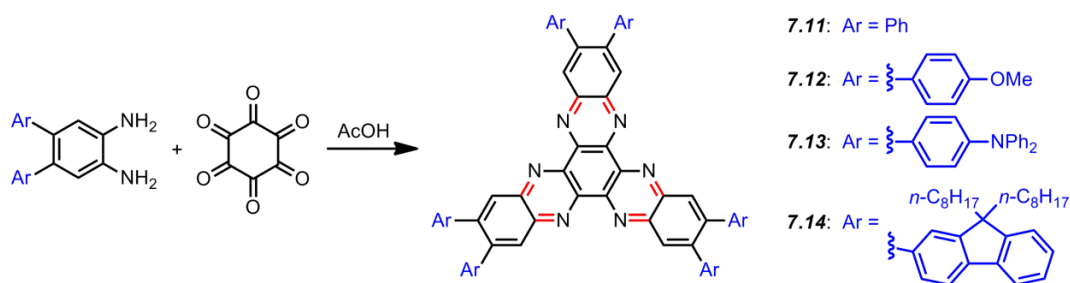
⁴⁴ Kohne, B.; Praefcke, K., "Eine Neue Und Einfache Synthese Des Dipyrzino [2, 3-F: 2', 3' -H]-Chinoxalin-Ringsystems," *Liebigs Annalen der Chemie* **1985**, *1985*, 522-528.

⁴⁵ (a) Baxter, P. N. W.; Lehn, J.-M.; Kneisel, B. O.; Baum, G.; Fenske, D., "The Designed Self-Assembly of Multicomponent and Multicompartamental Cylindrical Nanoarchitectures," *Chemistry—A European Journal* **1999**, *5*, 113-120. (b) Baxter, P.; Lehn, J.-M.; Decian, A.; Fischer, J., "Selbstorganisation Von Multikomponenten-Systemen: Spontane Bildung Eines Zylinderförmigen Komplexes Aus Fünf Liganden Und Sechs Metall-Ionen," *Angewandte Chemie* **1993**, *105*, 92-95.

demonstrated that a mixture of compound **7.10** and triphenylene exhibits a mesophase between 130 °C and 240 °C along with a hexagonal columnar structure.⁴⁶

Another synthetic route to these *N*-hetero star-shaped compounds was reported by Gao and co-workers (Scheme 7.9).⁴⁷ The three-fold condensation reactions between *ortho*-diaminobenzenes and cyclohexane-1,2,3,4,5,6-hexone afford the corresponding hexaazatriphenylenes (HATs, compounds **7.11** to **7.14**) in high yields (70 to 85% yields). In the studies, the compounds (**7.11** to **7.14**) were examined by electronic spectra and with potential measurements.

Scheme 7.9 Preparation of Functionalized Hexaazatriphenylene



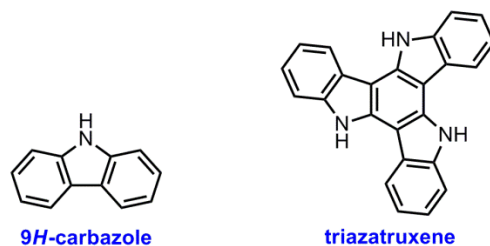
⁴⁶ (a) Arikainen, E. O.; Boden, N.; Bushby, R. J.; Lozman, O. R.; Vinter, J. G.; Wood, A., "Complimentary Polytopic Interactions," *Angewandte Chemie International Edition* **2000**, 39, 2333-2336. (b) Bushby, R. J.; Fisher, J.; Lozman, O. R.; Lange, S.; Lydon, J. E.; McLaren, S. R., "The Stability of Columns Comprising Alternating Triphenylene and Hexaphenyltriphenylene Molecules: Variations in the Structure of the Hexaphenyltriphenylene Component," *Liquid Crystals* **2006**, 33, 653-664.

⁴⁷ Gao, B.; Liu, Y.; Geng, Y.; Cheng, Y.; Wang, L.; Jing, X.; Wang, F., "Starburst Substituted Hexaazatriphenylene Compounds: Synthesis, Photophysical and Electrochemical Properties," *Tetrahedron Letters* **2009**, 50, 1649-1652.

7.2.5. Star-Shaped Oligomers with a Triazatruxene Core

Carbazole-based oligomeric and polymeric materials are known as excellent hole-transporting units mainly due to the electron-donating abilities of the nitrogen atom.⁴⁸ These materials have been investigated for the last couple of decades and have various applications in light-harvesting devices and molecular electronics. Triazatruxene is composed of three overlapping carbazole units (Figure 7.6) that function as electron-donating units for π -conjugated branches (e.g. oligofluorenes) to improve hole injection and transport.²¹

Figure 7.6 Carbazole and Triazatruxene



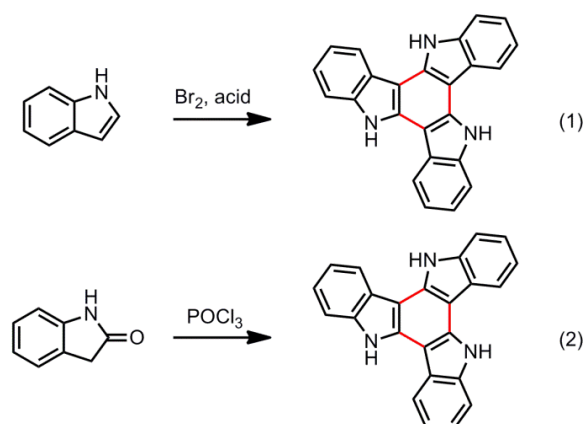
The synthesis of triazatruxene is usually performed by the trimerization of indole in the presence of bromine and an acid (Scheme 7.10, eq 1).⁴⁹ Alternatively, it can be synthesized

⁴⁸ Morin, J. F.; Leclerc, M.; Adès, D.; Siove, A., "Polycarbazoles: 25 Years of Progress," *Macromolecular Rapid Communications* **2005**, *26*, 761-778.

⁴⁹ Bocchi, V.; Palla, G., "Synthesis and Characterization of New Indole Trimers and Tetramers," *Tetrahedron* **1986**, *42*, 5019-5024.

by trimerizing 2-indolone with phosphoryl chloride (POCl_3), as reported by the Franceschin group (Scheme 7.10, eq 2).⁵⁰

Scheme 7.10 Synthesis of Triazatruxene



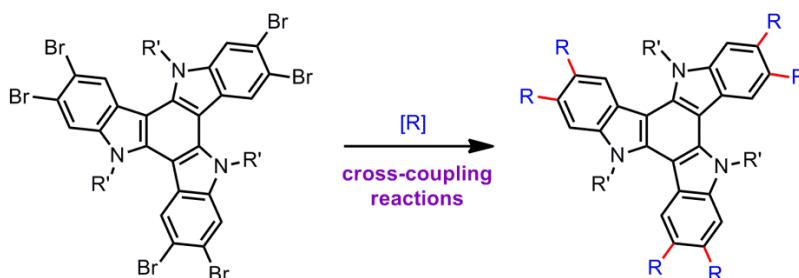
Since functionalized triazatruxenes exhibit unique optoelectronic properties, various triazatruxene derivatives have been prepared and examined. Generally, triazatruxenes derivatives are synthesized from hexabromotriazatruxene (Scheme 7.11).⁵¹ Various cross-coupling reactions, such as Stille,⁵² Sonogashira,⁵³ or Suzuki⁵⁴ coupling, can attach the conjugated arms to the core triazatruxene structure.

⁵⁰ Franceschin, M.; Ginnari-Satriani, L.; Alvino, A.; Ortaggi, G.; Bianco, A., "Study of a Convenient Method for the Preparation of Hydrosoluble Fluorescent Triazatruxene Derivatives," *European Journal of Organic Chemistry* **2010**, 2010, 134-141.

⁵¹ Robertson, N.; Parsons, S.; MacLean, E. J.; Coxall, R. A.; Mount, A. R., "Preparation, X-Ray Structure and Properties of a Hexabrominated, Symmetric Indole Trimer and Its TCNQ Adduct: A New Route to Functional Molecular Systems," *Journal of Materials Chemistry* **2000**, 10, 2043-2047.

⁵² Luo, J.; Zhao, B.; Shao, J.; Lim, K. A.; On Chan, H. S.; Chi, C., "Room-Temperature Discotic Liquid Crystals Based on Oligothiophenes-Attached and Fused Triazatruxenes," *Journal of Materials Chemistry* **2009**, 19, 8327-8334.

Scheme 7.11 Preparation of Triazatruxene Derivatives



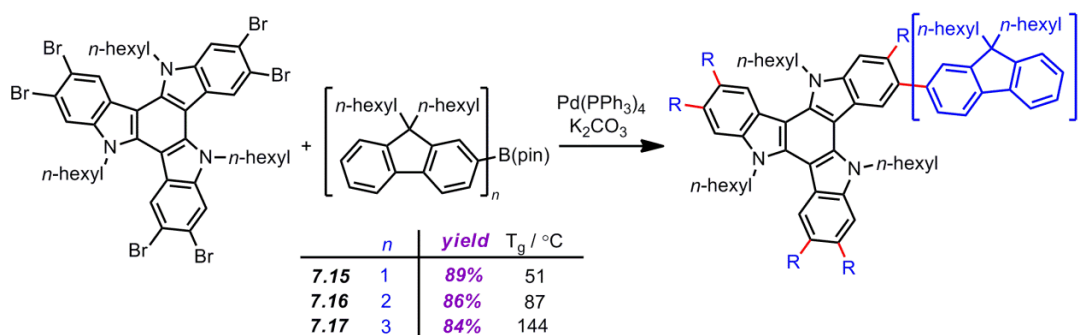
Some of six-armed triazatruxene derivatives have been synthesized by the Huang and co-workers (Scheme 7.11).⁵⁵ In this report, the desired products were prepared by the microwave-assisted sextuple Suzuki coupling reactions. Hexabromotriazatruxene was coupled with oligomeric fluorenyl boronic acids to furnish the first (7.15), second (7.16), and third (7.17) generation in 89%, 86%, and 84% yields, respectively.

⁵³ Gomez-Lor, B.; Alonso, B.; Omenat, A.; Serrano, J. L., "Electroactive C_3 Symmetric Discotic Liquid-Crystalline Triindoles," *Chemical Communications* **2006**, 5012-5014.

⁵⁴ Hiyosbi, H.; Kumagai, H.; Ooi, H.; Sonoda, T.; Mataka, S., "Donor- π -Acceptor Type Symmetric Cyclic Triindoles: Synthesis and Properties," *Heterocycles* **2007**, 72, 231-238.

⁵⁵ Lai, W.-Y.; Chen, Q.-Q.; He, Q.-Y.; Fan, Q.-L.; Huang, W., "Microwave-Enhanced Multiple Suzuki Couplings toward Highly Luminescent Starburst Monodisperse Macromolecules," *Chemical Communications* **2006**, 1959-1961.

Scheme 7.12 Preparations and Properties of Six-Armed Triazatruxenes



The optoelectronic properties of these compounds have been also investigated by the same group.⁵⁶ As the generation (*i.e.* the value of *n*) is increased, the absorption maximum is shifted to the lower energies. In the fluorescence experiments, a small redshift was observed from the 1st to the 2nd generation. Finally, these six-armed star compounds form amorphous solids with glass transition temperatures at 51 °C for the 1st, 87 °C for the 2nd, and 144 °C for the 3rd generation.

7.2.6. Summary

Some representative examples of star-shaped π -conjugated oligomers have been presented. The star-shaped oligomers possess better solubility and film-forming properties,

⁵⁶ (a) Lai, W. Y.; He, Q. Y.; Zhu, R.; Chen, Q. Q.; Huang, W., "Kinked Star-Shaped Fluorene/Triazatruxene Co-Oligomer Hybrids with Enhanced Functional Properties for High-Performance, Solution-Processed, Blue Organic Light-Emitting Diodes," *Advanced Functional Materials* **2008**, *18*, 265-276. (b) Lai, W.-Y.; Zhu, R.; Fan, Q.-L.; Hou, L.-T.; Cao, Y.; Huang, W., "Monodisperse Six-Armed Triazatruxenes: Microwave-Enhanced Synthesis and Highly Efficient Pure-Deep-Blue Electroluminescence," *Macromolecules* **2006**, *39*, 3707-3709. (c) Levermore, P. A.; Xia, R.; Lai, W.; Wang, X. H.; Huang, W.; Bradley, D. D. C., "Deep-Blue Light Emitting Triazatruxene Core/Oligo-Fluorene Branch Dendrimers for Electroluminescence and Optical Gain Applications," *Journal of Physics D: Applied Physics* **2007**, *40*, 1896.

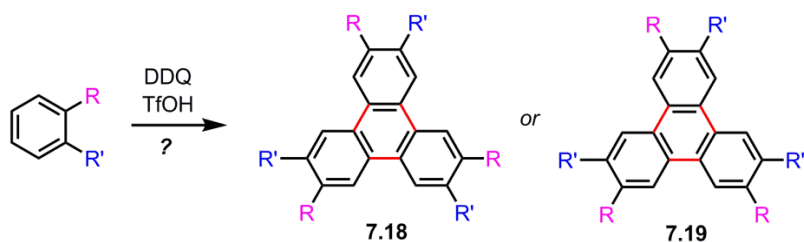
compared to the corresponding linear conjugated chains. These [n]stars have a wide range of applications in materials science, such as solar cells, field-effect transistors, light-emitting diodes, etc. Their ability of self-organizing and π stacking in crystals and liquid crystals are certainly noteworthy. It is certainly expected that coordinated efforts from multiple disciplines will be continuously made to synthesize and utilize these materials in various areas.

7.3. Method Development

7.3.1. Project Goals

During our investigations on the oxidative cyclotrimerization reactions leading to symmetrical trimers (as described in Chapter 6), we were also interested in employing substrates containing two different substituents (Scheme 7.13). The reactions of a monomer containing two different substituents would afford either a C_3 symmetrical trimer (7.18) or an unsymmetrical trimer (7.19). Furthermore, the regioselectivity of this process would provide deeper insights into the detailed mechanism of this process.

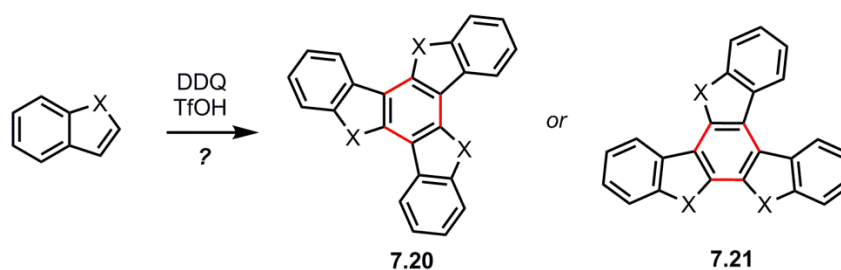
Scheme 7.13 Oxidative Coupling toward Triphenylene Derivatives



Also, we were interested in whether heterocyclic aromatic compounds, such as benzofuran, benzothiophene, or indole, would participate in this type of process. As described in Scheme 7.14, the oxidative cyclotrimerization reactions with these heterocycles could afford either symmetric truxene derivatives (7.20) or unsymmetrical isotruxene derivatives (7.21). The development of these processes would provide a novel synthetic

method to access symmetrical or unsymmetrical oligomers, which are useful as building blocks for various organic materials.

Scheme 7.14 Oxidative Coupling toward Truxene/Isotruxene Derivatives

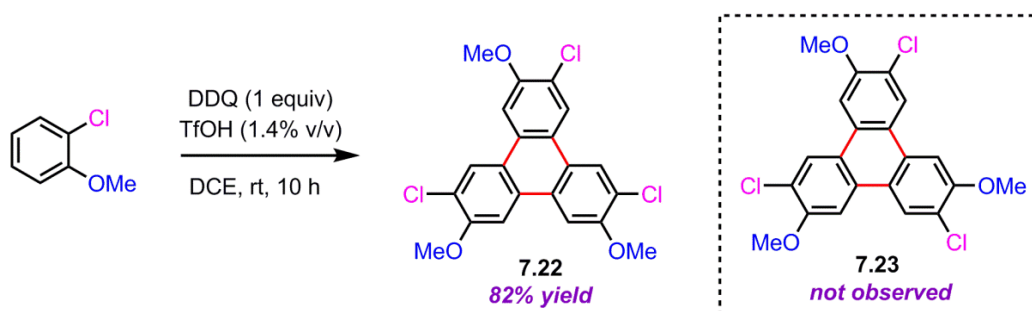


7.3.2. Oxidation toward Triphenylene Derivatives

7.3.2.1. Survey of Halogenated Anisoles

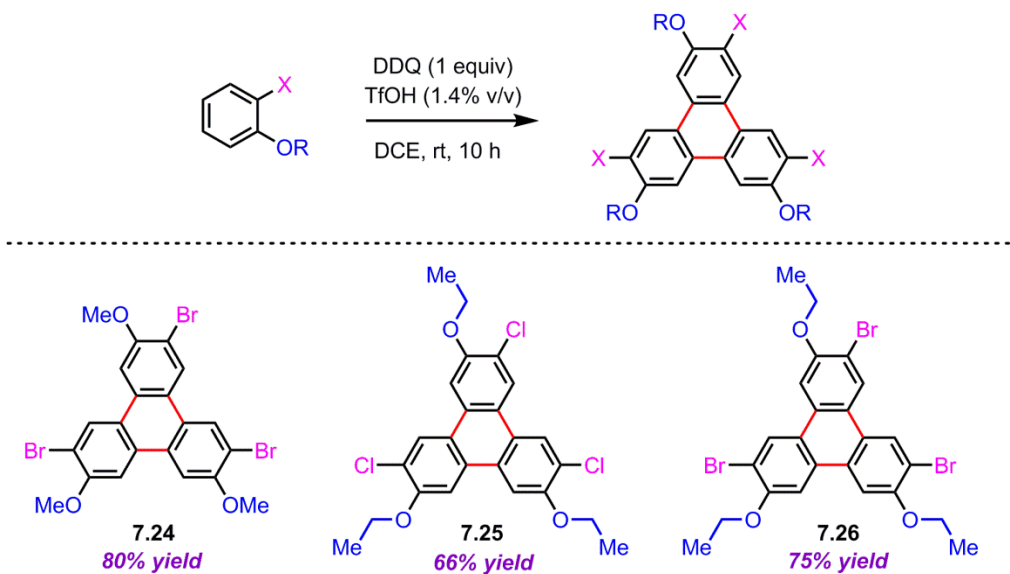
Our initial investigations involved oxidation reactions toward halogenated triphenylene derivatives. We chose halogenated anisoles as a starting material because they have both an electron-donating group (*i.e.* methoxy group) and a halogen that can be further functionalized. When 2-chloroanisole was subjected to the DDQ/TfOH oxidation reaction (1 equiv of DDQ and 1.4% v/v of trifluoromethanesulfonic acid), an unsymmetrical trimer (7.22) was obtained in 82% yield (Scheme 7.15). The reaction was highly regioselective; we did not observe the formation of a symmetrical trimer (7.23) from this process.

Scheme 7.15 Oxidative Cyclotrimerization of 2-Chloroanisole



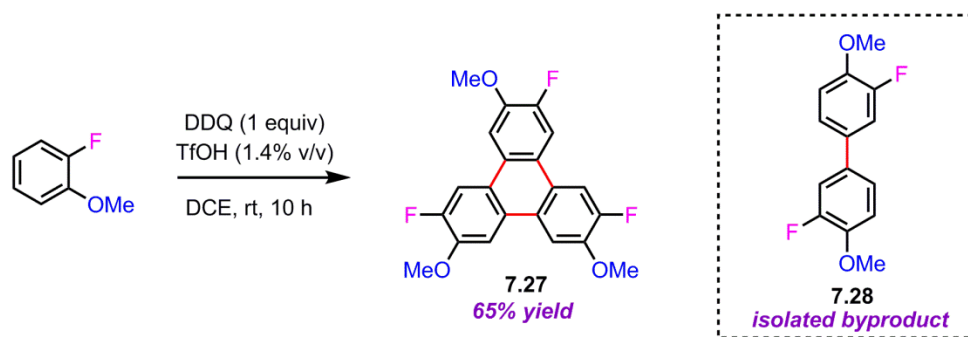
We also examined other halogenated anisoles and halogenated phenetoles (ethoxy benzenes). When 2-bromoanisole was subjected to the DDQ/acid reaction (1 equiv of DDQ and 1.4% v/v of TfOH), the corresponding unsymmetrical trimer (**7.24**) was obtained in 80% yield (Scheme 7.16). The reaction with 2-chlorophenetole afforded the unsymmetrical trimer (**7.25**) in 66% yield under the DDQ/triflic acid oxidation condition. In addition, when 2-bromophenetole was subjected to the DDQ/acid oxidation reaction, the corresponding trimer (**7.26**) was afforded in 75% yield.

Scheme 7.16 Oxidative Cyclotrimerization of Halogenated Anisoles and Phenetoles



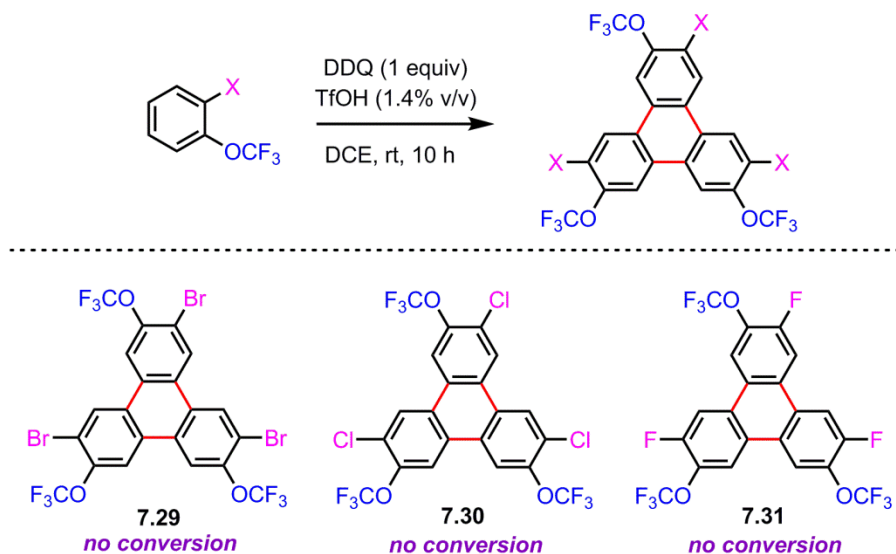
In order to obtain more information on the mechanistic pathway, we isolated a byproduct from the oxidation reaction with 2-fluoroanisole (Scheme 7.17). When 2-fluoroanisole was employed as a starting material in the DDQ/acid oxidative coupling reaction (with 1 equiv of DDQ and 1.4% v/v of TfOH), the corresponding unsymmetrical trimer (**7.27**) was obtained in 65% yield. The byproduct of this reaction turned out to be compound **7.28**; the identity of this compound provided more details on the reaction mechanism (see Section 7.4).

Scheme 7.17 Oxidative Cyclotrimerization of 2-Fluoroanisole



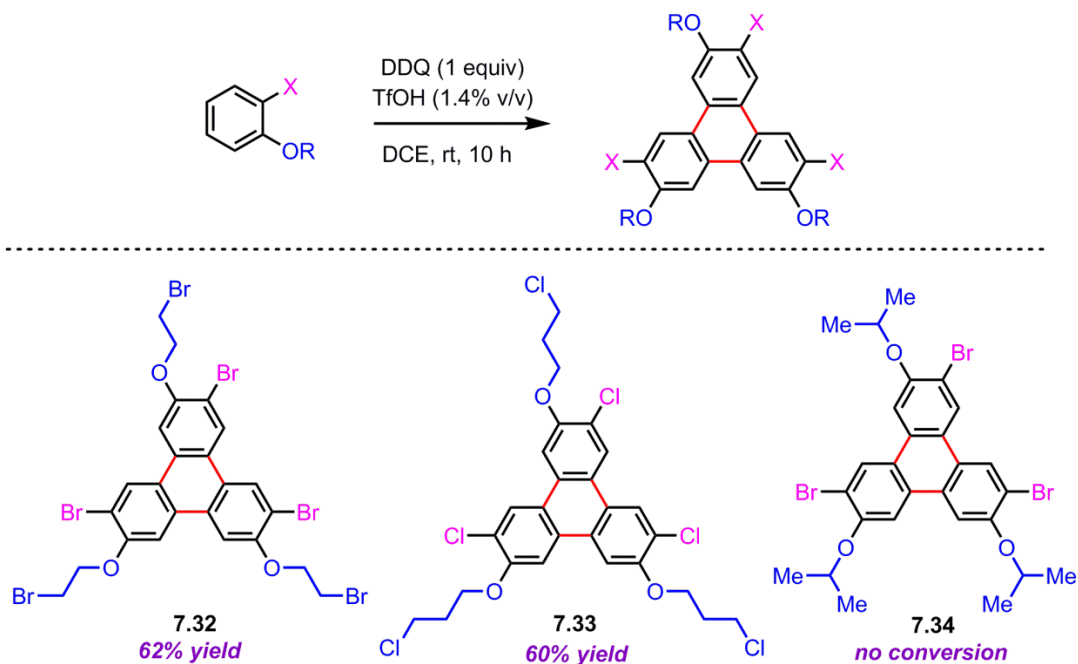
We also examined trifluoromethoxy benzenes to see whether they would have similar reactivity toward the intermolecular oxidative coupling reactions. As shown in Scheme 7.18, none of the halogenated trifluoromethoxy benzenes that were examined afforded cyclic trimers (**7.29**, **7.30** or **7.31**) in the oxidation reaction with DDQ and triflic acid. We speculated that the problem with these substrates is related to the insufficient electron-donating ability of the trifluoromethoxy groups.

Scheme 7.18 Oxidative Cyclotrimerization of Halogenated Trifluoromethoxy Benzenes



The reactivity of some alkyl-halogenated anisole derivatives toward the intermolecular oxidative cyclotrimerization reactions was examined (Scheme 7.19). When 1-(2-bromoethoxy)-2-bromobenzene was subjected to the DDQ/triflic acid oxidation reaction, the corresponding trimer (**7.32**) was afforded in good yield (62% yield). The reaction with 1-(3-chloropropoxy)-2-chlorobenzene afforded the corresponding trimerized product (**7.33**) in 60% yield. However, the reaction with 1-bromo-2-(isopropoxy)benzene did not give the desired product (**7.34**) under the DDQ/triflic acid oxidation condition.

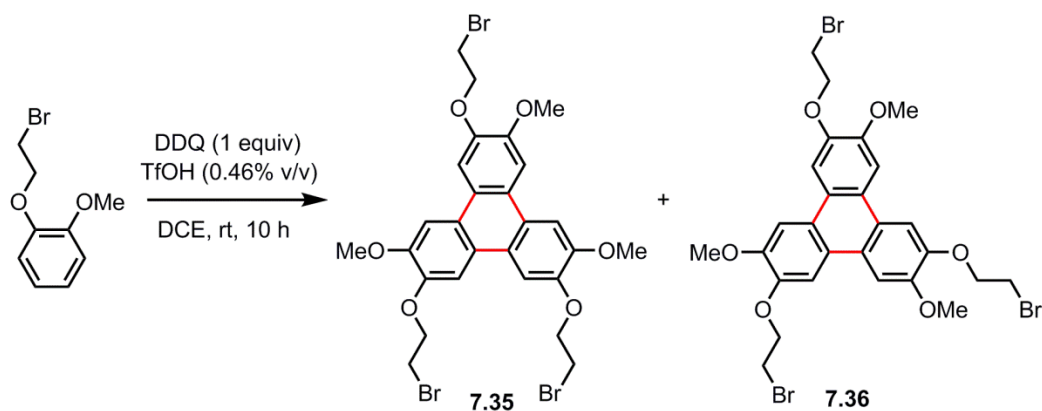
Scheme 7.19 Oxidative Cyclotrimerization of Halogenated Anisole Derivatives



7.3.2.2. Survey of Substituted Aromatic Compounds

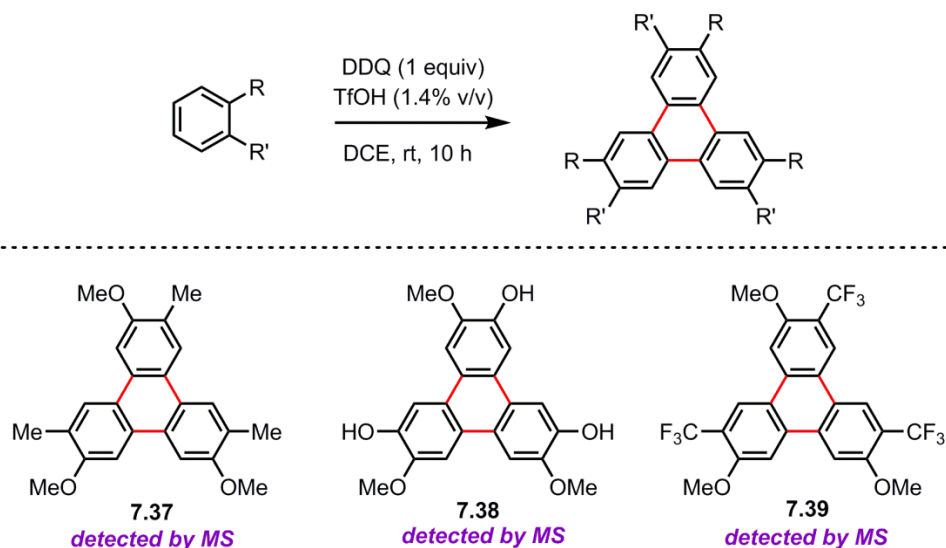
The reactivity of a dialkoxybenzene, 2-(2-bromoethoxy)anisole, toward the oxidative cyclotrimerization process was examined (Scheme 7.20). When 2-(2-bromoethoxy)anisole was employed as a starting material for the DDQ/acid oxidation reaction, both the corresponding unsymmetrical trimer (7.35) and the symmetrical trimer (7.36) were formed in 60% yield; the ratio of the two regioisomers was 9:1 (unsymmetrical: symmetrical).

Scheme 7.20 Oxidative Cyclotrimerization of Dialkoxy Benzene



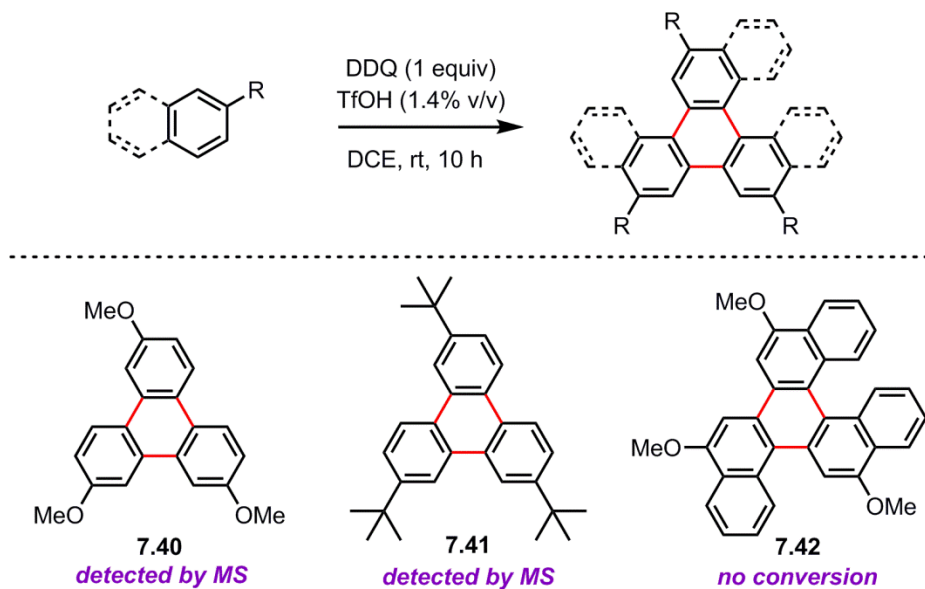
The reactivity of other anisole derivatives toward the oxidative coupling process was also examined. When 2-methylanisole was reacted with DDQ and triflic acid, the desired product (7.37) was given as a minor product (Scheme 7.21). This cyclic product was detected by mass spectrometry but not isolated. We also observed that the oxidative cyclotrimerization reaction of 2-hydroxyanisole furnished the corresponding trimer (7.38). When 2-trifluoromethylanisole was subjected to the DDQ/acid condition, the corresponding cyclic trimer (7.39) was formed but only as a minor product. The low yield of the process and the insolubility of these compounds made the purification process challenging.

Scheme 7.21 Oxidative Cyclotrimerization of Anisole Derivatives



We examined monosubstituted benzenes and naphthalenes for the oxidative coupling process. When anisole was employed as a starting material for the DDQ and triflic acid oxidation reaction, the corresponding product (**7.40**) was afforded (Scheme 7.22). This trimer was detected by mass spectrometry but not isolated. It was observed that the intermolecular cyclotrimerization reaction of *tert*-butylbenzene gave the corresponding trimer as a minor product (**7.41**). The insolubility of these products and accompanying byproducts made the isolation of these compounds difficult. When 1-methoxynaphthalene was subjected to the DDQ/triflic acid condition, the corresponding cyclic trimer (**7.42**) was not formed.

Scheme 7.22 Oxidative Cyclotrimerization of Monosubstituted Aromatic Compounds

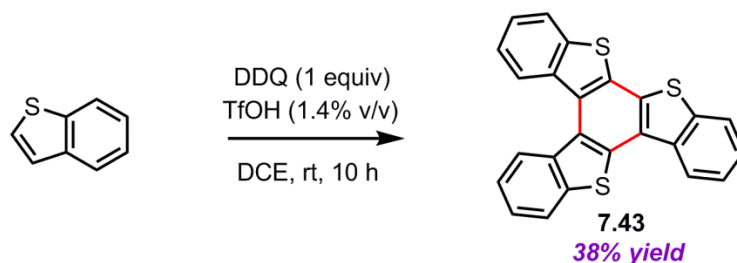


7.3.3. Oxidation toward Isotruxene Derivatives

7.3.3.1. Survey of Benzothiophenes and Thiophenes

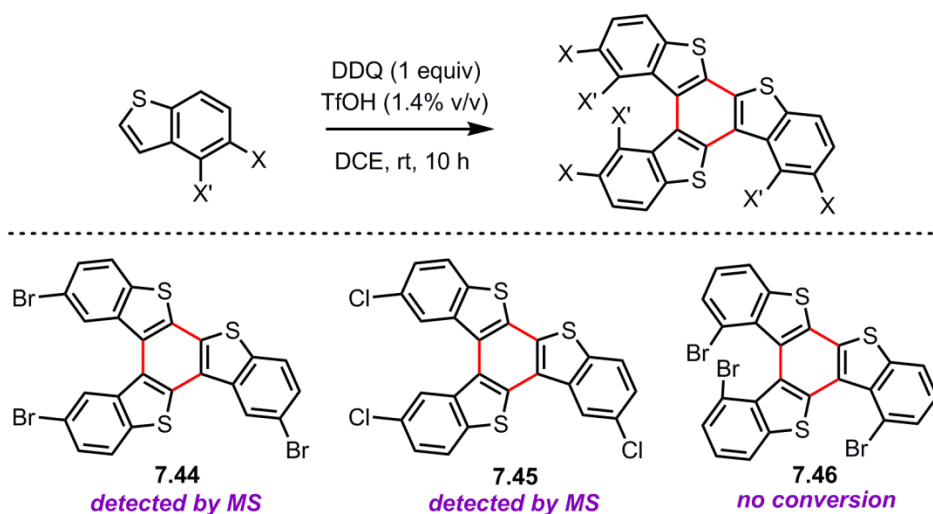
We were interested in whether heterocyclic aromatic compounds would participate in the intermolecular oxidative coupling process. When benzothiophene was employed as a starting material in the DDQ and triflic acid oxidation reaction, the corresponding trimer (7.43) was furnished in 38% yield (Scheme 7.23). The yield of this process was moderate, but the reaction was highly regioselective; a symmetrical trimer was not formed from this process.

Scheme 7.23 Oxidative Cyclotrimerization of Benzothiophene



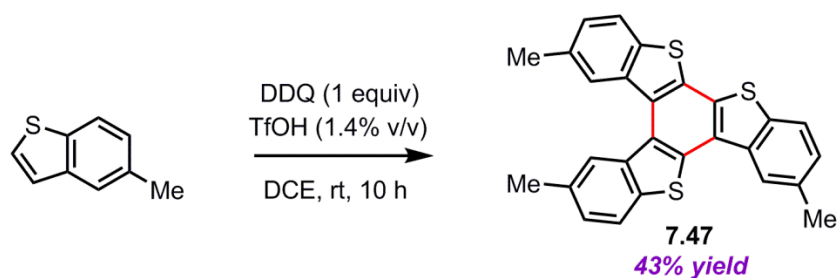
The reactivity of halogenated benzothiophenes toward the oxidative cyclotrimerization reaction was examined (Scheme 7.24). When 5-bromo-1-benzothiophene was employed as a starting material in the DDQ/acid oxidation reaction, the corresponding cyclized product (**7.44**) was afforded. The trimer was detected by mass spectrometry but not isolated. The intermolecular coupling reaction of 5-chloro-1-benzothiophene furnished the corresponding trimer (**7.45**), which was detected by mass spectrometry. The low efficiency of the process and the insolubility of the products made the isolation process challenging. However, when 4-bromo-1-benzothiophene was subjected to the DDQ/TfOH oxidation condition, the corresponding cyclic trimer (**7.46**) was not formed.

Scheme 7.24 Oxidative Cyclotrimerization of Halogenated Benzothiophenes



In addition, an alkylated heteroaromatic compound was examined (Scheme 7.25). When 5-methyl-1-benzothiophene was subjected to the DDQ/triflic acid oxidation reaction, the corresponding cyclic trimer (**7.47**) was furnished in 43% yield. This process was highly regioselective; a symmetrical trimer was not formed from this reaction.

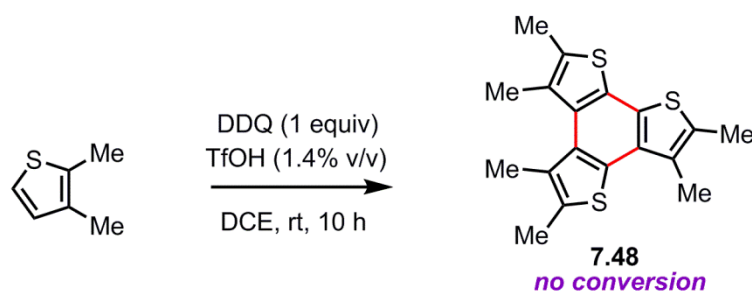
Scheme 7.25 Oxidative Cyclotrimerization of 5-Methyl-1-benzothiophene



We also examined the reactivity of substituted thiophenes toward the DDQ/triflic acid-mediated oxidative cyclic trimerization reaction (Scheme 7.26). When 2,3-

dimethylthiophene was employed as a starting material in the oxidative cyclization reaction, the desired product (7.48) was not formed.

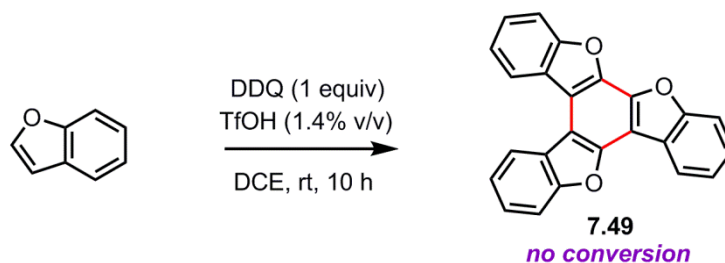
Scheme 7.26 Oxidative Cyclotrimerization of 2,3-Dimethylthiophene



7.3.3.2. Survey of Indoles and Benzofurans

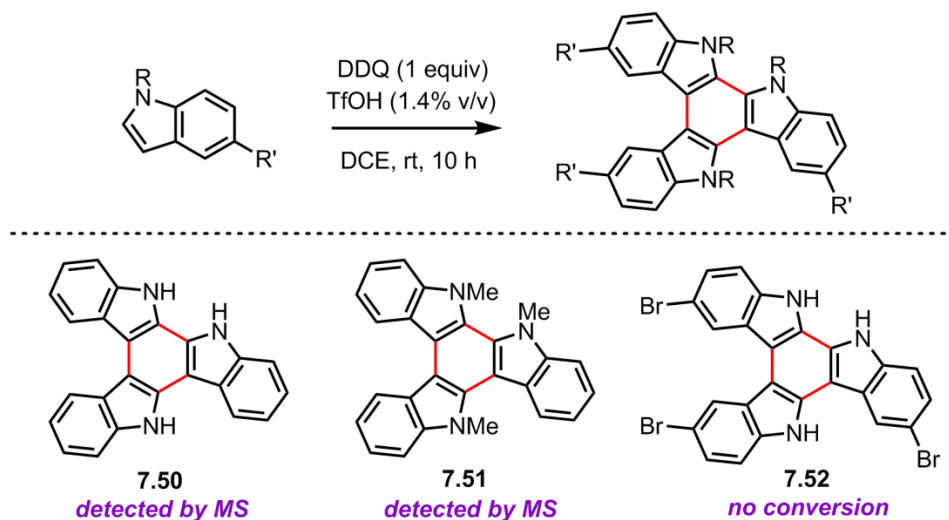
We were interested in whether other heterocyclic aromatic compounds, such as indoles and benzofurans, would participate in the oxidative cyclotrimerization process. Thus, the reactivity of benzofuran toward the DDQ/triflic acid-mediated oxidative cyclic trimerization reaction was investigated (Scheme 7.27). When benzofuran was employed as a starting material for the oxidative coupling reaction, the corresponding product (7.49) was not formed.

Scheme 7.27 Oxidative Cyclotrimerization of Benzofuran



We also examined indoles and indole derivatives for the oxidative coupling process (Scheme 7.28). When indole was subjected to the DDQ/acid oxidation coupling reaction, the corresponding product (7.50) was formed. The trimer was detected by mass spectrometry but not isolated. The intermolecular oxidative coupling reaction of 1-methylindole gave the corresponding trimer as a minor product (7.51). The formation of the trimer was detected by mass spectrometry. When 5-bromoindole was subjected to the DDQ/ acid condition, the corresponding cyclic trimer (7.52) was not afforded.

Scheme 7.28 Oxidative Cyclotrimerization of Indole and its Derivatives

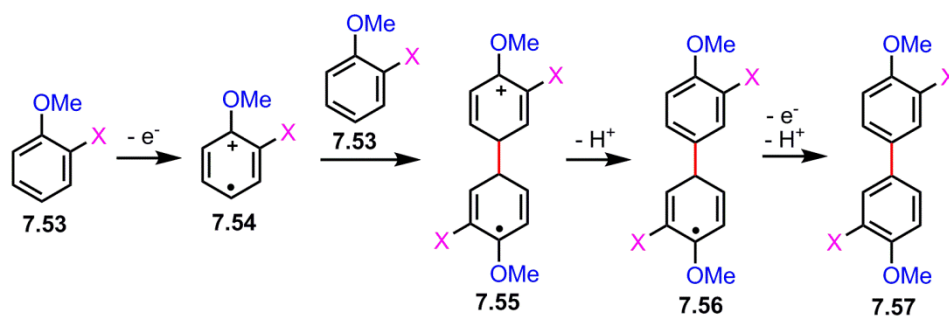


7.4. Mechanistic Considerations

As mentioned in the previous chapter, there are two possible mechanistic pathways for this type of processes (*i.e.* Scholl-type oxidation). One of them is an electron transfer mechanism, and the other one is a proton transfer mechanism. There has been a debate on which mechanistic pathway is operating for this process, and several theoretical investigations have been conducted. The experimental results of this chapter, which were obtained from the reactions with halogenated anisoles, provided useful information on the detailed mechanism for the Scholl-type oxidation process.

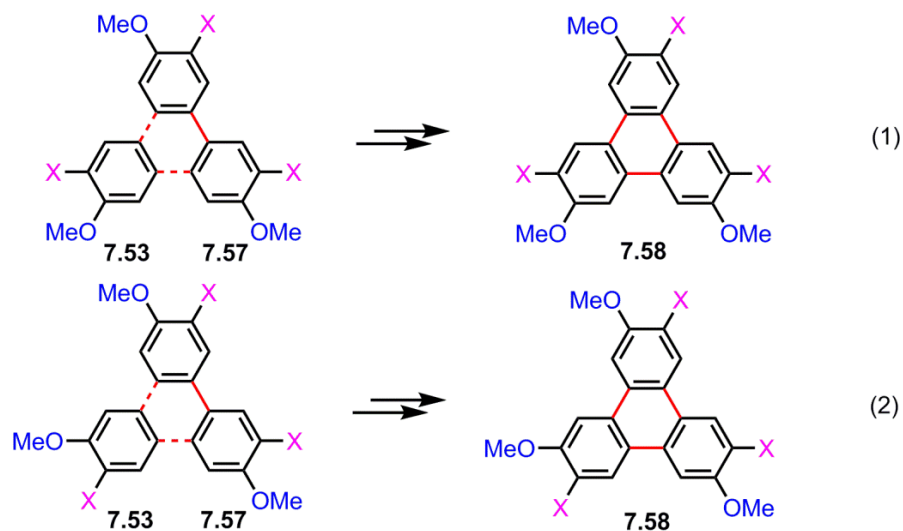
We considered both of the above proposed mechanisms for this oxidative cyclotrimerization process. If the electron transfer mechanism is operative as described in Scheme 7.29, a monomeric starting material **7.53** will lose one electron to generate a radical cation **7.54**. Then, an intermolecular coupling between the radical cation (**7.54**) and another monomer (**7.53**) will lead to the formation of a dimeric radical cation **7.55**. And, a loss of a proton from the radical cation (**7.55**) will generate a dimeric radical **7.56**. Then, the radical intermediate (**7.56**) will lose an electron and a proton to afford a neutral dimer intermediate (**7.57**). Notably, the two methoxy groups of the dimer (**7.57**) will end up *para* to each other.

Scheme 7.29 Dimer Formation via Electron Transfer Mechanism



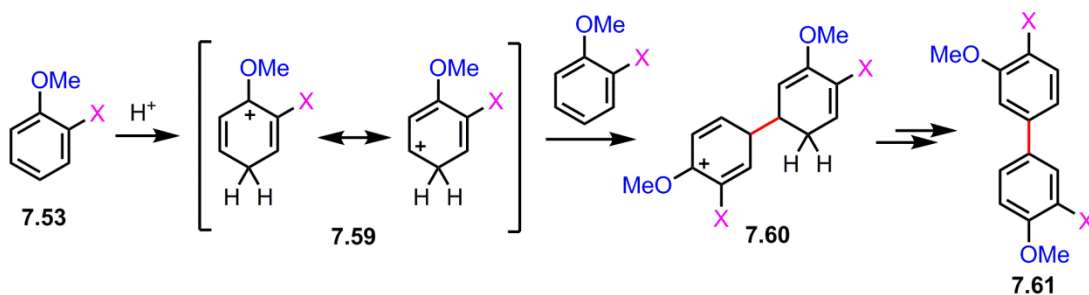
As described in Scheme 7.30, the final trimeric product (**7.58**) will be afforded by a coupling reaction between the dimer intermediate (**7.57**) and another monomer (**7.53**). Once the intermediate dimer (**7.57**) is formed, the product of this coupling reaction would be an unsymmetrical trimer, no matter what direction the monomer (**7.53**) approaches. In other words, the products from the two possible approaches (as shown in equations 1 and 2 of Scheme 7.30) would be identical. According to our experimental data, this unsymmetrical trimer was the observed reaction outcome.

Scheme 7.30 Trimer Formation via Electron Transfer Mechanism



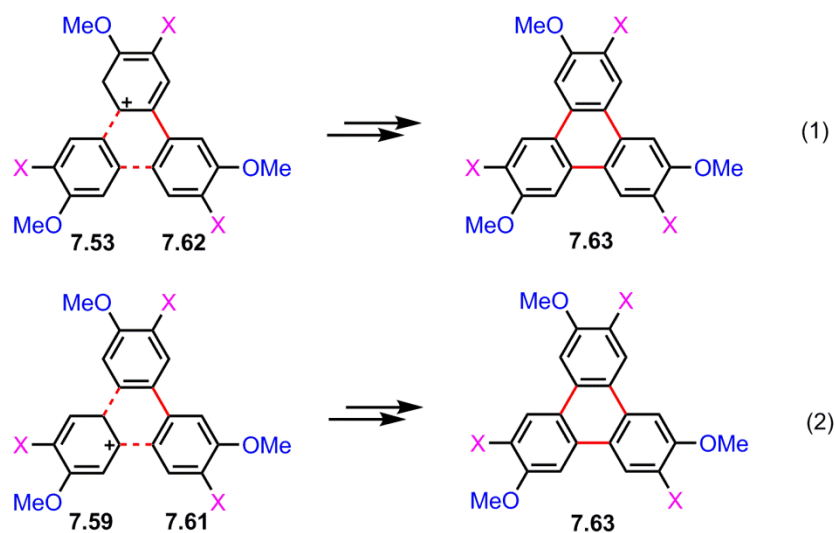
If a proton transfer mechanism were operative for this process, the reaction would involve different types of intermediates as described in Scheme 7.31. A monomer **7.53** would be protonated in the acidic condition to generate a monomeric cation **7.59**. Then, a coupling reaction between the cation (**7.59**) and another monomer (**7.53**) would lead to a dimeric cation **7.60**. Then, a neutral dimer intermediate (**7.61**) would be generated from the cation (**7.60**) via loss of a proton and H_2 . Notably, the dimer intermediate from this mechanism (**7.61**) possesses two methoxy groups that are not symmetrically disubstituted on the biphenyl core.

Scheme 7.31 Dimer Formation via Proton Transfer Mechanism



As shown in Scheme 7.32, the final trimer (**7.63**) will be formed by a coupling reaction between the dimer intermediate (**7.61**) and another monomer (**7.53**). There are two ways for these two components to be coupled. As described in equation 1 (Scheme 7.32), the protonated dimer (**7.62**) can be coupled with the neutral monomer (**7.53**) to give the corresponding product (**7.63**). Another way to form a trimer would be a coupling between the protonated monomer (**7.59**) and the neutral dimer (**7.61**), as shown in equation 2. From both pathways, the product expected from the coupling reaction would be a symmetrical trimer (**7.63**). In other words, the products from the two possible coupling modes (as shown in equations 1 and 2 of Scheme 7.32) would be identical. According to our experimental data, this symmetrical trimer was not the observed reaction outcome.

Scheme 7.32 Trimer Formation via Proton Transfer Mechanism



By employing halogenated anisoles as starting materials for the oxidative cyclotrimerization reactions, we were able to provide evidence for a specific mechanistic pathway. As mentioned above, the trimeric product expected from the electron transfer mechanism would be an unsymmetrical trimer. On the other hand, the product expected from the proton transfer mechanism would be a symmetrical trimer. Our experimental data suggest that these oxidative cyclotrimerization reactions follow the electron transfer pathway because unsymmetrical trimers were obtained as reaction products from the cyclotrimerization experiments with halogenated anisoles.

7.5. Conclusions and Outlook

The regioselective formation of cyclic trimers from substituted benzenes and heteroaromatic compounds has been demonstrated. This DDQ/TfOH method provides a simple and convenient synthetic route toward star-shaped oligomers containing triphenylene or isotruxene cores. Furthermore, the experimental outcome suggests that this oxidative process proceeds by an electron transfer mechanism. This is the first experimental evidence for mechanistic details on the Scholl-type oxidation.

7.6. Experimental Section

7.6.1. General Information

All reactions were performed in oven- or flame-dried glassware fitted with rubber septa under a positive pressure of nitrogen, unless otherwise stated. Air- and moisture-sensitive liquids were transferred via syringe or stainless steel cannula. Organic solvents were concentrated by rotary evaporation at various temperatures, unless otherwise noted. All work-up and purification procedures were carried out with reagent grade solvents under typical bench-top conditions. Analytical thin-layer chromatography (TLC) was performed using glass plates, which are pre-coated with silica gel 60 F254 (0.25 mm thickness) impregnated with a fluorescent indicator (254 nm). TLC plates were visualized by exposure to UV (ultraviolet) light, and then were stained with phosphomolybdic acid (PMA) in ethanol, potassium permanganate (KMnO₄) in water, or cerium(IV) sulfate and ammonium molybdate in sulfuric acid (CAM). Liquid chromatography was performed using forced flow (flash chromatography)⁵⁷ on silica gel (porosity = 60 Å, particle size = 32-63 μm) purchased from Sorbent Technologies. Medium pressure gradient chromatography was performed on a Teledyne Isco CombiFlash automated flash chromatography system with a 200-780 nm UV-vis variable wavelength detector.

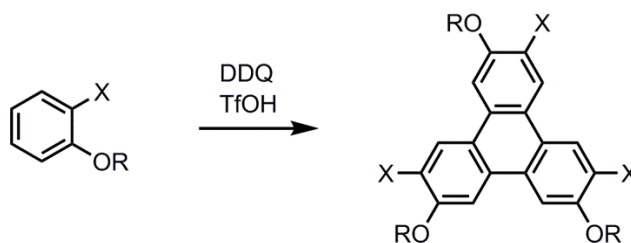
⁵⁷ Still, W. C.; Kahn, M.; Mitra, A., "Rapid Chromatographic Technique for Preparative Separations with Moderate Resolution," *The Journal of Organic Chemistry* **1978**, *43*, 2923-2925.

All commercially available chemicals and solvents were purchased from Sigma Aldrich, Acros, Strem, Alfa Aesar, Fisher, or TCI America and were used without purification with the following exceptions. Tetrahydrofuran (THF), methylene chloride (CH_2Cl_2), toluene, *N,N*-dimethylacetamide (DMAc), 1,2-dichlorobenzene (*o*-DCB), and carbon disulfide (CS_2) were dried and purified using a solvent purification system from Innovative Technology Inc.

Proton nuclear magnetic resonance (^1H NMR) spectra were recorded on either a Varian INOVA 500 (500 MHz) or a Varian VNMR 500 (500 MHz) at 23 °C unless specified otherwise. Proton chemical shifts are reported in ppm (parts per million, δ scale) downfield from tetramethylsilane and are referenced to residual protium in the NMR solvent as the internal standard (CHCl_3 : 7.26 ppm, C_6H_6 : 7.16 ppm). Data are reported as follows: chemical shift, integration, multiplicity (s = singlet, d = doublet, t = triplet, q = quartet, qn = quintet, br = broad, and m = multiplet), coupling constant (*J*) in hertz (Hz), and assignment. Carbon nuclear magnetic resonance (^{13}C NMR) spectra were recorded on either a Varian INOVA 500 (125 MHz) or a Varian VNMR 500 (125 MHz) with complete proton decoupling at 23 °C unless otherwise stated. Carbon chemical shifts are reported in ppm (parts per million, δ scale) downfield from tetramethylsilane and are referenced to the NMR solvent resonance as the internal standard (CDCl_3 : 77.16 ppm, C_6D_6 : 128.06 ppm).

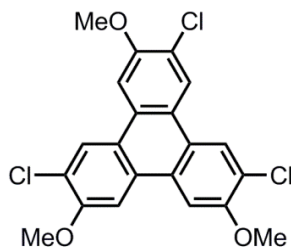
Melting points were determined with a Thomas-Hoover Unimelt capillary melting point apparatus and were uncorrected. Infrared (IR) spectra were recorded on a Bruker FT-

IR Alpha (ATR Mode) spectrophotometer, ν_{max} cm^{-1} . Data are represented as follows: frequency of absorption (cm^{-1}) and intensity of absorption (s = strong, m = medium, w = weak, and br = broad). Low resolution mass spectrometric analyses were performed using a Thermo Electron Corporation Finnigan Trace GC Ultra gas chromatograph unit connected to a Thermo Electron Corporation Finnigan Trace DSQ mass spectrometer with direct inlet capabilities. High-resolution mass spectra (HRMS) were obtained by the Boston College Mass Spectrometry Center using various TOF instruments.

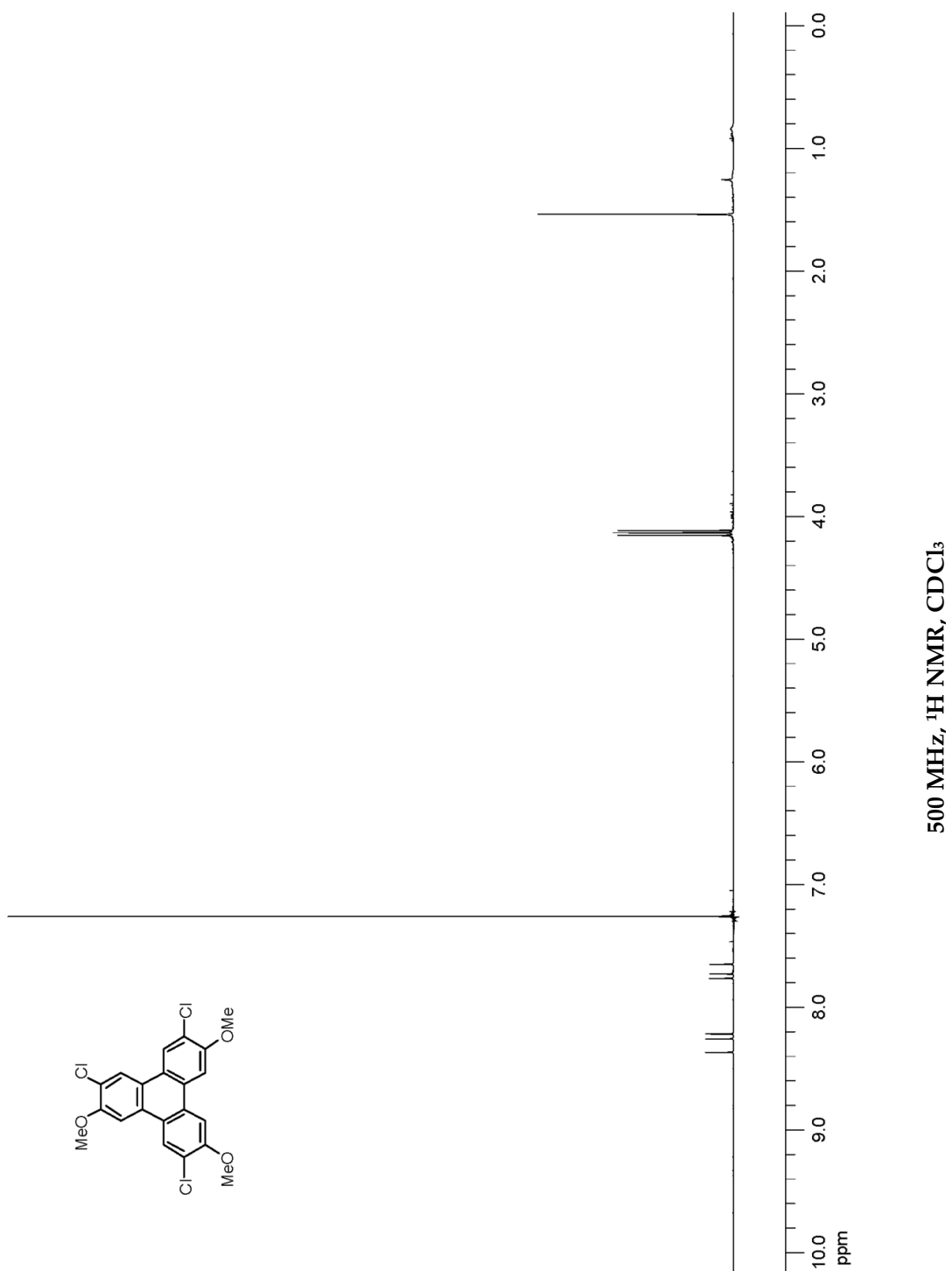
7.6.2. Experimental and Spectral Data**7.6.2.1. Representative Procedure for Oxidative Coupling of Anisoles**

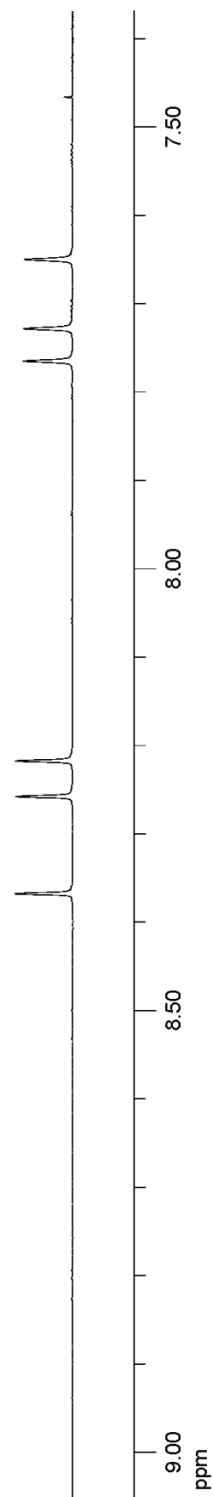
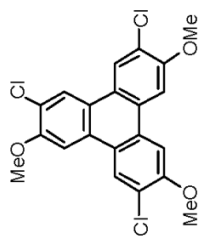
An oven-dried 20 mL scintillation vial, equipped with a magnetic stir-bar, was charged with the starting material (1.0 equiv), DDQ (1.0 equiv), trifluoromethanesulfonic acid (1.4% v/v, 3.0 equiv), and 1,2-dichloroethane (0.05 M). The reaction mixture was then allowed to stir at ambient temperature for 10 h. After this time, methanol (0.05M) was added, and the solution was then allowed to stir at ambient temperature for an additional hour. Upon addition of the methanol, some solids were precipitated out of the solution. Then, the solvent was removed from the heterogeneous mixture under reduced pressure. The crude material was purified by either recrystallization (methanol/DCM) or silica-gel column chromatography (hexanes/DCM) to give the title compounds.

7.6.2.2. 2,6,11-Trichloro-3,7,10-trimethoxytriphenylene

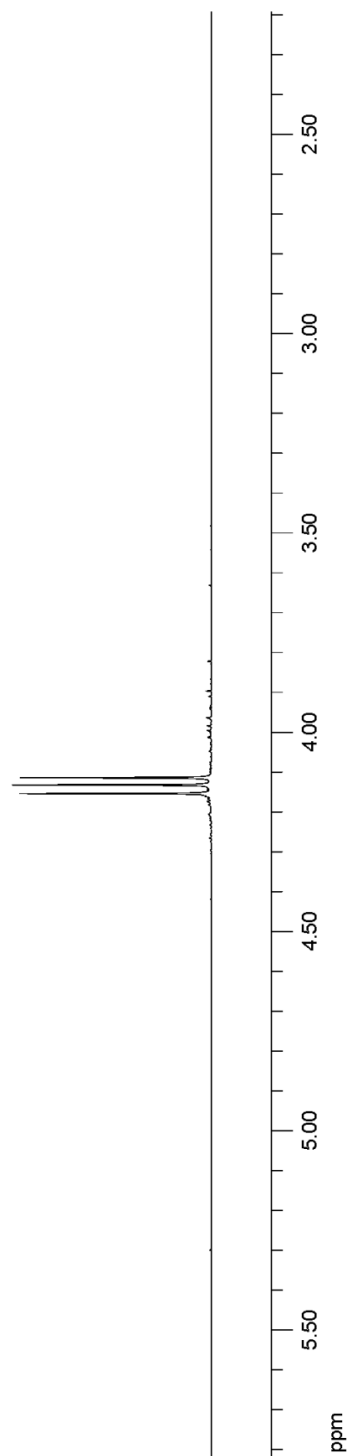
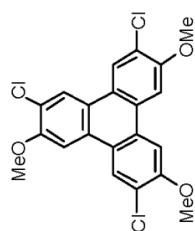


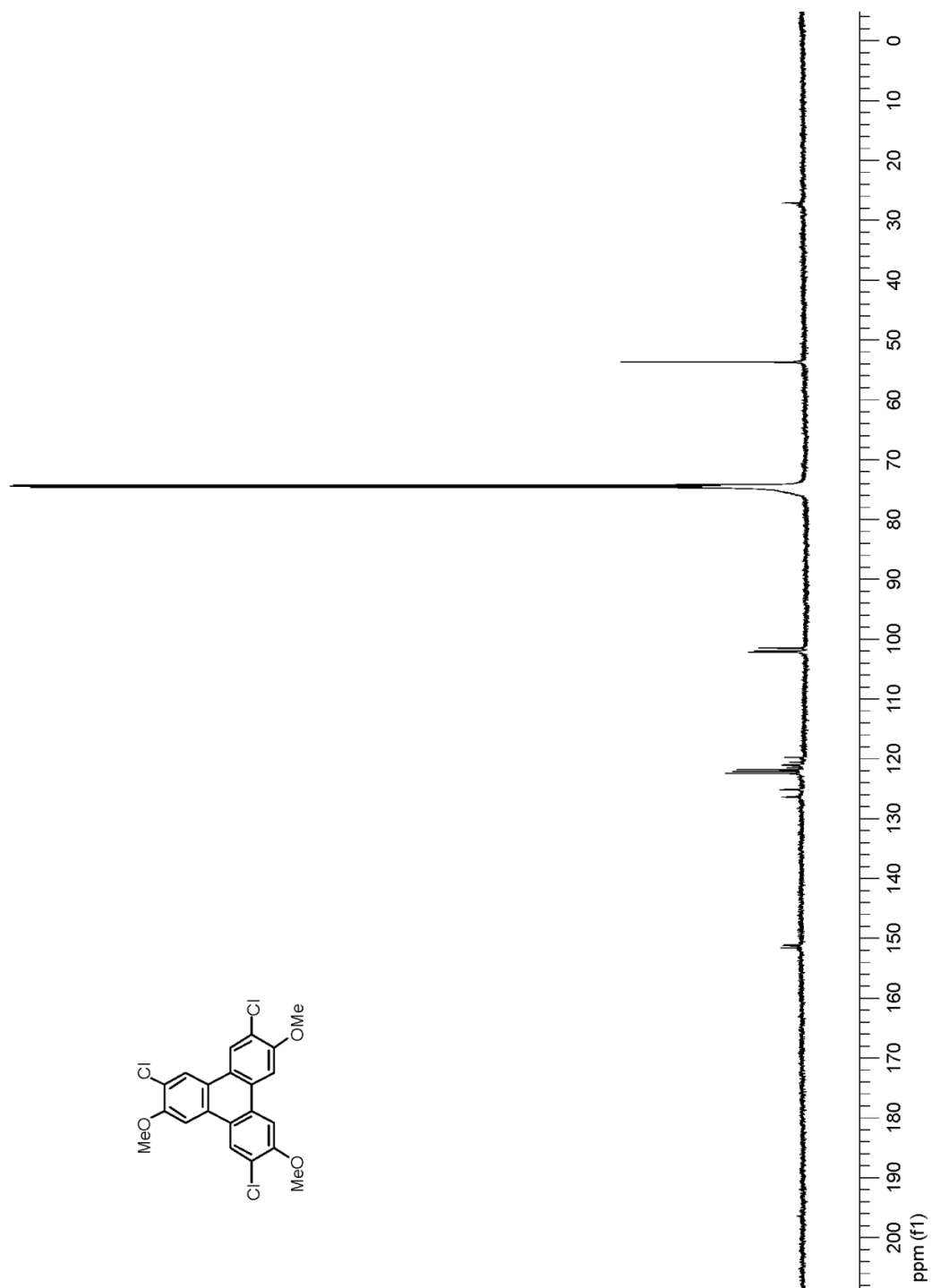
The general procedure described in Section 7.6.2.1 was followed on 0.10 mmol scale (14 mg) to obtain 2,6,11-trichloro-3,7,10-trimethoxytriphenylene as a white solid in 82% yield (34 mg). ^1H NMR (500 MHz, CDCl_3): δ 8.37 (s, 1H), 8.25 (s, 1H), 8.21 (s, 1H), 7.77 (s, 1H), 7.72 (s, 1H), 7.65 (s, 1H), 4.15 (s, 3H), 4.13 (s, 3H), 4.11 (s, 3H). ^{13}C NMR (150 MHz, CDCl_3): δ 151.6, 151.3, 151.1, 126.4, 125.2, 125.1, 122.5, 122.1, 121.9, 121.5, 121.2, 121.1, 121.0, 120.6, 119.8, 102.2, 102.0, 101.5, 53.7. HRMS (DART) calculated for $\text{C}_{21}\text{H}_{16}\text{Cl}_3\text{O}_3$ $[\text{M}+\text{H}]^+$: 421.0168, found: 421.0165.

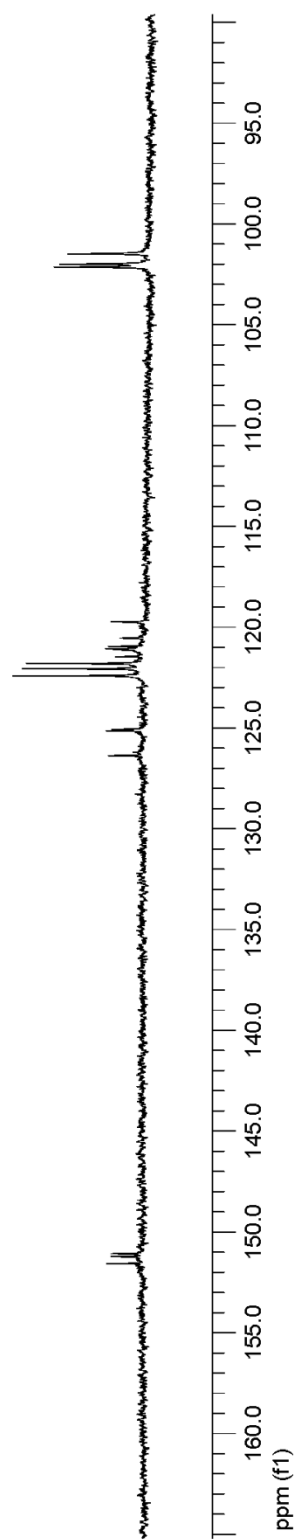
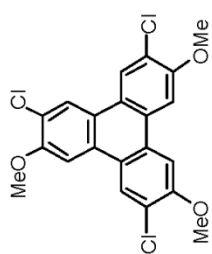


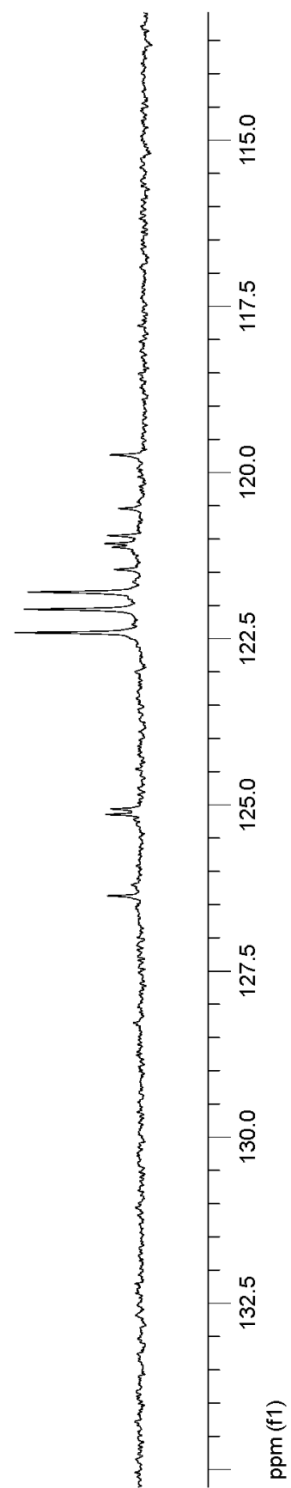
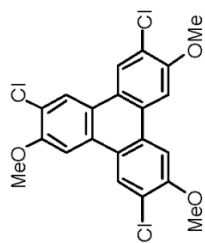


500 MHz, $^1\text{H NMR}$, CDCl_3

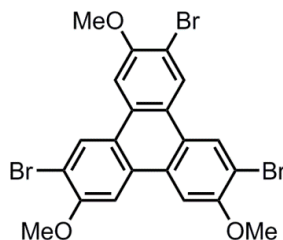
500 MHz, $^1\text{H NMR}$, CDCl_3

125 MHz, ^{13}C NMR, CDCl_3

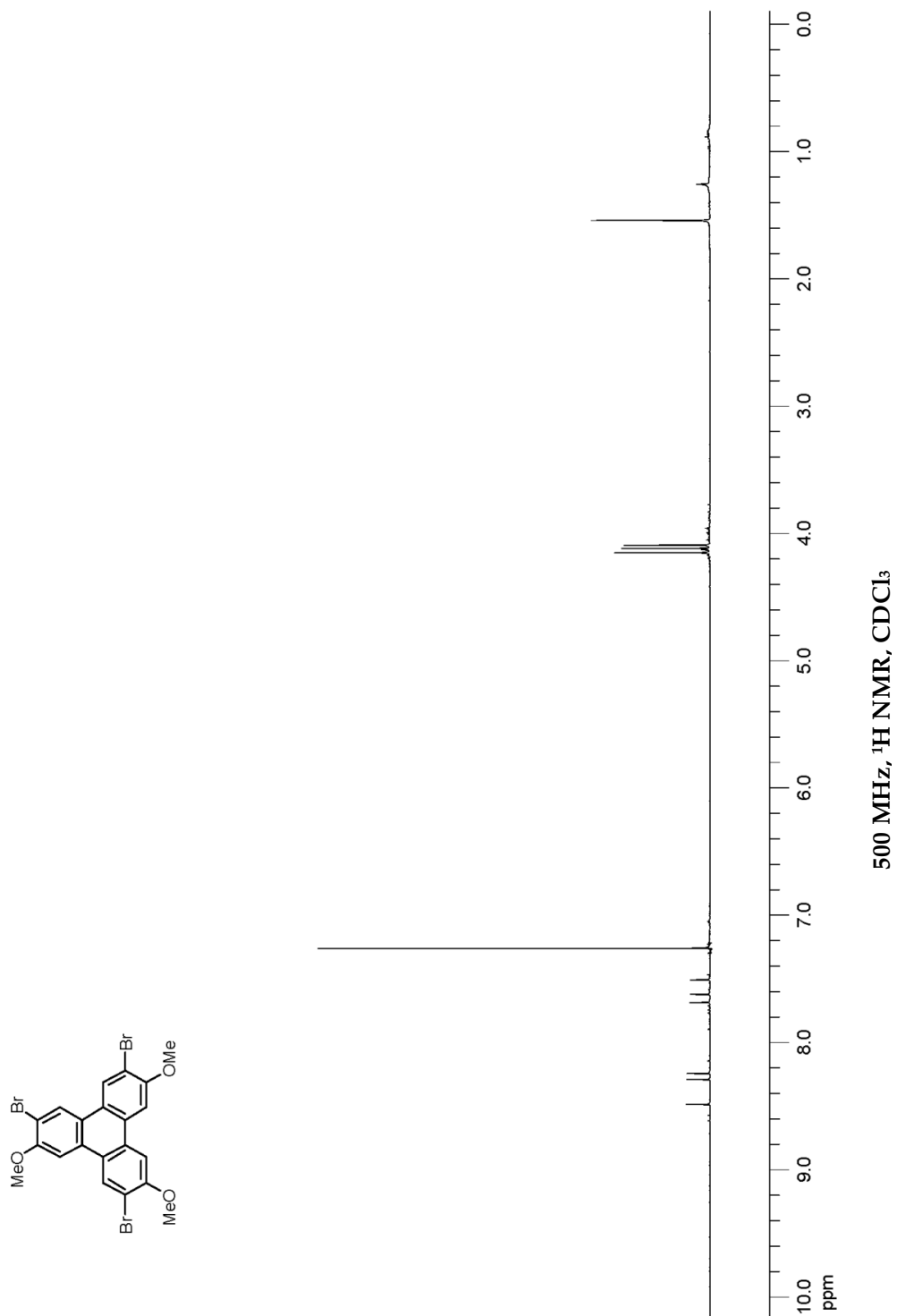
125 MHz, ^{13}C NMR, CDCl_3

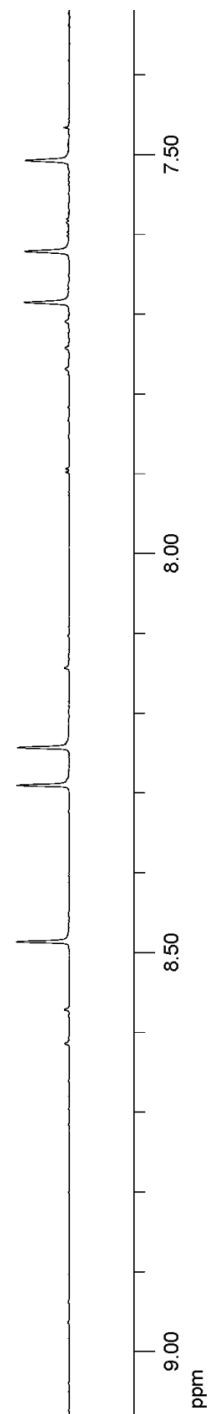
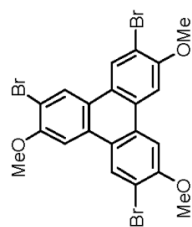
125 MHz, ^{13}C NMR, CDCl_3

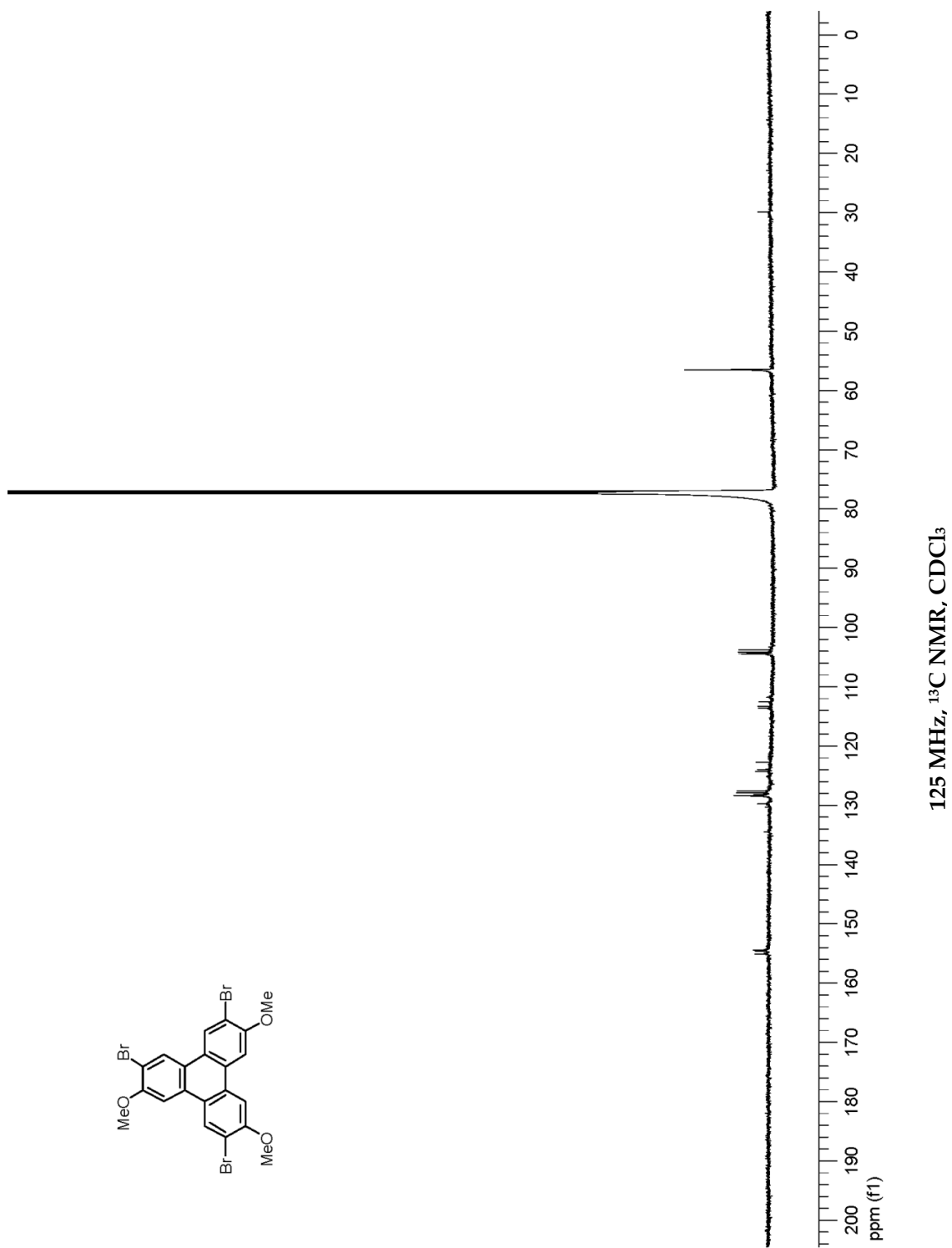
7.6.2.3. 2,6,11-Tribromo-3,7,10-trimethoxytriphenylene

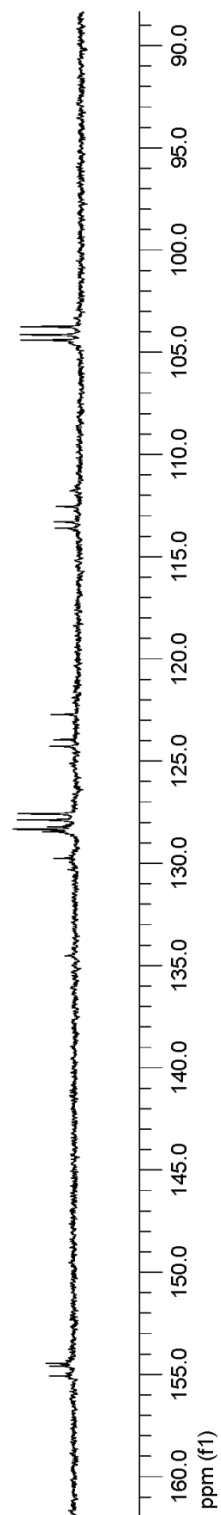
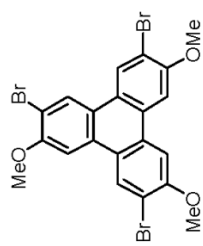


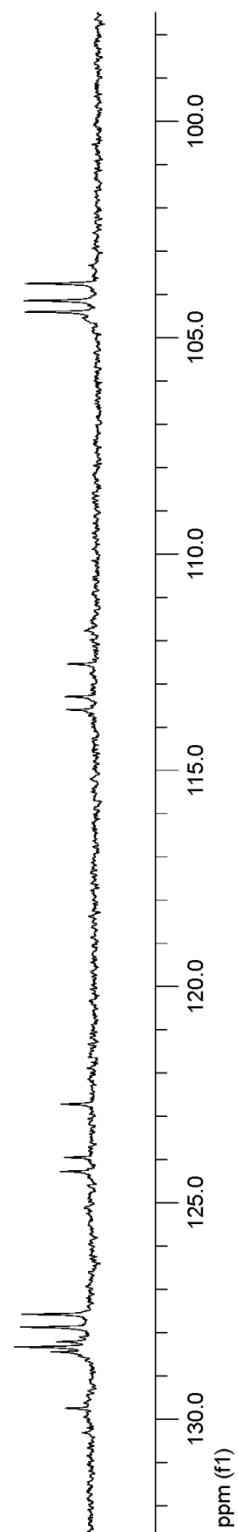
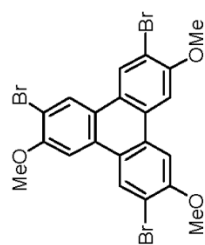
The general procedure described in Section 7.6.2.1 was followed on 0.10 mmol scale (19 mg) to obtain 2,6,11-tribromo-3,7,10-trimethoxytriphenylene as a white solid in 80% yield (42 mg). ^1H NMR (500 MHz, CDCl_3): δ 8.49 (s, 1H), 8.29 (s, 1H), 8.24 (s, 1H), 7.69 (s, 1H), 7.62 (s, 1H), 7.51 (s, 1H), 4.15 (s, 3H), 4.12 (s, 3H), 4.09 (s, 3H). ^{13}C NMR (150 MHz, CDCl_3): δ 155.1, 154.6, 154.5, 129.8, 128.5, 128.3, 128.2, 127.9, 127.6, 124.3, 124.0, 122.7, 113.6, 113.3, 112.6, 104.4, 104.2, 103.8, 56.5. HRMS (DART) calculated for $\text{C}_{21}\text{H}_{16}^{79}\text{Br}_2^{81}\text{BrO}_3$ $[\text{M}+\text{H}]^+$: 554.8629, found: 554.8648.



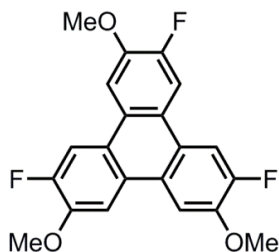
500 MHz, ¹H NMR, CDCl₃



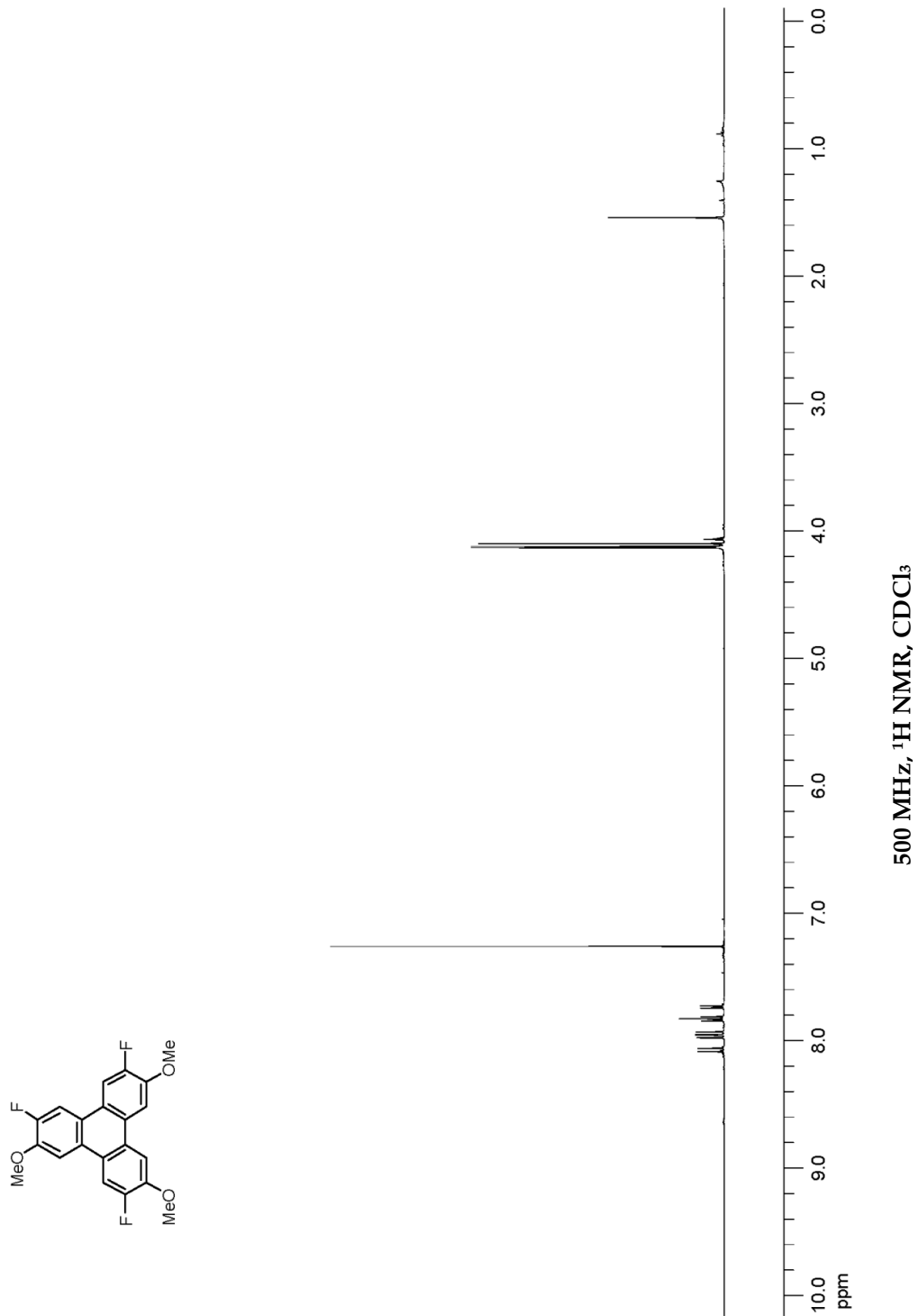
125 MHz, ^{13}C NMR, CDCl_3

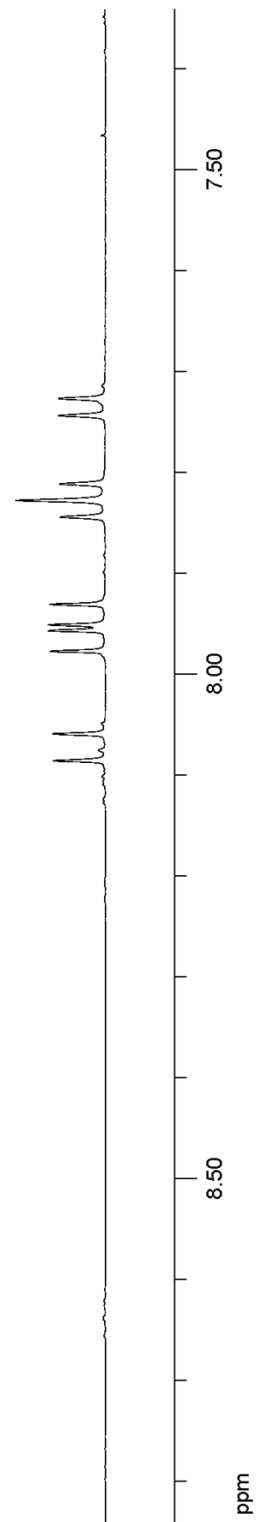
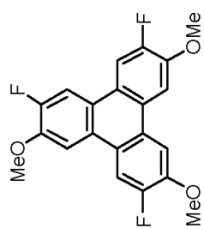
125 MHz, ^{13}C NMR, CDCl_3

7.6.2.4. 2,6,11-Trifluoro-3,7,10-trimethoxytriphenylene

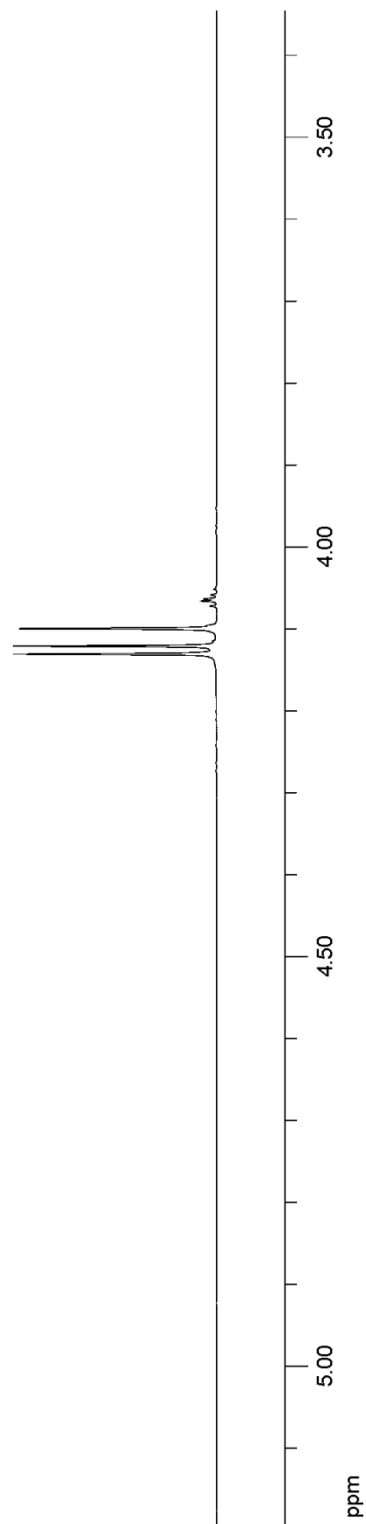
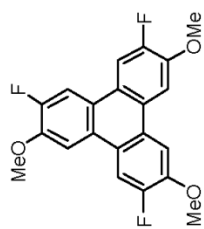


The general procedure described in Section 7.6.2.1 was followed on 0.10 mmol scale (13 mg) to obtain 2,6,11-trifluoro-3,7,10-trimethoxytriphenylene as a white solid in 65% yield (24 mg). ^1H NMR (500 MHz, CDCl_3): δ 8.07 (d, $J = 13.5$ Hz, 1H), 7.96 (d, $J = 12.5$ Hz, 1H), 7.94 (d, $J = 13.0$ Hz, 1H), 7.84 (d, $J = 8.5$ Hz, 1H), 7.82 (d, $J = 7.5$ Hz, 1H), 7.74 (d, $J = 8.5$ Hz, 1H), 4.13 (s, 3H), 4.12 (s, 3H), 4.10 (s, 3H). HRMS (DART) calculated for $\text{C}_{21}\text{H}_{16}\text{F}_3\text{O}_3$ $[\text{M}+\text{H}]^+$: 373.1052, found: 373.1062.

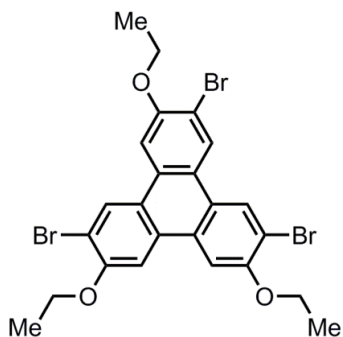




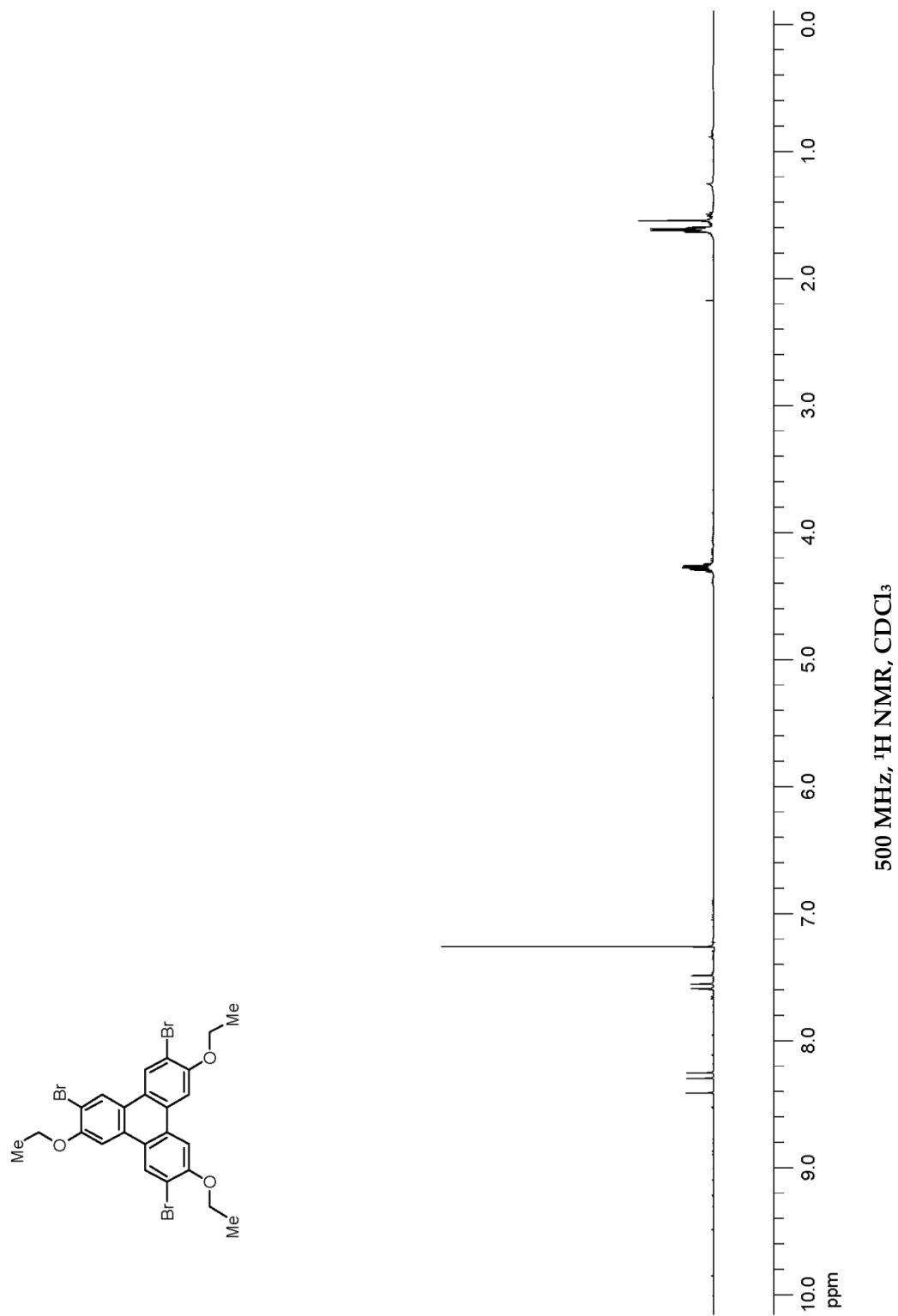
500 MHz, $^1\text{H NMR}$, CDCl_3

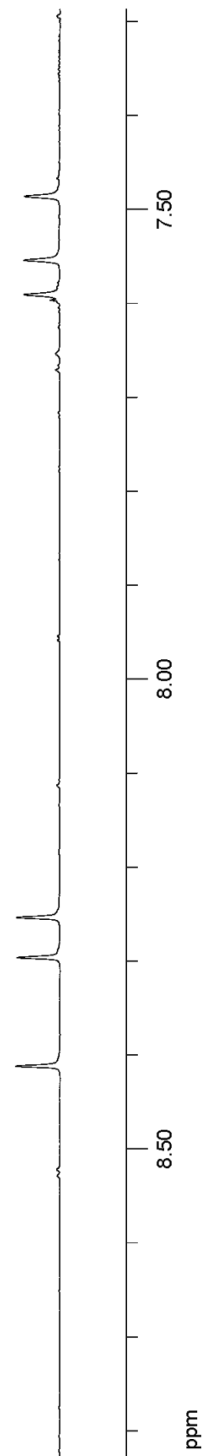
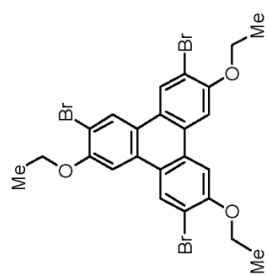
500 MHz, ^1H NMR, CDCl_3

7.6.2.5. 2,6,11-Tribromo-3,7,10-triethoxytriphenylene



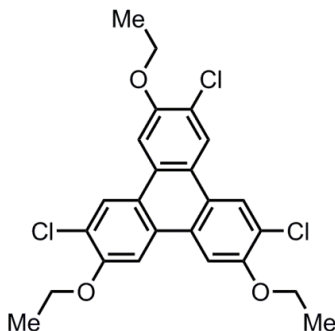
The general procedure described in Section 7.6.2.1 was followed on 0.10 mmol scale (20 mg) to obtain 2,6,11-tribromo-3,7,10-triethoxytriphenylene as a white solid in 75% yield (45 mg). ^1H NMR (500 MHz, CDCl_3): δ 8.41 (s, 1H), 8.30 (s, 1H), 8.25 (s, 1H), 7.59 (s, 1H), 7.55 (s, 1H), 7.49 (s, 1H), 4.29–4.26 (m, 6H), 1.64–1.60 (m, 9H). HRMS (DART) calculated for $\text{C}_{24}\text{H}_{22}^{79}\text{Br}_2^{81}\text{BrO}_3$ $[\text{M}+\text{H}]^+$: 596.9099, found: 596.9098.



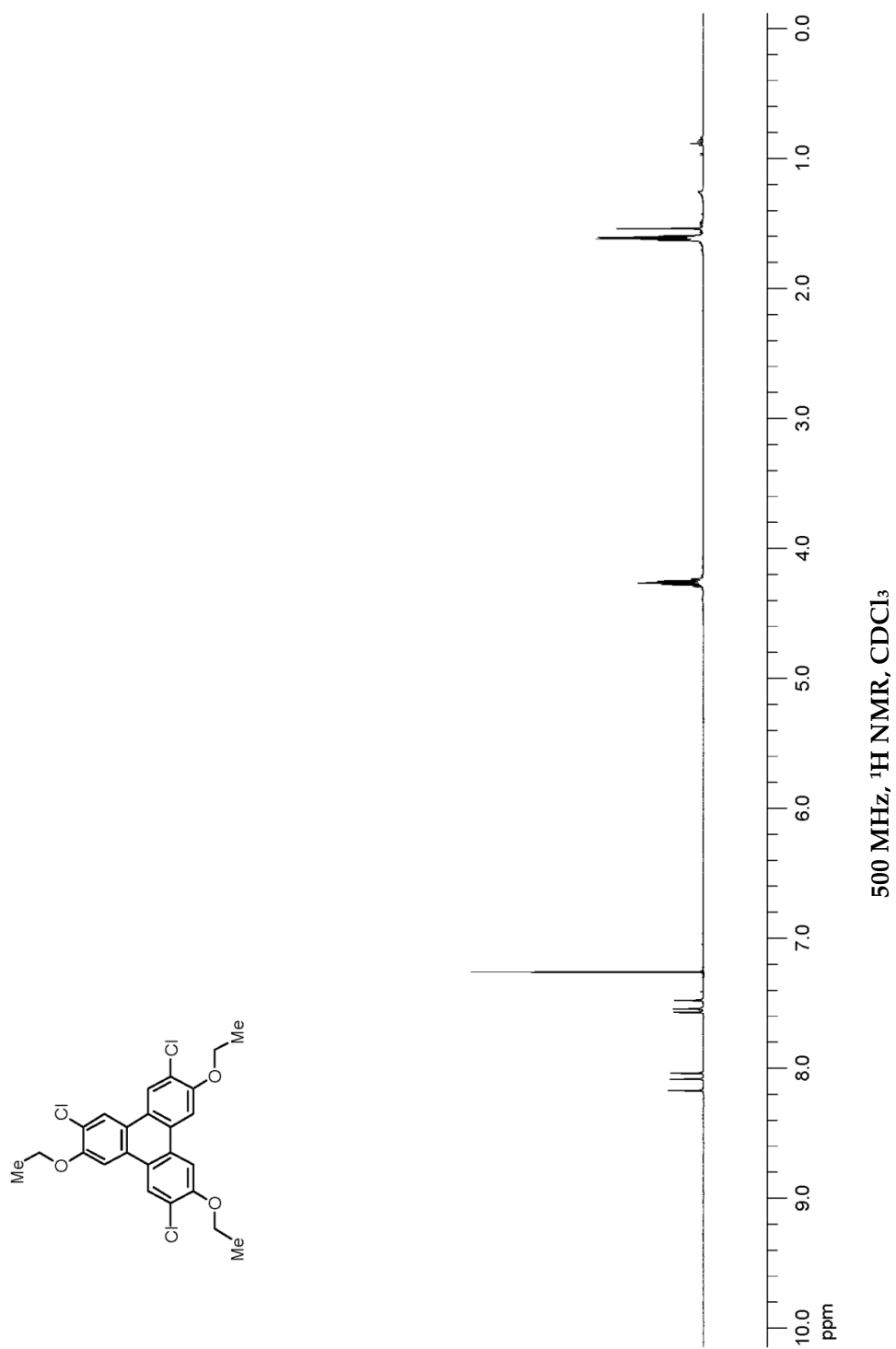


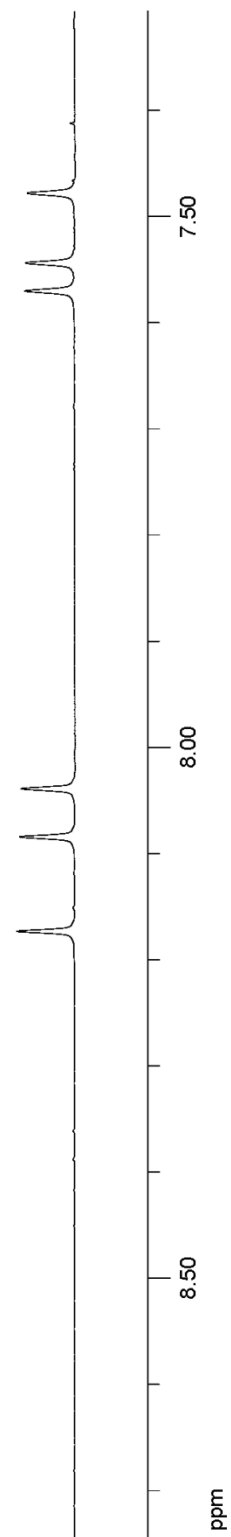
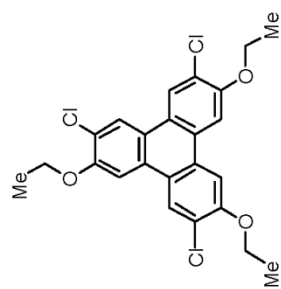
500 MHz, $^1\text{H NMR}$, CDCl_3

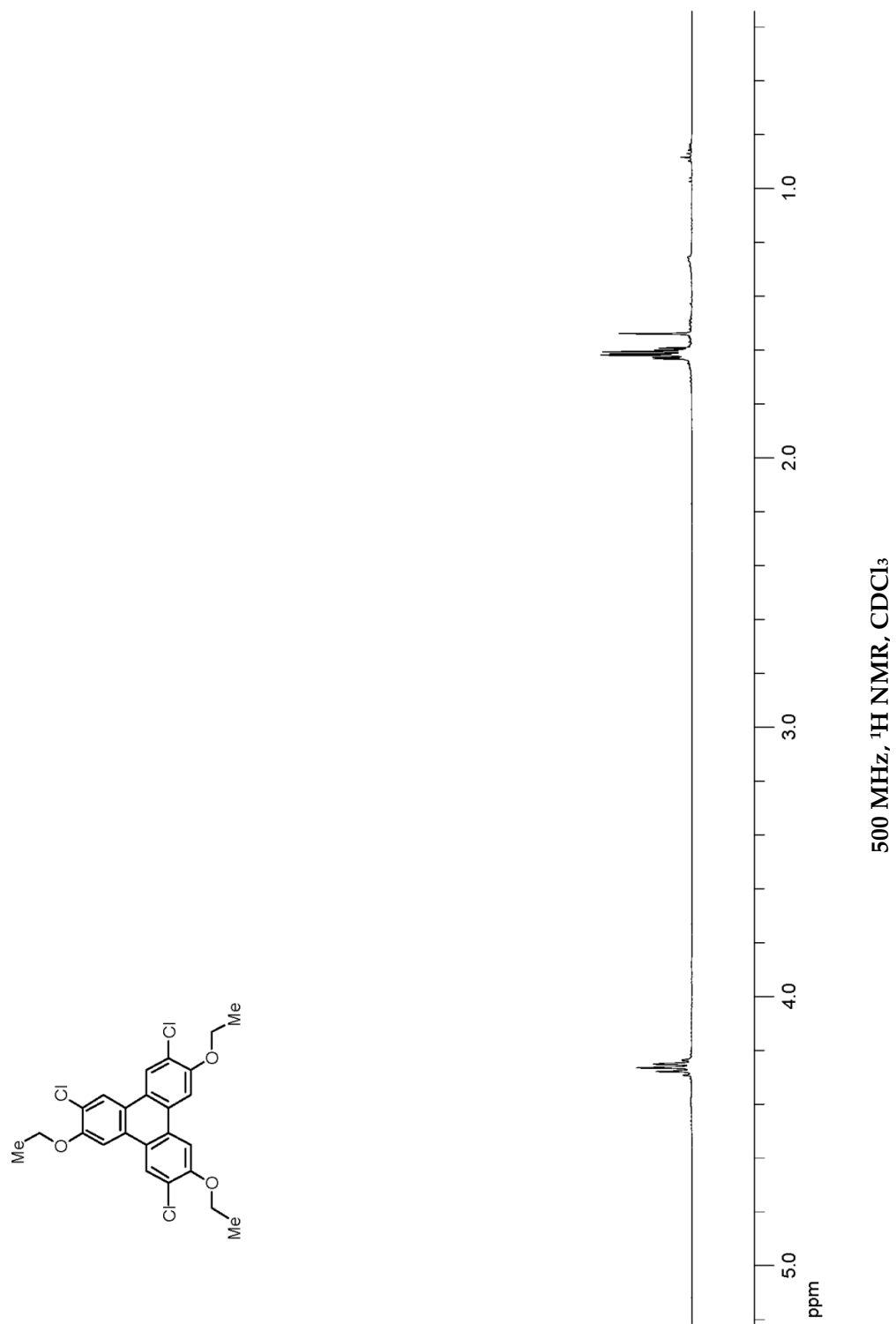
7.6.2.6. 2,6,11-Trichloro-3,7,10-triethoxytriphenylene

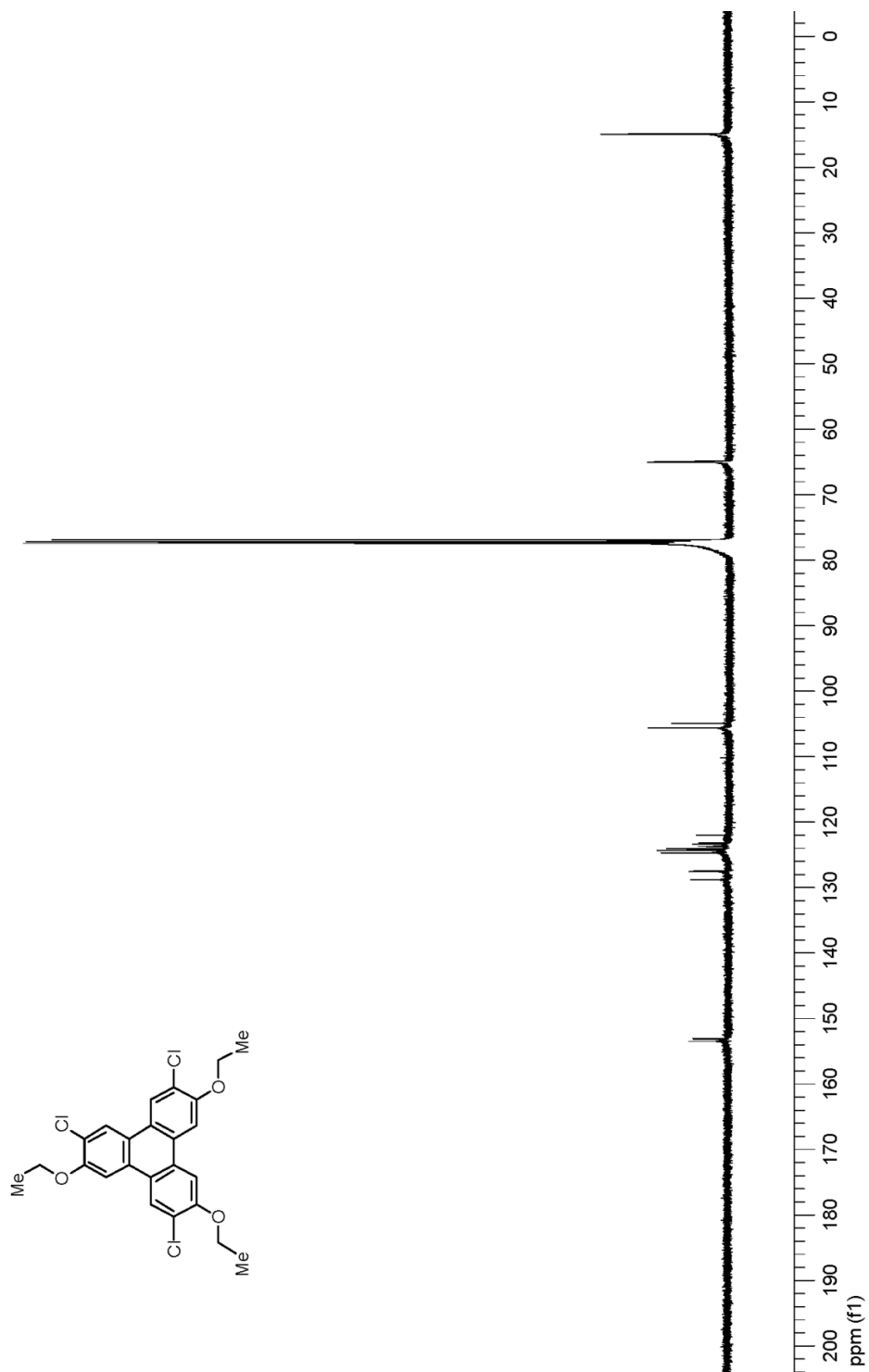


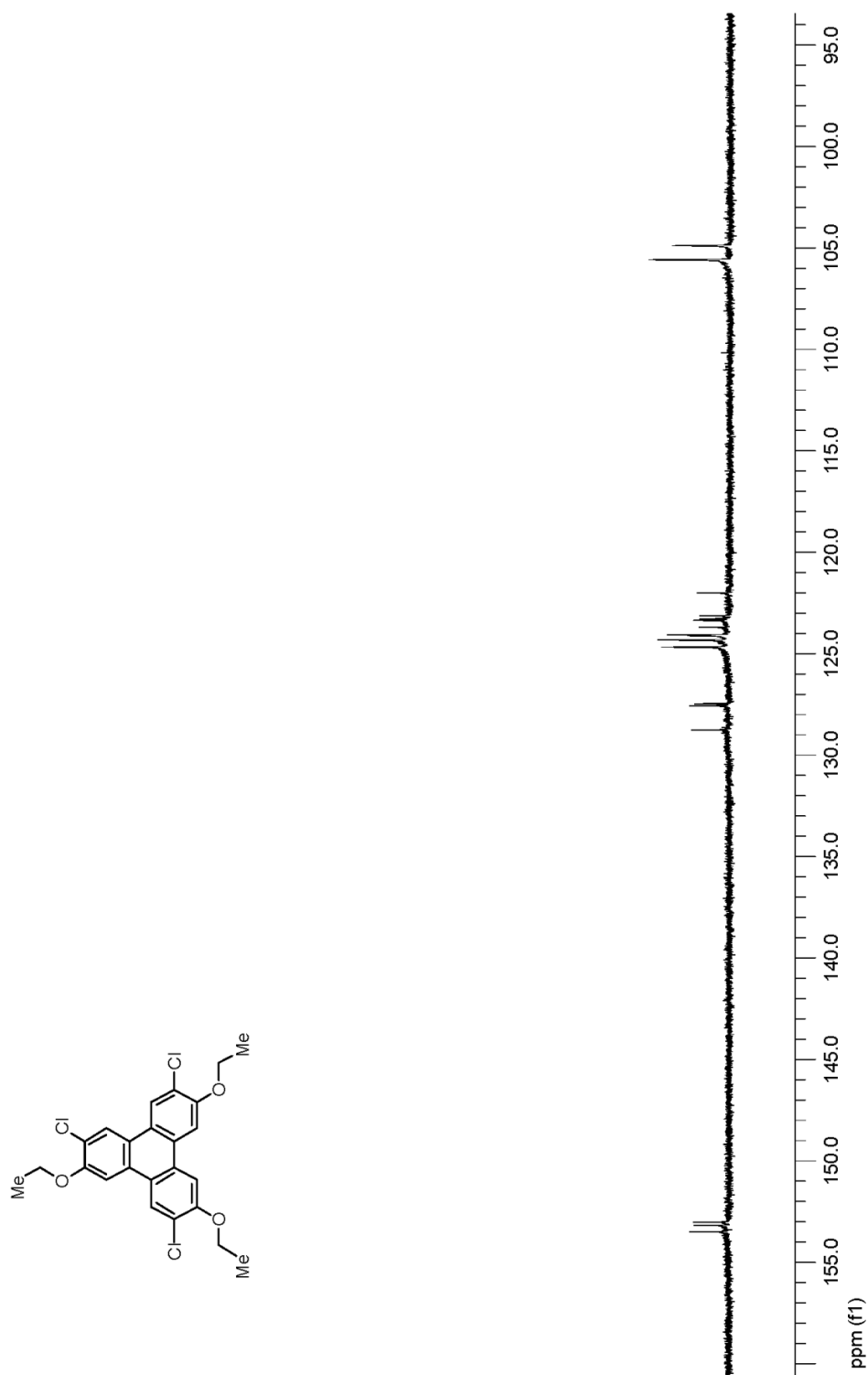
The general procedure described in Section 7.6.2.1 was followed on 0.10 mmol scale (16 mg) to obtain 2,6,11-trichloro-3,7,10-triethoxytriphenylene as a white solid in 66% yield (30 mg). ^1H NMR (500 MHz, CDCl_3): δ 8.17 (s, 1H), 8.08 (s, 1H), 8.04 (s, 1H), 7.57 (s, 1H), 7.54 (s, 1H), 7.48 (s, 1H), 4.27–4.25 (m, 6H), 1.63–1.60 (m, 9H). ^{13}C NMR (125 MHz, CDCl_3): δ 153.5, 153.2, 153.0, 128.8, 127.6, 127.5, 124.7, 124.3, 124.1, 124.0, 123.7, 123.4, 123.3, 123.1, 122.0, 105.6, 104.9, 65.0, 64.9, 15.0, 14.9. HRMS (DART) calculated for $\text{C}_{24}\text{H}_{22}\text{Cl}_3\text{O}_3$ $[\text{M}+\text{H}]^+$: 463.0634, found: 463.0632.

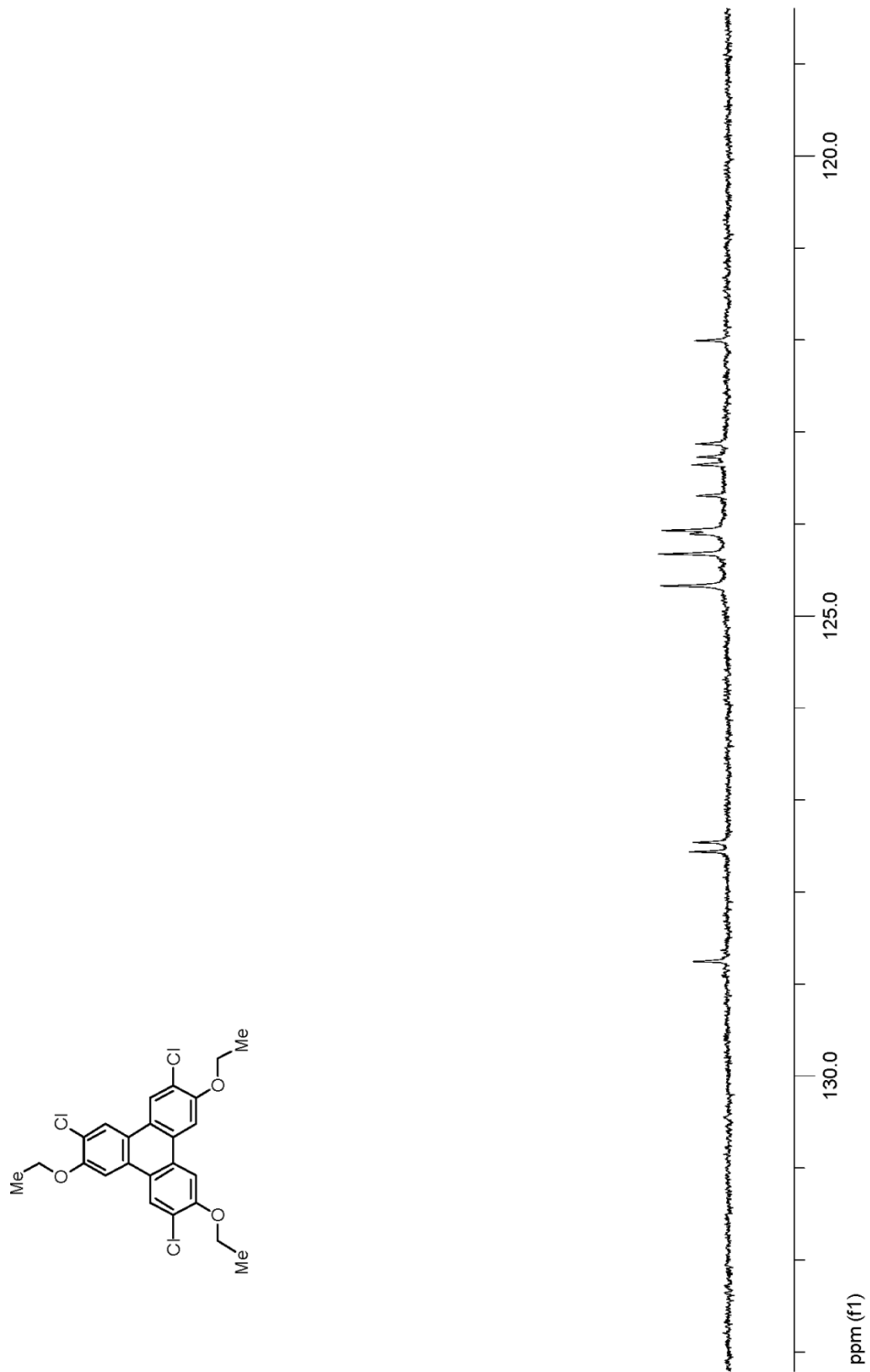


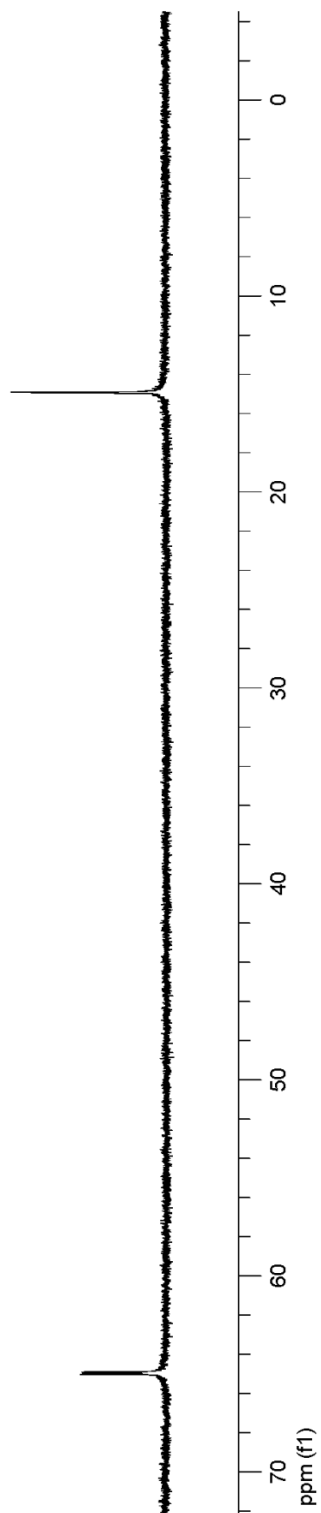
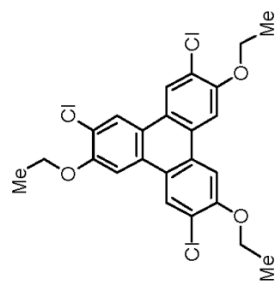
500 MHz, ¹H NMR, CDCl₃



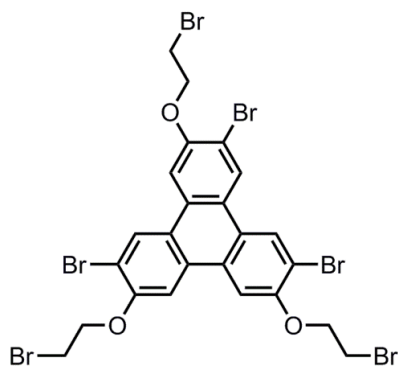
125 MHz, ^{13}C NMR, CDCl_3



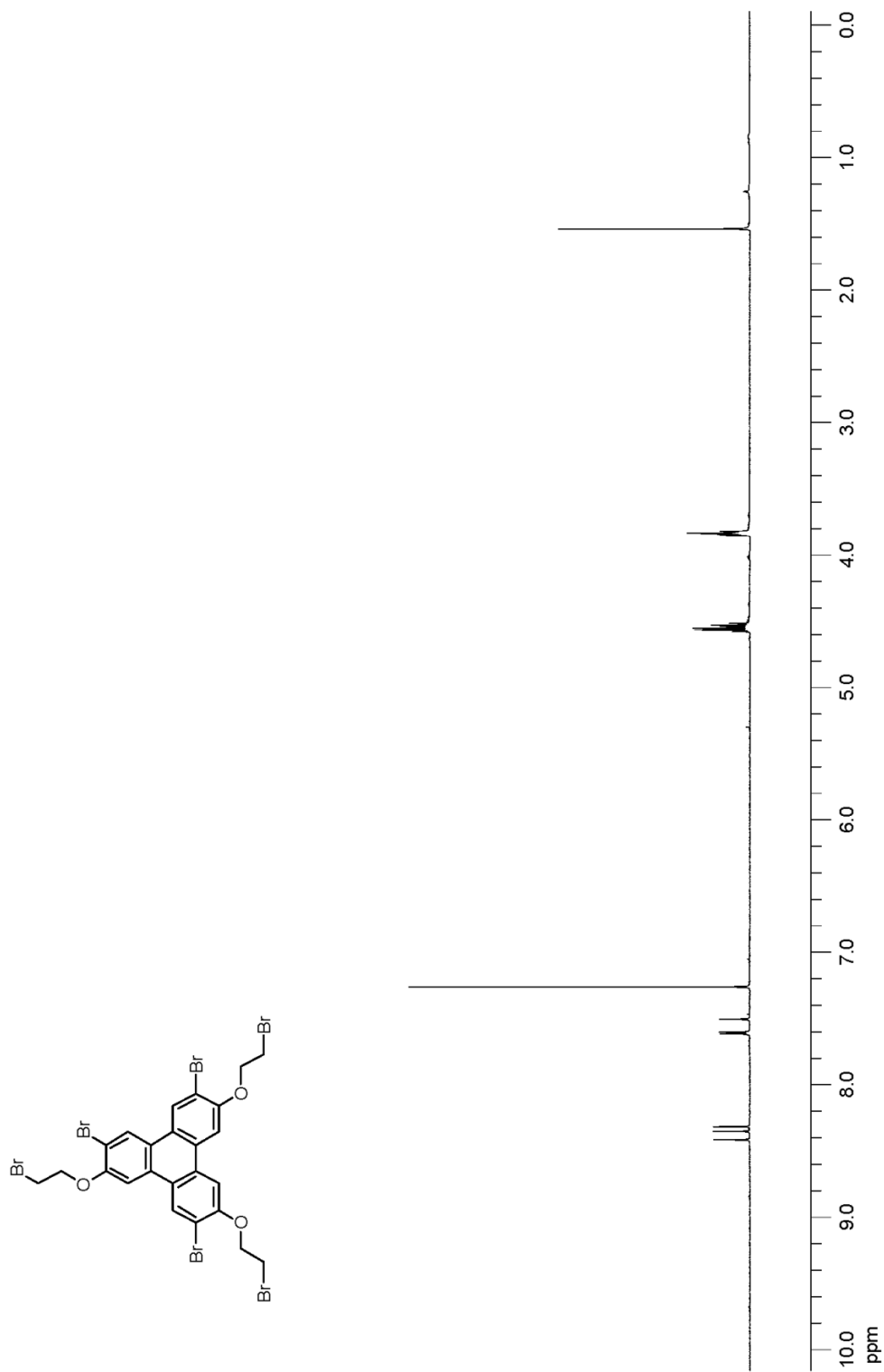


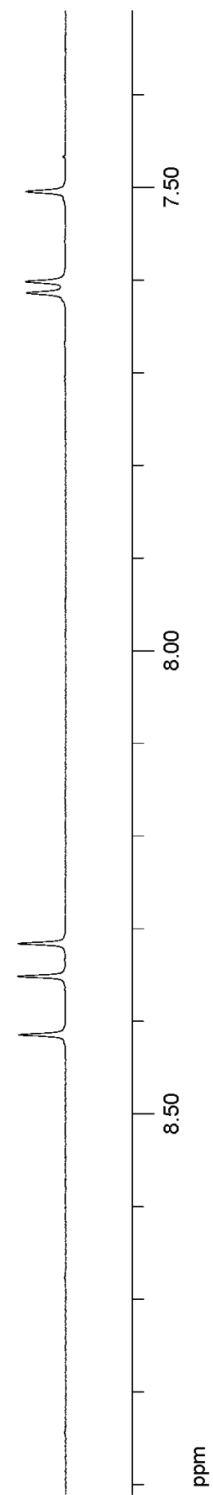
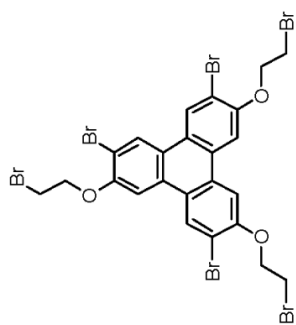
125 MHz, ¹³C NMR, CDCl₃

7.6.2.7. 2,6,11-Tribromo-3,7,10-tris(2-bromoethoxy)triphenylene

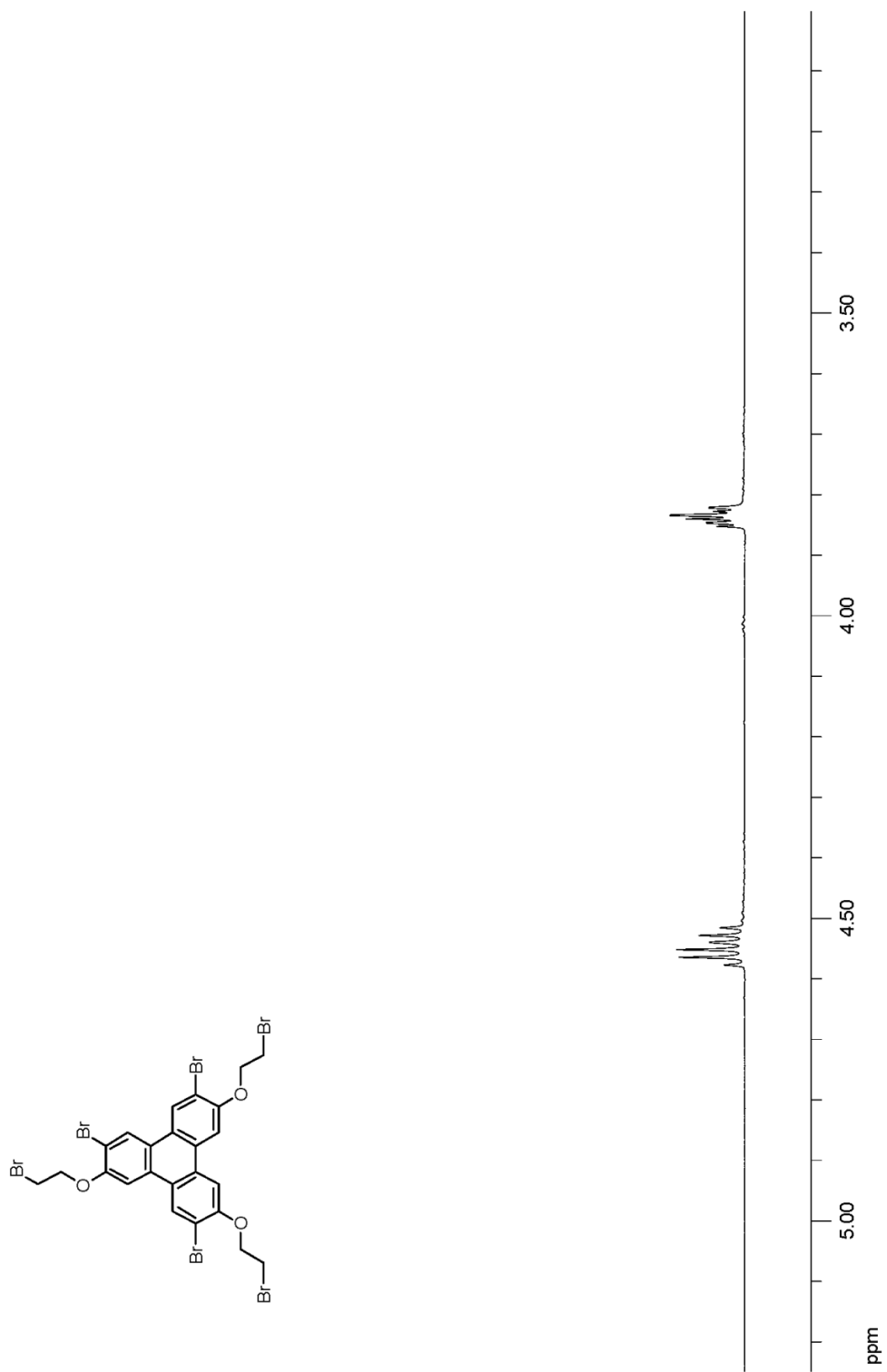


The general procedure described in Section 7.6.2.1 was followed on 0.10 mmol scale (28 mg) to obtain 2,6,11-tribromo-3,7,10-tris(2-bromoethoxy)triphenylene as a white solid in 62% yield (51 mg). ^1H NMR (500 MHz, CDCl_3): δ 8.41 (s, 1H), 8.35 (s, 1H), 8.32 (s, 1H), 7.61 (s, 1H), 7.60 (s, 1H), 7.51 (s, 1H), 4.56 (t, $J = 6.5$ Hz, 2H), 4.55 (t, $J = 6.5$ Hz, 2H), 4.53 (t, $J = 6.5$ Hz, 2H), 3.85–3.82 (m, 6H). HRMS (DART) calculated for $\text{C}_{24}\text{H}_{19}^{79}\text{Br}_3^{81}\text{Br}_3\text{O}_3$ $[\text{M}+\text{H}]^+$: 834.6373, found: 834.6350.

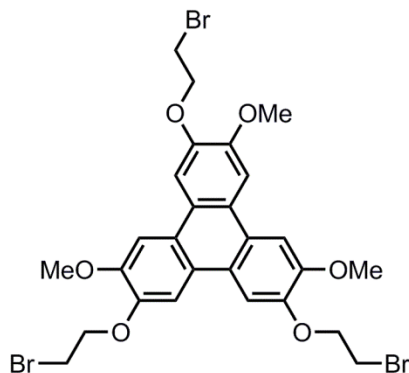




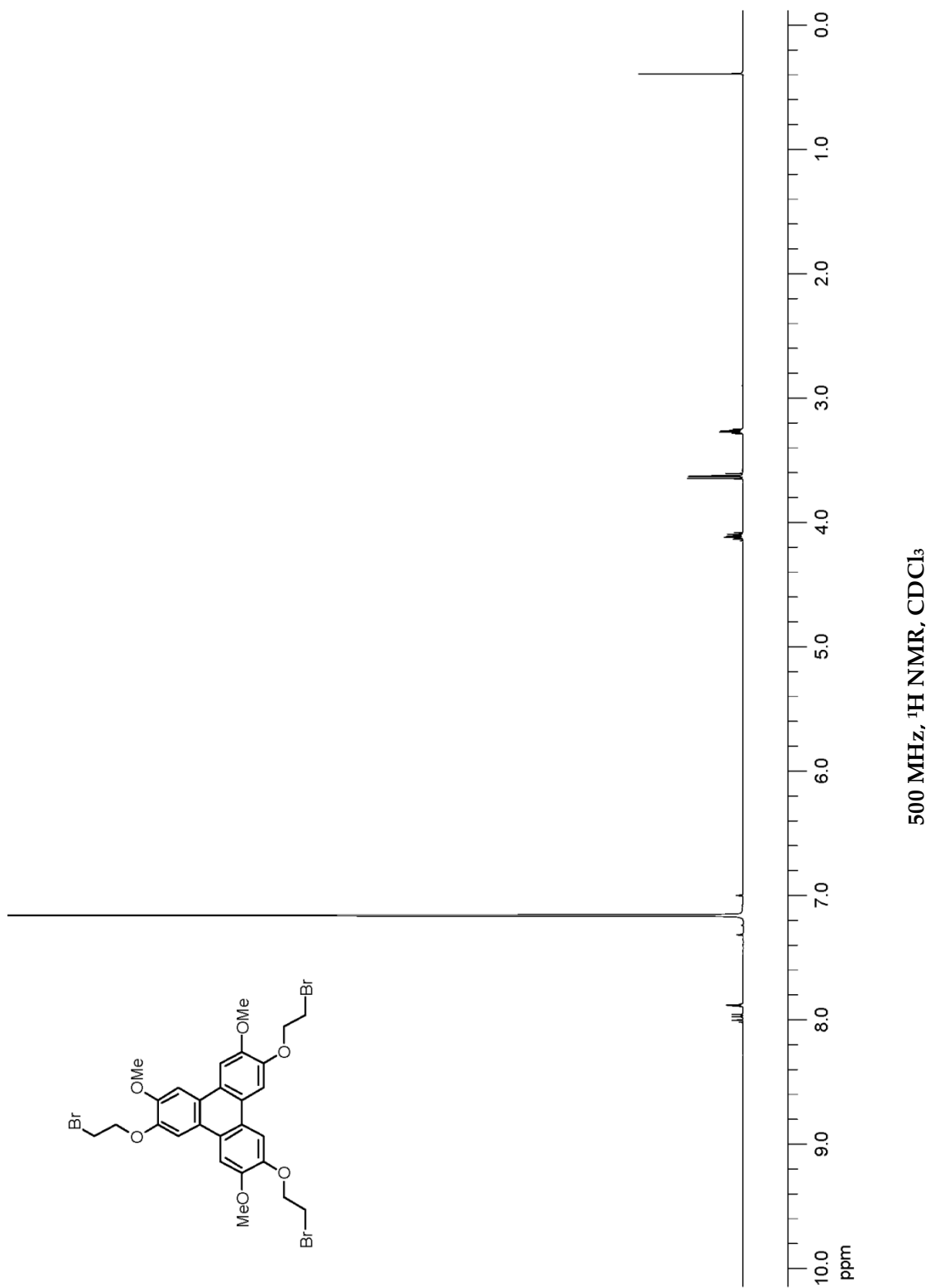
500 MHz, ¹H NMR, CDCl₃

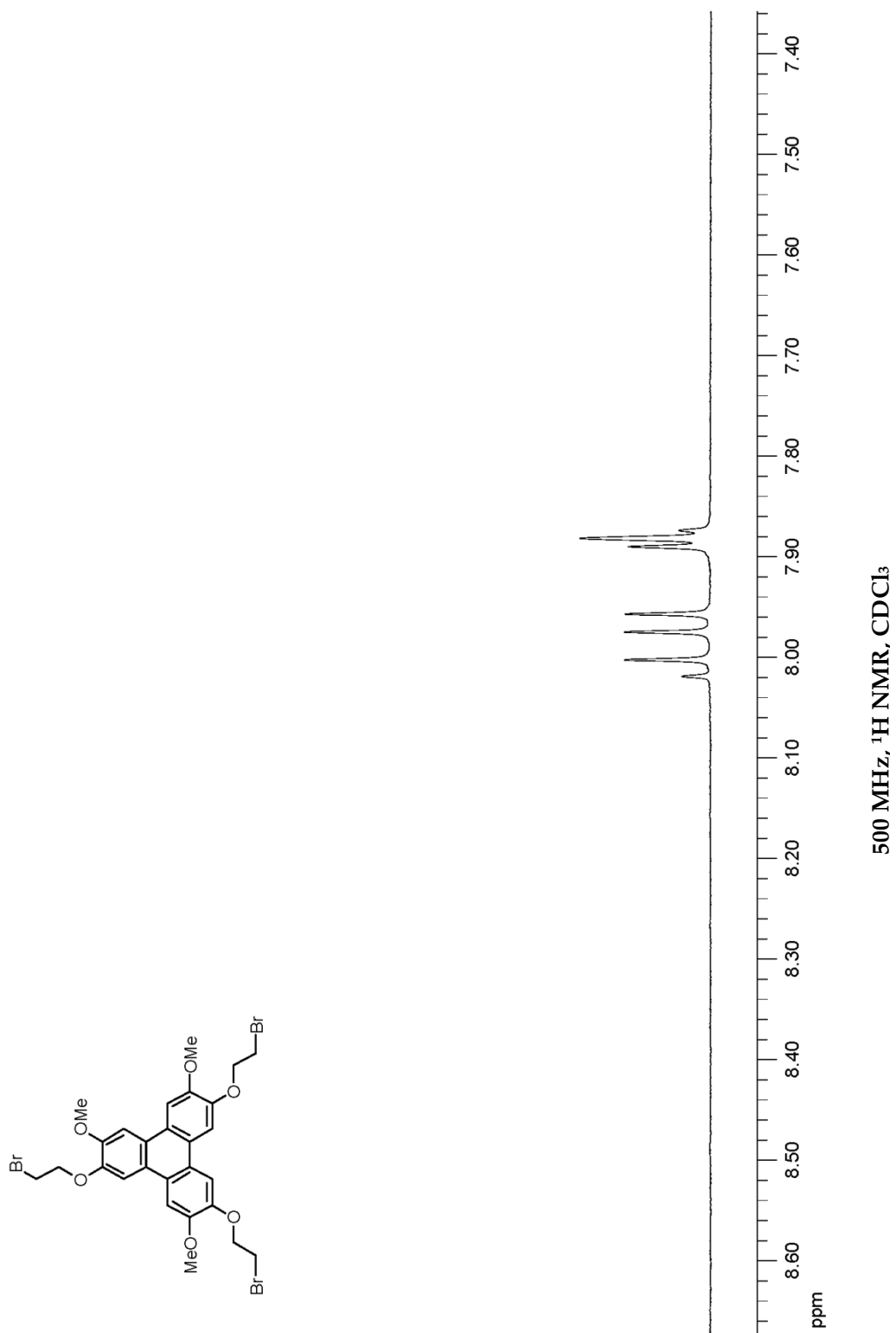


7.6.2.8. 2,6,11-Tris(2-bromoethoxy)-3,7,10-trimethoxytriphenylene

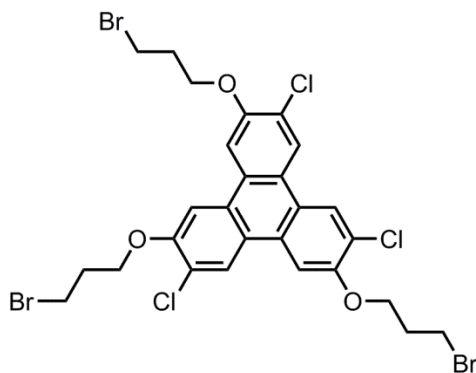


The general procedure described in Section 7.6.2.1 was followed on 0.10 mmol scale (23 mg) to obtain 2,6,11-tris(2-bromoethoxy)-3,7,10-trimethoxytriphenylene as a white solid in 60% yield (41 mg) as a mixture of regioisomers (9:1 for unsymmetrical:symmetrical). ^1H NMR (500 MHz, C_6D_6): δ 7.99 (s, 1H), 7.96 (s, 1H), 7.94 (s, 1H), 7.88 (s, 1H), 7.87 (s, 2H), 4.12–4.06 (m, 6H), 3.63 (s, 3H), 3.61 (s, 6H), 3.27–3.23 (m, 6H). HRMS (DART) calculated for $\text{C}_{27}\text{H}_{28}^{79}\text{Br}_3\text{O}_6$ $[\text{M}+\text{H}]^+$: 684.9436, found: 684.9450.

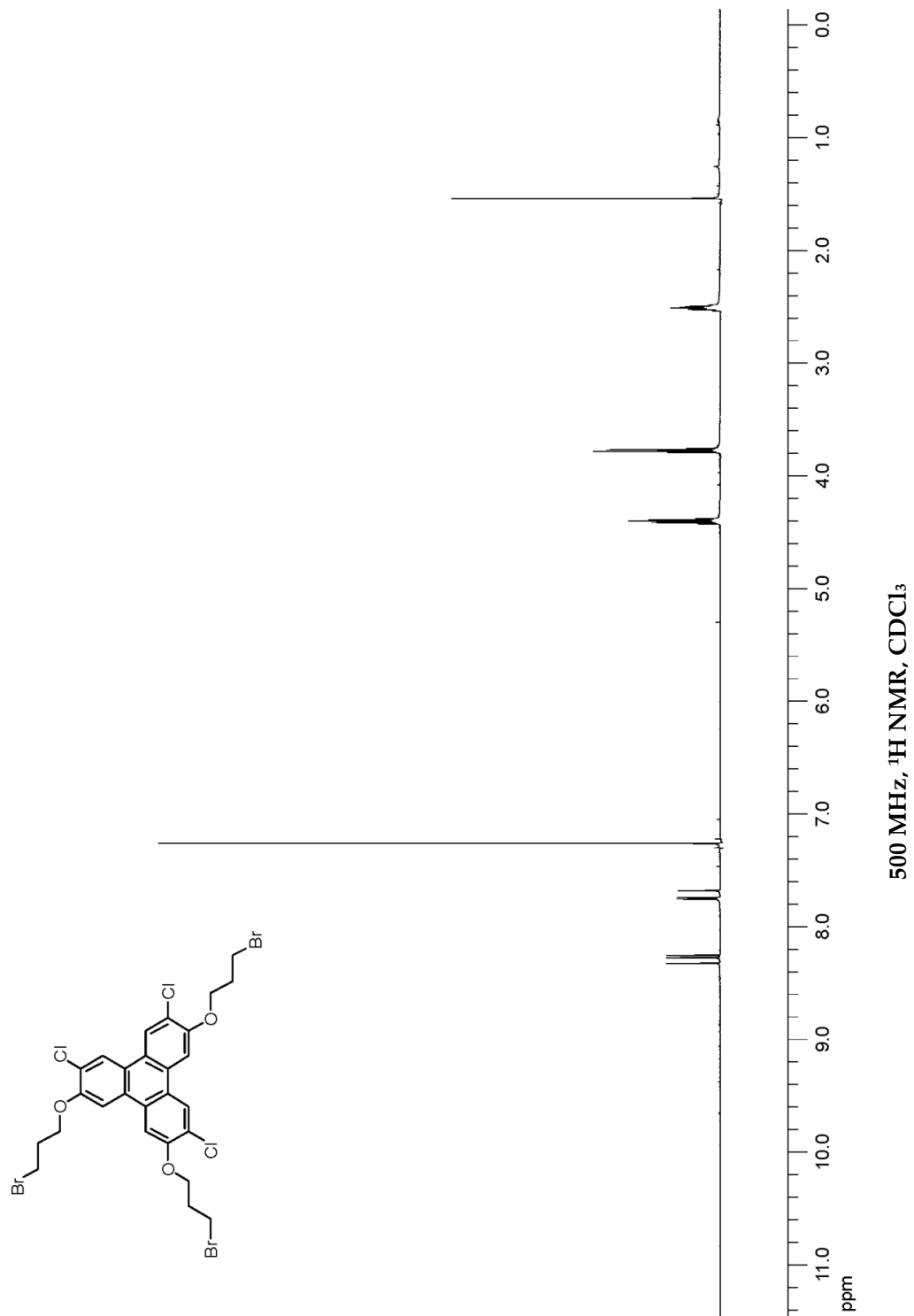


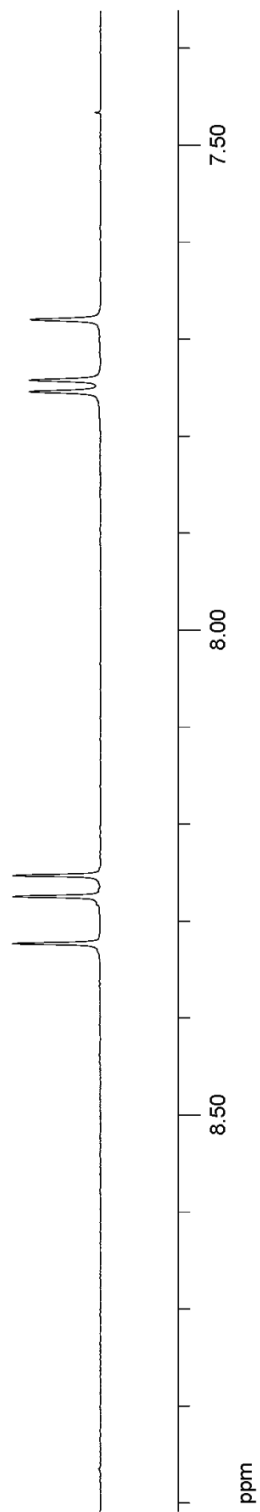
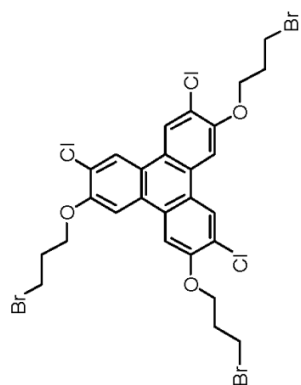


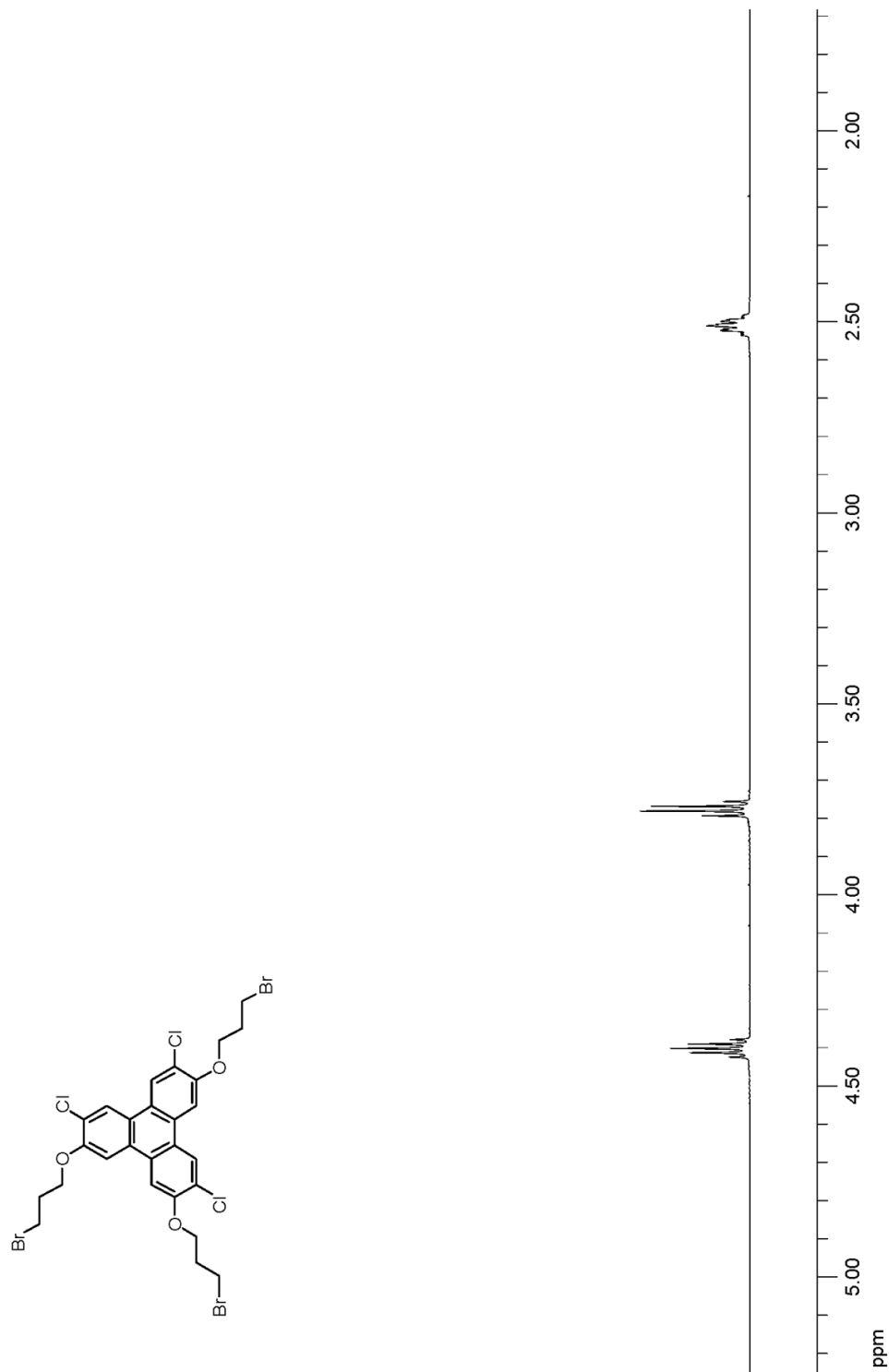
7.6.2.9. 2,6,11-Tris(3-bromopropoxy)-3,7,10-trichlorotriphenylene

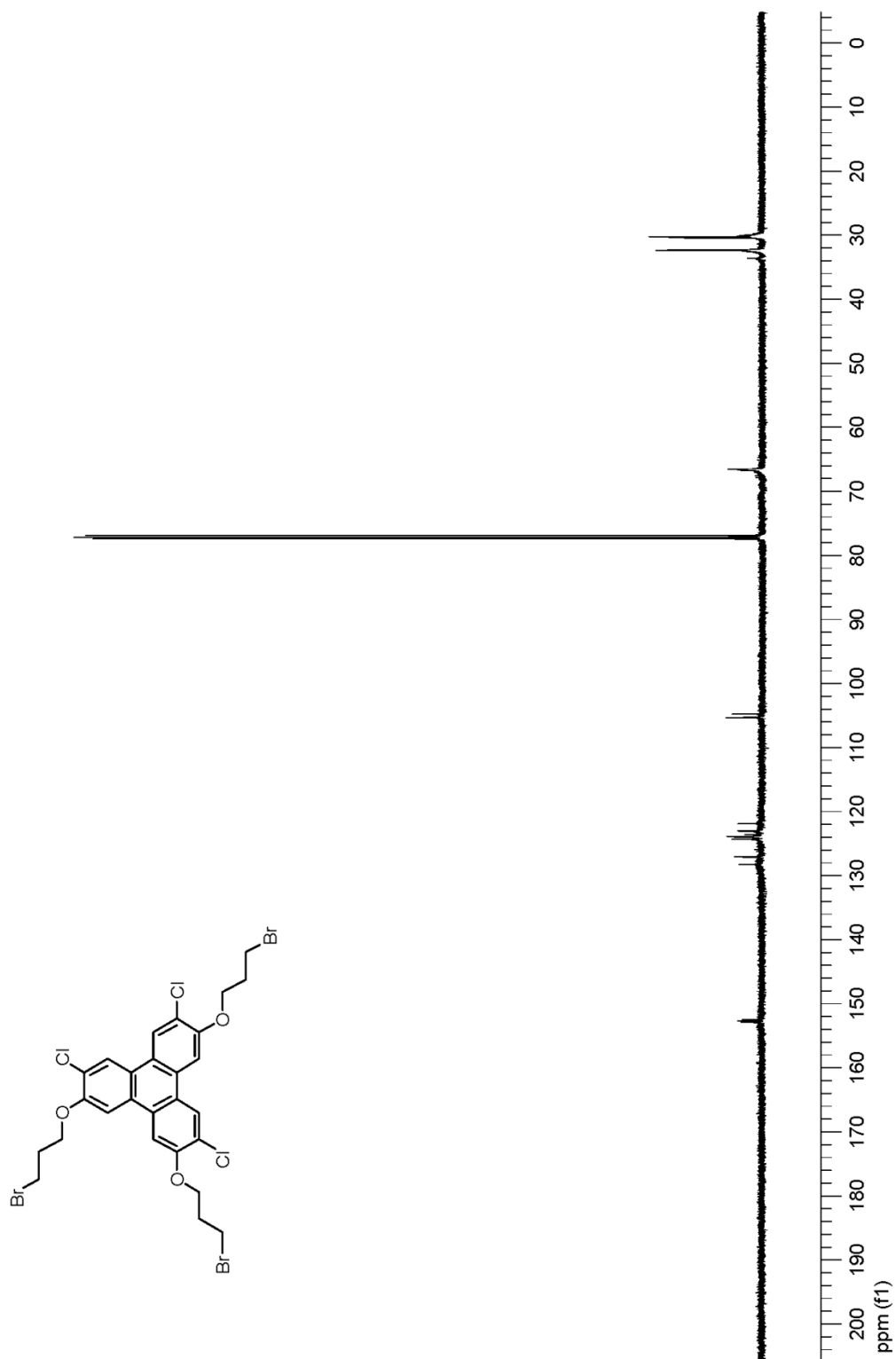


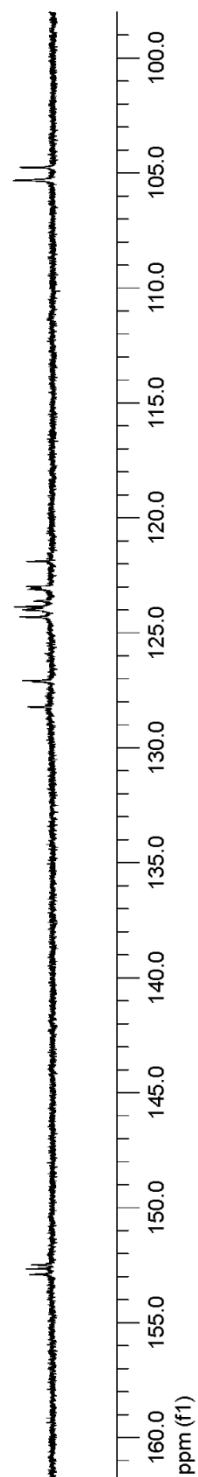
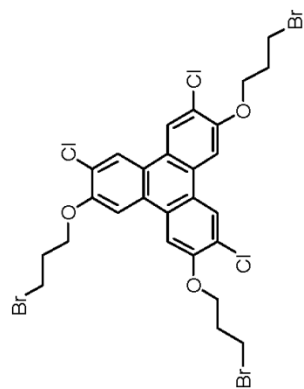
The general procedure described in Section 7.6.2.1 was followed on 0.10 mmol scale (25 mg) to obtain 2,6,11-tris(3-bromopropoxy)-3,7,10-trichlorotriphenylene as a white solid in 60% yield (44 mg). ^1H NMR (500 MHz, CDCl_3): δ 8.32 (s, 1H), 8.27 (s, 1H), 8.25 (s, 1H), 7.75 (s, 1H), 7.74 (s, 1H), 7.68 (s, 1H), 4.43–4.38 (m, 6H), 3.79–3.76 (m, 6H), 2.52–2.49 (m, 6H). ^{13}C NMR (125 MHz, CDCl_3): δ 152.9, 152.7, 152.5, 128.2, 127.1, 124.3, 124.0, 123.9, 123.8, 123.6, 123.1, 123.0, 121.9, 105.3, 104.7, 66.7, 66.6, 66.5, 32.4, 32.3, 32.2, 30.5, 30.4, 30.2. HRMS (DART) calculated for $\text{C}_{27}\text{H}_{25}^{79}\text{Br}^{81}\text{Br}_2\text{Cl}_3\text{O}_3$ $[\text{M}+\text{H}]^+$: 742.8379, found: 742.8399.

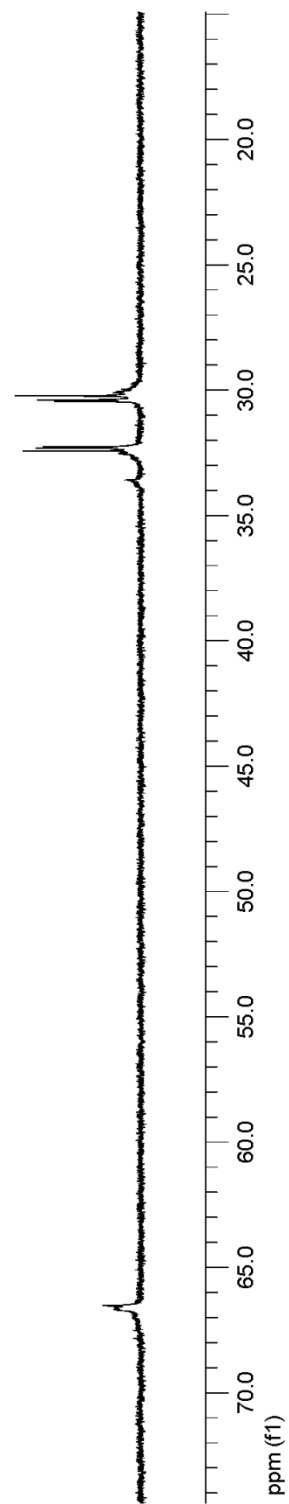
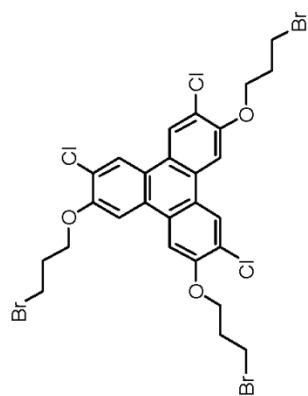


500 MHz, ¹H NMR, CDCl₃

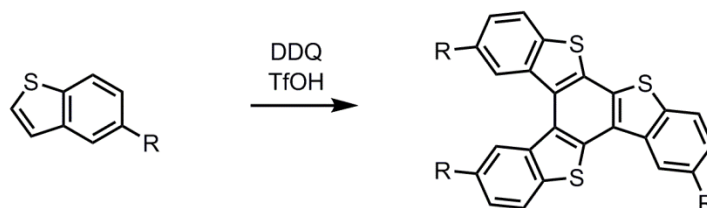




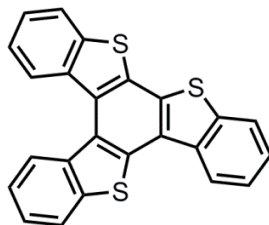
125 MHz, ^{13}C NMR, CDCl_3

125 MHz, ¹³C NMR, CDCl₃

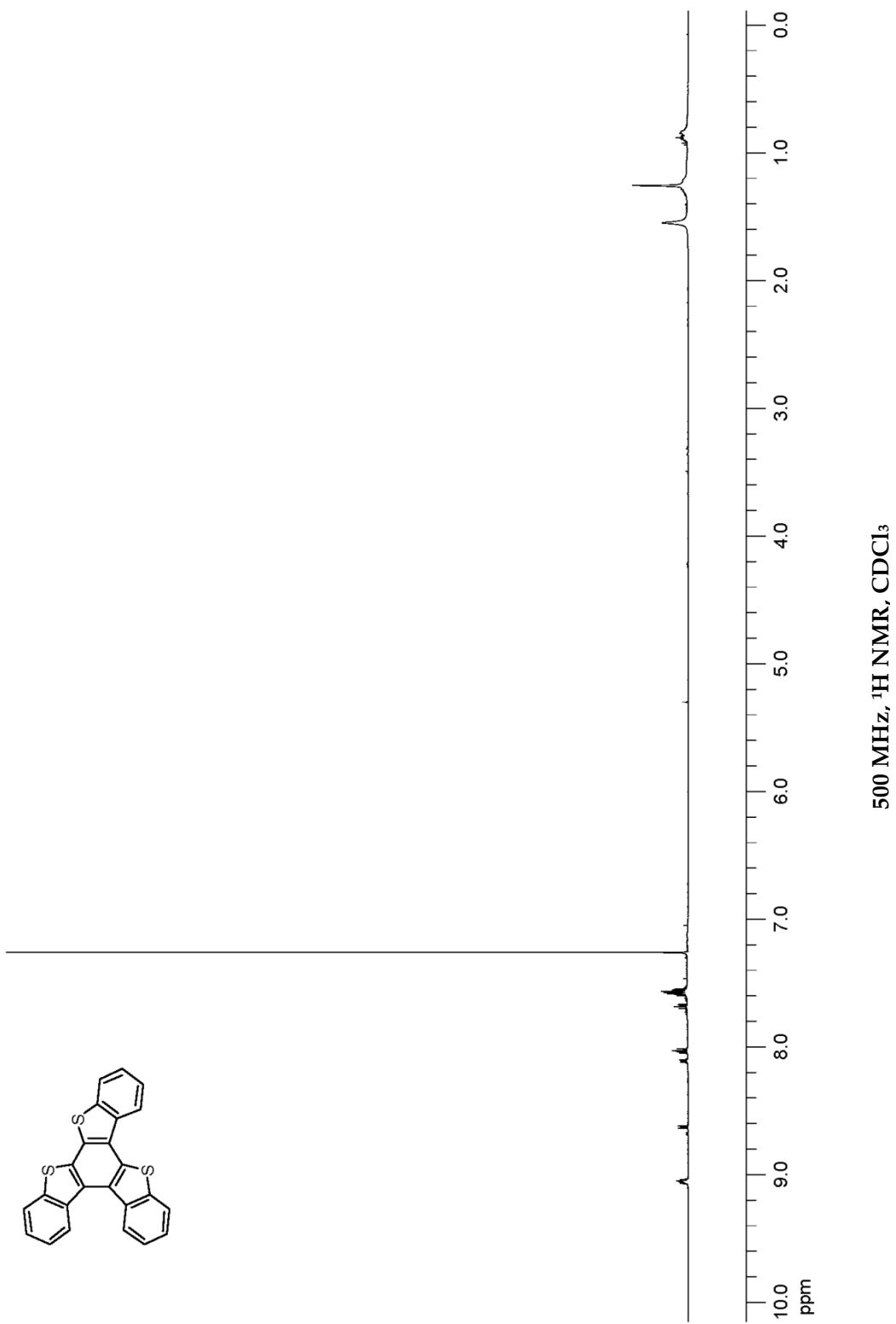
7.6.2.10. Representative Procedure for Coupling of Benzothiophenes

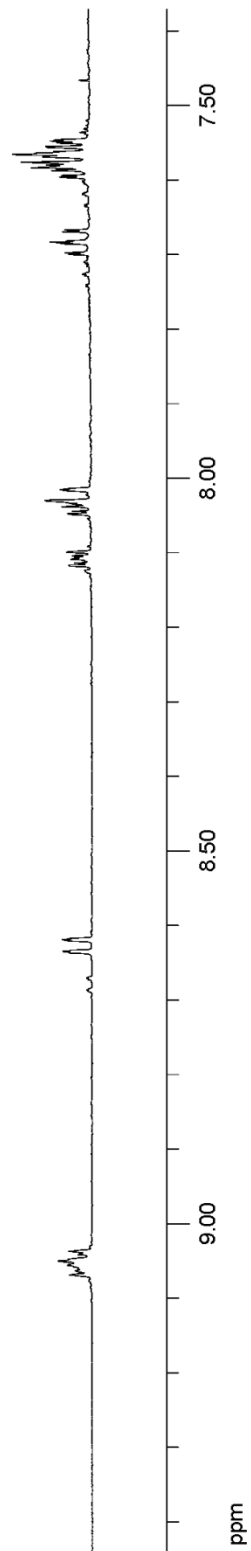
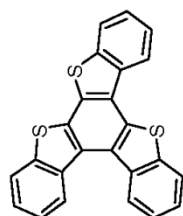


An oven-dried 20 mL scintillation vial, equipped with a magnetic stir-bar, was charged with the starting material (1.0 equiv), DDQ (1.0 equiv), trifluoromethanesulfonic acid (1.4% v/v, 3.0 equiv), and 1,2-dichloroethane (0.05 M). The reaction mixture was then allowed to stir at ambient temperature for 10 h. After this time, methanol (0.05M) was added, and the solution was then allowed to stir at ambient temperature for an additional hour. Upon addition of the methanol, some solids were precipitated out of the solution. Then, the solvent was removed from the heterogeneous mixture under reduced pressure. The crude material was purified by silica-gel column chromatography (hexanes/DCM) to give the title compounds.

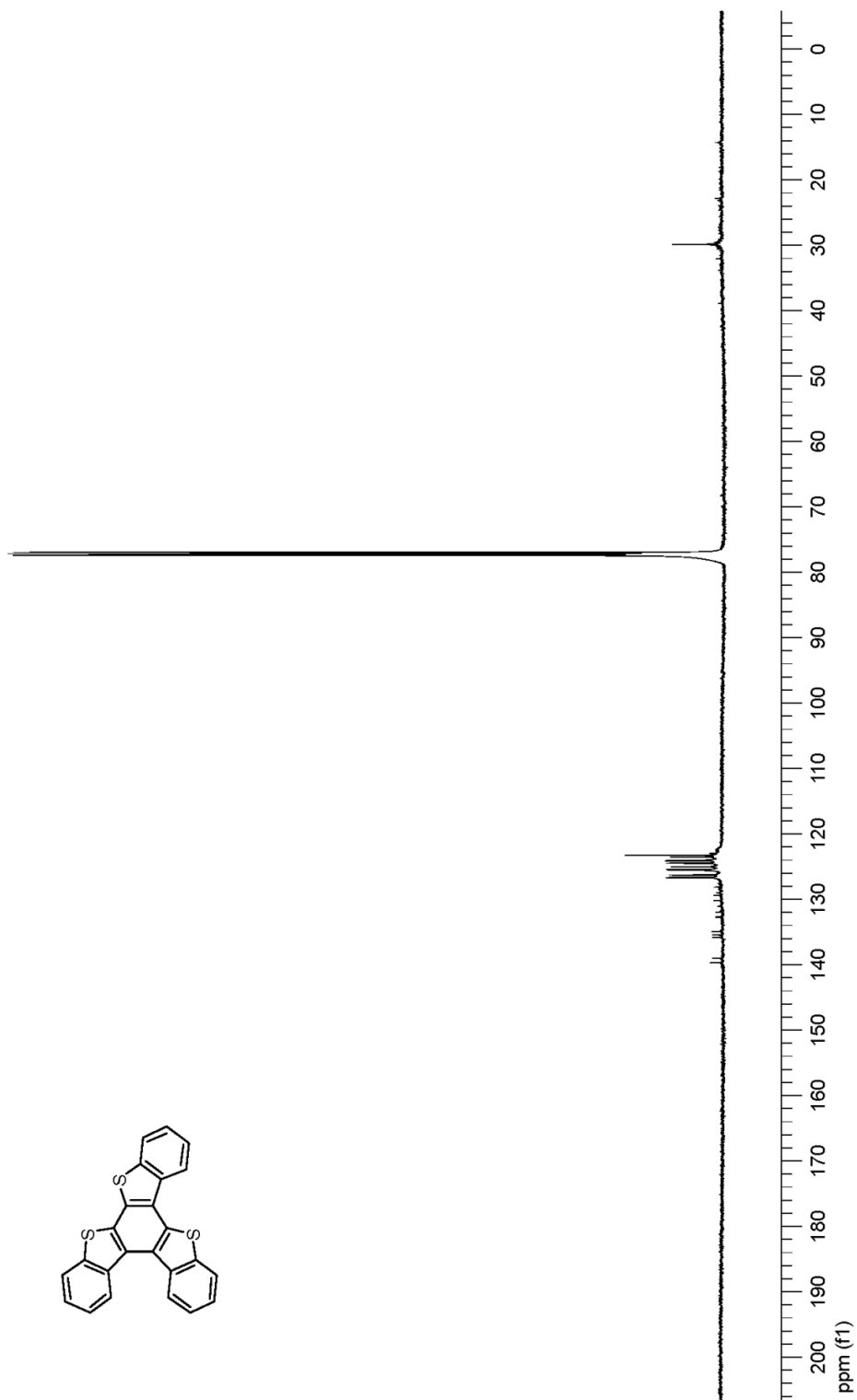
7.6.2.11. Benzo[1,2-*b*:3,4-*b'*:6,5-*b''*]tris[1]benzothiophene

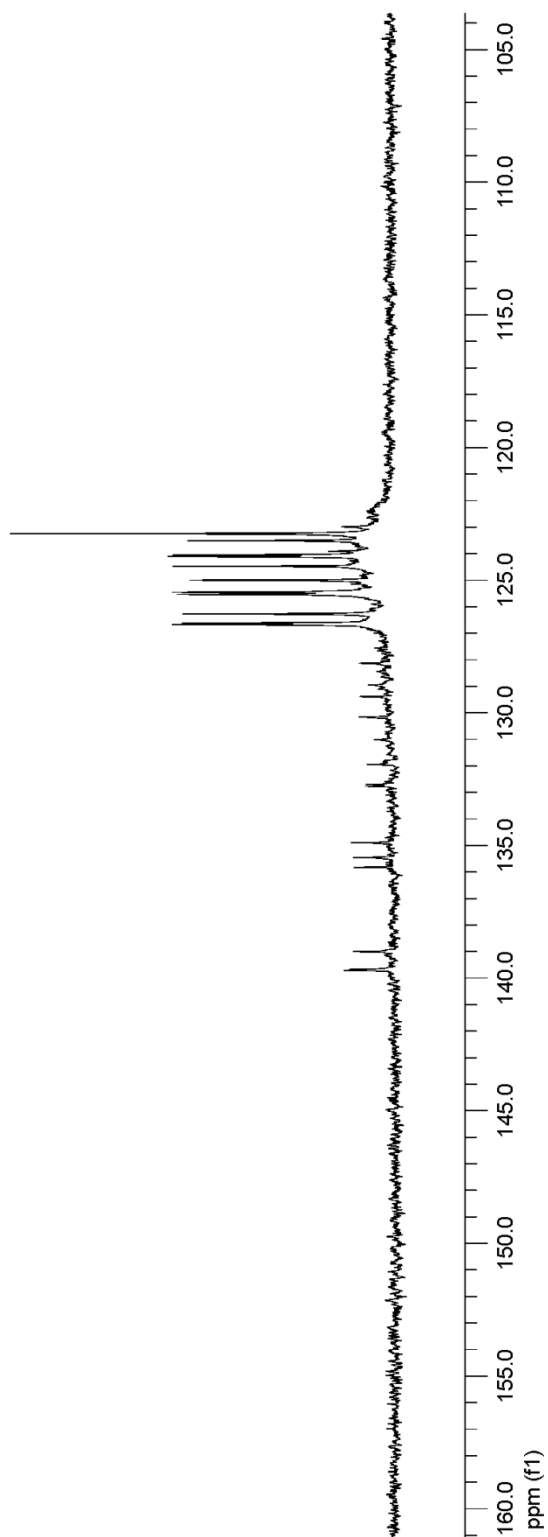
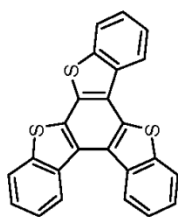
The general procedure described in Section 7.6.2.10 was followed on 0.10 mmol scale (13 mg) to obtain benzo[1,2-*b*:3,4-*b'*:6,5-*b''*]tris[1]benzothiophene as a pale yellow solid in 38% yield (15 mg). ^1H NMR (500 MHz, CDCl_3): δ 9.07–9.04 (m, 2H), 8.63 (d, $J = 8.0$ Hz, 1H), 8.11 (d, $J = 9.0$ Hz, 1H), 8.05–8.01 (m, 2H), 7.68 (t, $J = 8.0$ Hz, 2H), 7.60–7.54 (m, 4H). ^{13}C NMR (150 MHz, CDCl_3): δ 139.7, 139.6, 139.0, 135.8, 135.5, 134.9, 132.8, 132.7, 132.0, 130.2, 129.4, 128.1, 126.7, 126.6, 126.3, 125.5, 125.4, 125.0, 124.5, 124.1, 124.0, 123.5, 123.2. HRMS (DART) calculated for $\text{C}_{24}\text{H}_{13}\text{S}_3$ $[\text{M}+\text{H}]^+$: 397.0179, found: 397.0189.

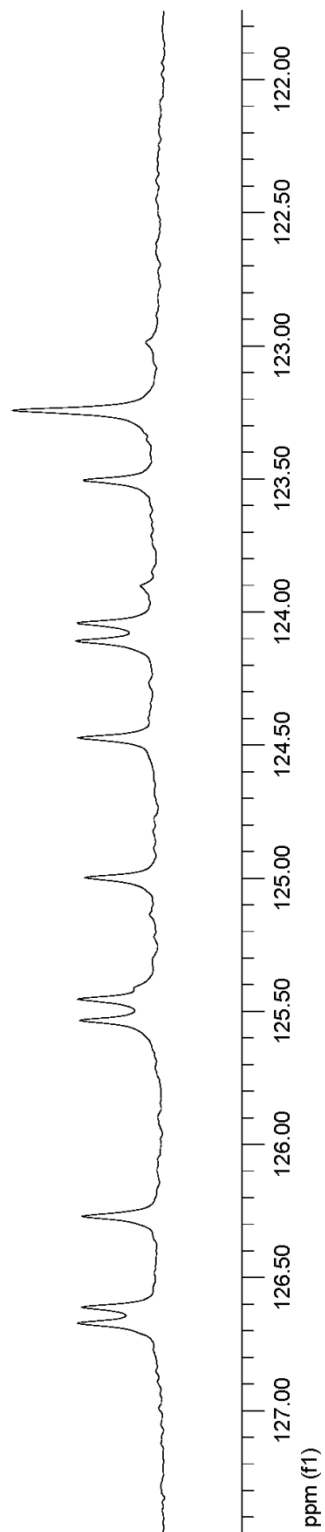
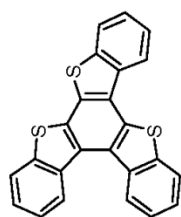


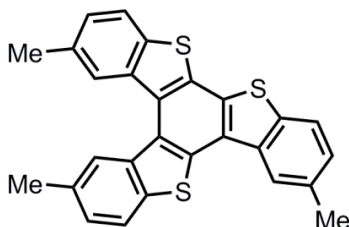


500 MHz, ^1H NMR, CDCl_3

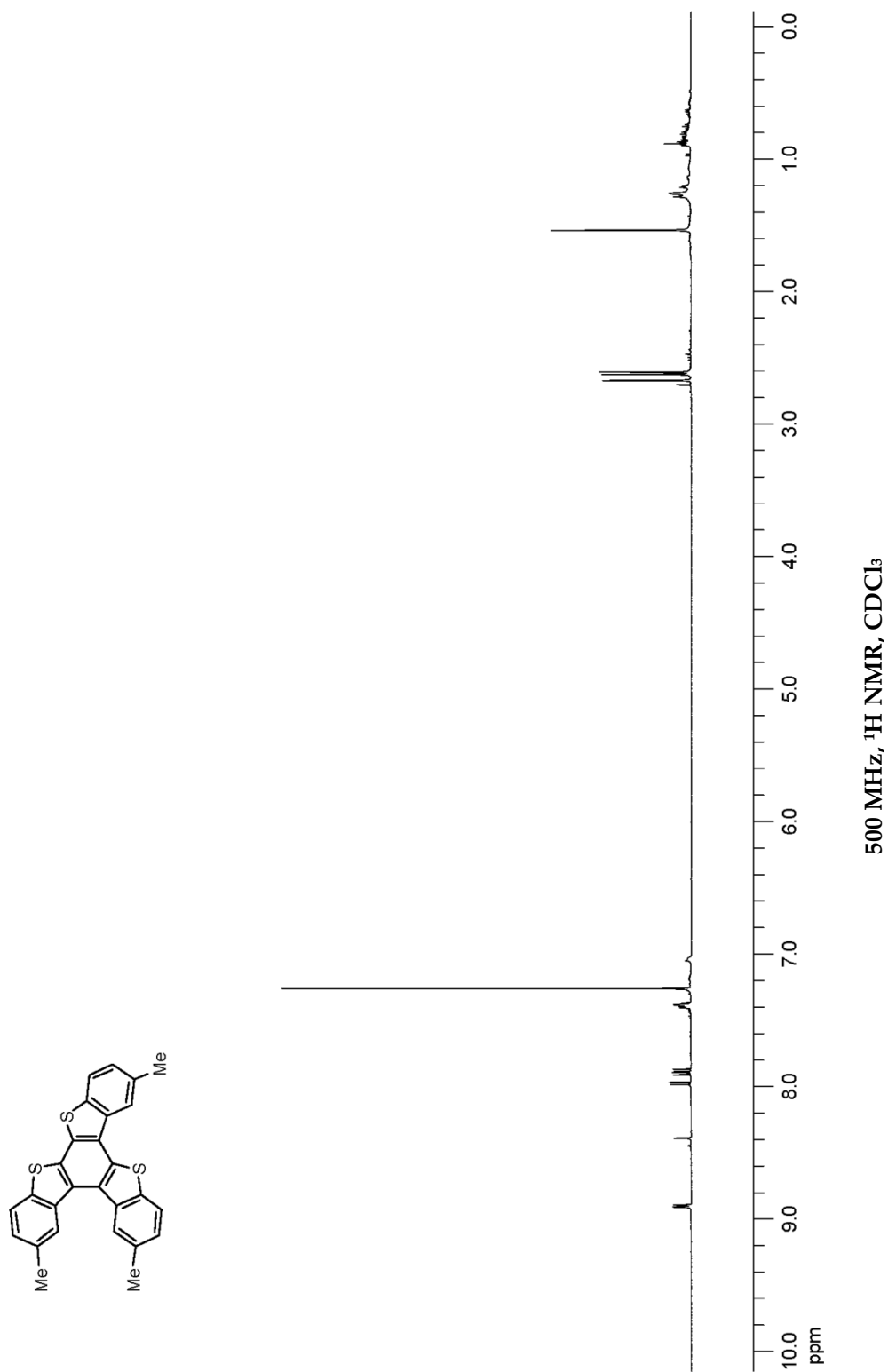


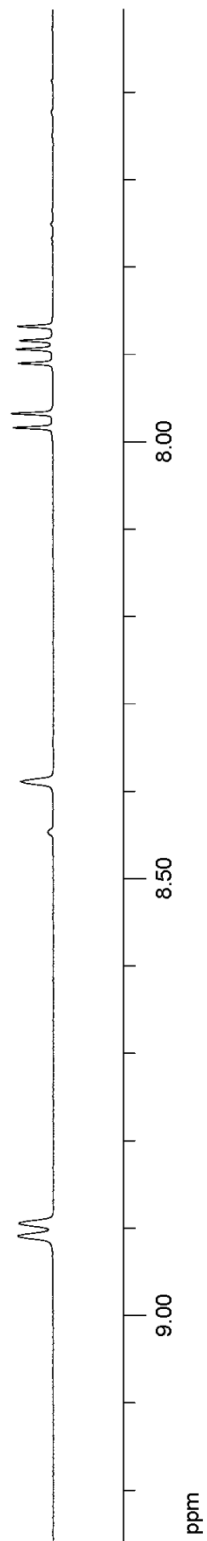
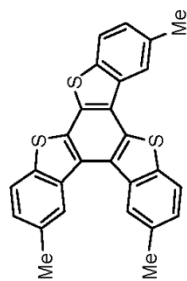
125 MHz, ^{13}C NMR, CDCl_3

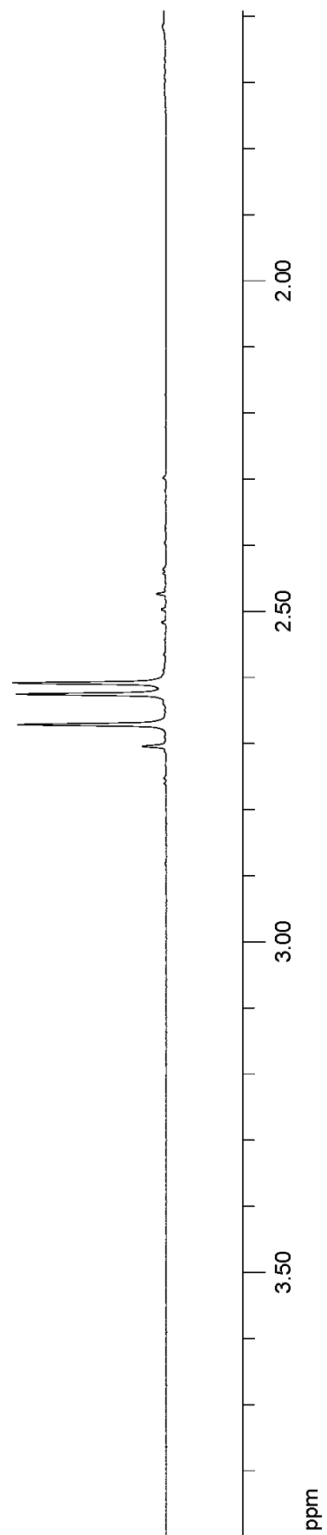
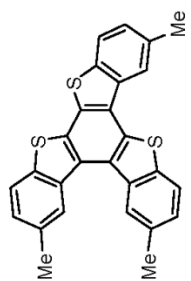
125 MHz, ^{13}C NMR, CDCl_3

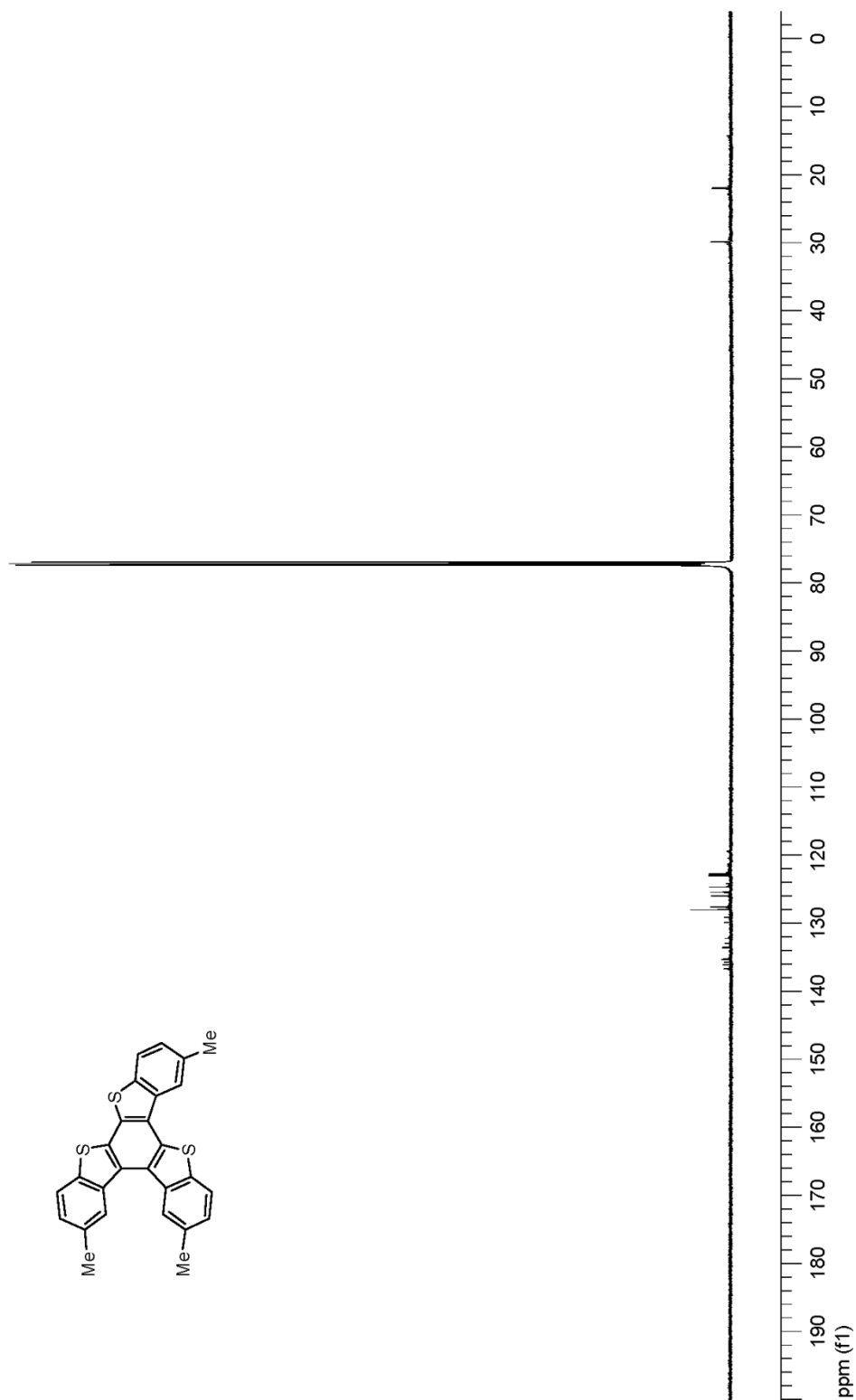
7.6.2.12. 2,7,14-Trimethylbenzo[1,2-*b*:3,4-*b'*:6,5-*b''*]tris[1]benzothiophene

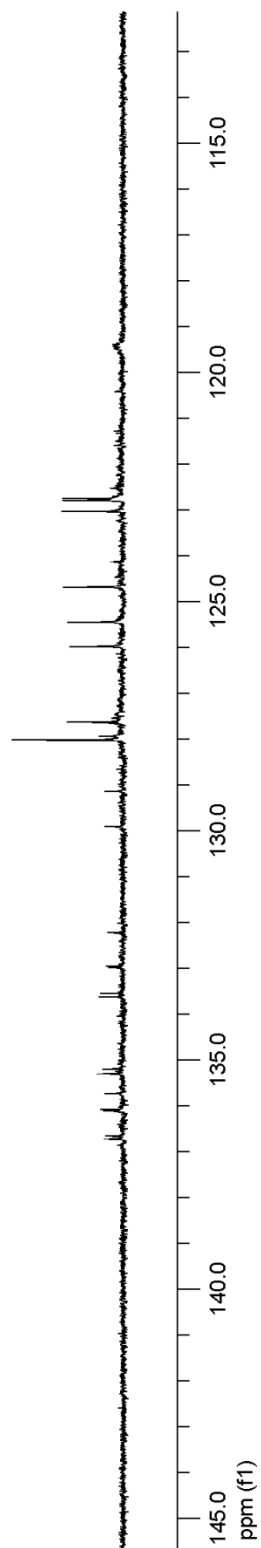
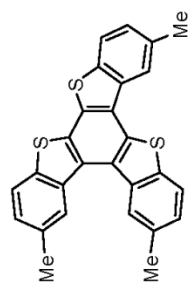
The general procedure described in Section 7.6.2.10 was followed on 0.10 mmol scale (15 mg) to obtain 2,7,14-trimethylbenzo[1,2-*b*:3,4-*b'*:6,5-*b''*]tris[1]benzothiophene as a pale yellow solid in 43% yield (19 mg). ^1H NMR (500 MHz, CDCl_3): δ 8.91 (s, 1H), 8.89 (s, 1H), 8.39 (s, 1H), 7.98 (d, $J = 8.5$ Hz, 1H), 7.90 (d, $J = 8.5$ Hz, 1H), 7.88 (d, $J = 8.0$ Hz, 1H), 7.40–7.37 (m, 3H), 2.67 (s, 3H), 2.63 (s, 3H), 2.61 (s, 3H). ^{13}C NMR (150 MHz, CDCl_3): δ 136.7, 136.6, 136.1, 136.0, 135.7, 135.3, 135.2, 133.6, 133.5, 132.9, 132.2, 130.0, 129.2, 128.0, 127.6, 126.0, 125.5, 124.7, 124.1, 123.0, 122.8, 122.7, 122.5, 22.1, 21.9, 21.8. HRMS (DART) calculated for $\text{C}_{27}\text{H}_{19}\text{S}_3$ $[\text{M}+\text{H}]^+$: 439.0649, found: 439.0653.

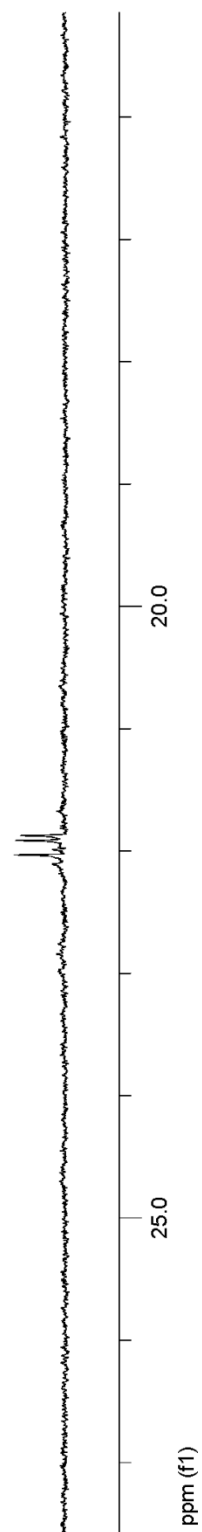
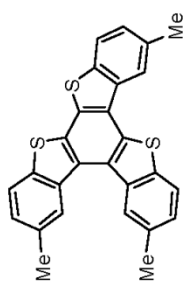


500 MHz, ^1H NMR, CDCl_3

500 MHz, ^1H NMR, CDCl_3



125 MHz, ^{13}C NMR, CDCl_3



125 MHz, ^{13}C NMR, CDCl_3